Symmetry Energy at supra-saturation densities studied with neutron-proton elliptic flows

P. Russotto
INFN-LNS, Catania, Italy
for
ASY-EOS II & NewCHIM collaborations

9/2/2018 10:15 AM

Introduction

The nuclear EOS describes the relation among energy, pressure, density, temperature and isospin asymmetry. It is a fundamental ingredient in nuclear physics and astrophysics.

Nuclear matter phase diagram (schematic)

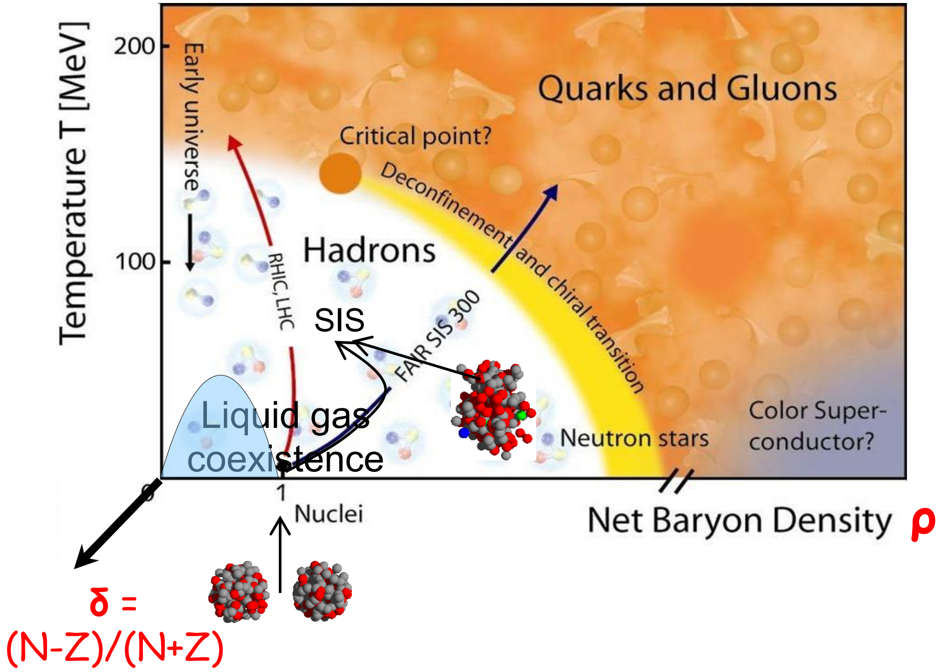

Introduction

The nuclear EOS describes the relation among energy, pressure, density, temperature and isospin asymmetry. It is a fundamental ingredient in nuclear physics and astrophysics.

Nuclear matter phase diagram (schematic)

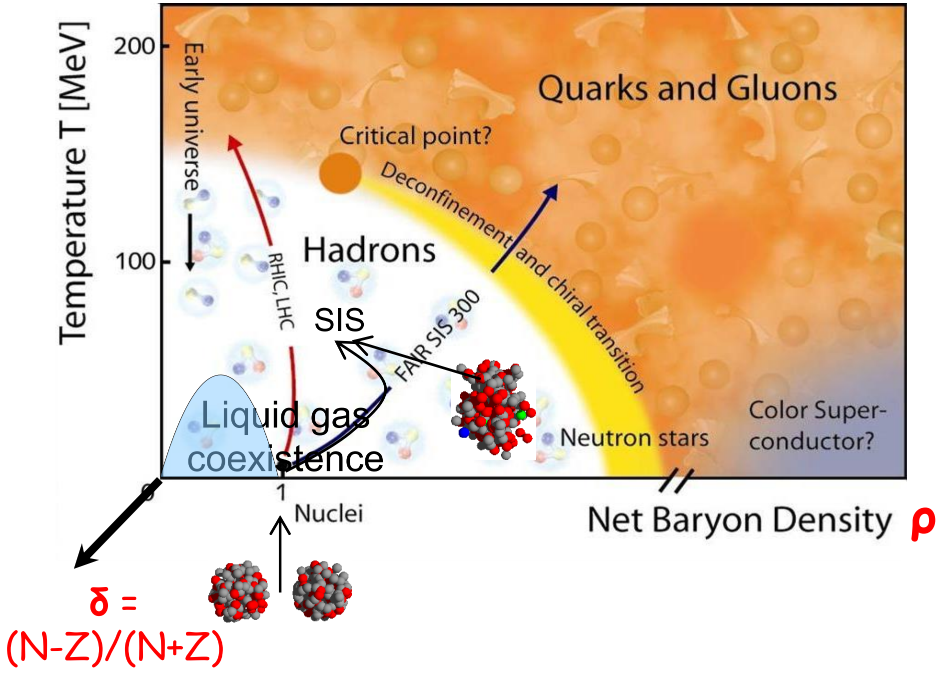

E/A(ρ, δ)=????

Introduction

The nuclear EOS describes the relation among energy, pressure, density, temperature and isospin asymmetry. It is a fundamental ingredient in nuclear physics and astrophysics.

Nuclear matter phase diagram (schematic)

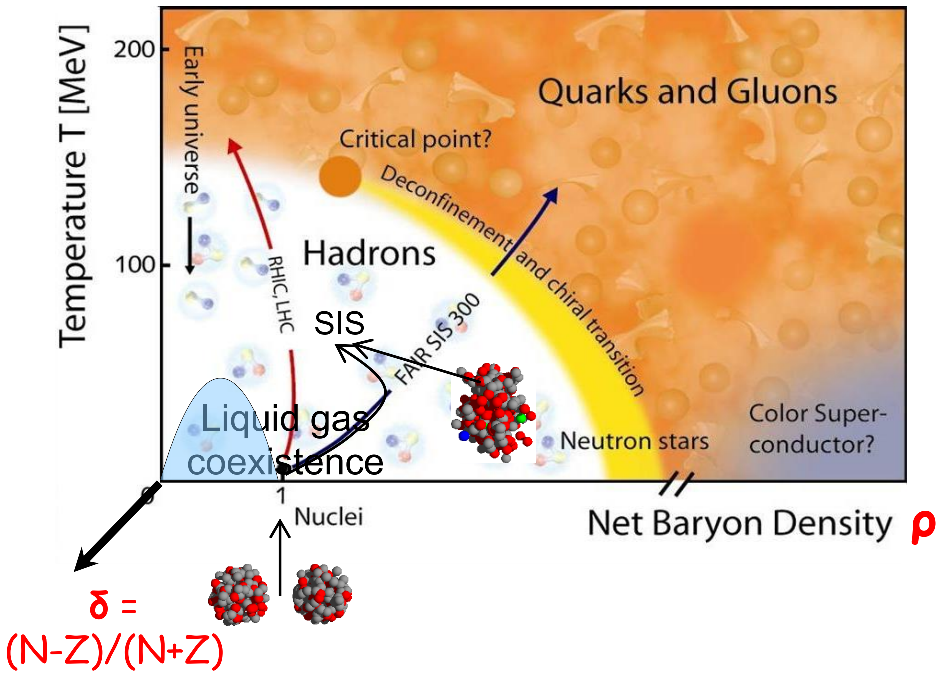

E/A(ρ, δ)=????

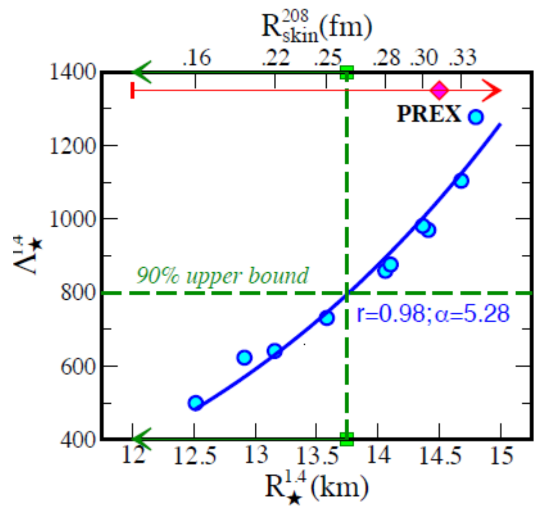

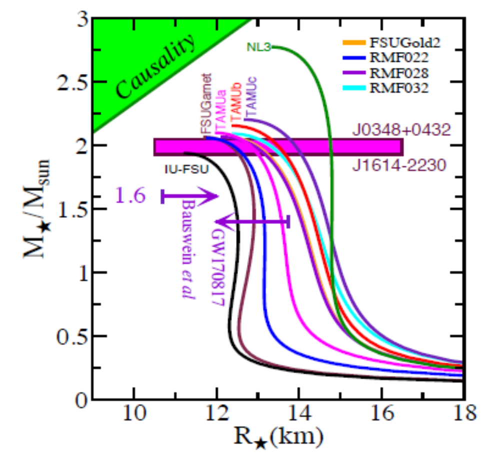

Fattoyev, Piekarewicz, Horowitz

Symmetry Energy at supra-saturation densities

$$E(\rho,\delta) = E(\rho,\delta=0) + E_{sym}(\rho)\delta^2 + \ldots$$

$$\delta = \frac{\rho_n - \rho_p}{\rho_n + \rho_p} = \frac{N-Z}{A}$$

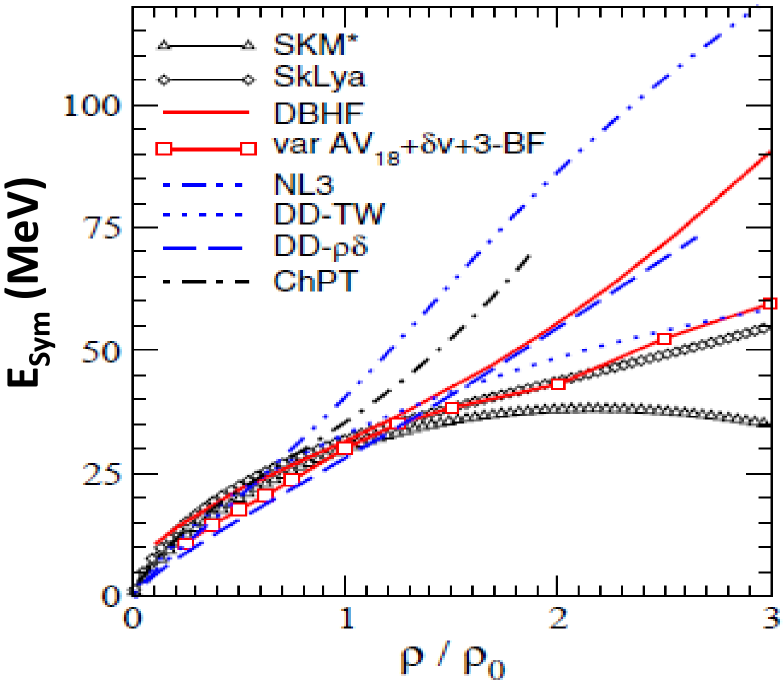

Fuchs and Wolter, EPJA 30 (2006)

Symmetry Energy at supra-saturation densities

$$E(\rho,\delta) = E(\rho,\delta=0) + E_{sym}(\rho)\delta^2 + \ldots$$

$$\delta = \frac{\rho_n - \rho_p}{\rho_n + \rho_p} = \frac{N-Z}{A}$$

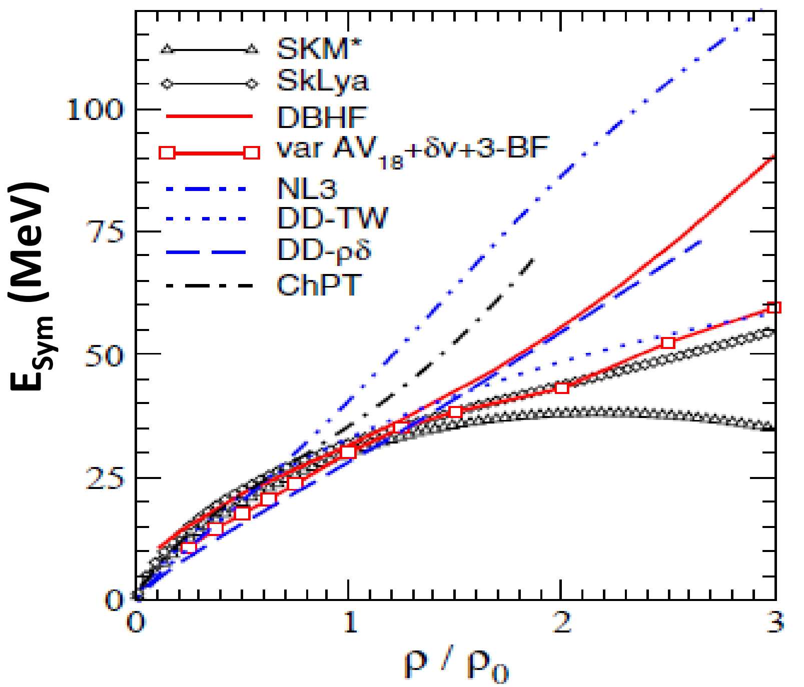

Fuchs and Wolter, EPJA 30 (2006)

- Phenomenological forces constrained around saturation and for nearly isospin-symmetric matter.
- Poor knowledge of effective forces in neutron-rich matter.
- Uncertainties in the nature of the three-neutron force.
- Uncertain extrapolations far from the saturation density.

Symmetry Energy at supra-saturation densities

$$E(\rho,\delta) = E(\rho,\delta=0) + E_{sym}(\rho)\delta^2 + \ldots$$

$$\delta = \frac{\rho_n - \rho_p}{\rho_n + \rho_p} = \frac{N-Z}{A}$$

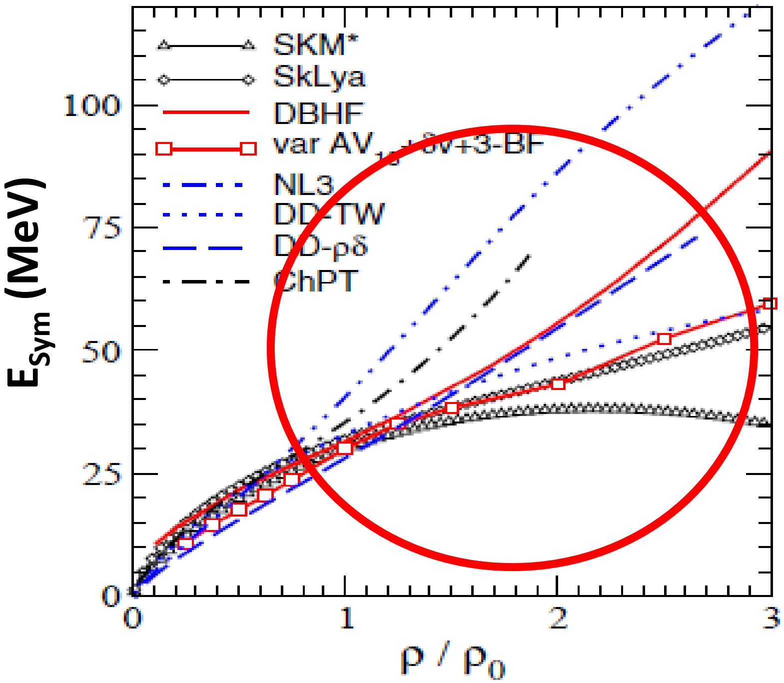

Fuchs and Wolter, EPJA 30 (2006)

- Phenomenological forces constrained around saturation and for nearly isospin-symmetric matter.
- Poor knowledge of effective forces in neutron-rich matter.
- Uncertainties in the nature of the three-neutron force.
- Uncertain extrapolations far from the saturation density.

Why high-density?

- Huge divergences
- Few constraints
- Astrophysical interest

Symmetry Energy at supra-saturation densities

$$E(\rho,\delta) = E(\rho,\delta=0) + E_{sym}(\rho)\delta^2 + \ldots$$

$$\delta = \frac{\rho_n - \rho_p}{\rho_n + \rho_p} = \frac{N-Z}{A}$$

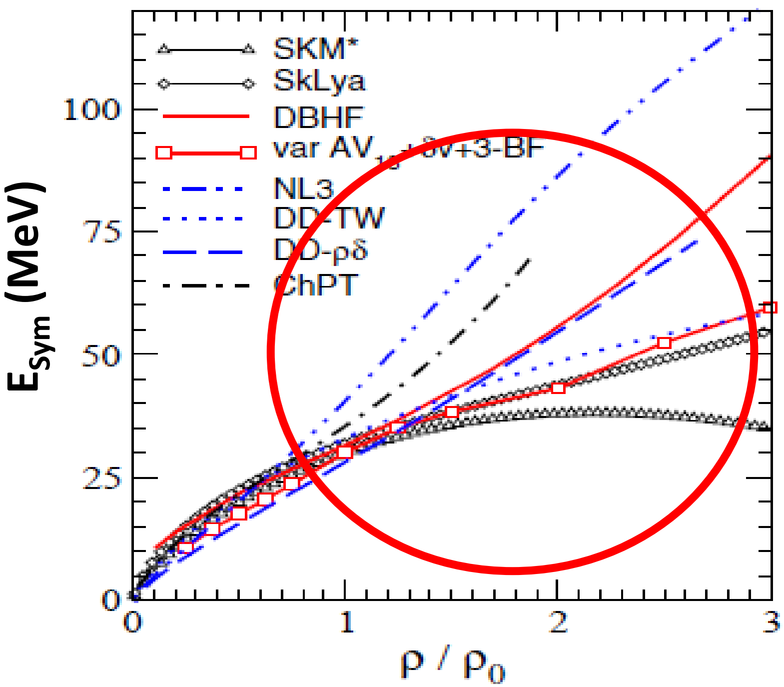

Fuchs and Wolter, EPJA 30 (2006)

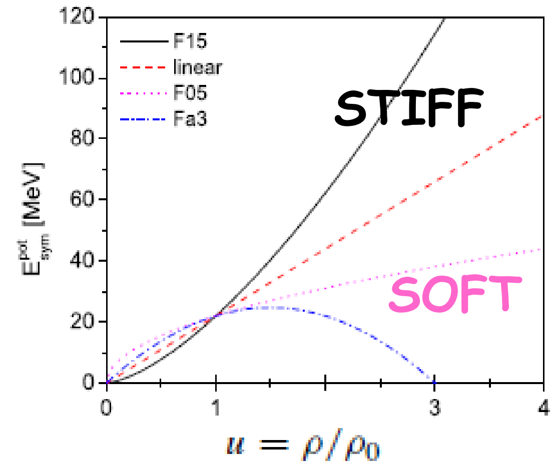

$$E_{sym} = E^{pot}_{sym} + E^{kin}_{sym} = 22\,\text{MeV} \cdot (\rho/\rho_0)^{\gamma} + 12\,\text{MeV} \cdot (\rho/\rho_0)^{2/3}$$

- Phenomenological forces constrained around saturation and for nearly isospin-symmetric matter.
- Poor knowledge of effective forces in neutron-rich matter.
- Uncertainties in the nature of the three-neutron force.
- Uncertain extrapolations far from the saturation density.

Why high-density?

- Huge divergences
- Few constraints
- Astrophysical interest

High densities observable: flows

$$\frac{dN}{d(\phi-\phi_R)}(y,p_t)=\frac{N_0}{2\pi}\left(1+2\sum_{n\geq 1}v_n\cos n(\phi-\phi_R)\right)$$

y = rapidity, pt = transverse momentum

ϕ_R = reaction plane orientation

High densities observable: flows

$$\frac{dN}{d(\phi-\phi_R)}(y,p_t)=\frac{N_0}{2\pi}\left(1+2\sum_{n\geq 1}v_n\cos n(\phi-\phi_R)\right)$$

y = rapidity, pt = transverse momentum
ϕ_R = reaction plane orientation

$$V_2(y,p_t)=\left\langle\frac{p_x^2-p_y^2}{p_t^2}\right\rangle$$

Elliptic flow: competition between in plane ($v_2>0$) and out-of-plane ejection ($v_2<0$)

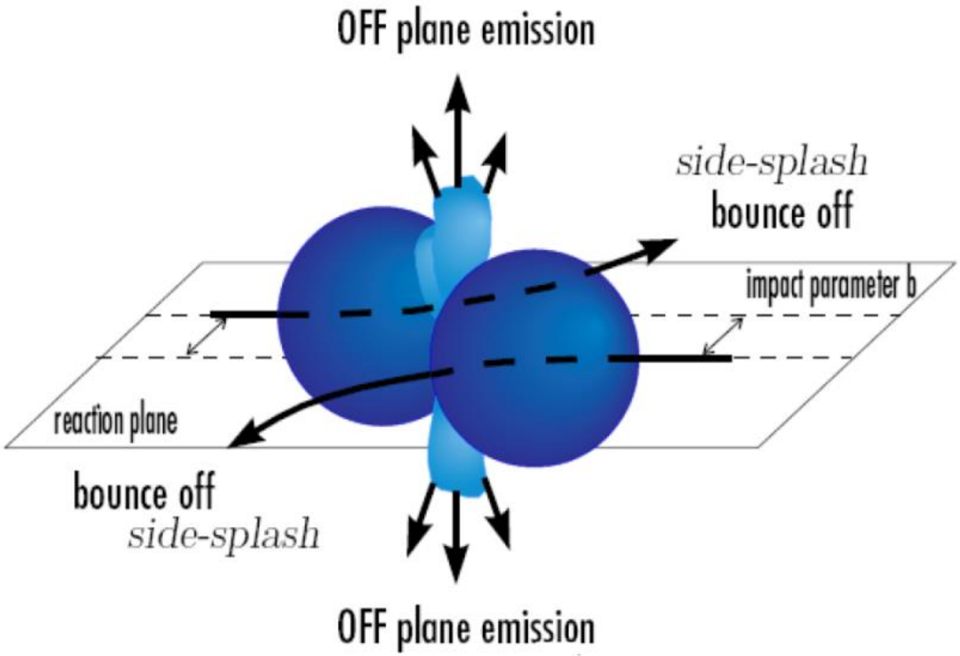

High densities observable: flows

$$\frac{dN}{d(\phi-\phi_R)}(y,p_t)=\frac{N_0}{2\pi}\left(1+2\sum_{n\geq1}v_n\cos n(\phi-\phi_R)\right)$$

y = rapidity, pt = transverse momentum
ϕ_R = reaction plane orientation

$$V_2(y,p_t)=\left\langle\frac{p_x^2-p_y^2}{p_t^2}\right\rangle$$

Elliptic flow: competition between in plane (v_2>0) and out-of-plane ejection (v_2<0)

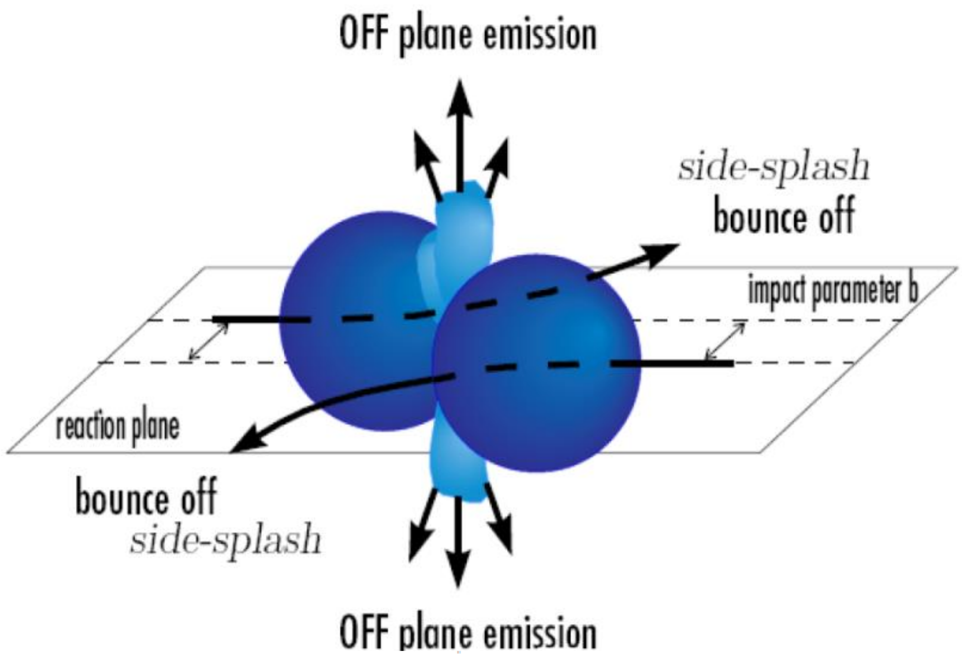

UrQMD :Au+Au @ 400 AMeV
5.5<b<7.5 fm

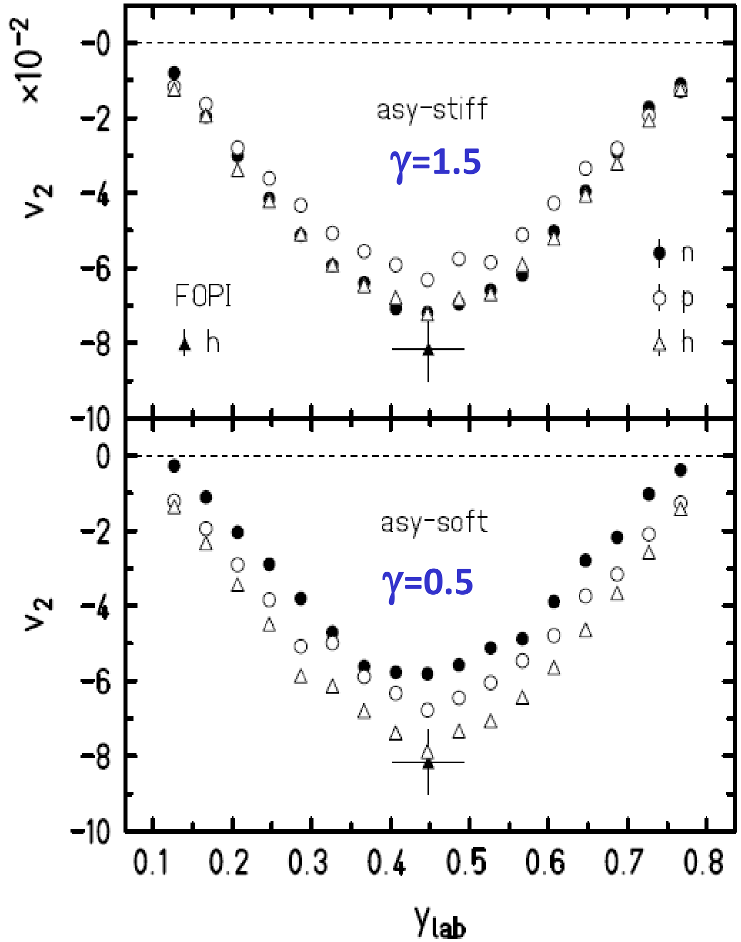

$$E_{sym}=E_{sym}^{pot}+E_{sym}^{kin}$$
$$=22\,\mathrm{MeV}\cdot(\rho/\rho_0)^{\gamma}+12\,\mathrm{MeV}\cdot(\rho/\rho_0)^{2/3}$$

Qingfeng Li, J. Phys. G31 1359-1374 (2005)
P.Russotto et al., Phys. Lett. B 697 (2011)

FOPI/LAND experiment on neutron squeeze out (1991)

Main observable
v_2^n/v_2^H

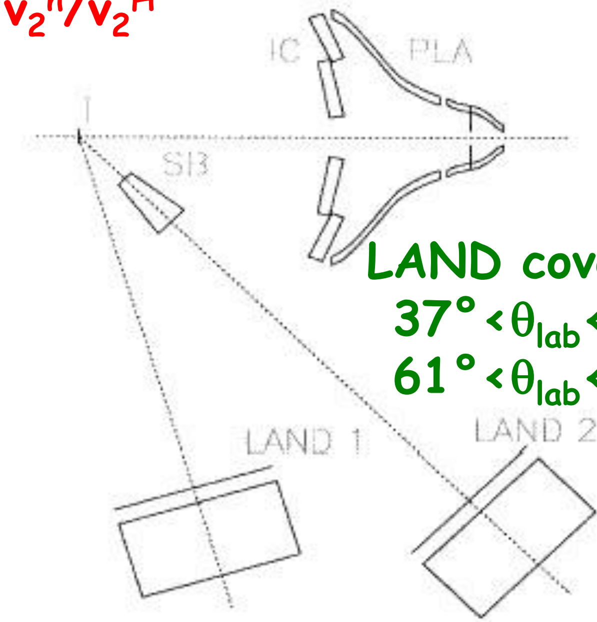

LAND coverage
$37° < \theta_{lab} < 53°$
$61° < \theta_{lab} < 85°$

UrQMD:
momentum dep. of isoscalar field
momentum dep. of NNECS
momentum independent power-law parameterization of the symmetry energy

$\gamma = 0.9 \pm 0.4$

L=83±26

Y. Leifels et al., PRL 71, 963 (1993)
P.Russotto et al., PLB 697 (2011)

FOPI/LAND experiment on neutron squeeze out (1991)

Main observable
v_2^n/v_2^H

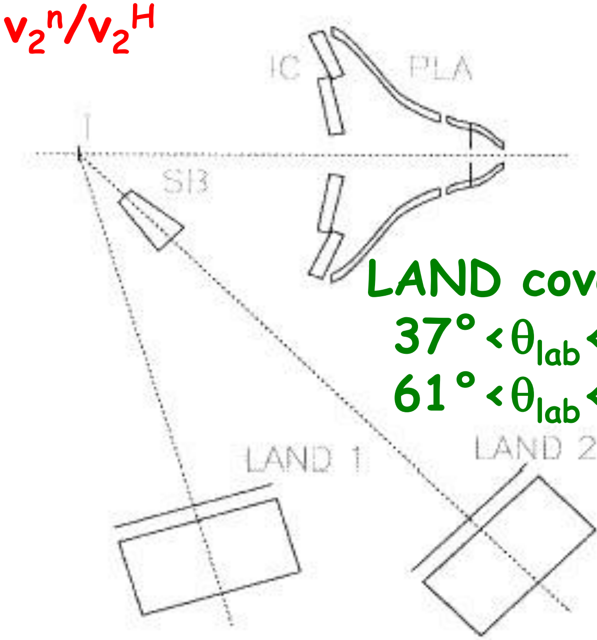

LAND coverage
$37° < \theta_{lab} < 53°$
$61° < \theta_{lab} < 85°$

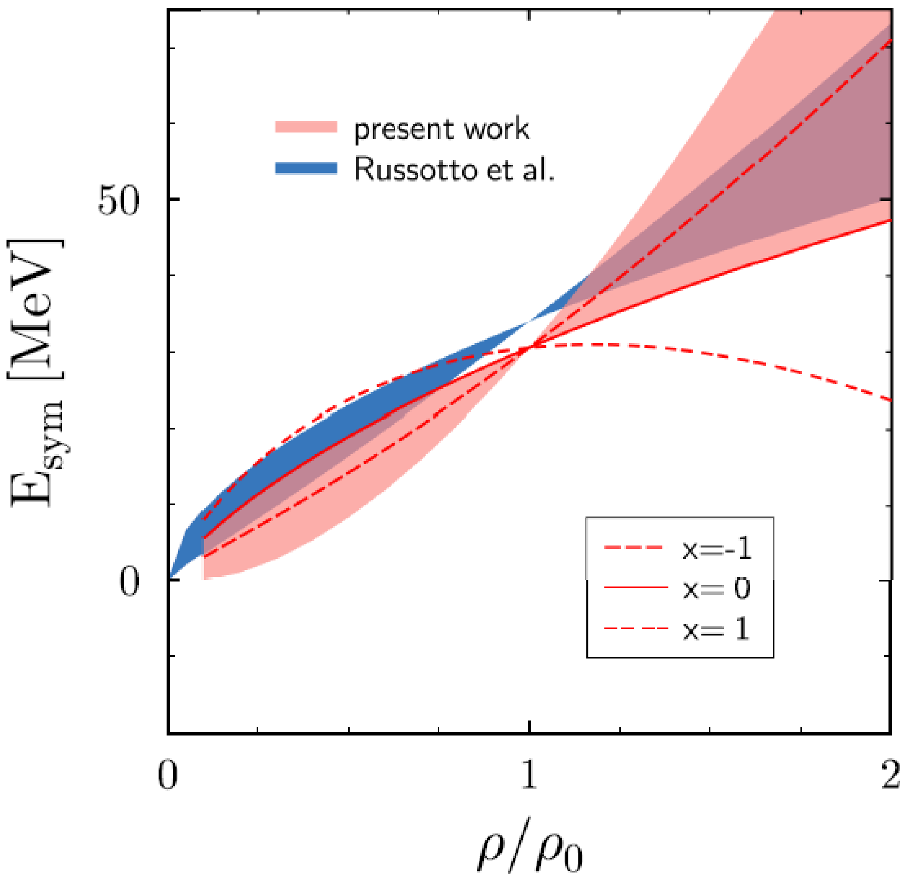

UrQMD:
momentum dep. of isoscalar field
momentum dep. of NNECS
momentum independent power-law
parameterization of the symmetry energy

$\gamma = 0.9 \pm 0.4$

L=83±26

Y. Leifels et al., PRL 71, 963 (1993)
P.Russotto et al., PLB 697 (2011)

Tübingen-QMD:
density dep. of NNECS
asymmetry dep. of NNECS
soft vs. hard EoS
width of wave packets
momentum dependent (Gogny inspired)
parameterization of the symmetry energy
M.D. Cozma et al. , PLB 700, 139 (2011) &
PRC88 044912 (2013)

ASY-EOS S394 experiment @ GSI Darmstadt (May 2011)

After re-analysis of Au+Au FOPI-LAND data (1991) P.Russotto et al., PLB 697 (2011)

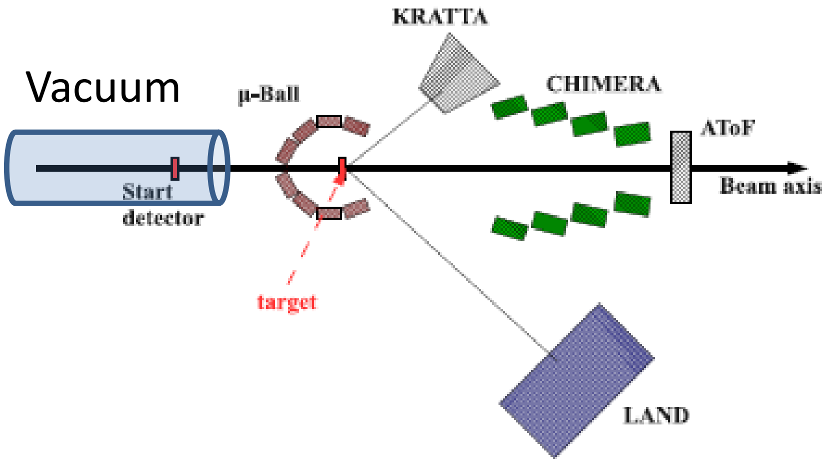

ASY-EOS S394 experiment @ GSI Darmstadt (May 2011)

After re-analysis of Au+Au FOPI-LAND data (1991) P.Russotto et al., PLB 697 (2011)

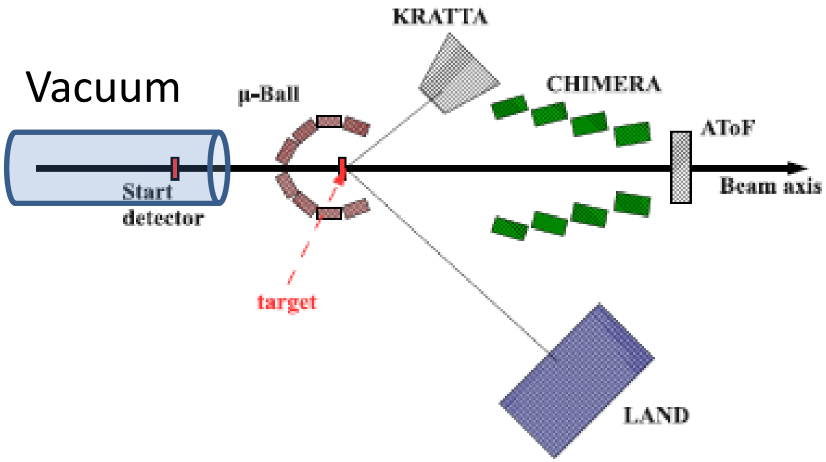

TOFWALL: **96 plastic bars; ToF, ΔE, X-Y position.**

Trigger, impact parameter and reaction plane determination

ASY-EOS S394 experiment @ GSI Darmstadt (May 2011)

After re-analysis of Au+Au FOPI-LAND data (1991) P.Russotto et al., PLB 697 (2011)

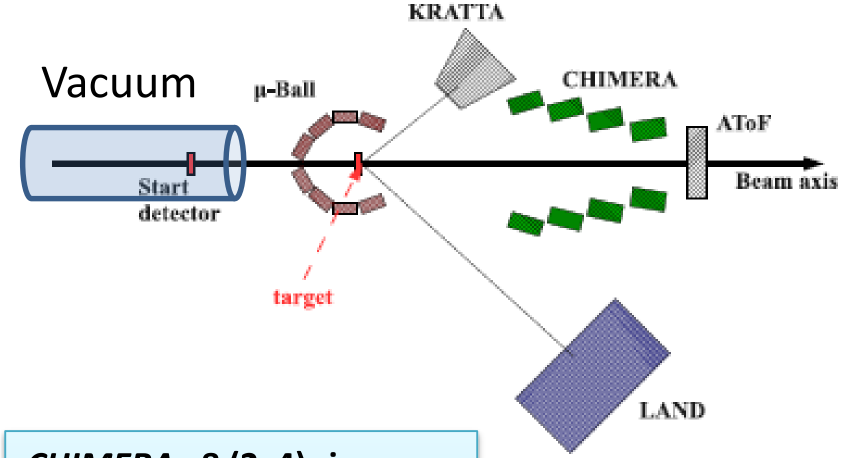

TOFWALL: **96 plastic bars; ToF, ΔE, X-Y position.**
Trigger, impact parameter and reaction plane determination

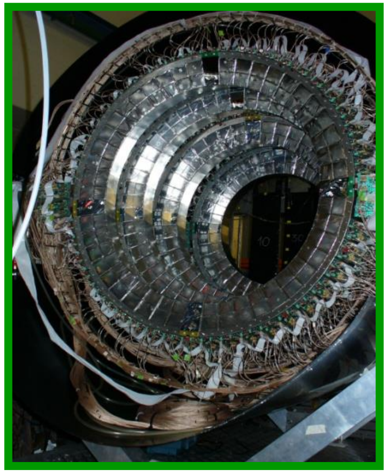

CHIMERA: **8 (2x4) rings, high granularity CsI(Tl), 352 detectors 7°<θ<20° + 16x2 pads silicon detectors. Light charged particle identification by PSD.**
Multiplicity, Z, A, Energy: impact parameter and reaction plane determination

ASY-EOS S394 experiment @ GSI Darmstadt (May 2011)

After re-analysis of Au+Au FOPI-LAND data (1991) P.Russotto et al., PLB 697 (2011)

μBall: 4 rings 50 CsI(Tl), Θ>60°. Discriminate target vs. reactions with air. Multiplicity and reaction plane measurements.

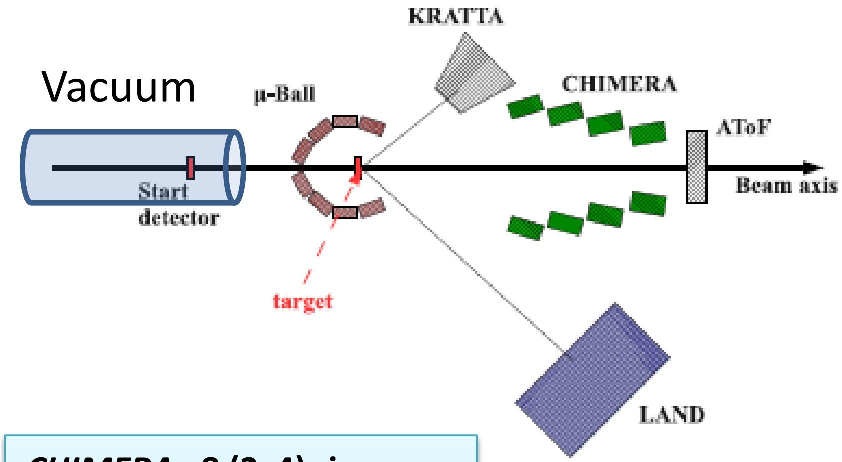

TOFWALL: 96 plastic bars; ToF, ΔE, X-Y position. Trigger, impact parameter and reaction plane determination

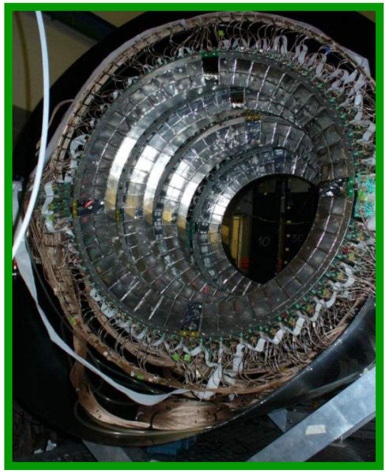

CHIMERA: 8 (2x4) rings, high granularity CsI(Tl), 352 detectors 7°<θ<20° + 16x2 pads silicon detectors. Light charged particle identification by PSD. Multiplicity, Z, A, Energy: impact parameter and reaction plane determination

ASY-EOS S394 experiment @ GSI Darmstadt (May 2011)

After re-analysis of Au+Au FOPI-LAND data (1991) P.Russotto et al., PLB 697 (2011)

μBall: **4 rings 50 CsI(Tl), Θ>60°. Discriminate target vs. reactions with air. Multiplicity and reaction plane measurements.**

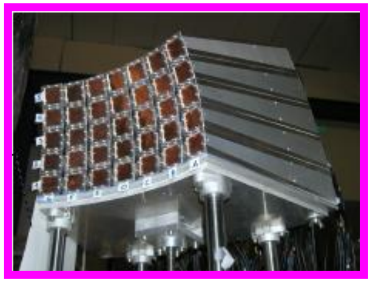

KraTTA: **35 (5x7) triple telescopes (Si-CsI-CsI) placed at 21°<Θ<60° with digital readout . Light particles and IMFs emitted at midrapidity**

TOFWALL: **96 plastic bars; ToF, ΔE, X-Y position. Trigger, impact parameter and reaction plane determination**

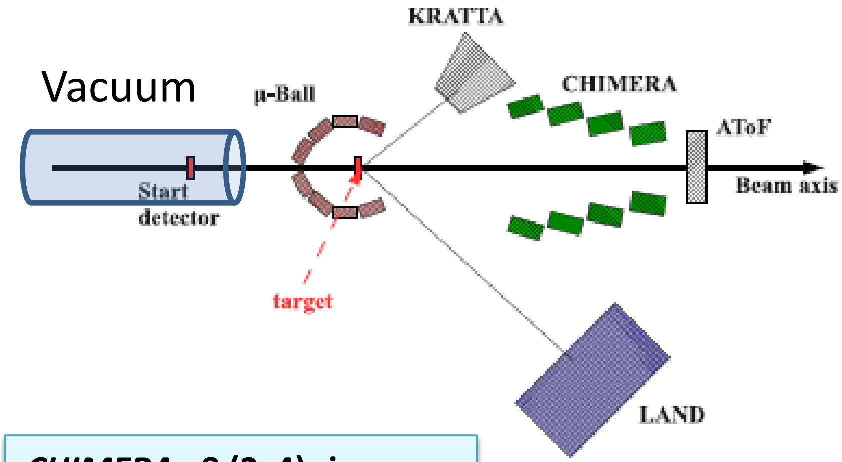

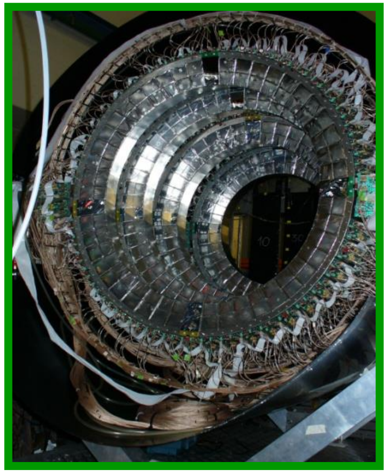

CHIMERA: **8 (2x4) rings, high granularity CsI(Tl), 352 detectors 7°<θ<20° + 16x2 pads silicon detectors. Light charged particle identification by PSD. Multiplicity, Z, A, Energy: impact parameter and reaction plane determination**

ASY-EOS S394 experiment @ GSI Darmstadt (May 2011)

After re-analysis of Au+Au FOPI-LAND data (1991) P.Russotto et al., PLB 697 (2011)

__µBall__: 4 rings 50 CsI(Tl), Θ>60°. Discriminate target vs. reactions with air. Multiplicity and reaction plane measurements.

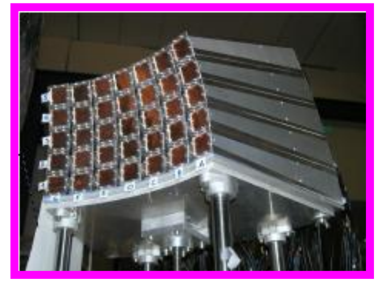

__KraTTA__: 35 (5x7) triple telescopes (Si-CsI-CsI) placed at 21°<Θ<60° with digital readout . Light particles and IMFs emitted at midrapidity

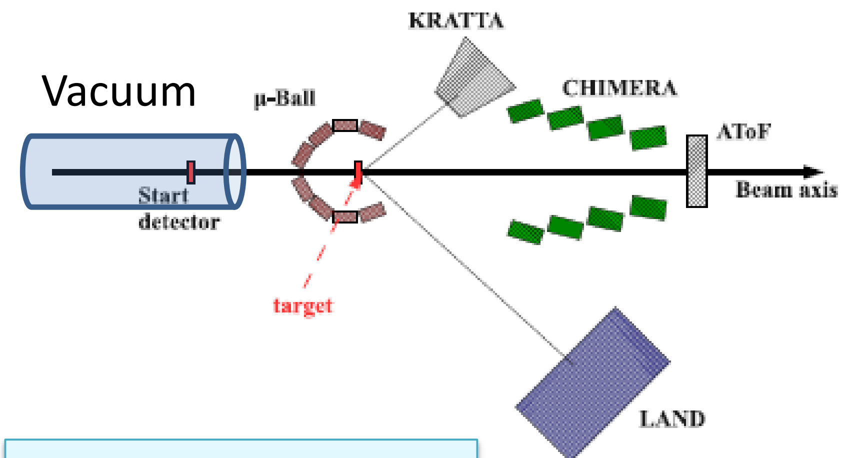

__TOFWALL__: 96 plastic bars; ToF, ΔE, X-Y position. Trigger, impact parameter and reaction plane determination

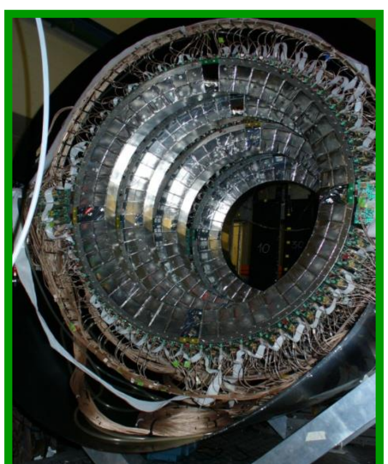

__CHIMERA__: 8 (2x4) rings, high granularity CsI(Tl), 352 detectors 7°<θ<20° + 16x2 pads silicon detectors. Light charged particle identification by PSD. Multiplicity, Z, A, Energy: impact parameter and reaction plane determination

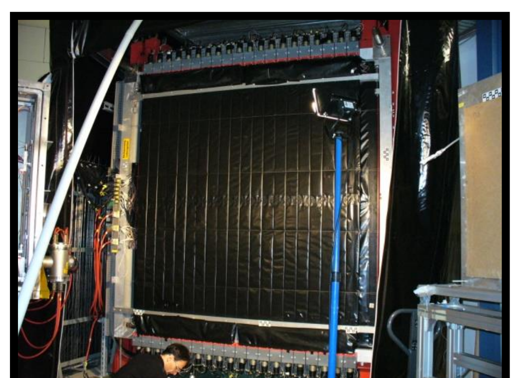

__LAND__: Large Area Neutron Detector . Plastic scintillators sandwiched with Fe 2x2x1 m^3 plus plastic veto wall. New Taquila front-end electronics. Neutrons and Hydrogen detection. Flow measurements

ASY-EOS S394 experiment @ GSI Darmstadt (May 2011)

After re-analysis of Au+Au FOPI-LAND data (1991) P.Russotto et al., PLB 697 (2011)

µBall: 4 rings 50 CsI(Tl), Θ>60°. Discriminate target vs. reactions with air. Multiplicity and reaction plane measurements.

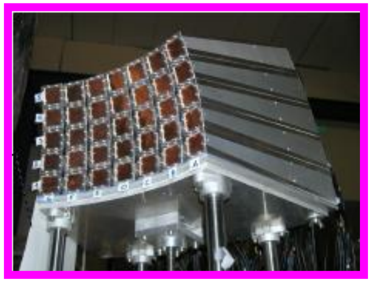

KraTTA: 35 (5x7) triple telescopes (Si-CsI-CsI) placed at 21°<Θ<60° with digital readout . Light particles and IMFs emitted at midrapidity

Shadow bar: evaluation of background neutrons in LAND

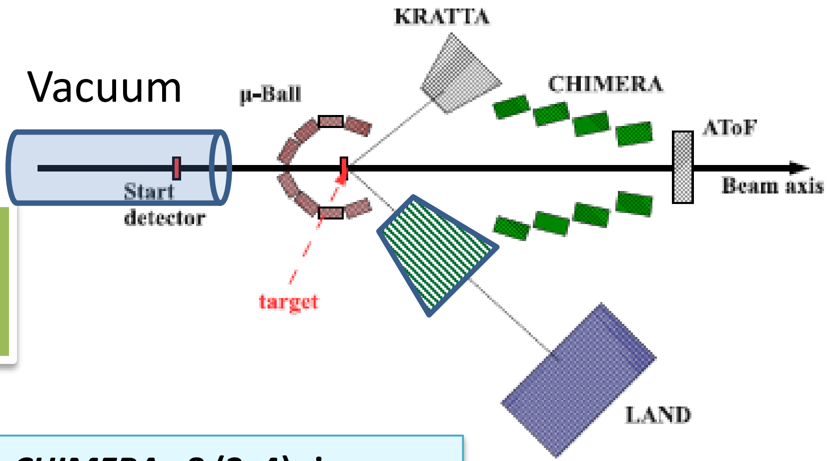

TOFWALL: 96 plastic bars; ToF, ΔE, X-Y position. Trigger, impact parameter and reaction plane determination

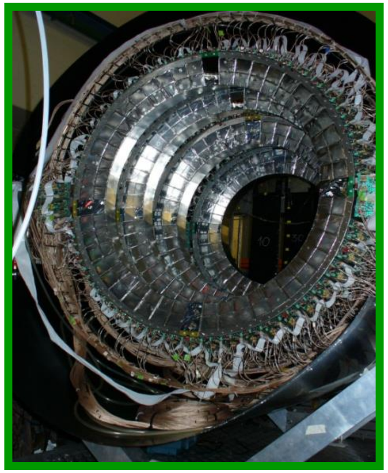

CHIMERA: 8 (2x4) rings, high granularity CsI(Tl), 352 detectors 7°<θ<20° + 16x2 pads silicon detectors. Light charged particle identification by PSD. Multiplicity, Z, A, Energy: impact parameter and reaction plane determination

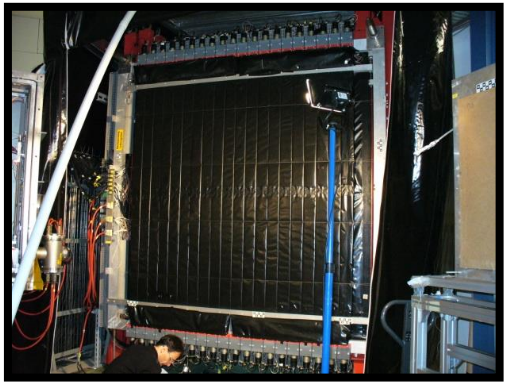

LAND: Large Area Neutron Detector . Plastic scintillators sandwiched with Fe 2x2x1 m^3 plus plastic veto wall. New Taquila front-end electronics. Neutrons and Hydrogen detection. Flow measurements

ASY-EOS results

Au+Au @ 400 AMeV b<7.5 fm

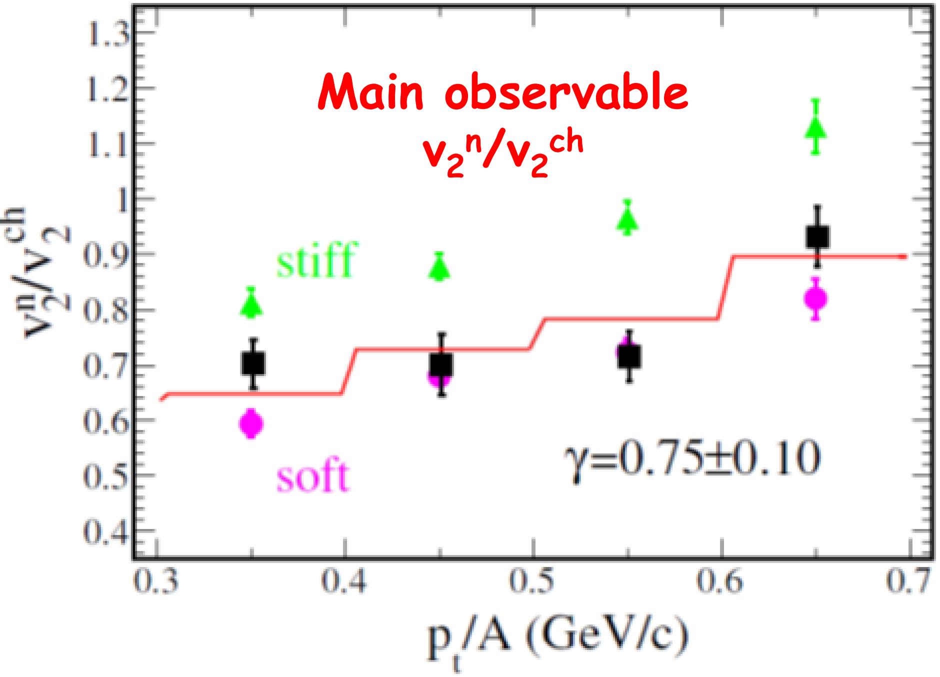

$$E_{sym} = S(\rho) = S_0 + \frac{L}{3}\left(\frac{\rho - \rho_o}{\rho_o}\right) + \frac{K_{sym}}{18}\left(\frac{\rho - \rho_o}{\rho_o}\right)^2 + \ldots,$$

ASY-EOS results

Au+Au @ 400 AMeV b<7.5 fm

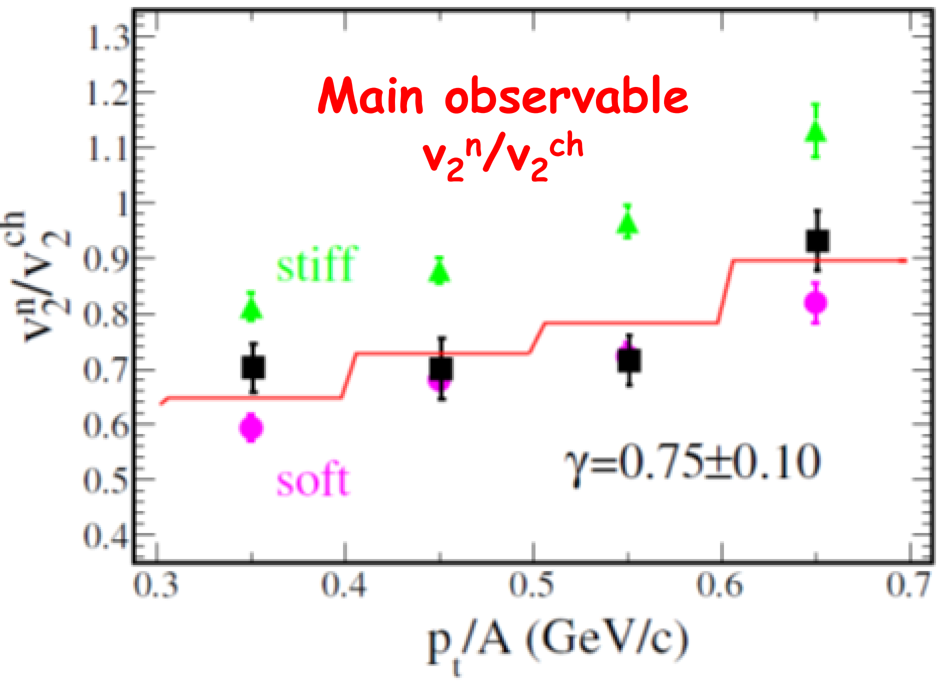

FOPI-LAND DATA : P.Russotto et al., Phys. Lett. B 697 (2011)

γ = 0.9 ± 0.4 ; L=83±26 MeV

$$E_{sym} = S(\rho) = S_0 + \frac{L}{3}\left(\frac{\rho - \rho_o}{\rho_o}\right) + \frac{K_{sym}}{18}\left(\frac{\rho - \rho_o}{\rho_o}\right)^2 + \ldots,$$

ASY-EOS results

Au+Au @ 400 AMeV b<7.5 fm

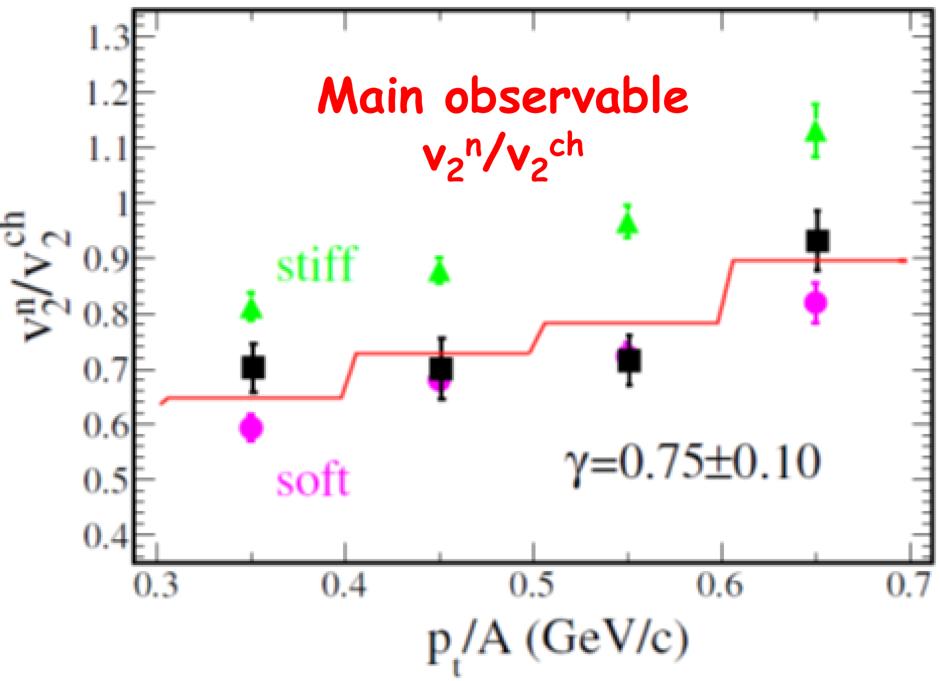

FOPI-LAND DATA : P.Russotto et al., Phys. Lett. B 697 (2011)

γ = 0.9 ± 0.4 ; L=83±26 MeV

ASY-EOS DATA: P. Russotto et al., PRC 94, 034608 (2016)

γ = 0.72± 0.19 ; L=72±13 MeV

$$E_{sym} = S(\rho) = S_0 + \frac{L}{3}\left(\frac{\rho-\rho_o}{\rho_o}\right) + \frac{K_{sym}}{18}\left(\frac{\rho-\rho_o}{\rho_o}\right)^2 + \ldots,$$

ASY-EOS results

Au+Au @ 400 AMeV b<7.5 fm

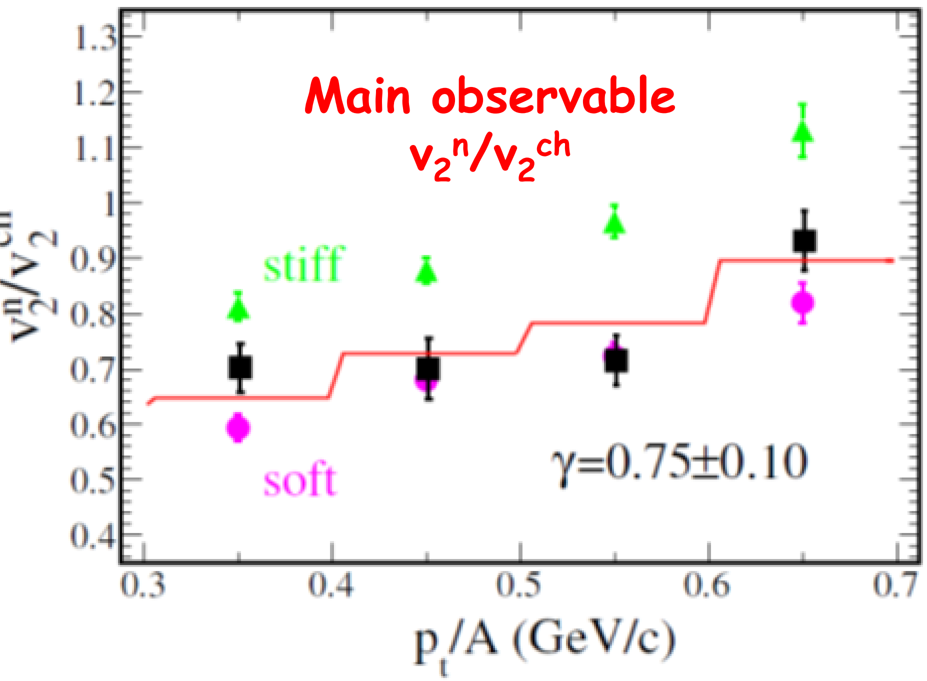

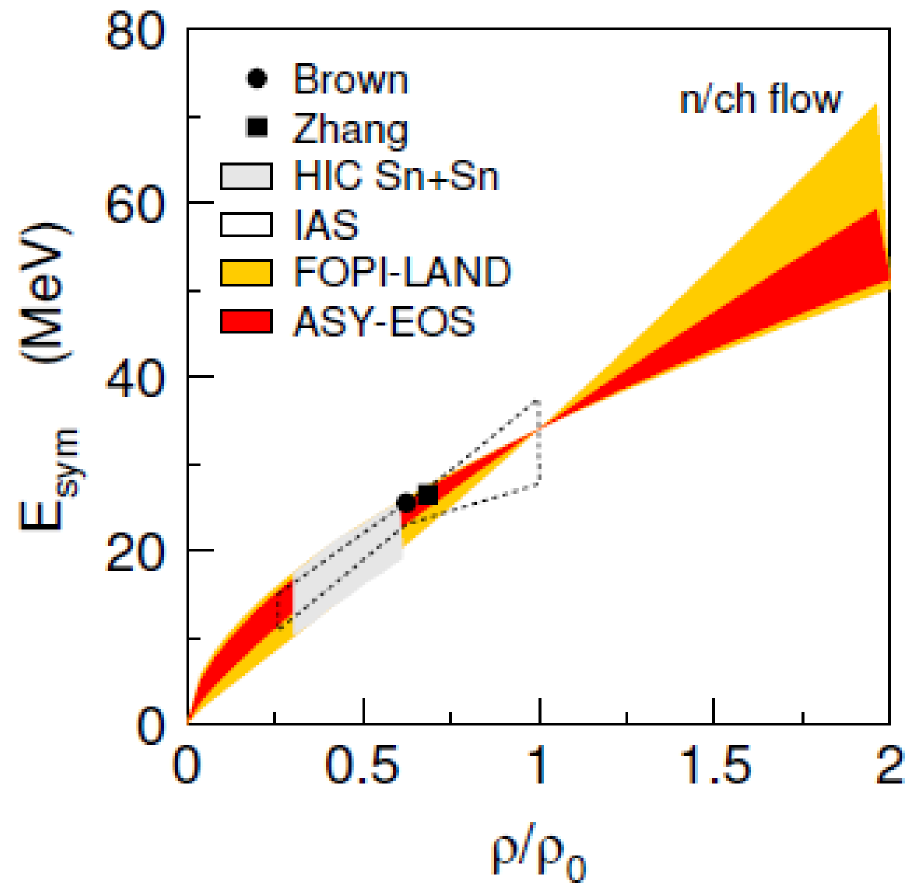

FOPI-LAND DATA : P.Russotto et al., Phys. Lett. B 697 (2011)

γ = 0.9 ± 0.4 ; L=83±26 MeV

ASY-EOS DATA: P. Russotto et al., PRC 94, 034608 (2016)

γ = 0.72± 0.19 ; L=72±13 MeV

HIC: (mainly Isospin diffusion for Sn+Sn): M.B. Tsang et al., PRC 86, 015803 (2012)

neutron skin thickness, binding energies,….: Brown, PRL 111, 232502 (2013); Zhang & Chen, Phys. Lett. B 726 (2013), Danielewicz & Lee, NPA922 (2014).

$$E_{sym} = S(\rho) = S_0 + \frac{L}{3}\left(\frac{\rho-\rho_o}{\rho_o}\right) + \frac{K_{sym}}{18}\left(\frac{\rho-\rho_o}{\rho_o}\right)^2 + \ldots,$$

ASY-EOS results

Au+Au @ 400 AMeV b<7.5 fm

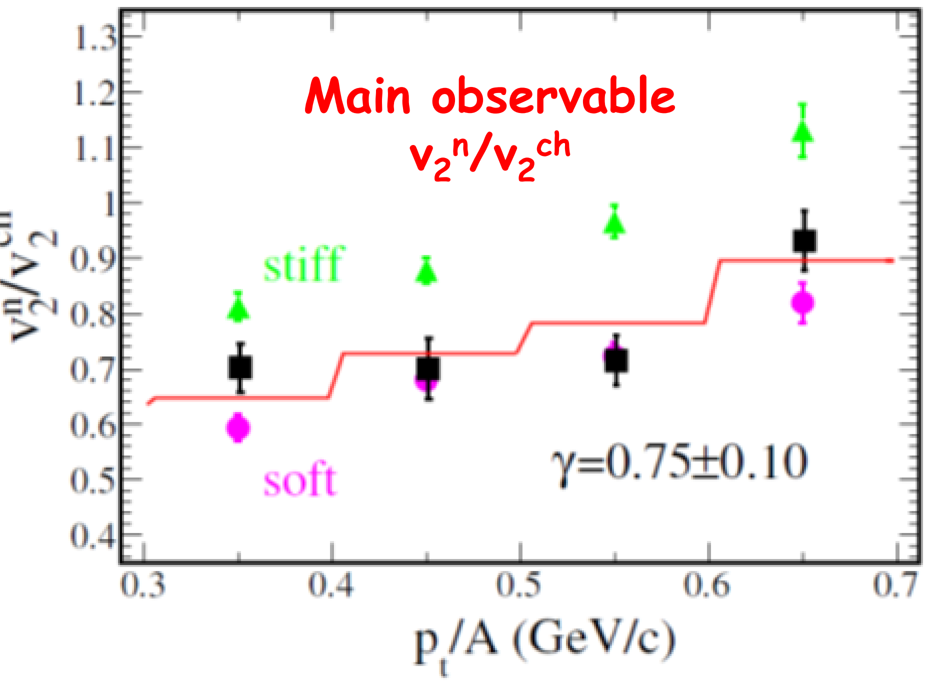

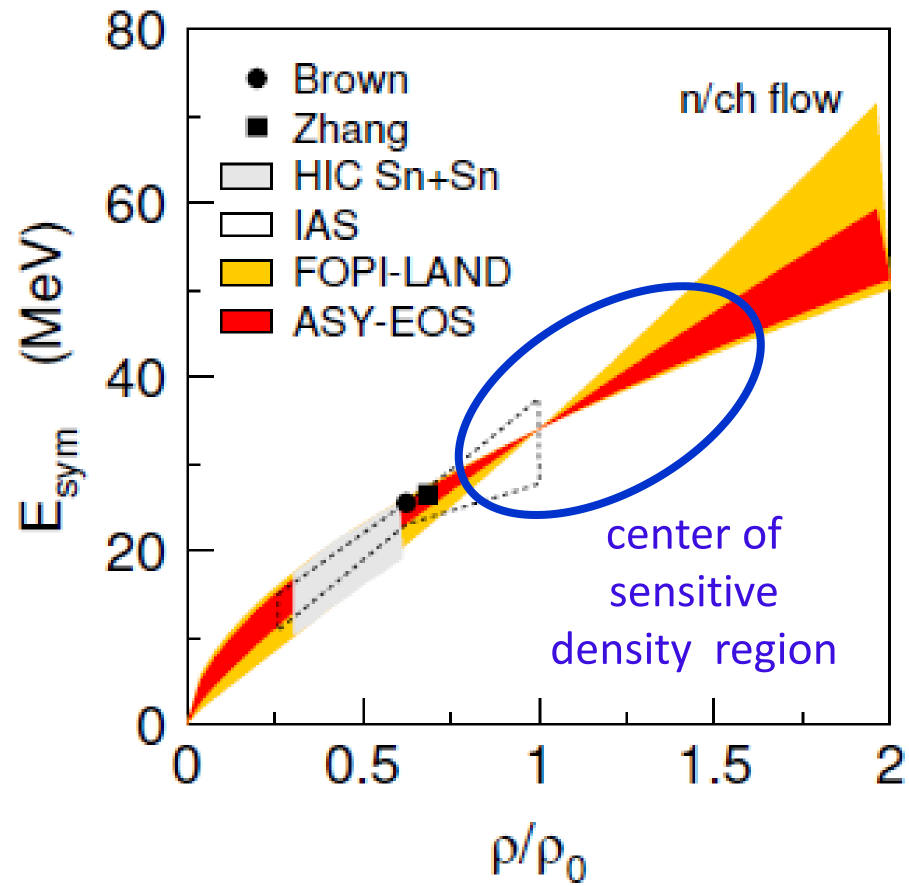

FOPI-LAND DATA : P.Russotto et al., Phys. Lett. B 697 (2011)

γ = 0.9 ± 0.4 ; L=83±26 MeV

ASY-EOS DATA: P. Russotto et al., PRC 94, 034608 (2016)

γ = 0.72± 0.19 ; L=72±13 MeV

HIC: (mainly Isospin diffusion for Sn+Sn): M.B. Tsang et al., PRC 86, 015803 (2012)

neutron skin thickness, binding energies,….: Brown, PRL 111, 232502 (2013); Zhang & Chen, Phys. Lett. B 726 (2013), Danielewicz & Lee, NPA922 (2014).

$$E_{sym} = S(\rho) = S_0 + \frac{L}{3}\left(\frac{\rho-\rho_o}{\rho_o}\right) + \frac{K_{sym}}{18}\left(\frac{\rho-\rho_o}{\rho_o}\right)^2 + \ldots,$$

ASY-EOS results

Au+Au @ 400 AMeV b<7.5 fm

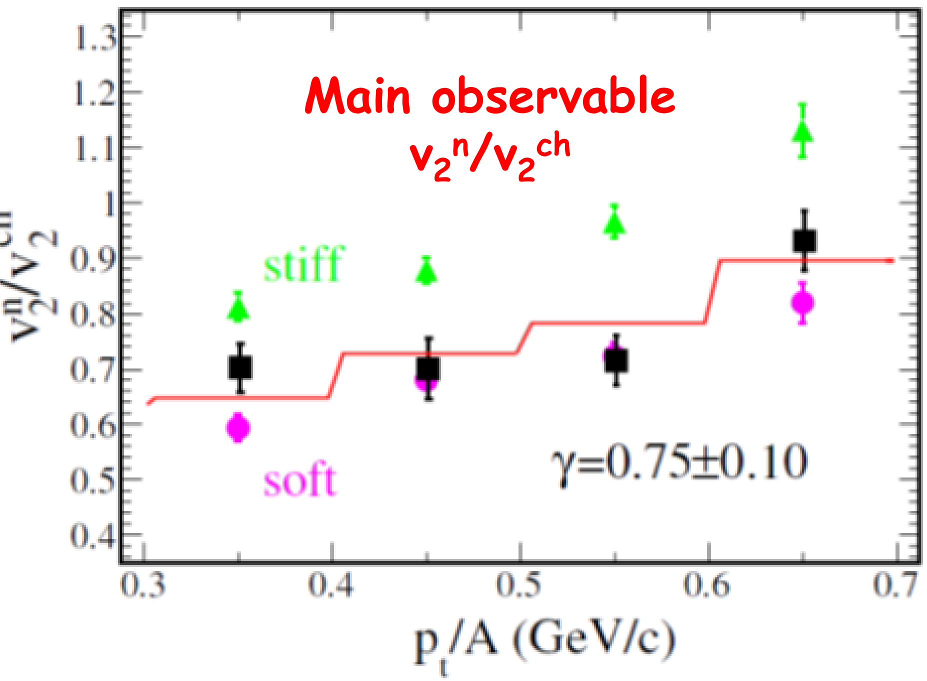

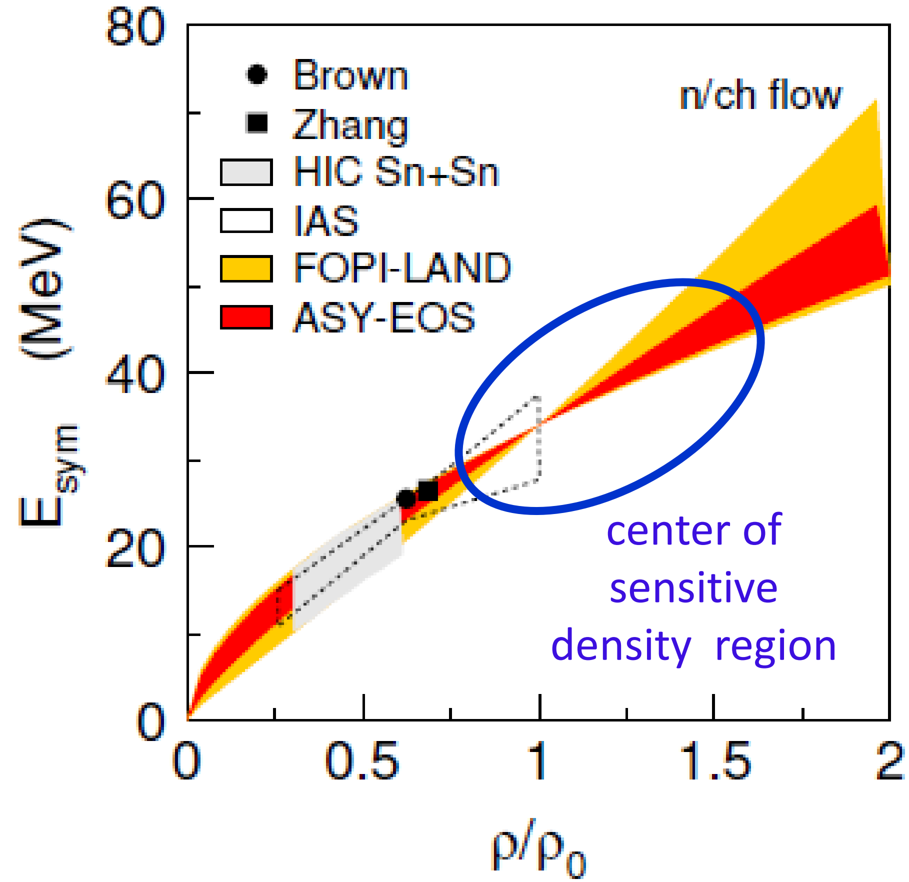

FOPI-LAND DATA : P.Russotto et al., Phys. Lett. B 697 (2011)

γ = 0.9 ± 0.4 ; L=83±26 MeV

ASY-EOS DATA: P. Russotto et al., PRC 94, 034608 (2016)

γ = 0.72± 0.19 ; L=72±13 MeV

$$E_{sym} = S(\rho) = S_0 + \frac{L}{3}\left(\frac{\rho-\rho_o}{\rho_o}\right) + \frac{K_{\rm sym}}{18}\left(\frac{\rho-\rho_o}{\rho_o}\right)^2 + \ldots,$$

HIC: (mainly Isospin diffusion for Sn+Sn): M.B. Tsang et al., PRC 86, 015803 (2012)

neutron skin thickness, binding energies,….: Brown, PRL 111, 232502 (2013); Zhang & Chen, Phys. Lett. B 726 (2013), Danielewicz & Lee, NPA922 (2014).

Next step? ASY-EOS II

ASY-EOS II: Symmetry energy @ higher density

Which densities can be explored in the early stage of the reaction ? (BUU calculations)

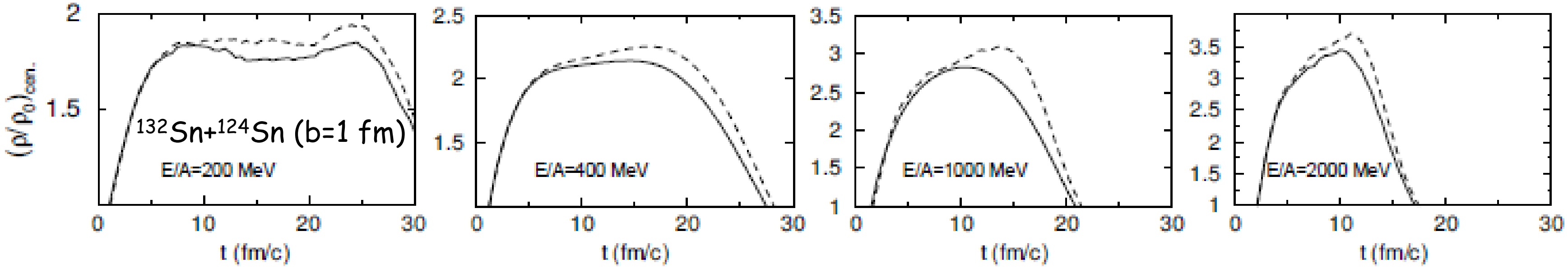

Bao-An Li, NPA 708 (2002)

ASY-EOS II: Symmetry energy @ higher density

Which densities can be explored in the early stage of the reaction ? (BUU calculations)

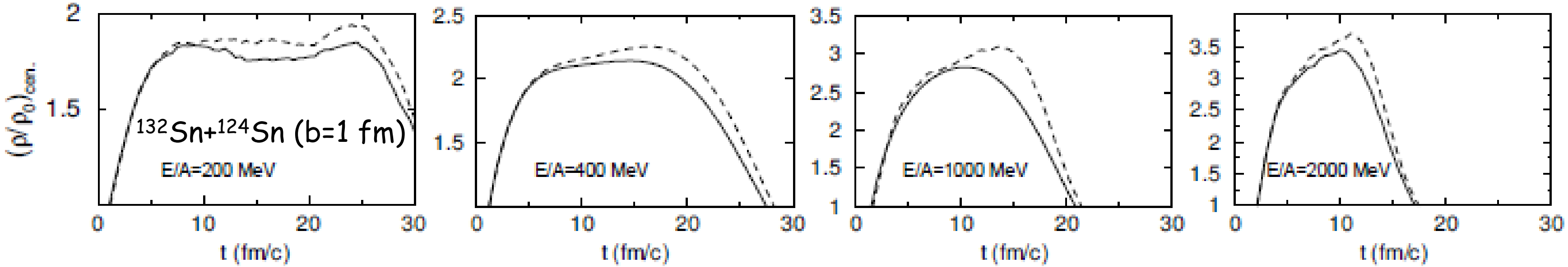

Bao-An Li, NPA 708 (2002)

Which densities are explored by the flow?
IQMD calculations for p

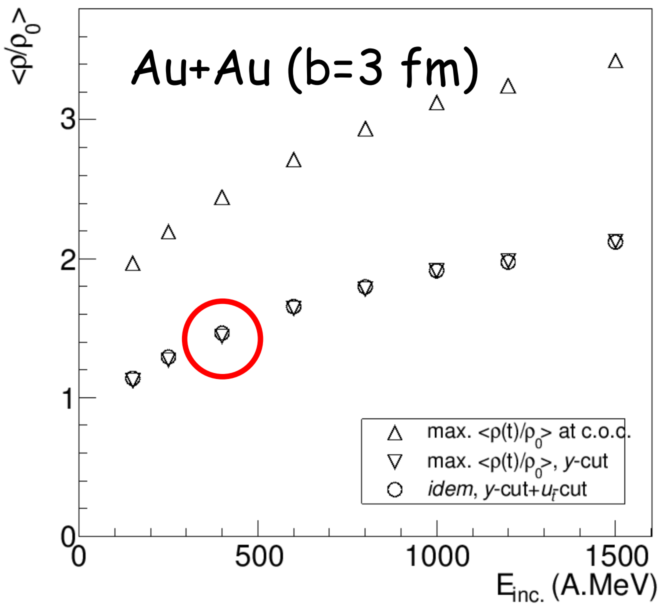

A. Le Fevre et al., NPA 945 (2016)

ASY-EOS II: Symmetry energy @ higher density

Which densities can be explored in the early stage of the reaction ? (BUU calculations)

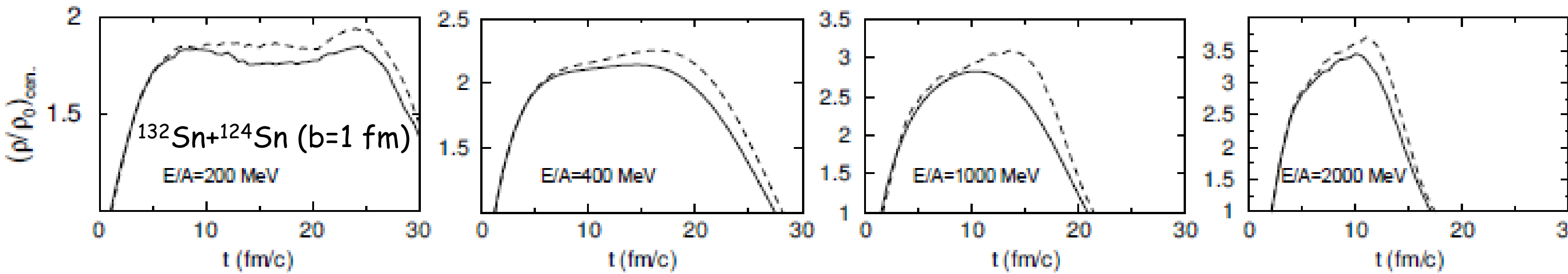

Bao-An Li, NPA 708 (2002)

Which densities are explored by the flow?
IQMD calculations for p

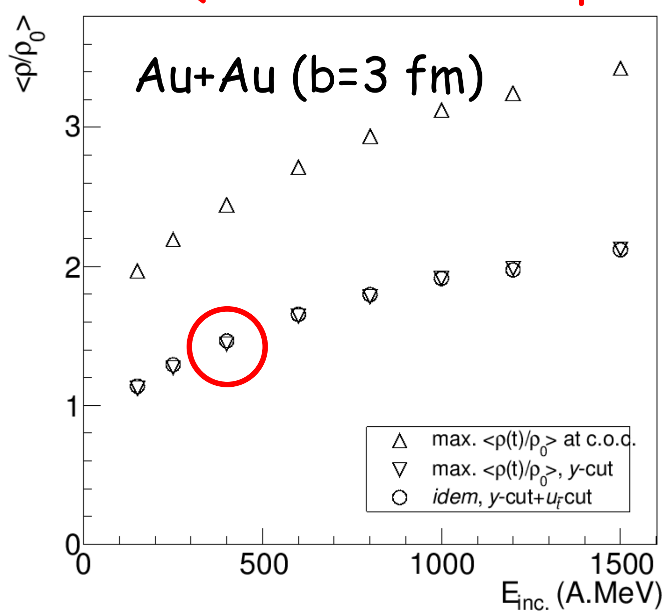

A. Le Fevre et al., NPA 945 (2016)

Sensitivity of DEFR to density

$$\mathrm{DEFR}^{(n,Y)}(\rho) = \frac{v_2^n}{v_2^Y}(x=-1,\rho) - \frac{v_2^n}{v_2^Y}(x=1,\rho)$$

$$V_{sym}(x,\tilde{\rho}) = \begin{cases} V_{sym}^{Gogny}(x,\tilde{\rho}) & \tilde{\rho} \leqslant \rho, \\ V_{sym}^{Gogny}(0,\tilde{\rho}) & \tilde{\rho} > \rho, \end{cases}$$

P. Russotto et al., PRC 94, (2016)

M.D. Cozma TuQMD calculations

ASY-EOS II: Symmetry energy @ higher density

Which densities can be explored in the early stage of the reaction ? (BUU calculations)

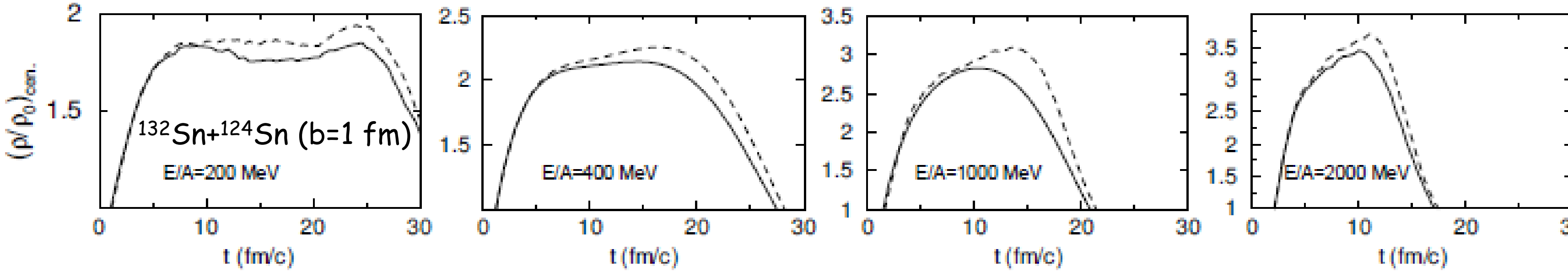

Bao-An Li, NPA 708 (2002)

Which densities are explored by the flow?
IQMD calculations for p

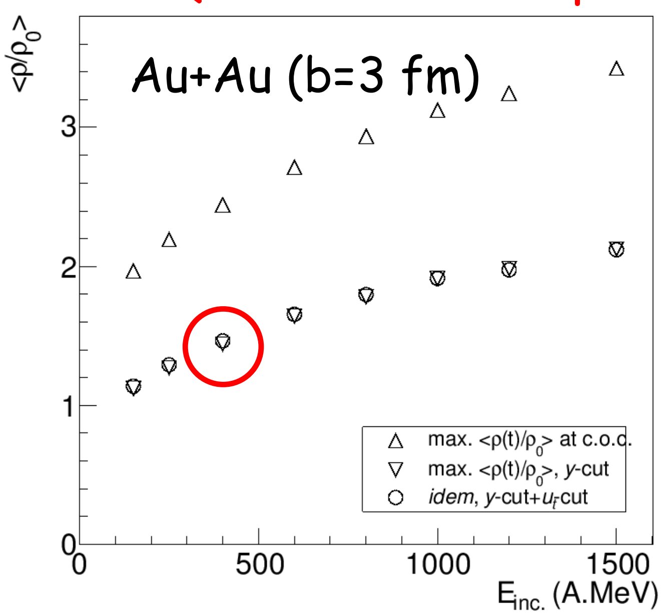

A. Le Fevre et al., NPA 945 (2016)

Sensitivity of DEFR to density

$$\mathrm{DEFR}^{(n,Y)}(\rho) = \frac{v_2^n}{v_2^Y}(x=-1,\rho) - \frac{v_2^n}{v_2^Y}(x=1,\rho)$$

Au+Au @ 400AMeV (b<7.5 fm)

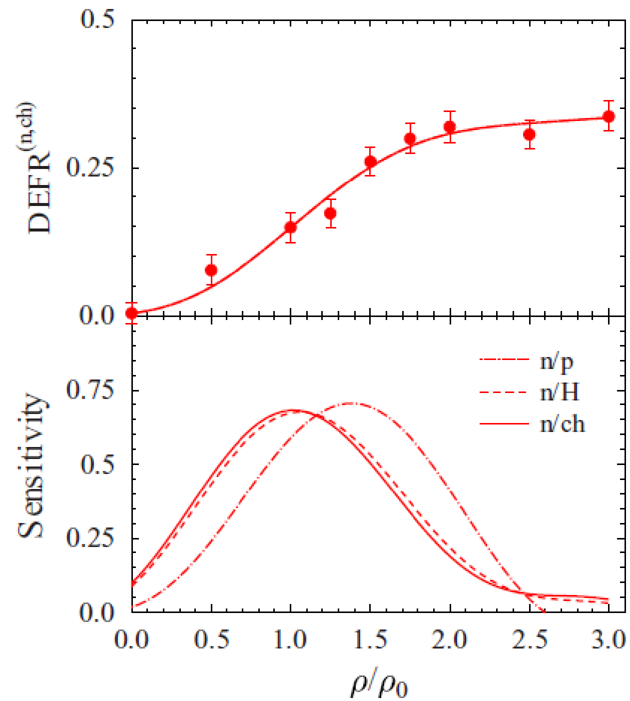

M.D. Cozma TuQMD calculations

P. Russotto et al.,PRC 94, (2016)

ASY-EOS II: Symmetry energy @ higher density

Which densities can be explored in the early stage of the reaction ? (BUU calculations)

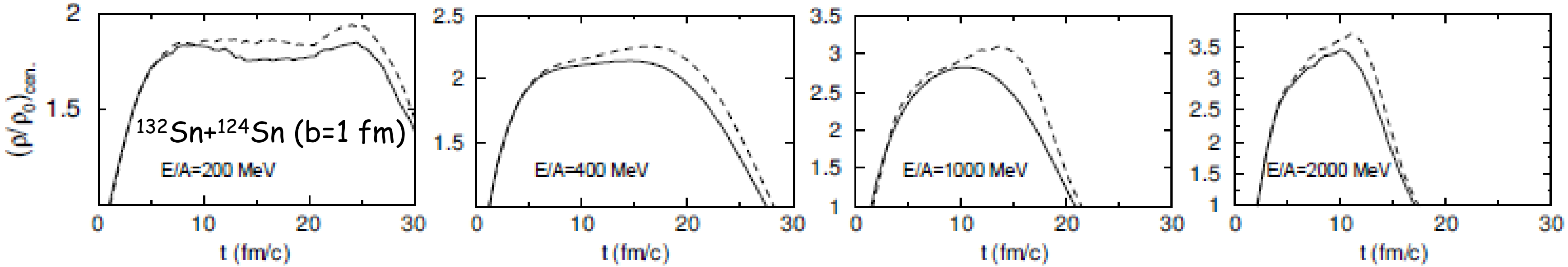

Bao-An Li, NPA 708 (2002)

Which densities are explored by the flow?
IQMD calculations for p

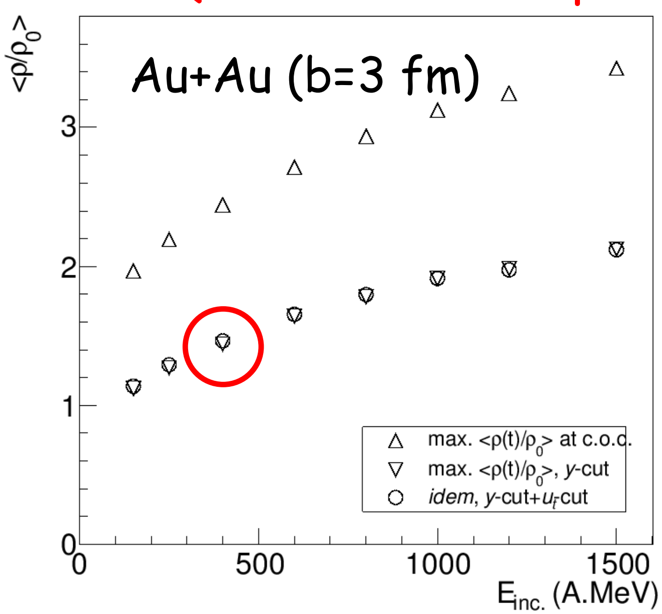

A. Le Fevre et al., NPA 945 (2016)

Sensitivity of DEFR to density

$$\mathrm{DEFR}^{(n,Y)}(\rho) = \frac{v_2^n}{v_2^Y}(x=-1,\rho) - \frac{v_2^n}{v_2^Y}(x=1,\rho)$$

Au+Au @ 400AMeV (b<7.5 fm)

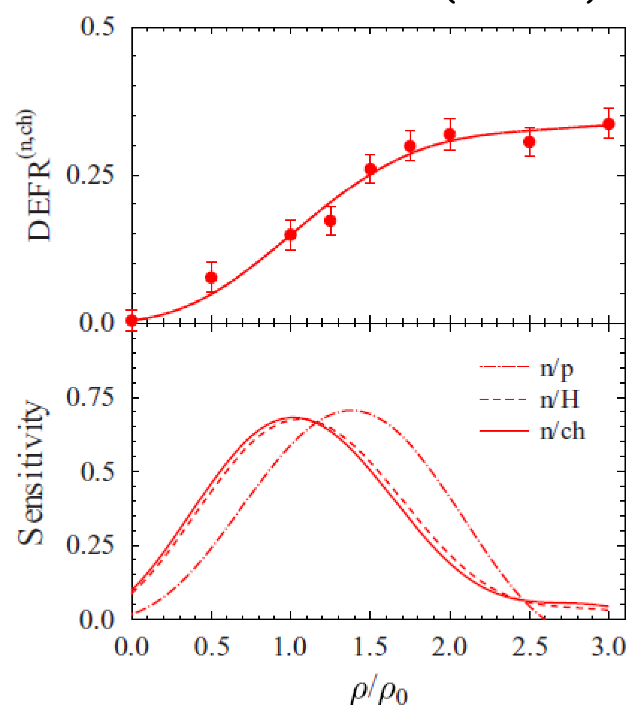

P. Russotto et al.,PRC 94, (2016)
M.D. Cozma TuQMD calculations

To explore higher densities:
1) raise the beam energy
2) use n-p observable

ASY-EOS II: UrQMD predictions

The systems/energies we would like to measure in the future campaign are:

$$
\begin{array}{lll}
{}^{197}\mathrm{Au} + {}^{197}\mathrm{Au} & \mathrm{at} & 400,\ 600,\ 1000\ \mathrm{AMeV} \\
{}^{132}\mathrm{Sn} + {}^{124}\mathrm{Sn} & \mathrm{at} & 400,\ 600\ \mathrm{AMeV} \\
{}^{106}\mathrm{Sn} + {}^{112}\mathrm{Sn} & \mathrm{at} & 400,\ 600\ \mathrm{AMeV}
\end{array}
$$

Measure excitation function to improve resolving power

ASY-EOS II: UrQMD predictions

The systems/energies we would like to measure in the future campaign are:

$$^{197}\mathrm{Au} + {}^{197}\mathrm{Au} \quad \text{at} \quad 400, 600, 1000 \text{ AMeV}$$
$$^{132}\mathrm{Sn} + {}^{124}\mathrm{Sn} \quad \text{at} \quad 400, 600 \text{ AMeV}$$
$$^{106}\mathrm{Sn} + {}^{112}\mathrm{Sn} \quad \text{at} \quad 400, 600 \text{ AMeV}$$

Measure excitation function to improve resolving power

At midvelocity b/bred <0.53

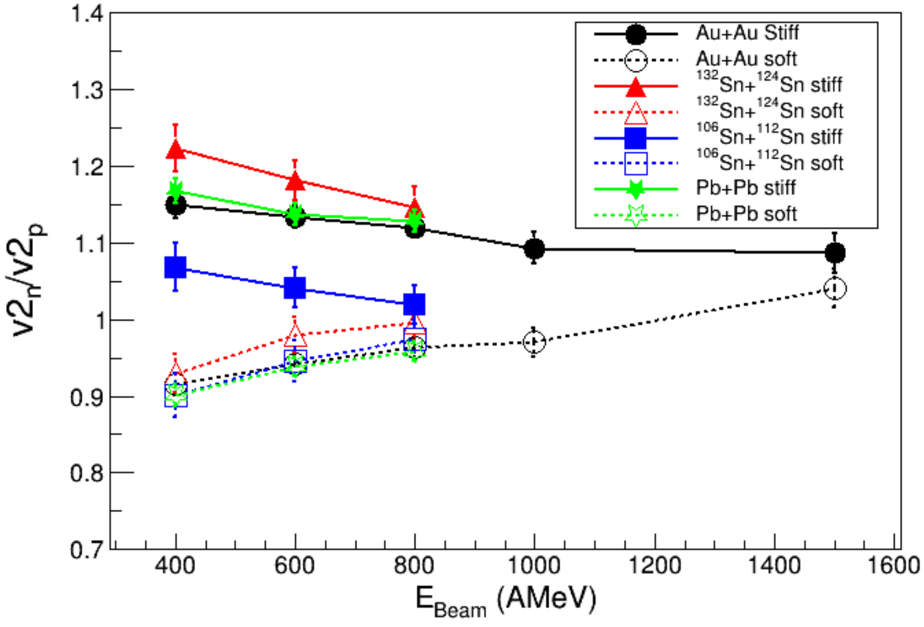

$$E_{sym} = 22\,\mathrm{MeV}\cdot(\rho/\rho_0)^{\gamma} + 12\,\mathrm{MeV}\cdot(\rho/\rho_0)^{2/3}$$

Stiff γ=1.5, Soft γ=0.5

ASY-EOS II: UrQMD predictions

The systems/energies we would like to measure in the future campaign are:

^{197}Au + ^{197}Au at 400, 600, 1000 AMeV
^{132}Sn + ^{124}Sn at 400, 600 AMeV
^{106}Sn + ^{112}Sn at 400, 600 AMeV

Measure excitation function to improve resolving power

At midvelocity b/bred <0.53

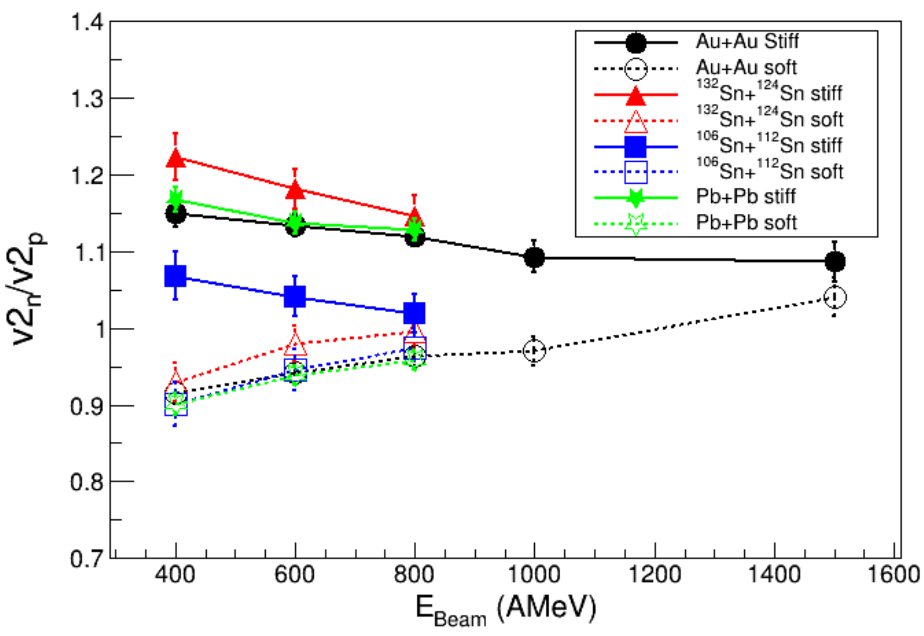

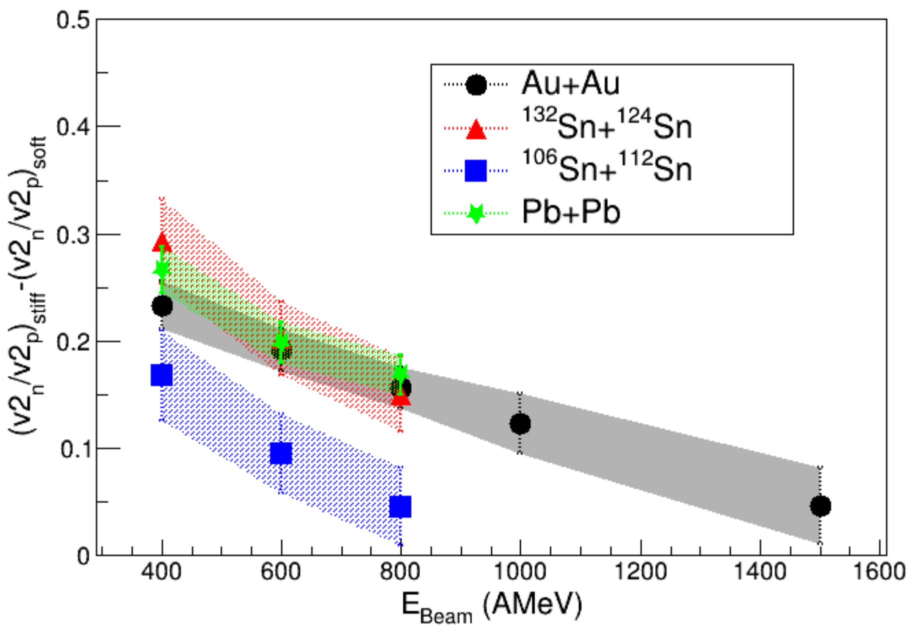

$$E_{sym} = 22\,\text{MeV} \cdot (\rho/\rho_0)^{\gamma} + 12\,\text{MeV} \cdot (\rho/\rho_0)^{2/3}$$

Stiff γ=1.5, Soft γ=0.5

ASY-EOS II "LOI"

PROPOSAL FOR BEAM-TIME IN 2018/2019

FOR

DETERMINATION OF SYMMETRY ENERGY AT SUPRA-NORMAL DENSITIES: A FEASIBILITY STUDY

ASY-EOS II Collaboration

SPOKESPERSON: P. Russotto[1]

PRINCIPAL INVESTIGATORS: A. Le Fèvre[2], Y. Leifels[2], J. Łukasik[3], P. Russotto[1]

PARTICIPANTS: M. Adamczyk[4], J. Benlliure[5], E. Bonnet[6], J. Brzychczyk[4], Ch. Caesar[2], P. Cammarata[7], Z. Chajecki[8], A. Chbihi[9], E. De Filippo[11], M. Famiano[12], I. Gašparić[13], B. Gnoffo[11,20], C. Guazzoni[21], T. Isobe[14], M. Jabłoński[4], M. Jastrząb[3], J. Kallunkathariyil[22], K. Kezzar[15], M. Kiš[2], P. Koczoń[2], A. Krasznahorkay[16], P. Lasko[3], K. Łojek[4], W.G. Lynch[8], P. Marini[18], N.S. Martorana[1,20], A.B. McIntosh[7], T. Murakami[19], A. Pagano[11], E.V. Pagano[1,20], M. Papa[11], P. Pawłowski[3], S. Pirrone[11], G. Politi[11,20], K. Pysz[3], L. Quattrocchi[11,20] F. Rizzo[1,20], W. Trautmann[2], A. Trifirò[23], M. Trimarchi[23], M.B. Tsang[8], A. Wieloch[4] and S.J. Yennello[7]
THEORY SUPPORT: J. Aichelin[6], M. Colonna[1], M.D. Cozma[10], P. Danielewicz[8], Ch. Hartnack[6], Q.F. Li[17] and Y. Wang[17]

INSTITUTIONS: [1]INFN-LNS, Catania, Italy; [2]GSI, Darmstadt, Germany; [3]IFJ PAN, Kraków, Poland; [4]Jagiellonian University, Kraków, Poland; [5]Universidade de Santiago de Compostela, Spain; [6]SUBATECH, Nantes, France; [7]Texas A&M University Cyclotron Institute, College Station, USA; [8]NSCL/MSU, East Lansing, USA; [9]GANIL, Caen, France; [10]IFIN-HH, Bucharest, Romania; [11]INFN-Sezione di Catania, Italy; [12]Western Michigan University, Kalamazoo, MI, USA; [13]RBI, Zagreb, Croatia; [14]RIKEN, Wako-shi, Japan; [15]King Saud University, Riyadh, Saudi Arabia; [16]Institute for Nuclear Research, Debrecen, Hungary; [17]School of Science, Huzhou University, P.R. China; [18]CEA, DAM, DIF, Arpajon, France; [19]Kyoto University, Japan; [20]Università di Catania, Italy; [21] Politecnico di Milano and INFN-Sezione di Milano, Italy; [22]CEA, Saclay, France; [23]Dipartimento di Scienze MIFT, Univ. di Messina, Italy.

≈55 signatures from 23 institutions

ASY-EOS II: the set-up

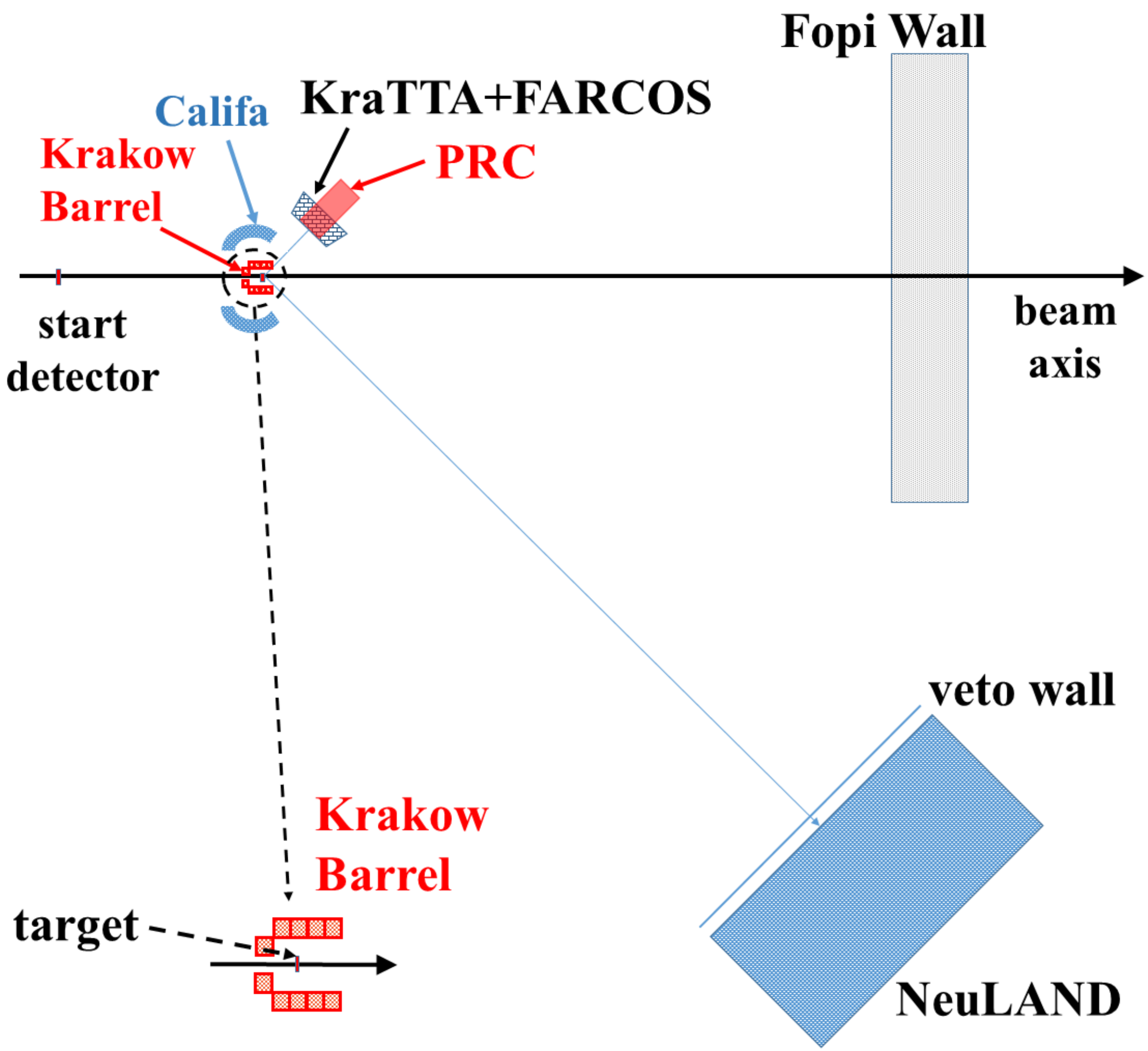

ASY-EOS II: the set-up

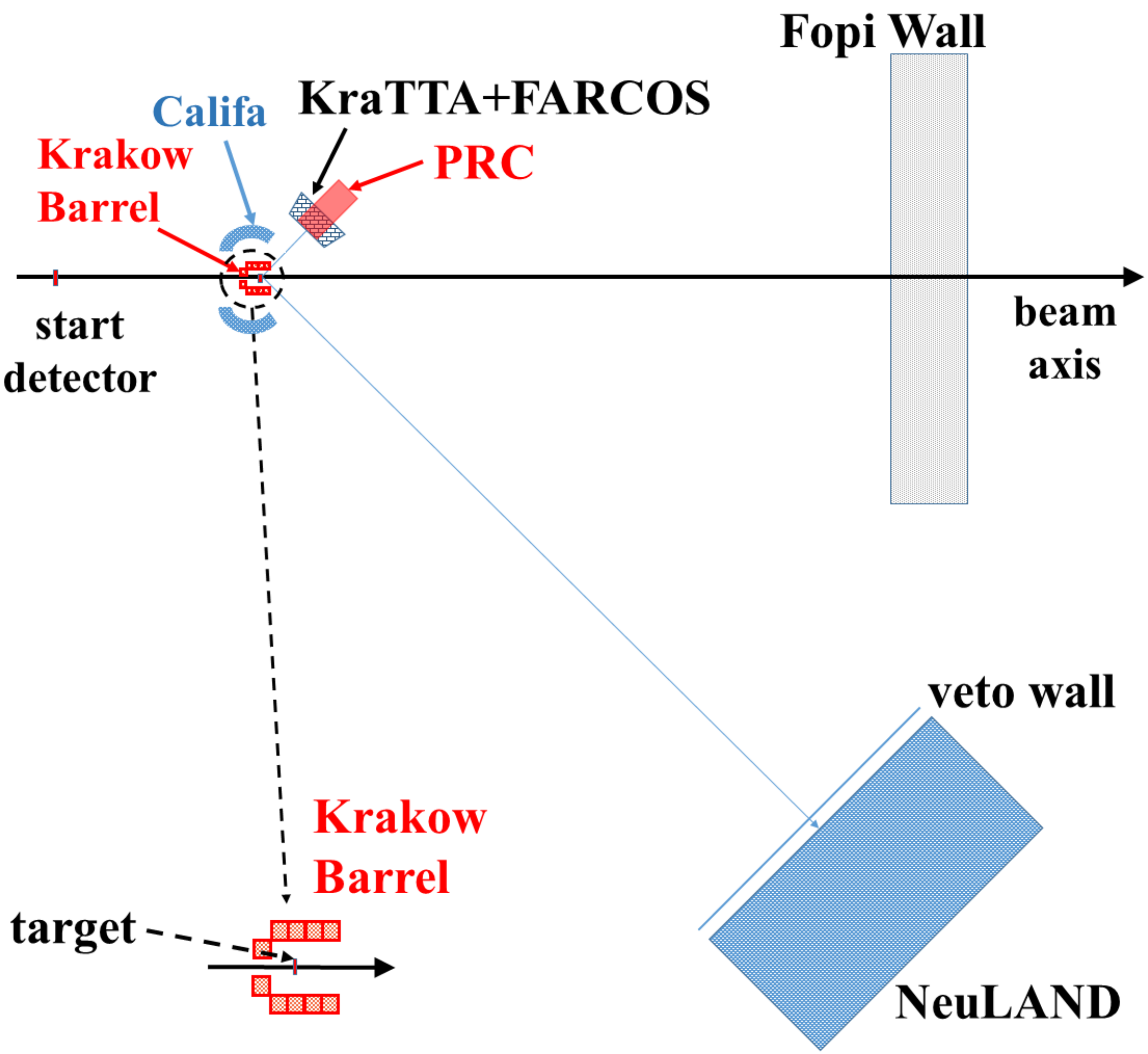

Krab: 5 rings of fast scinitillating fibers read-out by SiPM

Fopi-Wall: plastic scintillating forward wall

NeuLAND: 3000 plastic scintillator bars (250x5x5 cm^3) n,p detector

ASY-EOS II: the set-up

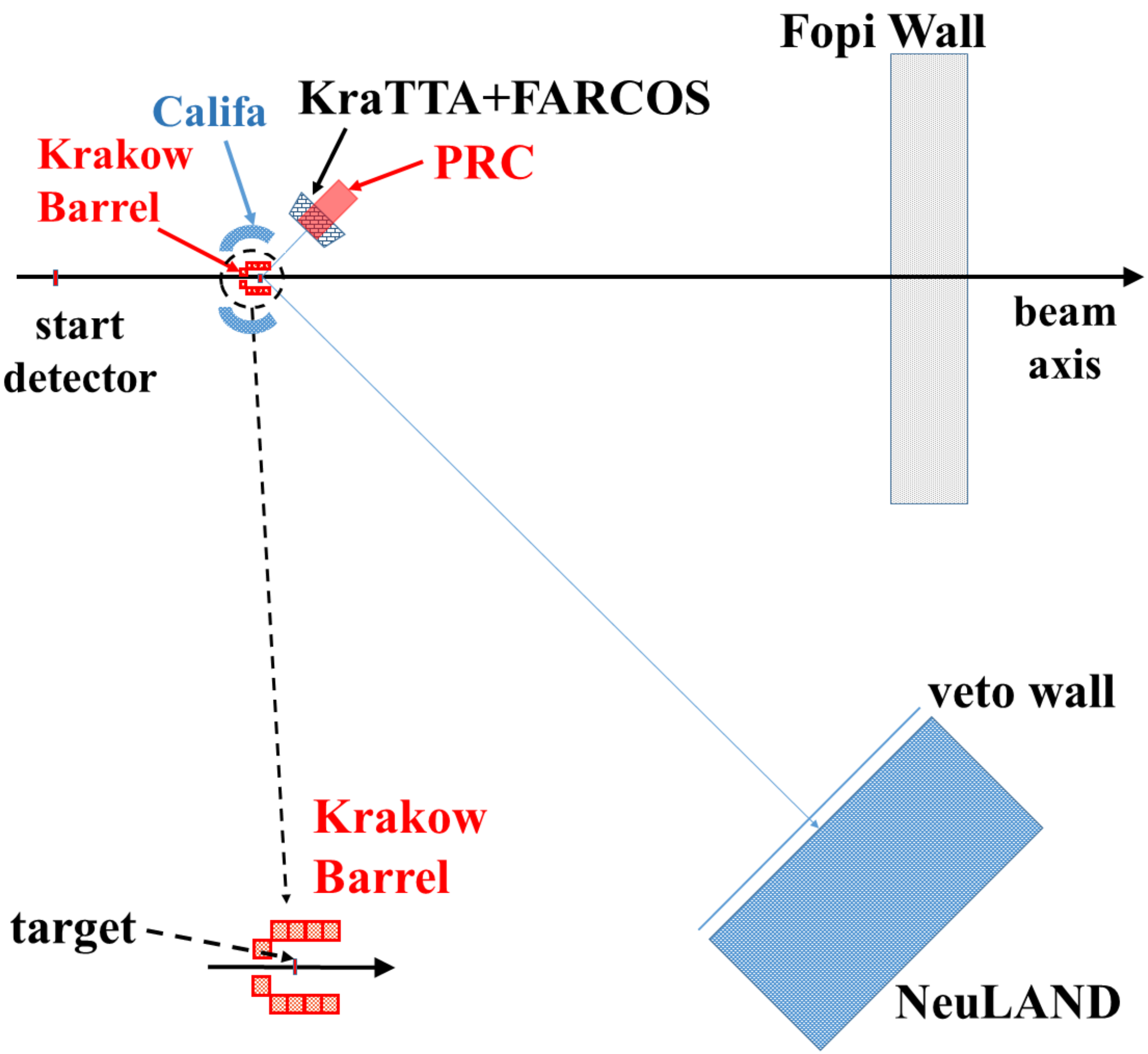

Krab: 5 rings of fast scinitillating fibers read-out by SiPM

Fopi-Wall: plastic scintillating forward wall

NeuLAND: 3000 plastic scintillator bars (250x5x5 cm^3) n,p detector

KraTTA (Si-Si-Csi-CsI-Si): Flows and yields of LCP at mid-rapidity

FARCOS (2xDSSSD-CsI): LCP at mid-rapidity (high angular resolution)

Califa (CsI): LCP at target-rapidity

Pion Range Counter (stack of plastics): π^+ and π^- at mid-rapidity

ASY-EOS: TuQMD predictions

L and KSym sensitivities

$$S(\rho) = S_0 + \frac{L}{3}\left(\frac{\rho - \rho_o}{\rho_o}\right) + \frac{K_{\text{sym}}}{18}\left(\frac{\rho - \rho_o}{\rho_o}\right)^2 + \ldots,$$

$$\Delta np(h)EFR = \left[\frac{v_2^n}{v_2^{p(h)}}\right]_{(a)} - \left[\frac{v_2^n}{v_2^{p(h)}}\right]_{(b)}$$

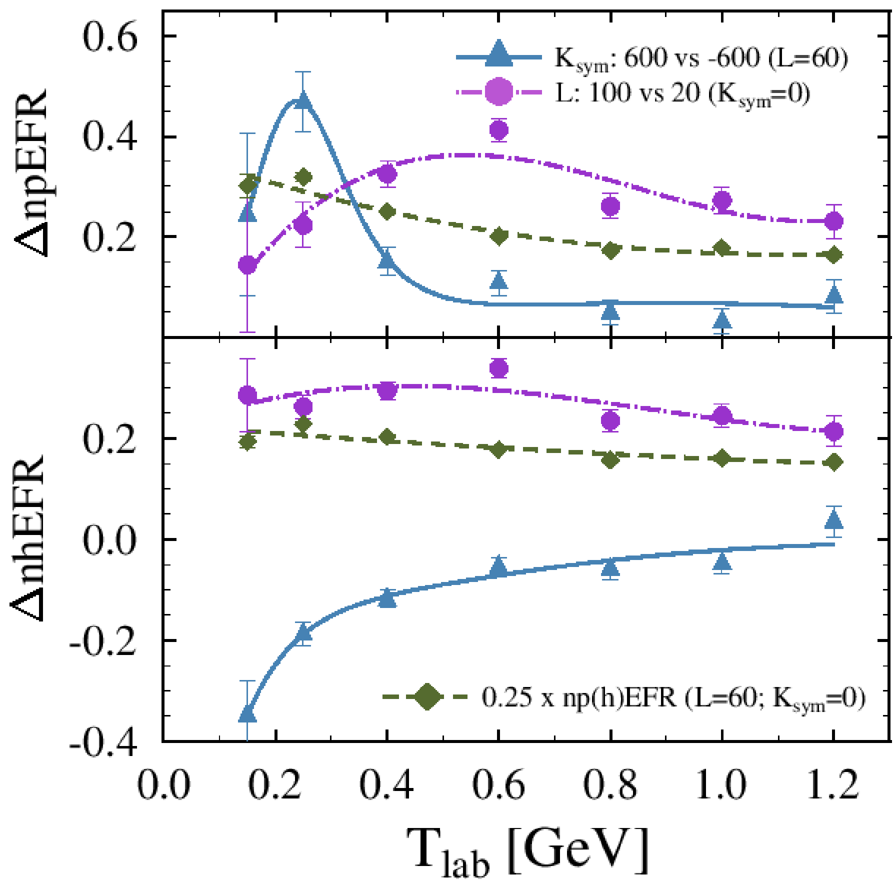

M.D Cozma, EPJA
arXiv:1706.01300

Au+Au b<7.5 fm

ASY-EOS: TuQMD predictions

L and KSym sensitivities

$$S(\rho) = S_0 + \frac{L}{3}\left(\frac{\rho - \rho_o}{\rho_o}\right) + \frac{K_{sym}}{18}\left(\frac{\rho - \rho_o}{\rho_o}\right)^2 + \ldots,$$

$$\Delta np(h)EFR = \left[\frac{v_2^n}{v_2^{p(h)}}\right]_{(a)} - \left[\frac{v_2^n}{v_2^{p(h)}}\right]_{(b)}$$

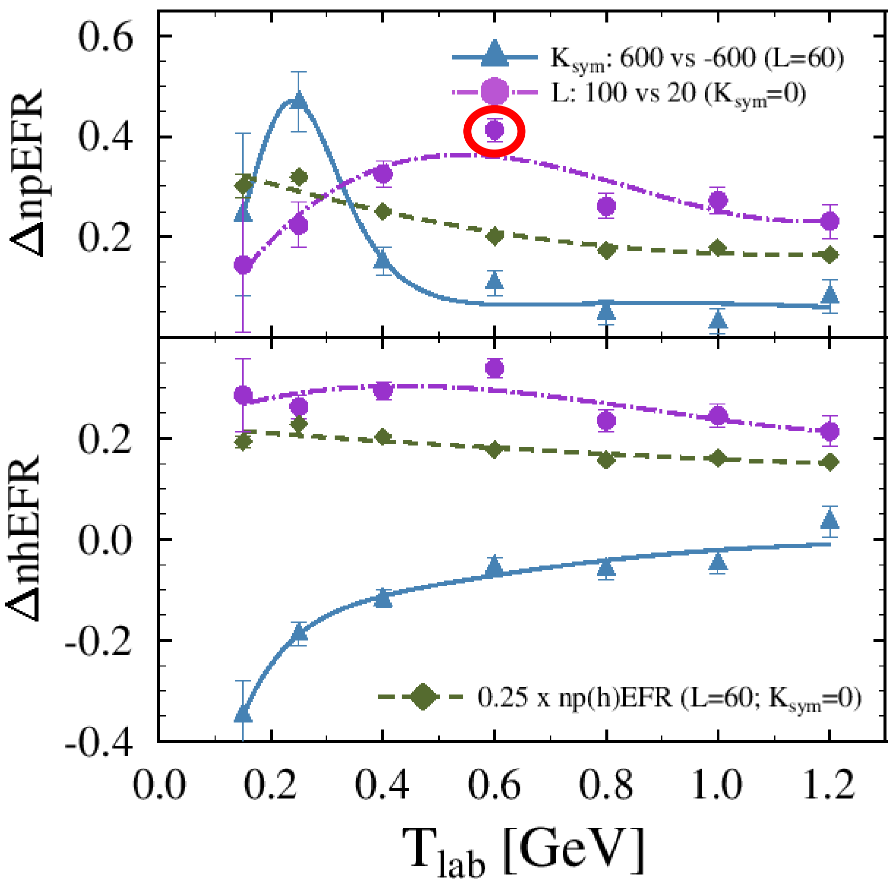

M.D Cozma, EPJA
arXiv:1706.01300

Au+Au b<7.5 fm

ASY-EOS: TuQMD predictions

L and KSym sensitivities

$$S(\rho) = S_0 + \frac{L}{3}\left(\frac{\rho - \rho_o}{\rho_o}\right) + \frac{K_{sym}}{18}\left(\frac{\rho - \rho_o}{\rho_o}\right)^2 + \ldots,$$

$$\Delta np(h)EFR = \left[\frac{v_2^n}{v_2^{p(h)}}\right]_{(a)} - \left[\frac{v_2^n}{v_2^{p(h)}}\right]_{(b)}$$

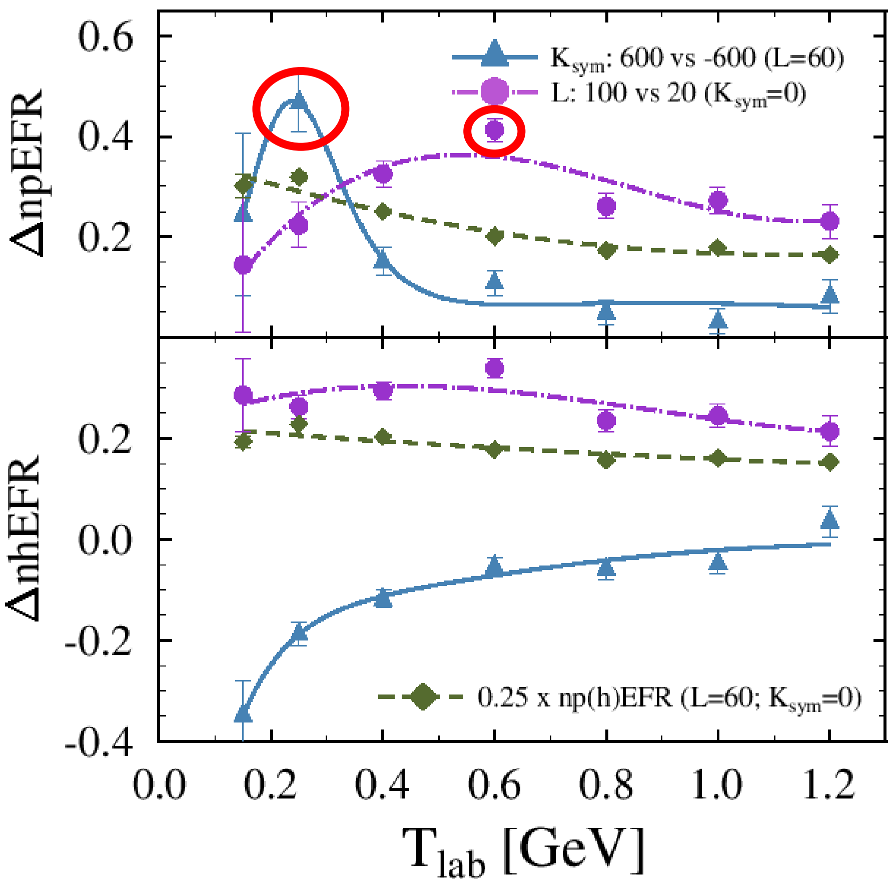

M.D Cozma, EPJA
arXiv:1706.01300

Au+Au b<7.5 fm

Constraints for L and K_{sym}

- Free of systematical uncertainties (cMDI2) neutron-proton v_2^n/v_2^p

$$\begin{aligned} L &= 84 \pm 30(\mathrm{exp}) \pm 18(\mathrm{th})\ \mathrm{MeV} \\ K_{sym} &= 30 \pm 142(\mathrm{exp}) \pm 85(\mathrm{th})\ \mathrm{MeV}\,. \end{aligned}$$

- Full MDI2 freedom

neutron-proton v_2^n/v_2^p+neutron-charged part. v_2^n/v_2^{ch}

$$\begin{aligned} L &= 85 \pm 22(\mathrm{exp}) \pm 20(\mathrm{th}) \pm 12(\mathrm{sys})\ \mathrm{MeV} \\ K_{sym} &= 96 \pm 315(\mathrm{exp}) \pm 170(\mathrm{th}) \pm 166(\mathrm{sys})\ \mathrm{MeV} \end{aligned}$$

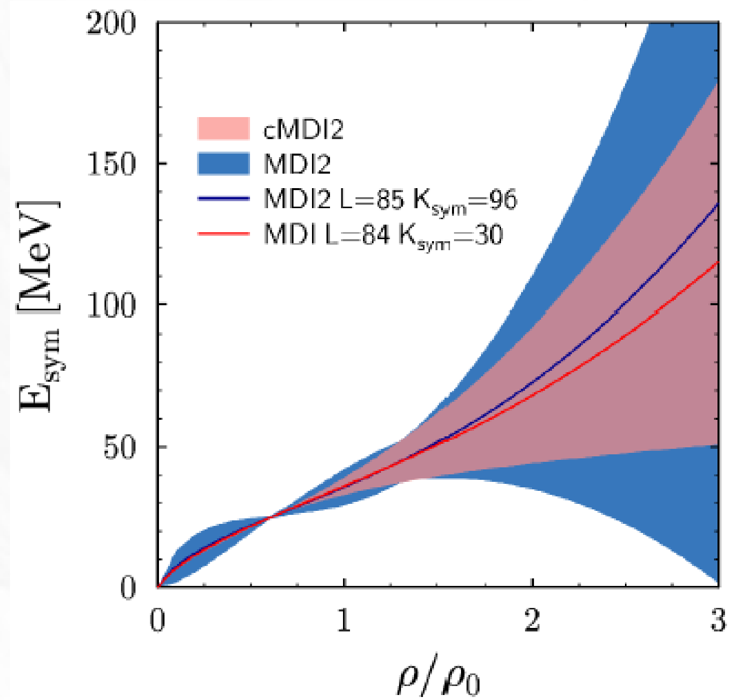

- Isovector compressibility: $K_\tau = K_{sym} - 6L - \frac{J_0}{K_0} L$

$$\begin{aligned} K_\tau &= -354 \pm 228\ \ \mathrm{MeV(cMDI2)} \\ K_\tau &= -290 \pm 421\ \ \mathrm{MeV(MDI2)}\,. \end{aligned}$$

Literature:
ISGMR: -500±100 MeV
Gogny interaction: -370±100 MeV

arXiv:1706.01300 [nucl-th]

UrQMD prediction for pions

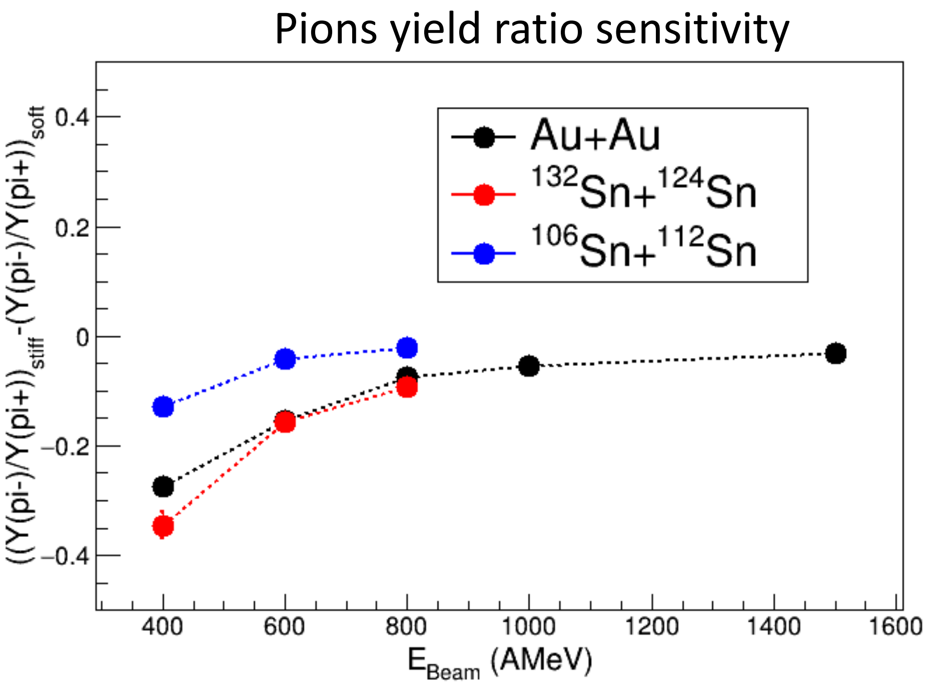

UrQMD prediction for pions

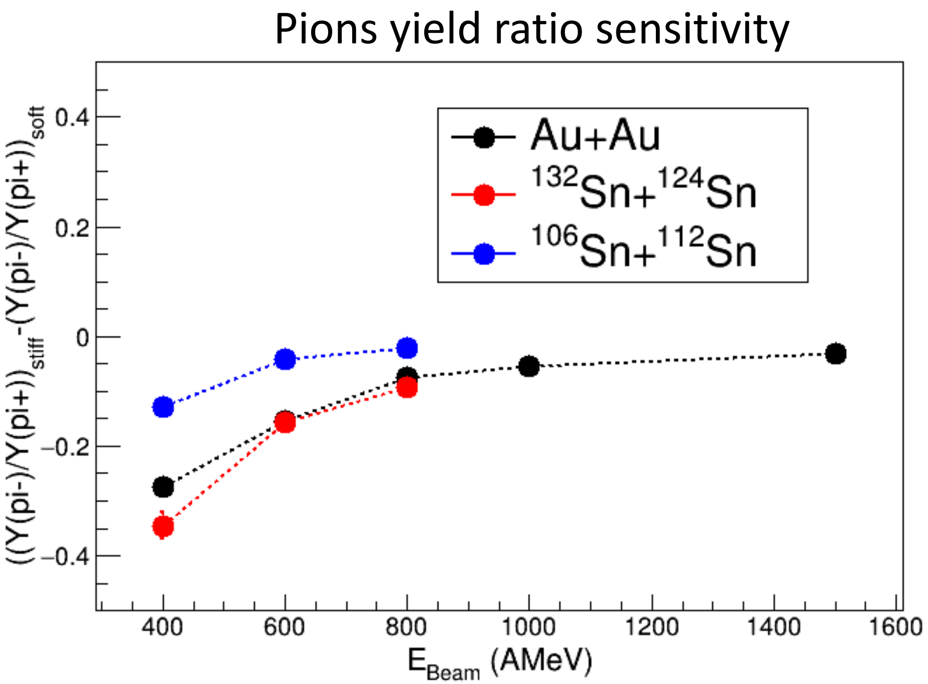

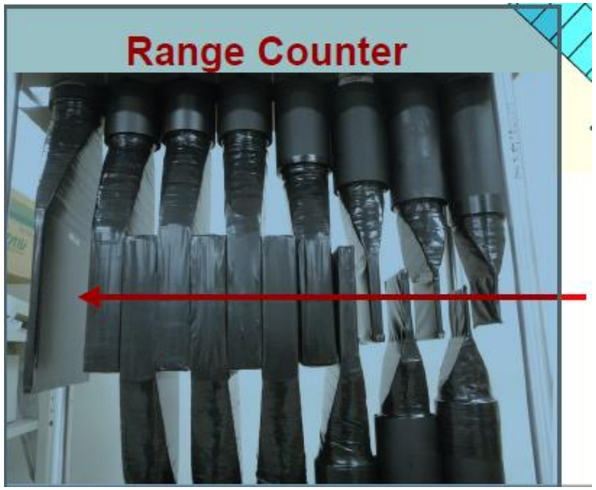

UrQMD prediction for pions

Pions yield ratio sensitivity

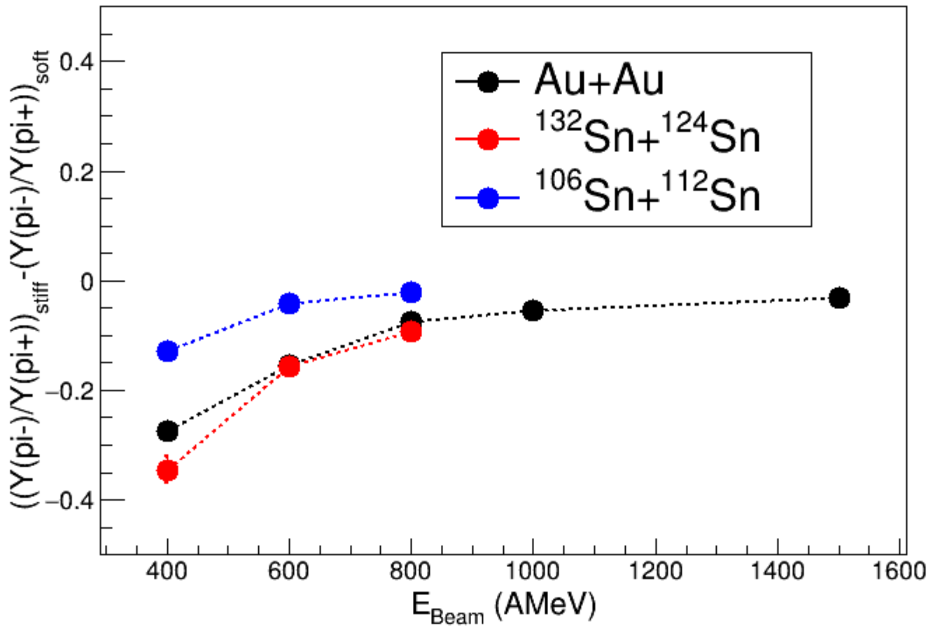

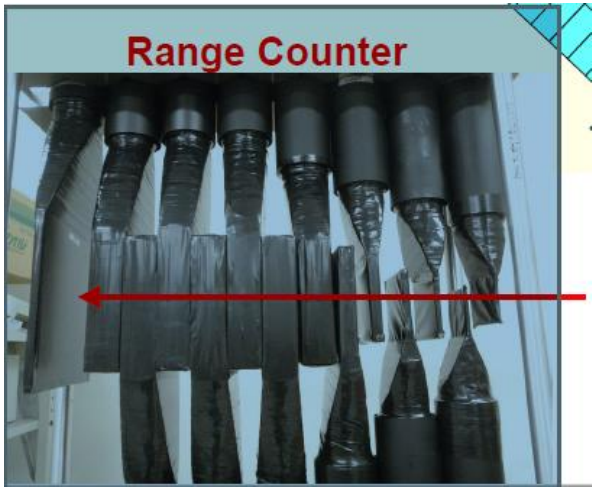

132Sn + 124Sn
108Sn + 112Sn
124Sn + 112Sn
112Sn + 124Sn ~270 MeV/u

Transport 2017 MSU
Mizuki Nishimura

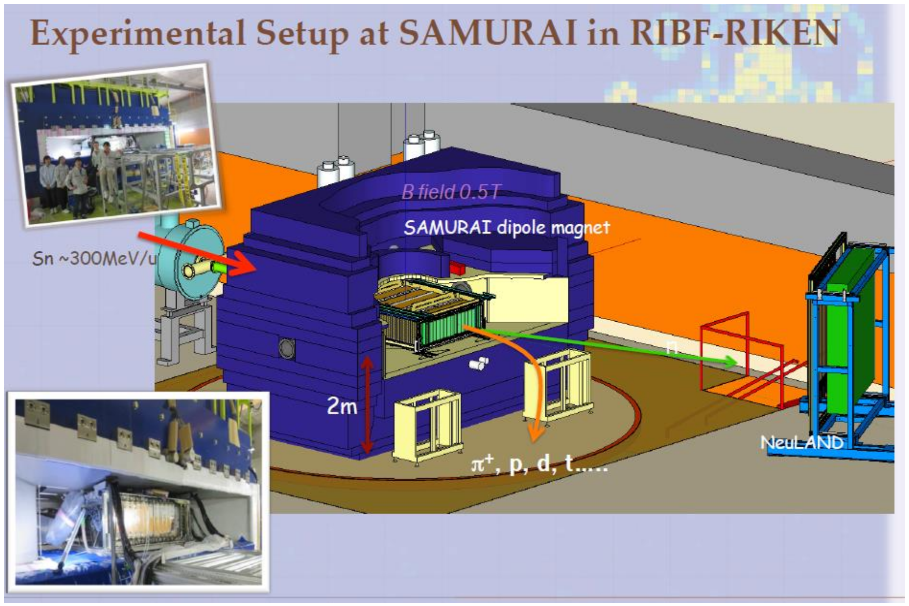

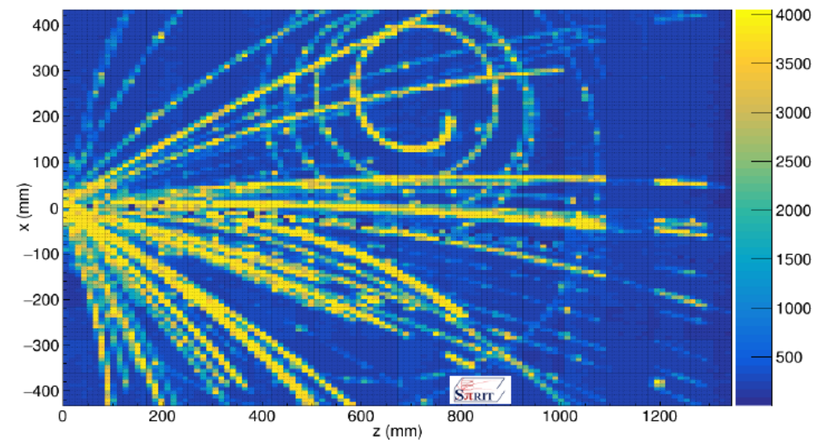

Figure 13: (Color online) Single event recorded with the SπRIT TPC following the reaction of a ^{132}Sn beam accelerated to 270 MeV/u on a solid ^{124}Sn target located at the entrance to the detector ($x = 0$, $z = 0$). Several light ions are produced whose trajectories are slightly curved in the magnetic field. In this event, a pion was also produced as evidenced by the spiral trajectory in the upper half of the figure.

Conclusions

Symmetry Energy:

- Low densities: several constraints quite consistent
- High density:
  - n/p flows: “our” observable for constraining the high-density dependence of the symmetry energy
  - ASY-EOS data analysis is done, new constraint obtained
  - pions: Spirit results will come!
- Work on code consistency needed…everywhere!
- Possibility of new (and better) experiments on n,p flows (& pions?) @ GSI
- International collaborations and efforts

Conclusions

Symmetry Energy:

- Low densities: several constraints quite consistent
- High density:
  - n/p flows: "our" observable for constraining the high-density dependence of the symmetry energy
  - ASY-EOS data analysis is done, new constraint obtained
  - pions: Spirit results will come!
- Work on code consistency needed…everywhere!
- Possibility of new (and better) experiments on n,p flows (& pions?) @ GSI
- International collaborations and efforts

Clepsydra nebula as seen from Hubble telescope (PJ)

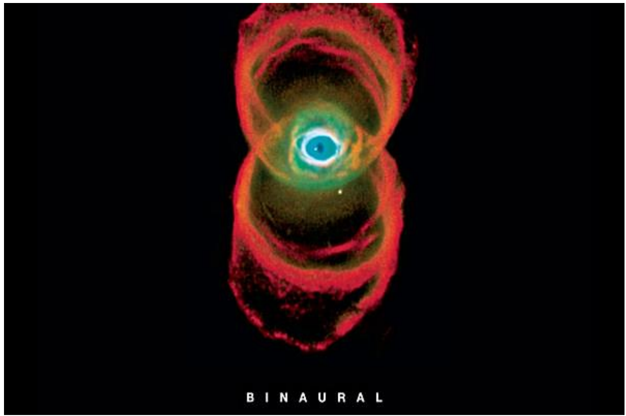

ASY-EOS results

Au+Au @ 400 AMeV b<7.5 fm

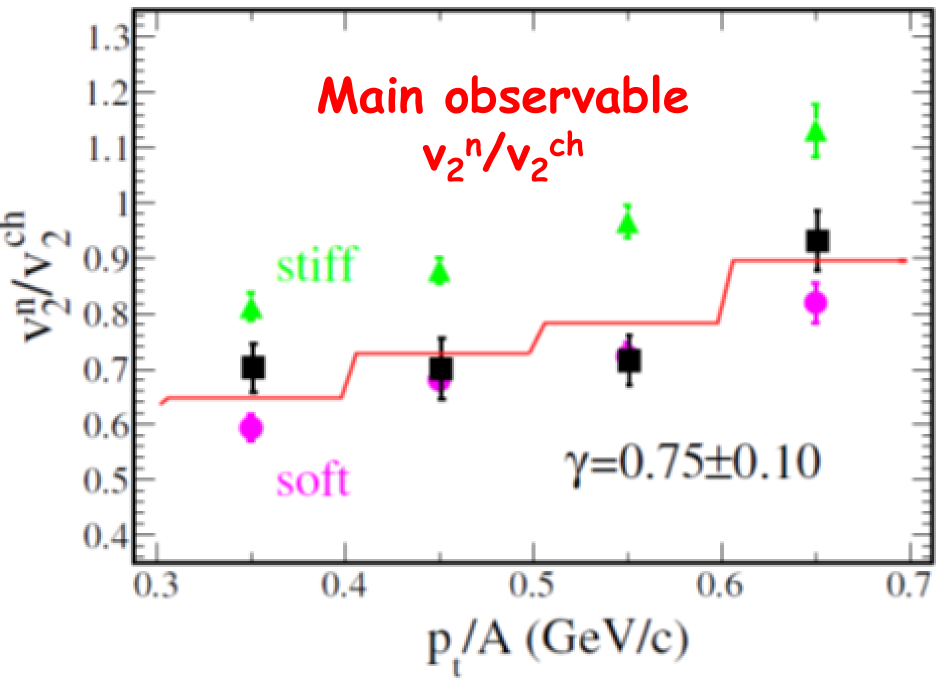

$$E_{sym} = S(\rho) = S_0 + \frac{L}{3}\left(\frac{\rho - \rho_o}{\rho_o}\right) + \frac{K_{sym}}{18}\left(\frac{\rho - \rho_o}{\rho_o}\right)^2 + \ldots,$$

ASY-EOS results

Au+Au @ 400 AMeV   b<7.5 fm

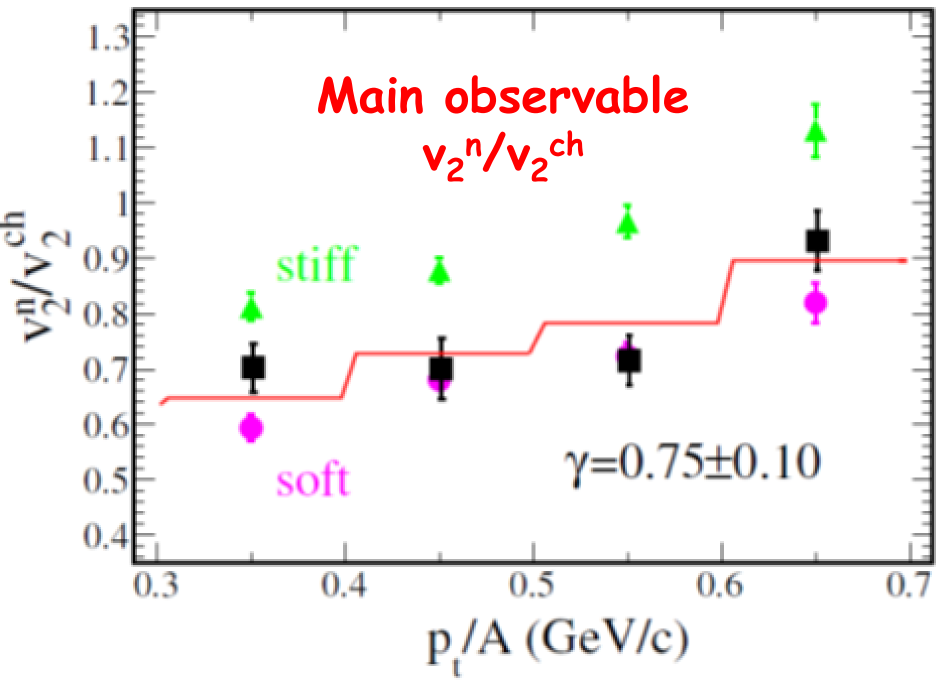

FOPI-LAND DATA : P.Russotto et al., Phys. Lett. B 697 (2011)

γ = 0.9 ± 0.4 ; L=83±26 MeV

$$E_{sym} = S(\rho) = S_0 + \frac{L}{3}\left(\frac{\rho - \rho_o}{\rho_o}\right) + \frac{K_{sym}}{18}\left(\frac{\rho - \rho_o}{\rho_o}\right)^2 + \ldots,$$

ASY-EOS results

Au+Au @ 400 AMeV b<7.5 fm

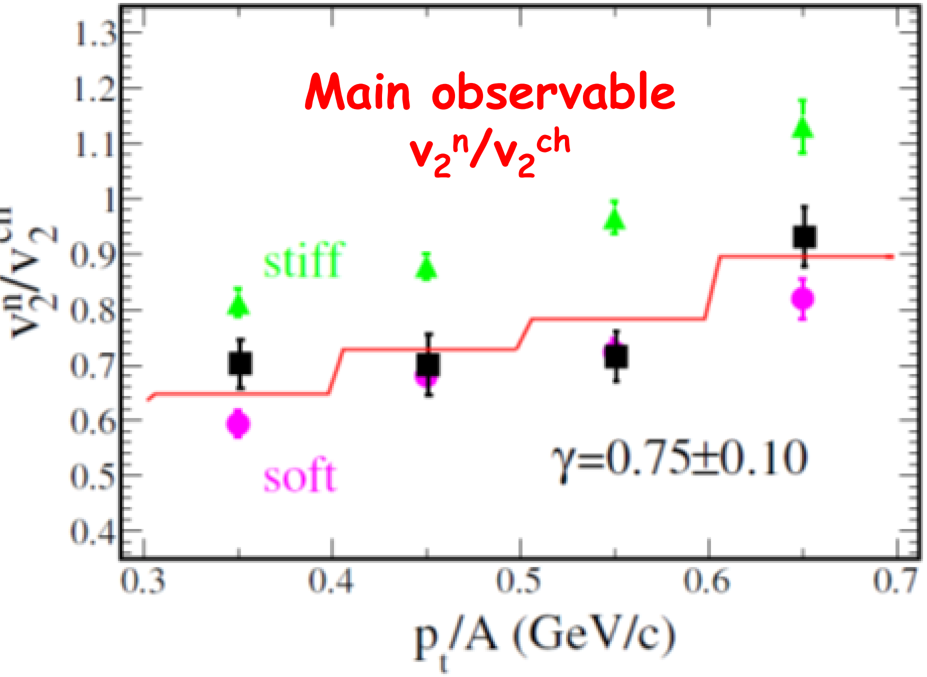

FOPI-LAND DATA : P.Russotto et al., Phys. Lett. B 697 (2011)

γ = 0.9 ± 0.4 ; L=83±26 MeV

ASY-EOS DATA: P. Russotto et al., PRC 94, 034608 (2016)

γ = 0.72± 0.19 ; L=72±13 MeV

$$E_{sym} = S(\rho) = S_0 + \frac{L}{3}\left(\frac{\rho-\rho_o}{\rho_o}\right) + \frac{K_{\mathrm{sym}}}{18}\left(\frac{\rho-\rho_o}{\rho_o}\right)^2 + \ldots,$$

ASY-EOS results

Au+Au @ 400 AMeV b<7.5 fm

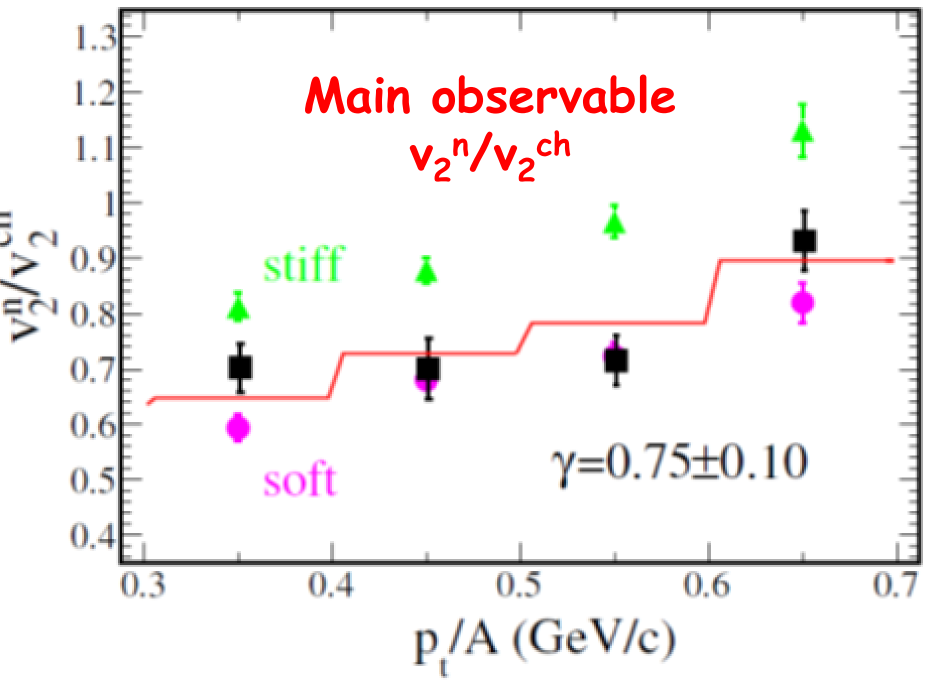

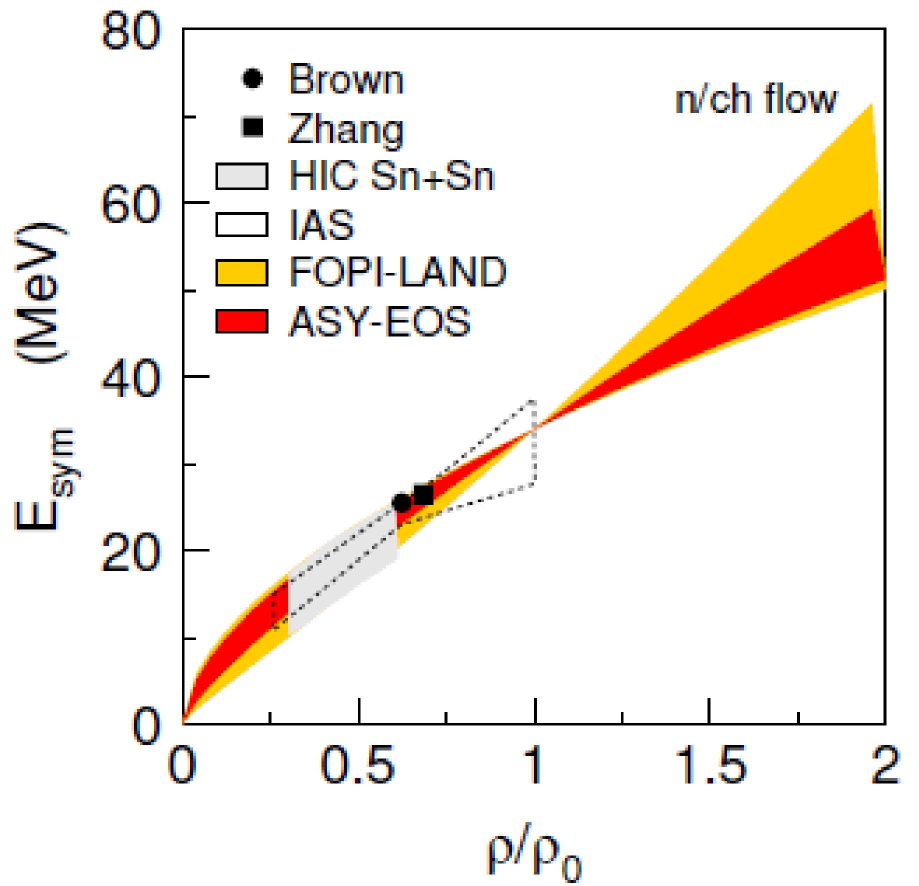

FOPI-LAND DATA : P.Russotto et al., Phys. Lett. B 697 (2011)

γ = 0.9 ± 0.4 ; L=83±26 MeV

ASY-EOS DATA: P. Russotto et al., PRC 94, 034608 (2016)

γ = 0.72± 0.19 ; L=72±13 MeV

HIC: (mainly Isospin diffusion for Sn+Sn): M.B. Tsang et al., PRC 86, 015803 (2012)

neutron skin thickness, binding energies,….: Brown, PRL 111, 232502 (2013); Zhang & Chen, Phys. Lett. B 726 (2013), Danielewicz & Lee, NPA922 (2014).

$$E_{sym} = S(\rho) = S_0 + \frac{L}{3}\left(\frac{\rho-\rho_o}{\rho_o}\right) + \frac{K_{sym}}{18}\left(\frac{\rho-\rho_o}{\rho_o}\right)^2 + \ldots,$$

ASY-EOS results

Au+Au @ 400 AMeV b<7.5 fm

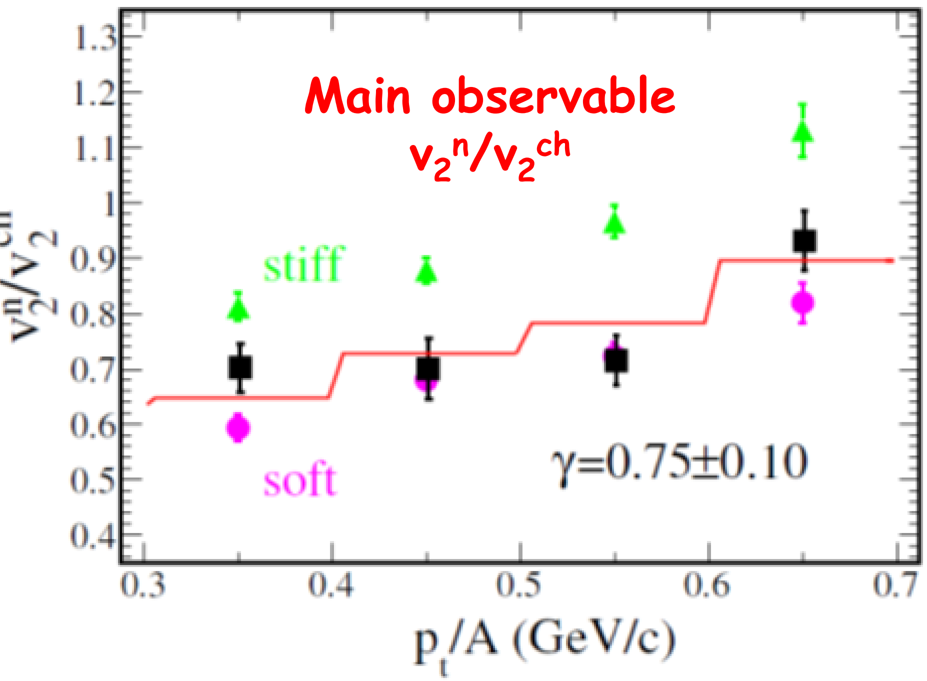

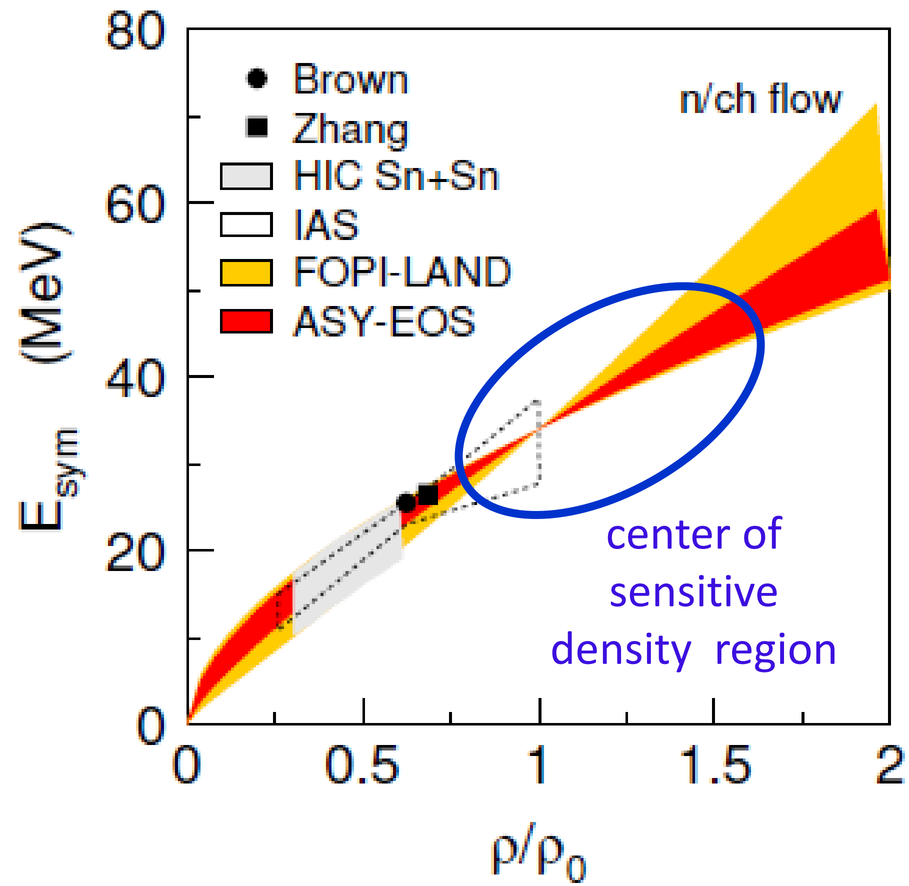

FOPI-LAND DATA : P.Russotto et al., Phys. Lett. B 697 (2011)
γ = 0.9 ± 0.4 ; L=83±26 MeV

ASY-EOS DATA: P. Russotto et al., PRC 94, 034608 (2016)
γ = 0.72± 0.19 ; L=72±13 MeV

HIC: (mainly Isospin diffusion for Sn+Sn):
M.B. Tsang et al., PRC 86, 015803 (2012)

neutron skin thickness, binding energies,….:
Brown, PRL 111, 232502 (2013); Zhang & Chen, Phys. Lett. B 726 (2013), Danielewicz & Lee, NPA922 (2014).

$$E_{sym} = S(\rho) = S_0 + \frac{L}{3}\left(\frac{\rho-\rho_o}{\rho_o}\right) + \frac{K_{sym}}{18}\left(\frac{\rho-\rho_o}{\rho_o}\right)^2 + \ldots,$$

ASY-EOS results

Au+Au @ 400 AMeV b<7.5 fm

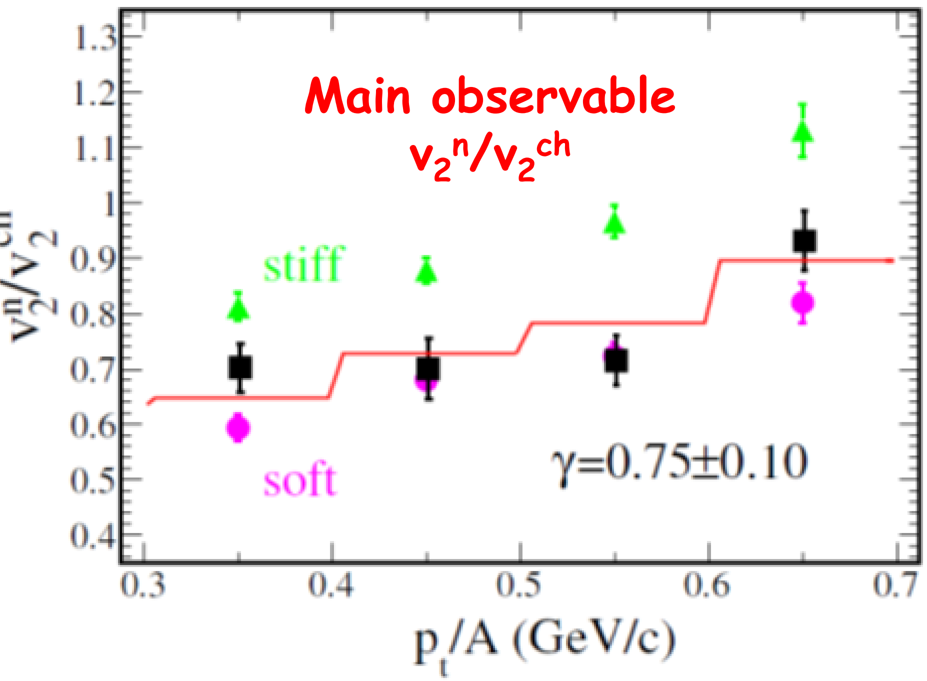

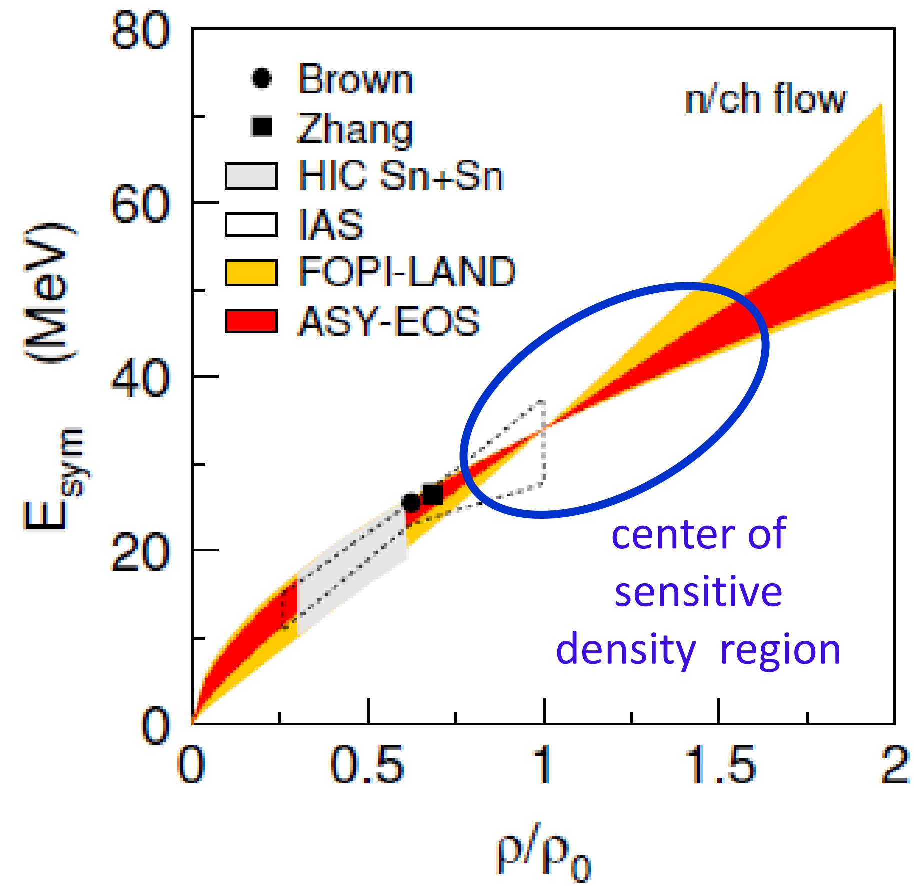

FOPI-LAND DATA : P.Russotto et al., Phys. Lett. B 697 (2011)

γ = 0.9 ± 0.4 ; L=83±26 MeV

ASY-EOS DATA: P. Russotto et al., PRC 94, 034608 (2016)

γ = 0.72± 0.19 ; L=72±13 MeV

$$E_{sym} = S(\rho) = S_0 + \frac{L}{3}\left(\frac{\rho-\rho_o}{\rho_o}\right) + \frac{K_{sym}}{18}\left(\frac{\rho-\rho_o}{\rho_o}\right)^2 + \ldots,$$

HIC: (mainly Isospin diffusion for Sn+Sn): M.B. Tsang et al., PRC 86, 015803 (2012)

neutron skin thickness, binding energies,….: Brown, PRL 111, 232502 (2013); Zhang & Chen, Phys. Lett. B 726 (2013), Danielewicz & Lee, NPA922 (2014).

Next step? ASY-EOS II

UrQMD and IQMD prediction for pions

Pions yield ratio senstivity

UrQMD

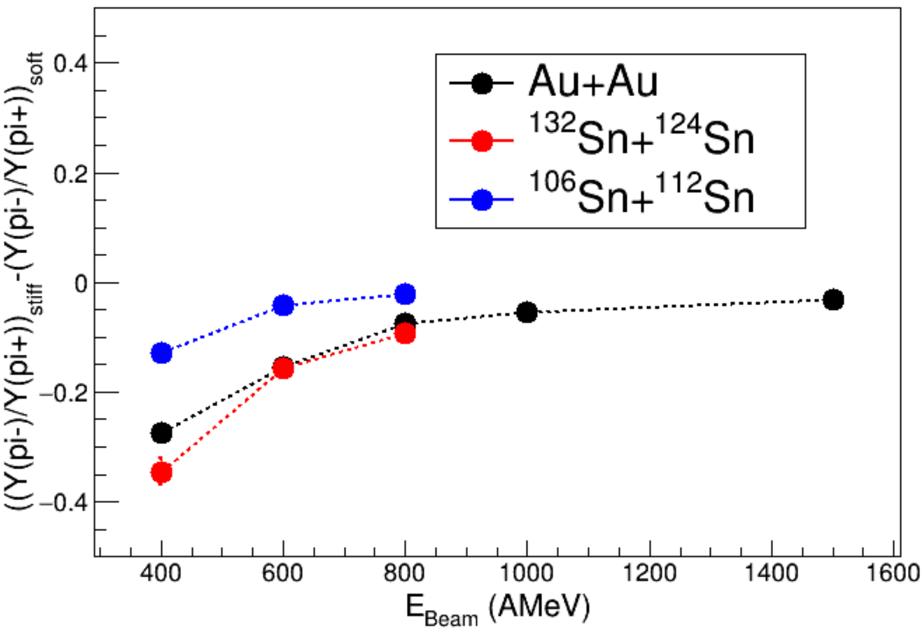

UrQMD and IQMD prediction for pions

Pions yield ratio senstivity

IQMD

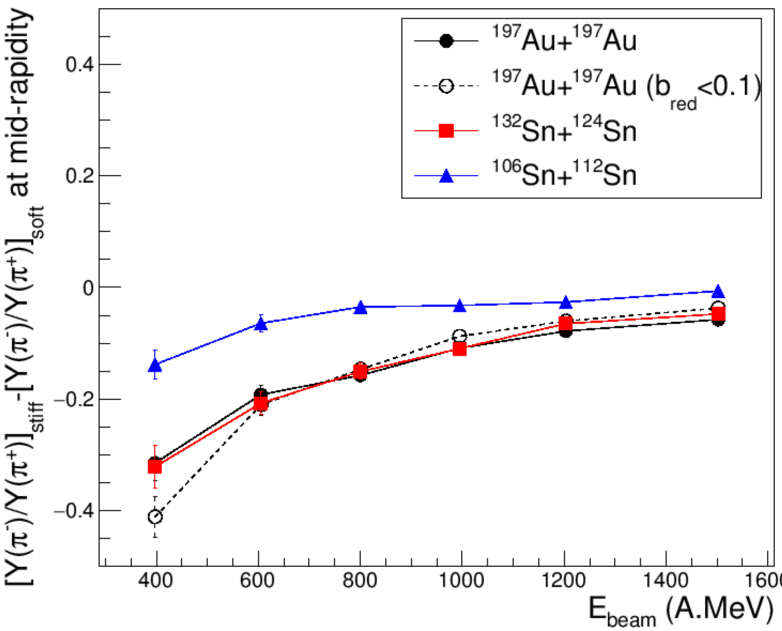

A. Le Fevre calculations

UrQMD

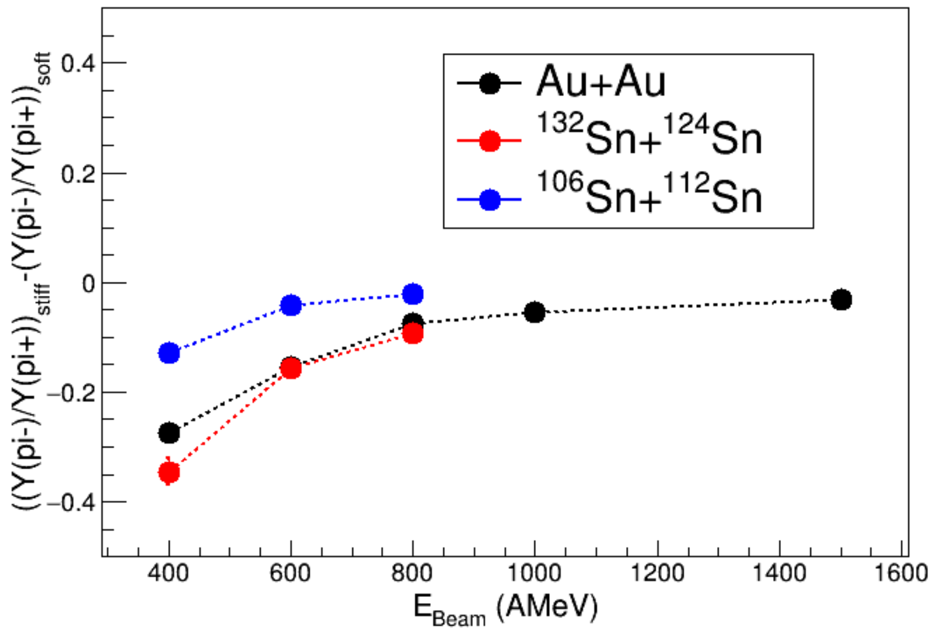

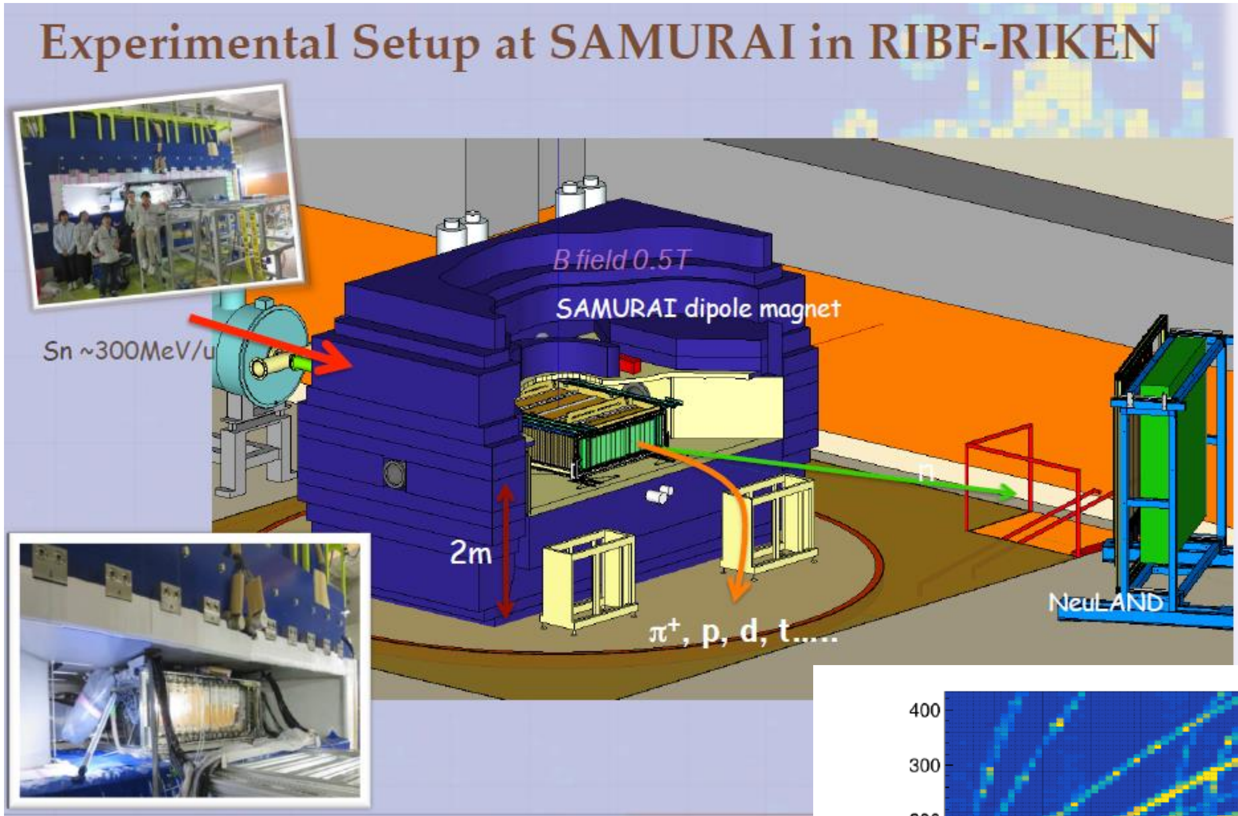

Transport 2017 MSU
Mizuki Nishimura

132Sn + 124Sn
108Sn + 112Sn
124Sn + 112Sn
112Sn + 124Sn ~300 MeV/u

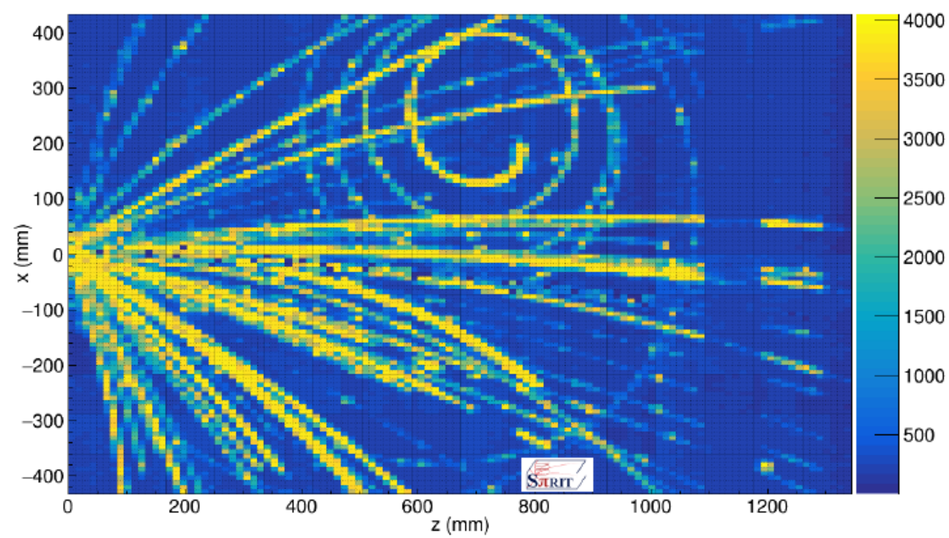

Figure 13: (Color online) Single event recorded with the SπRIT TPC following the reaction of a ^{132}Sn beam accelerated to 270 MeV/u on a solid ^{124}Sn target located at the entrance to the detector ($x = 0$, $z = 0$). Several light ions are produced whose trajectories are slightly curved in the magnetic field. In this event, a pion was also produced as evidenced by the spiral trajectory in the upper half of the figure.

Introduction

The nuclear EOS describes the relation among energy, pressure, density, temperature and isospin asymmetry. It is a fundamental ingredient in nuclear physics and astrophysics.

Nuclear matter phase diagram (schematic)

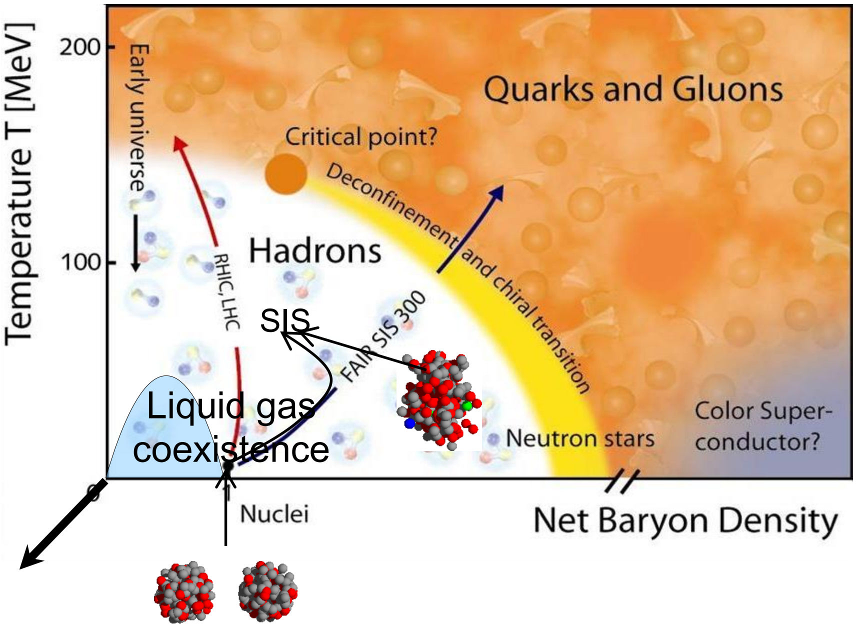

Introduction

The nuclear EOS describes the relation among energy, pressure, density, temperature and isospin asymmetry. It is a fundamental ingredient in nuclear physics and astrophysics.

Question: how E/A depends on the density ρ and isospin asymmetry δ=(N-Z)/(N+Z)

E/A(ρ, δ)=????

Nuclear matter phase diagram (schematic)

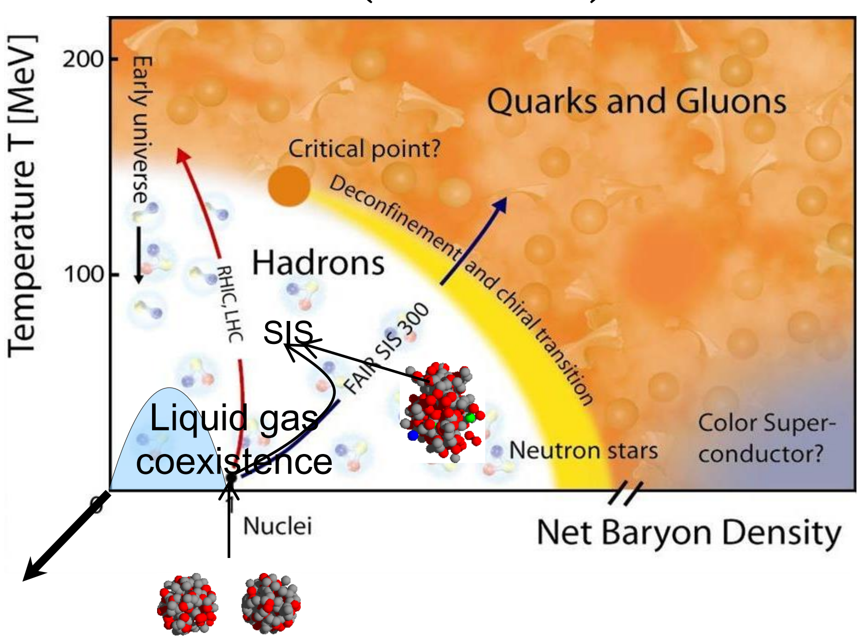

Introduction

The nuclear EOS describes the relation among energy, pressure, density, temperature and isospin asymmetry. It is a fundamental ingredient in nuclear physics and astrophysics.

Question: how E/A depends on the density ρ and isospin asymmetry δ=(N-Z)/(N+Z)

E/A(ρ, δ)=????

Nuclear matter phase diagram (schematic)

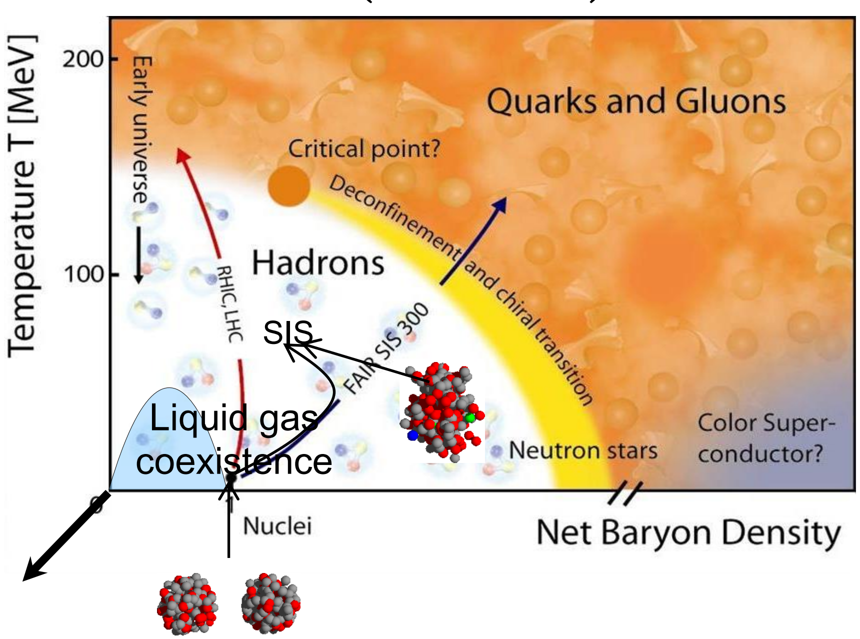

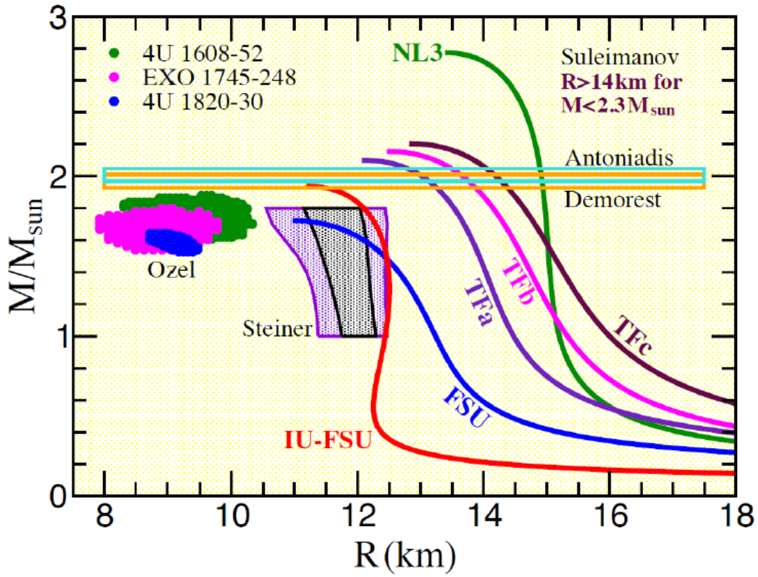

J. Piekarewicz, arXiv:1805.04780v1

Constraints of the Symmetry Energy

$$S(\rho) = S_0 + \frac{L}{3}\left(\frac{\rho-\rho_0}{\rho_0}\right) + \frac{K_{sym}}{18}\left(\frac{\rho-\rho_0}{\rho_0}\right)^2 + \dots$$

Terrestrial laboratories

- **Several constraints (quite consistent among them) around and below ρ_0**
- **Few constraints above ρ_0**

Constraints of the Symmetry Energy

$$S(\rho) = S_0 + \frac{L}{3}\left(\frac{\rho-\rho_0}{\rho_0}\right) + \frac{K_{sym}}{18}\left(\frac{\rho-\rho_0}{\rho_0}\right)^2 + \ldots$$

Quantity:	$E_{sym}(\rho_0)$ (MeV)	$L(\rho_0)$ (MeV)
2013 global average	31.6	58.9
“Standard deviation”	0.92	16.5
Average of “error bars”	2.66	16.0

Terrestrial laboratories

- **Several constraints (quite consistent among them) around and below ρ_0**
- **Few constraints above ρ_0**

Bao-An Li and Xiao Han
Phys. Lett. B727, 276 (2013)

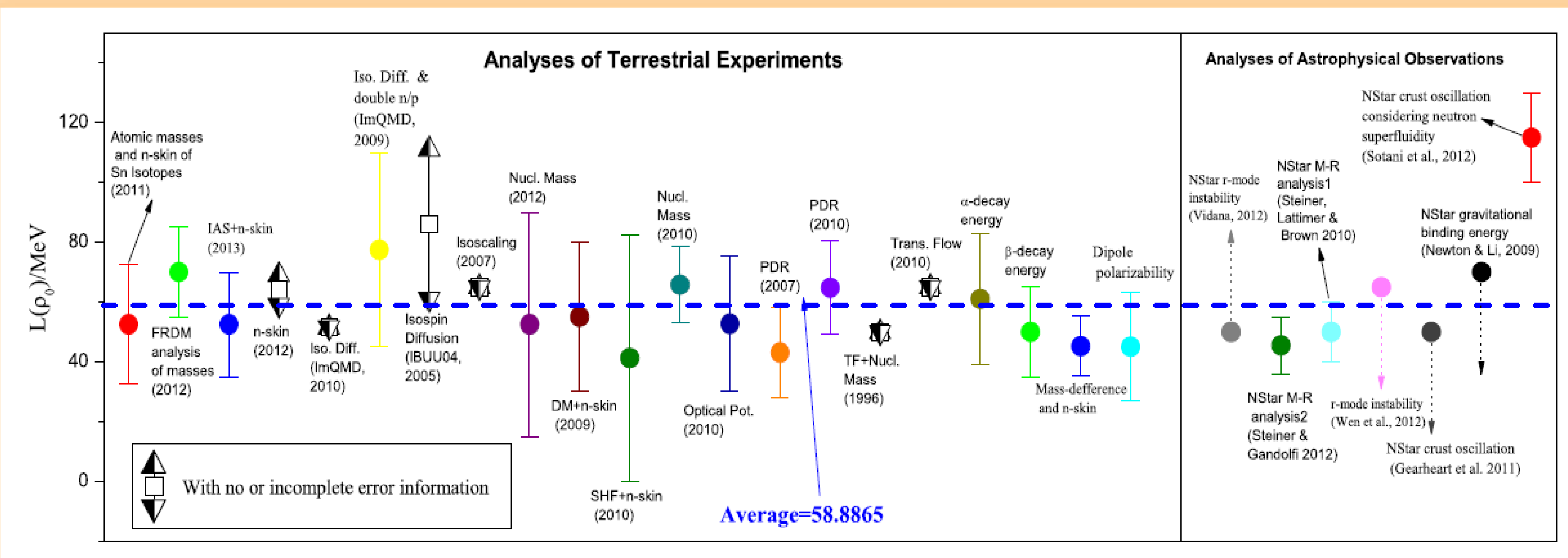

Constraints of the Symmetry Energy

$$S(\rho) = S_0 + \frac{L}{3}\left(\frac{\rho-\rho_0}{\rho_0}\right) + \frac{K_{sym}}{18}\left(\frac{\rho-\rho_0}{\rho_0}\right)^2 + \ldots.$$

Quantity:	$E_{sym}(\rho_0)$ (MeV)	$L(\rho_0)$ (MeV)
2013 global average	31.6	58.9
"Standard deviation"	0.92	16.5
Average of "error bars"	2.66	16.0

Terrestrial laboratories

- **Several constraints (quite consistent among them) around and below ρ_0**
- **Few constraints above ρ_0**

Bao-An Li and Xiao Han
Phys. Lett. B727, 276 (2013)

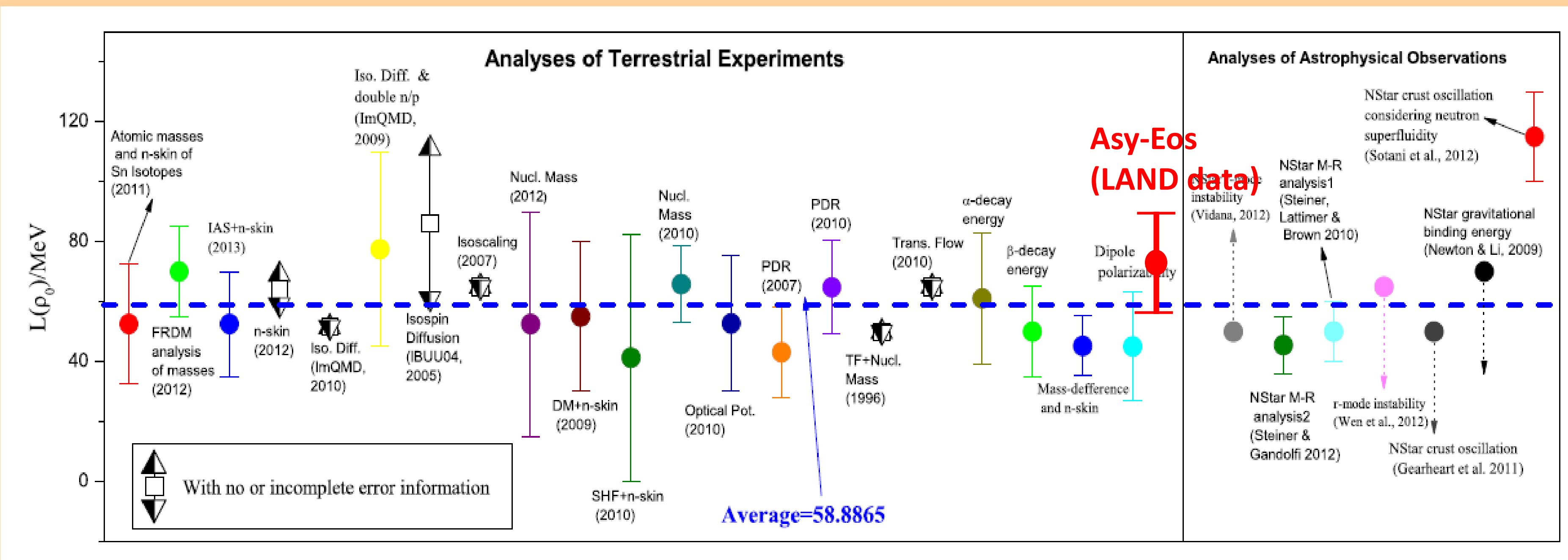

EOS for nuclear matter and Symmetry Energy

$$E(\rho,\delta) = E(\rho,\delta=0) + E_{sym}(\rho)\delta^2 + \ldots$$

$$\delta = \frac{\rho_n - \rho_p}{\rho_n + \rho_p} = \frac{N-Z}{A}$$

EOS for nuclear matter and Symmetry Energy

$$E(\rho,\delta) = E(\rho,\delta=0) + E_{sym}(\rho)\delta^2 + \ldots$$

$$\delta = \frac{\rho_n - \rho_p}{\rho_n + \rho_p} = \frac{N-Z}{A}$$

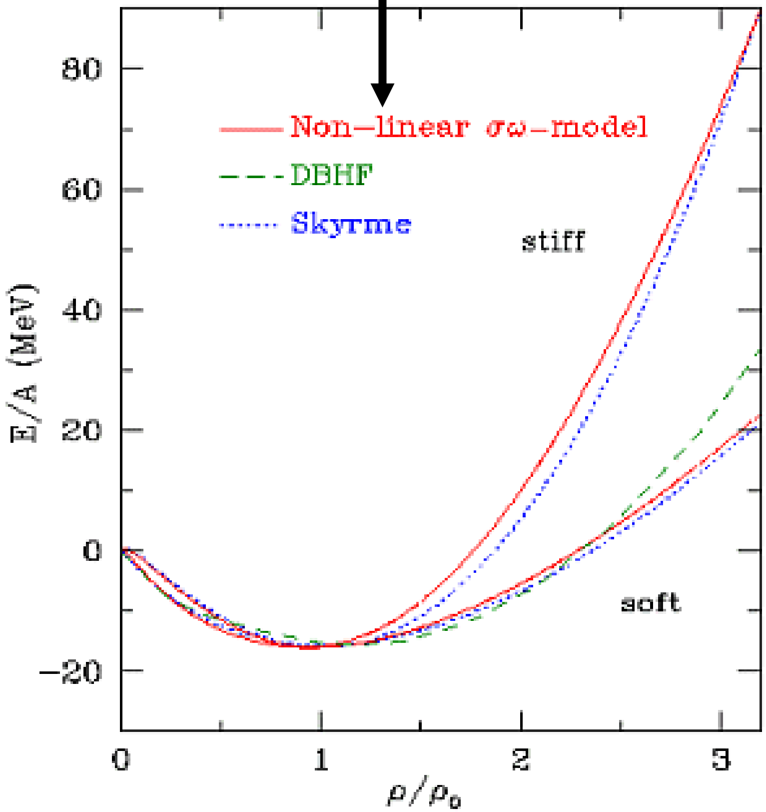

"How much energy is needed to compress hadronic matter?"

P. Danielewicz et al., Science 298 (2002)
C. Fuchs et al., PRL 86 (2001) 1974
Youngblood et al., PRL82 691 (1999)
A. Le Fevre et al., Nucl. Phys. A 945 (2016)

EOS for nuclear matter and Symmetry Energy

$$E(\rho,\delta) = E(\rho,\delta=0) + E_{sym}(\rho)\delta^2 + \ldots$$

$$\delta = \frac{\rho_n - \rho_p}{\rho_n + \rho_p} = \frac{N-Z}{A}$$

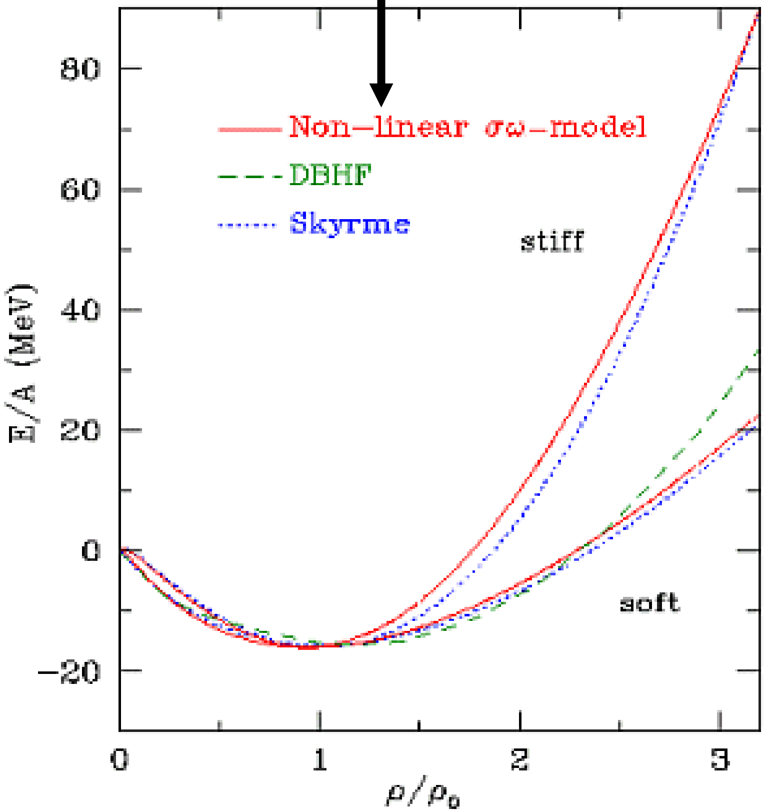

"How much energy is needed to compress hadronic matter?"

P. Danielewicz et al., Science 298 (2002)
C. Fuchs et al., PRL 86 (2001) 1974
Youngblood et al., PRL82 691 (1999)
A. Le Fevre et al., Nucl. Phys. A 945 (2016)

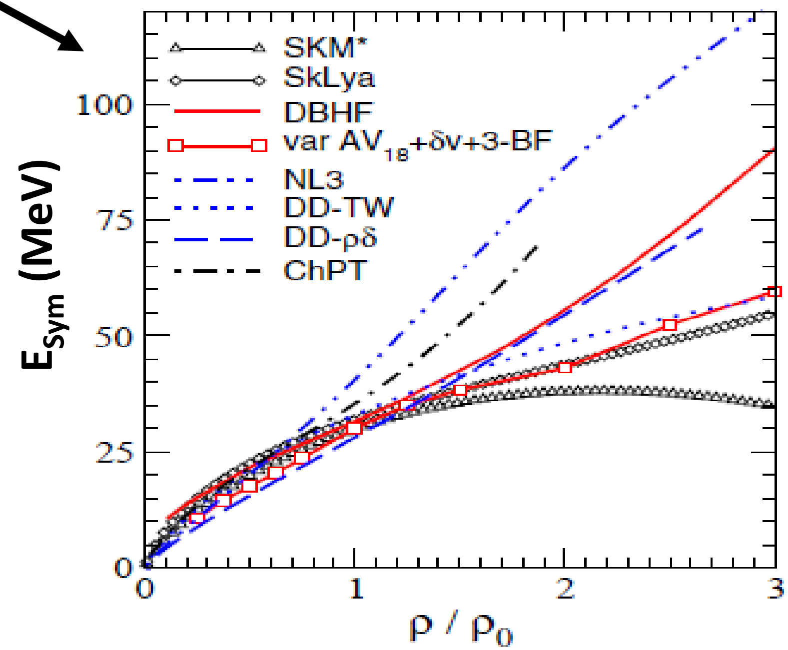

From Ab initio calculations (red) and phenomenological approaches

Fuchs and Wolter, EPJA 30 (2006)

EOS for nuclear matter and Symmetry Energy

$$E(\rho,\delta) = E(\rho,\delta=0) + E_{sym}(\rho)\delta^2 + \ldots$$

$$\delta = \frac{\rho_n - \rho_p}{\rho_n + \rho_p} = \frac{N-Z}{A}$$

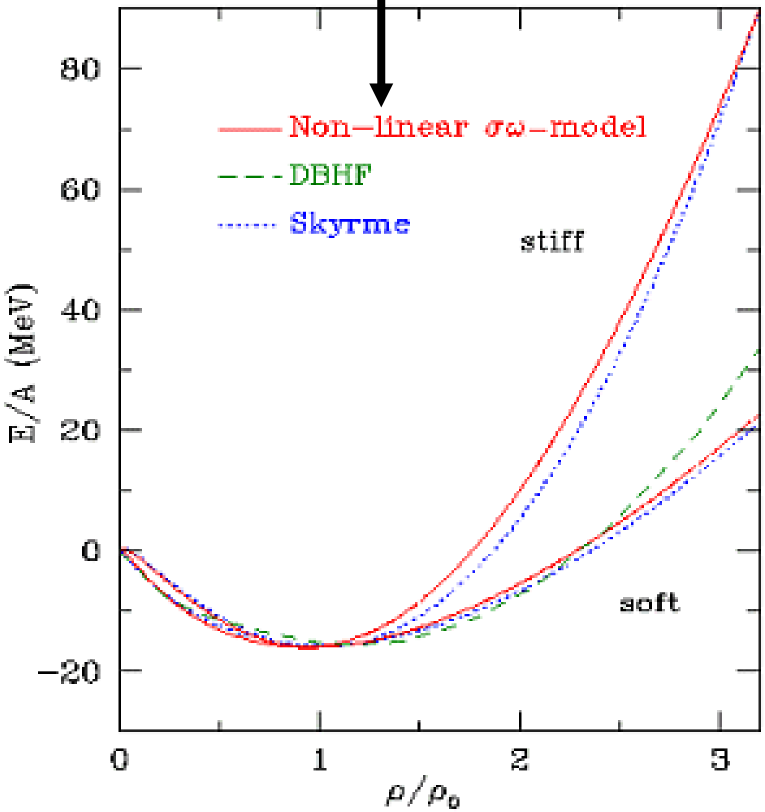

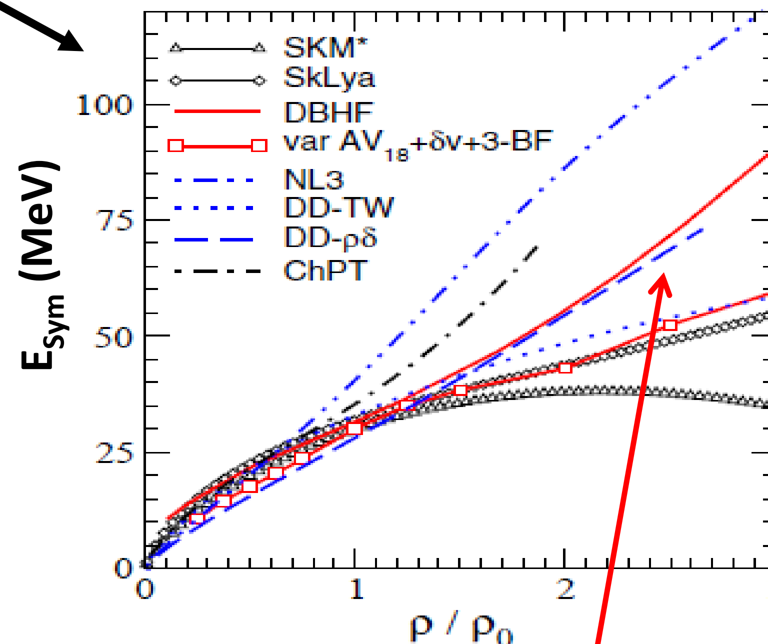

From Ab initio calculations (red) and phenomenological approaches

Fuchs and Wolter, EPJA 30 (2006)

"How much energy is needed to compress hadronic matter?"

P. Danielewicz et al., Science 298 (2002)
C. Fuchs et al., PRL 86 (2001) 1974
Youngblood et al., PRL82 691 (1999)
A. Le Fevre et al., Nucl. Phys. A 945 (2016)

High density…so important!

ASY-EOS II: LOI results

For your proposal S464 (LoI)[1] the G-PAC formulated the following evaluation with which I concur:

Regarding the LoI "Determination of Symmetry Energy at Supra-Normal Densities: a feasibility study" (Proposal S464), the committee appreciates the need to determine the energy symmetry of the nuclear matter equation of state including exploration of beam intensities reached for radioactive neutron rich and neutron deficient Sn isotopes. In light of the above, the committee encourages the applicants to submit this as a regular proposal to the G-PAC.

I would like to encourage your continued interest in the experimental program at GSI/FAIR, and hope that you will continue to propose experiments to future calls for proposals, and in particular, I am looking forward to a proposal on this in a next 'call'.

High density symmetry energy in relativistic heavy ion collisions

Which densities can be explored in the early stage of the reaction ?

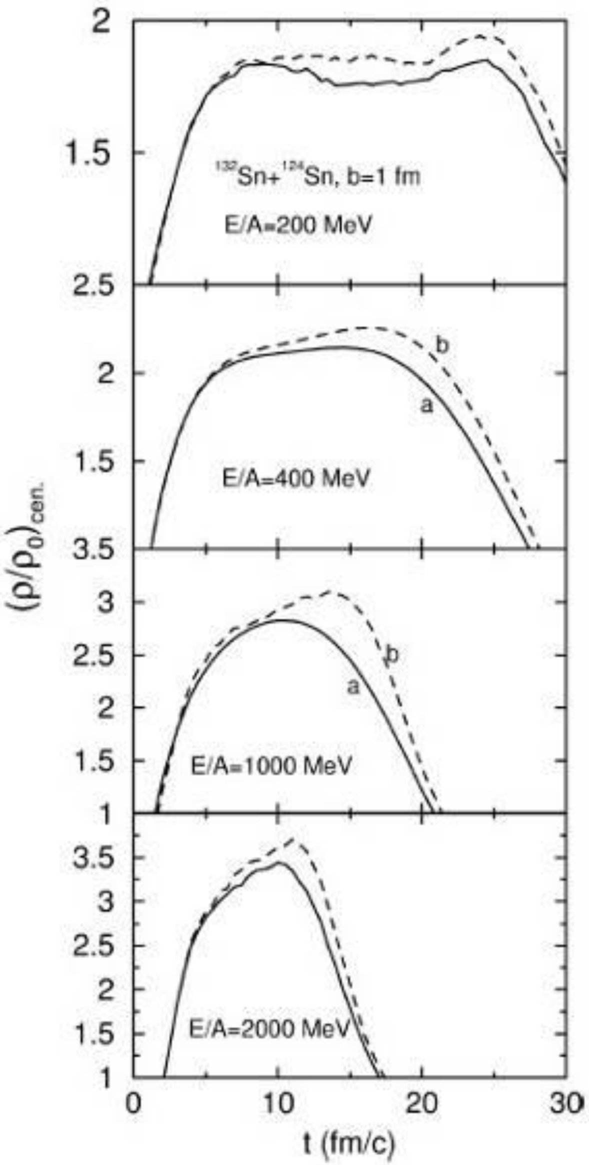

Bao-An Li, NPA 708 (2002)

High density symmetry energy in relativistic heavy ion collisions

Which densities can be explored in the early stage of the reaction ?

B.A. Li et al., PRC71 (2005)

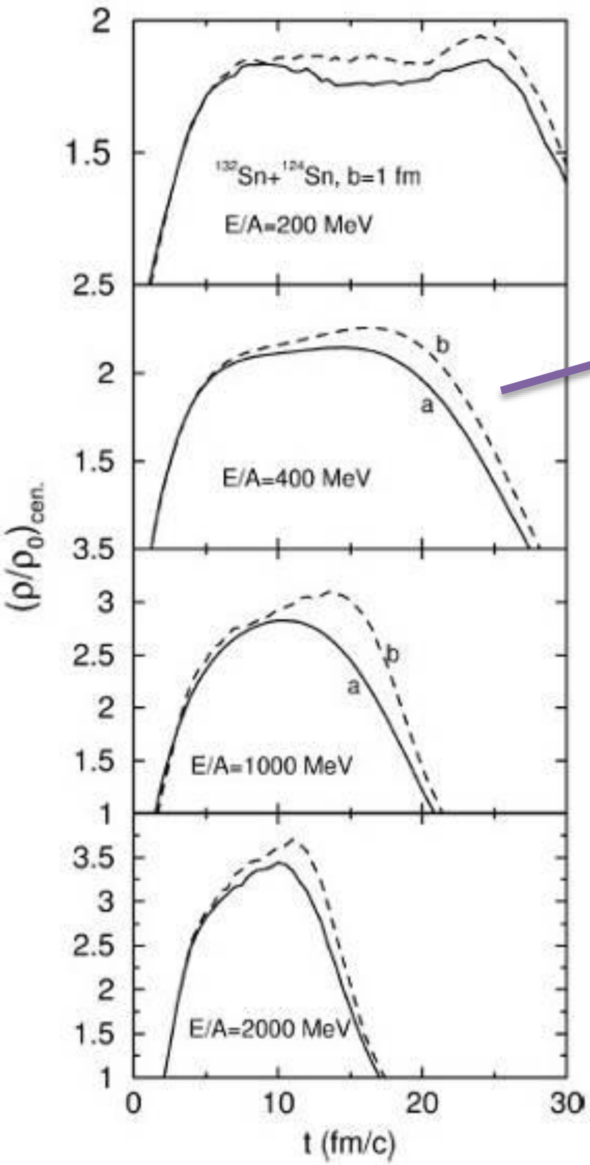

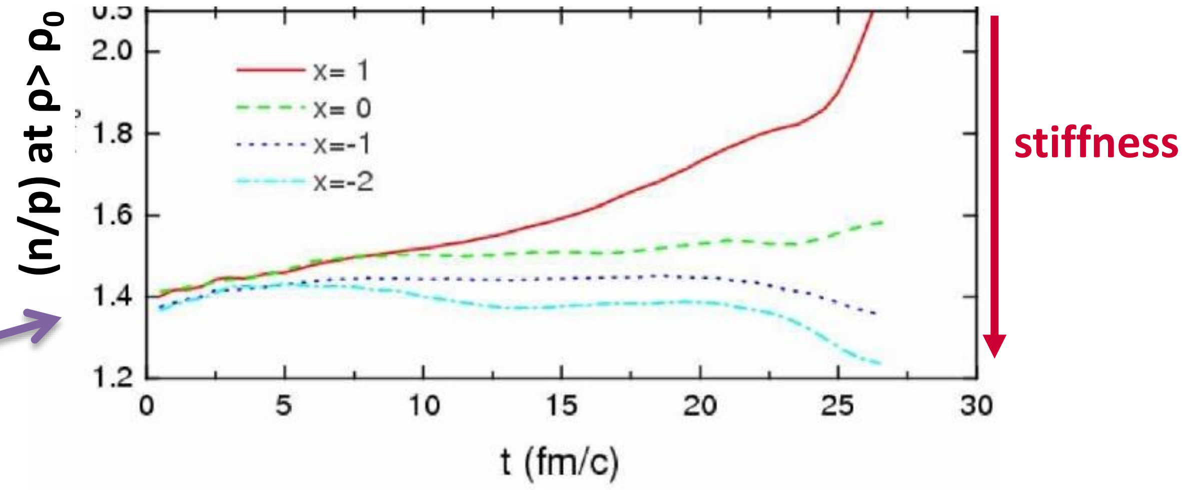

Bao-An Li, NPA 708 (2002)

High density symmetry energy in relativistic heavy ion collisions

Which densities can be explored in the early stage of the reaction ?

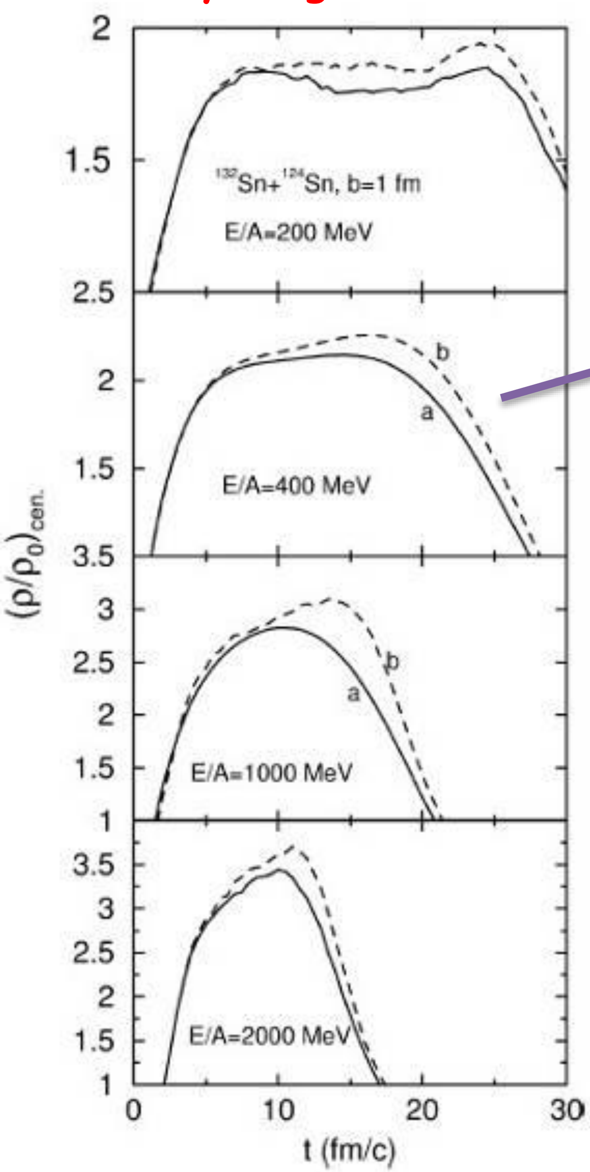

Bao-An Li, NPA 708 (2002)

B.A. Li et al., PRC71 (2005)

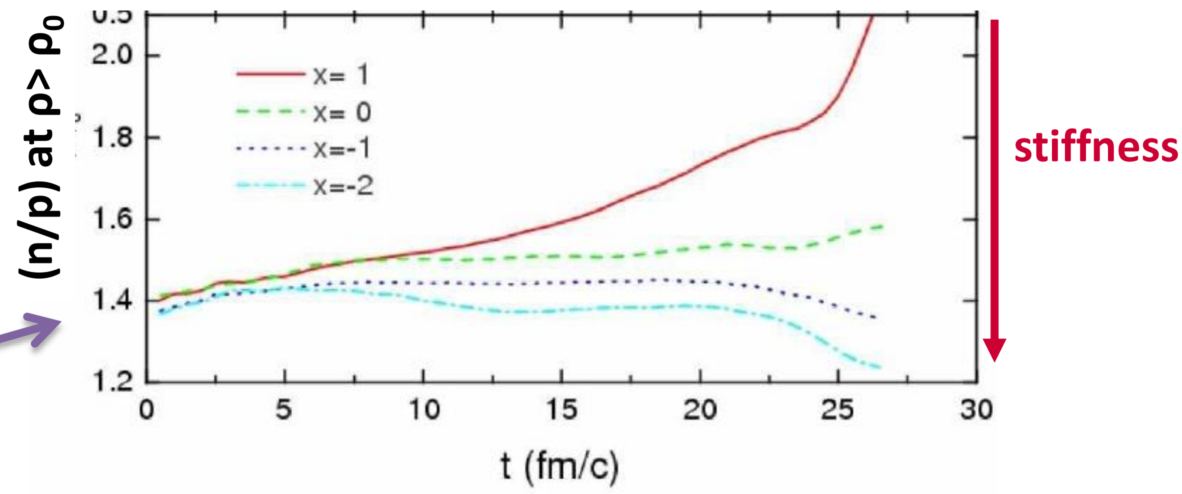

- N/Z of high density regions sensitive to $E_{sym}(\rho)$
- High $\rho > \rho_0$: asy-stiff more repulsive on neutrons

High density symmetry energy in relativistic heavy ion collisions

Which densities can be explored in the early stage of the reaction ?

B.A. Li et al., PRC71 (2005)

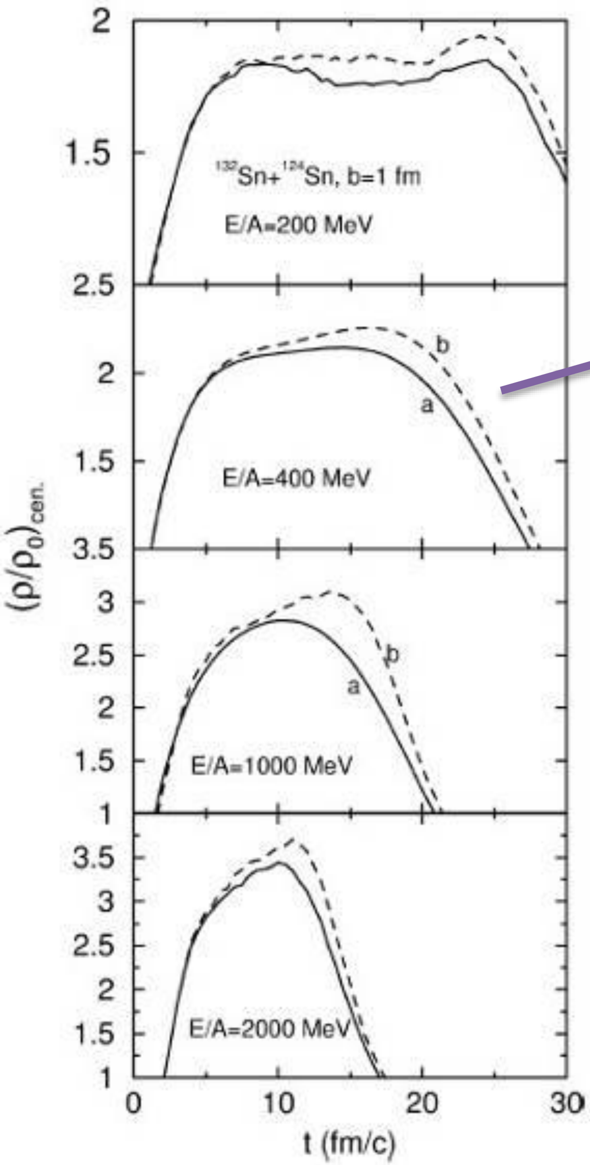

Bao-An Li, NPA 708 (2002)

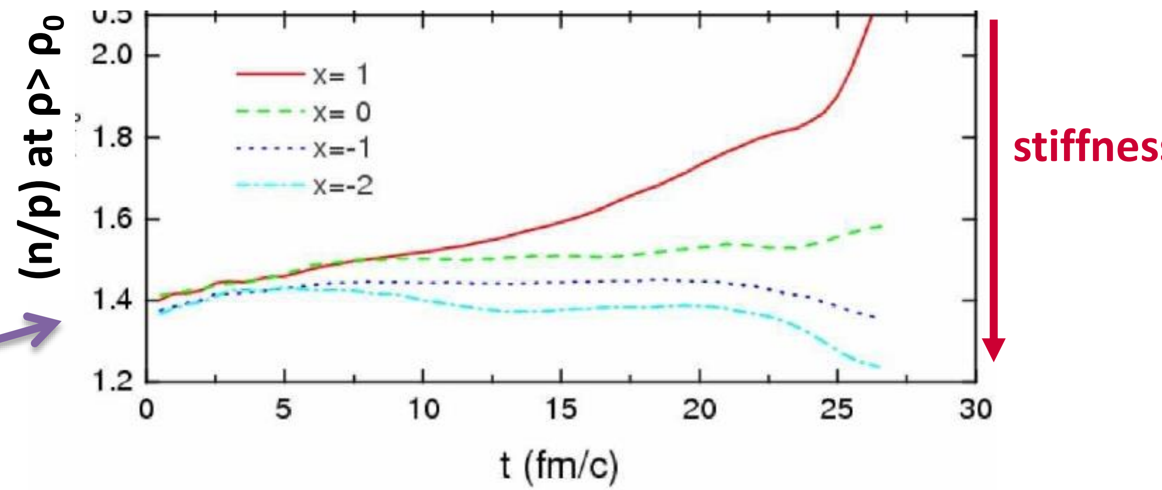

- N/Z of high density regions sensitive to $E_{sym}(\rho)$
- High $\rho > \rho_0$: asy-stiff more repulsive on neutrons

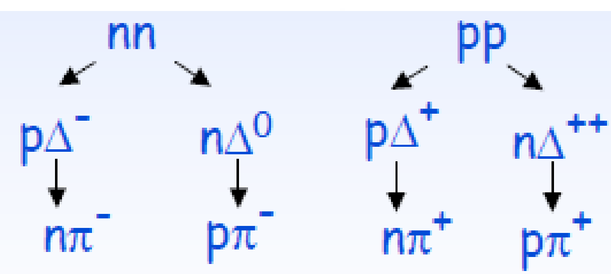

NN collisions in high density regions

π^-/π^+ reflecting the $(N/Z)_{dense}$

π^-/π^+ sensitive to $E_{sym}(\rho)$ at high ρ

High density symmetry energy in relativistic heavy ion collisions

Which densities can be explored in the early stage of the reaction ?

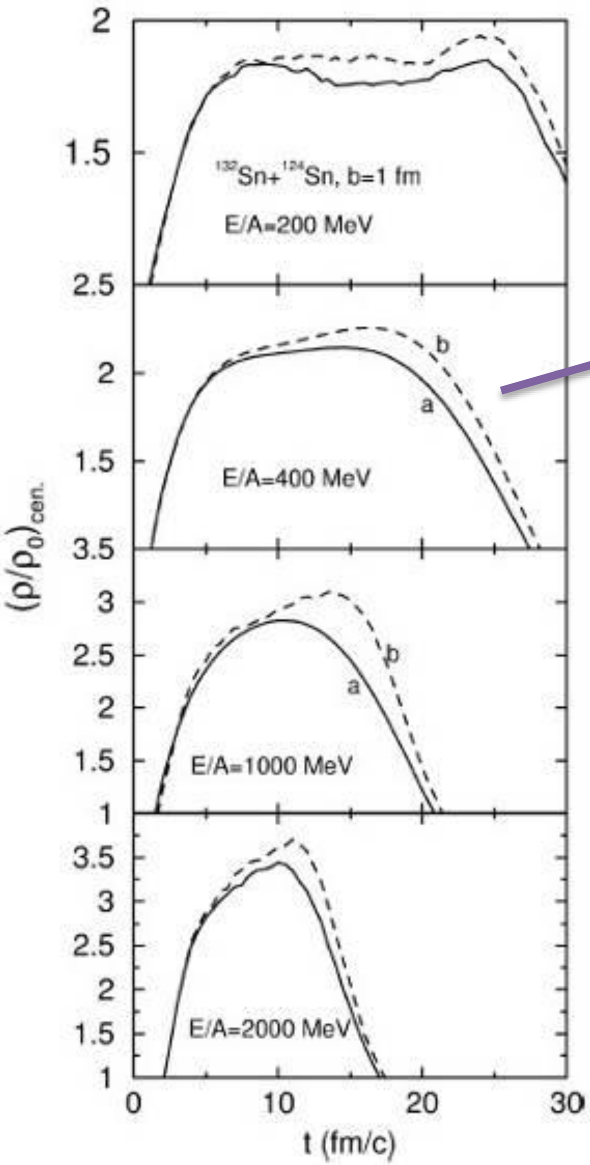

Bao-An Li, NPA 708 (2002)

B.A. Li et al., PRC71 (2005)

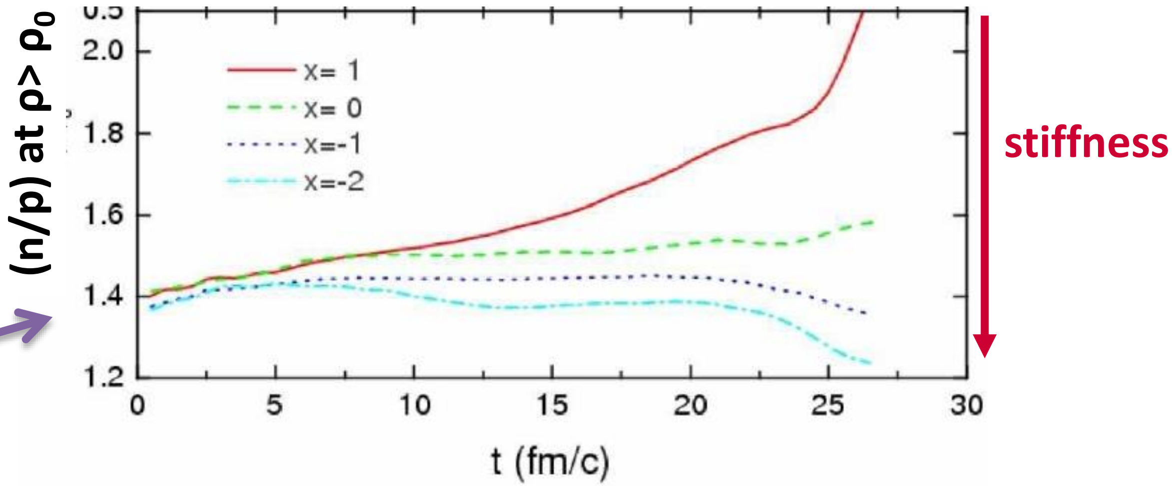

- N/Z of high density regions sensitive to $E_{sym}(\rho)$
- High $\rho>\rho_0$: asy-stiff more repulsive on neutrons

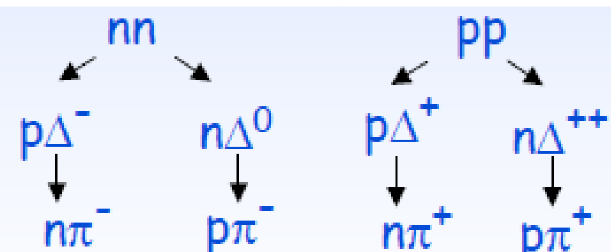

NN collisions in high density regions

$\pi-/\pi+$ reflecting the $(N/Z)_{dense}$

$\pi-/\pi+$ sensitive to $E_{sym}(\rho)$ at high ρ

But results are strongly model dependent (up to now) !

Esym at high density: pions yield

Z. Xiao et al., PRL 102 (09)

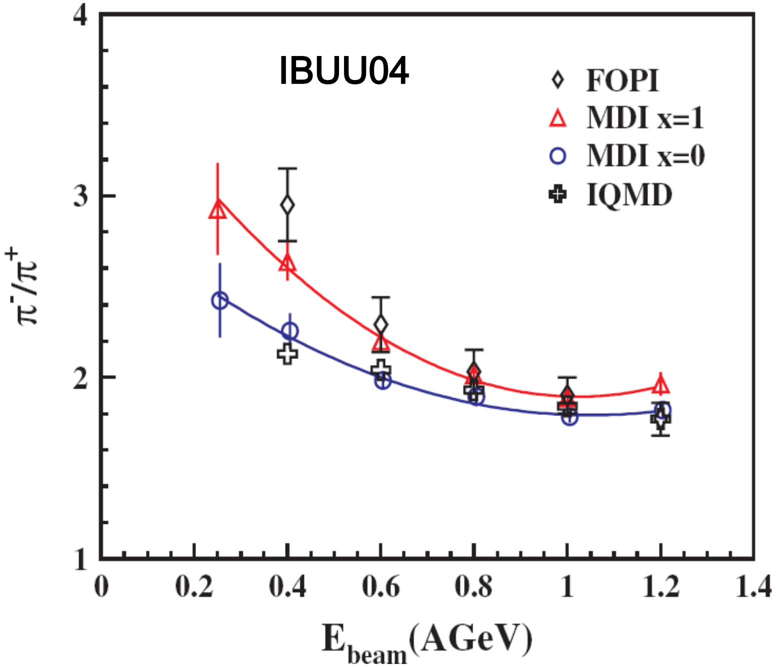

Ferini, et al., NPA 762 (2005)

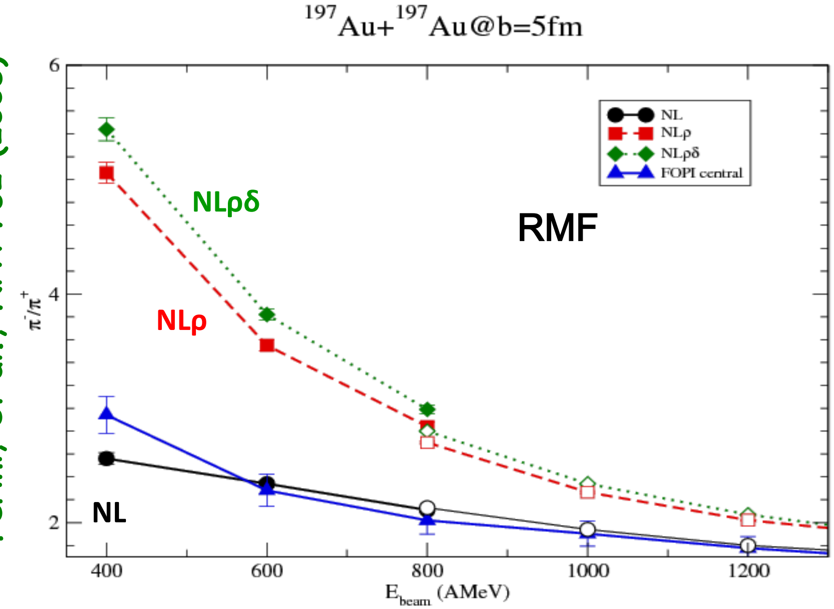

Z.Q. Feng, PLB 683 (2010)

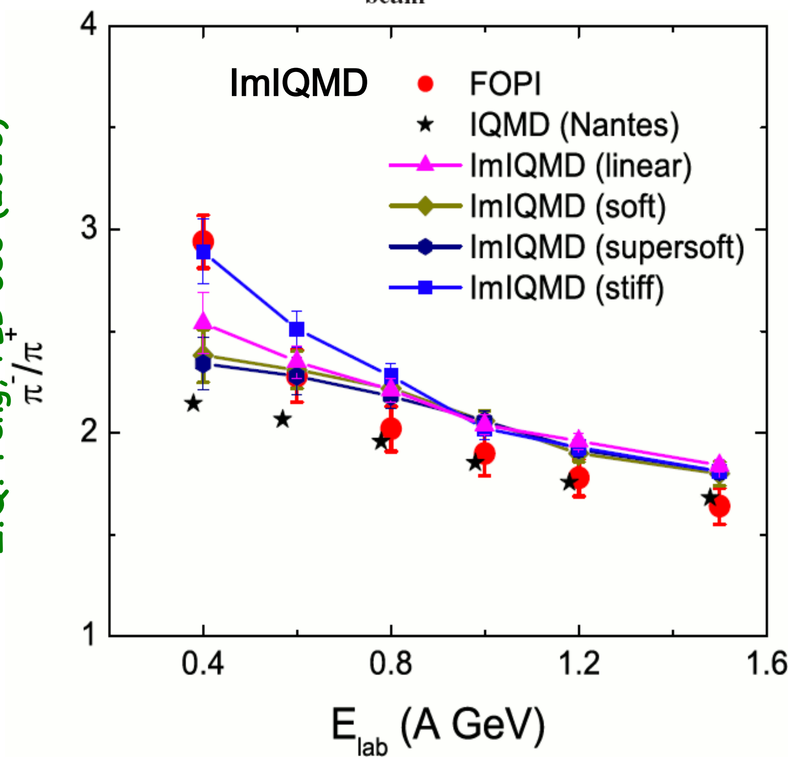

W.J. Xie , at al., PLB 718 (2013)

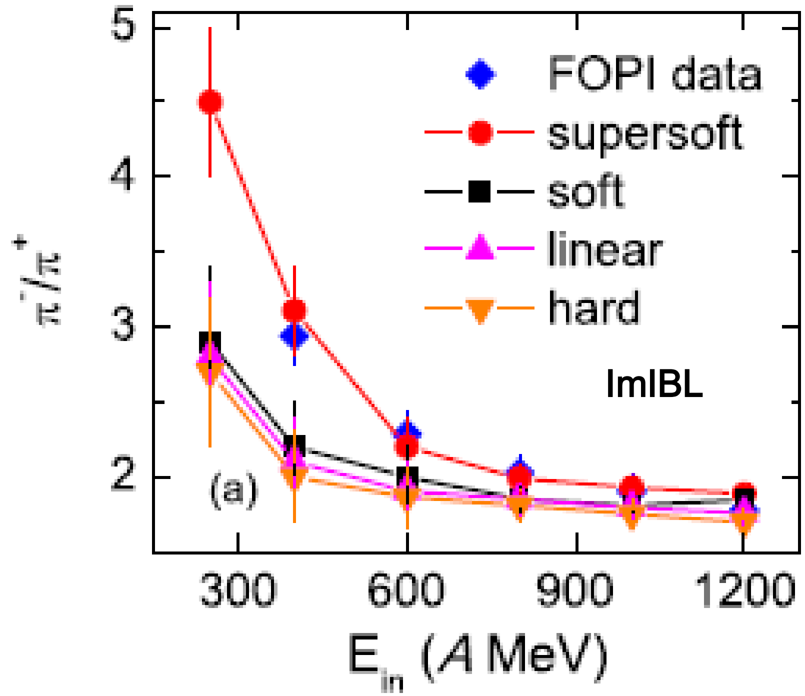

Esym at high density: pions yield

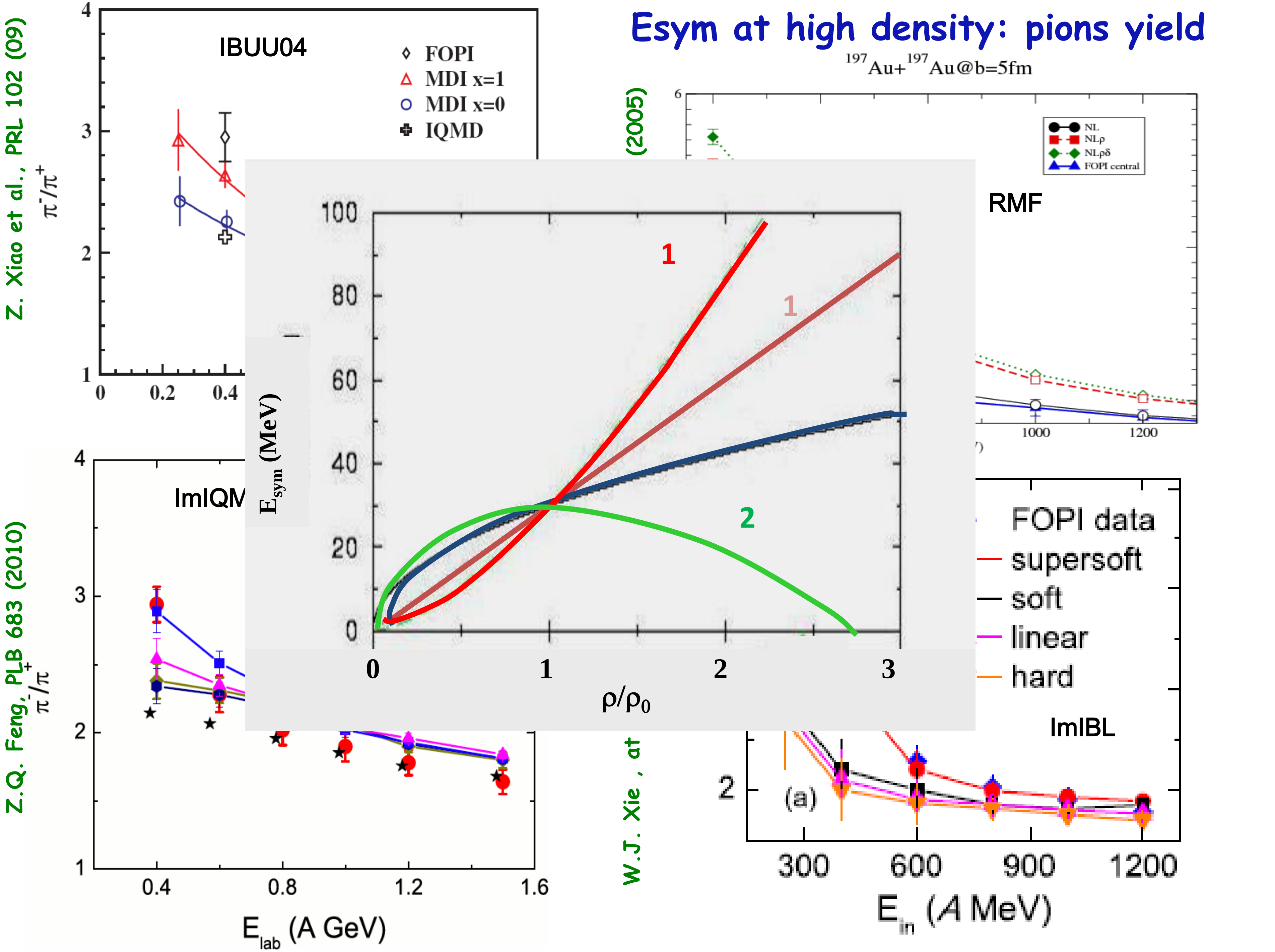

UrQMD prediction for pions

$^{197}Au+^{197}Au$ @ 400, 600, 800, 1000,1500 AMeV

$^{132}Sn+^{124}Sn$ @ 400, 600, 800 AMeV

$^{106}Sn+^{112}Sn$ @ 400, 600, 800 AMeV

for $b/b_{red}<0.53$

Pions yield ratio

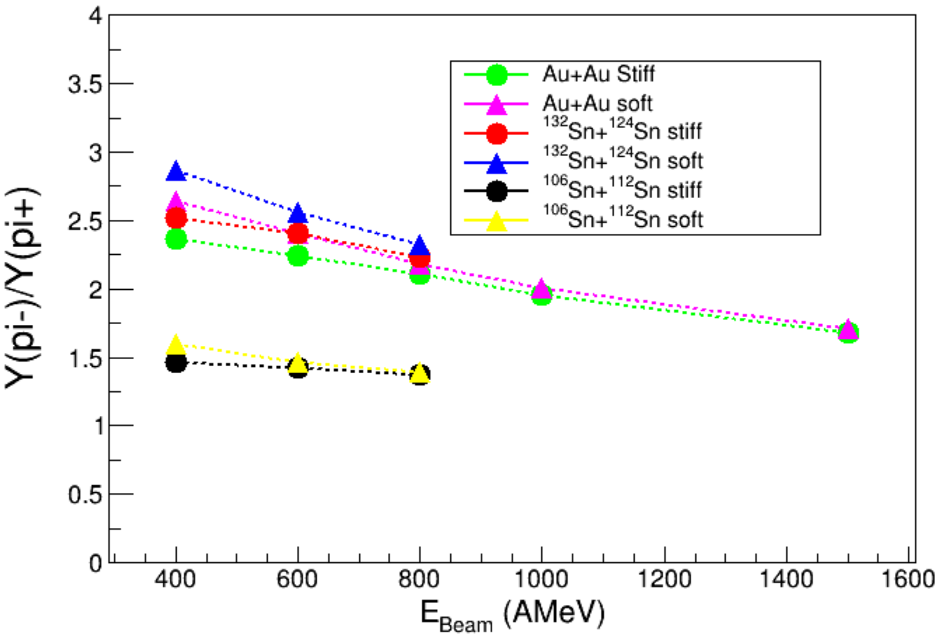

Sensitivity

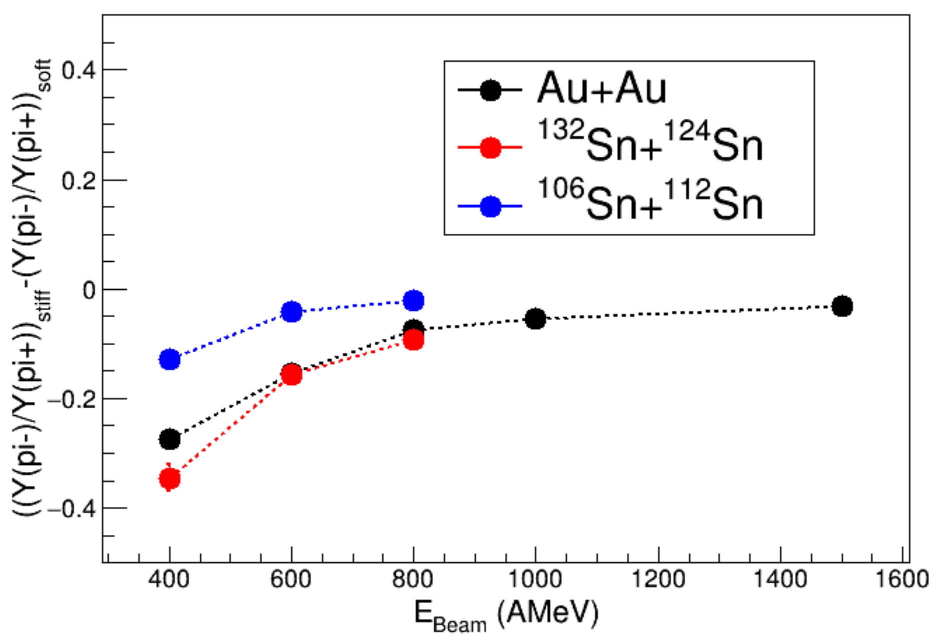

..but
no sensitivity to E_{Sym} in yields ratio as a function of p_t or E_{kin}^{cm} in (this version) of UrQMD

Can NeuLAND measure pi+ and pi-?

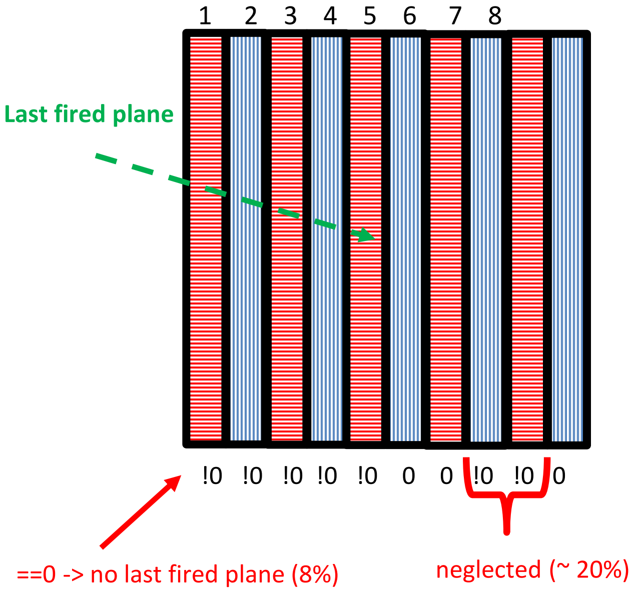

Analysis on sum of QDC signals in the planes

Protons

pi+

pi-

Can NeuLAND measure pi+ and pi-?

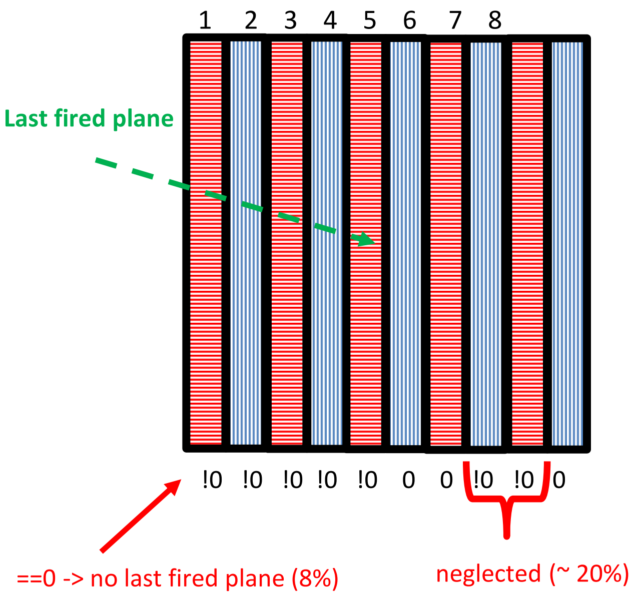

Analysis on sum of QDC signals in the planes

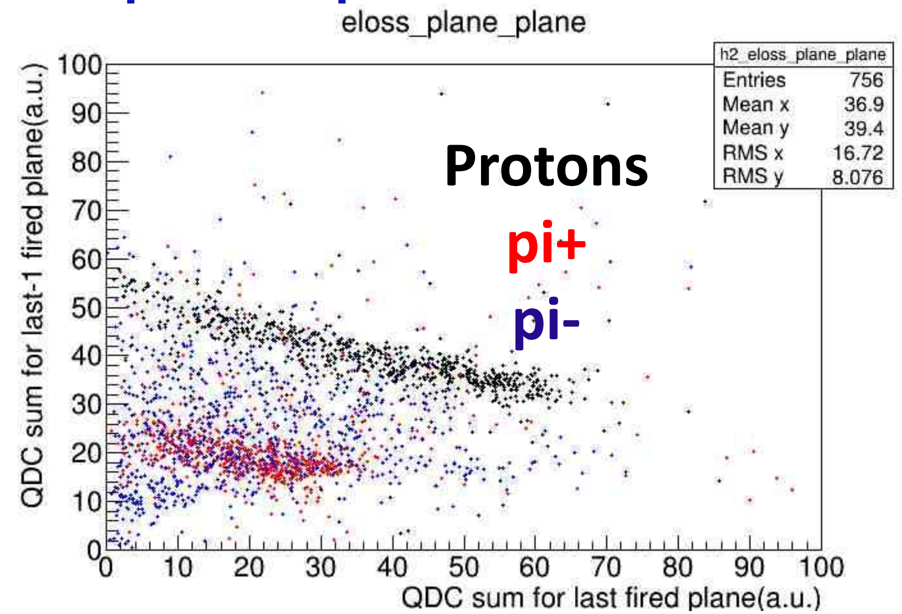

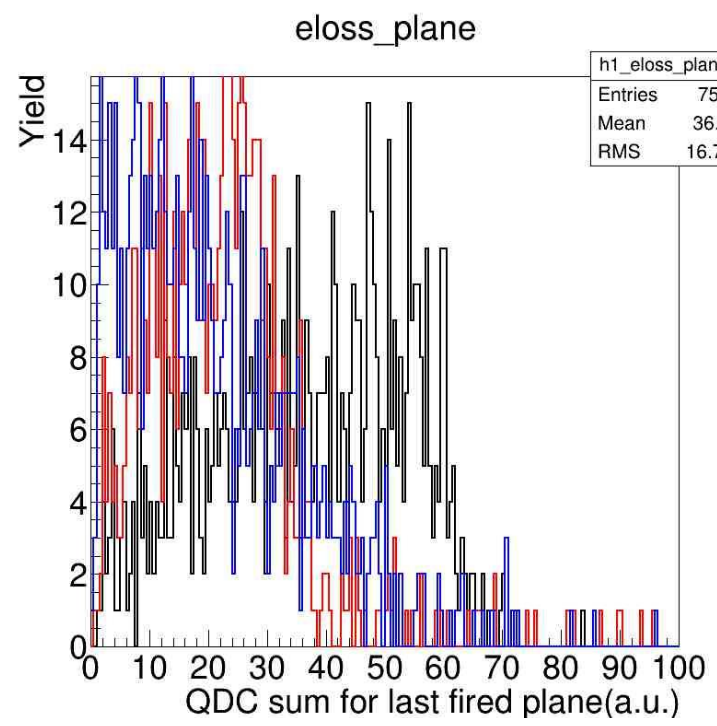

Can NeuLAND measure pi+ and pi-?

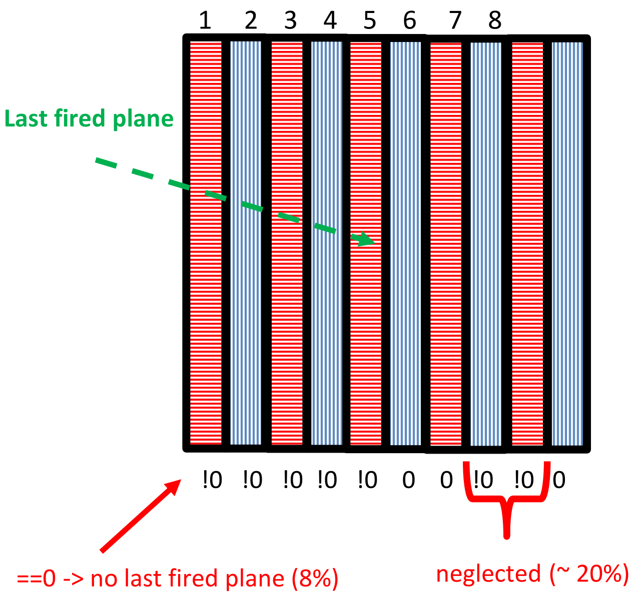

Analysis on sum of QDC signals in the planes

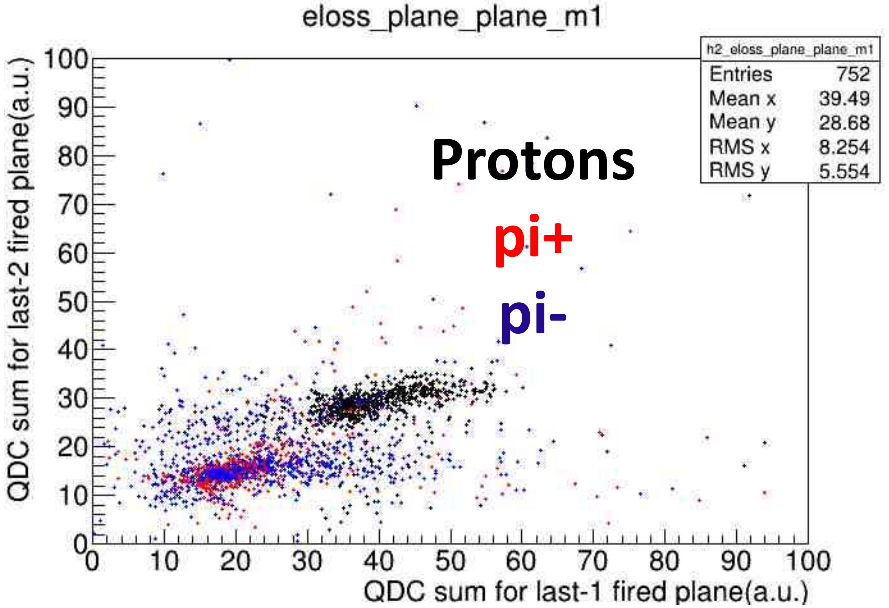

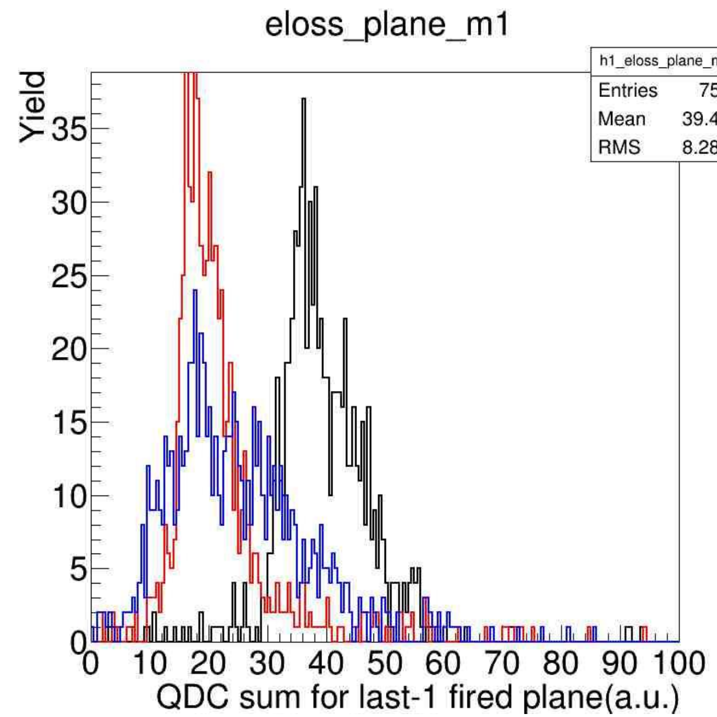

Can NeuLAND measure pi+ and pi-?

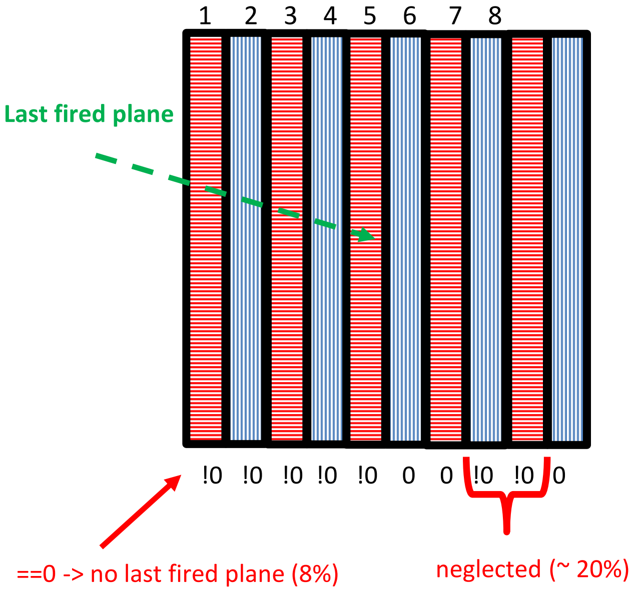

Analysis on sum of QDC signals in the planes

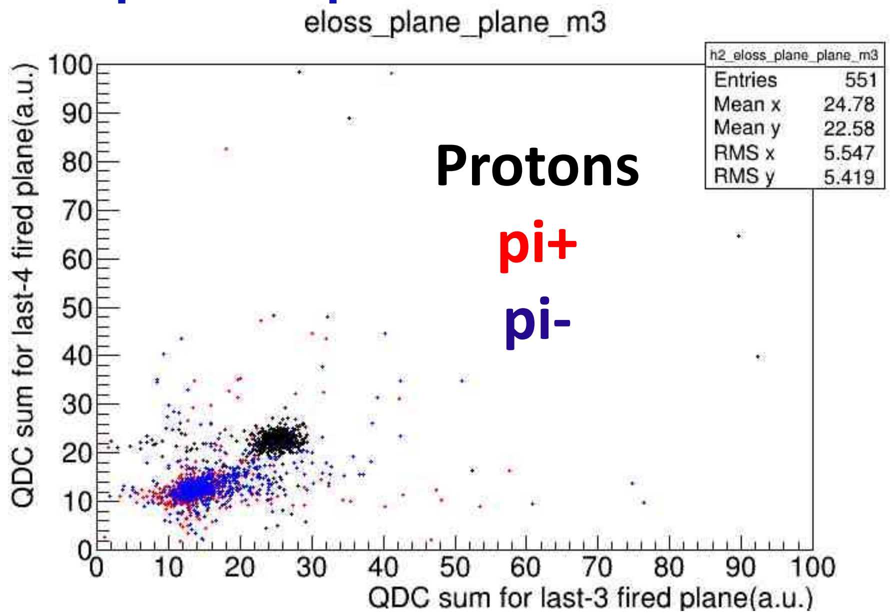

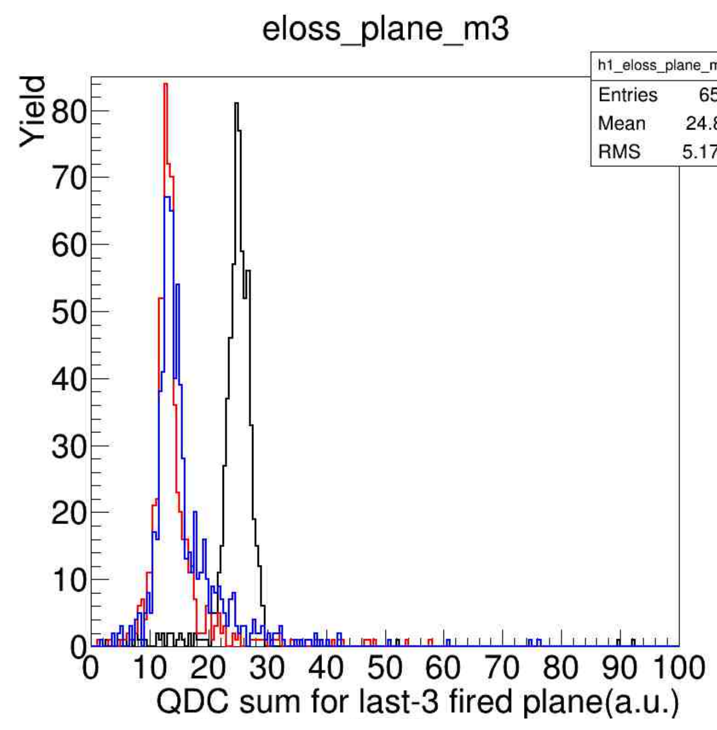

Can NeuLAND measure pi+ and pi-?

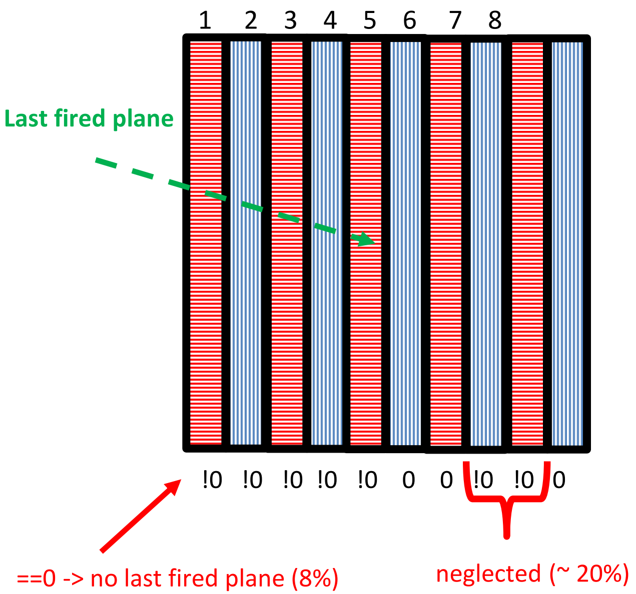

Analysis on sum of QDC signals in the planes

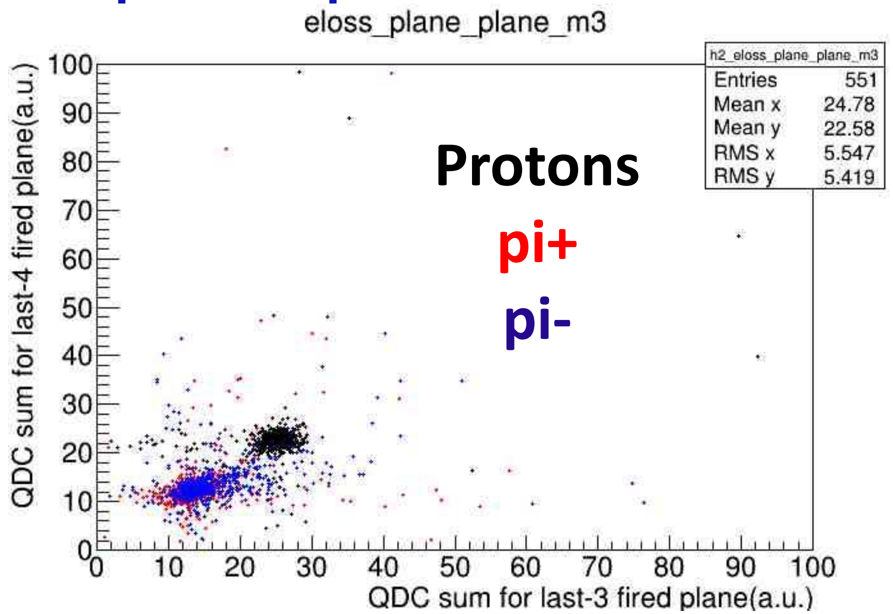

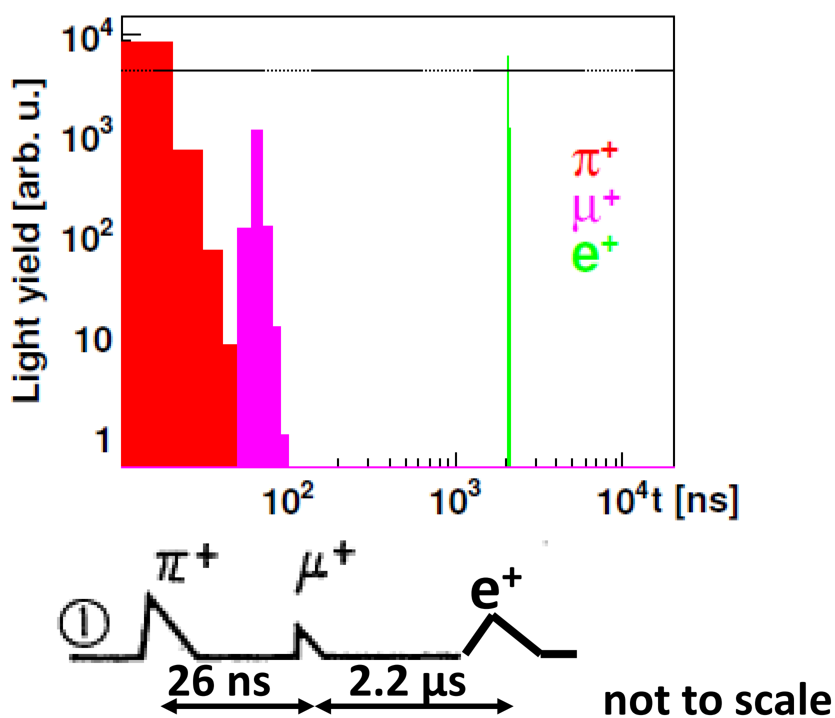

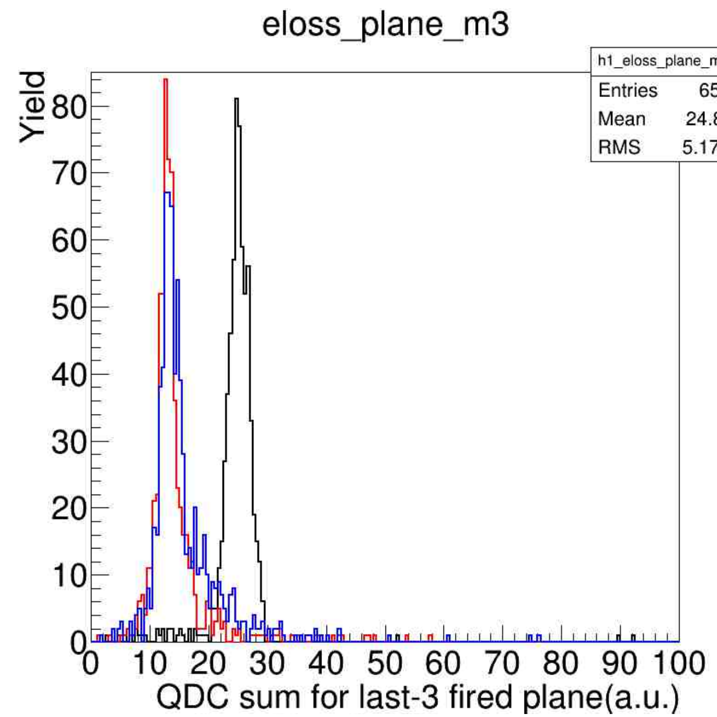

Can NeuLAND measure pi+ and pi-?

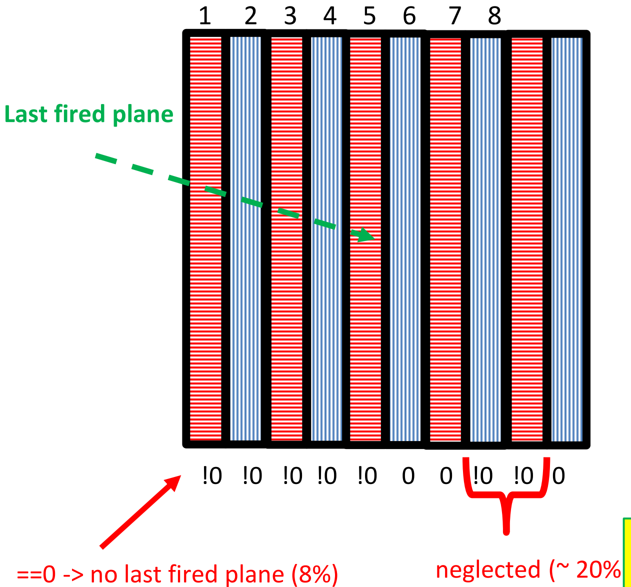

Analysis on sum of QDC signals in the planes

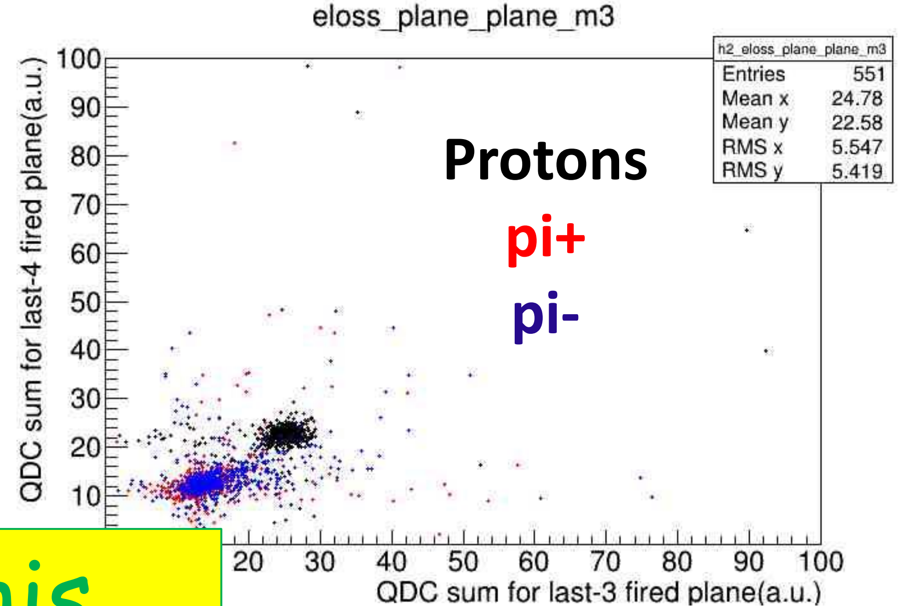

Is this feasible?

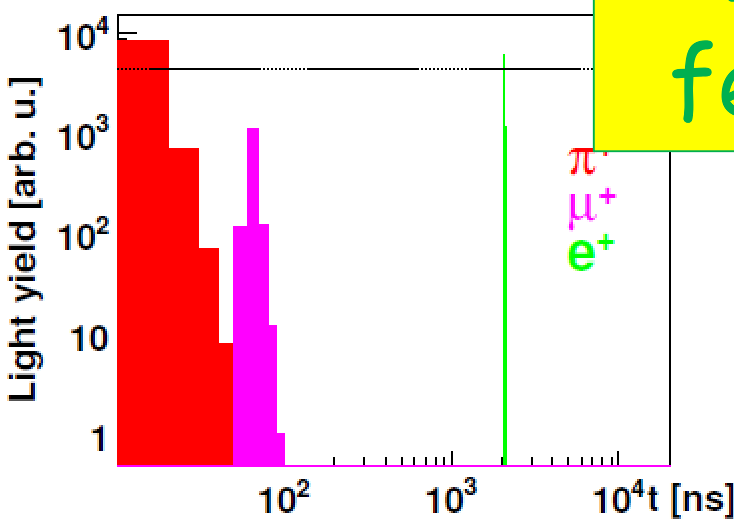

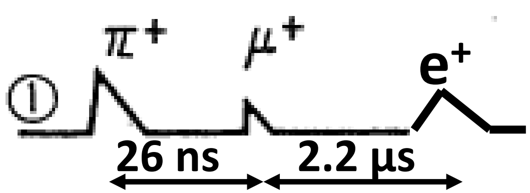

not to scale

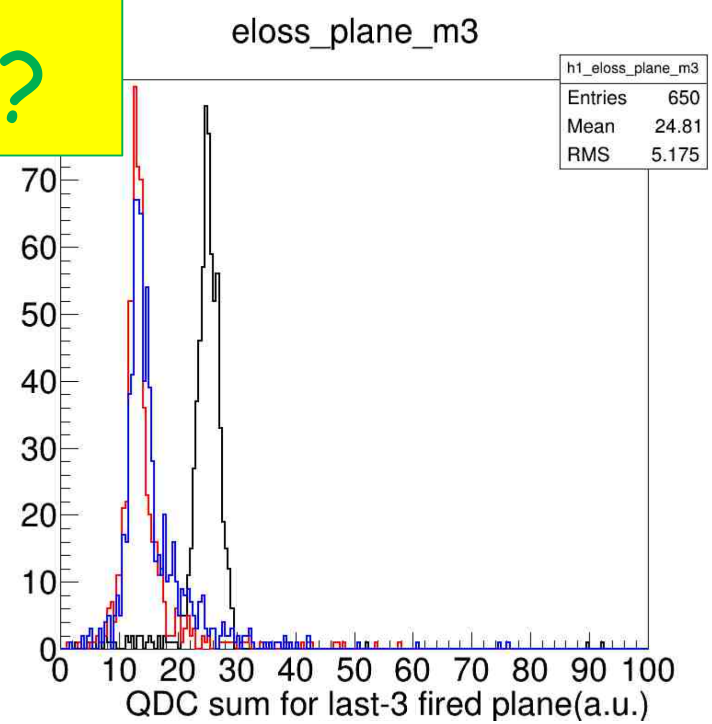

PHYSICAL REVIEW C **95**, 044614 (2017)

Pion production in rare-isotope collisions

M. B. Tsang,[1,2] J. Estee,[1,2] H. Setiawan,[1,2] W. G. Lynch,[1,2] J. Barney,[1,2] M. B. Chen,[2] G. Cerizza,[1] P. Danielewicz,[1,2] J. Hong,[1,2] P. Morfouace,[1] R. Shane,[1] S. Tangwancharoen,[1,2] K. Zhu,[1,2] T. Isobe,[3] M. Kurata-Nishimura,[3] J. Lukasik,[4] T. Murakami,[5] Z. Chajecki,[6] and SπRIT Collaboration

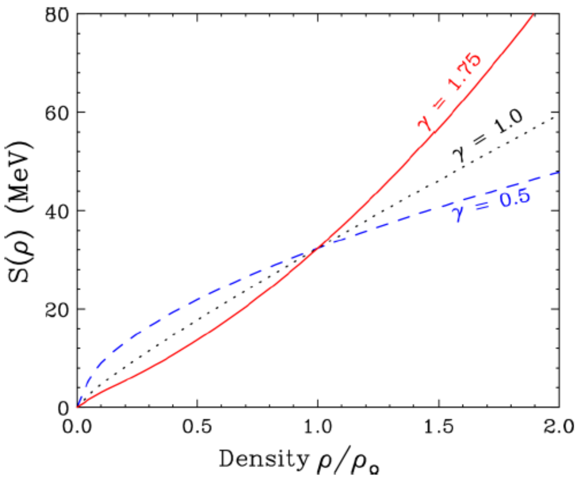

FIG. 1. The density dependence of the symmetry energy is shown for three different values of the parameter γ of Eq. (2) that controls the density dependence of the potential-energy component of the symmetry energy.

$$S(\rho) = S_{\text{kin}}\left(\frac{\rho}{\rho_0}\right)^{2/3} + S_{\text{int}}\left(\frac{\rho}{\rho_0}\right)^{\gamma},$$

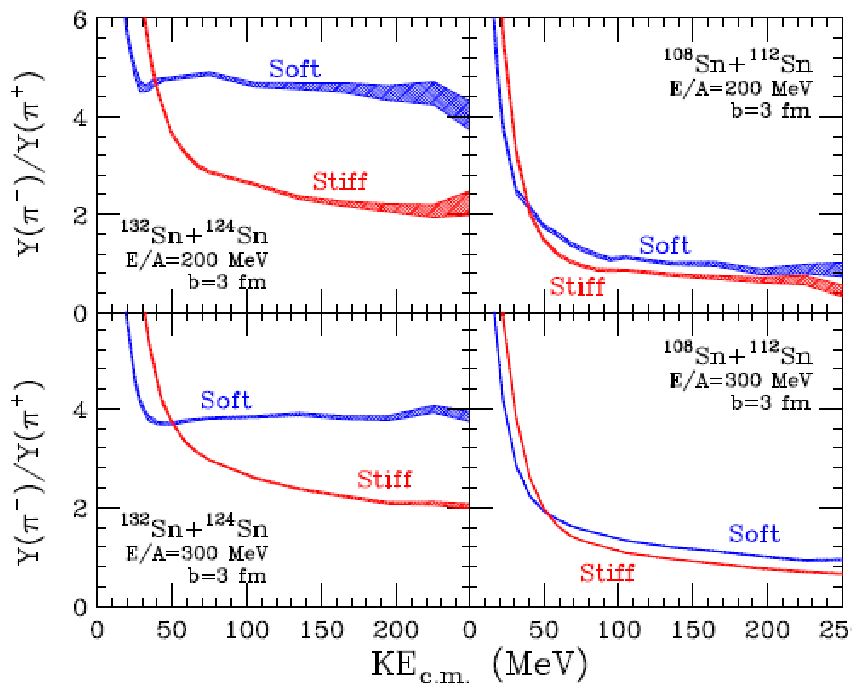

FIG. 4. Comparison of π^-/π^+ spectral ratios from central ($b =$ 3 fm) collisions of ^{132}Sn + ^{124}Sn (left panels) and ^{108}Sn + ^{112}Sn (right panels) reactions at the incident beam energies of 200 MeV (upper panels) and 300 MeV (lower panels) per nucleon. Calculations for both soft ($\gamma = 0.5$) and stiff ($\gamma = 1.75$) symmetry energies are shown.

PHYSICAL REVIEW C **95**, 044614 (2017)

Pion production in rare-isotope collisions

M. B. Tsang,[1,2] J. Estee,[1,2] H. Setiawan,[1,2] W. G. Lynch,[1,2] J. Barney,[1,2] M. B. Chen,[2] G. Cerizza,[1] P. Danielewicz,[1,2] J. Hong,[1,2] P. Morfouace,[1] R. Shane,[1] S. Tangwancharoen,[1,2] K. Zhu,[1,2] T. Isobe,[3] M. Kurata-Nishimura,[3] J. Lukasik,[4] T. Murakami,[5] Z. Chajecki,[6] and SπRIT Collaboration

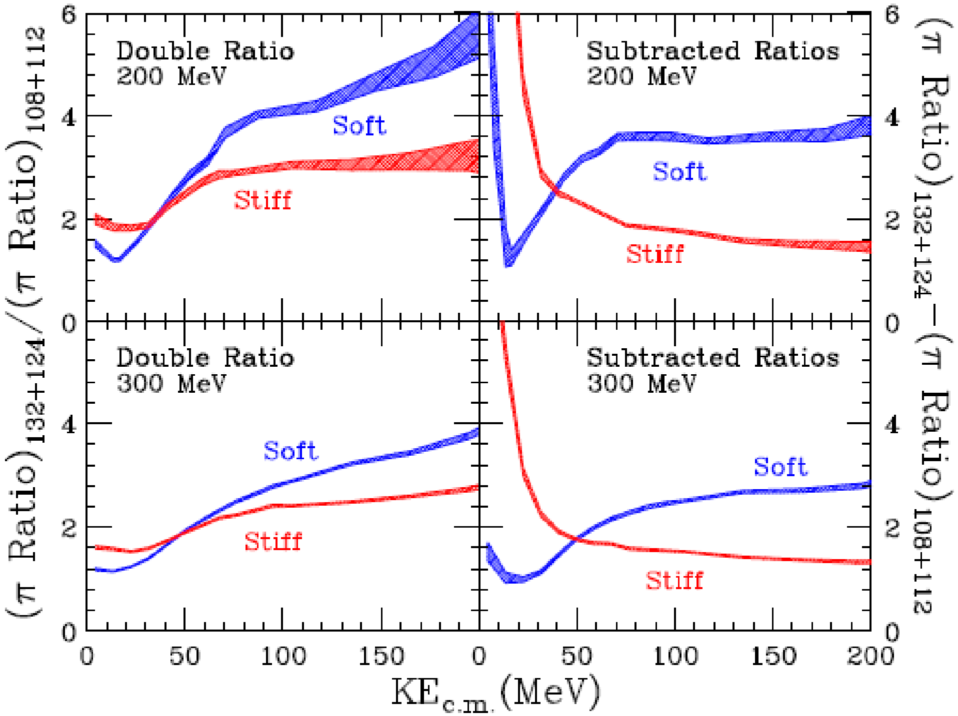

FIG. 5. Double ratios (left panels) and difference (right panels) of π^-/π^+ spectral ratios from central ($b = 3$ fm) collisions of ^{132}Sn + ^{124}Sn and ^{108}Sn + ^{112}Sn reactions at the incident beam energies of 200 MeV (upper panels) and 300 MeV (lower panels) per nucleon. Calculations for both soft ($\gamma = 0.5$) and stiff ($\gamma = 1.75$) symmetry energies are shown.

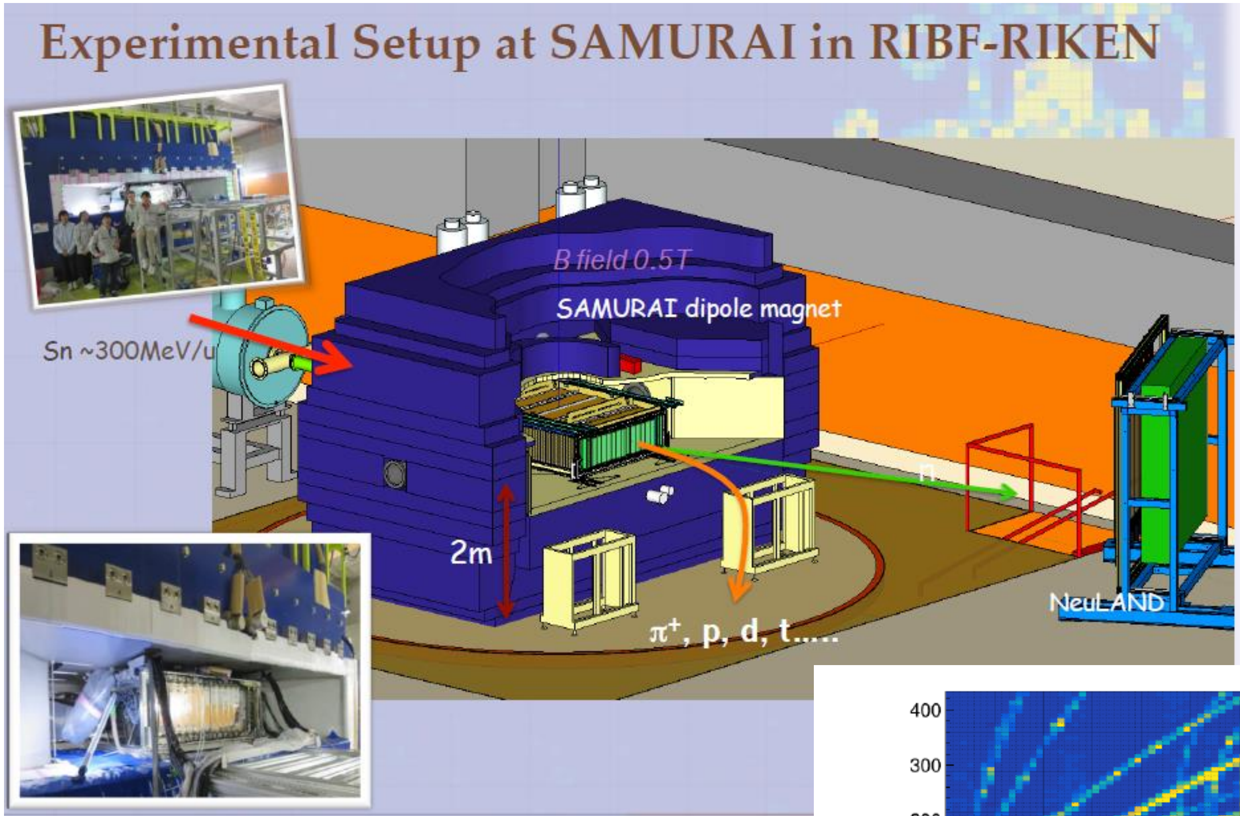

Transport 2017 MSU
Mizuki Nishimura

132Sn + 124Sn
108Sn + 112Sn
124Sn + 112Sn
112Sn + 124Sn ~300 MeV/u

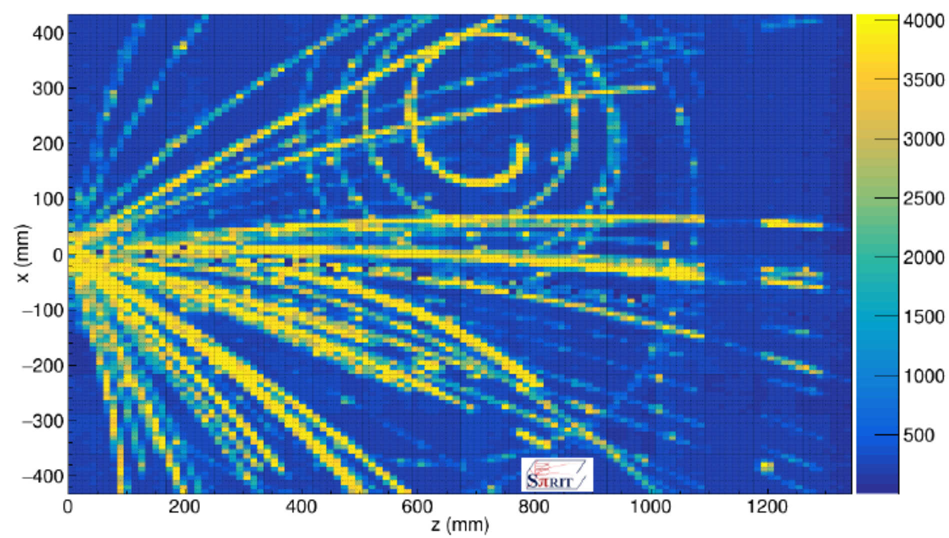

Figure 13: (Color online) Single event recorded with the SπRIT TPC following the reaction of a ^{132}Sn beam accelerated to 270 MeV/u on a solid ^{124}Sn target located at the entrance to the detector ($x = 0$, $z = 0$). Several light ions are produced whose trajectories are slightly curved in the magnetic field. In this event, a pion was also produced as evidenced by the spiral trajectory in the upper half of the figure.

Nuclear symmetry energy probed by the π^-/π^+ ratio

Gao-Chan Yong[1], Yuan Gao[2], Gao-Feng Wei[3], and Wei Zuo[1,4]
[1] *Institute of Modern Physics, Chinese Academy of Sciences, Lanzhou 730000, China*
[2] *School of Information Engineering, Hangzhou Dianzi University, Hangzhou 310018, China*
[3] *Shanxi Key Laboratory of Surface Engineering and Remanufacturing, School of Mechanical and Material Engineering, Xi'an University, Xi'an 710065, China*
[4] *University of Chinese Academy of Sciences, Beijing 100049, China*

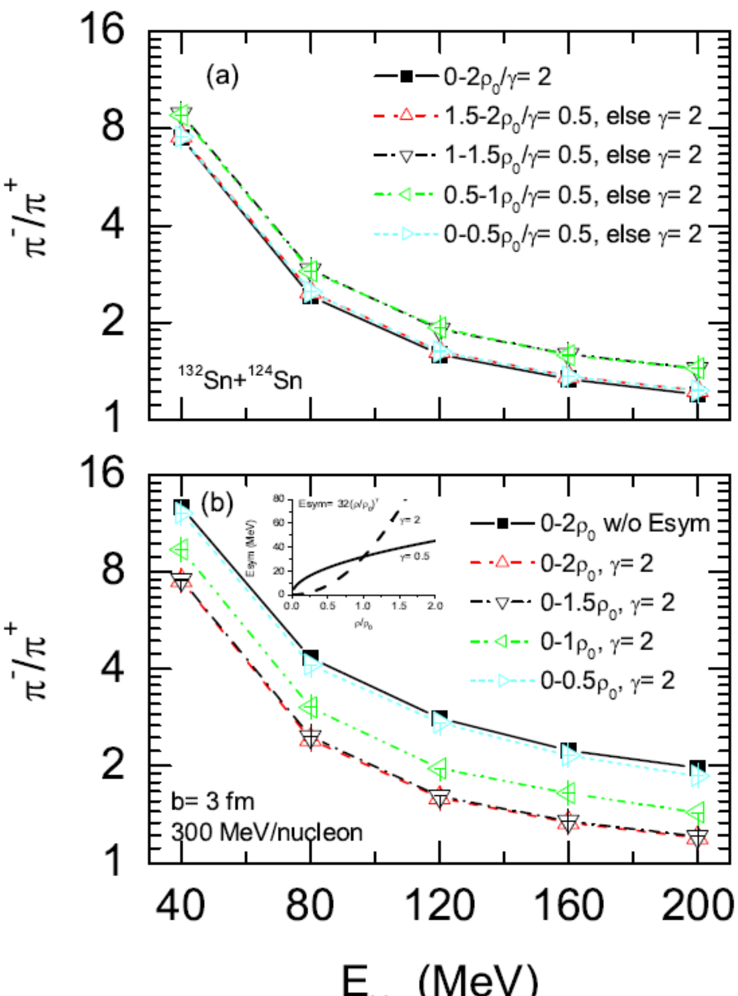

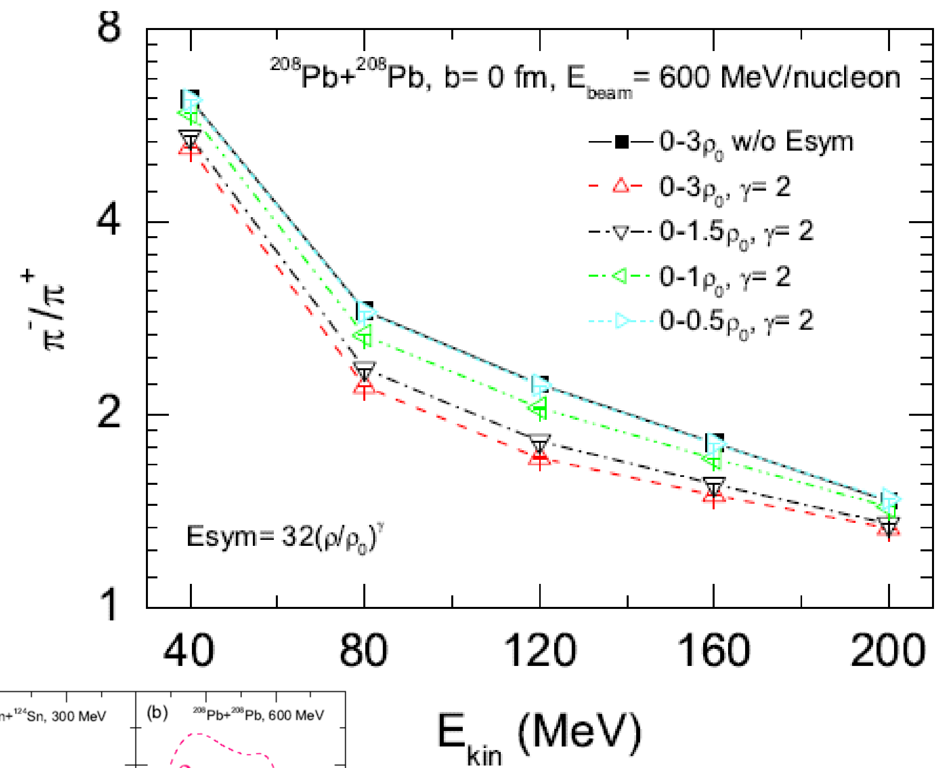

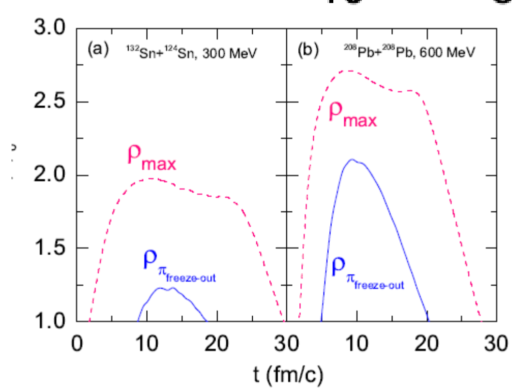

arXiv:1704.05166 [nucl-th]

Difference between $^{132}Sn + ^{124}Sn$ and $^{108}Sn + ^{112}Sn$ collisions

W.G. Lynch talk @ NuSym 2014

E/A =120 MeV

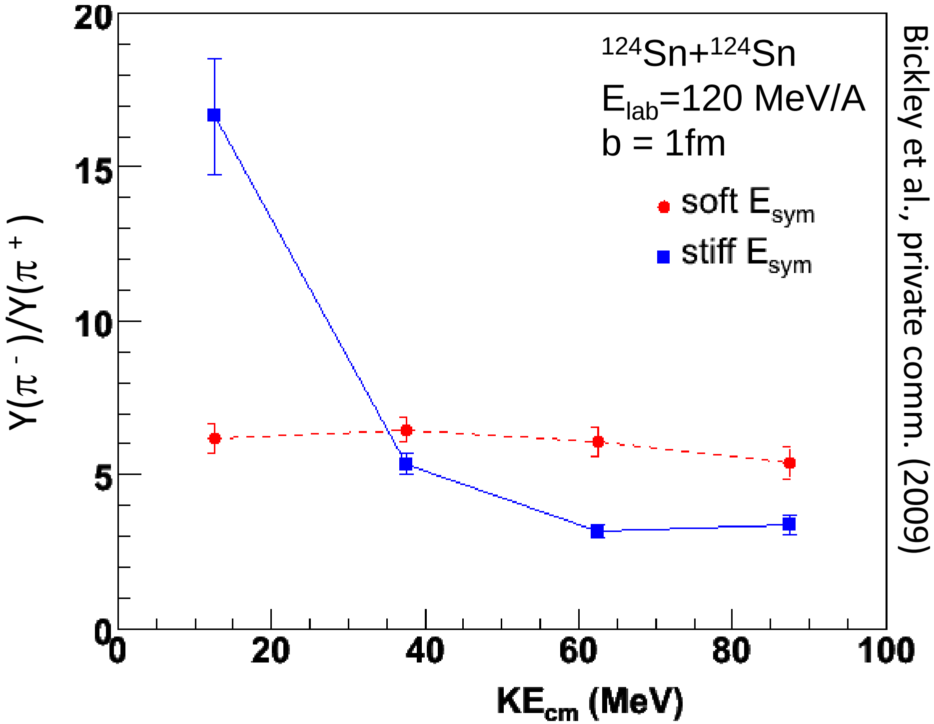

Bickley et al., private comm. (2009)

E/A = 300 MeV

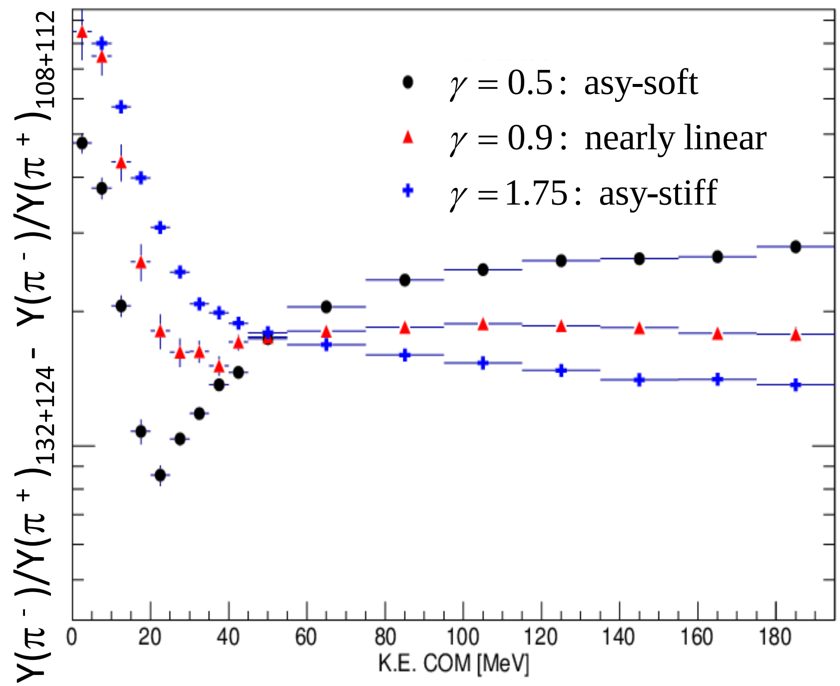

J. Hong, P. Danielewicz, private communicatons (2013)

- Pion ratio depends strongly on the symmetry energy.
- Ratios of spectra are more sensitive than ratios of integrated yields.
  - Integrated yields at E/A≥400 MeV suggest soft symmetry energy at $\rho \geq 2.5\rho_0$ (Xiao PRL, 102, 062502 (2009)
- Built two TPC's to probe these observables
  - E/A<150 MeV at MSU and E/A=200-350 MeV at RIKEN (probes $\rho \approx 2\rho_0$).

Difference between ^{132}Sn+ ^{124}Sn and ^{108}Sn+ ^{112}Sn collisions

W.G. Lynch talk @ NuSym 2014

E/A =120 MeV

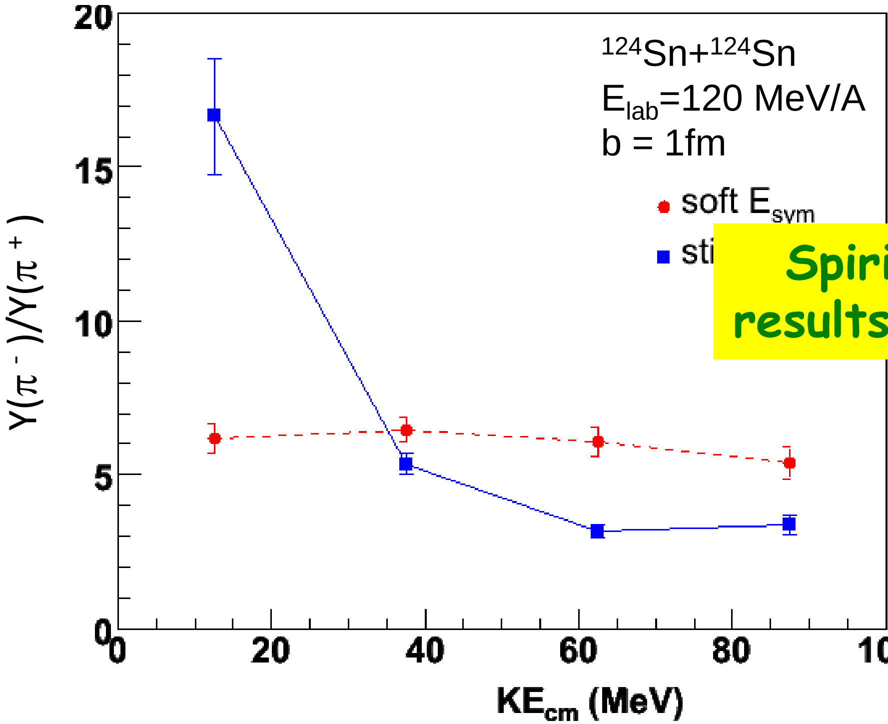

Bickley et al., ... omm. (2009)

Spirit at Riken results coming soon

E/A = 300 MeV

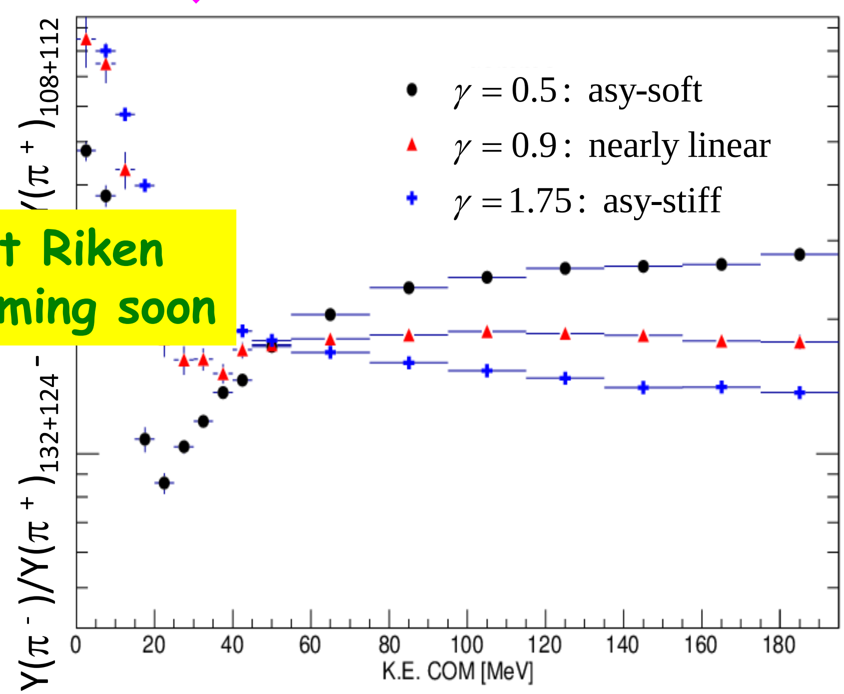

J. Hong, P. Danielewicz, private communicatons (2013)

- Pion ratio depends strongly on the symmetry energy.
- Ratios of spectra are more sensitive than ratios of integrated yields.
  - Integrated yields at E/A≥400 MeV suggest soft symmetry energy at $\rho \geq 2.5\rho_0$ (Xiao PRL, 102, 062502 (2009)
- Built two TPC's to probe these observables
  - E/A<150 MeV at MSU and E/A=200-350 MeV at RIKEN (probes $\rho \approx 2\rho_0$).

ASY-EOS S394 experiment @ GSI Darmstadt (May 2011)

Au+Au @ 400 AMeV

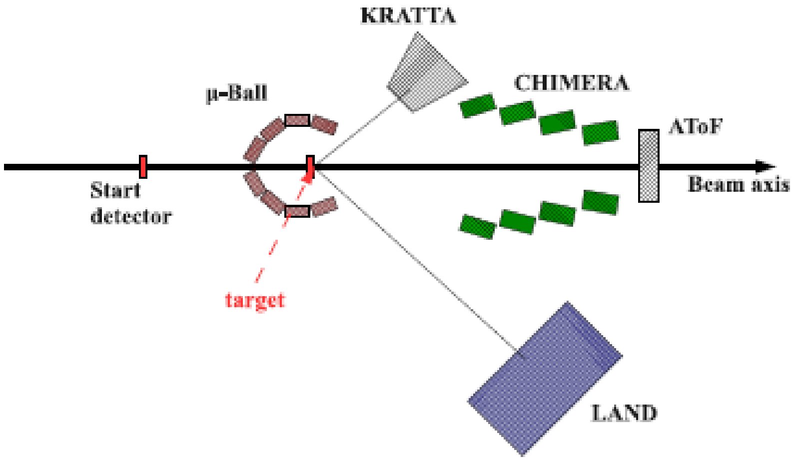

ASY-EOS S394 experiment @ GSI Darmstadt (May 2011)

Au+Au @ 400 AMeV

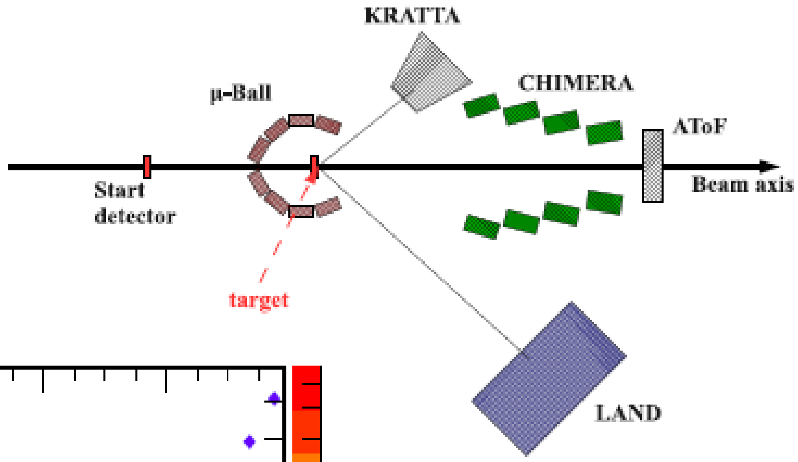

P. Russotto et al., PRC 94, 034608 (2016).

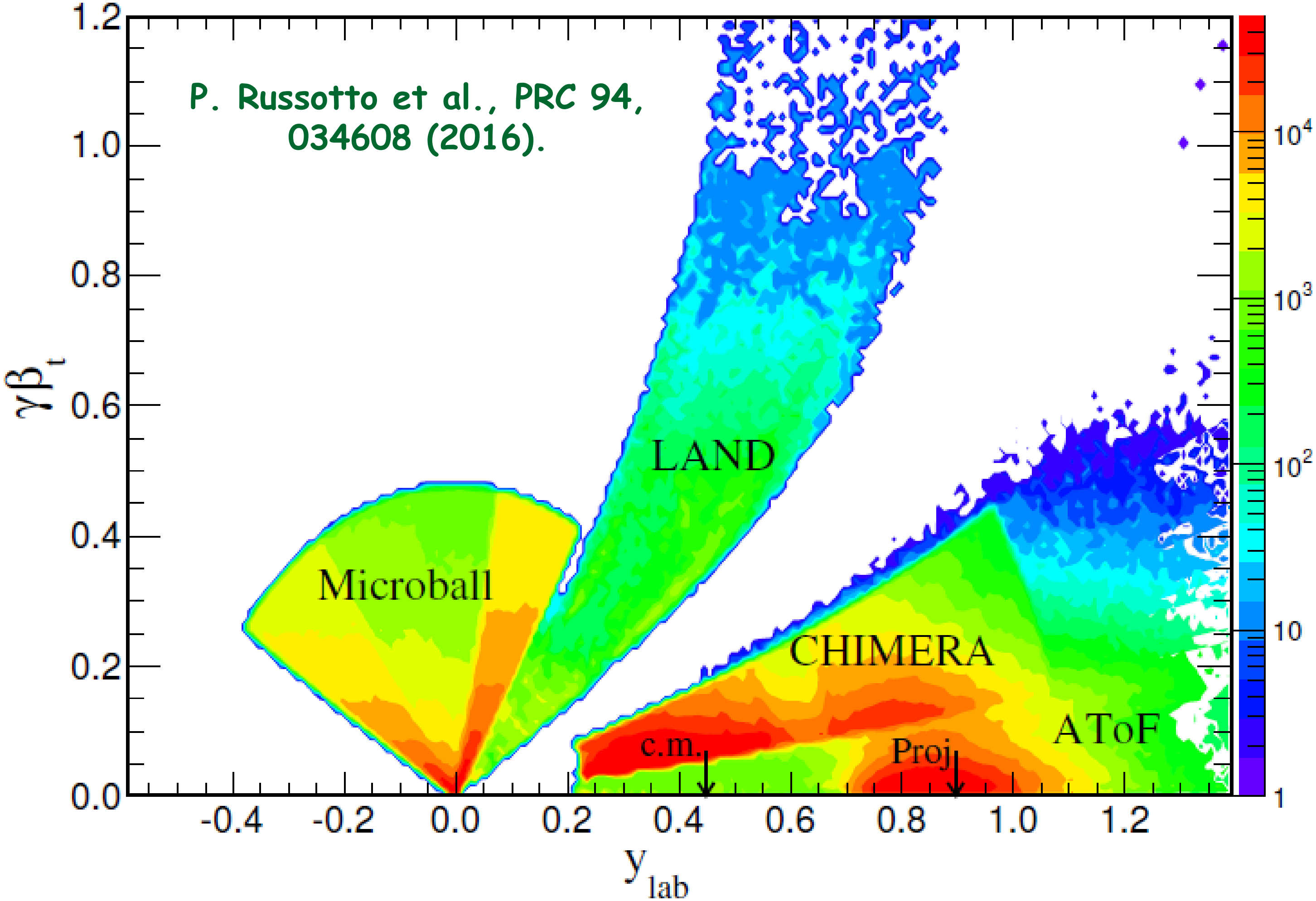

ASY-EOS S394 experiment @ GSI Darmstadt (May 2011)

Au+Au @ 400 AMeV

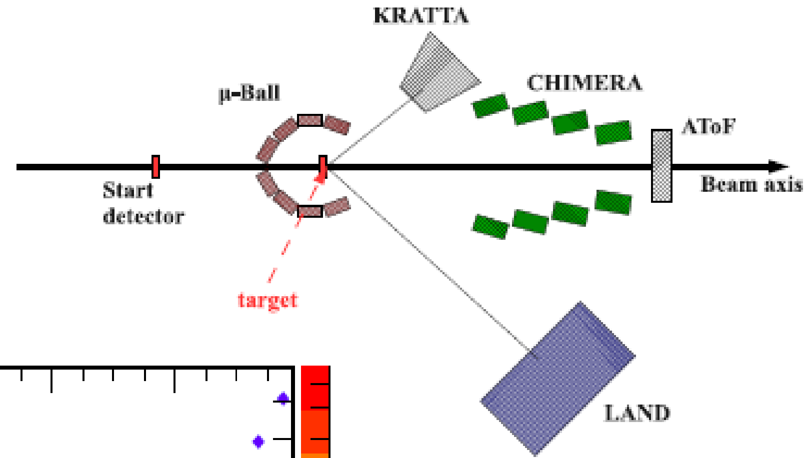

P. Russotto et al., PRC 94, 034608 (2016).

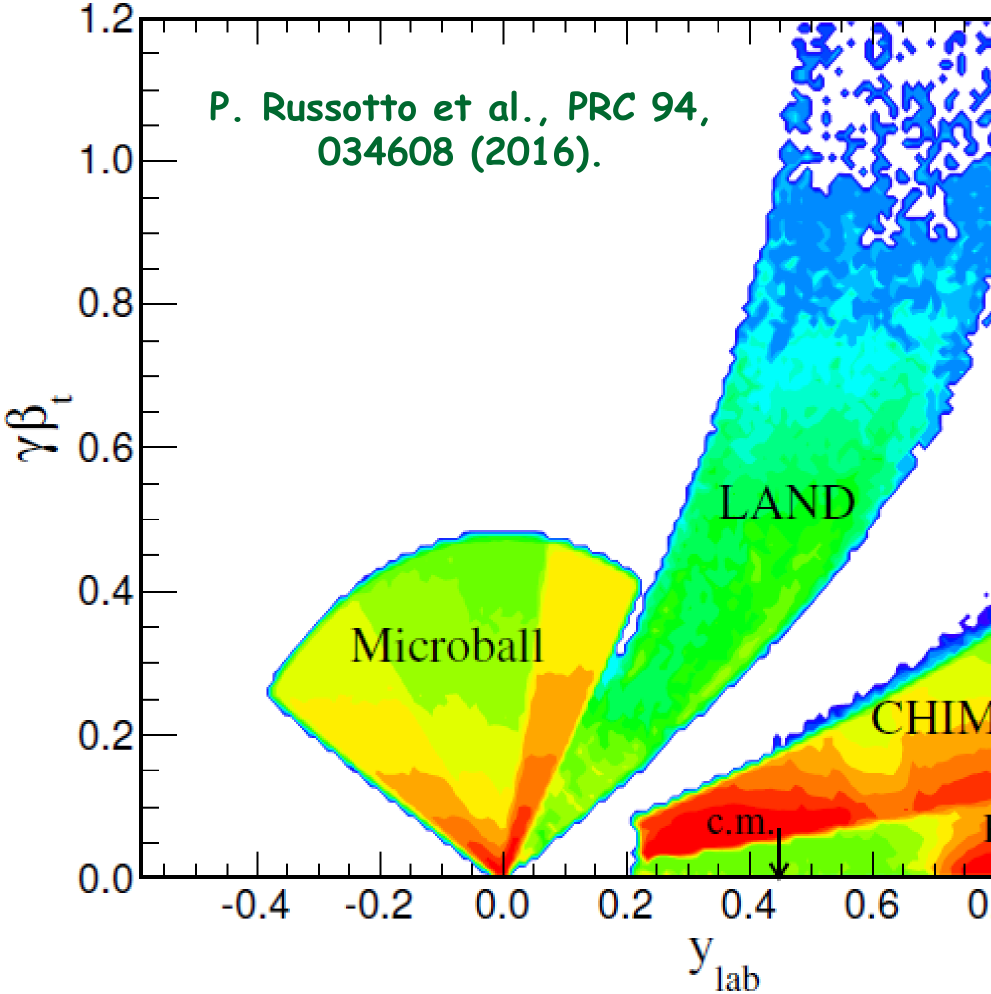

KRATTA:
J. Lukasik et al.,
Nucl. Instr. Meth.
709 (2013) 120128

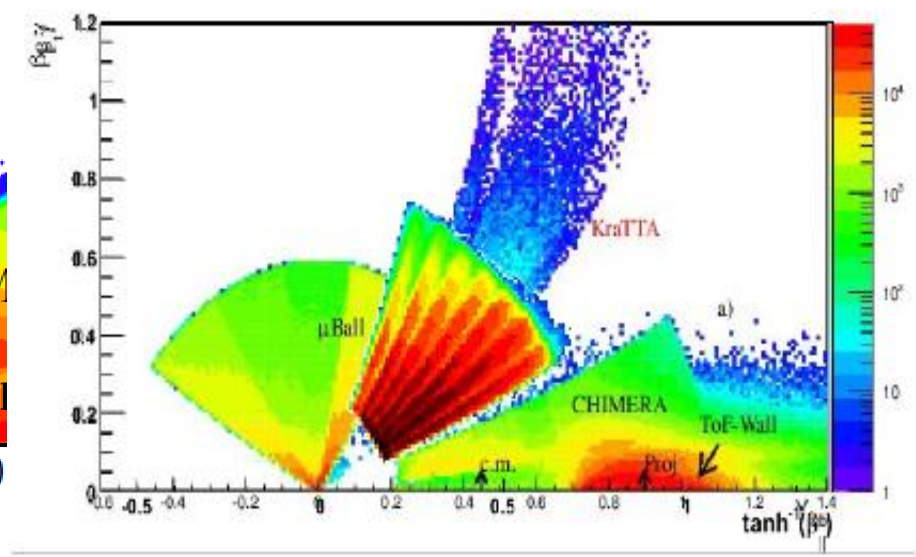

ASY-EOS II: IQMD and TuQMD predictions

IQMD

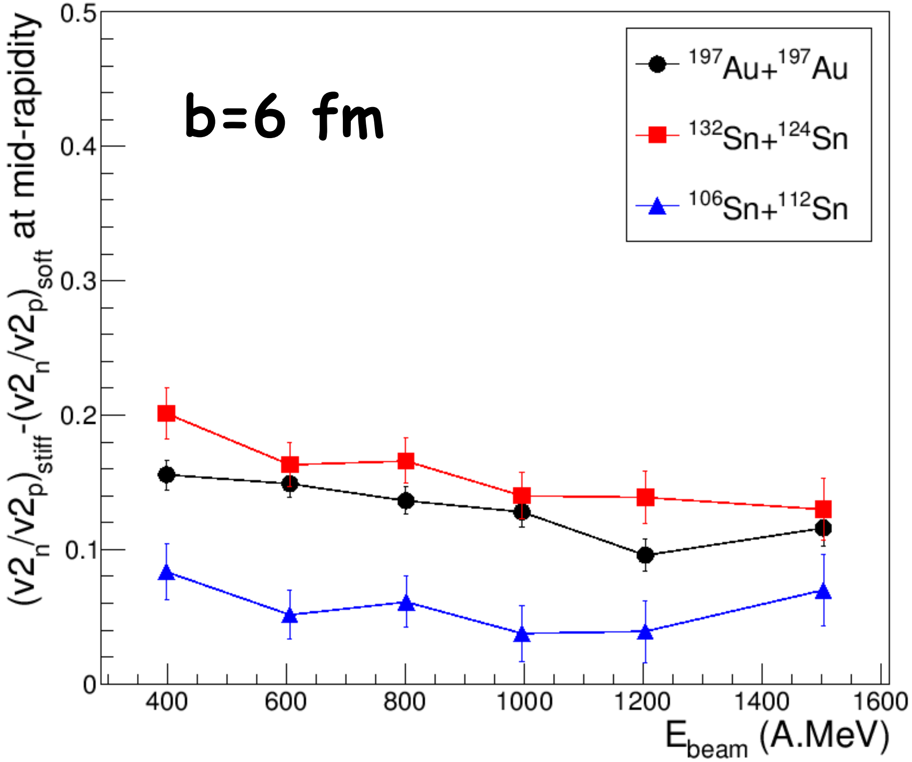

A. Le Fevre calculations

ASY-EOS II: IQMD and TuQMD predictions

IQMD

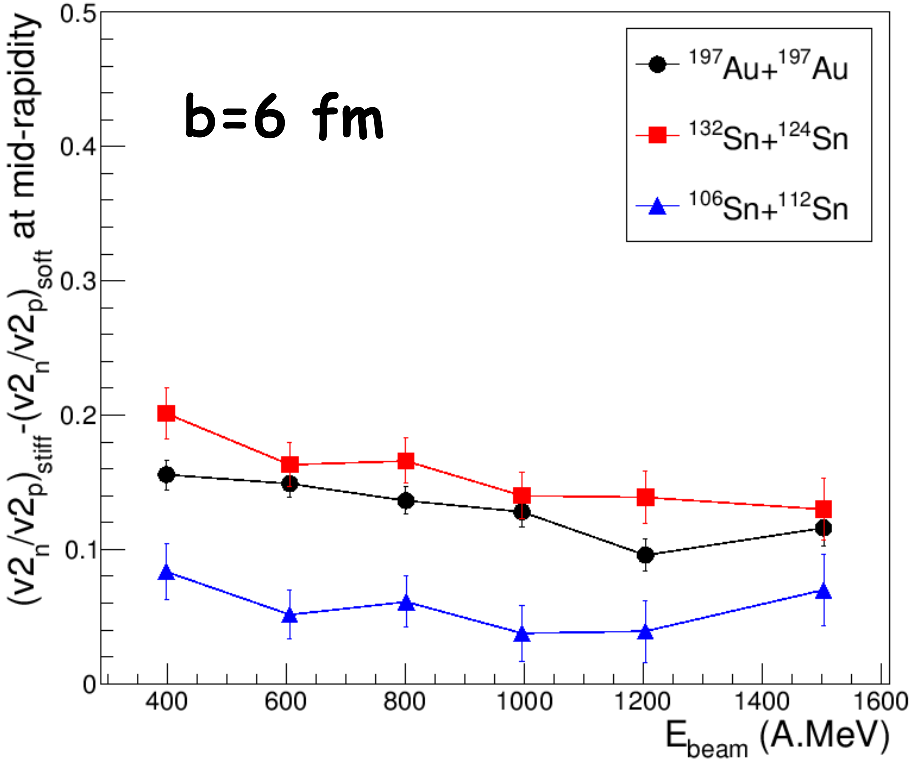

A. Le Fevre calculations

TuQMD
but using x=-2 (super-stiff) and x=2 (super-soft)

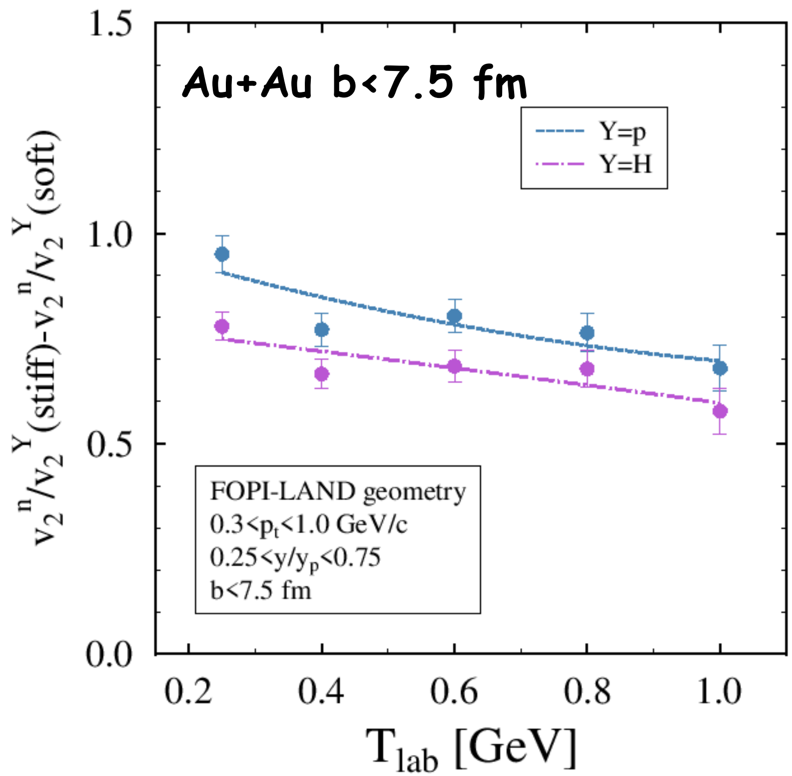

M.D Cozma calculations

NeuLAND @ FAIR/GSI

TDR finalized in Oct 2011 and submitted

- total volume 2.5x2.5x3 m^3
- each bar readout by two PMT
- 3000 modules (plastic scintillator bars) 250x5x5 cm^3
- 30 double planes with 100 bars each, bars in neighboring planes
- mutually perpendicular
- $\sigma_t \leq 150$ ps and $\sigma_{x,y,z} \leq 1.5$ cm
- one-neutron efficiency ~95% for energies 200-1000 MeV
- multi-neutron detection capability

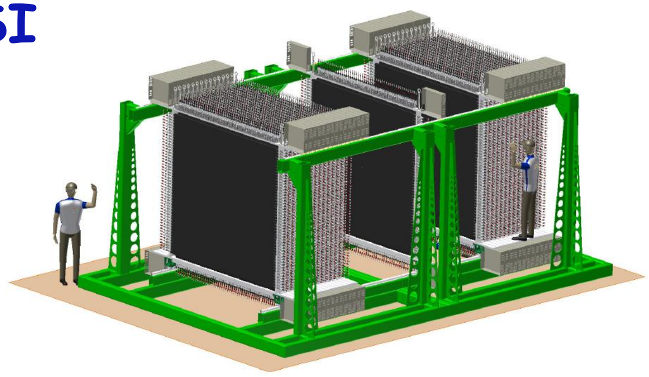

I. Gasparic AsyEOS2012 workshop, 6.9.2012, Siracusa, Italy

NeuLAND @ FAIR/GSI

TDR finalized in Oct 2011 and submitted

- total volume 2.5x2.5x3 m^3
- each bar readout by two PMTs
- 3000 modules (plastic scintillator bars) 250x5x5 cm^3
- 30 double planes with 100 bars each, bars in neighboring planes
- mutually perpendicular
- $\sigma_t \leq 150$ ps and $\sigma_{x,y,z} \leq 1.5$ cm
- one-neutron efficiency ~95% for energies 200-1000 MeV
- multi-neutron detection capability

I know that!!! ……

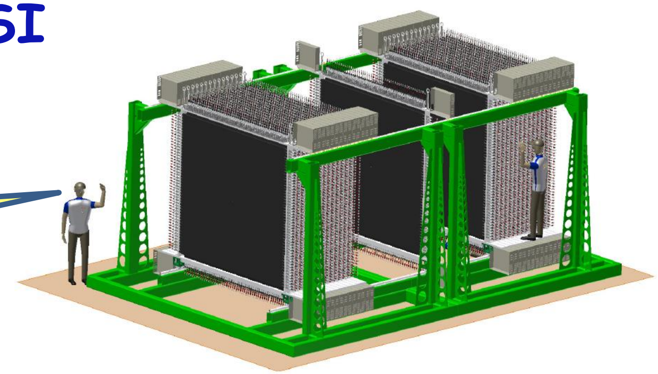

I. Gasparic AsyEOS2012 workshop, 6.9.2012, Siracusa, Italy

NeuLAND @ FAIR/GSI

TDR finalized in Oct 2011 and submitted

- total volume 2.5x2.5x3 m^3
- each bar readout by two PMT
- 3000 modules (plastic scintillator bars) 250x5x5 cm^3
- 30 double planes with 100 bars each, bars in neighboring planes
- mutually perpendicular
- $\sigma_t \leq 150$ ps and $\sigma_{x,y,z} \leq 1.5$ cm
- one-neutron efficiency ~95% for energies 200-1000 MeV
- multi-neutron detection capability

I know that!!!......

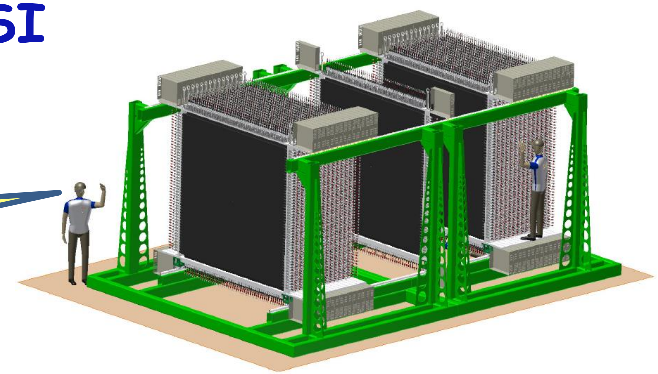

I. Gasparic AsyEOS2012 workshop, 6.9.2012, Siracusa, Italy

The NeuLAND demonstrator was part of the Sπrit TPC experiment carried out at RIKEN. Charged particles and neutrons stemming from central collisions of ^{108,112,124,132}Sn on ^{112,124} Sn target.

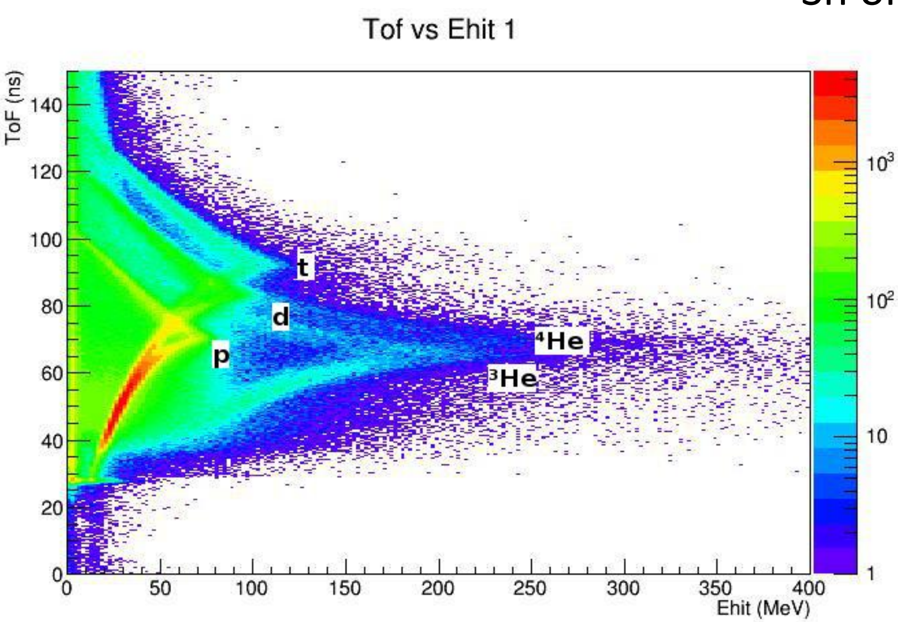

Particle ID plot from the 1st NeuLAND plane

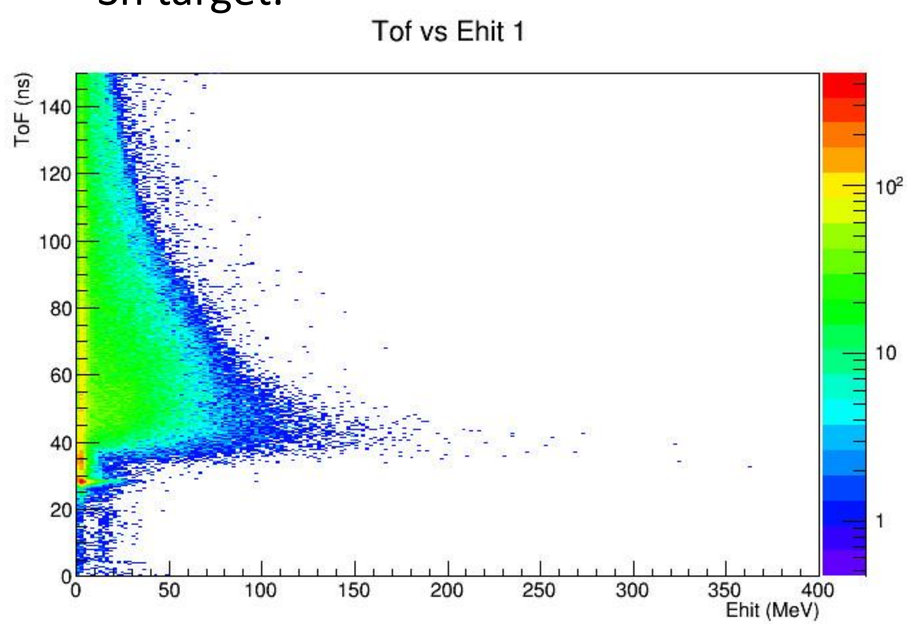

including a condition that no VETO hit was registered in the event

NeuLAND @ FAIR/GSI

TDR finalized in Oct 2011 and submitted
- total volume 2.5x2.5x3 m^3
- each bar readout by two PMT
- 3000 modules (plastic scintillator bars) 250x5x5 cm^3
- 30 double planes with 100 bars each, bars in neighboring planes
- mutually perpendicular
- $\sigma_t \leq 150$ ps and $\sigma_{x,y,z} \leq 1.5$ cm
- one-neutron efficiency ~95% for energies 200-1000 MeV
- multi-neutron detection capability

I know that!!!......

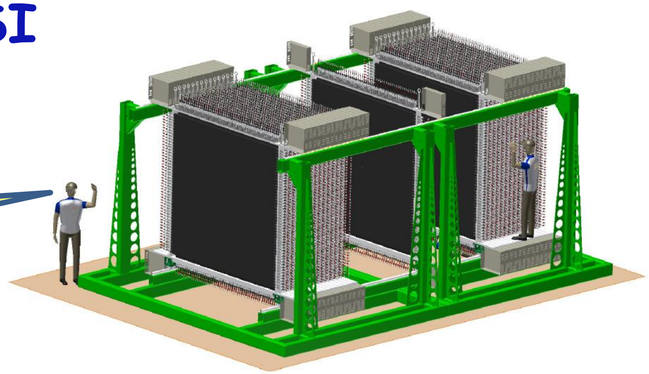

I. Gasparic AsyEOS2012 workshop, 6.9.2012, Siracusa, Italy

The NeuLAND demonstrator was part of the Sπrit TPC experiment carried out at RIKEN. Charged particles and neutrons stemming from central collisions of ^{108,112,124,132}Sn on ^{112,124} Sn target.

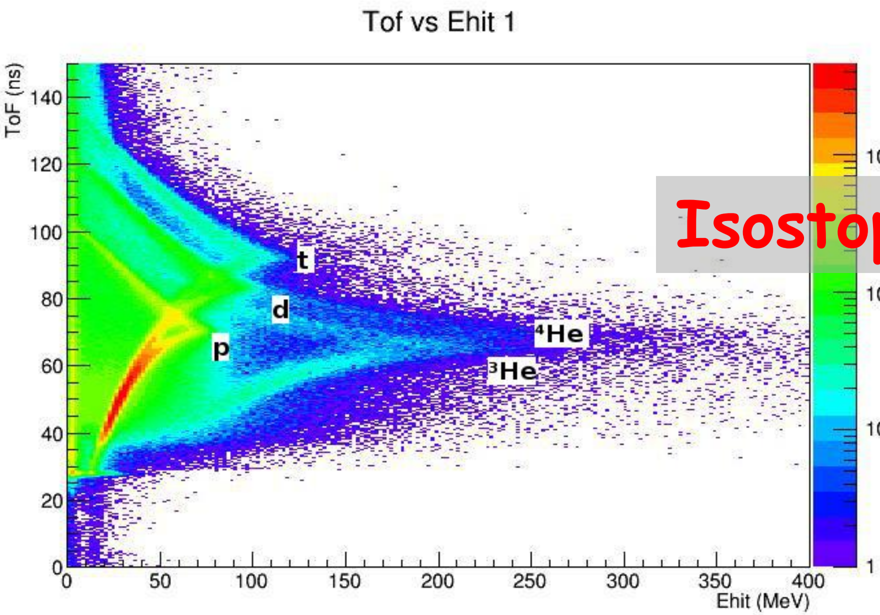

Isotopic resolution!

Particle ID plot from the 1st NeuLAND plane

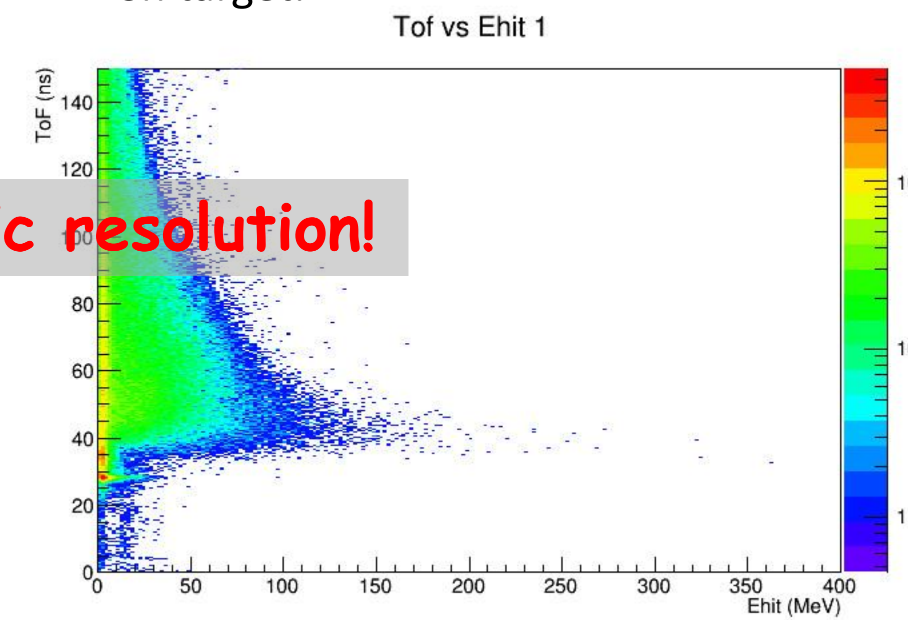

including a condition that no VETO hit was registered in the event

FOPI forward wall

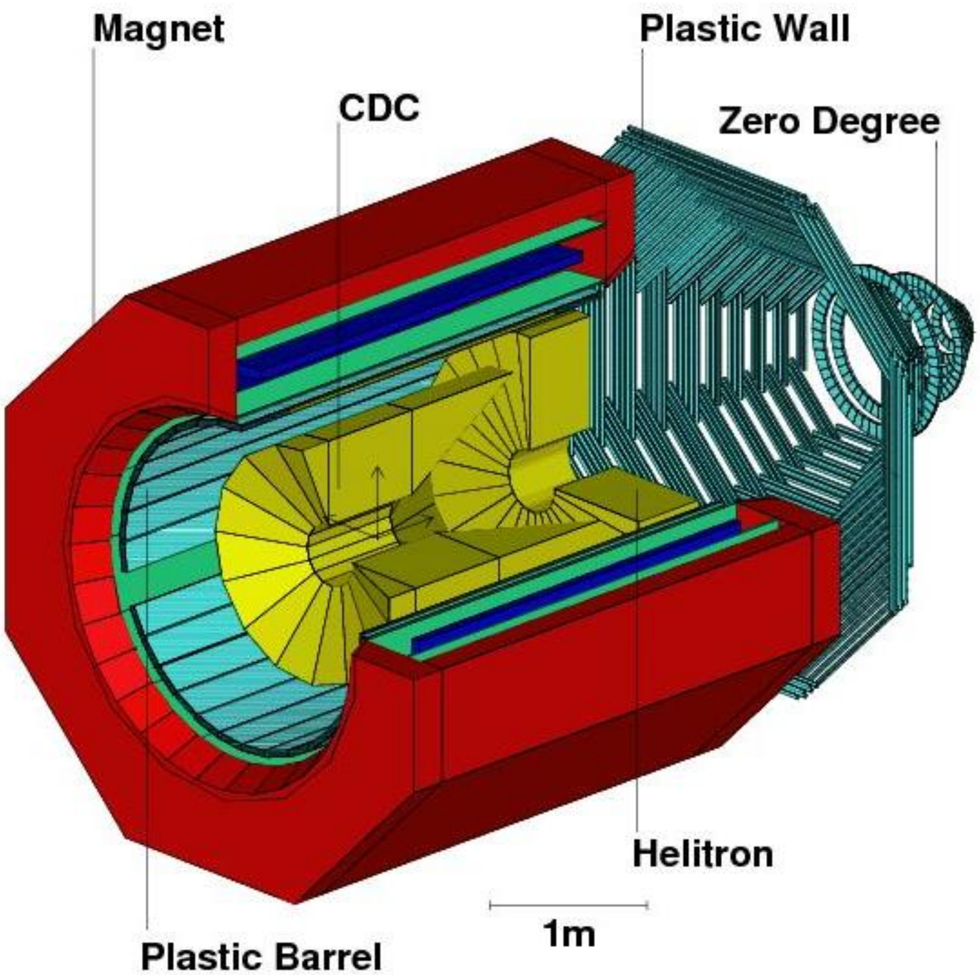

Figure 2.1: Schematic drawing of the FOPI detector.

2.10 The Forward Wall

The forward wall covers polar angles from 1.2 ° to 30 ° and the full azimuthal range. It consists of two parts: the outer wall called "Plastic Wall" (PLAWA) and the inner wall called "Zero Degree" (ZD).

2.10.1 The Plastic Wall (PLAWA)

Like the Plastic Barrel the Plastic Wall is made of 512 plastic scintillator strips divided into eight sectors. Each sector is composed of 64 strips. The light produced by a charged particle on a given strip is read out at both ends of the strip via photo multipliers. Each strip delivers four signals, two energies (E_L,E_R) and two times (t_L,t_R). The energy loss ΔE of a particle is proportional to $\sqrt{E_L \cdot E_R}$ and its time of flight is proportional to $\frac{1}{2} \cdot (t_L + t_R)$. The position of a particle hitting the PLAWA is given by the angular position of the strip which fired. The time resolution is linked to the active length of the scintillator strip, thus it varies from 80 ps for strips in the inner sector to 120 ps for strips in the outer sector. The resolution of the hit position varies from 1.2 cm to 2.0 cm [74, 75].

2.10.2 The Zero Degree Detector

This detector covers polar angles from 1.2 ° to 7.0 ° and consists of 252 plastic scintillator strips grouped into 7 concentric rings. Each module is read out by only one photo multiplier and delivers the energy loss (ΔE) and the time of flight of charged particles. The time resolution of this detector is about 200 ps.

Study for the new Krakow Barrel (J. Lukasik group)

Trigger/Reaction Plane detector around the target:

- 5 rings of 4x4 mm^2 fast scintillating fibers (e.g. BCF-20) read out by SiPMs
- covers angles from 30° to 165°,
- segmentation assures more or less uniform count rates for Au+Au at 1 AGeV,
- geometrical efficiency ~95%
- ~10% of charged particles involved in multihits,
- ~5% multihit probability
- sufficiently large for radioactive beams
- sufficiently small and lightweight not to disturb neutrons
- min radius - 6 cm,
- max radius - 12 cm
- length 43 cm
- 180 segments in forward rings
- 90 segments in backward ring
- 810 channels

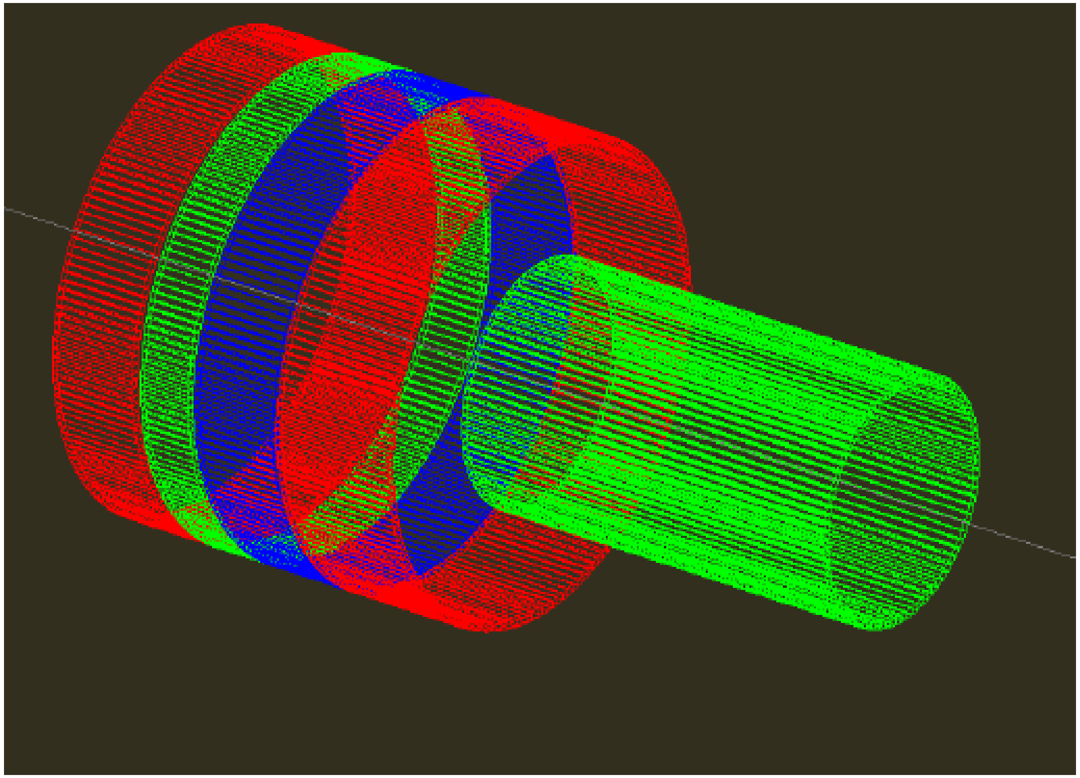

Study for the new Krakow Barrel (J. Lukasik group)

Trigger/Reaction Plane detector around the target:

- 5 rings of 4x4 mm^2 fast scintillating fibers (e.g. BCF-20) read out by SiPMs
- covers angles from 30^o to 165^o,
- segmentation assures more or less uniform count rates for Au+Au at 1 AGeV,
- geometrical efficiency ~95%
- ~10% of charged particles involved in multihits,
- ~5% multihit probability
- sufficiently large for radioactive beams
- sufficiently small and lightweight not to disturb neutrons
- min radius - 6 cm,
- max radius - 12 cm
- length 43 cm
- 180 segments in forward rings
- 90 segments in backward ring
- 810 channels

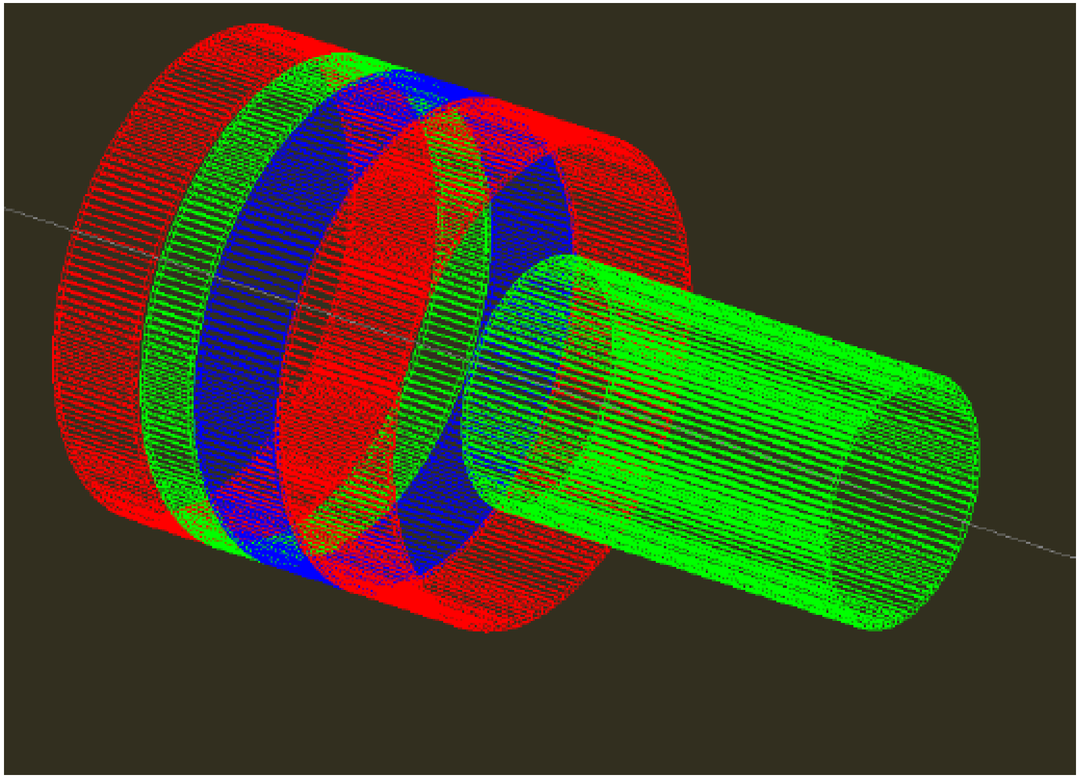

- **Fast enough to trigger**
- **Transparent to neutrons**
- **Highly segmented**
- **Background reduction**
- **Inside (a part of) Califa???**

Study for the new Krakow Barrel (J. Lukasik group)

Trigger/Reaction Plane detector around the target:

- 5 rings of 4x4 mm^2 fast scintillating fibers (e.g. BCF-20) read out by SiPMs
- covers angles from 30° to 165°,
- segmentation assures more or less uniform count rates for Au+Au at 1 AGeV,
- geometrical efficiency ~95%
- ~10% of charged particles involved in multihits,
- ~5% multihit probability
- sufficiently large for radioactive beams
- sufficiently small and lightweight not to disturb neutrons
- min radius - 6 cm,
- max radius - 12 cm
- length 43 cm
- 180 segments in forward rings
- 90 segments in backward ring
- 810 channels

Project already approved on Monday!

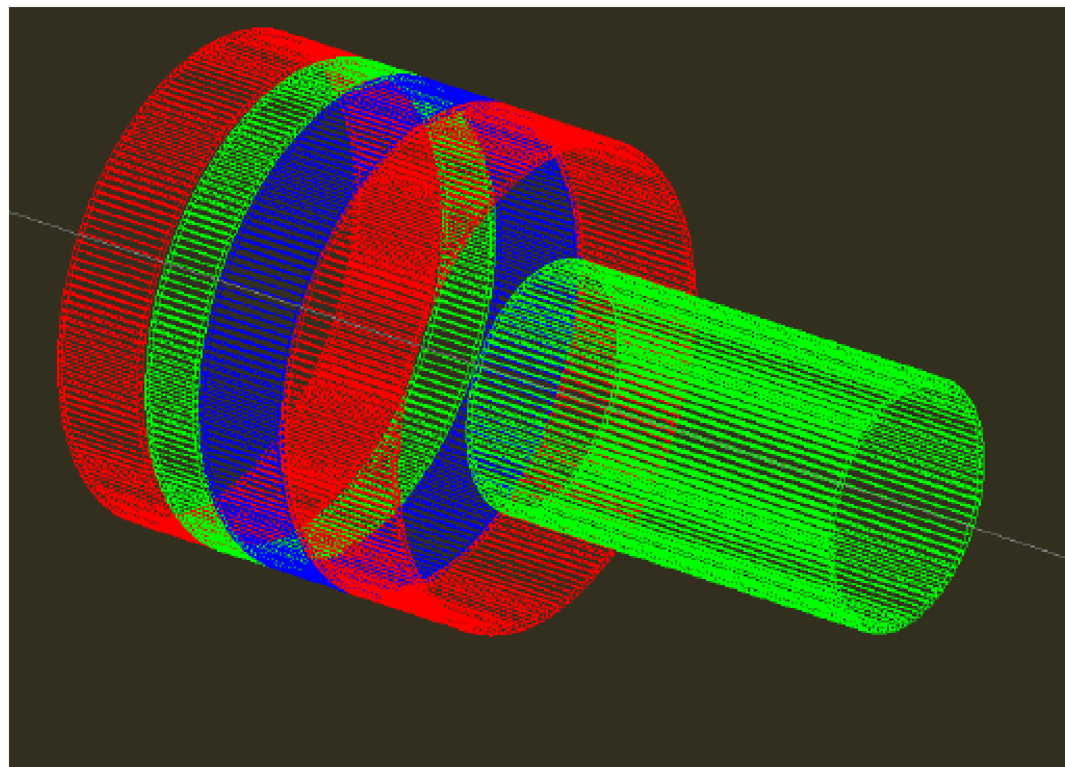

- **Fast enough to trigger**
- **Transparent to neutrons**
- **Highly segmented**
- **Background reduction**
- **Inside (a part of) Califa???**

Krakow Barrel

Background reduction: CHIMERA-MicroBall correlation in ASY-EOS exp

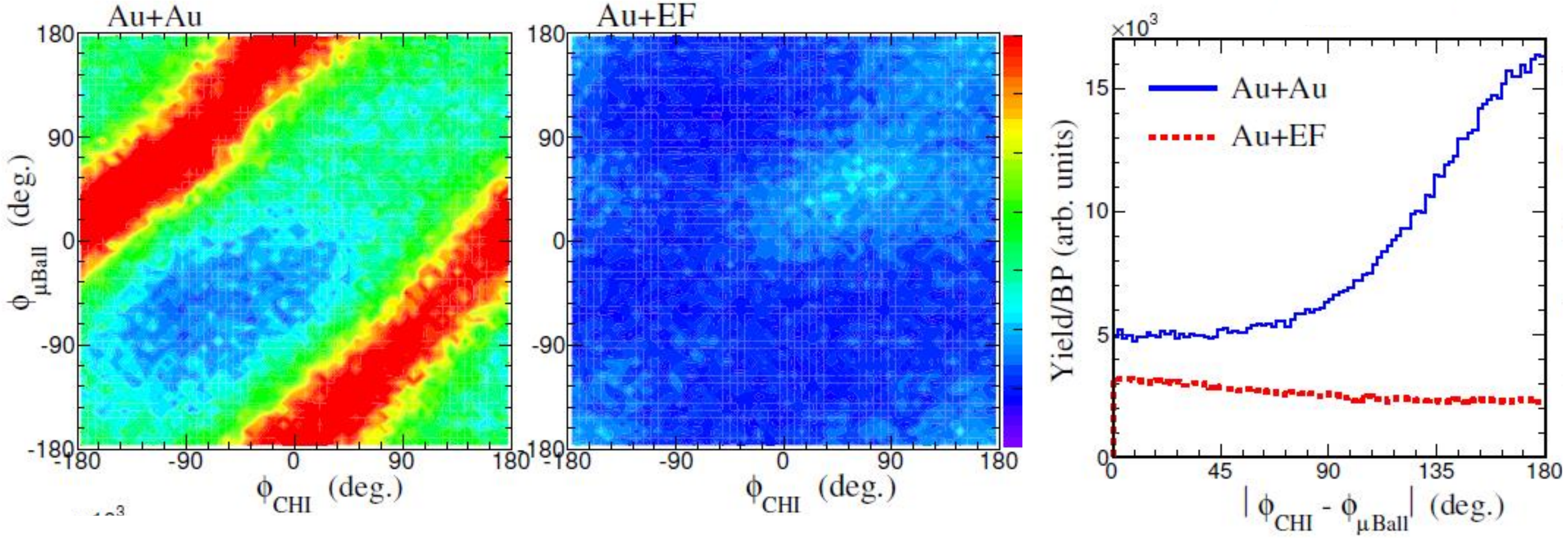

Krakow Barrel

Background reduction: CHIMERA-MicroBall correlation in ASY-EOS exp

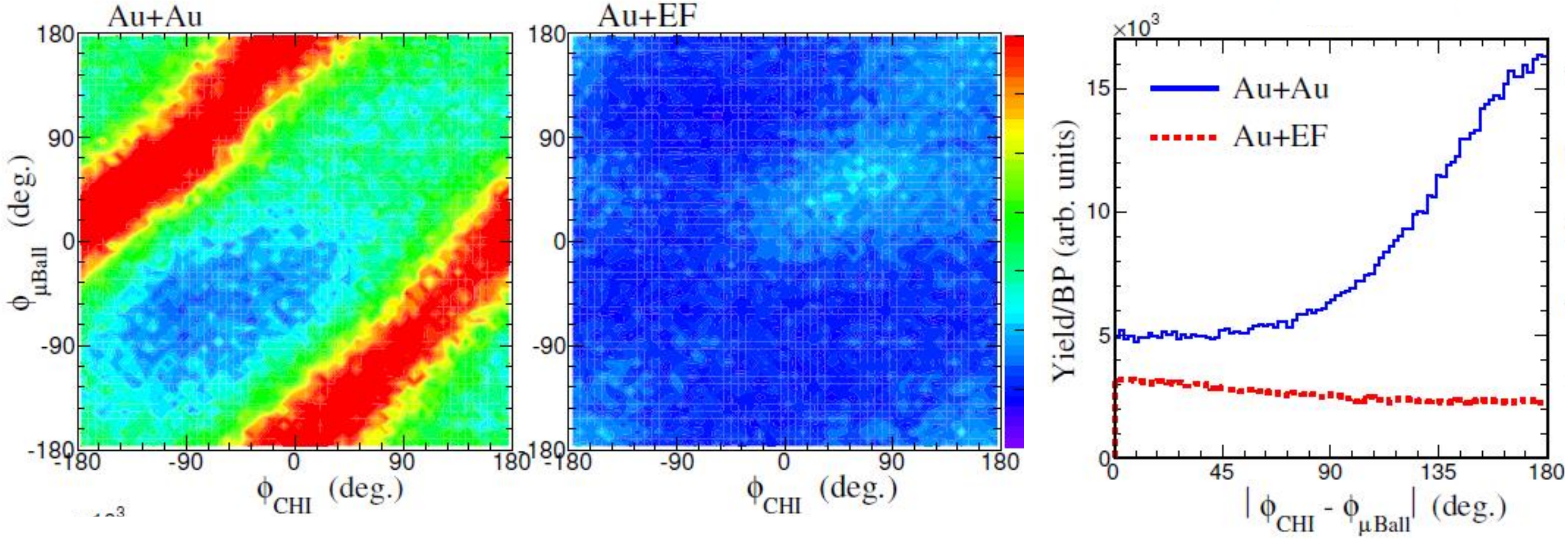

UrQMD + clustering: Au+Au 1000 AMeV, 0-10 fm, 200 fm/c

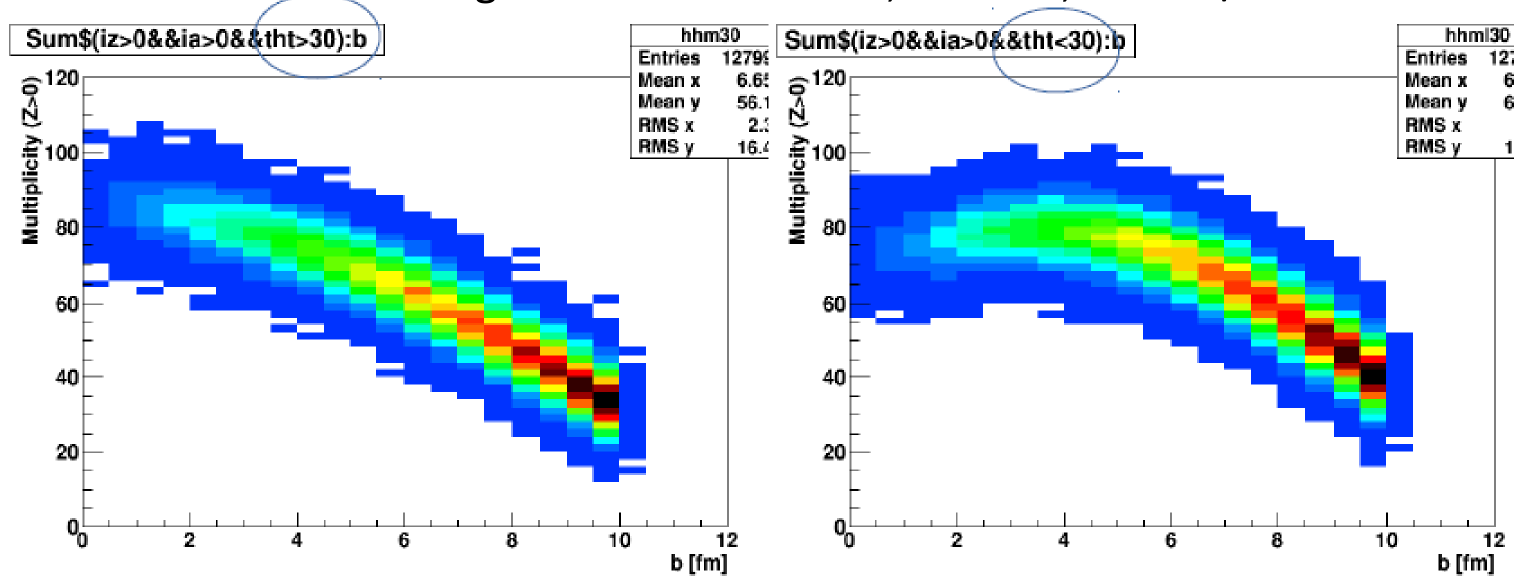

KraTTA & FARCOS

35 modules (5 x7), 20.7°<θ<63.5°
40 cm from target.
Digitized with 100 MHz, 14 bits Flash ADCs

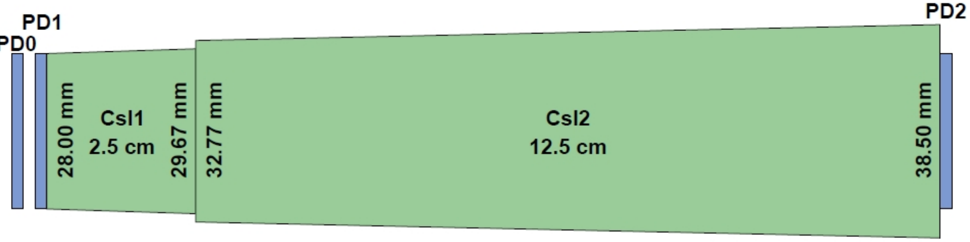

Au+Au @ 400 A.MeV
3.35<b<6 fm (c2)
θ_{lab} cut as LAND

J. Lukasik et al., NIM A 709, 120 (2013)

S. Kupny Ph. D (2014)

KraTTA & FARCOS

35 modules (5 x7), 20.7°<θ<63.5°
40 cm from target.
Digitized with 100 MHz, 14 bits Flash ADCs

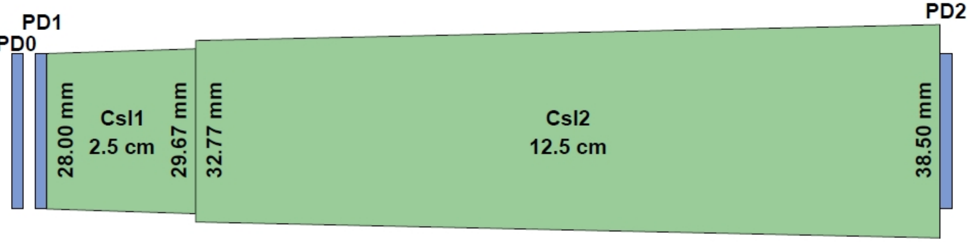

Au+Au @ 400 A.MeV
3.35<b<6 fm (c2)
θ_{lab} cut as LAND

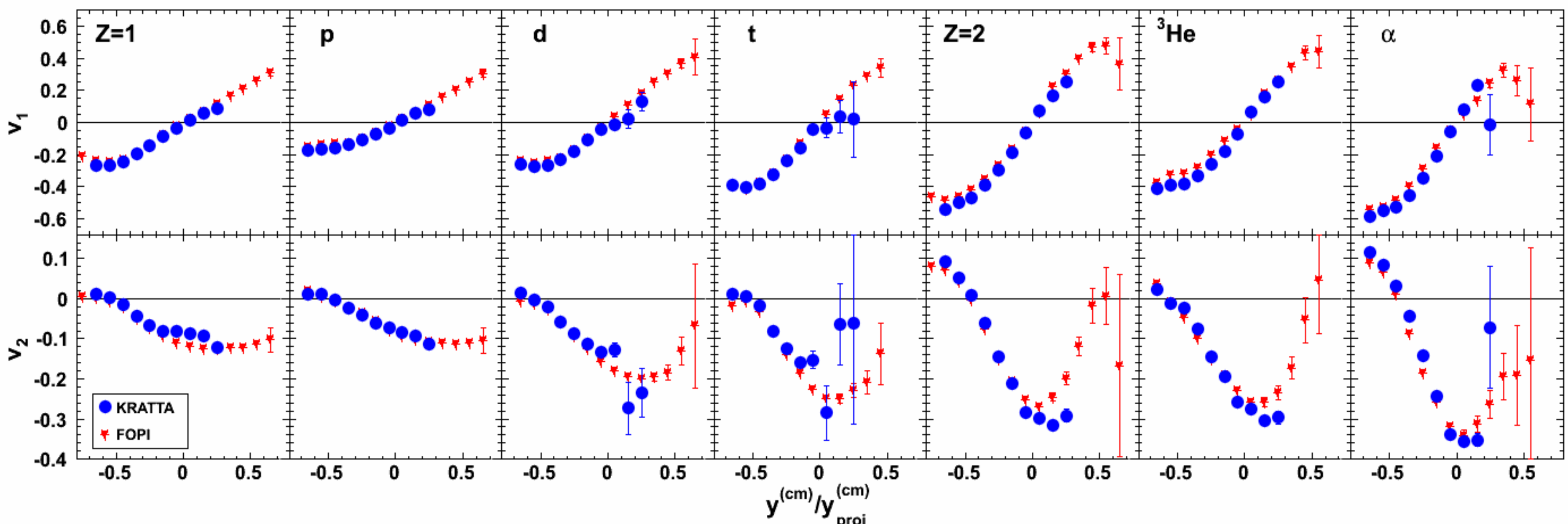

J. Lukasik et al., NIM A 709, 120 (2013)

S. Kupny Ph. D (2014)

KraTTA & FARCOS

35 modules (5 x7), 20.7°<θ<63.5°
40 cm from target.
Digitized with 100 MHz, 14 bits Flash ADCs

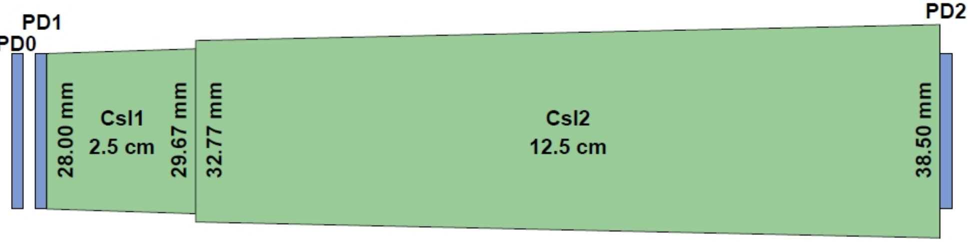

132 channels by each cluster

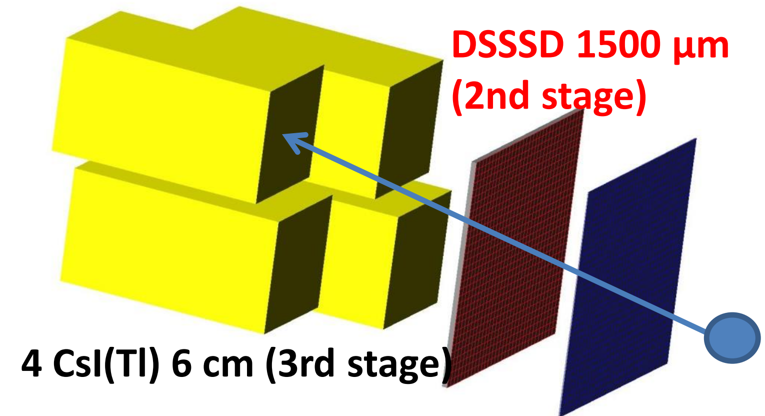

High angular and energy resolution

Au+Au @ 400 A.MeV
3.35<b<6 fm (c2)
θ_{lab} cut as LAND

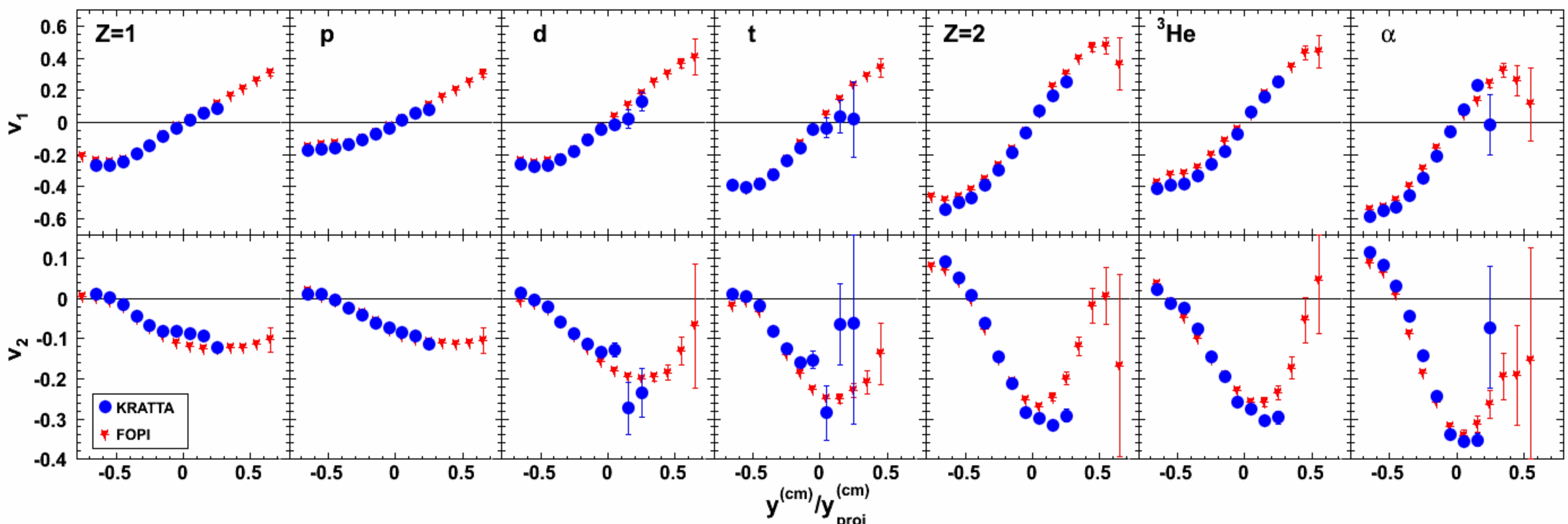

J. Lukasik et al., NIM A 709, 120 (2013)

S. Kupny Ph. D (2014)

Pion Range Counter

Beam energy dependence of charged pion ratio in ^{28}Si + In reactions

M. Sako[a,b,1,*], T. Murakami[a,b], Y. Nakai[b], Y. Ichikawa[a], K. Ieki[c], S. Imajo[a], T. Isobe[b], M. Matsushita[c], J. Murata[c], S. Nishimura[b], H. Sakurai[b], R.D. Sameshima[a], and E. Takada[d]

[a]Department of Physics, Kyoto University, Kyoto 606-8502, Japan
[b]RIKEN Nishina Center for Accelerator-Based Scienece, RIKEN, Saitama 351-0198, Japan
[c]Department of Physics, Rikkyo University, Tokyo 171-8501, Japan
[d]National Institute of Radiological Sciences, Chiba 263-8555, Japan

https://arxiv.org/abs/1409.3322v1

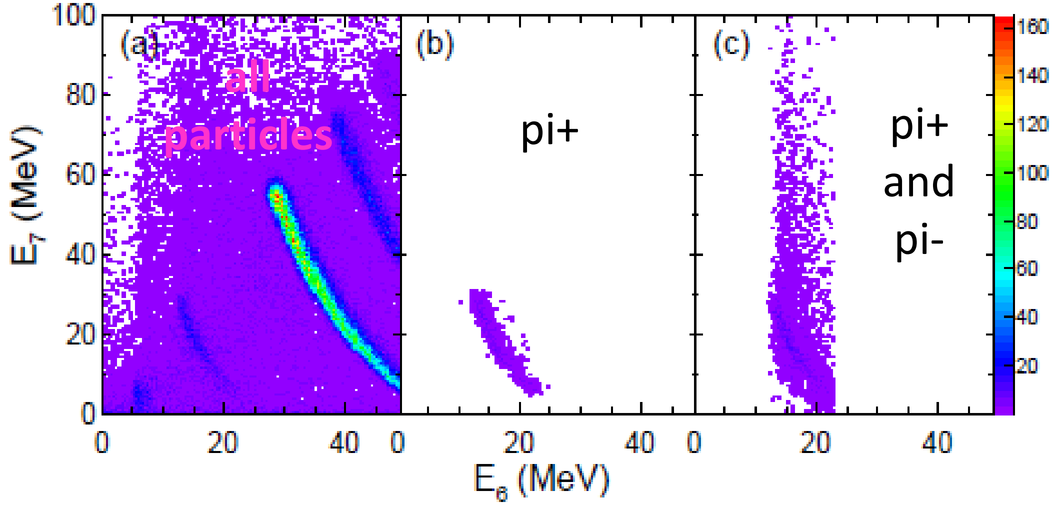

Figure 1: (Color online) Correlation of E_7 vs. E_6 with a beam energy of 600 MeV/nucleon at 60°. (a) All events with the condition of S_7. (b)π^+ event with the selection of a double pulse. (c) Charged pion events with the condition of S_7 and G_7.

The experiment was performed at the PH2 beam-line of the Heavy Ion Medical Accelerator in Chiba (HIMAC) in the National Institute of Radiological Science (NIRS). ^{28}Si beams were accelerated up to 400, 600, and 800 MeV/nucleon with a heavy-ion synchrotron. Typical beam intensities were about 1×10^7 particles per spill in a 3.3 sec cycle. A self-supporting natural indium plate (329 mg/cm^2 thick) was placed in a small vacuum chamber located at the end of the PH2-line.

The PRC consisted of 13 layers, where each layer was coupled to a fast photomultiplier tube (PMT) at the one end through a light guide. Here the 13 layers were numbered from i=1 to 13 beginning from the first trigger counter. The first two layers, which were each 2 mm thick, were used for triggering the data acquisition. Of the remaining 11 layers, two were 5 mm thick, one was10 mm thick, one was 15 mm thick, and seven were 30 mm thick. To veto charged particles penetrating the PRC, another plastic scintillator (5 mm thick) was placed behind the PRC.

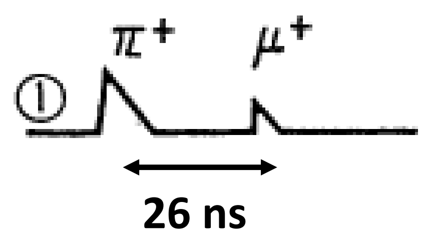

ASY-EOS II…not a true proposal

ASY-EOS II…not a true proposal

- **test of RIBs yield in cave C**

Beam Time Request. In order to make realistic estimates of the beam time for the future experiments it is of fundamental importance to know the incoming beam rate of the ^{132}Sn and ^{106}Sn secondary beams in Cave C target station. Therefore, for the current proposal we request 12 shifts (4 days) to test the intensities

the velocity of the ion. The mass is then directly deduced. *The requested 12 shifts could be shared with an experiment proposed by the R3B collaboration, which aims to measure the dipole excitation of neutron rich tin isotopes. During this experiment, beam intensities of neutron rich tin isotopes will be deduced.*

ASY-EOS II…not a true proposal

- **test of RIBs yield in cave C**

BEAM TIME REQUEST. In order to make realistic estimates of the beam time for the future experiments it is of fundamental importance to know the incoming beam rate of the ^{132}Sn and ^{106}Sn secondary beams in Cave C target station. Therefore, for the current proposal we request 12 shifts (4 days) to test the intensities

the velocity of the ion. The mass is then directly deduced. *The requested 12 shifts could be shared with an experiment proposed by the R3B collaboration, which aims to measure the dipole excitation of neutron rich tin isotopes. During this experiment, beam intensities of neutron rich tin isotopes will be deduced.*

- **test of detectors**

In addition to the production and transport test, we request 9 shifts (3 days) of stable beam. The test beam is necessary to commission the new devices we plan to use, NeuLAND, CALIFA, FARCOS, Krakow Barrel and the upgraded version of the PRC, and to optimize the already existing devices to the new operating conditions. It will allow us to construct and debug the interface between the front-end electronics and DAQ system. A Gold beam of 400A MeV would be best suited for this purpose, but any other heavy primary beam of similar energy could be used. *It was negotiated with the R3B collaboration to do such measurements - if possible - in parallel to their experimental campaigns.*

ASY-EOS II: plans?

It would be great if someone of you could come at

Open ASY-EOS II Collaboration Meeting

14-15 December 2017 *Catania & Caltagirone, Sicily, Italy*

Participation to the collaboration meeting is open to everyone is interested and not restricted to the ASY-EOS II collaboration members.

https://agenda.infn.it/conferenceDisplay.py?confId=14424

My conclusions @ NuSYM2017

Symmetry Energy:

- Low densities: several constraints quite consistent
- High density:
  - n/p flows: "our" observable for constraining the high-density dependence of the symmetry energy
  - ASY-EOS data analysis is done, new constraint obtained
  - pions: Spirit results will come!
- Work on code consistency needed…everywhere!
- Possibility of new (and better) experiments on n,p flows (& pions?) @ GSI
- International collaborations and efforts

My conclusions @ NuSYM2017

Symmetry Energy:

- Low densities: several constraints quite consistent
- High density:
  - n/p flows: "our" observable for constraining the high-density dependence of the symmetry energy
  - ASY-EOS data analysis is done, new constraint obtained
  - pions: Spirit results will come!
- Work on code consistency needed…everywhere!
- Possibility of new (and better) experiments on n,p flows (& pions?) @ GSI
- International collaborations and efforts

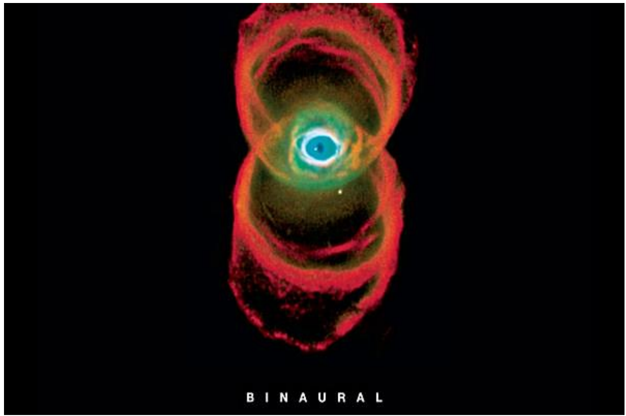

Clepsydra nebula as seen from Hubble telescope (PJ)

My conclusions @ NuSYM2017

Symmetry Energy:

- Low densities: several constraints quite consistent
- High density:
  - n/p flows: "our" observable for constraining the high-density dependence of the symmetry energy
  - ASY-EOS data analysis is done, new constraint obtained
  - pions: Spirit results!
- Work on code consistency needed…everywhere!
- Possibility of new (and better) experiments on n,p flows (& pions?) @ GSI
- International collaborations and efforts

My conclusions @ NuSYM2017

Symmetry Energy:

- Low densities: several constraints quite consistent
- High density:
  - n/p flows: "our" observable for constraining the high-density dependence of the symmetry energy
  - ASY-EOS data analysis is done, new constraint obtained
  - pions: Spirit results!
- Work on code consistency needed…everywhere!
- Possibility of new (and better) experiments on n,p flows (& pions?) @ GSI
- International collaborations and efforts

On the road…..

ASY-EOS II proposal

Determination of Symmetry Energy at Supra-Normal Densities: a feasibility study

ASY-EOS II Collaboration

Spokesperson: P. Russotto[1]

Principal Investigators: A. Le Fèvre[2], Y. Leifels[2], J. Łukasik[3], P. Russotto[1]

Participants: M. Adamczyk[4], J. Benlliure[5], E. Bonnet[6], J. Brzychczyk[4], Ch. Caesar[2], P. Cammarata[7], Z. Chajecki[8], A. Chbihi[9], E. De Filippo[11], M. Famiano[12], I. Gašparić[13], B. Gnoffo[11,20], C. Guazzoni[21], T. Isobe[14], M. Jabłoński[4], M. Jastrząb[3], J. Kallunkathariyil[22], K. Kezzar[15], M. Kiš[2], P. Koczoń[2], A. Krasznahorkay[16], P. Lasko[3], K. Łojek[4], W.G. Lynch[8], P. Marini[18], N.S. Martorana[1,20], A.B. McIntosh[7], T. Murakami[19], A. Pagano[11], E.V. Pagano[1,20], M. Papa[11], P. Pawłowski[3], S. Pirrone[11], G. Politi[11,20], K. Pysz[3], L. Quattrocchi[11,20] F. Rizzo[1,20], W. Trautmann[2], A. Trifirò[23], M. Trimarchi[23], M.B. Tsang[8], A. Wieloch[4] and S.J. Yennello[7]

Theory Support: J. Aichelin[6], M. Colonna[1], M.D. Cozma[10], P. Danielewicz[8], Ch. Hartnack[6], Q.F. Li[17] and Y. Wang[17]

Institutions: [1]INFN-LNS, Catania, Italy; [2]GSI, Darmstadt, Germany; [3]IFJ PAN, Kraków, Poland; [4]Jagiellonian University, Kraków, Poland; [5]Universidade de Santiago de Compostela, Spain; [6]SUBATECH, Nantes, France; [7]Texas A&M University Cyclotron Institute, College Station, USA; [8]NSCL/MSU, East Lansing, USA; [9]GANIL, Caen, France; [10]IFIN-HH, Bucharest, Romania; [11]INFN-Sezione di Catania, Italy; [12]Western Michigan University, Kalamazoo, MI, USA; [13]RBI, Zagreb, Croatia; [14]RIKEN, Wako-shi, Japan; [15]King Saud University, Riyadh, Saudi Arabia; [16]Institute for Nuclear Research, Debrecen, Hungary; [17]School of Science, Huzhou University, P.R. China; [18]CEA, DAM, DIF, Arpajon, France; [19]Kyoto University, Japan; [20]Università di Catania, Italy; [21] Politecnico di Milano and INFN-Sezione di Milano, Italy; [22]CEA, Saclay, France; [23]Dipartimento di Scienze MIFT, Univ. di Messina, Italy.

UrQMD prediction for pions

$^{197}Au+^{197}Au$ @ 400, 600, 800, 1000,1500 AMeV (0.039+0.039)

$^{132}Sn+^{124}Sn$ @ 400, 600, 800 AMeV (0.059+0.037)

$^{106}Sn+^{112}Sn$ @ 400, 600, 800 AMeV (0.003+0.011)

b/bred <0.53

Pions yield ratio

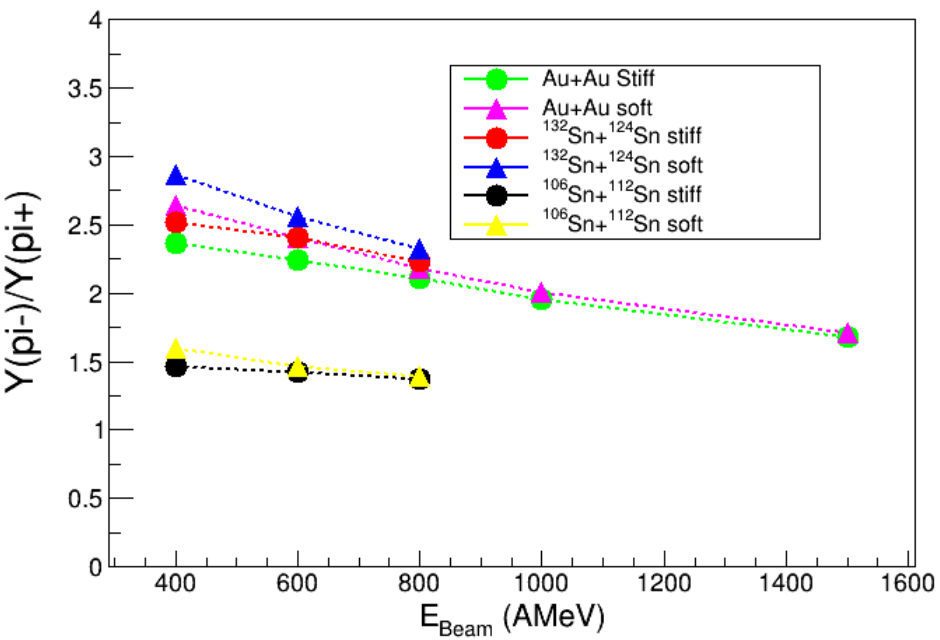

Sensitivity

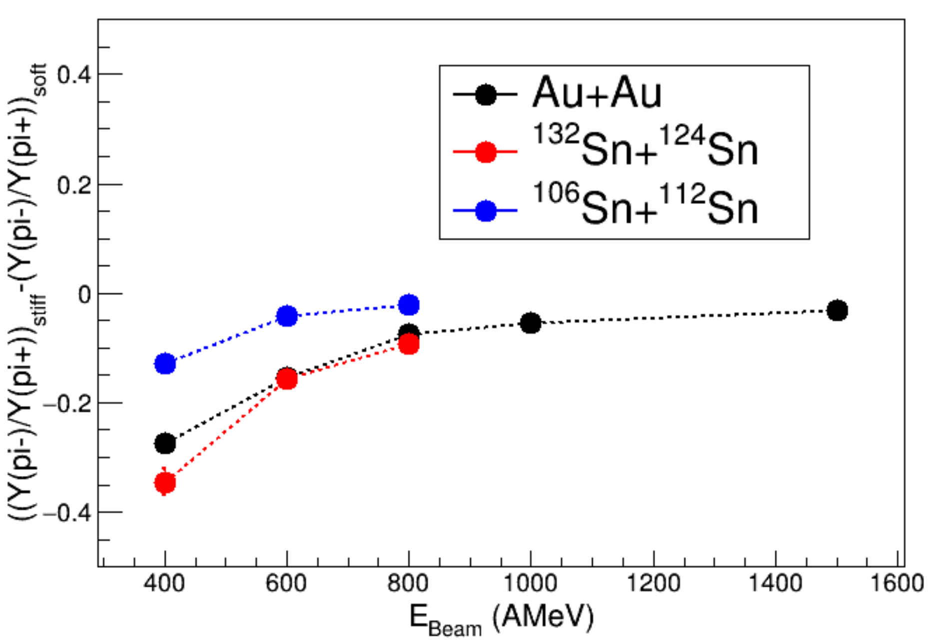

Beam energy dependence of charged pion ratio in ^{28}Si + In reactions

M. Sako[a,b,1,*], T. Murakami[a,b], Y. Nakai[b], Y. Ichikawa[a], K. Ieki[c], S. Imajo[a], T. Isobe[b], M. Matsushita[c], J. Murata[c], S. Nishimura[b], H. Sakurai[b], R.D. Sameshima[a], and E. Takada[d]

[a]Department of Physics, Kyoto University, Kyoto 606-8502, Japan
[b]RIKEN Nishina Center for Accelerator-Based Scienece, RIKEN, Saitama 351-0198, Japan
[c]Department of Physics, Rikkyo University, Tokyo 171-8501, Japan
[d]National Institute of Radiological Sciences, Chiba 263-8555, Japan

https://arxiv.org/abs/1409.3322v1

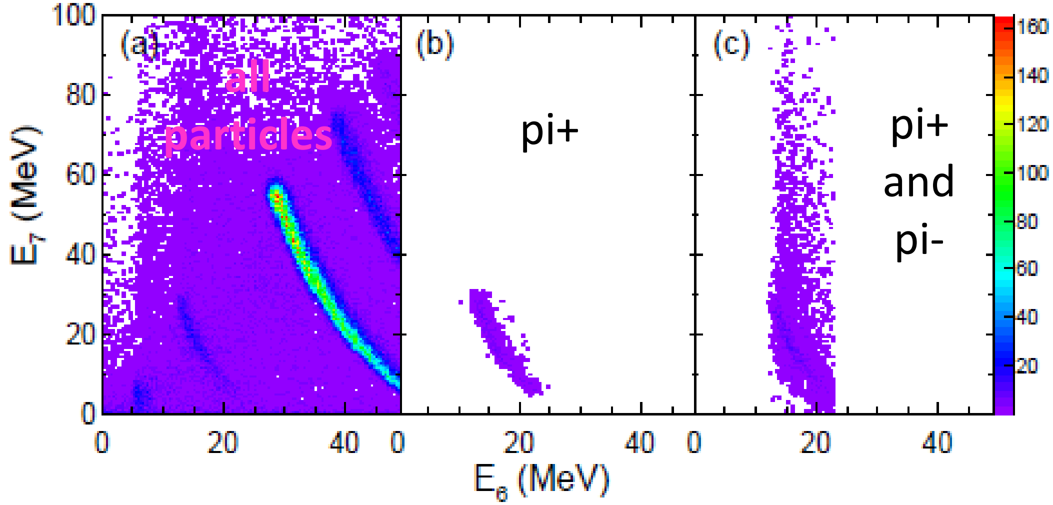

Figure 1: (Color online) Correlation of E_7 vs. E_6 with a beam energy of 600 MeV/nucleon at 60°. (a) All events with the condition of S_7. (b)π^+ event with the selection of a double pulse. (c) Charged pion events with the condition of S_7 and G_7.

The experiment was performed at the PH2 beam-line of the Heavy Ion Medical Accelerator in Chiba (HIMAC) in the National Institute of Radiological Science (NIRS). ^{28}Si beams were accelerated up to 400, 600, and 800 MeV/nucleon with a heavy-ion synchrotron. Typical beam intensities were about 1×10^7 particles per spill in a 3.3 sec cycle. A self-supporting natural indium plate (329 mg/cm^2 thick) was placed in a small vacuum chamber located at the end of the PH2-line.

Introduction

The nuclear EOS describes the relation among energy, pressure, density, temperature and isospin asymmetry of nuclear matter. It is a fundamental ingredient in nuclear physics and astrophysics.

Introduction

The nuclear EOS describes the relation among energy, pressure, density, temperature and isospin asymmetry of nuclear matter. It is a fundamental ingredient in nuclear physics and astrophysics.

Nuclear matter phase diagram (schematic)

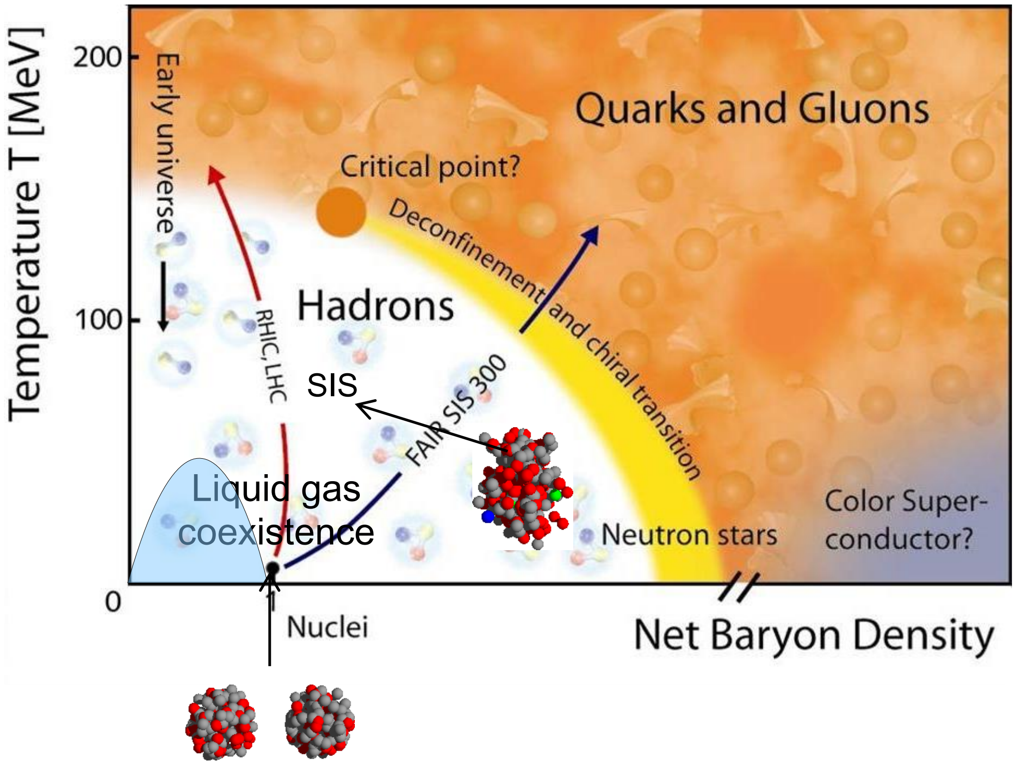

Introduction

The nuclear EOS describes the relation among energy, pressure, density, temperature and isospin asymmetry of nuclear matter. It is a fundamental ingredient in nuclear physics and astrophysics.

Nuclear matter phase diagram (schematic)

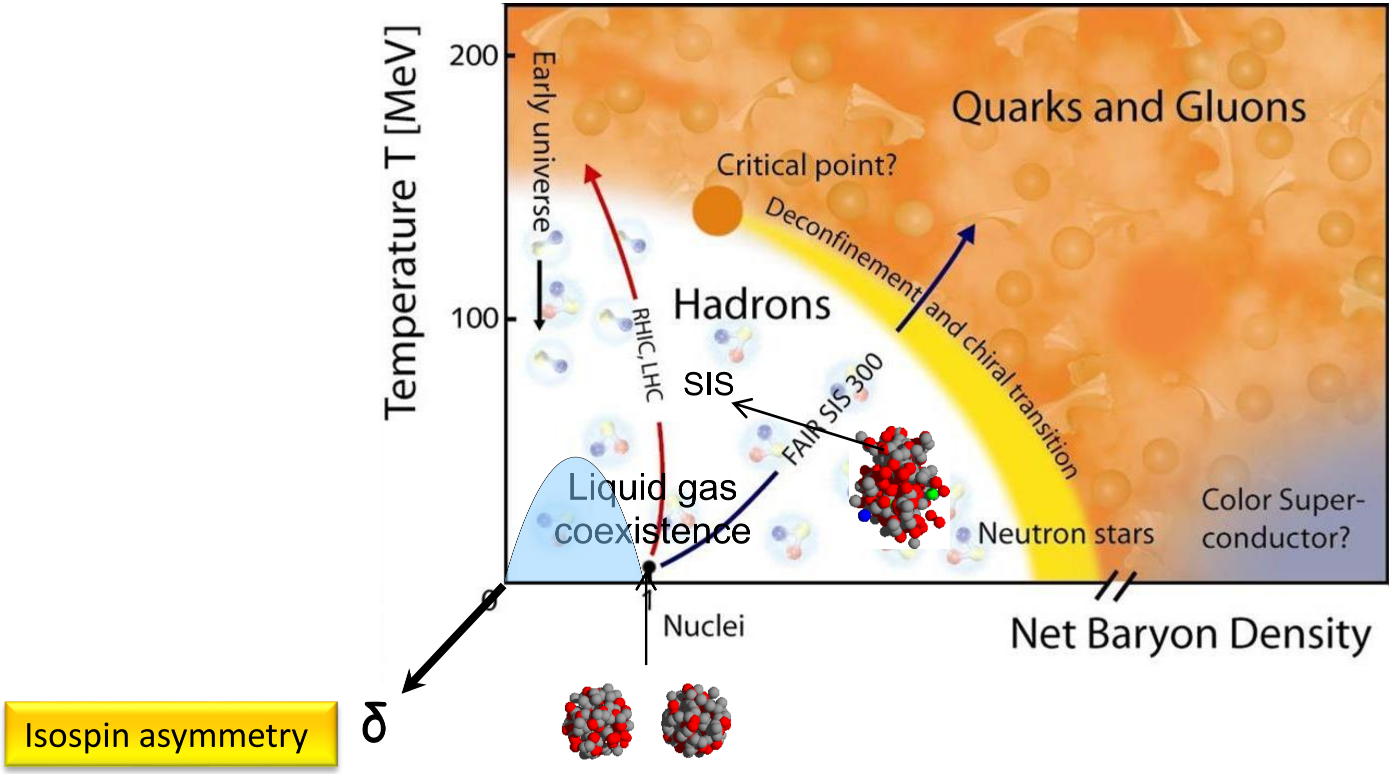

Introduction

The nuclear EOS describes the relation among energy, pressure, density, temperature and isospin asymmetry of nuclear matter. It is a fundamental ingredient in nuclear physics and astrophysics.

Question:

how E/A depends on the density ρ and isospin asymmetry δ=(N-Z)/(N+Z) ,

that is, E/A(ρ, δ)=????

Nuclear matter phase diagram (schematic)

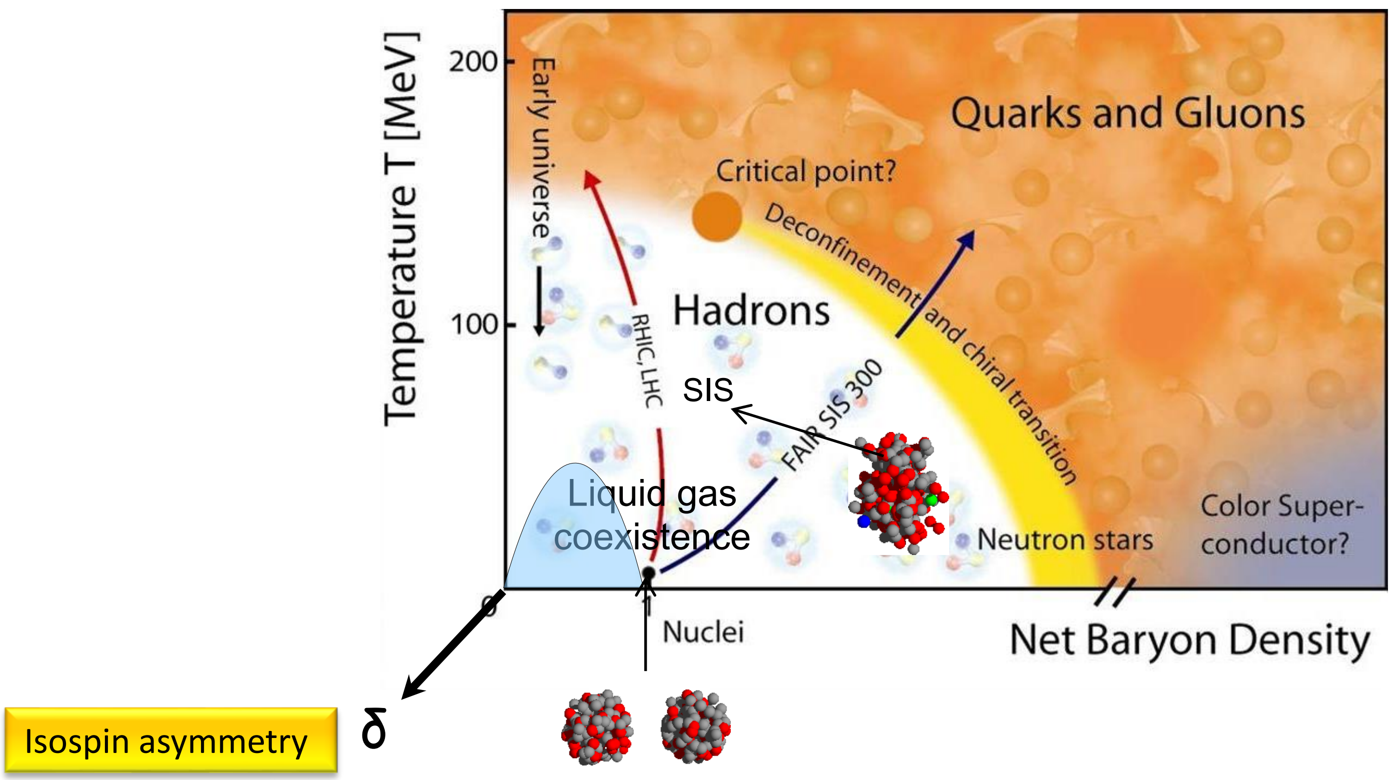

Introduction

The nuclear EOS describes the relation among energy, pressure, density, temperature and isospin asymmetry of nuclear matter. It is a fundamental ingredient in nuclear physics and astrophysics.

Question:

how E/A depends on the density ρ and isospin asymmetry δ=(N-Z)/(N+Z) ,

that is, E/A(ρ, δ)=????

Nuclear matter phase diagram (schematic)

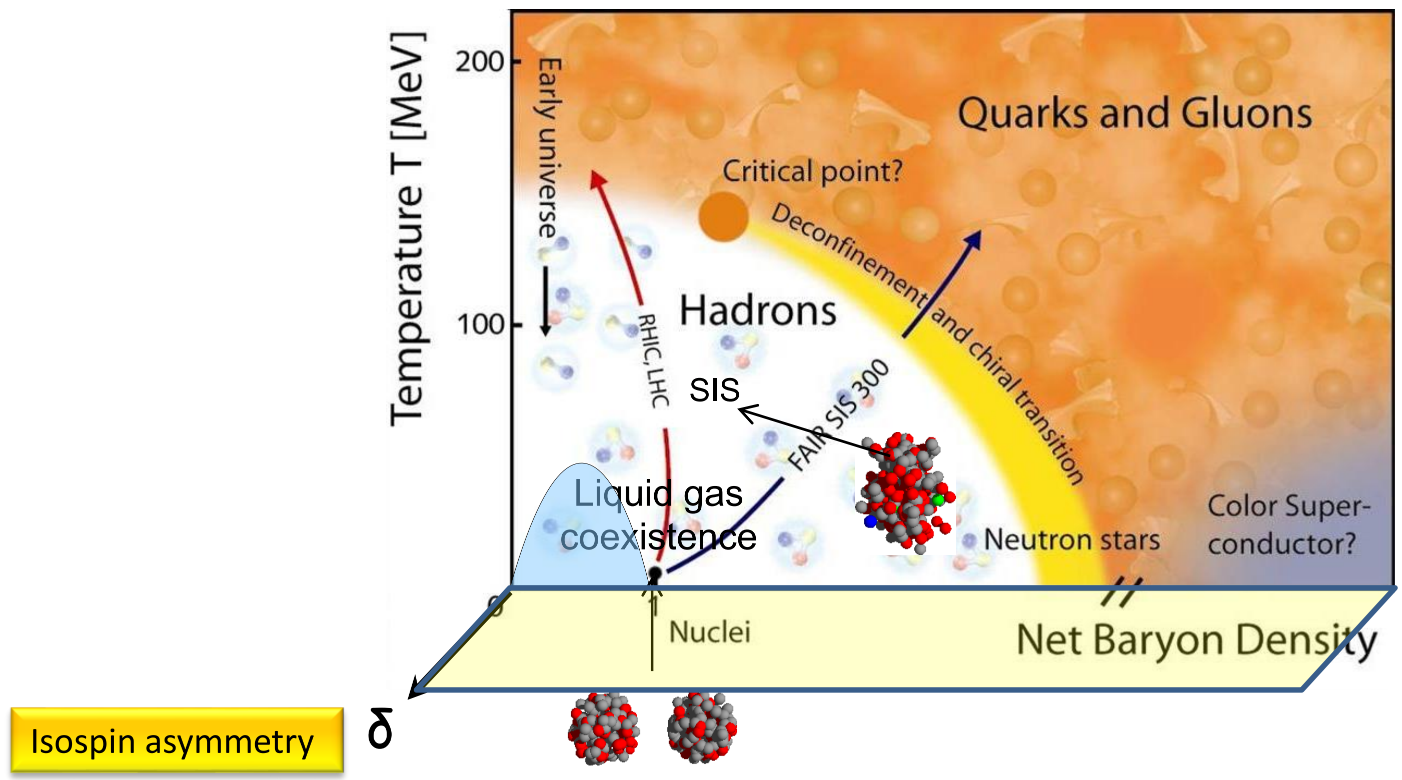

EOS for nuclear matter and Symmetry Energy

$$E(\rho,\delta) = E(\rho,\delta=0) + E_{sym}(\rho)\delta^2 + \ldots$$

$$\delta = \frac{\rho_n - \rho_p}{\rho_n + \rho_p} = \frac{N-Z}{A}$$

EOS for nuclear matter and Symmetry Energy

$$E(\rho,\delta) = E(\rho,\delta=0) + E_{sym}(\rho)\delta^2 + \ldots$$

$$\delta = \frac{\rho_n - \rho_p}{\rho_n + \rho_p} = \frac{N-Z}{A}$$

EOS for nuclear matter and Symmetry Energy

$$E(\rho,\delta) = E(\rho,\delta=0) + E_{sym}(\rho)\delta^2 + \dots$$

$$\delta = \frac{\rho_n - \rho_p}{\rho_n + \rho_p} = \frac{N-Z}{A}$$

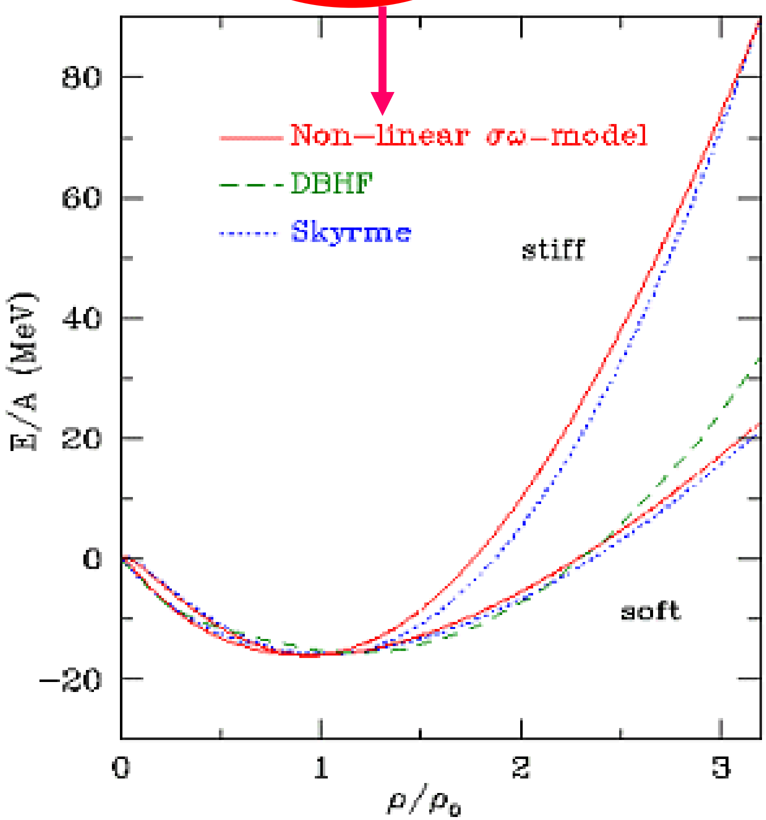

"How much energy is needed to compress hadronic matter?"

P. Danielewicz et al., Science 298 (2002)
C. Fuchs et al., PRL 86 (2001) 1974
Youngblood et al., PRL82 691 (1999)
A. Le Fevre et al., Nucl. Phys. A 945 (2016)

EOS for nuclear matter and Symmetry Energy

$$E(\rho,\delta) = E(\rho,\delta=0) + E_{sym}(\rho)\delta^2 + \ldots$$

$$\delta = \frac{\rho_n - \rho_p}{\rho_n + \rho_p} = \frac{N-Z}{A}$$

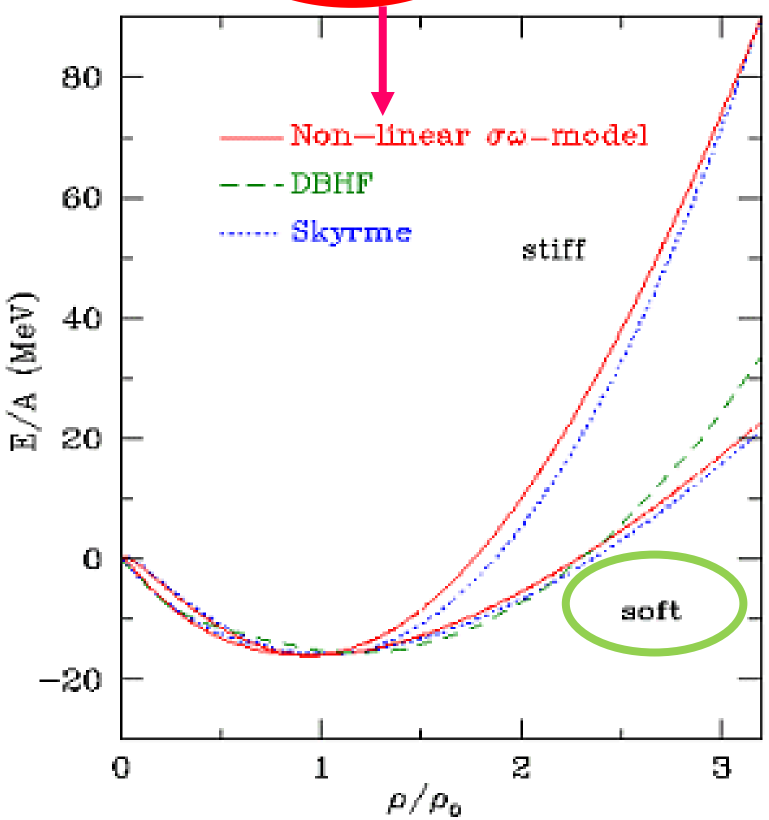

"How much energy is needed to compress hadronic matter?"

P. Danielewicz et al., Science 298 (2002)
C. Fuchs et al., PRL 86 (2001) 1974
Youngblood et al., PRL82 691 (1999)
A. Le Fevre et al., Nucl. Phys. A 945 (2016)

EOS for nuclear matter and Symmetry Energy

$$E(\rho,\delta) = E(\rho,\delta=0) + E_{sym}(\rho)\delta^2 + ...$$

$$\delta = \frac{\rho_n - \rho_p}{\rho_n + \rho_p} = \frac{N-Z}{A}$$

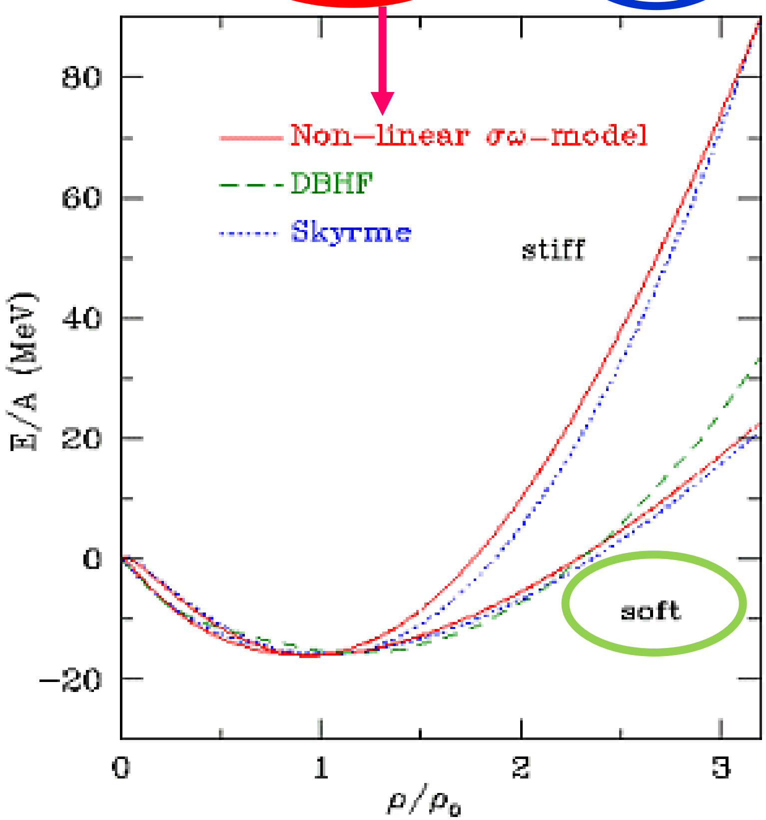

"How much energy is needed to compress hadronic matter?"

P. Danielewicz et al., Science 298 (2002)
C. Fuchs et al., PRL 86 (2001) 1974
Youngblood et al., PRL82 691 (1999)
A. Le Fevre et al., Nucl. Phys. A 945 (2016)

EOS for nuclear matter and Symmetry Energy

$$E(\rho,\delta) = E(\rho,\delta=0) + E_{sym}(\rho)\delta^2 + \ldots$$

$$\delta = \frac{\rho_n - \rho_p}{\rho_n + \rho_p} = \frac{N-Z}{A}$$

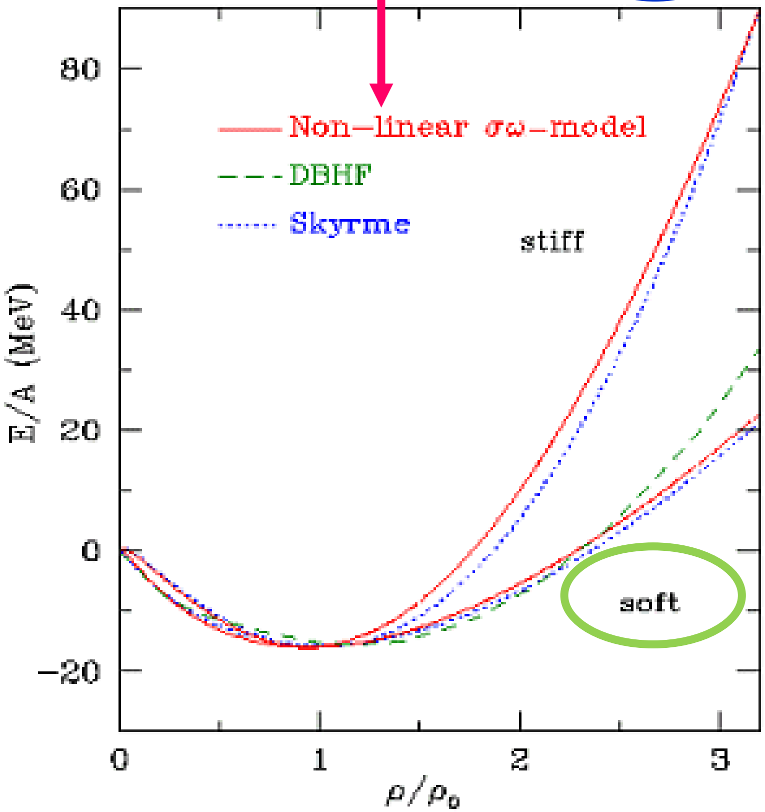

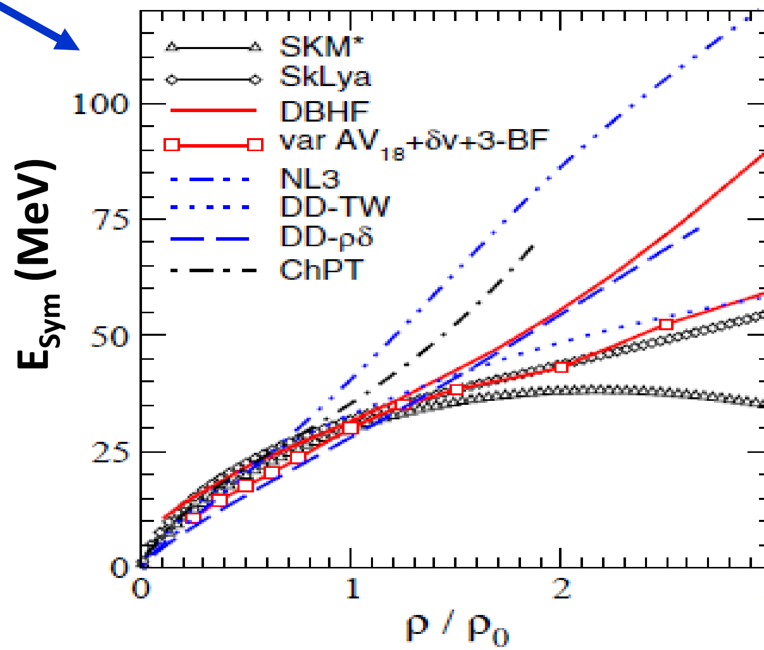

"How much energy is needed to compress hadronic matter?"

From Ab initio calculations (red) and phenomenological approaches

Fuchs and Wolter, EPJA 30 (2006)

P. Danielewicz et al., Science 298 (2002)
C. Fuchs et al., PRL 86 (2001) 1974
Youngblood et al., PRL82 691 (1999)
A. Le Fevre et al., Nucl. Phys. A 945 (2016)

EOS for nuclear matter and Symmetry Energy

$$E(\rho,\delta) = E(\rho,\delta=0) + E_{sym}(\rho)\delta^2 + \ldots$$

$$\delta = \frac{\rho_n - \rho_p}{\rho_n + \rho_p} = \frac{N-Z}{A}$$

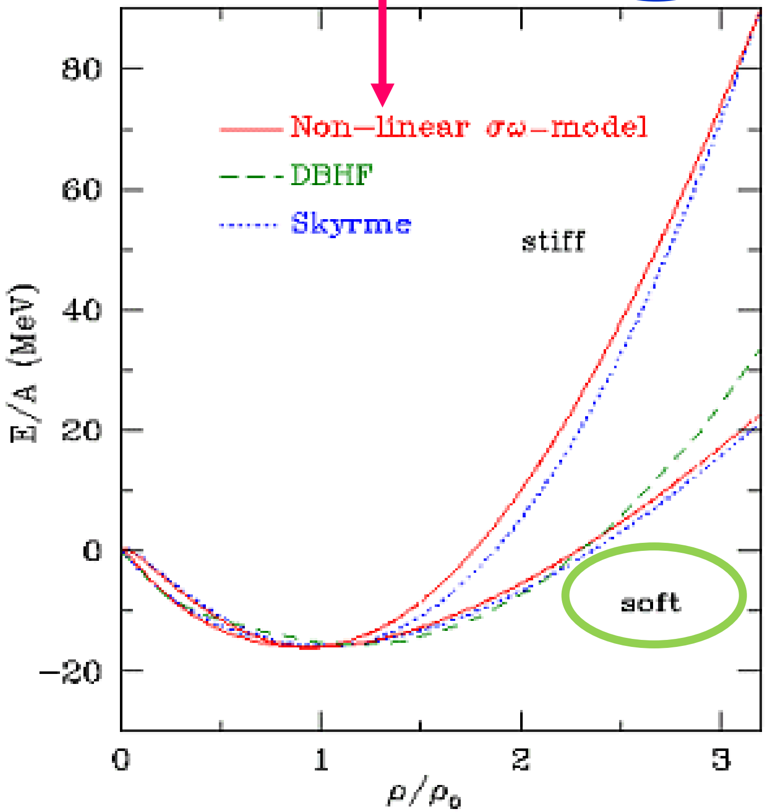

"How much energy is needed to compress hadronic matter?"

P. Danielewicz et al., Science 298 (2002)
C. Fuchs et al., PRL 86 (2001) 1974
Youngblood et al., PRL82 691 (1999)
A. Le Fevre et al., Nucl. Phys. A 945 (2016)

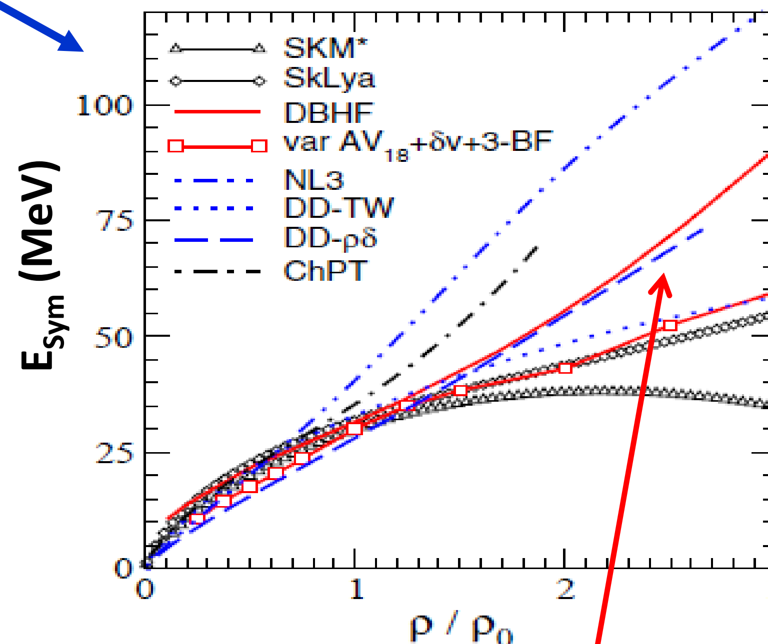

From Ab initio calculations (red) and phenomenological approaches

Fuchs and Wolter, EPJA 30 (2006)

High density…so important!

Study of the density dependence of the symmetry energy

Z. Xiao, Bao-An Li et al., PRL 102, 062502 (2009)

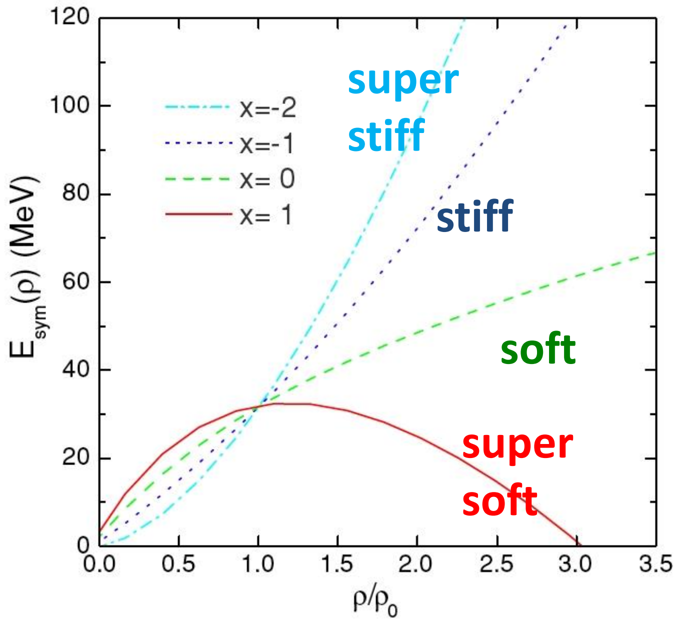

UrQMD: power law coefficient γ

$$E_{sym} = E_{sym}^{kin} + E_{sym}^{pot}$$
$$= 12\text{MeV}\cdot(\rho/\rho_0)^{2/3} + 22\text{MeV}\cdot(\rho/\rho_0)^{\gamma}$$

Study of the density dependence of the symmetry energy

Density $\rho <\approx \rho_0$ (sub- and around saturation density, $\rho_0 = 0.17\ fm^{-3}$)

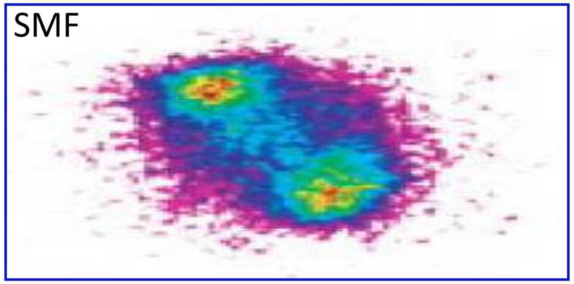

Isospin Transport properties in HI collisions at Fermi Energies, (diffusion, fractionation, migration), flows, n/p emission , clusterization….

Nuclear structure (IAS), Resonances (PDR,GDR), n skin thickness …

Z. Xiao, Bao-An Li et al., PRL 102, 062502 (2009)

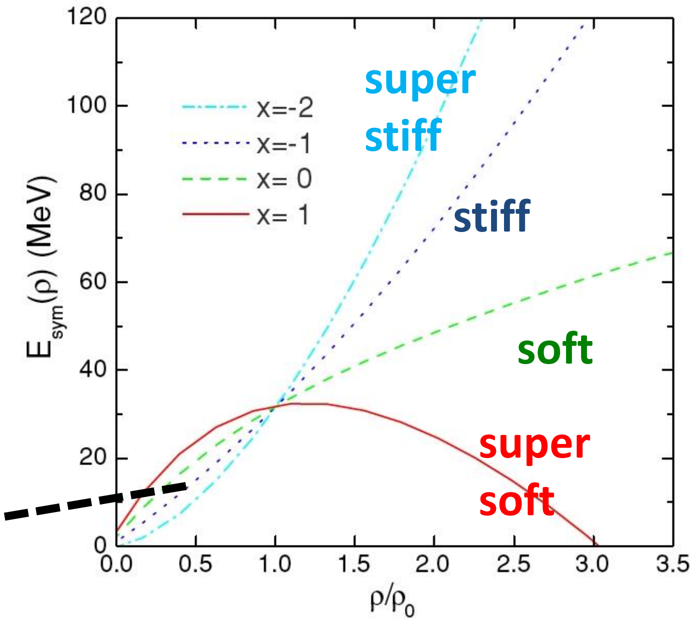

UrQMD: power law coefficient γ

$$E_{sym} = E_{sym}^{kin} + E_{sym}^{pot}$$
$$= 12MeV \cdot (\rho/\rho_0)^{2/3} + 22MeV \cdot (\rho/\rho_0)^{\gamma}$$

Study of the density dependence of the symmetry energy

Density $\rho <\approx \rho_0$ (sub- and around saturation density, $\rho_0=0.17\ fm^{-3}$)

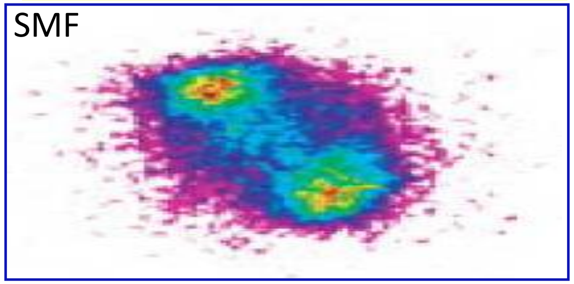

Isospin Transport properties in HI collisions at Fermi Energies, (diffusion, fractionation, migration), flows, n/p emission , clusterization….

Nuclear structure (IAS), Resonances (PDR,GDR), n skin thickness …

Z. Xiao, Bao-An Li et al., PRL 102, 062502 (2009)

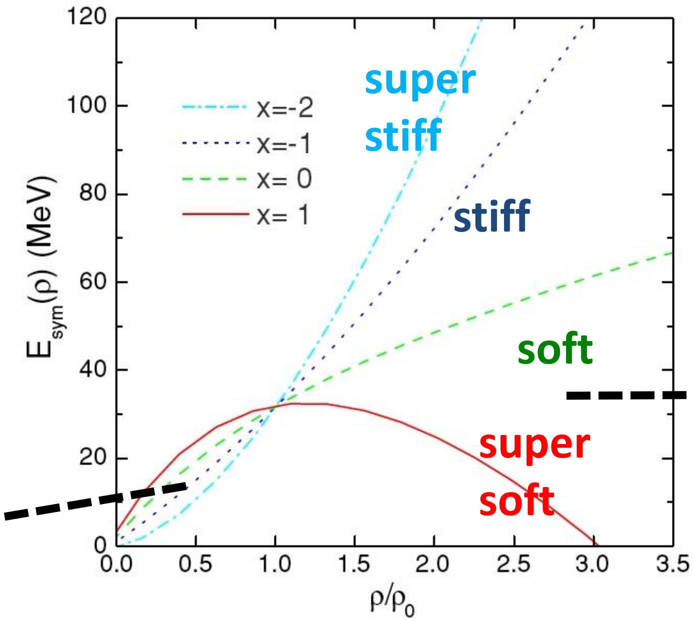

UrQMD: power law coefficient γ

$$E_{sym} = E_{sym}^{kin} + E_{sym}^{pot}$$
$$= 12MeV\cdot(\rho/\rho_0)^{2/3} + 22MeV\cdot(\rho/\rho_0)^{\gamma}$$

Density $\rho>\rho_0$ (supra-saturation): connected with *neutron stars, supernovae expl.*

Pre-equilibrium emission, particle production (π,K), collective flows in relativistic HI collisions

Study of the density dependence of the symmetry energy

Density $\rho <\approx \rho_0$ (sub- and around saturation density, ρ_0=0.17 fm^{-3})

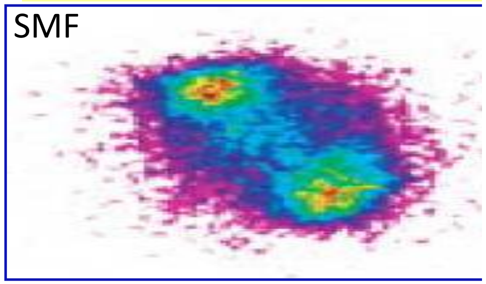

Isospin Transport properties in HI collisions at Fermi Energies, (diffusion, fractionation, migration), flows, n/p emission , clusterization

Nuclear structure (IAS), Resonances (PDR,GDR), n skin thickness …

Z. Xiao, Bao-An Li et al., PRL 102, 062502 (2009)

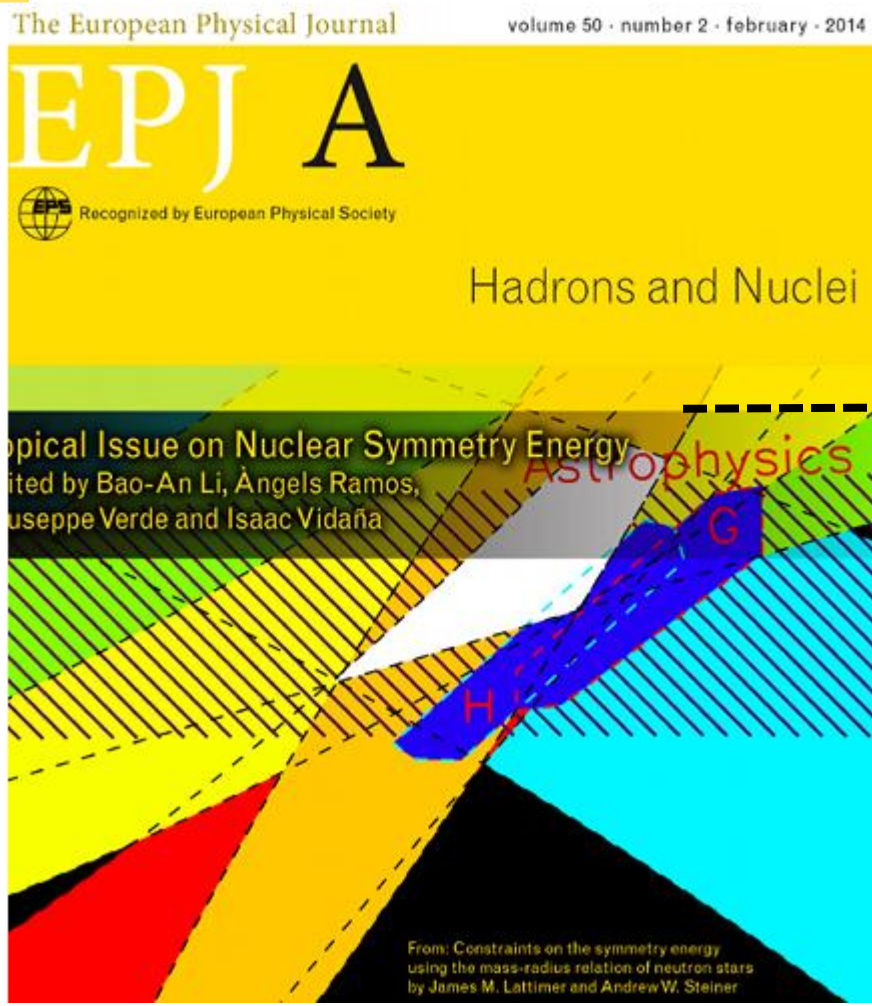

See Eur. Phys. J. A, 50 2 (2014) topical issue on Symmetry Energy

Density $\rho > \rho_0$ (supra-saturation): connected with *neutron stars, supernovae expl.*

Pre-equilibrium emission, particle production (π,K), collective flows in relativistic HI collisions

High densities: flows

$$\frac{dN}{d(\phi-\phi_R)}(y,p_t)=\frac{N_0}{2\pi}\left(1+2\sum_{n\geq 1} v_n \cos n(\phi-\phi_R)\right)$$

Y = rapidity
pt = transverse momentum

$$V_2(y,p_t)=\left\langle \frac{p_x^2-p_y^2}{p_t^2}\right\rangle$$

Elliptic flow: competition between in plane ($v_2>0$) and out-of-plane ejection ($v_2<0$)

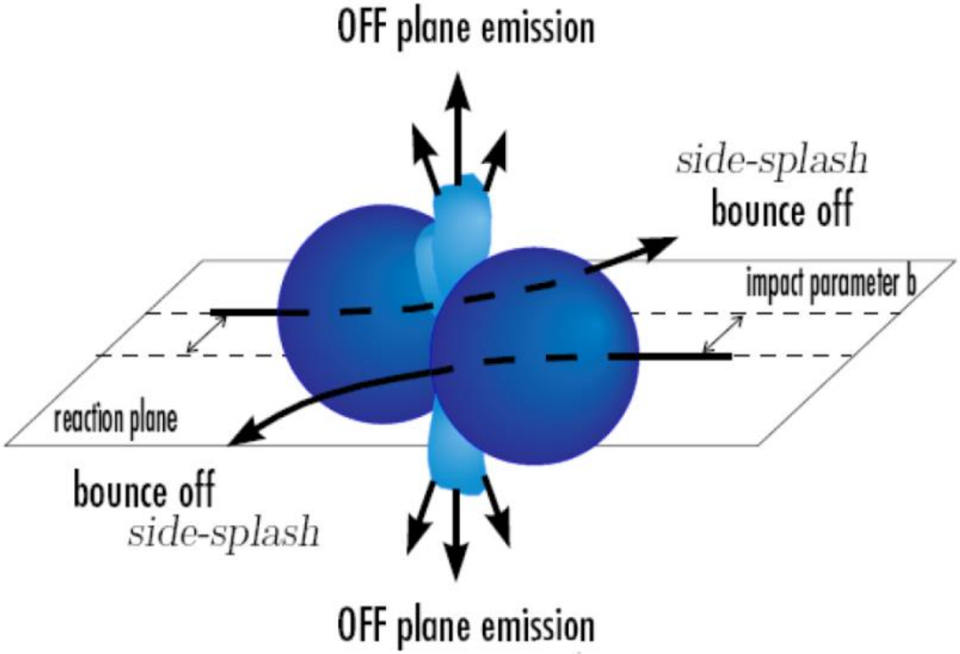

High densities: flows

$$\frac{dN}{d(\phi-\phi_R)}(y,p_t)=\frac{N_0}{2\pi}\left(1+2\sum_{n\geq1}v_n\cos n(\phi-\phi_R)\right)$$

Y = rapidity
pt = transverse momentum

UrQMD :Au+Au @ 400 AMeV
5.5<b<7.5 fm

$$V_2(y,p_t)=\left\langle\frac{p_x^2-p_y^2}{p_t^2}\right\rangle$$

Elliptic flow: competition between in plane (v_2>0) and out-of-plane ejection (v_2<0)

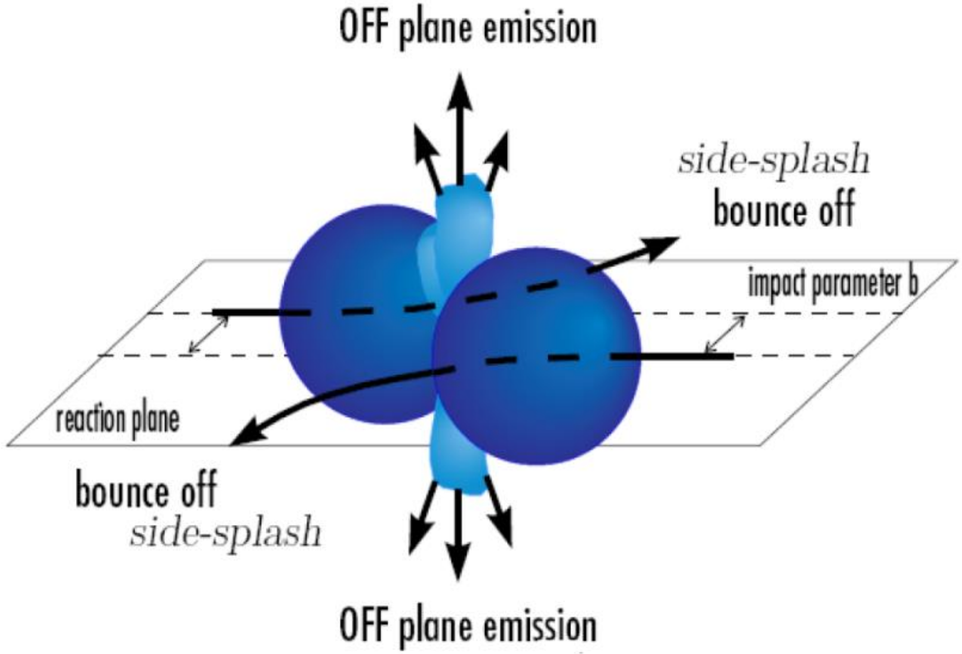

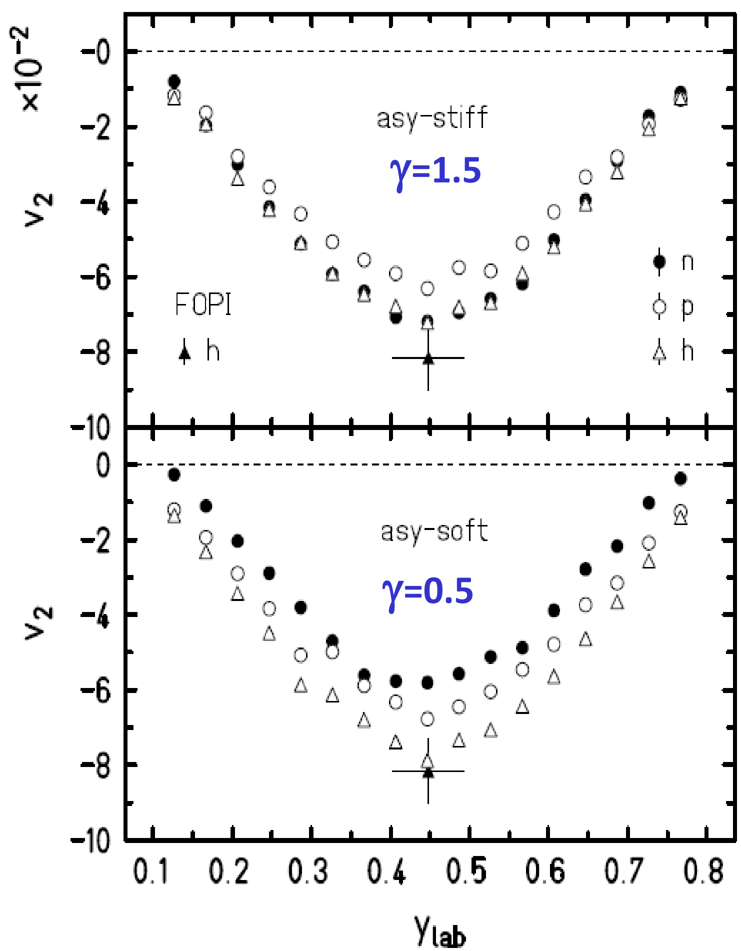

$$E_{sym}=E_{sym}^{pot}+E_{sym}^{kin}$$
$$=22\,\text{MeV}\cdot(\rho/\rho_0)^\gamma+12\,\text{MeV}\cdot(\rho/\rho_0)^{2/3}$$

Qingfeng Li, J. Phys. G31 1359-1374 (2005)
P.Russotto et al., Phys. Lett. B 697 (2011)

FOPI/LAND experiment on neutron squeeze out (1991)

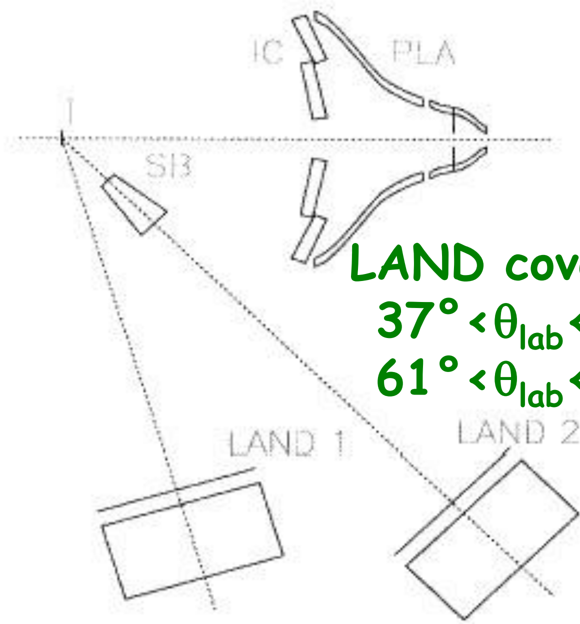

LAND coverage
$37° < \theta_{lab} < 53°$
$61° < \theta_{lab} < 85°$

UrQMD:
momentum dep. of isoscalar field
momentum dep. of NNECS
momentum independent power-law
parameterization of the symmetry energy

$$\gamma = 0.9 \pm 0.4$$

$$L = 83 \pm 26$$

Y. Leifels et al., PRL 71, 963 (1993)
P.Russotto et al., PLB 697 (2011)

FOPI/LAND experiment on neutron squeeze out (1991)

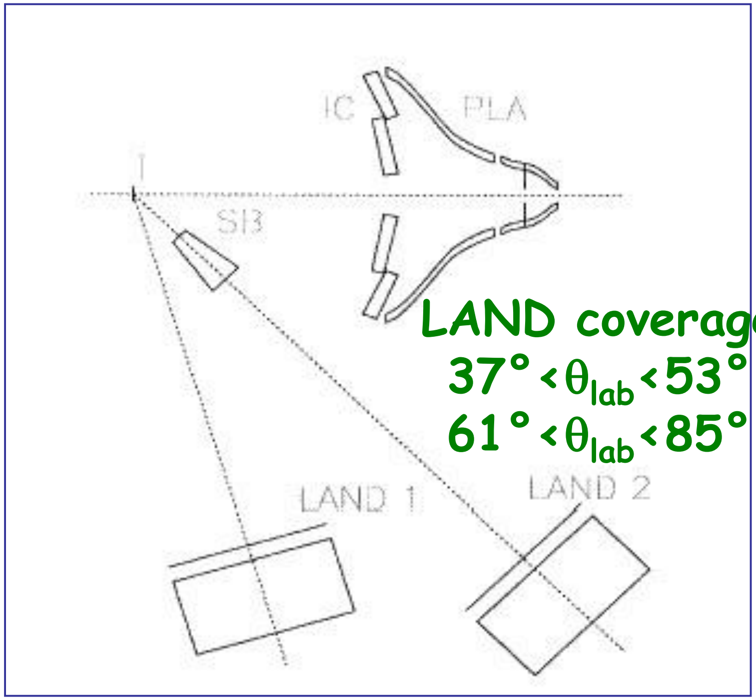

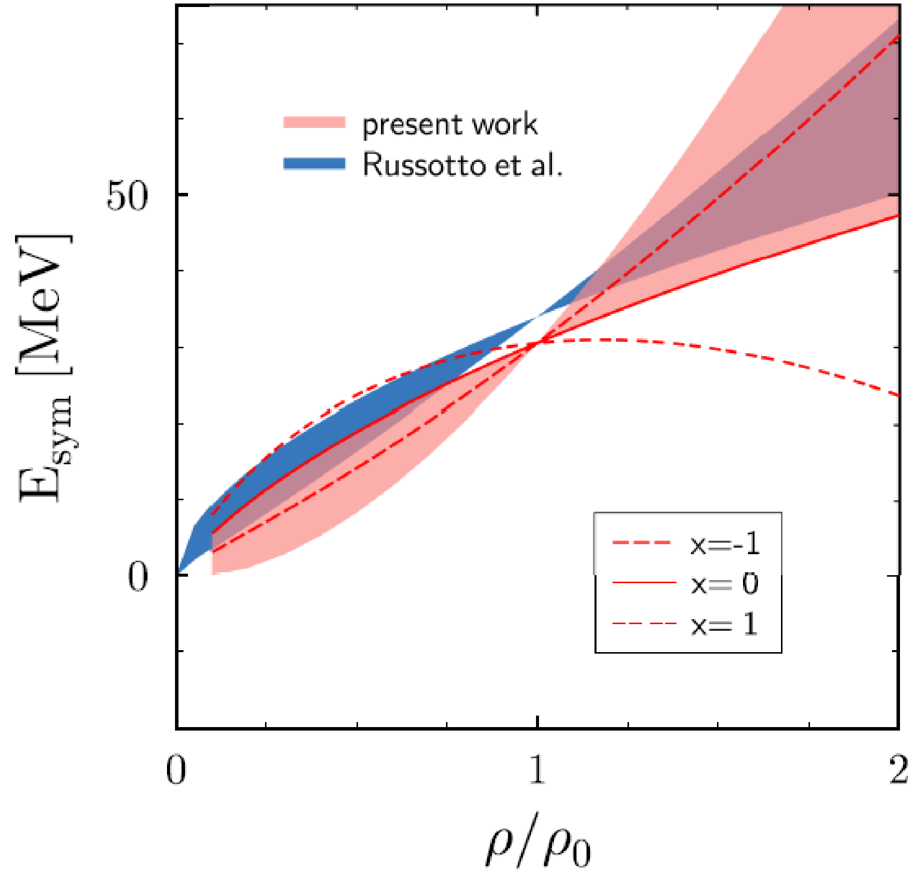

UrQMD:

momentum dep. of isoscalar field

momentum dep. of NNECS

momentum independent power-law parameterization of the symmetry energy

$\gamma = 0.9 \pm 0.4$

$L = 83 \pm 26$

Tübingen-QMD:

density dep. of NNECS

asymmetry dep. of NNECS

soft vs. hard EoS

width of wave packets

momentum dependent (Gogny inspired) parameterization of the symmetry energy

M.D. Cozma et al. , PLB 700, 139 (2011) & PRC88 044912 (2013)

Y. Leifels et al., PRL 71, 963 (1993)

P.Russotto et al., PLB 697 (2011)

ASY-EOS S394 experiment @ GSI Darmstadt (May 2011)

Au+Au, $^{96}Zr+^{96}Zr$, $^{96}Ru+^{96}Ru$ @ 400 AMev

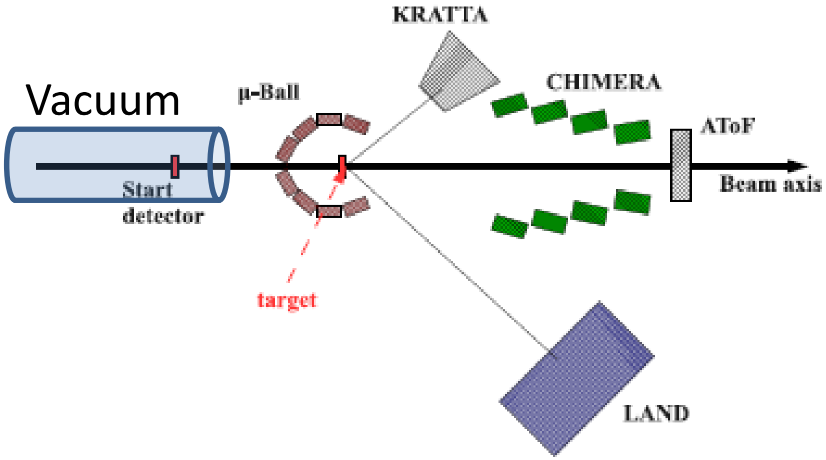

ASY-EOS S394 experiment @ GSI Darmstadt (May 2011)

Au+Au, $^{96}Zr+^{96}Zr$, $^{96}Ru+^{96}Ru$ @ 400 AMev

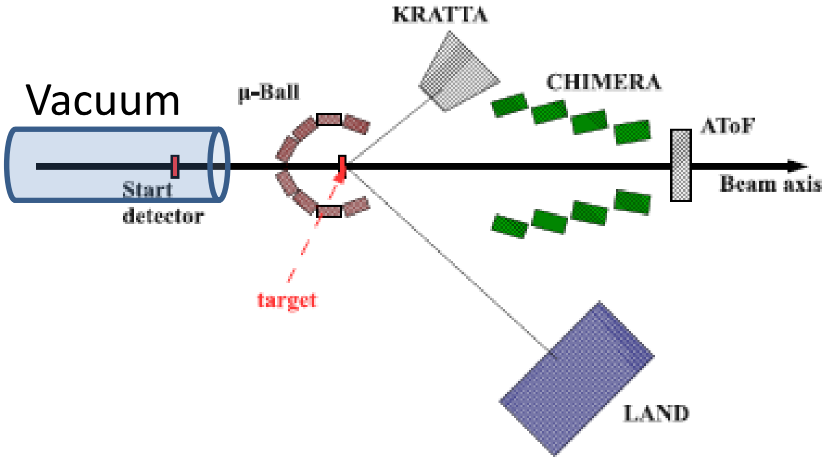

TOFWALL: **96 plastic bars; ToF, ΔE, X-Y position.**
Trigger, impact parameter and reaction plane determination

ASY-EOS S394 experiment @ GSI Darmstadt (May 2011)

Au+Au, $^{96}Zr+^{96}Zr$, $^{96}Ru+^{96}Ru$ @ 400 AMev

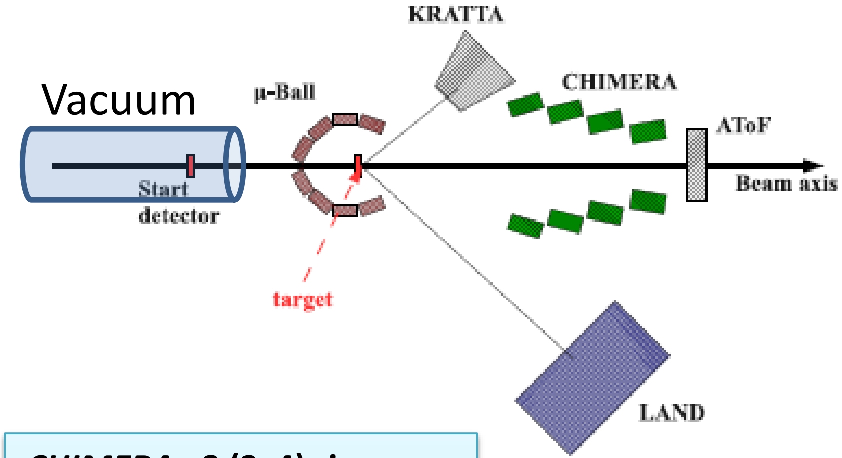

TOFWALL: 96 plastic bars; ToF, ΔE, X-Y position. Trigger, impact parameter and reaction plane determination

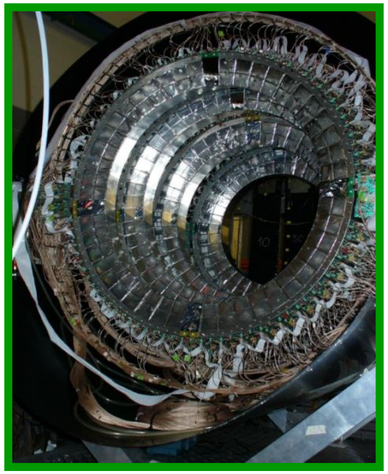

CHIMERA: 8 (2x4) rings, high granularity CsI(Tl), 352 detectors 7°<θ<20° + 16x2 pads silicon detectors. Light charged particle identification by PSD. Multiplicity, Z, A, Energy: impact parameter and reaction plane determination

ASY-EOS S394 experiment @ GSI Darmstadt (May 2011)

Au+Au, $^{96}Zr+^{96}Zr$, $^{96}Ru+^{96}Ru$ @ 400 AMev

***μBall*:** 4 rings 50 CsI(Tl), Θ>60°. Discriminate target vs. reactions with air. Multiplicity and reaction plane measurements.

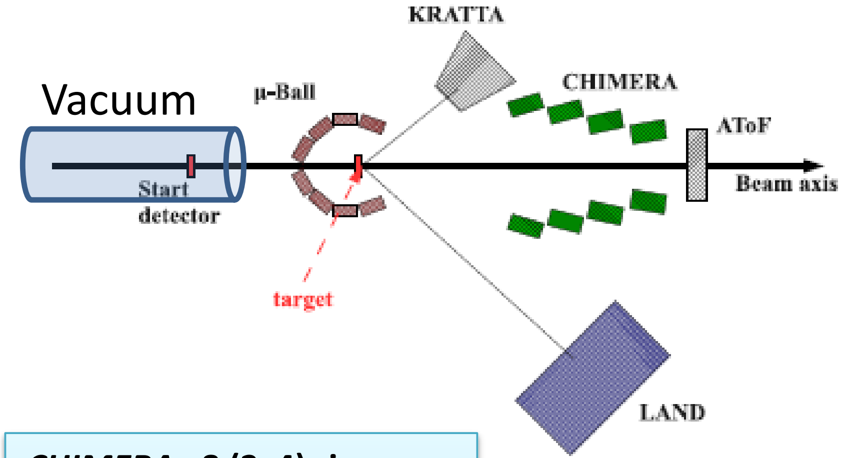

***TOFWALL*:** 96 plastic bars; ToF, ΔE, X-Y position. Trigger, impact parameter and reaction plane determination

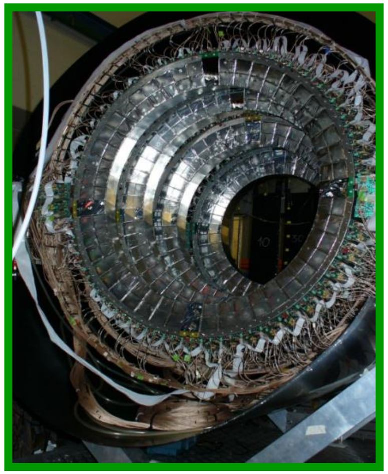

***CHIMERA*:** 8 (2x4) rings, high granularity CsI(Tl), 352 detectors 7°<θ<20° + 16x2 pads silicon detectors. Light charged particle identification by PSD. Multiplicity, Z, A, Energy: impact parameter and reaction plane determination

ASY-EOS S394 experiment @ GSI Darmstadt (May 2011)

Au+Au, $^{96}Zr+^{96}Zr$, $^{96}Ru+^{96}Ru$ @ 400 AMev

μBall: 4 rings 50 CsI(Tl), Θ>60°. Discriminate target vs. reactions with air.
Multiplicity and reaction plane measurements.

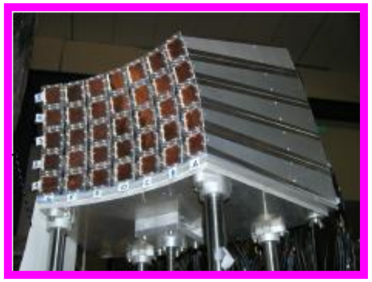

KraTTA: 35 (5x7) triple telescopes (Si-CsI-CsI) placed at 21°<Θ<60° with digital readout . Light particles and IMFs emitted at midrapidity

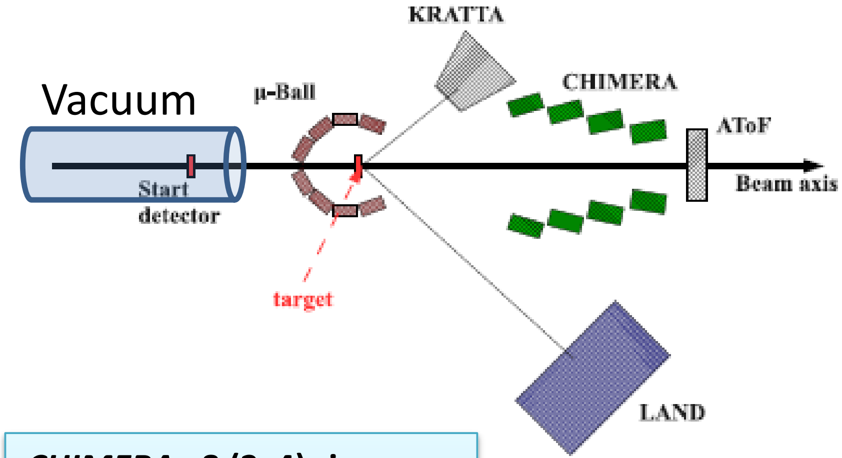

TOFWALL: 96 plastic bars; ToF, ΔE, X-Y position. Trigger, impact parameter and reaction plane determination

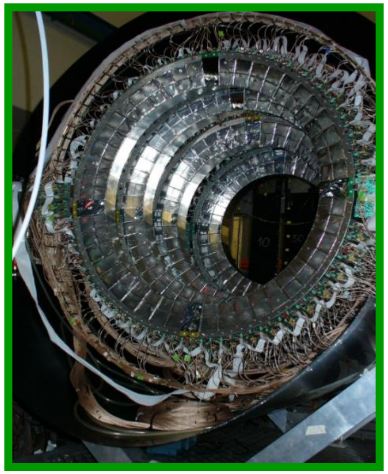

CHIMERA: 8 (2x4) rings, high granularity CsI(Tl), 352 detectors 7°<θ<20° + 16x2 pads silicon detectors. Light charged particle identification by PSD. Multiplicity, Z, A, Energy: impact parameter and reaction plane determination

ASY-EOS S394 experiment @ GSI Darmstadt (May 2011)

Au+Au, $^{96}Zr+^{96}Zr$, $^{96}Ru+^{96}Ru$ @ 400 AMev

μBall: 4 rings 50 CsI(Tl), Θ>60°. Discriminate target vs. reactions with air. Multiplicity and reaction plane measurements.

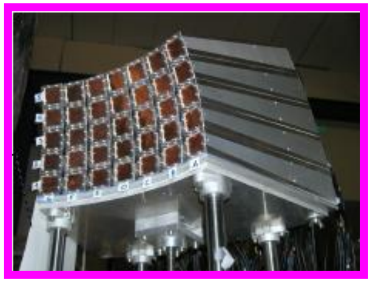

KraTTA: 35 (5x7) triple telescopes (Si-CsI-CsI) placed at 21°<Θ<60° with digital readout . Light particles and IMFs emitted at midrapidity

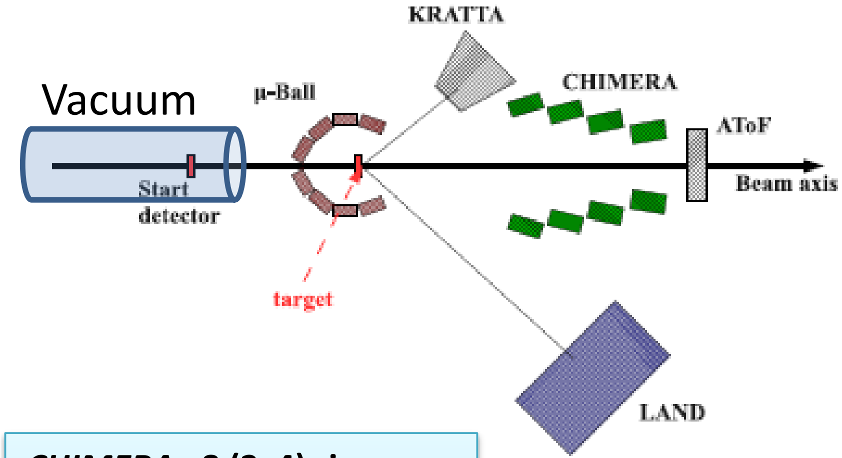

TOFWALL: 96 plastic bars; ToF, ΔE, X-Y position. Trigger, impact parameter and reaction plane determination

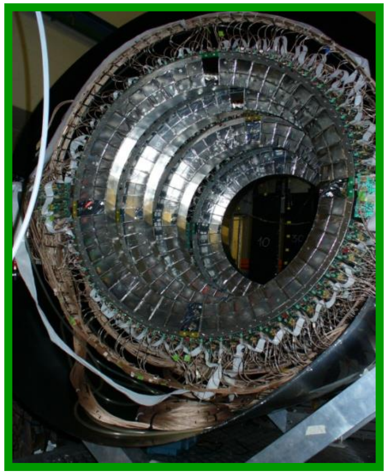

CHIMERA: 8 (2x4) rings, high granularity CsI(Tl), 352 detectors 7°<θ<20° + 16x2 pads silicon detectors. Light charged particle identification by PSD. Multiplicity, Z, A, Energy: impact parameter and reaction plane determination

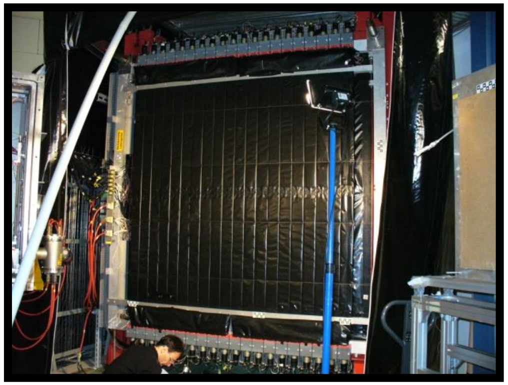

LAND: Large Area Neutron Detector . Plastic scintillators sandwiched with Fe 2x2x1 m^3 plus plastic veto wall. New Taquila front-end electronics. Neutrons and Hydrogen detection. Flow measurements

ASY-EOS S394 experiment @ GSI Darmstadt (May 2011)

Au+Au, $^{96}Zr+^{96}Zr$, $^{96}Ru+^{96}Ru$ @ 400 AMev

μBall: 4 rings 50 CsI(Tl), Θ>60°. Discriminate target vs. reactions with air. Multiplicity and reaction plane measurements.

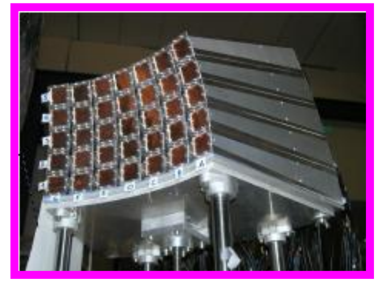

KraTTA: 35 (5x7) triple telescopes (Si-CsI-CsI) placed at 21°<Θ<60° with digital readout . Light particles and IMFs emitted at midrapidity

Shadow bar: evaluation of background neutrons in LAND

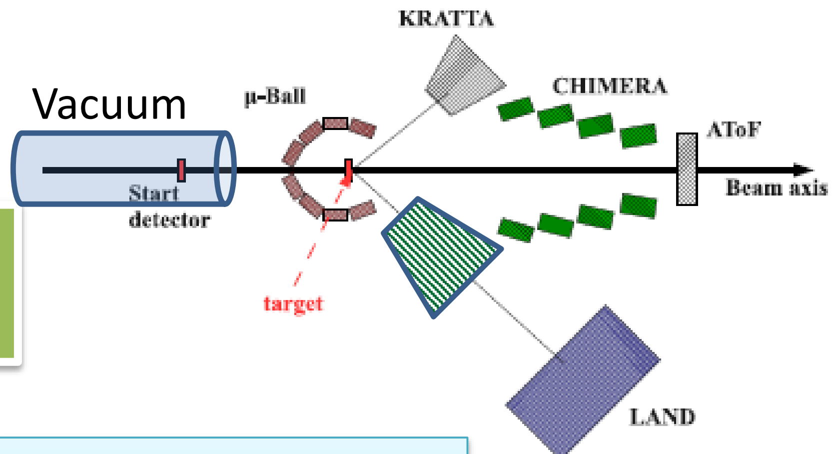

TOFWALL: 96 plastic bars; ToF, ΔE, X-Y position. Trigger, impact parameter and reaction plane determination

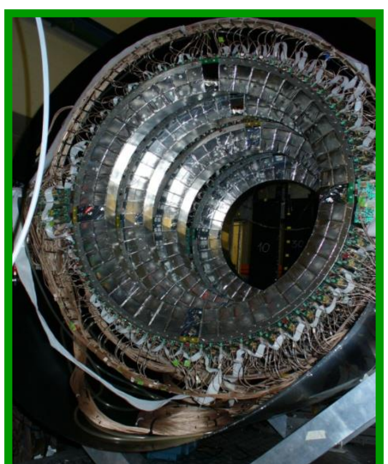

CHIMERA: 8 (2x4) rings, high granularity CsI(Tl), 352 detectors 7°<θ<20° + 16x2 pads silicon detectors. Light charged particle identification by PSD. Multiplicity, Z, A, Energy: impact parameter and reaction plane determination

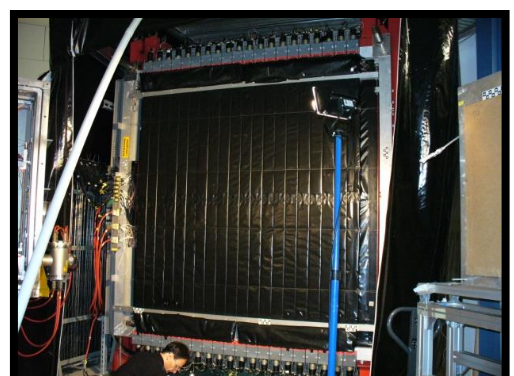

LAND: Large Area Neutron Detector . Plastic scintillators sandwiched with Fe 2x2x1 m^3 plus plastic veto wall. New Taquila front-end electronics. Neutrons and Hydrogen detection. Flow measurements

Au+Au @ 400 A.MeV: Some kinematics

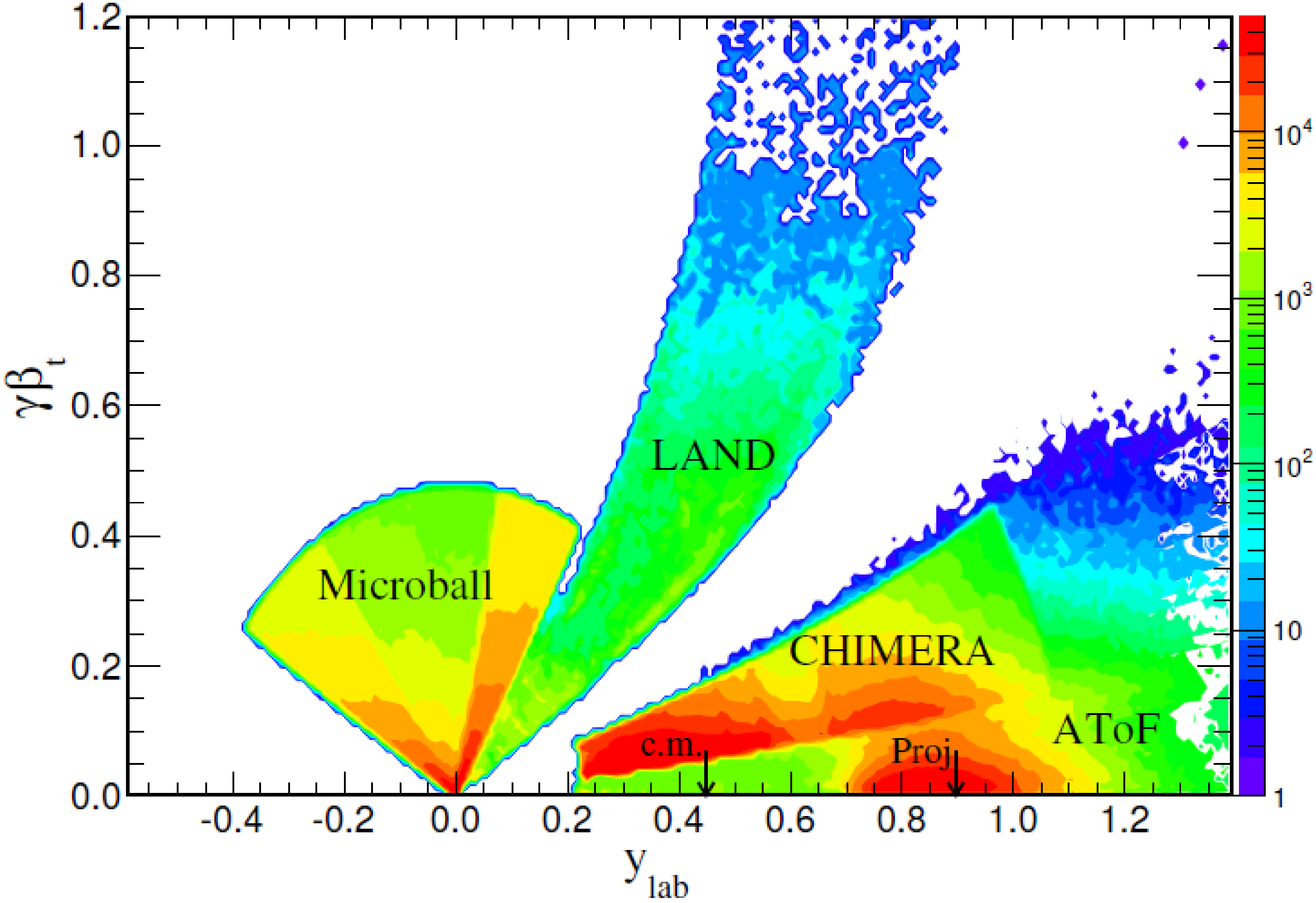

P. Russotto et al., EPJA 50, 38 (2014).
P. Russotto et al., PRC 94, 034608 (2016).

Au+Au @ 400 A.MeV: Some kinematics

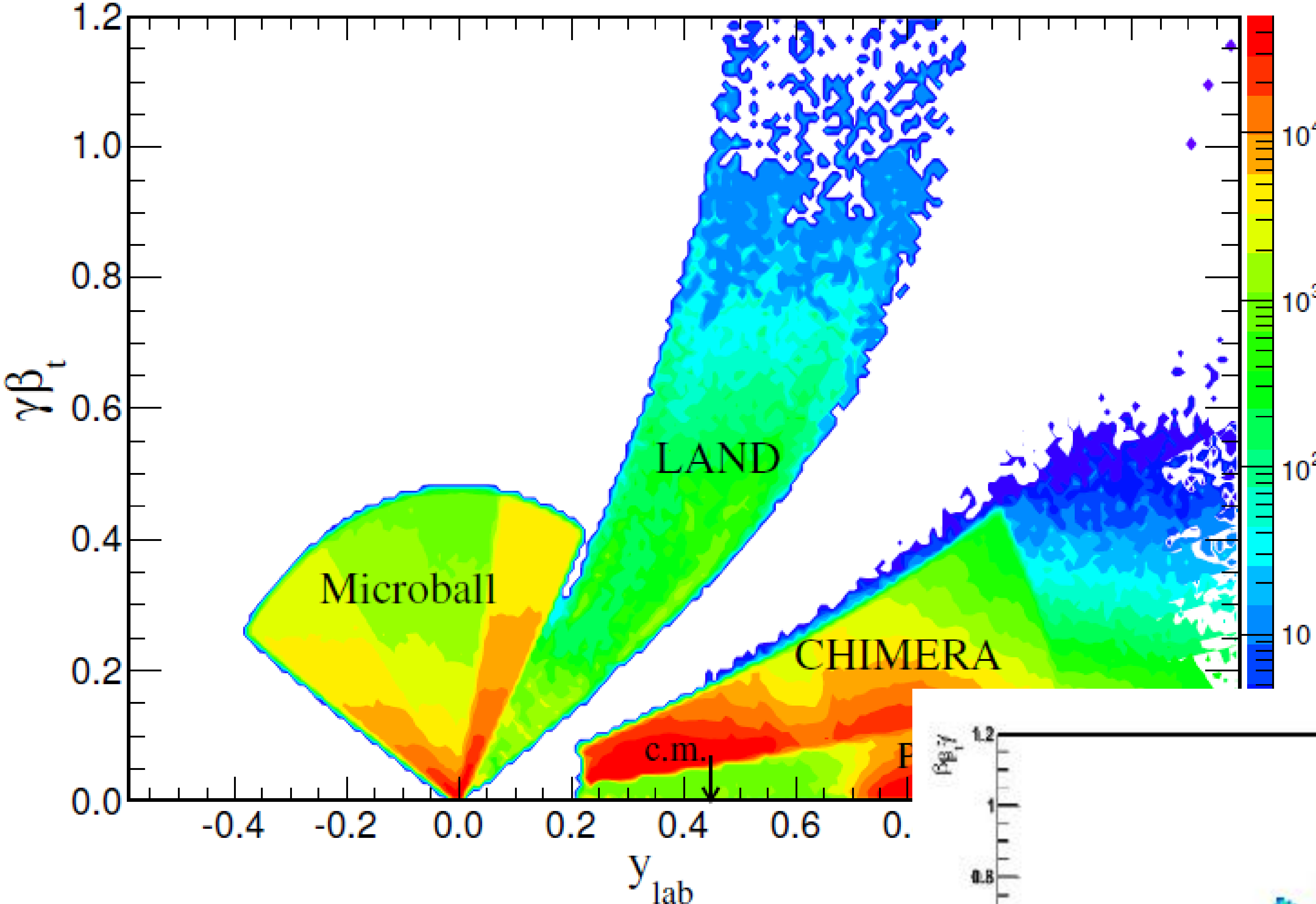

KRATTA:
J. Lukasik et al.,
Nucl. Instr. Meth.
709 (2013) 120128

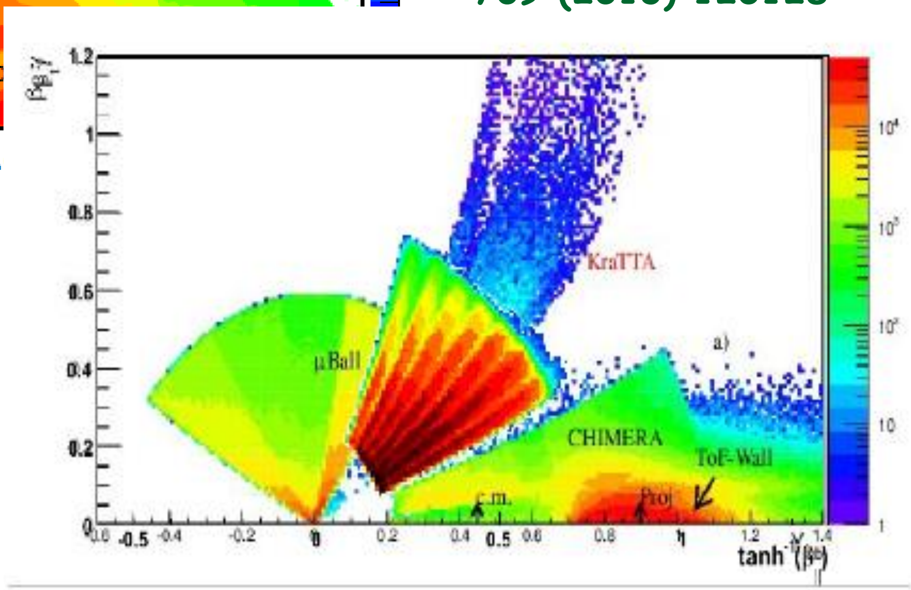

P. Russotto et al., EPJA 50, 38 (2014).
P. Russotto et al., PRC 94, 034608 (2016).

Results…

Au+Au @ 400 AMeV b<7.5 fm

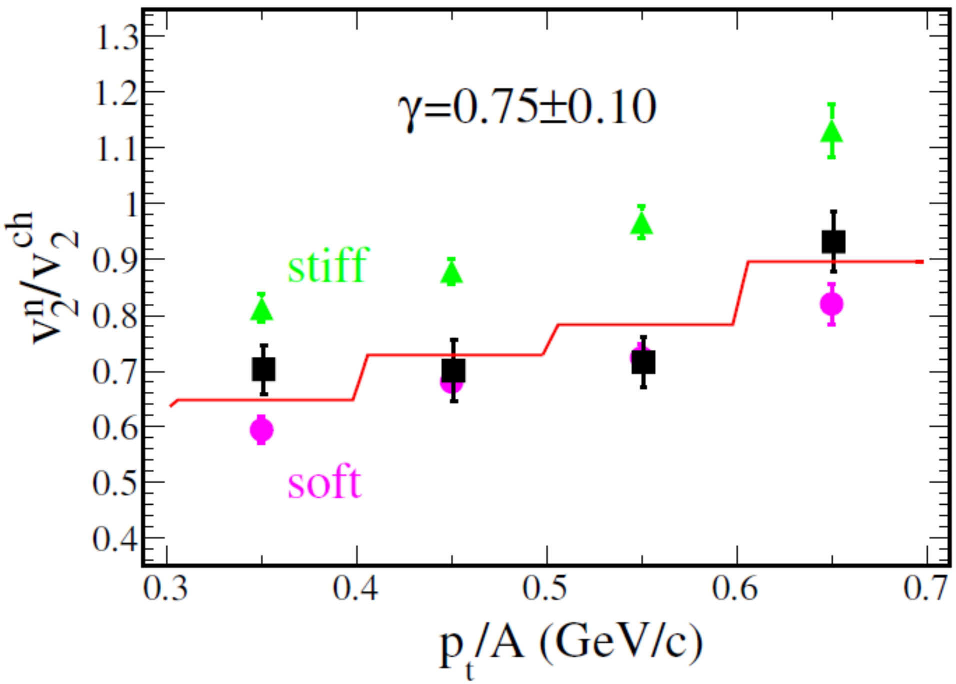

Results…

Au+Au @ 400 AMeV b<7.5 fm

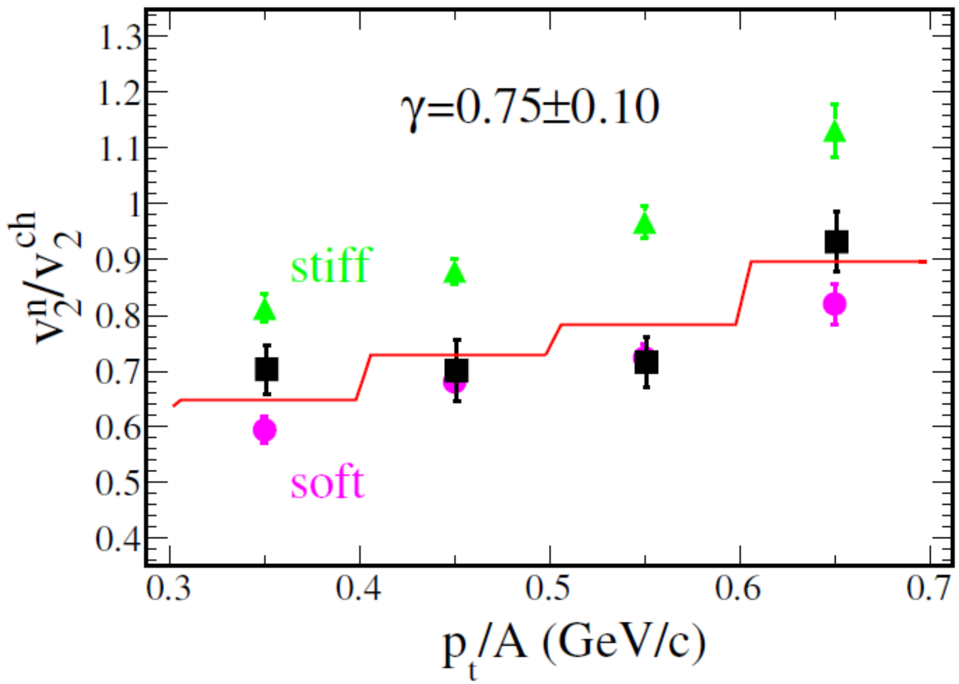

FOPI-LAND DATA : P.Russotto et al., Phys. Lett. B 697 (2011)

γ = 0.9 ± 0.4 ; L=83±26

Results…

Au+Au @ 400 AMeV b<7.5 fm

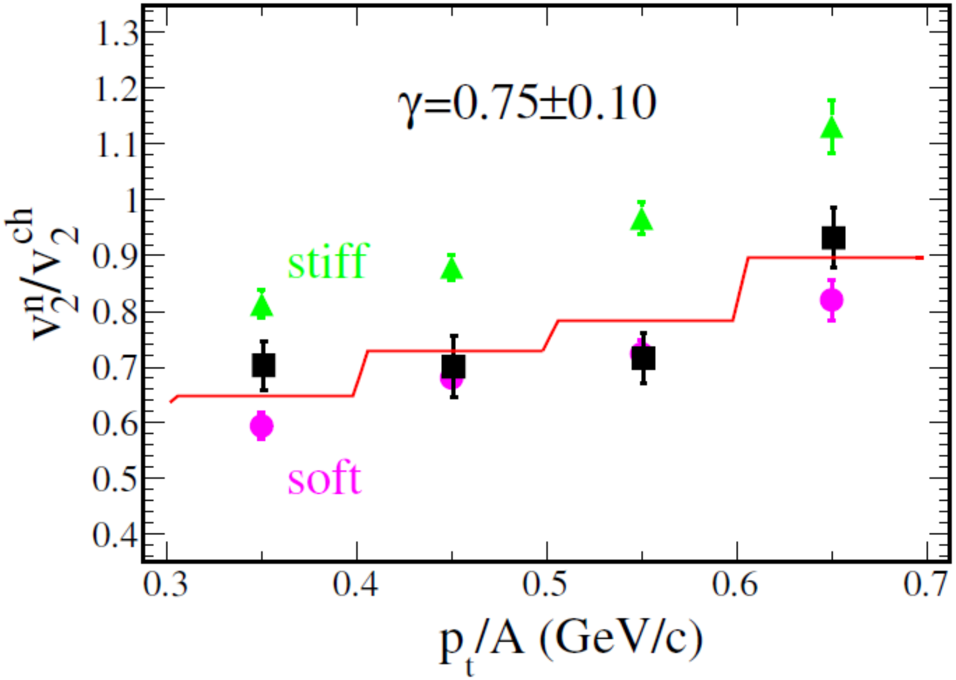

FOPI-LAND DATA : P.Russotto et al., Phys. Lett. B 697 (2011)

γ = 0.9 ± 0.4 ; L=83±26

ASY-EOS DATA: P. Russotto et al., PRC 94, 034608 (2016)

γ = 0.72± 0.19 ; L=72±13

Results…

Au+Au @ 400 AMeV b<7.5 fm

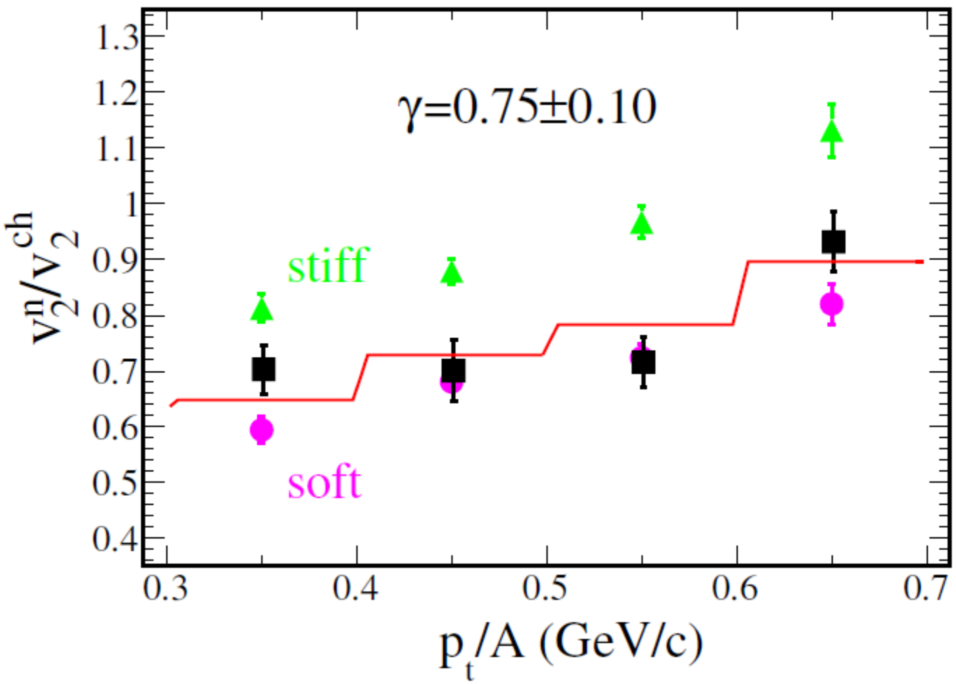

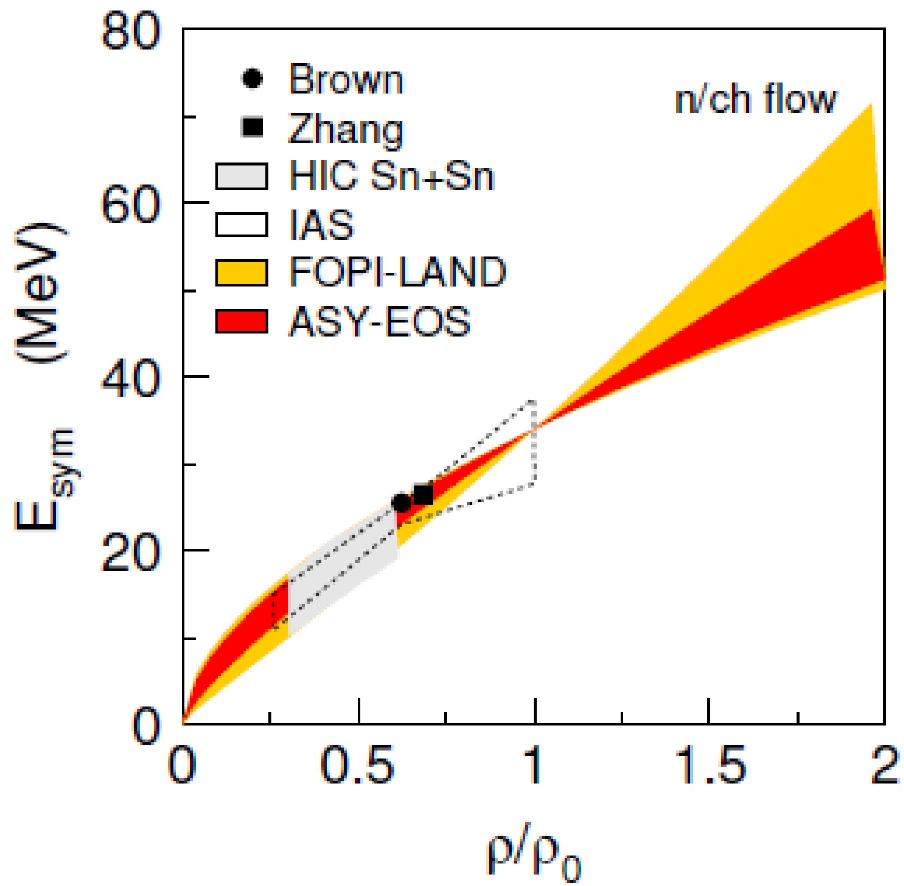

FOPI-LAND DATA : P.Russotto et al., Phys. Lett. B 697 (2011)
γ = 0.9 ± 0.4 ; L=83±26

ASY-EOS DATA: P. Russotto et al., PRC 94, 034608 (2016)
γ = 0.72± 0.19 ; L=72±13

HIC: (mainly Isospin diffusion for Sn+Sn) M.B. Tsang et al., PRC 86, 015803 (2012)

neutron skin thickness, binding energies,….: Brown, PRL 111, 232502 (2013); Zhang & Chen, Phys. Lett. B 726 (2013), Danielewicz & Lee, NPA922 (2014).

Results…

Au+Au @ 400 AMeV b<7.5 fm

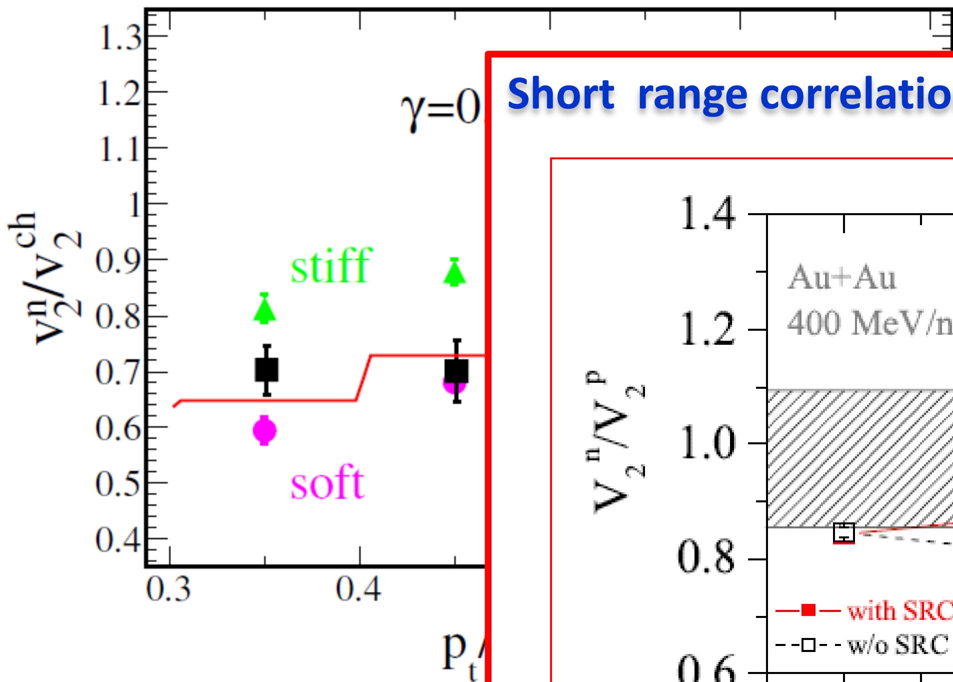

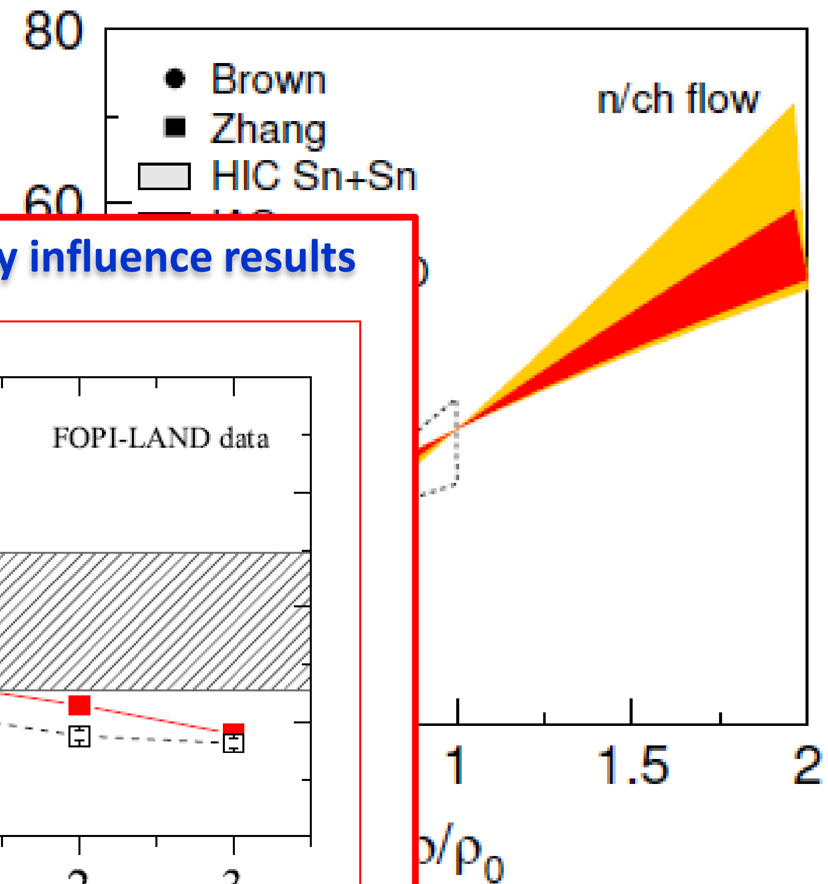

Short range correlations may influence results

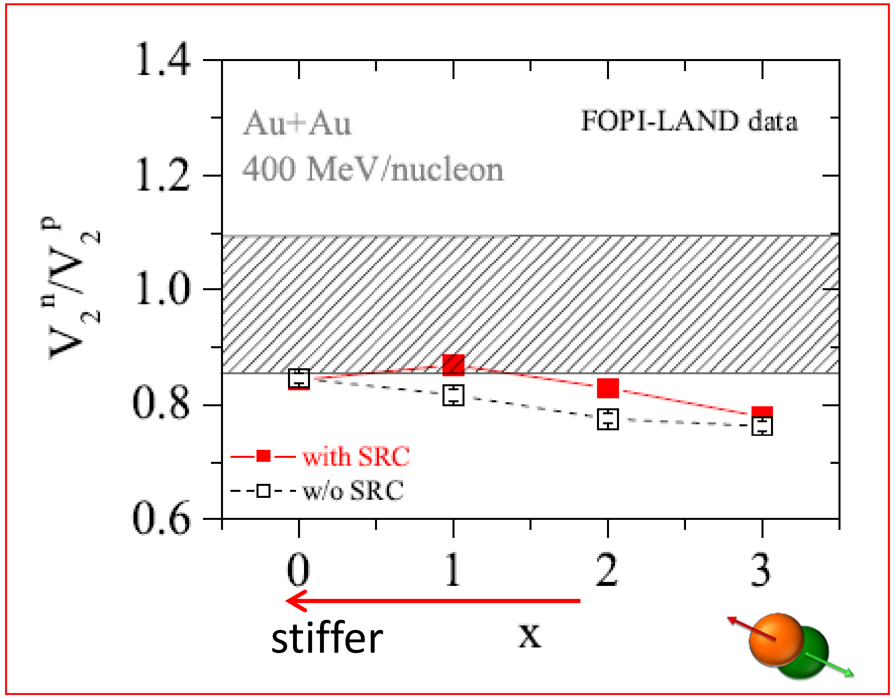

*Gao-Chan Yong, Phys. Rev. C **93**, 044610 (2016)*

*F. Zhang, Gao-Chan Yong, EPJA **52**, 350 (2016)*

FOPI-LAND DAT
al., Phys. Let
γ = 0.9 ± 0

ASY-EOS DATA: P. Russotto et al., PRC 94, 034608 (2016)
γ = 0.72± 0.19 ; L=72±13

n diffusion for
et al., PRC 86,

hickness, binding energies,….: Brown, PRL 111, 232502 (2013); Zhang & Chen, Phys. Lett. B 726 (2013), Danielewicz & Lee, NPA922 (2014).

UrQMD prediction for some interesting beams (and δ^2)

$^{197}Au+^{197}Au$ @ 400, 600, 800, 1000,1500 AMeV (0.039+0.039)

$^{132}Sn+^{124}Sn$ @ 400, 600, 800 AMeV (0.059+0.037)

$^{106}Sn+^{112}Sn$ @ 400, 600, 800 AMeV (0.003+0.011)

At midvelocity b/bred <0.53

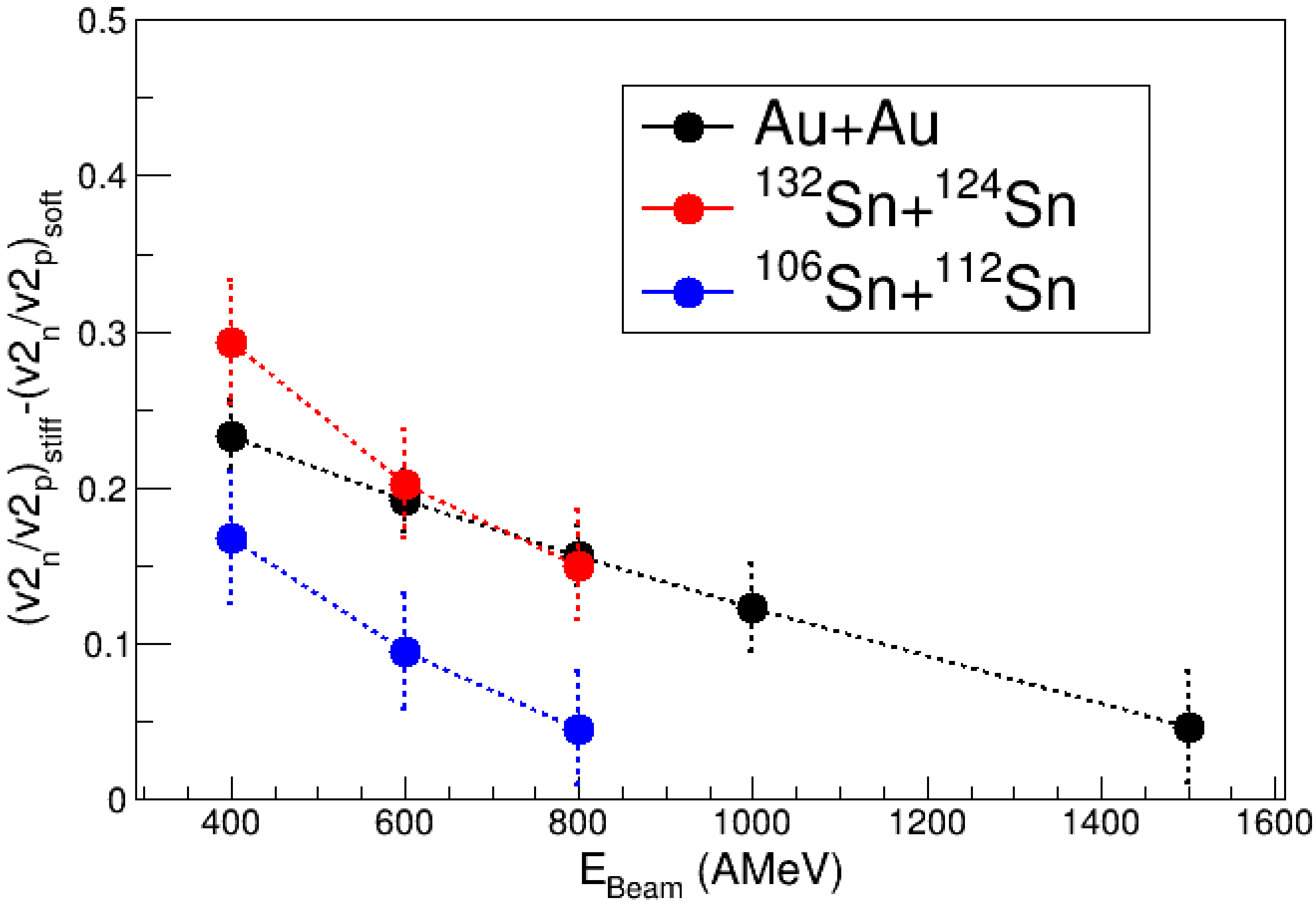

FUTURE Possibilities

NeuLAND @ FAIR/GSI

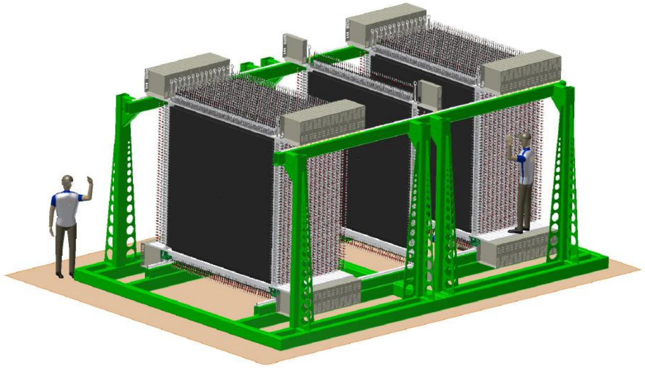

- TDR finalized in Oct 2011 and submitted
- total volume $2.5 \times 2.5 \times 3\ m^3$
- each bar readout by two PMT
- 3000 modules (plastic scintillator bars) $250 \times 5 \times 5\ cm^3$
- 30 double planes with 100 bars each, bars in neighboring planes
- mutually perpendicular
- $\sigma_t \leq 150$ ps and $\sigma_{x,y,z} \leq 1.5$ cm
- one-neutron efficiency ~95% for energies 200-1000 MeV
- multi-neutron detection capability

I. Gasparic AsyEOS2012 workshop, 6.9.2012, Siracusa, Italy

FUTURE Possibilities

NeuLAND @ FAIR/GSI

- TDR finalized in Oct 2011 and submitted
- total volume 2.5x2.5x3 m^3
- each bar readout by two PMTs
- 3000 modules (plastic scintillator bars) 250x5x5 cm^3
- 30 double planes with 100 bars each, bars in neighboring planes
- mutually perpendicular......
- $\sigma_t \leq 150$ ps and $\sigma_{x,y,z} \leq 1.5$ cm
- one-neutron efficiency ~95% for energies 200-1000 MeV
- multi-neutron detection capability

I know that!!!

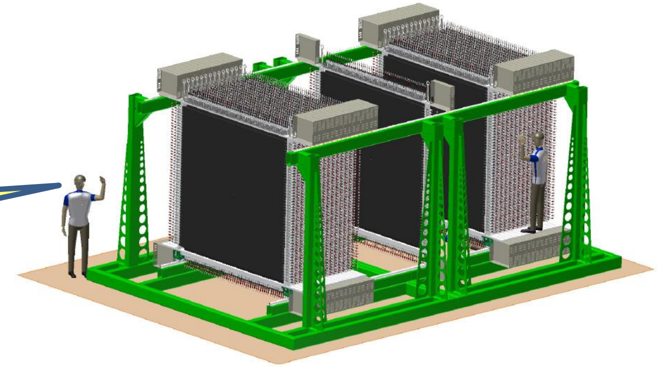

I. Gasparic AsyEOS2012 workshop, 6.9.2012, Siracusa, Italy

FUTURE Possibilities

NeuLAND @ FAIR/GSI

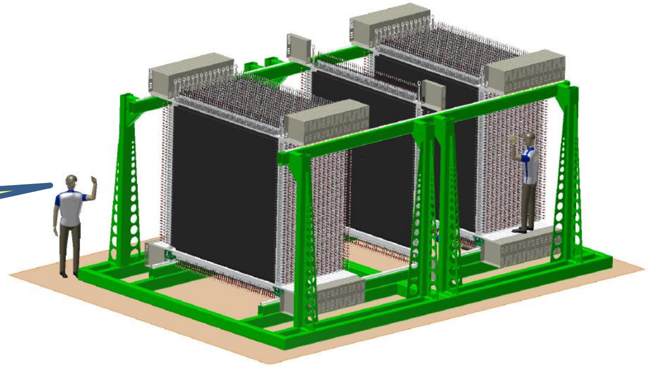

- TDR finalized in Oct 2011 and submitted
- total volume 2.5x2.5x3 m^3
- each bar readout by two PMTs
- 3000 modules (plastic scintillator bars) 250x5x5 cm^3
- 30 double planes with 100 bars each, bars in neighboring planes
- mutually perpendicular......
- $\sigma_t \leq 150$ ps and $\sigma_{x,y,z} \leq 1.5$ cm
- one-neutron efficiency ~95% for energies 200-1000 MeV
- multi-neutron detection capability

I know that!!!

I. Gasparic AsyEOS2012 workshop, 6.9.2012, Siracusa, Italy

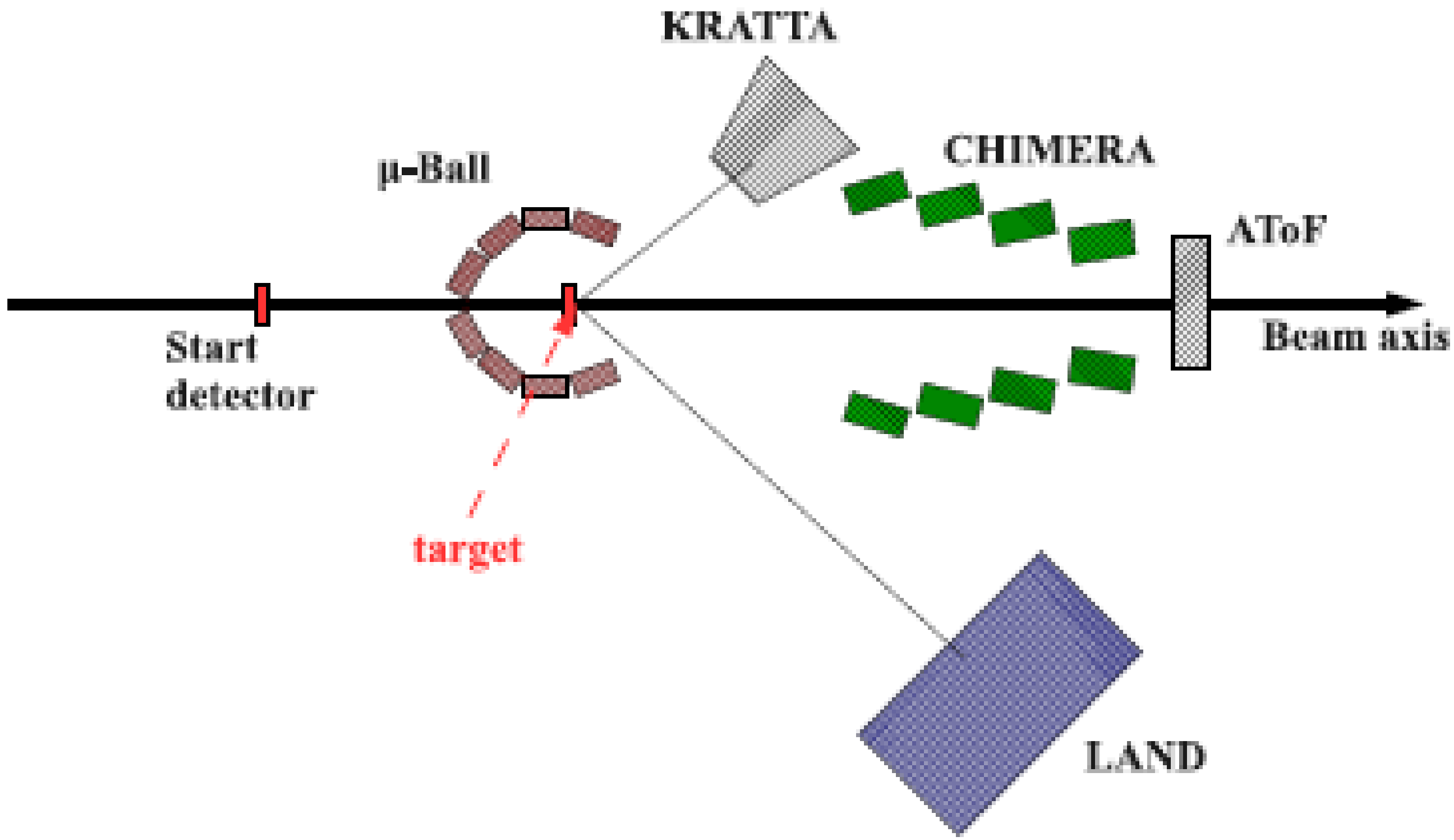

FUTURE Possibilities

NeuLAND @ FAIR/GSI

- TDR finalized in Oct 2011 and submitted
- total volume 2.5x2.5x3 m^3
- each bar readout by two PMTs
- 3000 modules (plastic scintillator bars) 250x5x5 cm^3
- 30 double planes with 100 bars each, bars in neighboring planes
- mutually perpendicular
- $\sigma_t \leq 150$ ps and $\sigma_{x,y,z} \leq 1.5$ cm
- one-neutron efficiency ~95% for energies 200-1000 MeV
- multi-neutron detection capability

I know that!!!......

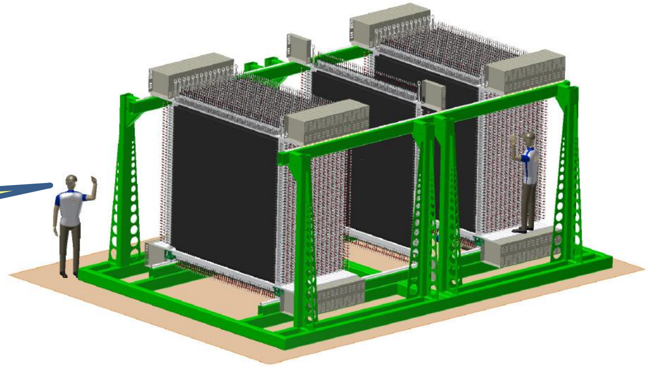

I. Gasparic AsyEOS2012 workshop, 6.9.2012, Siracusa, Italy

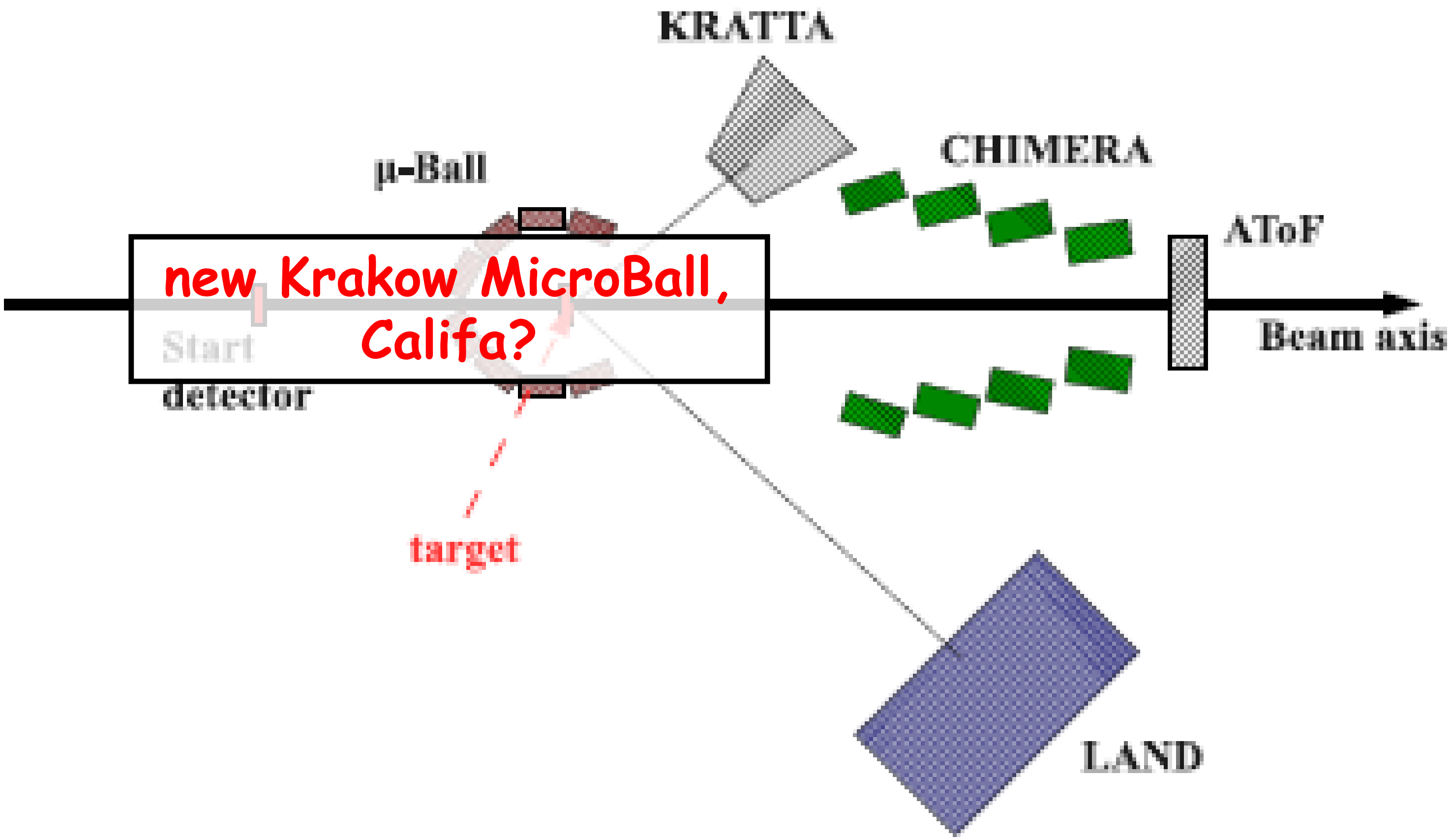

FUTURE Possibilities

NeuLAND @ FAIR/GSI

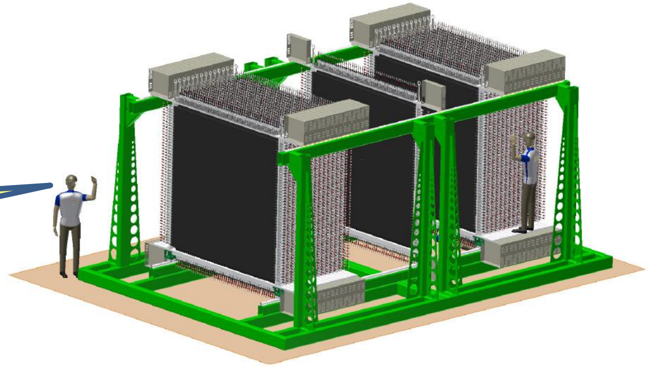

- TDR finalized in Oct 2011 and submitted
- total volume $2.5x2.5x3\ m^3$
- each bar readout by two P
- 3000 modules (plastic scintillator bars) $250x5x5\ cm^3$
- 30 double planes with 100 bars each, bars in neighboring planes
- mutually perpendicular ......
- $\sigma_t \leq 150$ ps and $\sigma_{x,y,z} \leq 1.5$ cm
- one-neutron efficiency ~95% for energies 200-1000 MeV
- multi-neutron detection capability

I know that!!!

I. Gasparic AsyEOS2012 workshop, 6.9.2012, Siracusa, Italy

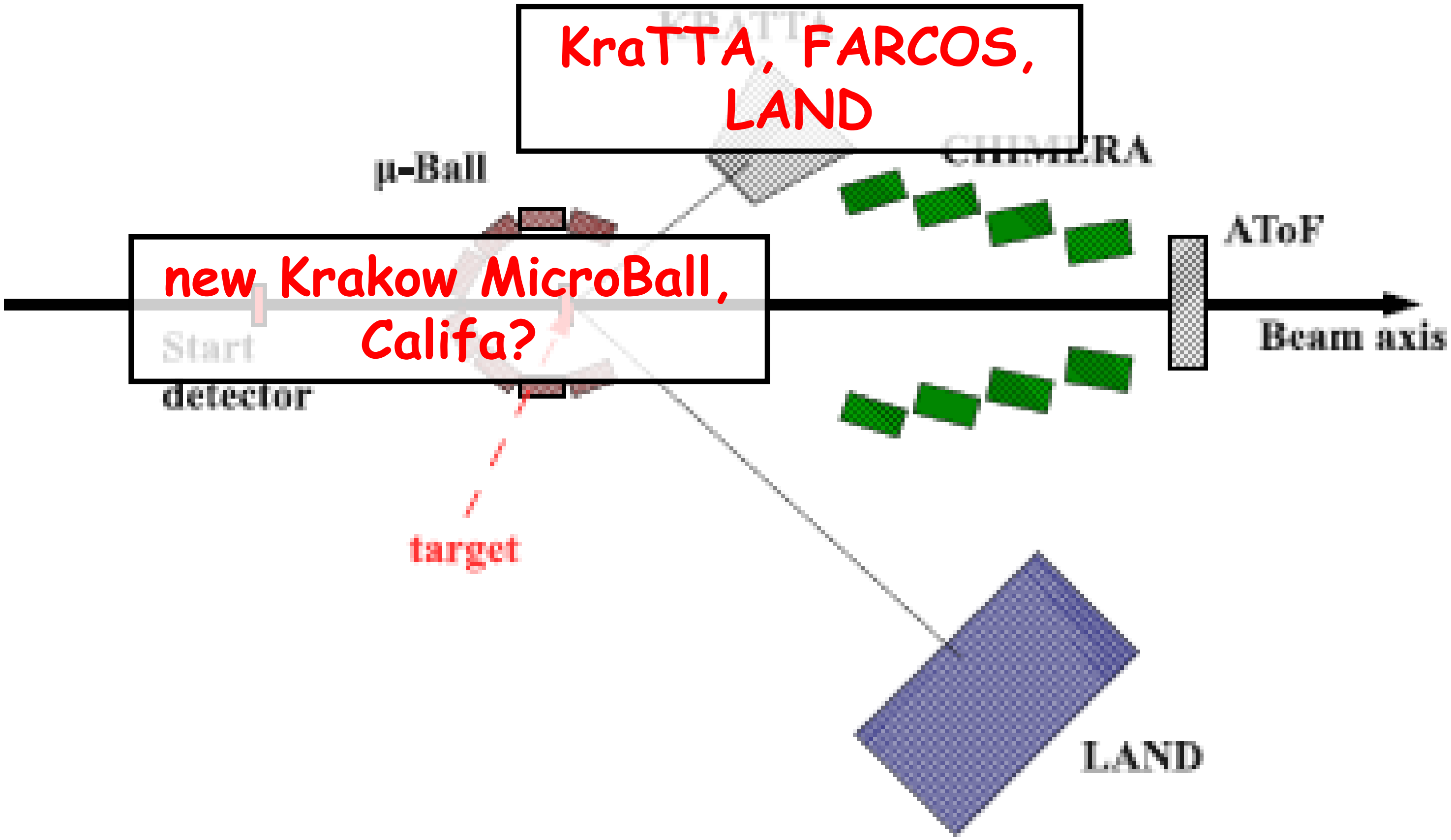

FUTURE Possibilities

NeuLAND @ FAIR/GSI

- TDR finalized in Oct 2011 and submitted
- total volume 2.5x2.5x3 m^3
- each bar readout by two PMT
- 3000 modules (plastic scintillator bars) 250x5x5 cm^3
- 30 double planes with 100 bars each, bars in neighboring planes
- mutually perpendicular
- $\sigma_t \leq 150$ ps and $\sigma_{x,y,z} \leq 1.5$ cm
- one-neutron efficiency ~95% for energies 200-1000 MeV
- multi-neutron detection capability

I know that!!!......

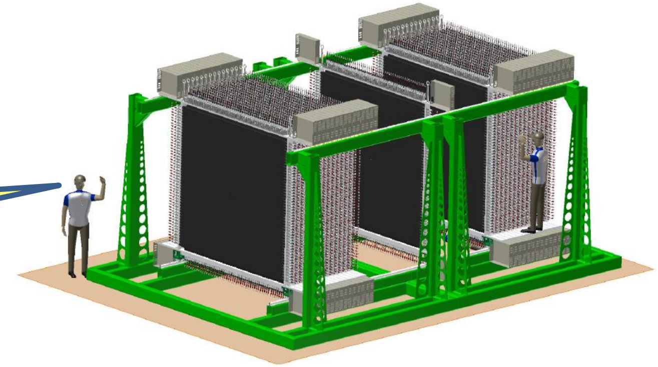

I. Gasparic AsyEOS2012 workshop, 6.9.2012, Siracusa, Italy

KraTTA, FARCOS, LAND

new Krakow MicroBall, Califa?

Fopi Forward Wall

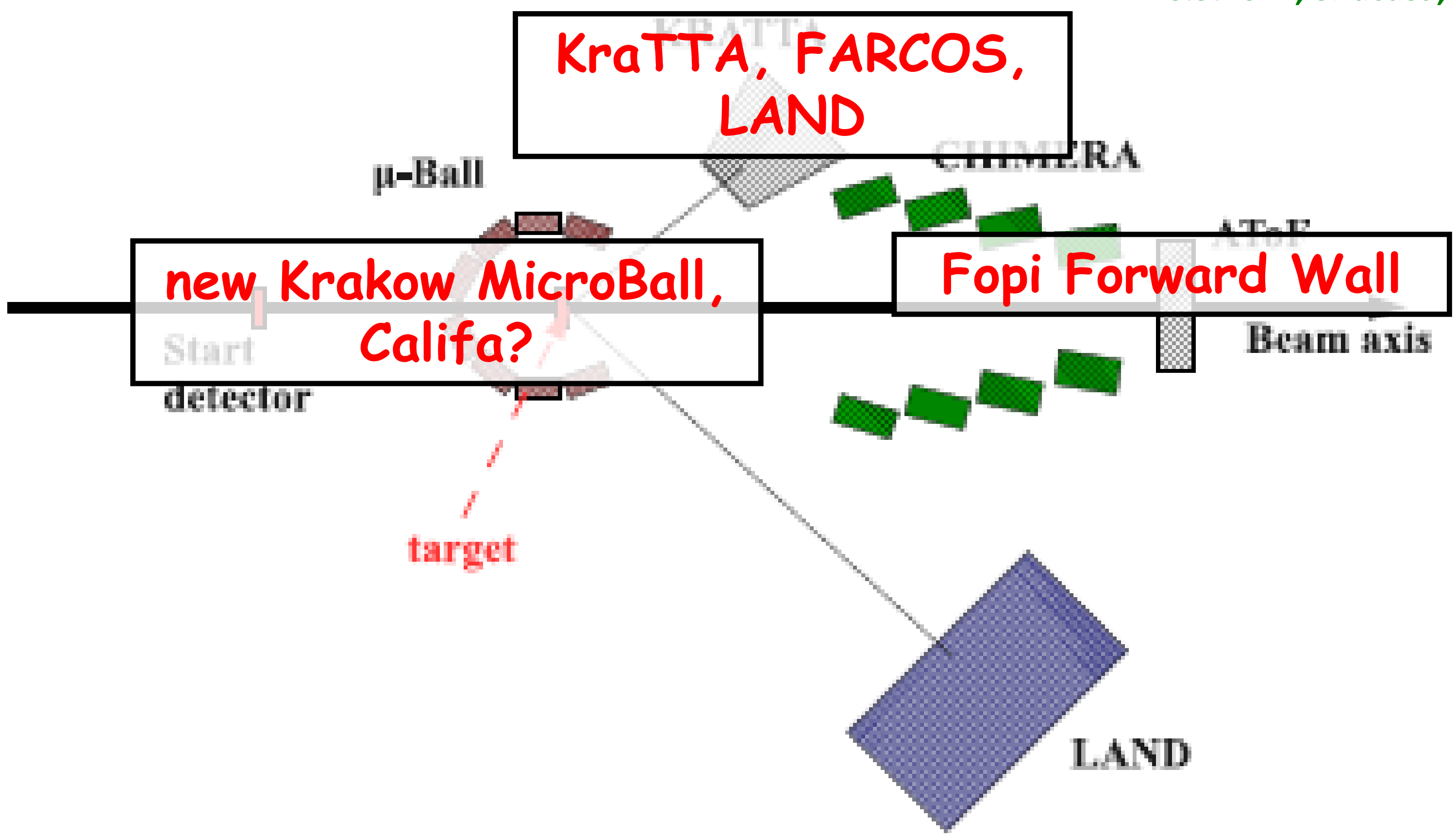

FUTURE Possibilities

NeuLAND @ FAIR/GSI

- TDR finalized in Oct 2011 and submitted
- total volume 2.5x2.5x3 m^3
- each bar readout by two PMTs
- 3000 modules (plastic scintillator bars) 250x5x5 cm^3
- 30 double planes with 100 bars each, bars in neighboring planes
- mutually perpendicular......
- $\sigma_t \leq 150$ ps and $\sigma_{x,y,z} \leq 1.5$ cm
- one-neutron efficiency ~95% for energies 200-1000 MeV
- multi-neutron detection capability

I know that!!!

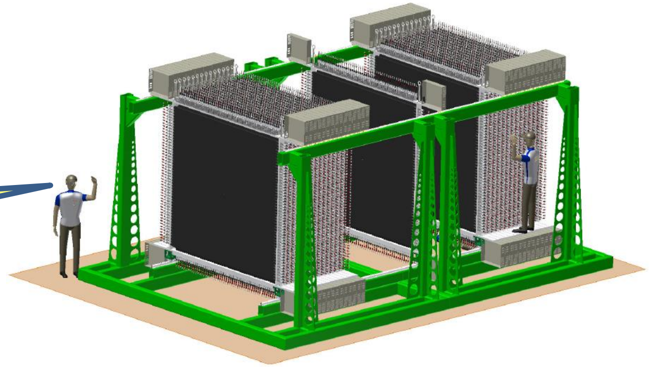

I. Gasparic AsyEOS2012 workshop, 6.9.2012, Siracusa, Italy

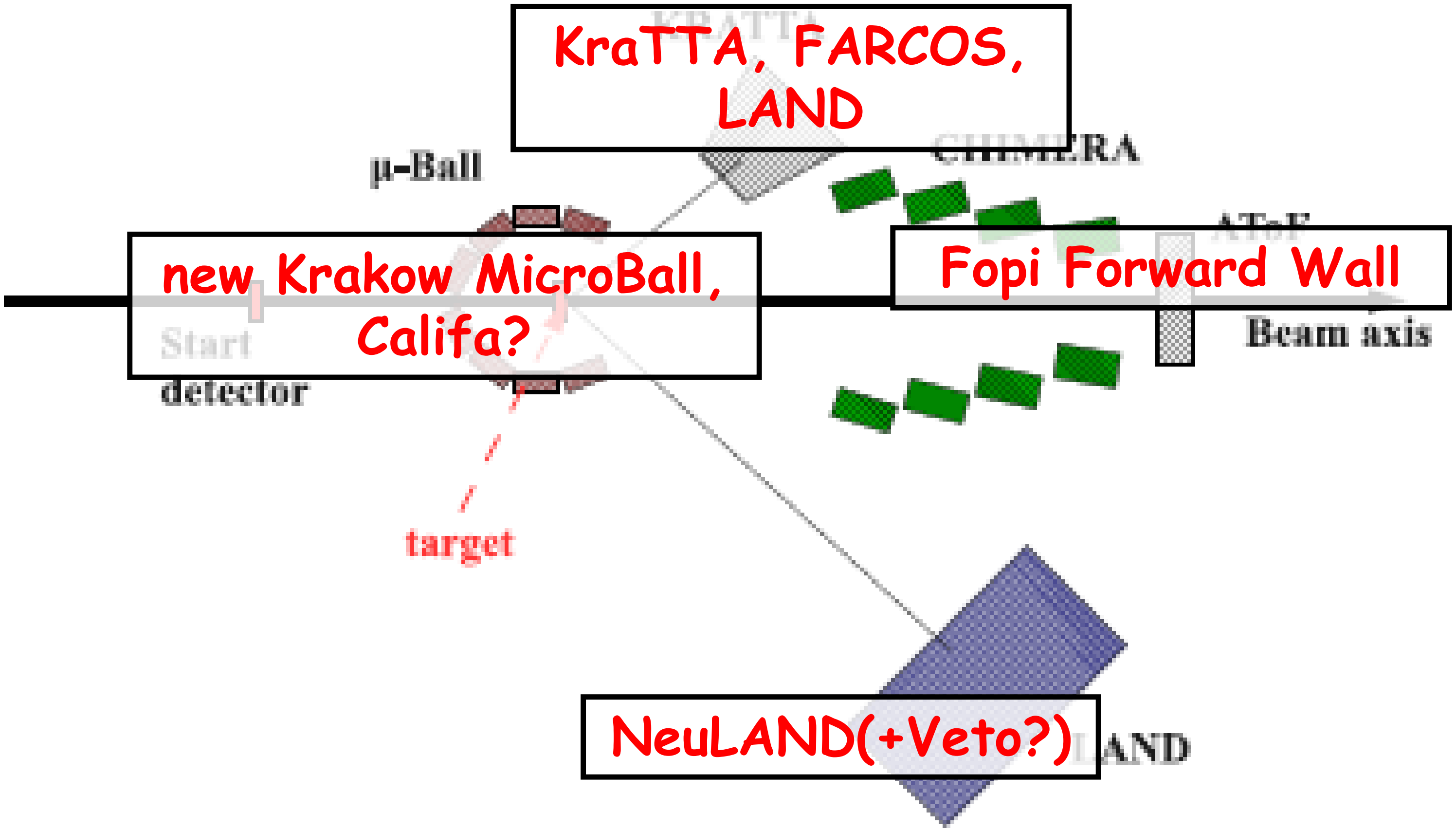

FOPI forward wall

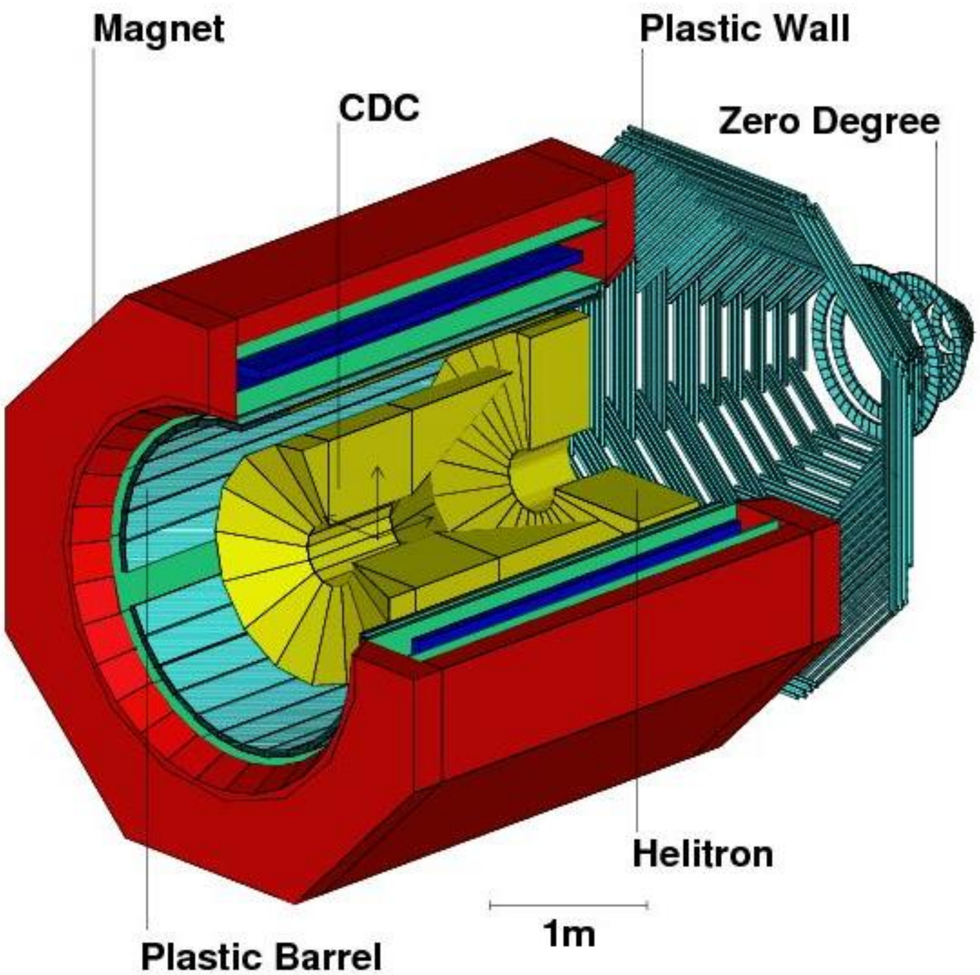

Figure 2.1: Schematic drawing of the FOPI detector.

2.10 The Forward Wall

The forward wall covers polar angles from 1.2 ° to 30 ° and the full azimuthal range. It consists of two parts: the outer wall called "Plastic Wall" (PLAWA) and the inner wall called "Zero Degree" (ZD).

2.10.1 The Plastic Wall (PLAWA)

Like the Plastic Barrel the Plastic Wall is made of 512 plastic scintillator strips divided into eight sectors. Each sector is composed of 64 strips. The light produced by a charged particle on a given strip is read out at both ends of the strip via photo multipliers. Each strip delivers four signals, two energies (E_L,E_R) and two times (t_L,t_R). The energy loss ΔE of a particle is proportional to $\sqrt{E_L \cdot E_R}$ and its time of flight is proportional to $\frac{1}{2} \cdot (t_L + t_R)$. The position of a particle hitting the PLAWA is given by the angular position of the strip which fired. The time resolution is linked to the active length of the scintillator strip, thus it varies from 80 ps for strips in the inner sector to 120 ps for strips in the outer sector. The resolution of the hit position varies from 1.2 cm to 2.0 cm [74, 75].

2.10.2 The Zero Degree Detector

This detector covers polar angles from 1.2 ° to 7.0 ° and consists of 252 plastic scintillator strips grouped into 7 concentric rings. Each module is read out by only one photo multiplier and delivers the energy loss (ΔE) and the time of flight of charged particles. The time resolution of this detector is about 200 ps.

NeuLAND can do that

The NeuLAND demonstrator was part of the Sπrit TPC experiment carried out at RIKEN, see April news. In contrast to earlier experiments, the NeuLAND demonstrator joined, here, the detector seeing both charged particles and neutrons stemming from central collisions of $^{108,112,124,132}Sn$ on ^{112,124} Sn target.

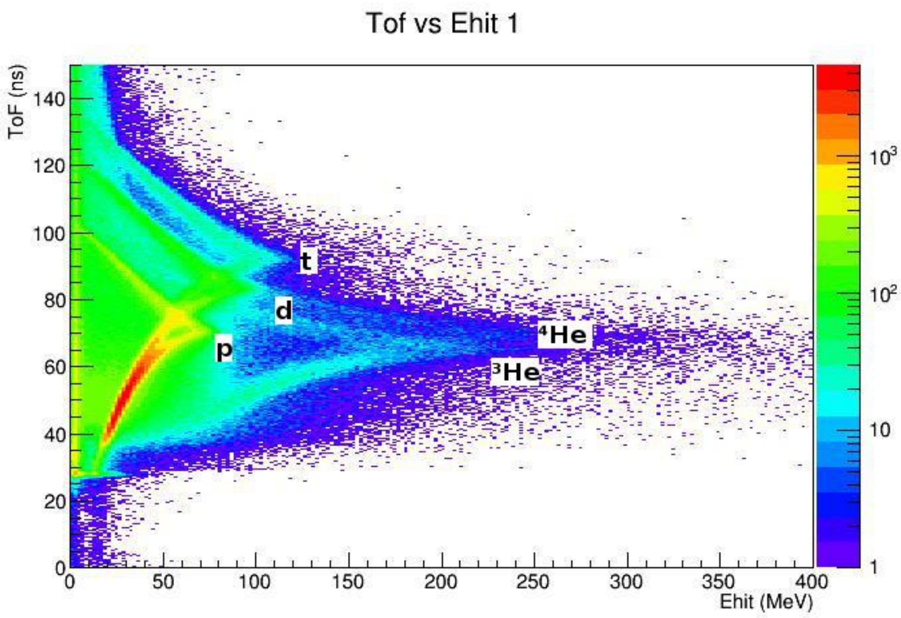

Figure 1: Particle ID plot from the 1st NeuLAND plane

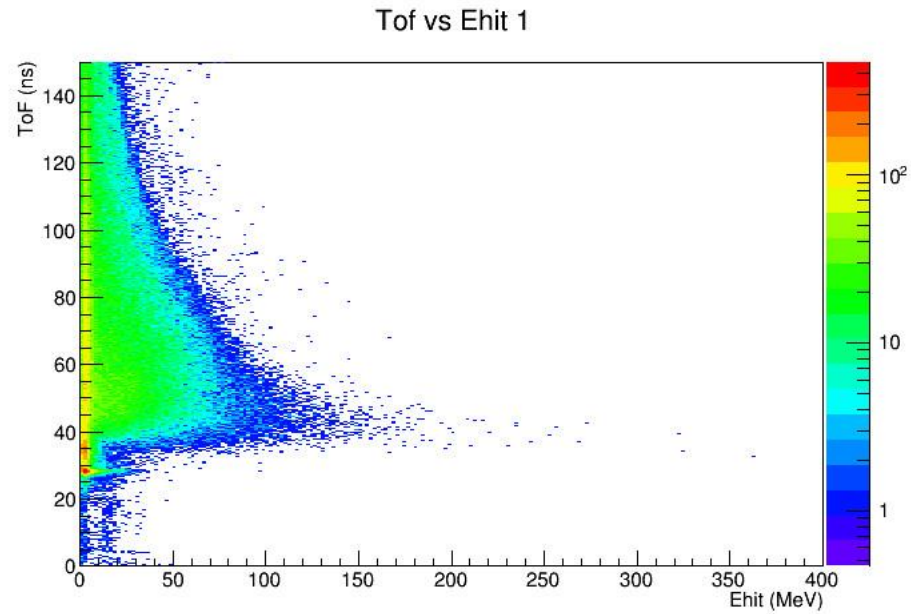

Figure 2: Same as Figure 1 but including a condition that no VETO hit was registered in the event.

NeuLAND can do that

The NeuLAND demonstrator was part of the Sπrit TPC experiment carried out at RIKEN, see April news. In contrast to earlier experiments, the NeuLAND demonstrator joined, here, the detector seeing both charged particles and neutrons stemming from central collisions of ^{108,112,124,132}Sn on ^{112,124} Sn target.

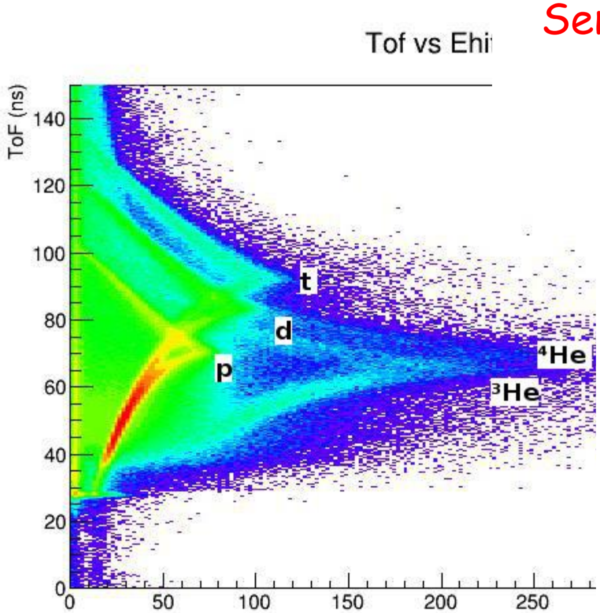

Sensitivity of observables to density.
TuQMD calculations

P. Russotto et al.Phys. Rev. C94, 014609 (2016)

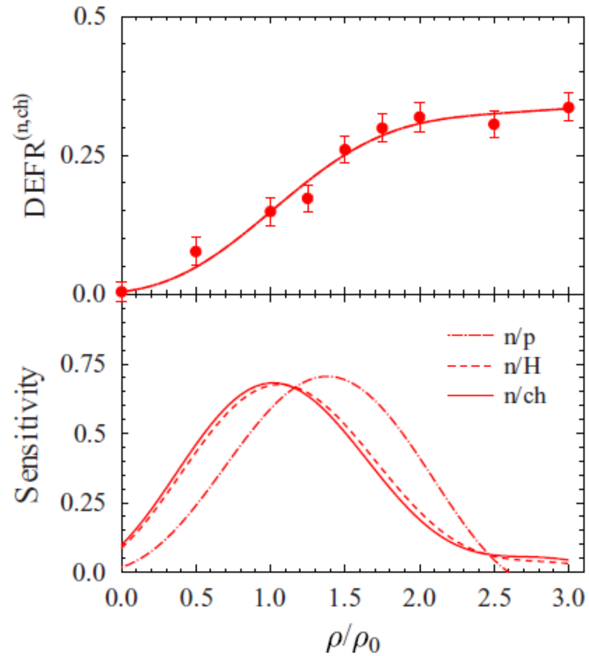

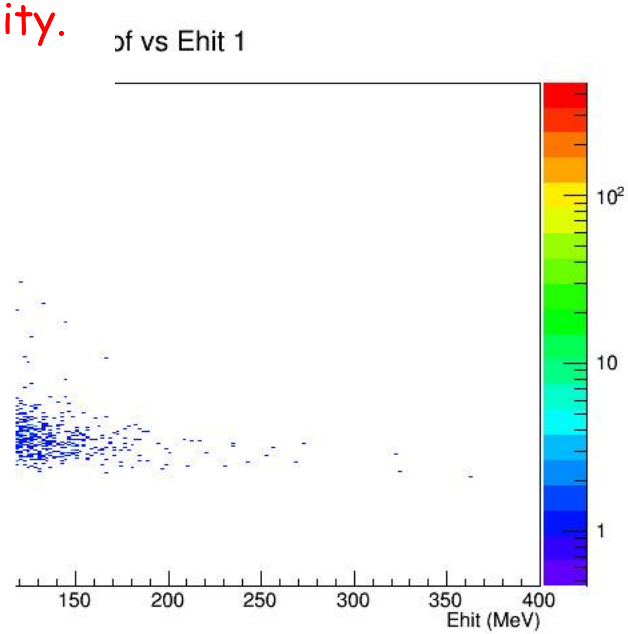

Figure 1: Particle ID plot fr
1st NeuLAND plane

e as Figure 1 but including a
t no VETO hit was registered in

UrQMD prediction for pions

$^{197}Au+^{197}Au$ @ 400, 600, 800, 1000,1500 AMeV (0.039+0.039)

$^{132}Sn+^{124}Sn$ @ 400, 600, 800 AMeV (0.059+0.037)

$^{106}Sn+^{112}Sn$ @ 400, 600, 800 AMeV (0.003+0.011)

b/bred <0.53

Pions yield ratio

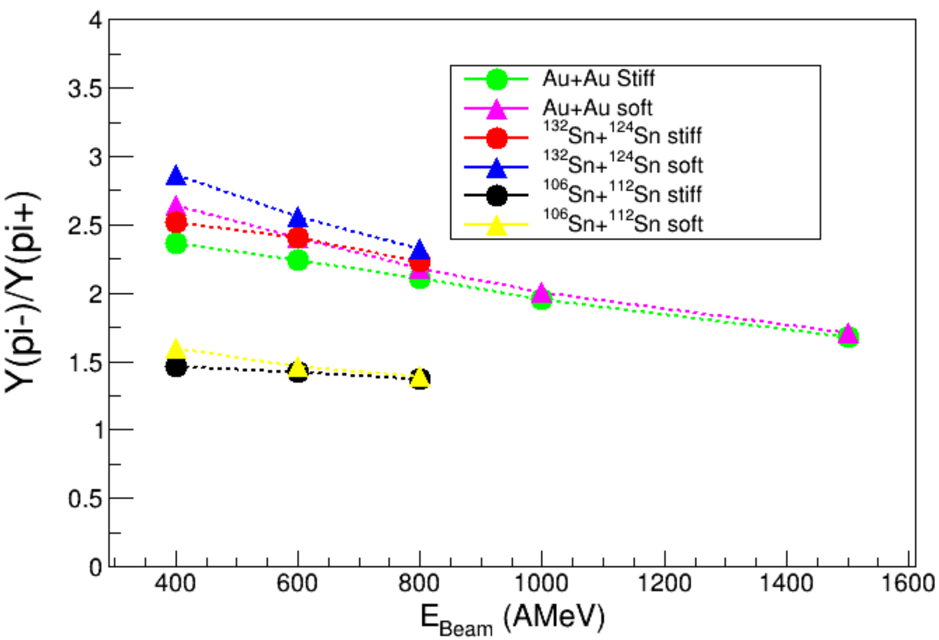

Sensitivity

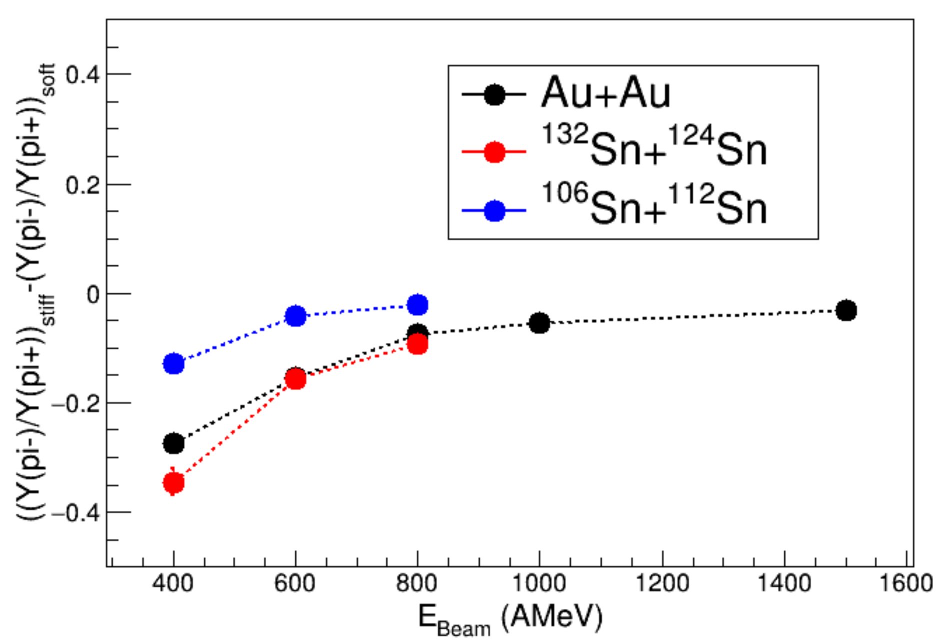

Can NeuLAND measure pi+ and pi-?

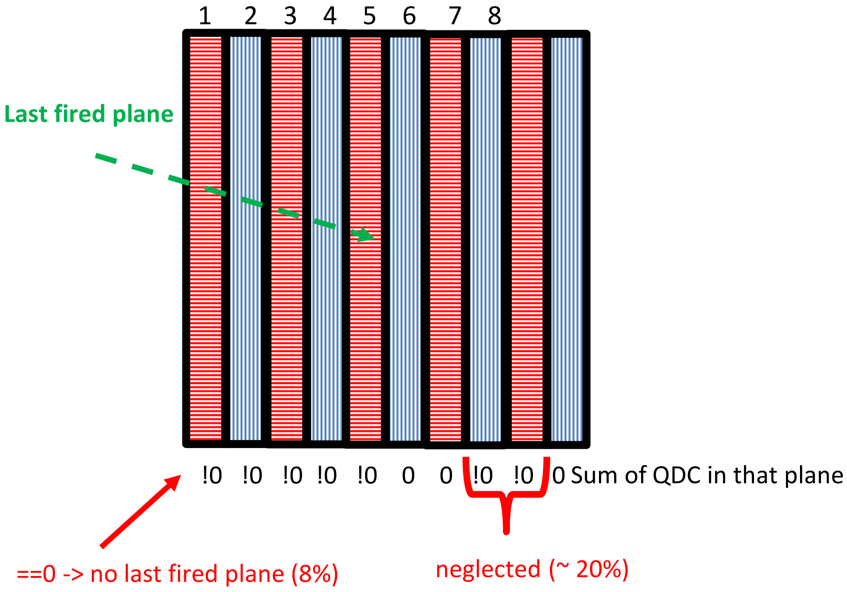

Protons

pi+

pi-

Can NeuLAND measure pi+ and pi-?

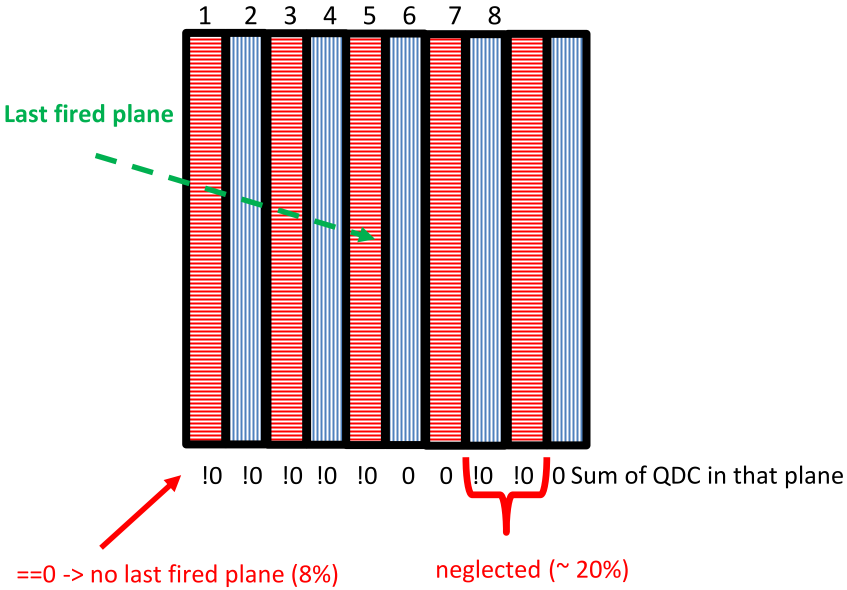

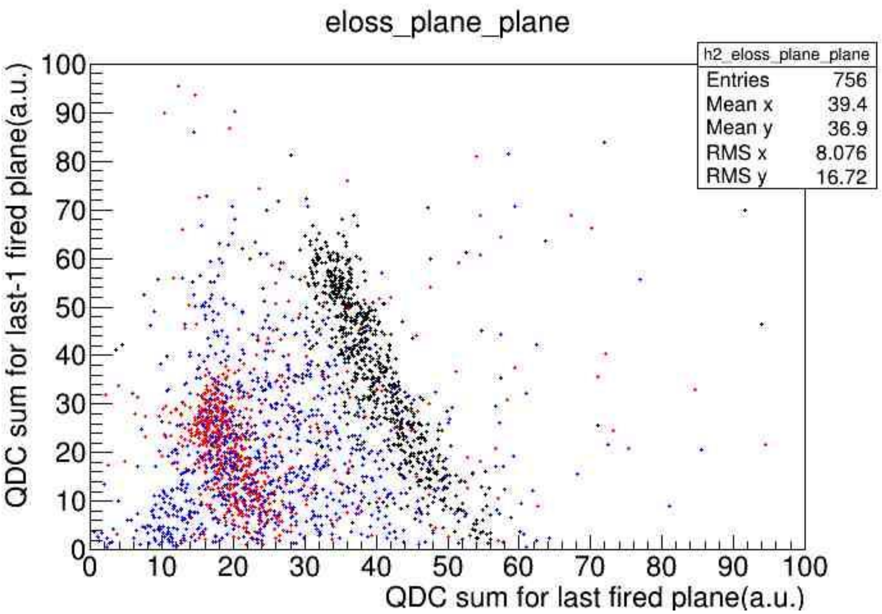

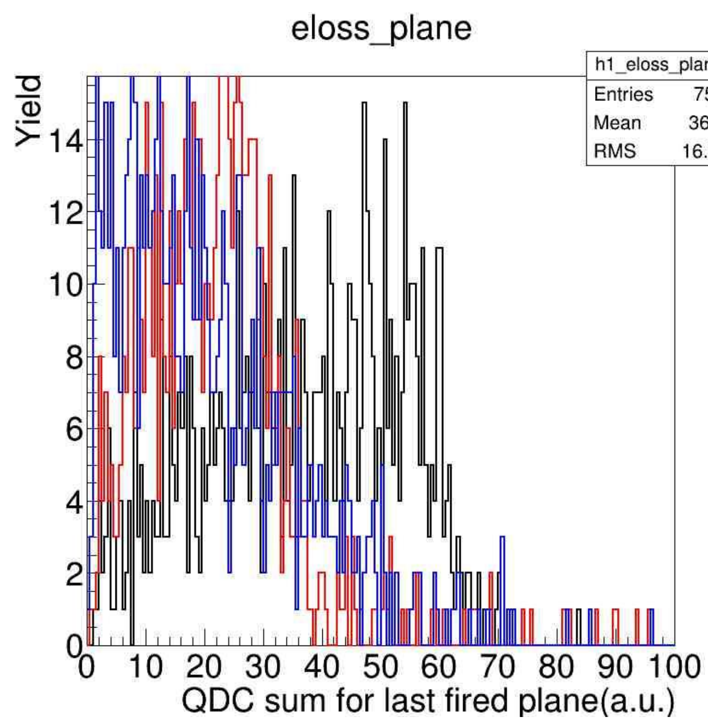

Protons
pi+
pi-

Can NeuLAND measure pi+ and pi-?

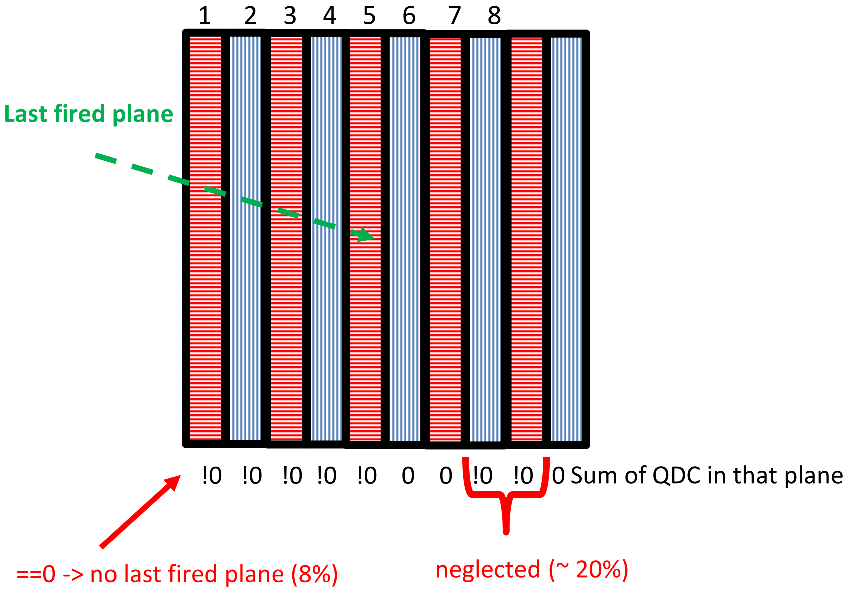

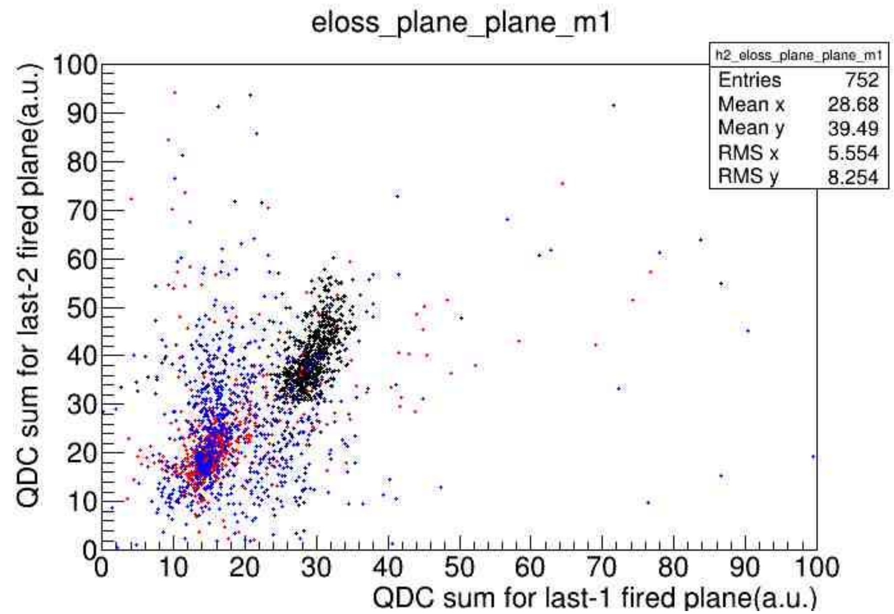

Protons
pi+
pi-

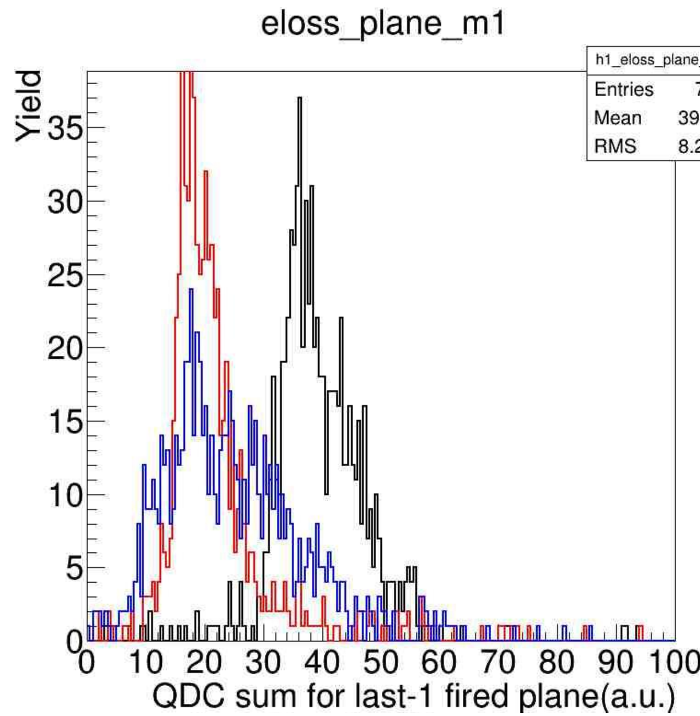

Can NeuLAND measure pi+ and pi-?

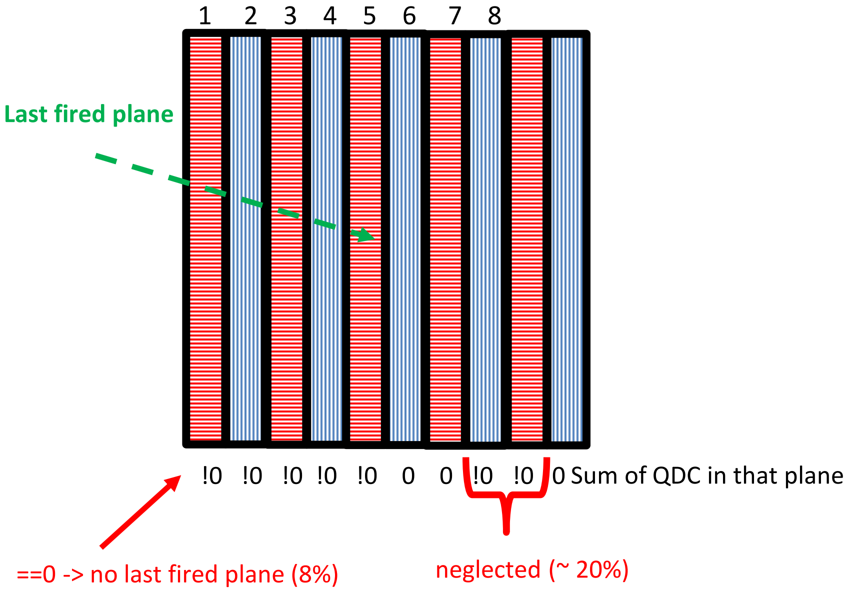

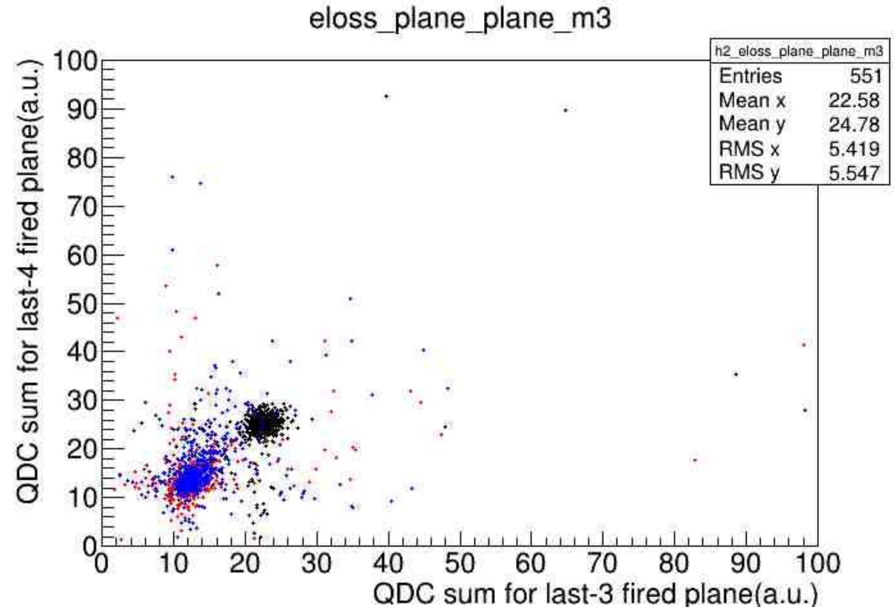

Protons
pi+
pi-

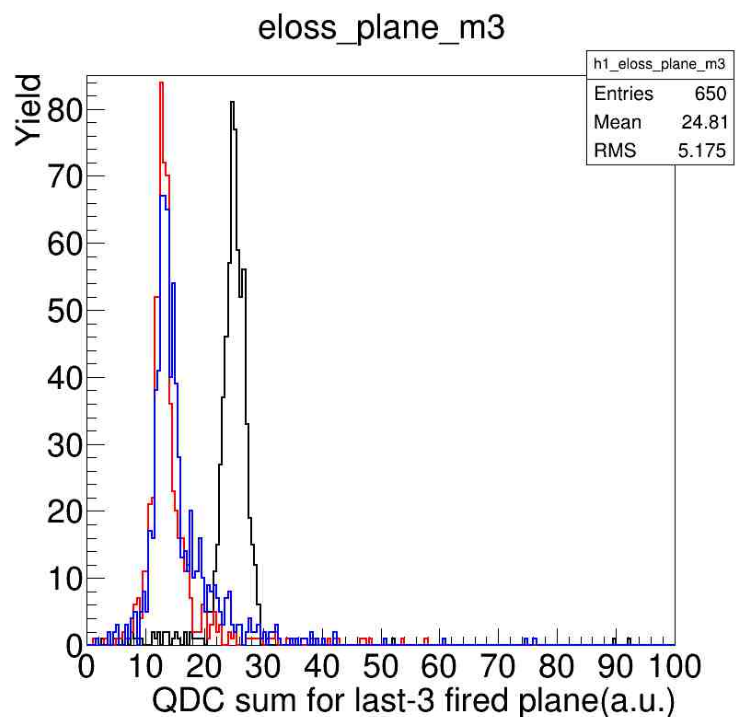

Can NeuLAND measure pi+ and pi-?

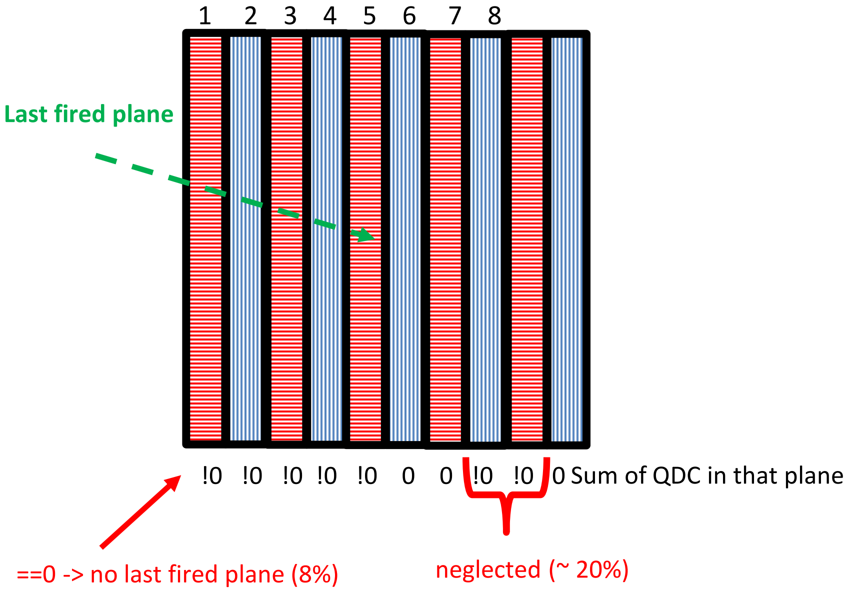

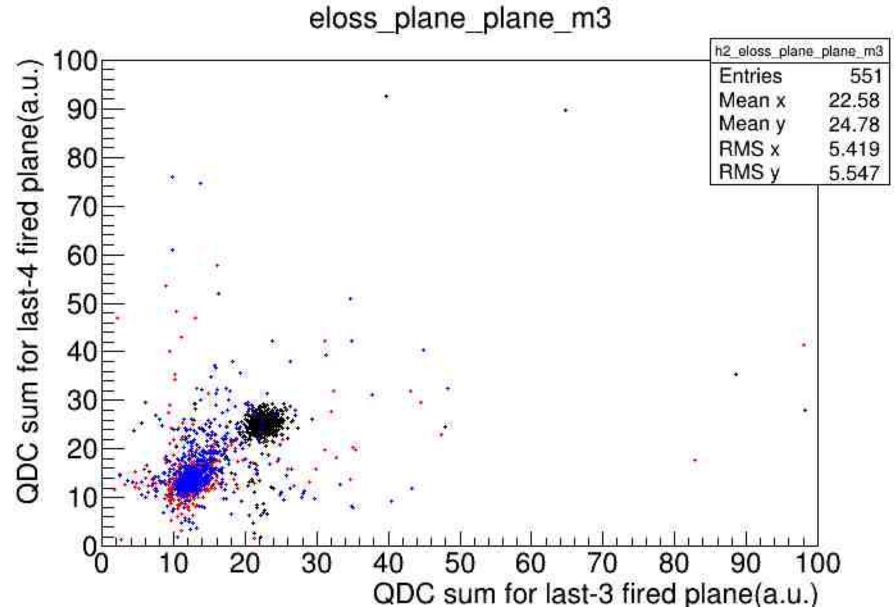

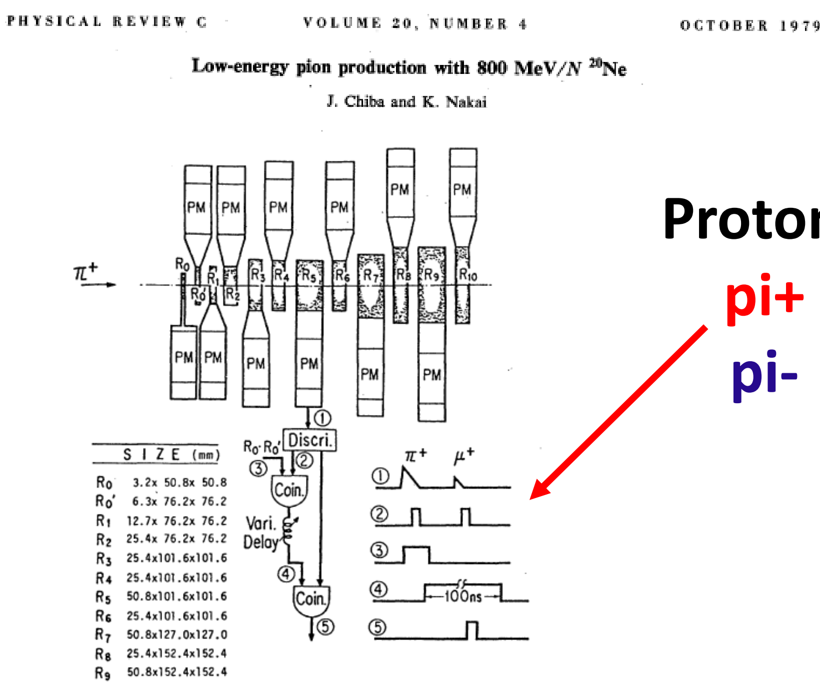

PHYSICAL REVIEW C VOLUME 20, NUMBER 4 OCTOBER 1979

Low-energy pion production with 800 MeV/N ^{20}Ne

J. Chiba and K. Nakai

SIZE (mm)	
R_0	3.2x 50.8x 50.8
R_0'	6.3x 76.2x 76.2
R_1	12.7x 76.2x 76.2
R_2	25.4x 76.2x 76.2
R_3	25.4x101.6x101.6
R_4	25.4x101.6x101.6
R_5	50.8x101.6x101.6
R_6	25.4x101.6x101.6
R_7	50.8x127.0x127.0
R_8	25.4x152.4x152.4
R_9	50.8x152.4x152.4
R_{10}	25.4x152.4x152.4

Protons

pi+

pi-

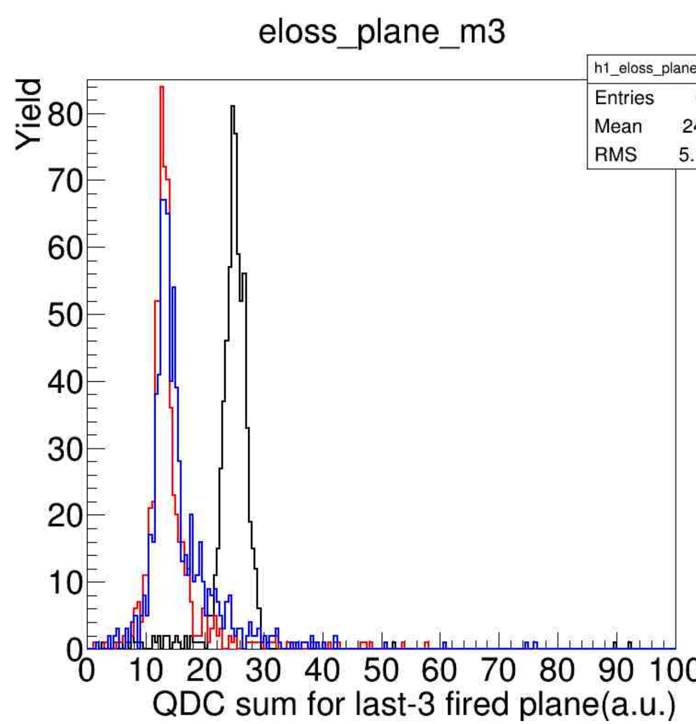

Study for a new Micro-Ball, by J. Lukasik (Krakow)

UrQMD + clustering: Au+Au 1000 AMeV, 0-10 fm, 200 fm/c

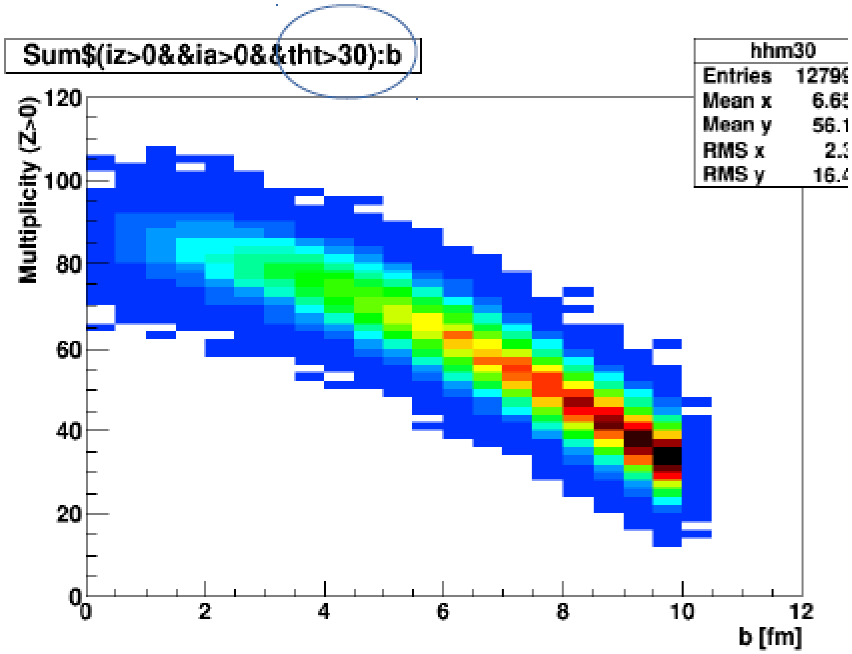

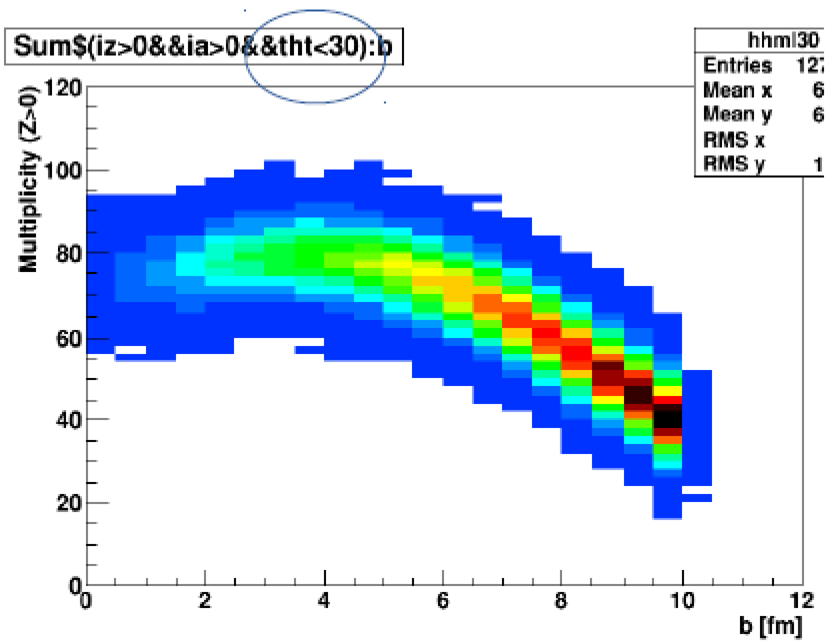

better correlation

Study for a new Micro-Ball, by J. Lukasik (Krakow)

Trigger/Reaction Plane detector around the target:

- 5 rings of 4x4 mm^2 fast scintillating fibers (e.g. BCF-20) read out by SiPMs
- covers angles from 30° to 165°,
- segmentation assures more or less uniform count rates for Au+Au at 1 AGeV,
- geometrical efficiency ~95%
- ~10% of charged particles involved in multihits,
- ~5% multihit probability
- sufficiently large for radioactive beams
- sufficiently small and lightweight not to disturb neutrons
- min radius - 6 cm,
- max radius - 12 cm
- length 43 cm
- 180 segments in forward rings
- 90 segments in backward ring
- 810 channels

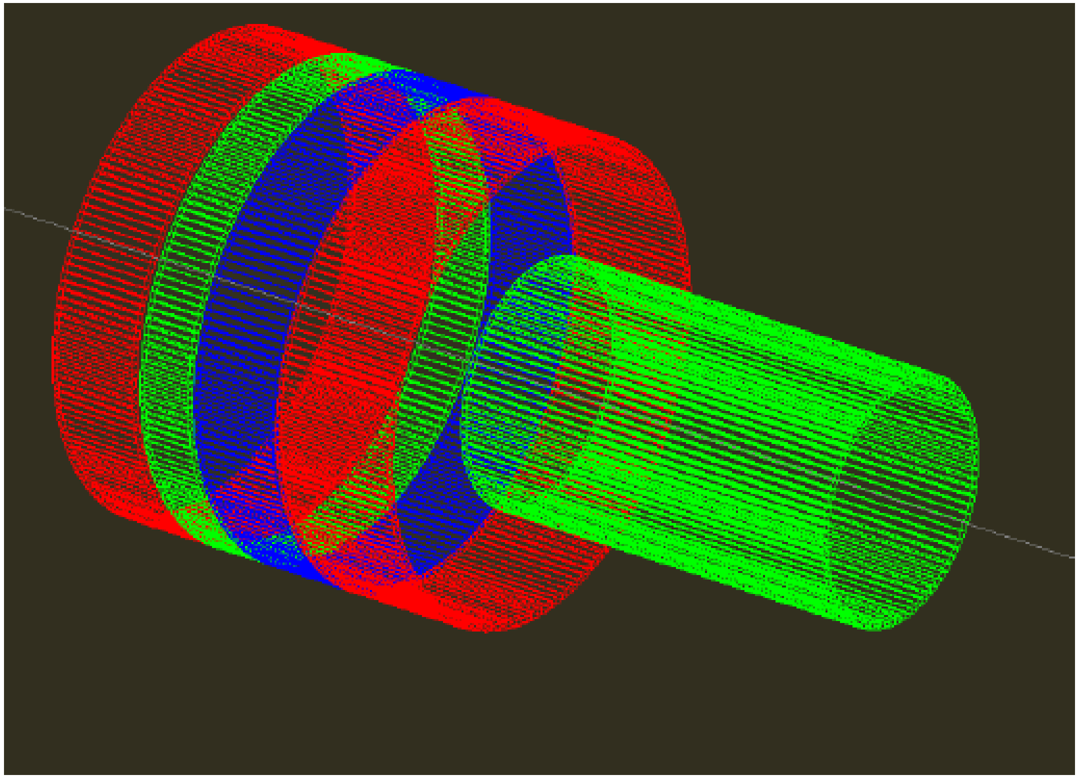

Conclusions

Symmetry Energy:

- Low densities: several constraints quite consistent
- High density:
  - pion constraints not consistent (up to now)
  - n/p flows suggests…a route "Towards a model-independent constraint of the high-density dependence of the symmetry energy"
  - ASY-EOS data analysis is done, new constraint obtained
  - For pions: Spirit results will come
- Work on code consistency needed…everywhere
- New and better experiments on n,p flows (& pions?) possible only at @ GSI
- International collaborations and efforts

Conclusions

Symmetry Energy:

- Low densities: several constraints quite consistent
- High density:
  - pion constraints not consistent (up to now)
  - n/p flows suggests…a route "Towards a model-independent constraint of the high-density dependence of the symmetry energy"
  - ASY-EOS data analysis is done, new constraint obtained
  - For pions: Spirit results will come
- Work on code consistency needed…everywhere
- New and better experiments on n,p flows (& pions?) possible only at @ GSI
- International collaborations and efforts

On the road.....

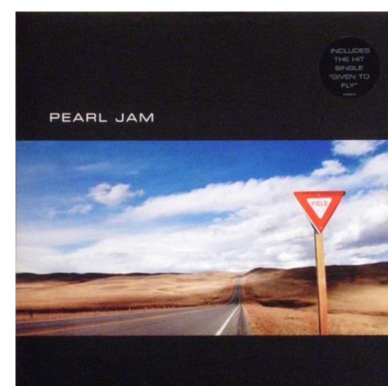

THE ASYEOS COLLABORATION

P. Russotto,[1] S. Gannon,[2] S. Kupny,[3] P. Lasko,[3] L. Acosta,[4,5] M. Adamczyk,[3] A. Al-Ajlan,[6] M. Al-Garawi,[7] S. Al-Homaidhi,[6] F. Amorini,[4] L. Auditore,[8,9] T. Aumann,[10,11] Y. Ayyad,[12] Z. Basrak,[13] J. Benlliure,[12] M. Boisjoli,[14] K. Boretzky,[11] J. Brzychczyk,[3] A. Budzanowski,[15,*] C. Caesar,[10] G. Cardella,[1] P. Cammarata,[16] Z. Chajecki,[17] M. Chartier,[2] A. Chbihi,[14] M. Colonna,[4] M. D. Cozma,[18] B. Czech,[15] E. De Filippo,[1] M. Di Toro,[4,19] M. Famiano,[20] I. Gašparić,[10,13] L. Grassi,[13] C. Guazzoni,[21,22] P. Guazzoni,[21,23] M. Heil,[11] L. Heilborn,[16] R. Introzzi,[24] T. Isobe,[25] K. Kezzar,[7] M. Kiš,[11] A. Krasznahorkay,[26] N. Kurz,[11] E. La Guidara,[1] G. Lanzalone,[4,27] A. Le Fèvre,[11] Y. Leifels,[11] R. C. Lemmon,[28] Q. F. Li,[29] I. Lombardo,[30,31] J. Łukasik,[15] W. G. Lynch,[17] P. Marini,[14,16,32] Z. Matthews,[2] L. May,[16] T. Minniti,[1] M. Mostazo,[12] A. Pagano,[1] E. V. Pagano,[4,19] M. Papa,[1] P. Pawłowski,[15] S. Pirrone,[1] G. Politi,[1,19] F. Porto,[4,19] W. Reviol,[33] F. Riccio,[21,22] F. Rizzo,[4,19] E. Rosato,[30,31,*] D. Rossi,[10,11] S. Santoro,[8,9] D. G. Sarantites,[33] H. Simon,[11] I. Skwirczynska,[15] Z. Sosin,[3,*] L. Stuhl,[26] W. Trautmann,[11] A. Trifirò,[8,9] M. Trimarchi,[8,9] M. B. Tsang,[17] G. Verde,[1,34] M. Veselsky,[35] M. Vigilante,[30,31] Yongjia Wang,[29] A. Wieloch,[3] P. Wigg,[2] J. Winkelbauer,[17] H. H. Wolter,[36] P. Wu,[2] S. Yennello,[16] P. Zambon,[21,22] L. Zetta,[21,23] and M. Zoric[13]

[1] *INFN-Sezione di Catania, I-95123 Catania, Italy*
[2] *University of Liverpool, Physics Department, Liverpool L69 7ZE, United Kingdom*
[3] *M. Smoluchowski Institute of Physics, Jagiellonian University, Pl-30-348 Kraków, Poland*
[4] *INFN-Laboratori Nazionali del Sud, I-95123 Catania, Italy*
[5] *Instituto de Física, Universidad Nacional Autónoma de México, A.P. 20-364, México 01000 D.F., Mexico*
[6] *KACST, Riyadh, Saudi Arabia*
[7] *Physics Department, King Saud University, Riyadh, Saudi Arabia*
[8] *INFN-Gruppo Collegato di Messina, I-98166 Messina, Italy*
[9] *Dipartimento di Scienze Matematiche e Informatiche, Scienze Fisiche e Scienze della Terra, University of Messina, I-98166 Messina, Italy*
[10] *Technische Universität Darmstadt, D-64289 Darmstadt, Germany*
[11] *GSI Helmholtzzentrum für Schwerionenforschung GmbH, D-64291 Darmstadt, Germany*
[12] *Universidade de Santiago de Compostela, 15782 Santiago de Compostela, Spain*
[13] *Ruđer Bošković Institute, HR-10002 Zagreb, Croatia*
[14] *GANIL, CEA et IN2P3-CNRS, F-14076 Caen, France*
[15] *H. Niewodniczański Institute of Nuclear Physics, Pl-31342 Kraków, Poland*
[16] *Department of Chemistry and Cyclotron Institute, Texas A&M University, College Station, TX-77843, USA*
[17] *Department of Physics and Astronomy and NSCL, Michigan State University, East Lansing, MI-48824, USA*
[18] *IFIN-HH, Reactorului 30, 077125 Măgurele-Bucharest, Romania*
[19] *Dipartimento di Fisica e Astronomia-Università, I-95123 Catania, Italy*
[20] *Western Michigan University, Kalamazoo, MI-49008, USA*
[21] *INFN-Sezione di Milano, I-20133 Milano, Italy*
[22] *Dipartimento di Elettronica, Informazione e Bioingegneria, Politecnico di Milano, I-20133 Milano, Italy*
[23] *Dipartimento di Fisica, Università degli Studi di Milano, I-20133 Milano, Italy*
[24] *INFN and DISAT, Politecnico di Torino, I-10129 Torino, Italy*
[25] *RIKEN, Wako, Saitama 351-0198, Japan*
[26] *Institute for Nuclear Research (MTA Atomki), P.O. Box 51, H-4001 Debrecen, Hungary*
[27] *Università degli Studi di Enna "Kore", I-94100 Enna, Italy*
[28] *STFC Daresbury Laboratory, Warrington WA4 4AD, United Kingdom*
[29] *School of Science, Huzhou University, Huzhou 313000, P.R. China*
[30] *INFN-Sezione di Napoli, I-80126 Napoli, Italy*
[31] *Dipartimento di Fisica "Ettore Pancini", Università di Napoli Federico II, I-80126 Napoli, Italy*
[32] *CENBGn Université de Bordeaux, CNRS/IN2P3, F-33175 Gradignan, France*
[33] *Chemistry Department, Washington University, St. Louis, MO-63130, USA*
[34] *Institut de Physique Nucléaire, IN2P3-CNRS et Université Paris-Sud, F-91406 Orsay, France*
[35] *Institute of Physics, Slovak Academy of Sciences, 84511 Bratislava 45, Slovakia*
[36] *Fakultät für Physik, Universität München, D-85748 Garching, Germany*

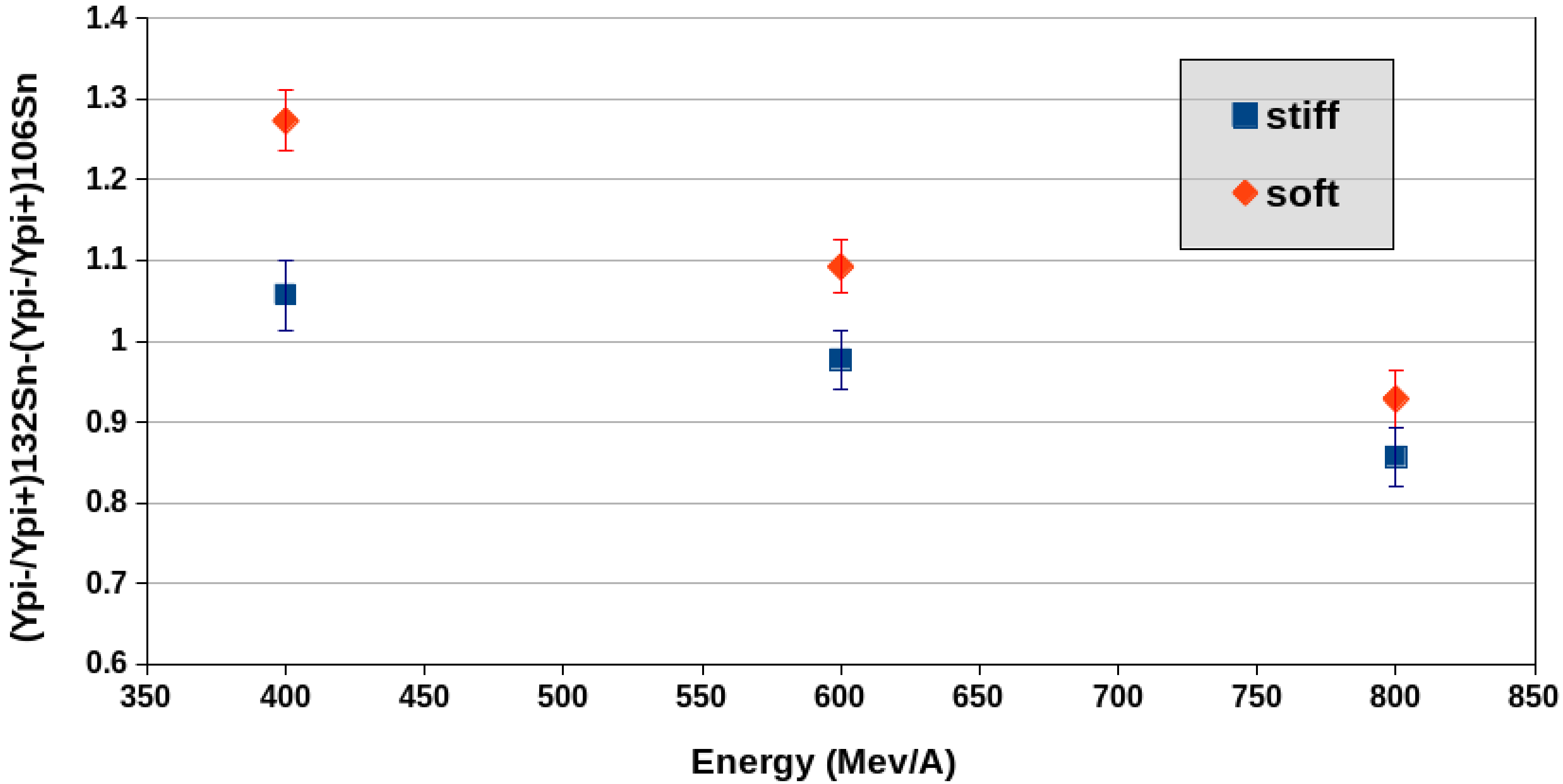
1.4
1.3
1.2
1.1
1
0.9
0.8
0.7
0.6
(Ypi-/Ypi+)132Sn-(Ypi-/Ypi+)106Sn
350
400
450
500
550
600
650
700
750
800
850
Energy (Mev/A)
stiff
soft

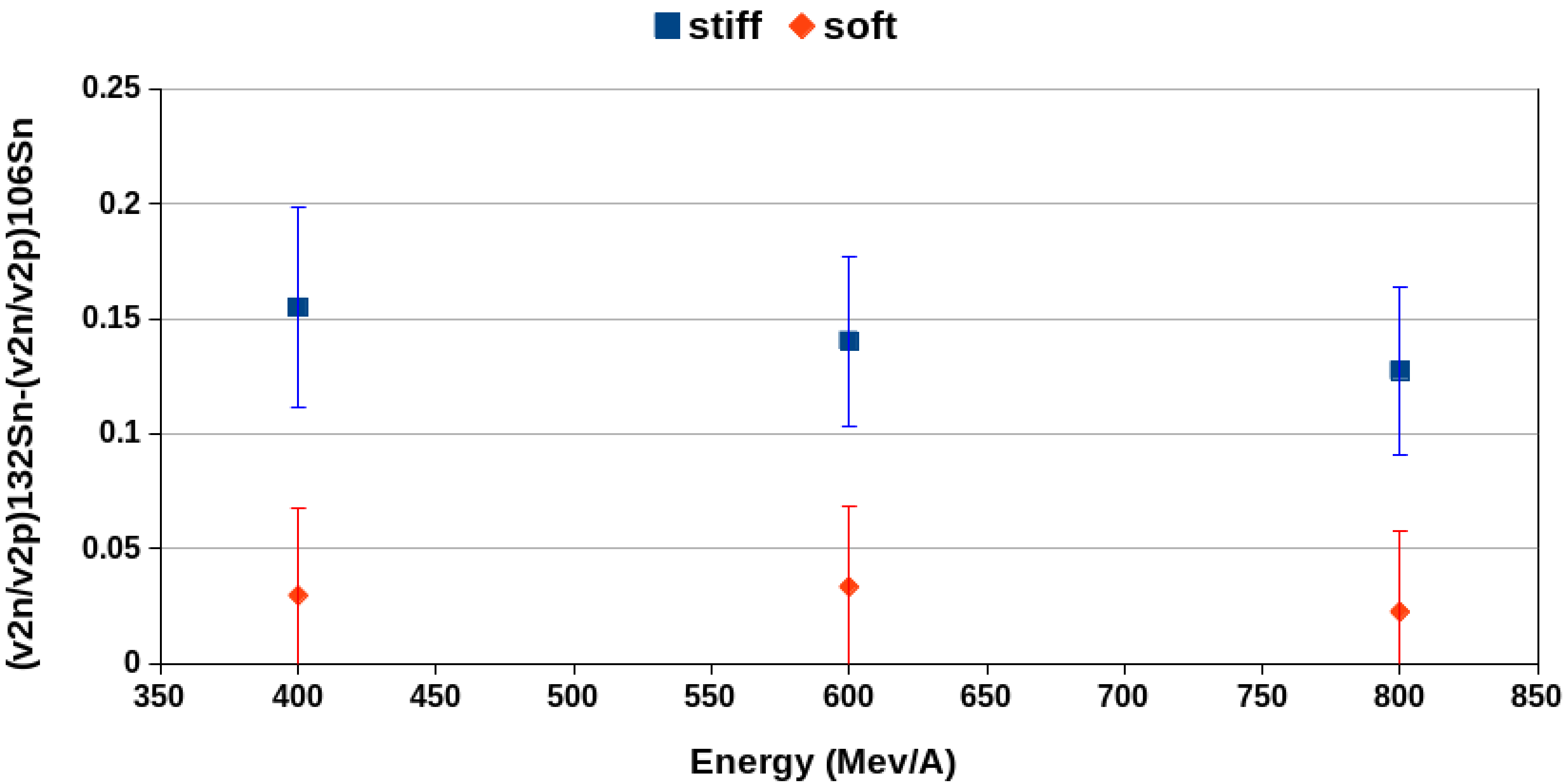
stiff
soft
0.25
0.2
0.15
0.1
0.05
0
(v2n/v2p)132Sn-(v2n/v2p)106Sn
350
400
450
500
550
600
650
700
750
800
850
Energy (Mev/A)

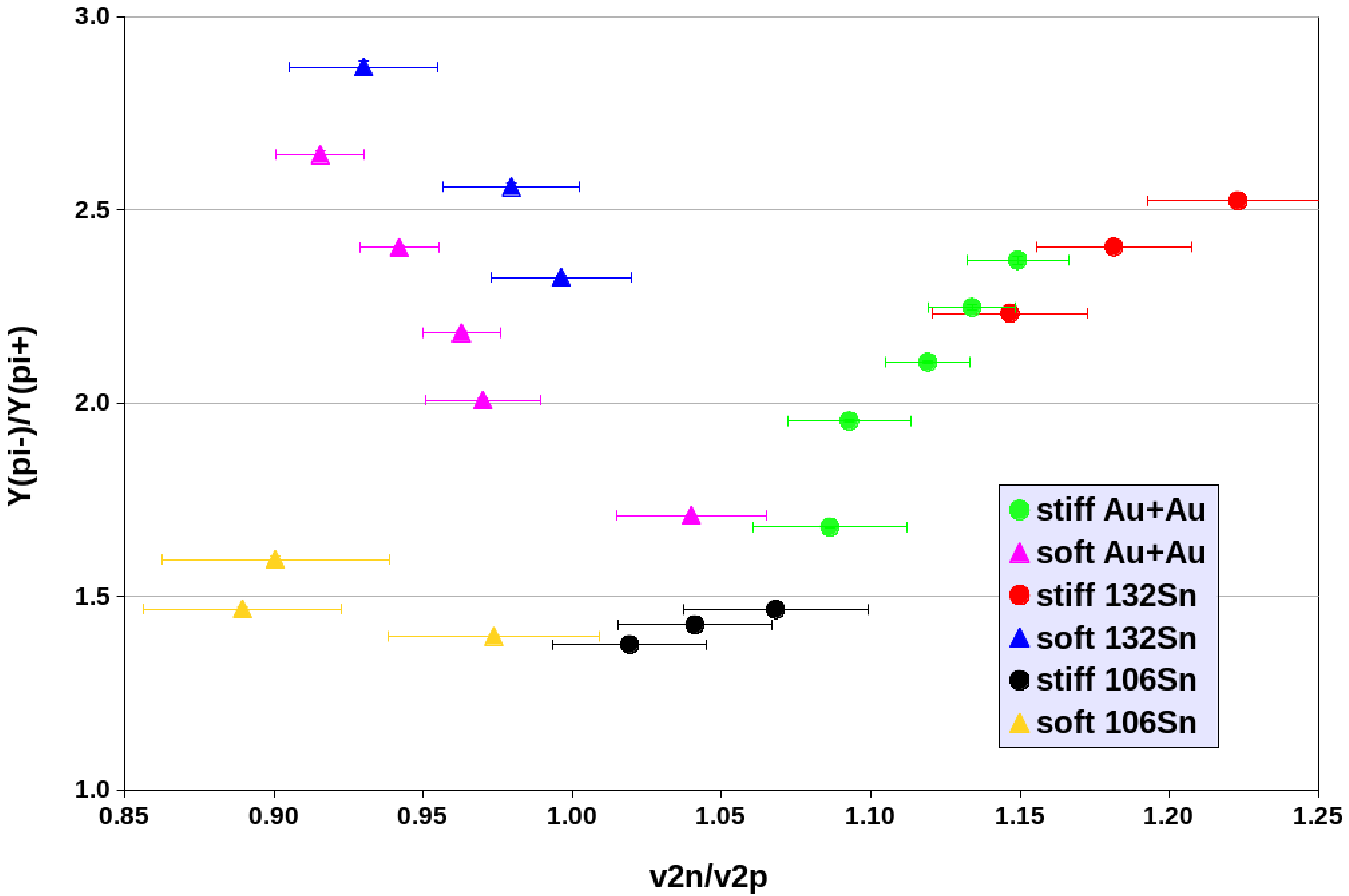

3.0
2.5
2.0
1.5
1.0
0.85
0.90
0.95
1.00
1.05
1.10
1.15
1.20
1.25
Y(pi-)/Y(pi+)
v2n/v2p
stiff Au+Au
soft Au+Au
stiff 132Sn
soft 132Sn
stiff 106Sn
soft 106Sn

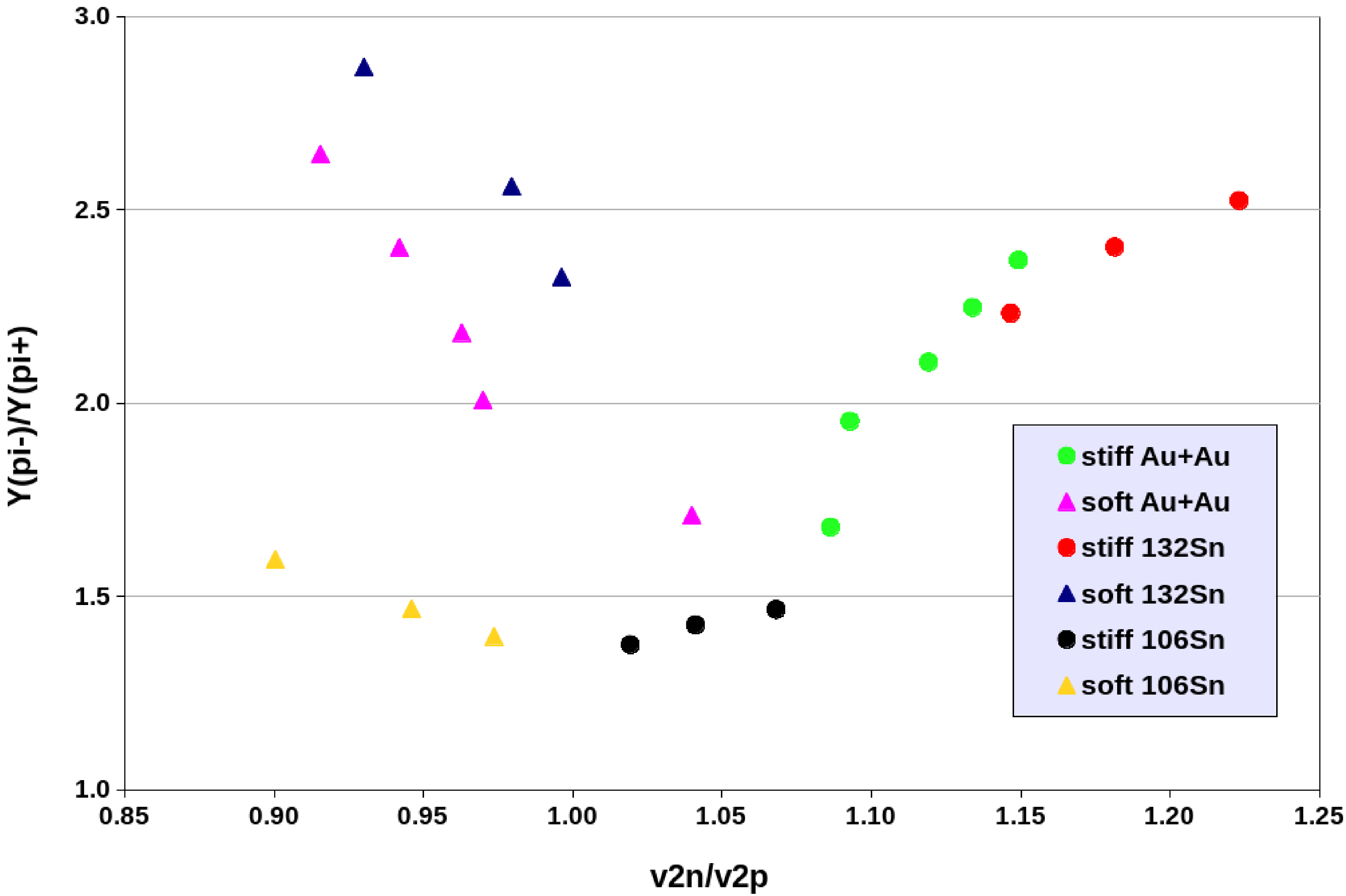

3.0
2.5
2.0
1.5
1.0
Y(pi-)/Y(pi+)
0.85
0.90
0.95
1.00
1.05
1.10
1.15
1.20
1.25
v2n/v2p
stiff Au+Au
soft Au+Au
stiff 132Sn
soft 132Sn
stiff 106Sn
soft 106Sn

31/03/17

LAST PAPER 13/03/2017

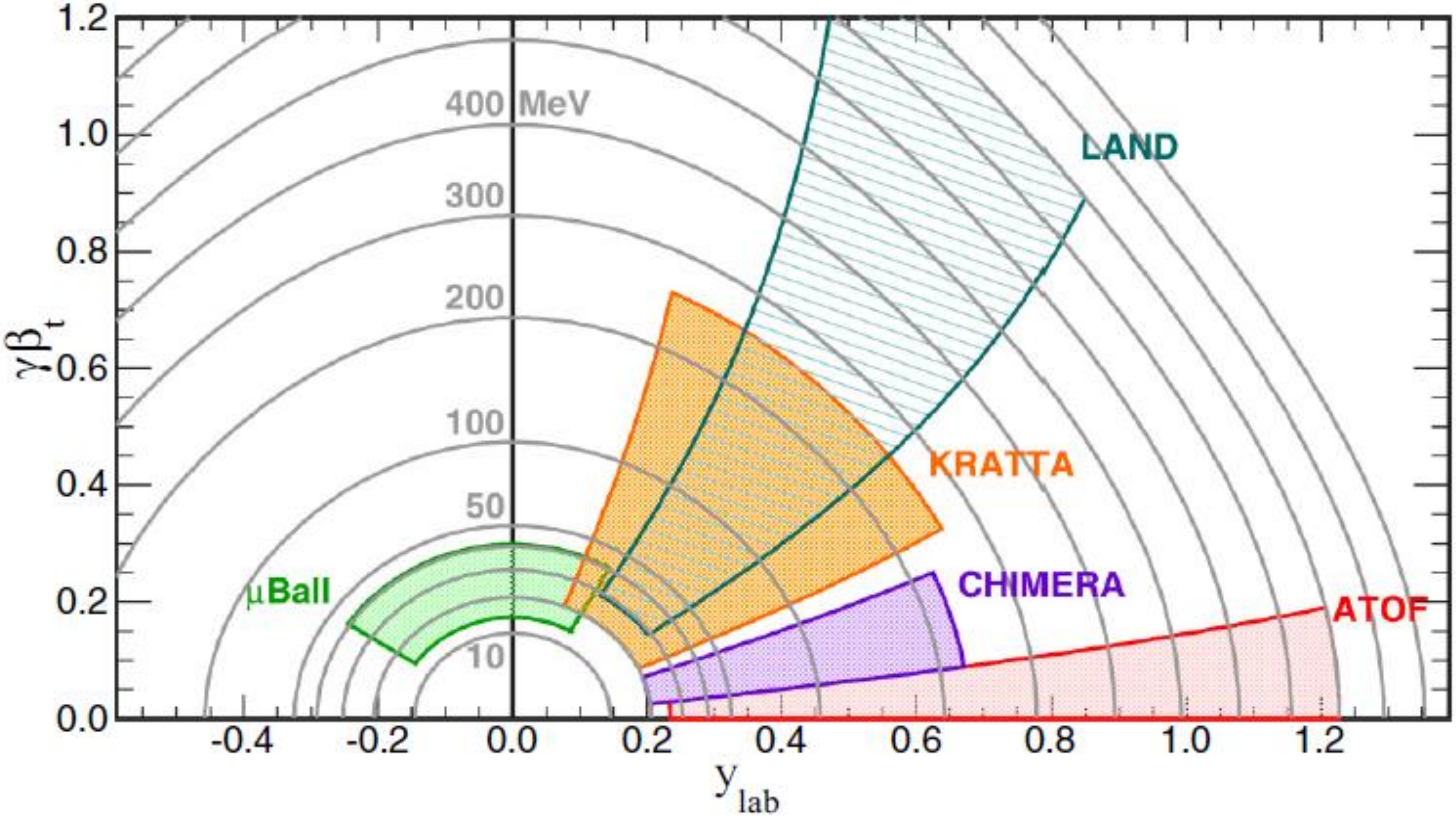

400 MeV
300
200
100
50
10
LAND
KRATTA
CHIMERA
ATOF
μBall
$\gamma\beta_t$
y_{lab}
1.2
1.0
0.8
0.6
0.4
0.2
0.0
-0.4
-0.2
0.0
0.2
0.4
0.6
0.8
1.0
1.2

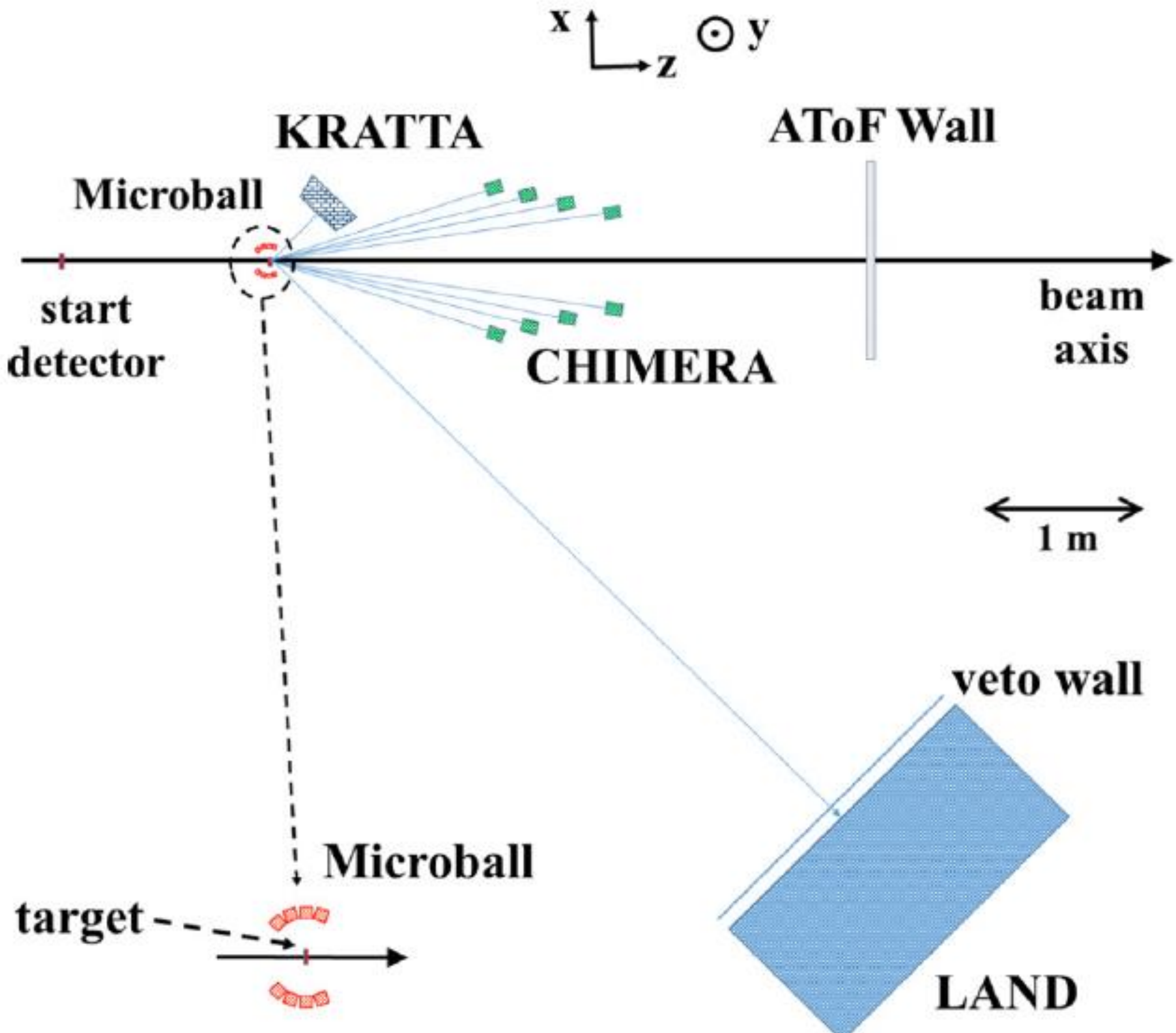
x
z
y
KRATTA
AToF Wall
Microball
start
detector
CHIMERA
beam
axis
1 m
veto wall
Microball
target
LAND

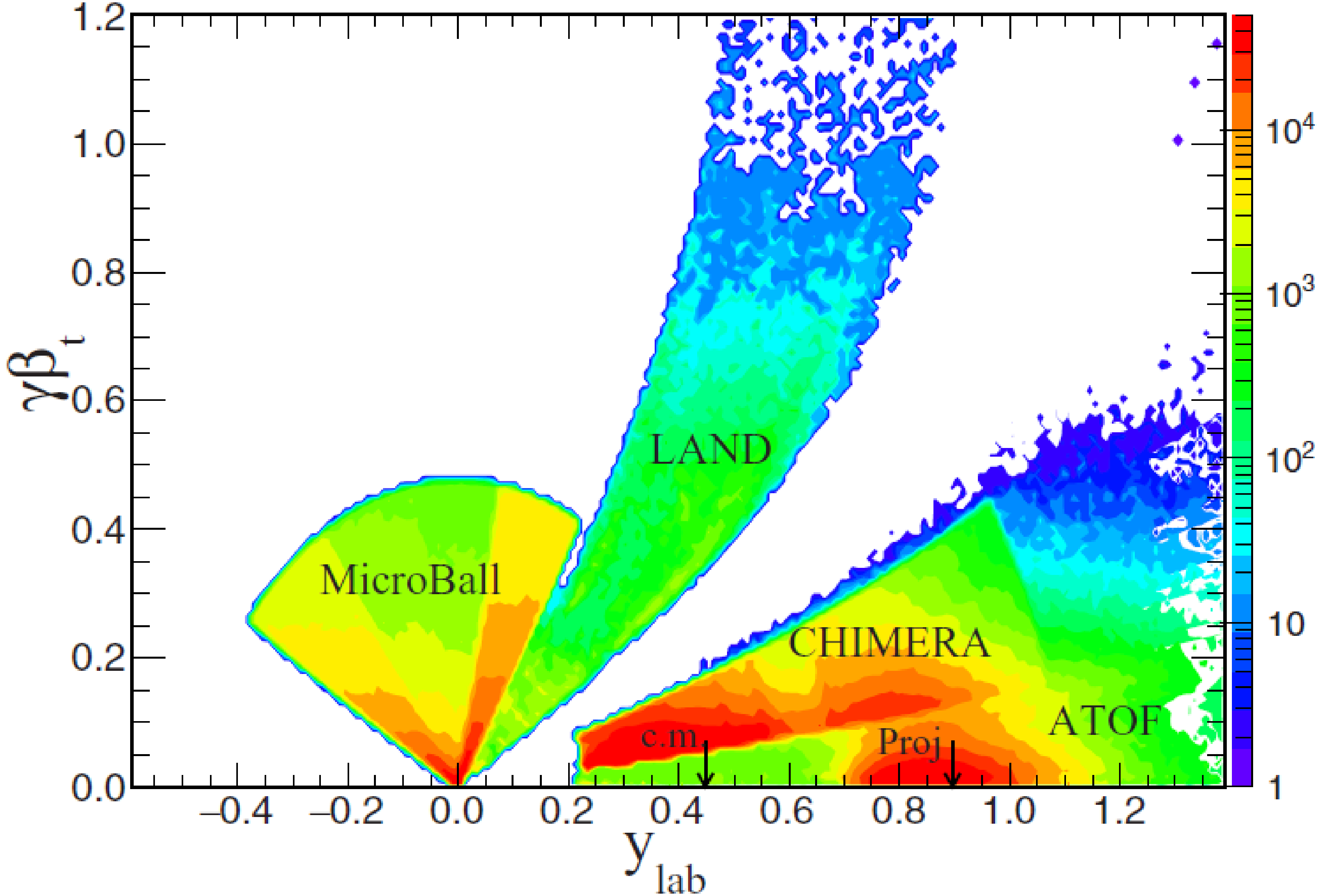

1.2
1.0
0.8
0.6
0.4
0.2
0.0
−0.4
−0.2
0.0
0.2
0.4
0.6
0.8
1.0
1.2
γβt
ylab
MicroBall
LAND
CHIMERA
ATOF
c.m.
Proj
10^4
10^3
10^2
10
1

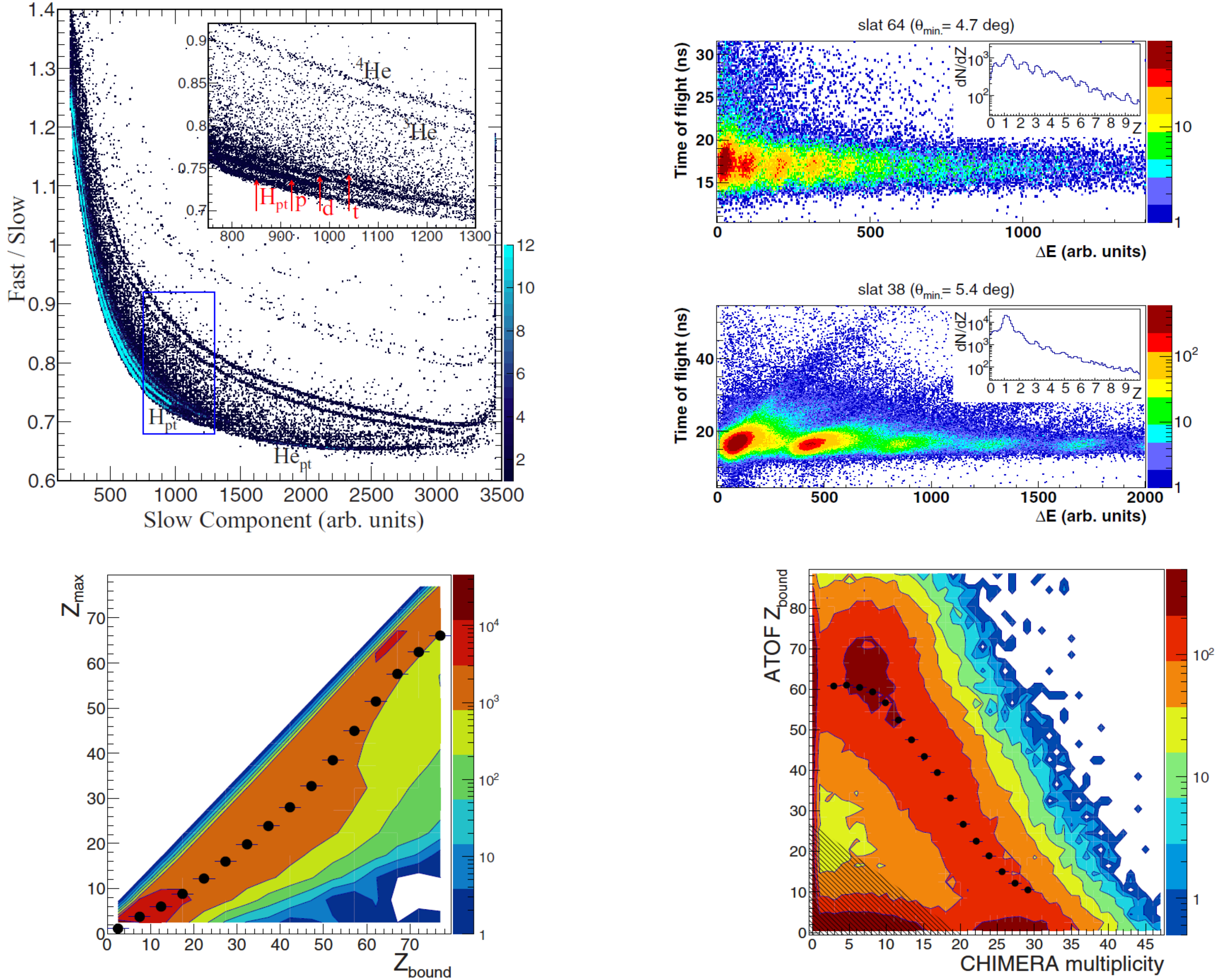
Fast / Slow
Slow Component (arb. units)
4He
3He
H_pt p d t
H_pt
He_pt
slat 64 (θmin.= 4.7 deg)
Time of flight (ns)
ΔE (arb. units)
dN/dZ
Z
slat 38 (θmin.= 5.4 deg)
Time of flight (ns)
ΔE (arb. units)
dN/dZ
Z
Z_max
Z_bound
ATOF Z_bound
CHIMERA multiplicity

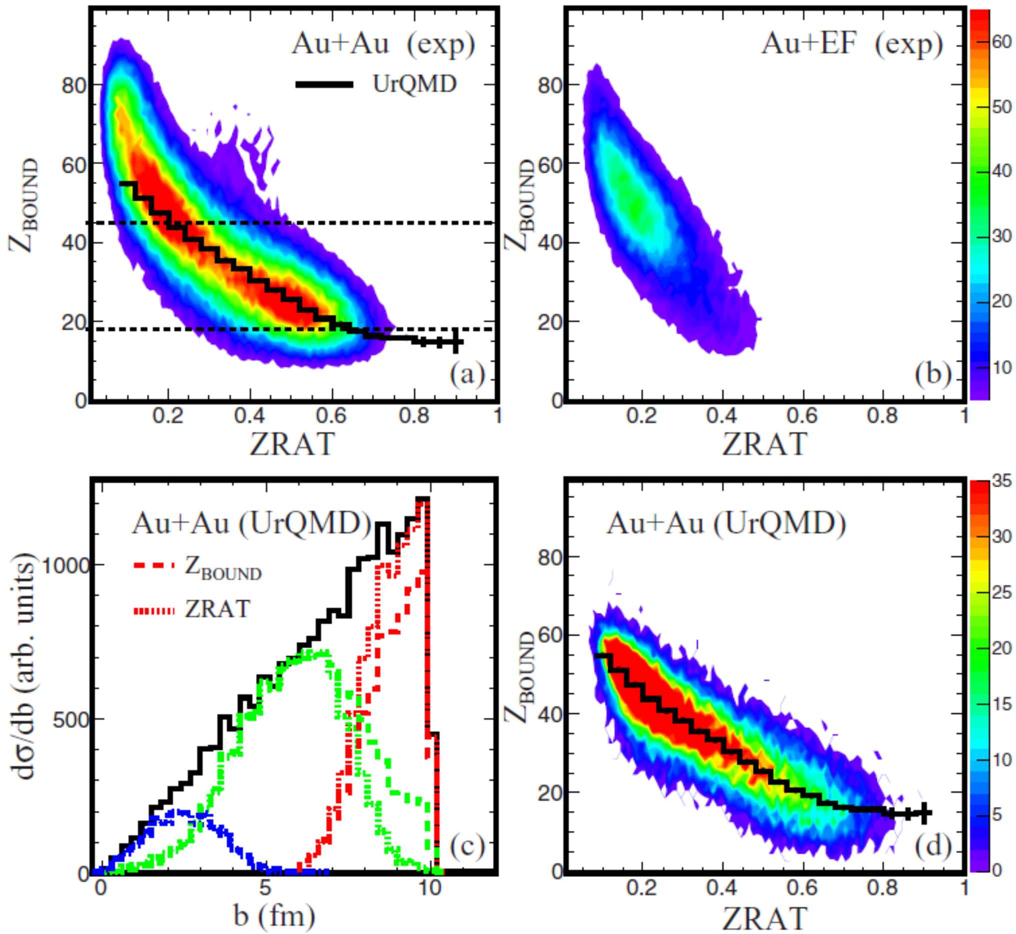

Au+Au (exp)
UrQMD
Au+EF (exp)
Au+Au (UrQMD)
Z_{BOUND}
ZRAT
(a)
(b)
(c)
(d)
$d\sigma/db$ (arb. units)
b (fm)

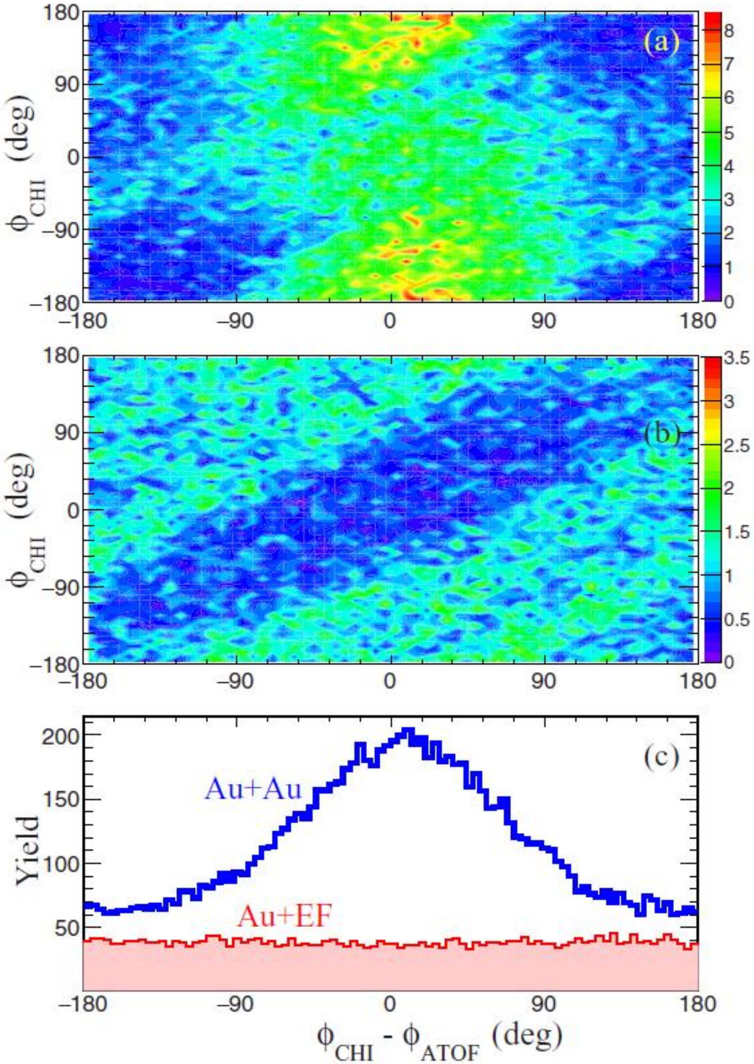

(a)
(b)
(c)
ϕ_{CHI} (deg)
Yield
Au+Au
Au+EF
ϕ_{CHI} - ϕ_{ATOF} (deg)

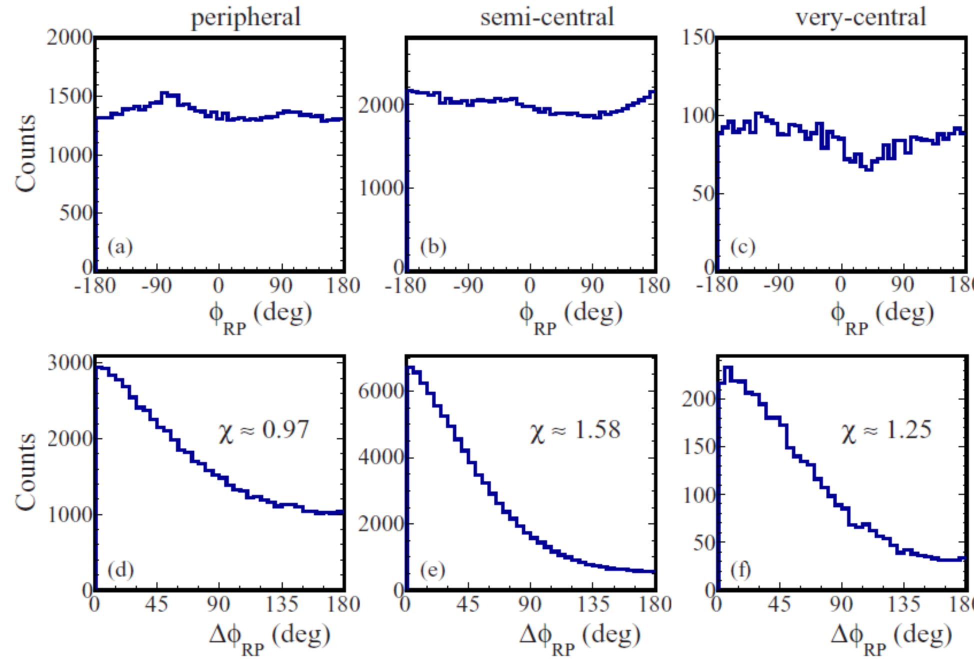

peripheral
semi-central
very-central
Counts
(a)
(b)
(c)
ϕ_{RP} (deg)
(d)
(e)
(f)
$\chi \approx 0.97$
$\chi \approx 1.58$
$\chi \approx 1.25$
$\Delta\phi_{RP}$ (deg)

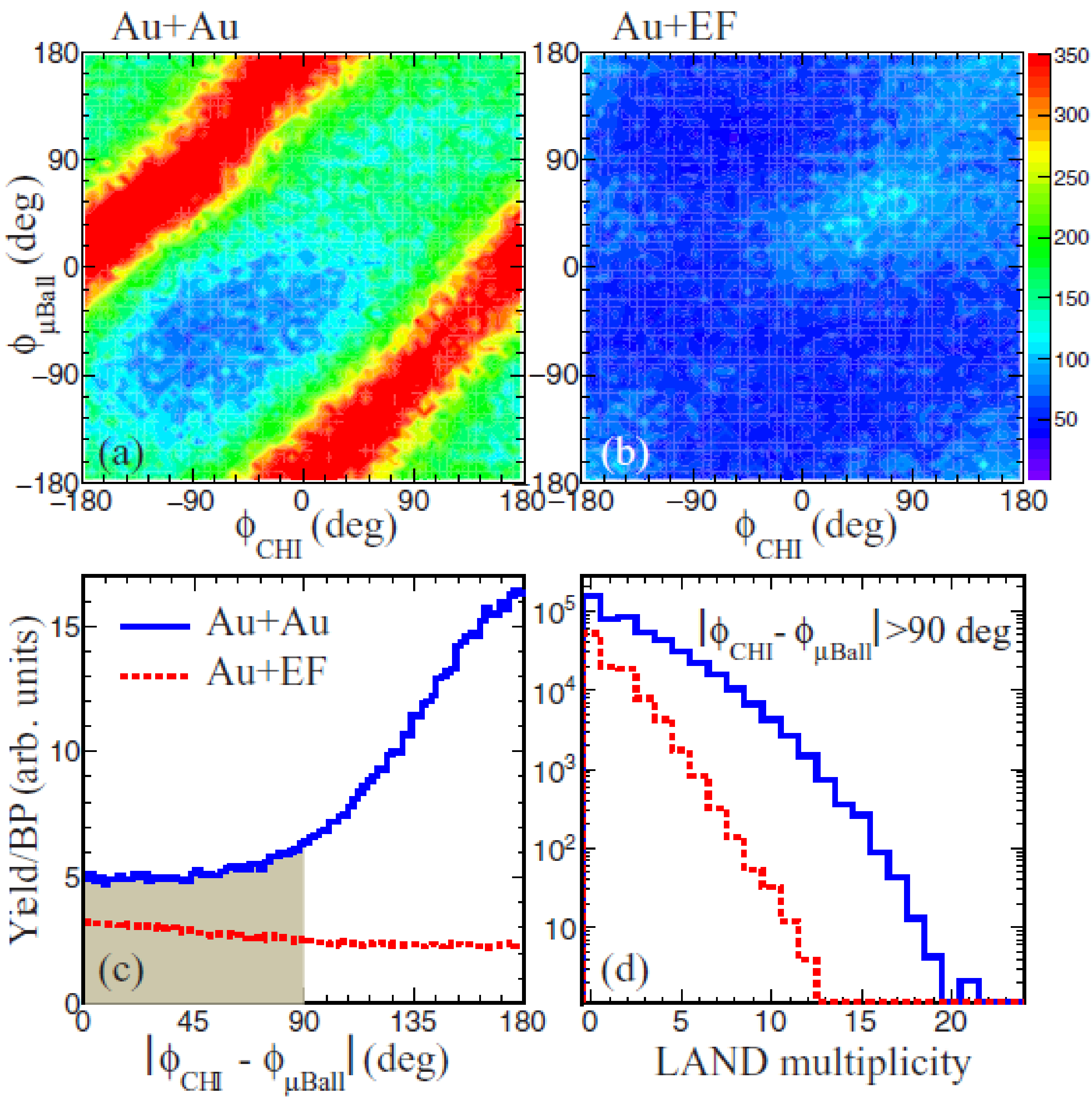

Au+Au
Au+EF
(a)
(b)
(c)
(d)
$\phi_{\mu Ball}$ (deg)
ϕ_{CHI} (deg)
ϕ_{CHI} (deg)
Yeld/BP (arb. units)
Au+Au
Au+EF
$|\phi_{CHI} - \phi_{\mu Ball}|$ (deg)
$|\phi_{CHI} - \phi_{\mu Ball}|$>90 deg
LAND multiplicity

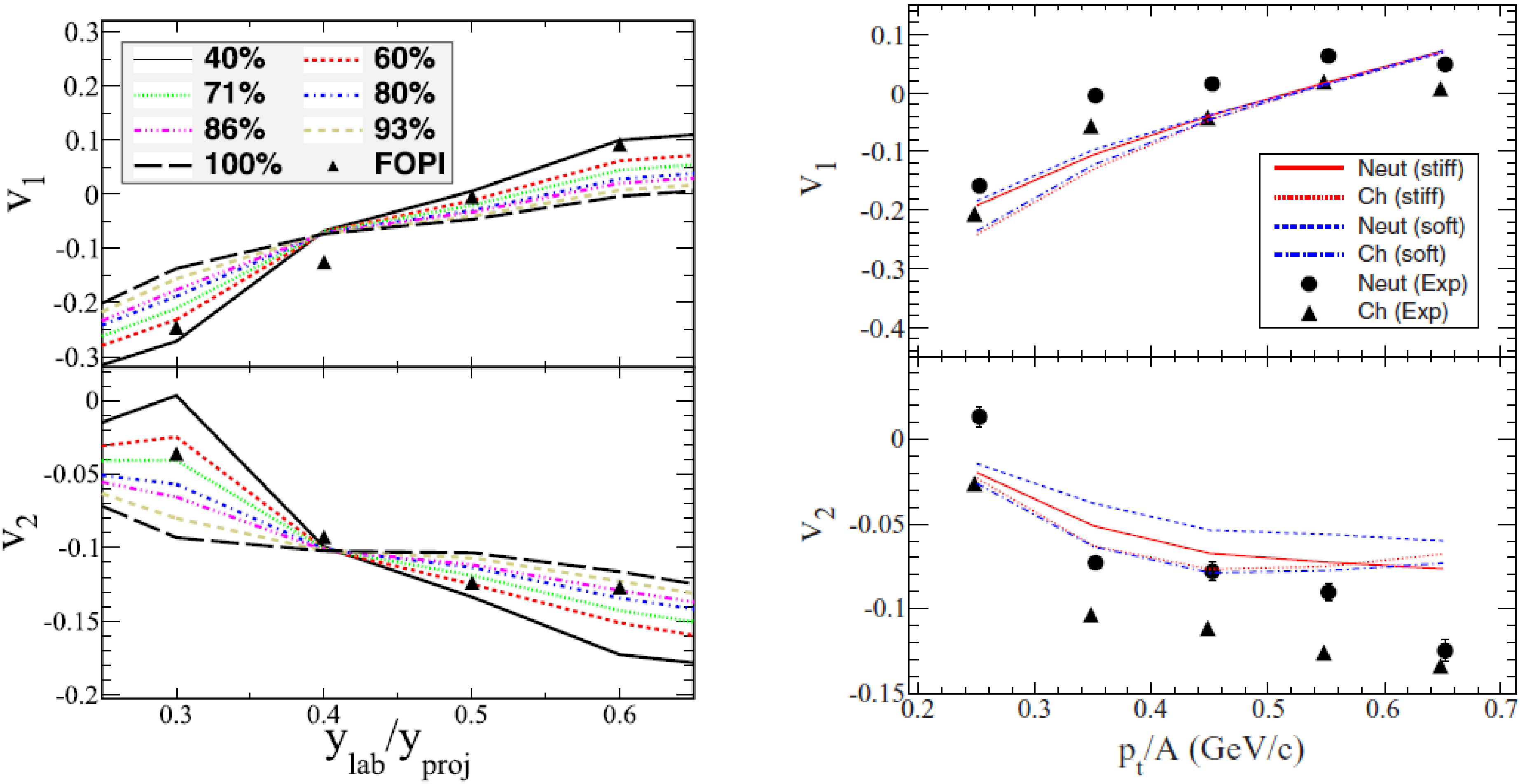

40%
60%
71%
80%
86%
93%
100%
FOPI
v_1
v_2
y_{lab}/y_{proj}
Neut (stiff)
Ch (stiff)
Neut (soft)
Ch (soft)
Neut (Exp)
Ch (Exp)
p_t/A (GeV/c)

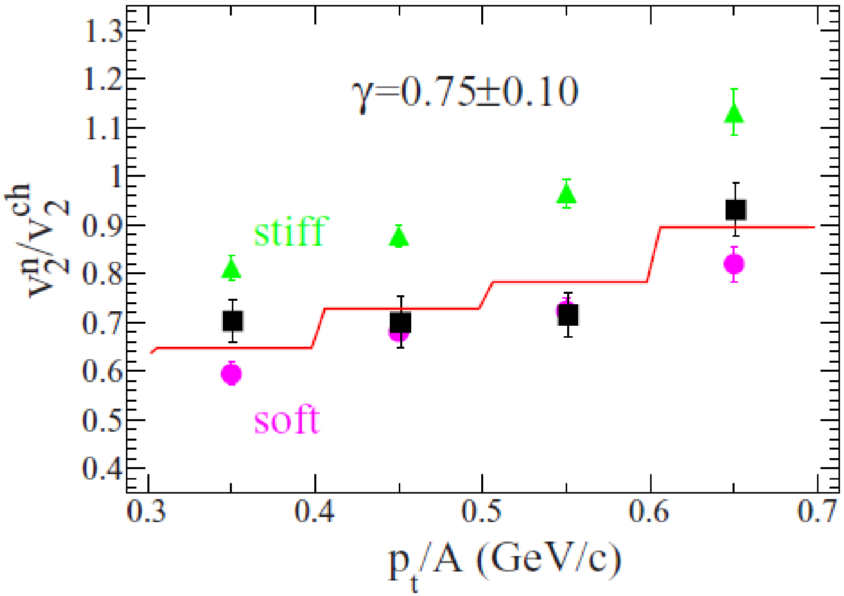
γ=0.75±0.10
stiff
soft
v_2^n/v_2^{ch}
p_t/A (GeV/c)

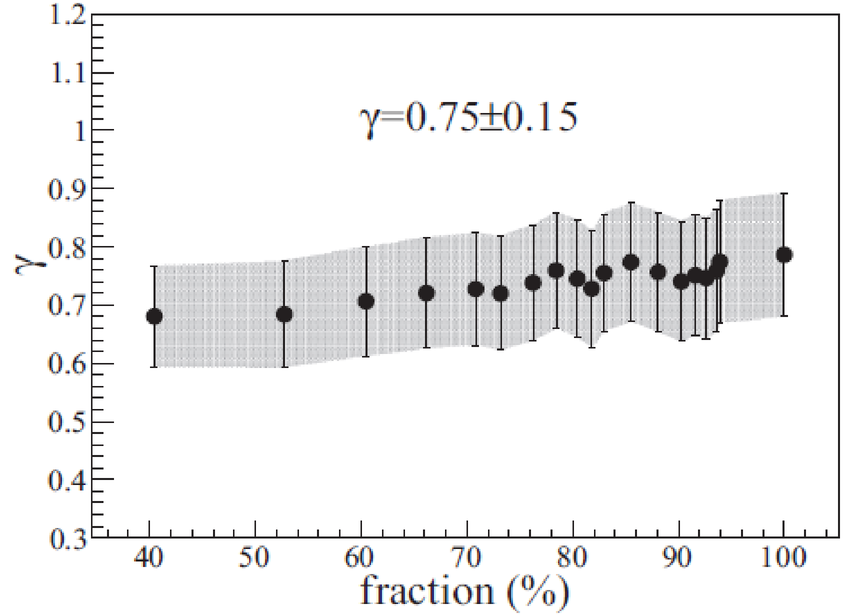
γ=0.75±0.15
γ
fraction (%)

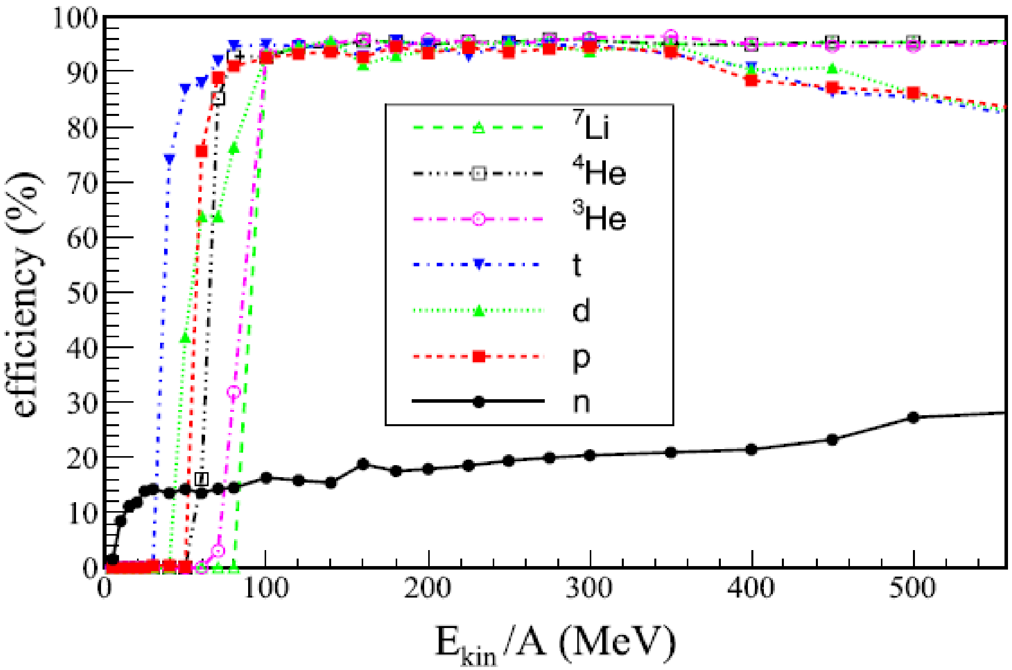
^{7}Li
^{4}He
^{3}He
t
d
p
n
efficiency (%)
E_{kin}/A (MeV)

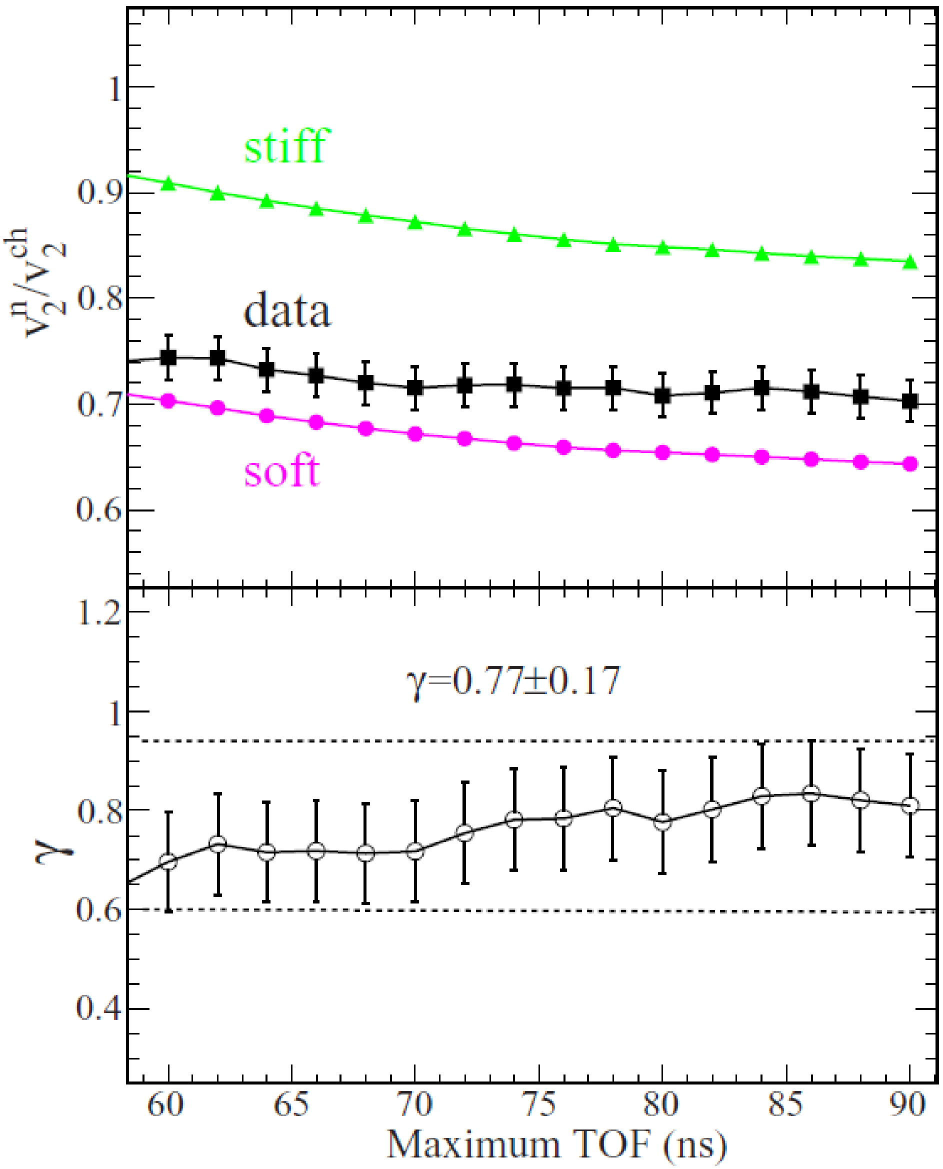

stiff
data
soft
γ=0.77±0.17
v_2^n/v_2^{ch}
γ
Maximum TOF (ns)

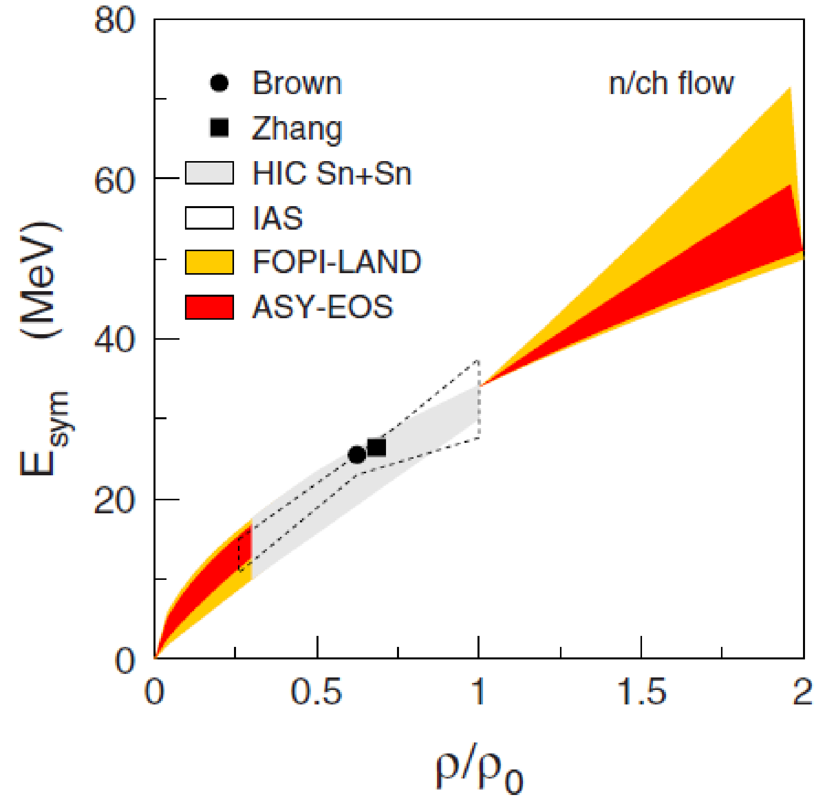

Brown
Zhang
HIC Sn+Sn
IAS
FOPI-LAND
ASY-EOS
n/ch flow
E_{sym} (MeV)
ρ/ρ_0

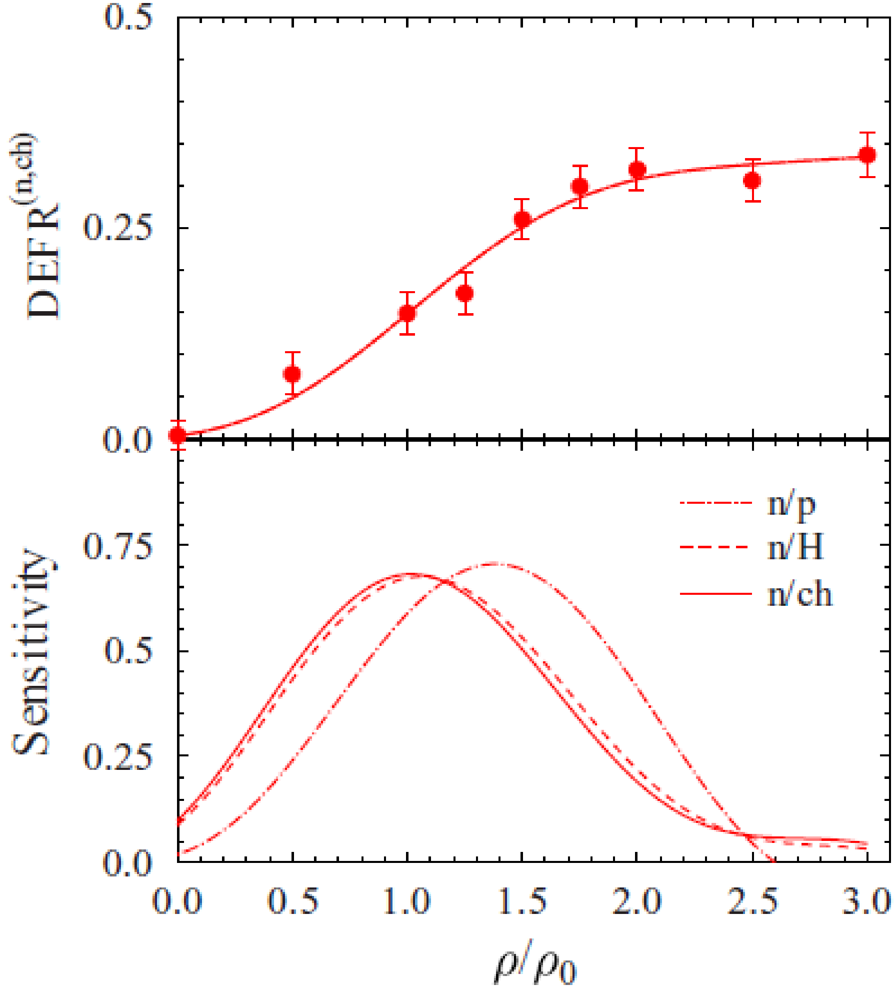

0.5
0.25
0.0
DEF R$^{(n,ch)}$
n/p
n/H
n/ch
0.75
0.5
0.25
0.0
Sensitivity
0.0
0.5
1.0
1.5
2.0
2.5
3.0
ρ/ρ_0

FARCOS

Experimental PERSPECTIVES in CHIMERA group : The FARCOS project

Starting prototype: 4 telescopes : NEWCHIM (2015-2019 final planning 20 telescopes)

Year	Tel.	Operation
2015	6	test acq. GET for FARCOS construction of 2 telescopes purchase of final GET electronics
2016	10	test dual gain module test GET electronic +DAQ Study of alignment system
2017	14(10)	test new asic pre-amplifiars final design modular support implementation asic pre-amplifier new DAQ VME+ GET running First experiments with new Chimera+Farcos front-end
2018	18(?)	Construction of new telescopes
2019	20+2	20 telescopes ready
. . . . .		

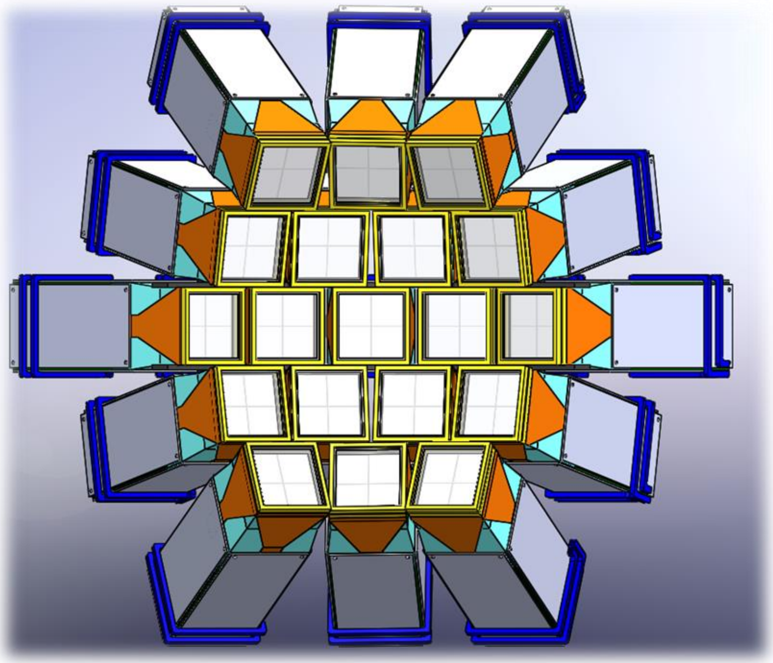

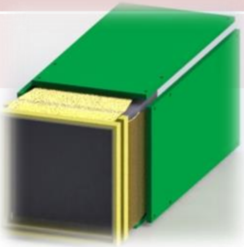

Final cost prediction: ≈< 1 M€

132 channels by each cluster

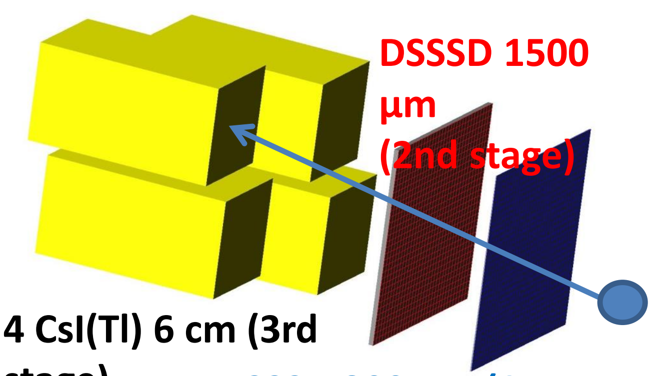

SIKO experiment
University of Birmingnam & CHIMERA collaboration

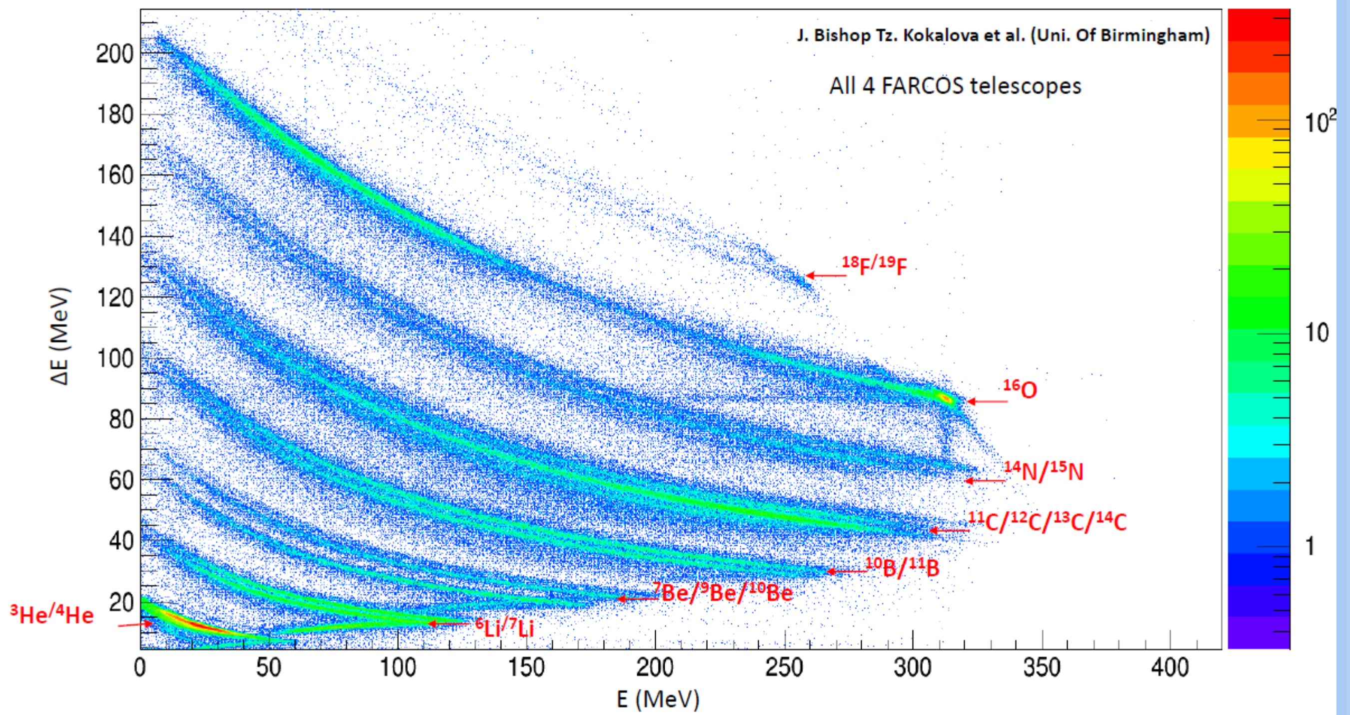

DAN

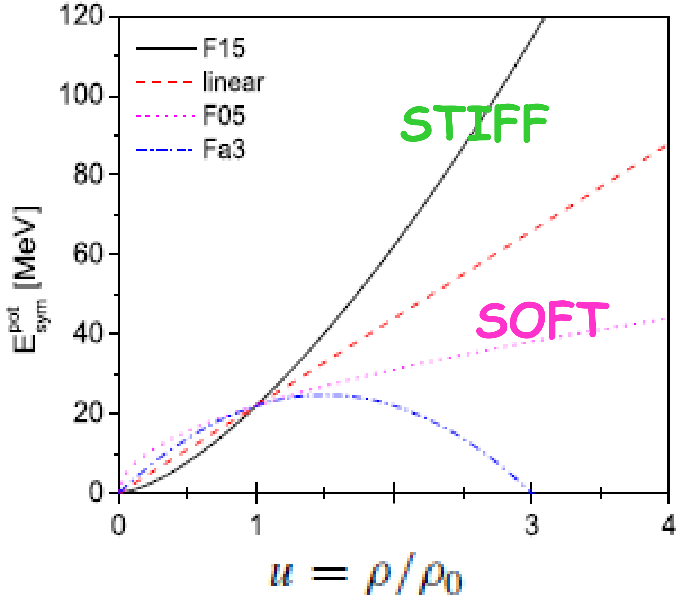

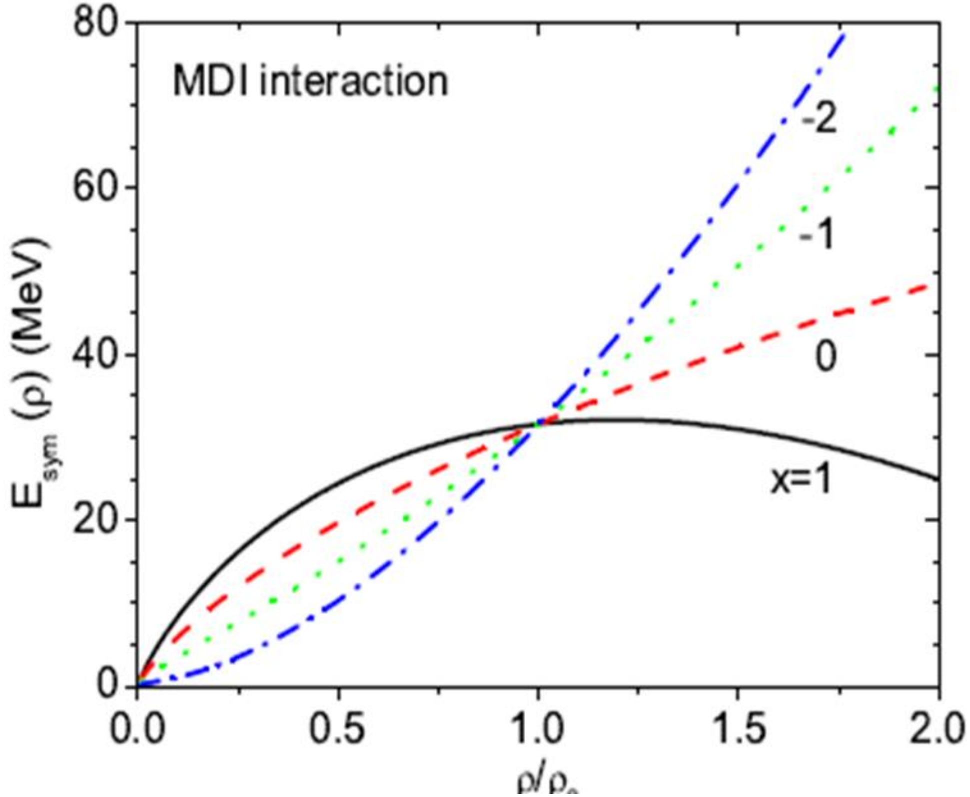

$$E_{sym} = E_{sym}^{pot} + E_{sym}^{kin}$$
$$= 22\,\text{MeV} \cdot (\rho/\rho_0)^{\gamma} + 12\,\text{MeV} \cdot (\rho/\rho_0)^{2/3}$$

new: result obtained with Tübingen QMD*)

M.D. Cozma, PLB 700, 139 (2011); arXiv:1102.2728

difference of neutron and proton squeeze-outs
Au + Au @ 400 A MeV

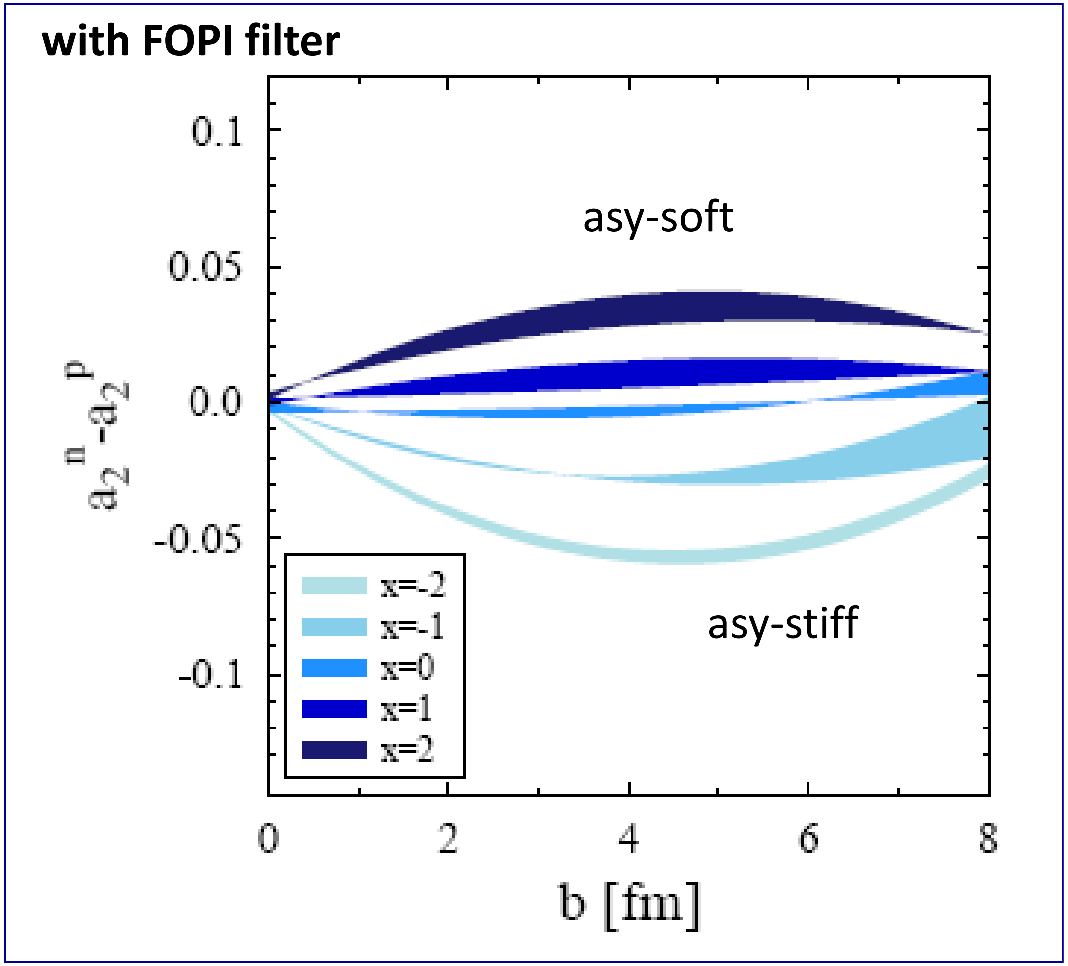

- $a_2 = 2v_2$
- with FOPI filter
- bands show uncertainty due to isoscalar field "soft to hard"

conclusion in paper:
super-soft not compatible with FOPI-LAND data

* V.S. Uma Maheswari, C. Fuchs, Amand Faessler, L. Sehn, D.S. Kosov, Z. Wang, NPA 628 (1998)

new: result obtained with Tübingen QMD*)

M.D. Cozma, PLB 700, 139 (2011); arXiv:1102.2728

difference of neutron and proton squeeze-outs
Au + Au @ 400 A MeV

with FOPI filter

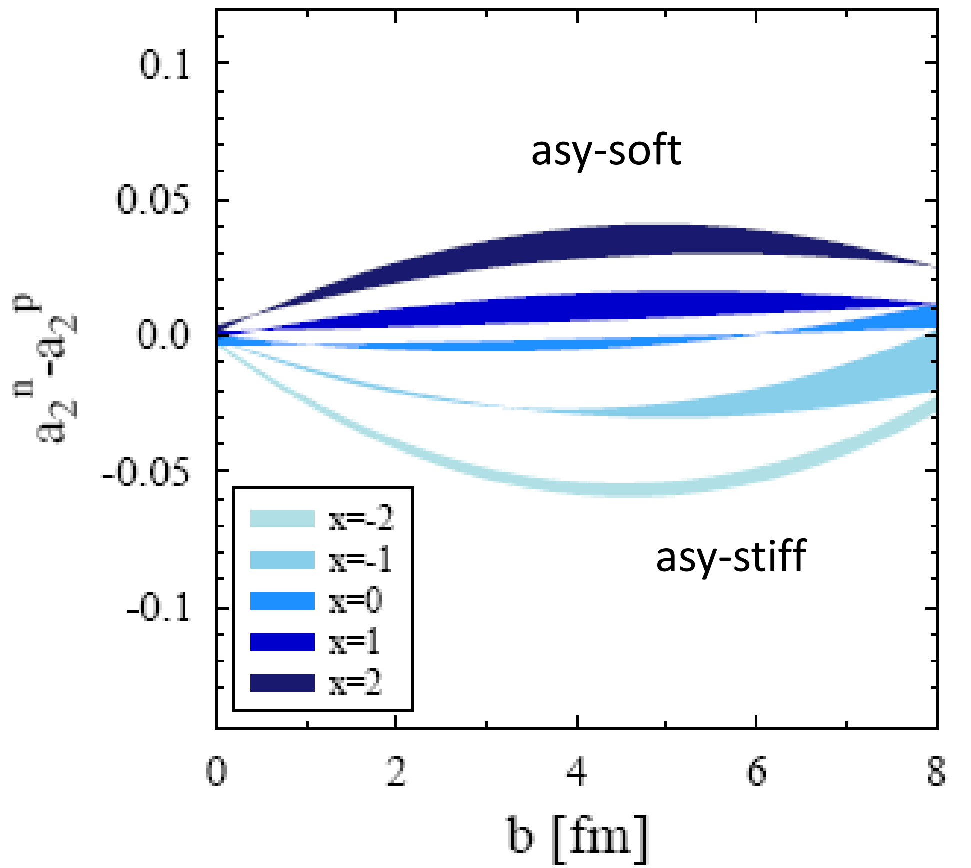

- $a_2 = 2v_2$
- with FOPI filter
- bands show uncertainty due to isoscalar field "soft to hard"

conclusion in paper:
super-soft not compatible with FOPI-LAND data

UrQMD:
momentum dep. of isoscalar field
momentum dep. of NNECS

T-QMD:
density dep. of NNECS
asymmetry dep. of NNECS
soft vs. hard EoS
width of wave packets

* V.S. Uma Maheswari, C. Fuchs, Amand Faessler, L. Sehn, D.S. Kosov, Z. Wang, NPA 628 (1998)

results with Tübingen QMD and momentum dependent forces*

*M.D. Cozma, PLB 700, 139 (2011); arXiv:1102.2728

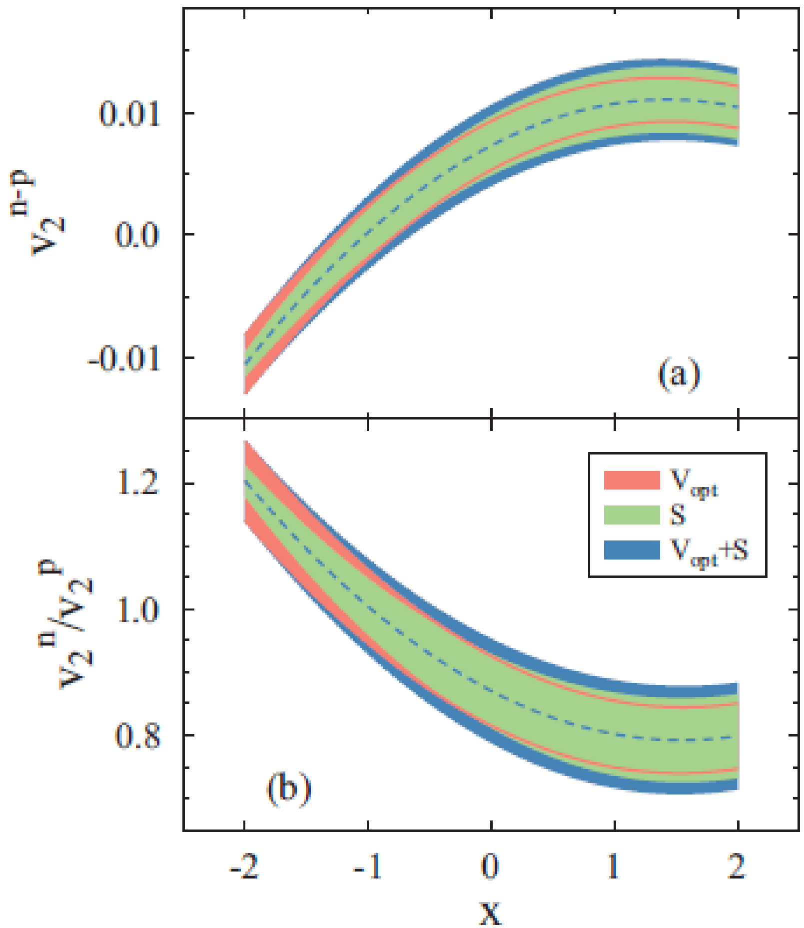

FIG. 1. (Color online) Variations in the values of the impact parameter integrated ($b \leqslant 7.5$ fm) npEFD (a) and npEFR (b) due to different choices for the optical potential (V_{opt}), parametrization of symmetry-energy (S) as well as the combined, quadratically added, uncertainty.

M.D. Cozma et al., Towards a model-independent constraint of the high-density dependence of the symmetry energy,

arXiv:1305.5417 [nucl-th] PRC88 044912 (2013)

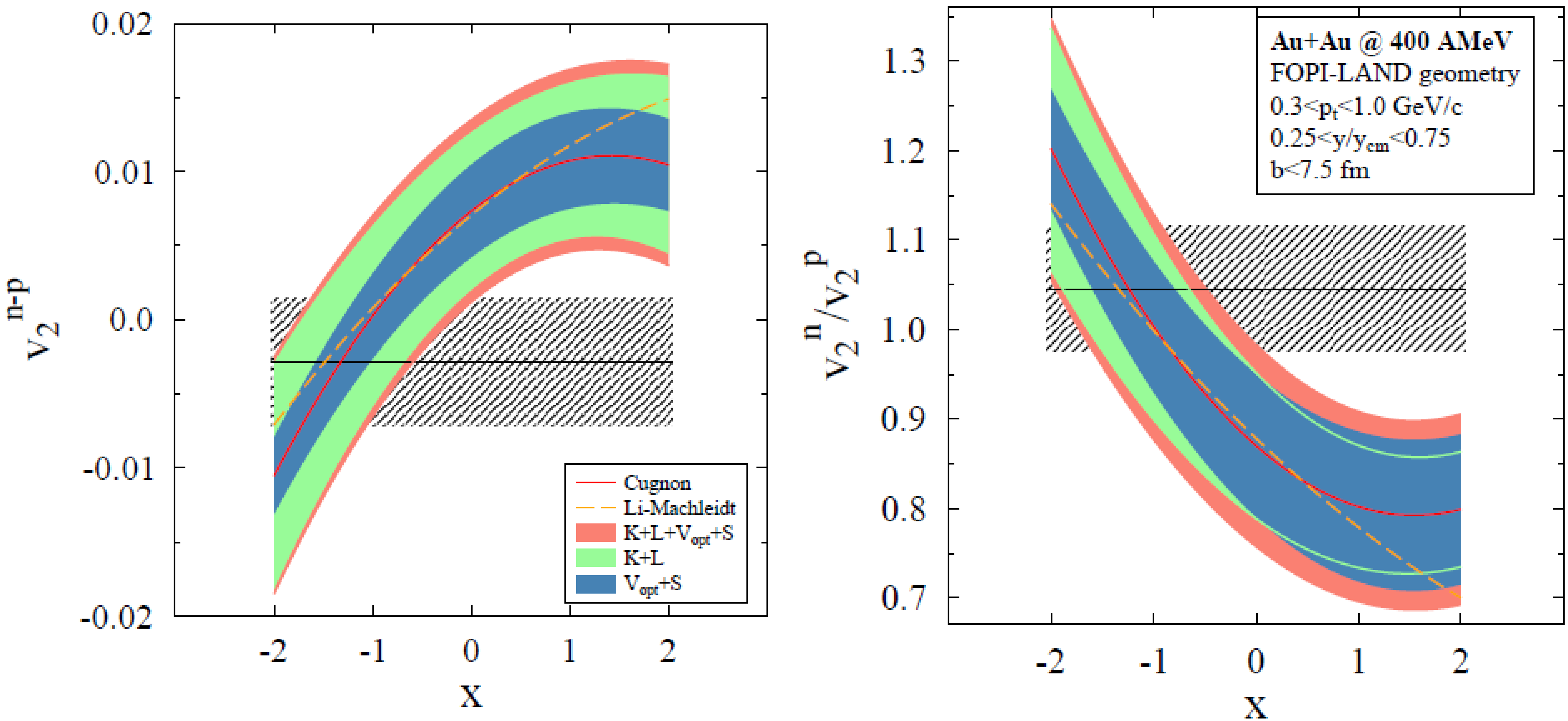

FIG. 2: Model dependence of npEFD and npEFR and comparison with FOPI-LAND experimental data, integrated over impact parameter b≤7.5 fm. Sensitivity to the different model parameters, compressibility modulus (K), width of nucleon wave function (L), optical potential (V_{opt}) and parametrization of the symmetry energy (S) are displayed. The total model dependence is obtained by adding, in quadrature, individual sensitivities.

Results with Tübingen QMD

UrQMD:
momentum dep. of isoscalar field
momentum dep. of NNECS
momentum independent power-law
parameterization of the symmetry energy

Tübingen-QMD:
density dep. of NNECS
asymmetry dep. of NNECS
soft vs. hard EoS
width of wave packets
momentum dependent (Gogny inspired)
parameterization of the symmetry energy

M.D. Cozma, PLB 700, 139 (2011);
arXiv:1102.2728

x =-1.35±1.25

M.D. Cozma et al., Towards a model-independent constraint of the high-density dependence of the symmetry energy

arXiv:1305.5417 [nucl-th] PRC88 044912 (2013)

Au+Au 400 A MeV b< 7.5 fm

stiffnes

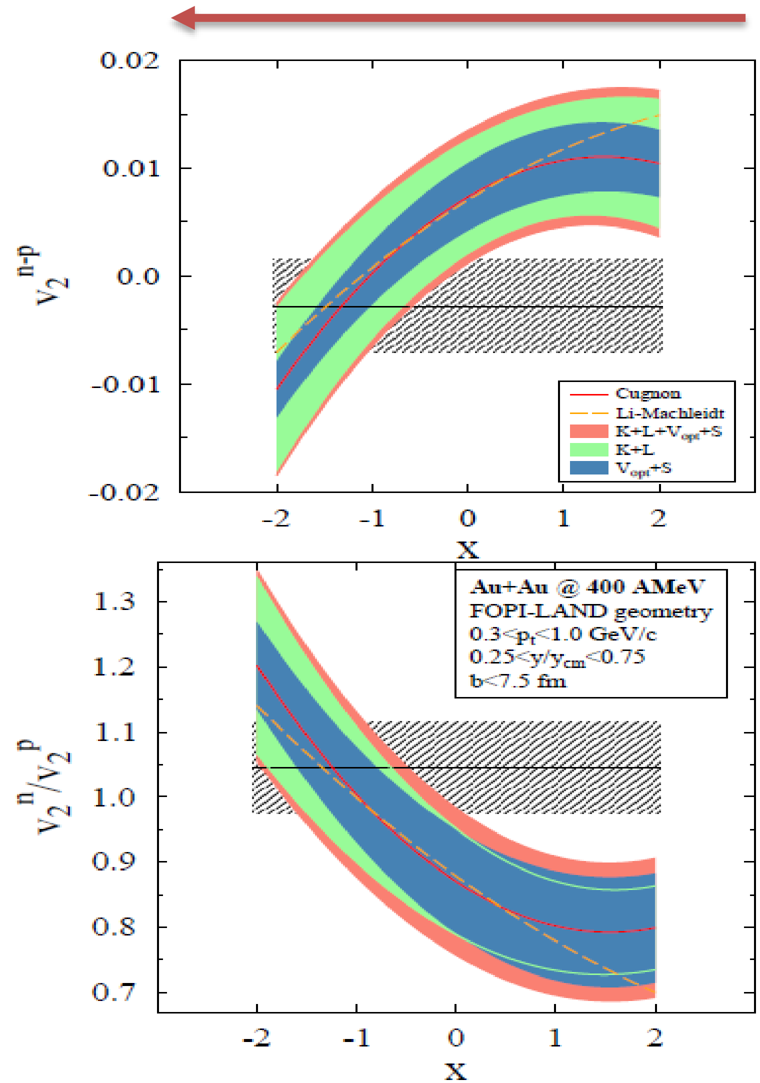

FIG. 2: Model dependence of npEFD and npEFR and comparison with FOPI-LAND experimental data, integrated over impact parameter b≤7.5 fm. Sensitivity to the different model parameters, compressibility modulus (K), width of nucleon wave function (L), optical potential (V_{opt}) and parametrization of the symmetry energy (S) are displayed. The total model dependence is obtained by adding, in quadrature, individual sensitivities.

CHIMERA

CHIMERA activity at LNS

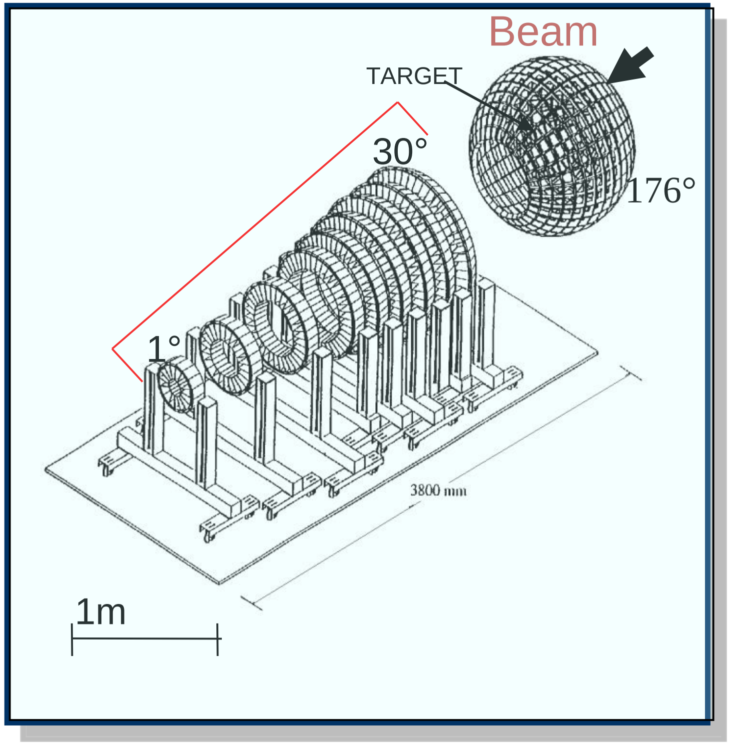

1192 telescopes

94 % of 4π

Several Id. technique

Low thresholds

E. De Filippo & A. Pagano, EPJA 50 2 (2014)

CHIMERA activity at LNS

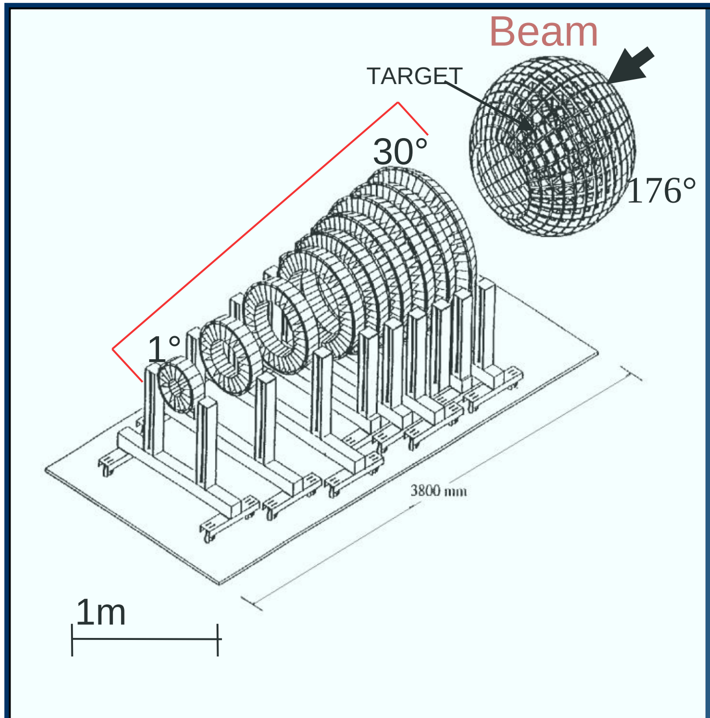

1192 telescopes

94 % of 4π

Several Id. technique

Low thresholds

Study of:

- Reaction mechanisms of Heavy-Ion collisions at Fermi and low energies
- Influence of Isospin on reaction mechanism
- Density dependence of Symmetry Energy at sub-saturation density
- New break-up mechanisms and exotic decaying in heavy (Au+Au) sytems
- In flight production and tagging of RIB
- Transfer reaction with light RIB
- Neutron and gamma detection
- Digital pulse sampling analysis
- Building of FARCOS correlator

E. De Filippo & A. Pagano, EPJA 50 2 (2014)

CHIMERA activity at LNS

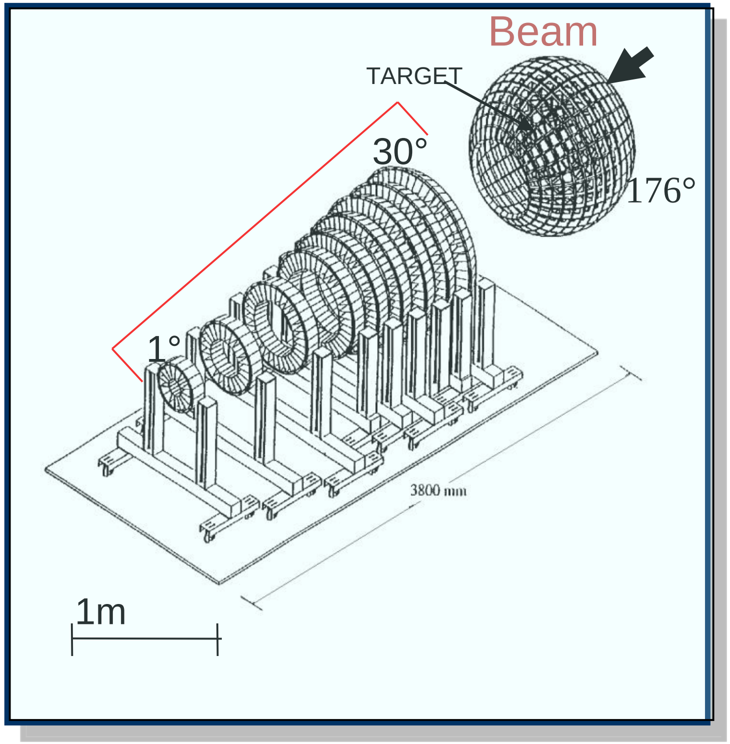

1192 telescopes

94 % of 4π

Several Id. technique

Low thresholds

Study of:

- Reaction mechanisms of Heavy-Ion collisions at Fermi and low energies
- Influence of Isospin on reaction mechanism
- Density dependence of Symmetry Energy at sub-saturation density
- New break-up mechanisms and exotic decaying in heavy (Au+Au) sytems
- In flight production and tagging of RIB
- Transfer reaction with light RIB
- Neutron and gamma detection
- Digital pulse sampling analysis
- Building of FARCOS correlator

E. De Filippo & A. Pagano, EPJA 50 2 (2014)

CHIMERA activity at LNS

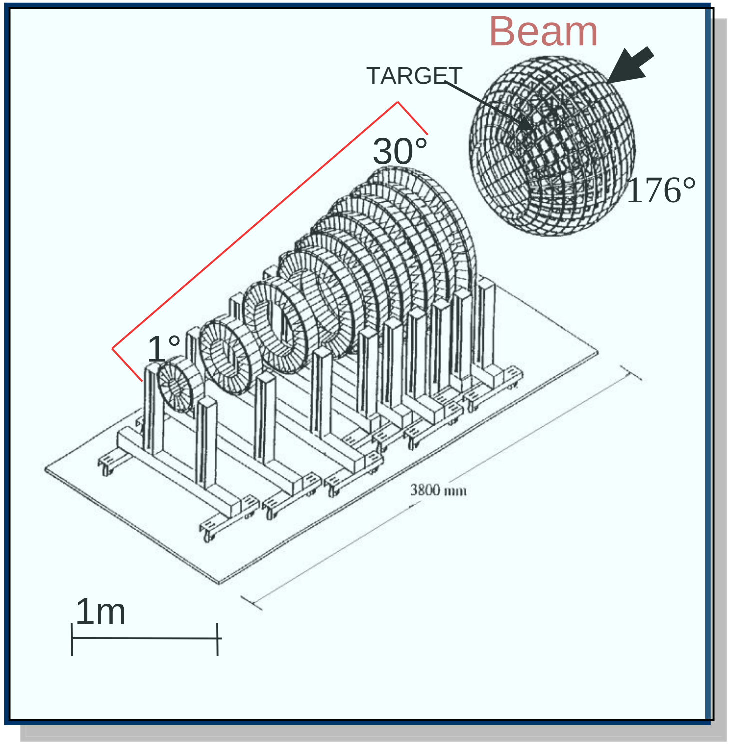

1192 telescopes

94 % of 4π

Several Id. technique

Low thresholds

a) the concept of CHIMERA detector was first discussed by A.Pagano et al., 2nd Japan-Italy Joint Symposium '95 - perspectives in H.I Physics, RIKEN 1995
b) First results were presented by A.Pagano et al., 5th Italy-Japan Symposium, Naples, 2004

CHIMERA activity at LNS

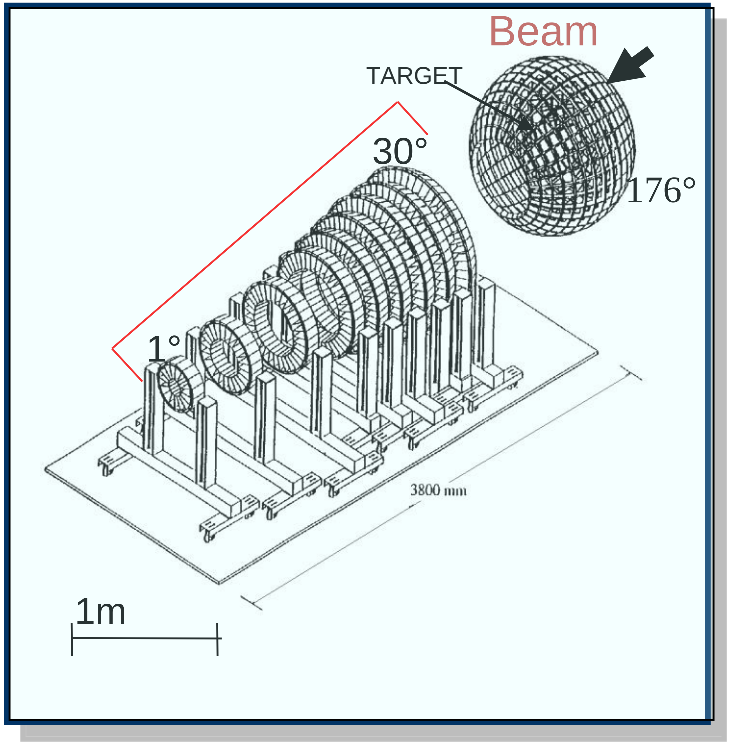

1192 telescopes

94 % of 4π

Several Id. technique

Low thresholds

a) the concept of CHIMERA detector was first discussed by A.Pagano et al., 2nd Japan-Italy Joint Symposium '95 - perspectives in H.I Physics, RIKEN 1995
b) First results were presented by A.Pagano et al., 5th Italy-Japan Symposium, Naples, 2004

Study of:

- Reaction mechanisms of Heavy-Ion collisions at Fermi and low energies
- Influence of Isospin on reaction mechanism
- Density dependence of Symmetry Energy at sub-saturation density
- New break-up mechanisms and exotic decaying in heavy (Au+Au) sytems
- In flight production and tagging of RIB
- Transfer reaction with light RIB
- Neutron and gamma detection
- Digital pulse sampling analysis
- Building of FARCOS correlator

CHIMERA activity at LNS

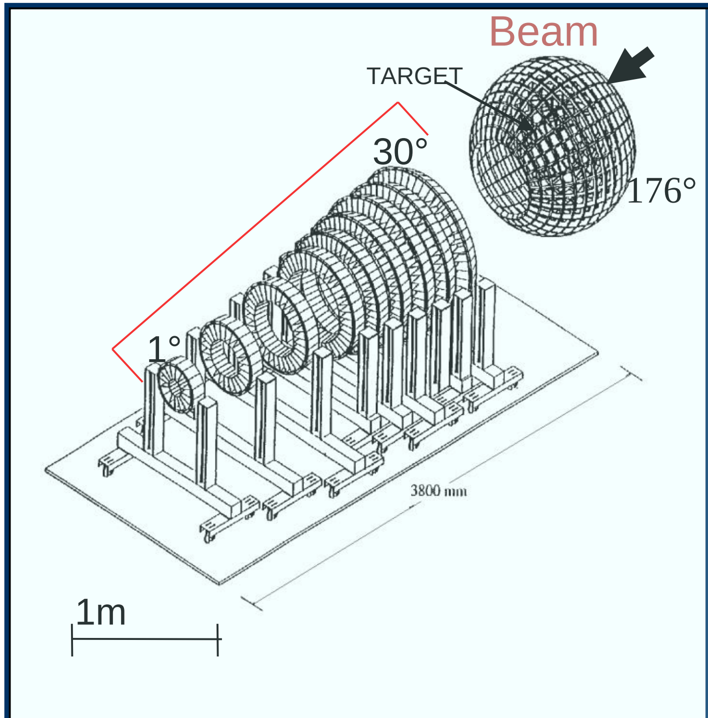

1192 telescopes

94 % of 4π

Several Id. technique

Low thresholds

a) the concept of CHIMERA detector was first discussed by A.Pagano et al., 2nd Japan-Italy Joint Symposium '95 - perspectives in H.I Physics, RIKEN 1995
b) First results were presented by A.Pagano et al., 5th Italy-Japan Symposium, Naples, 2004

Study of:

- Reaction mechanisms of Heavy-Ion collisions at Fermi and low energies
- Influence of Isospin on reaction mechanism
- Density dependence of Symmetry Energy at sub-saturation density
- New break-up mechanisms and exotic decaying in heavy (Au+Au) sytems
- In flight production and tagging of RIB
- Transfer reaction with light RIB
- Neutron and gamma detection
- Digital pulse sampling analysis
- Building of FARCOS correlator

CHIMERA multi-detector

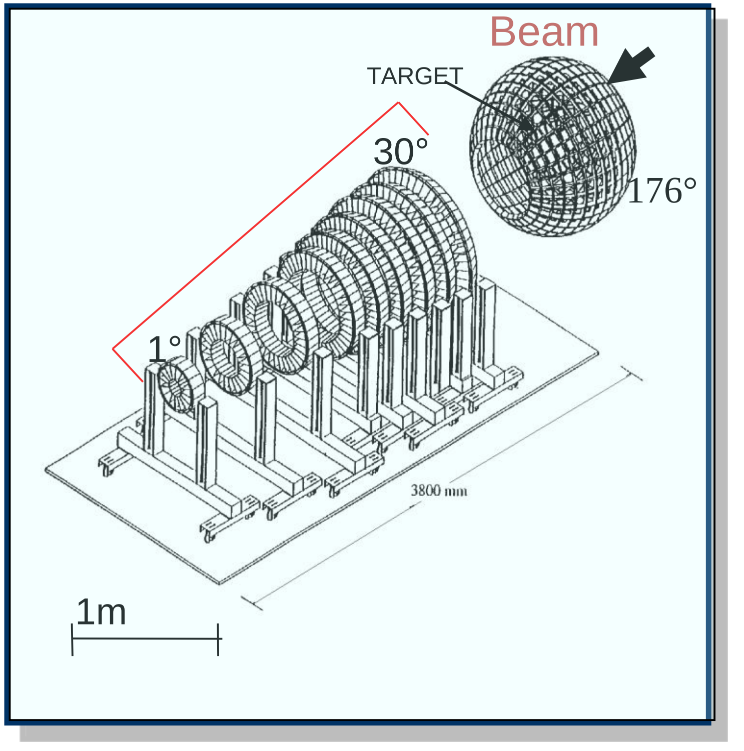

CHIMERA multi-detector

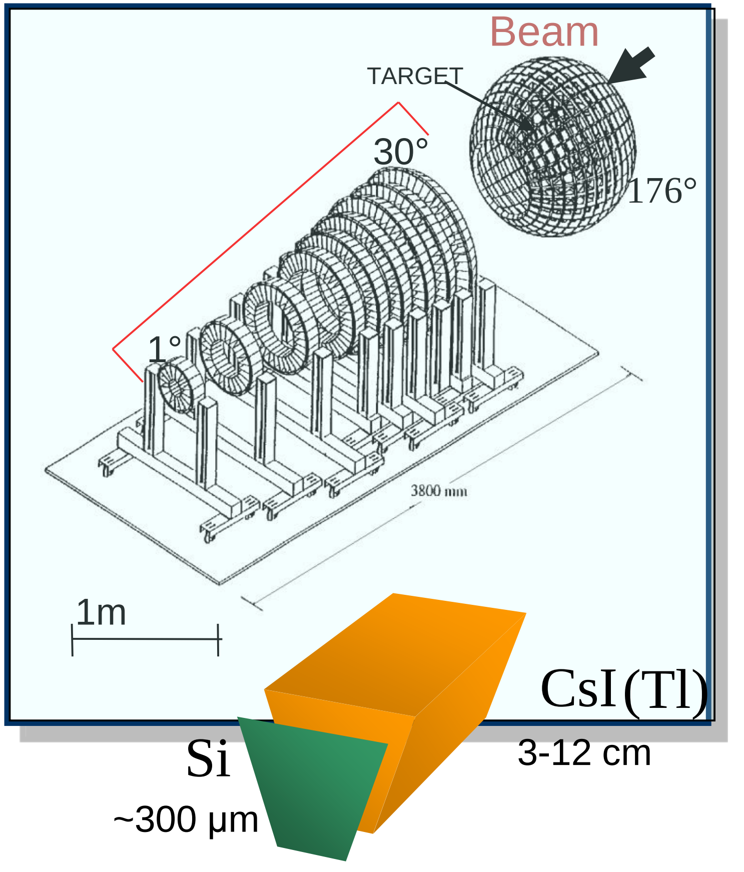

CHIMERA multi-detector

$\Delta E(Si)$-$E(CsI)$

Charge Z for particles punching throught the Si detector

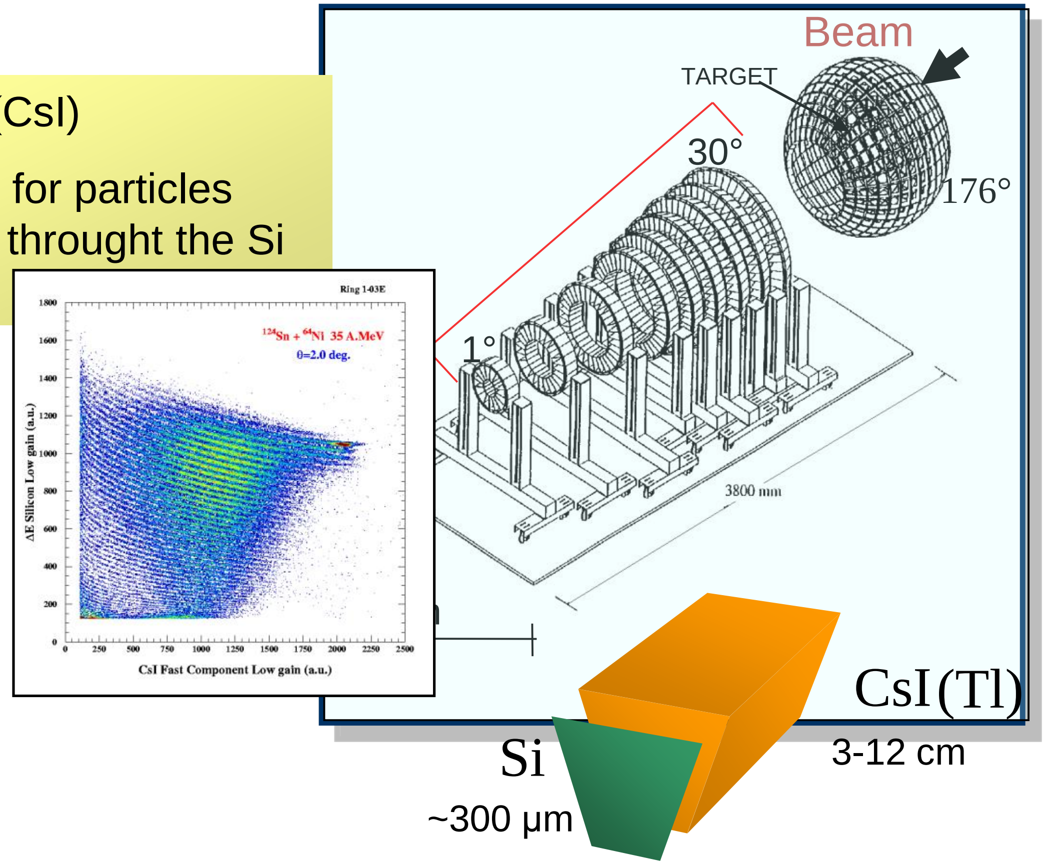

CHIMERA multi-detector

ΔE(Si)-E(CsI)

Charge Z for particles punching throught the Si detector

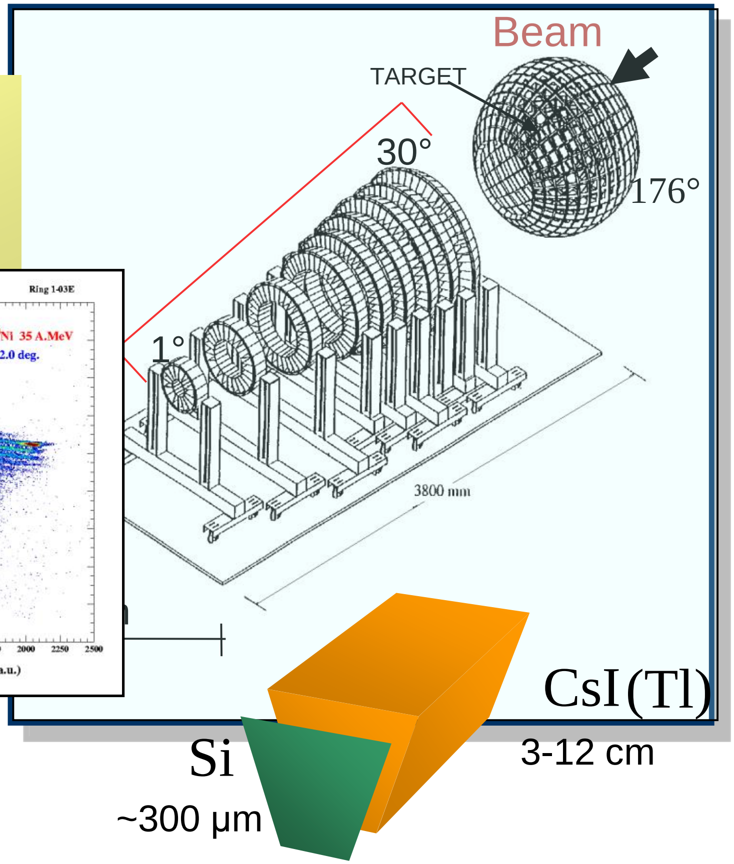

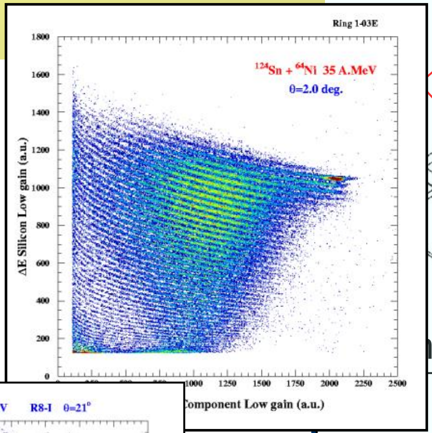

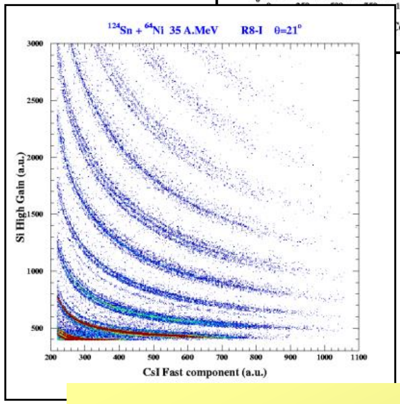

ΔE(Si)-E(CsI)

Charge Z and A for light ions (Z<9) punching throught the Si detector

CHIMERA multi-detector

ΔE(Si)-E(CsI)

Charge Z for particles punching throught the Si detector

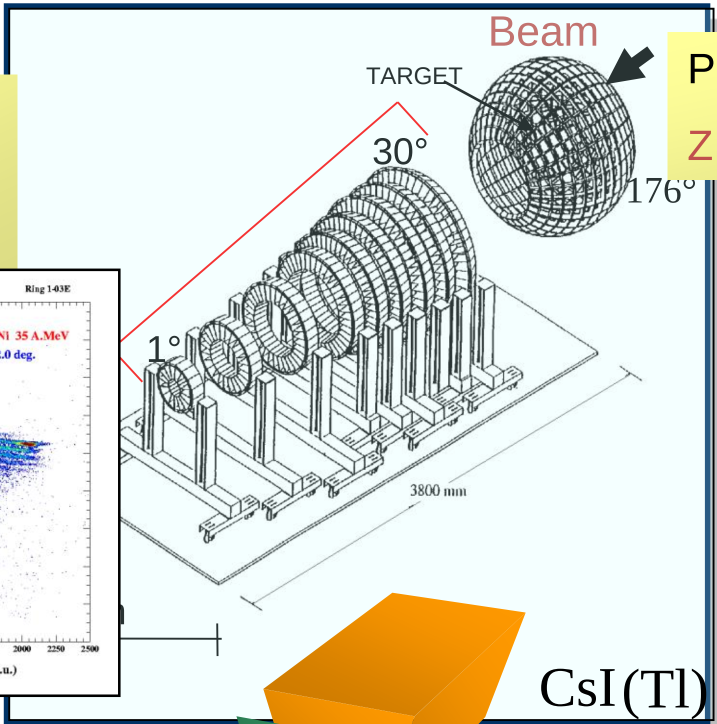

PSD in CsI(Tl)

Z and A for light charged particles

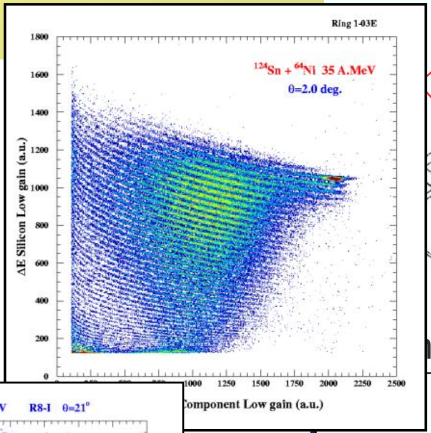

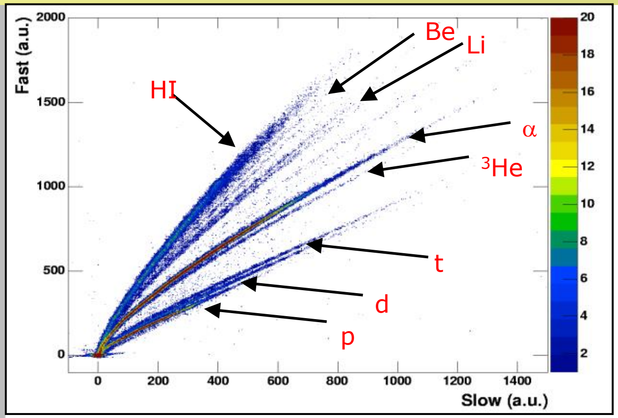

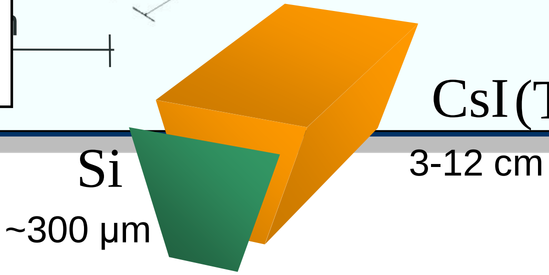

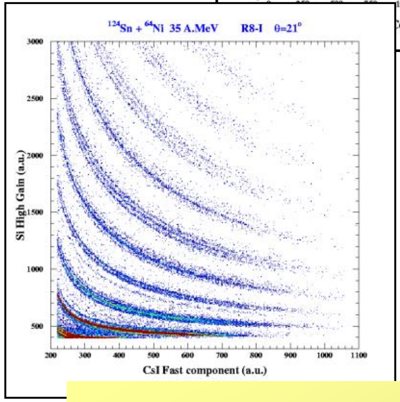

ΔE(Si)-E(CsI)

Charge Z and A for light ions (Z<9) punching throught the Si detector

CHIMERA multi-detector

ΔE(Si)-E(CsI)

Charge Z for particles punching throught the Si detector

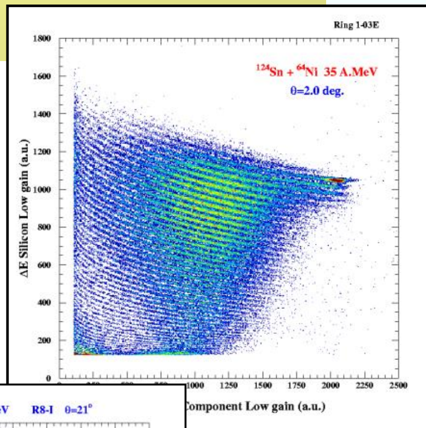

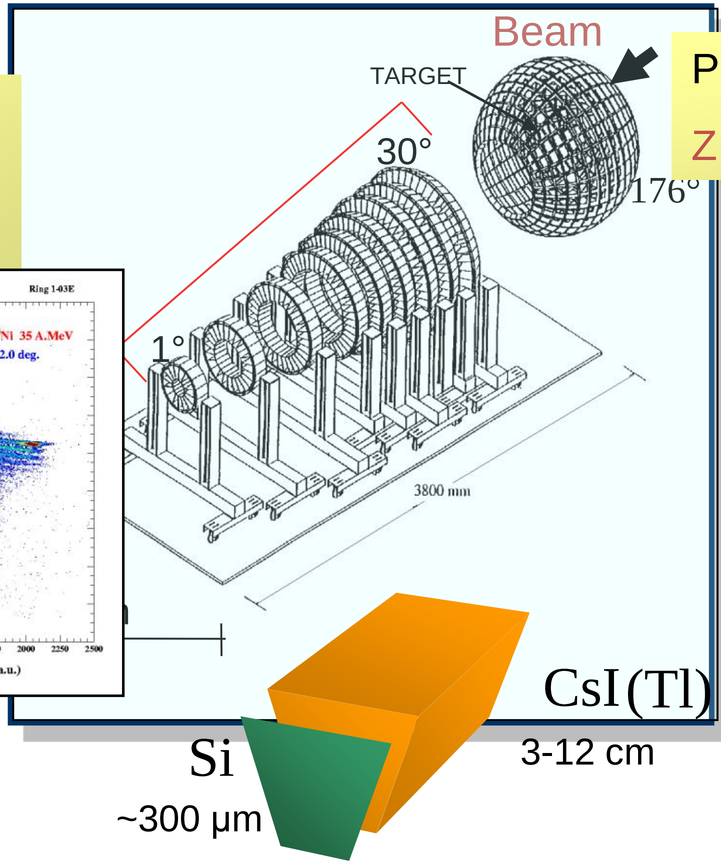

PSD in CsI(Tl)

Z and A for light charged particles

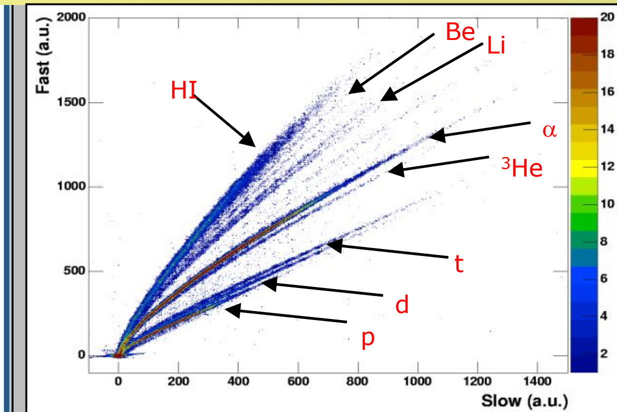

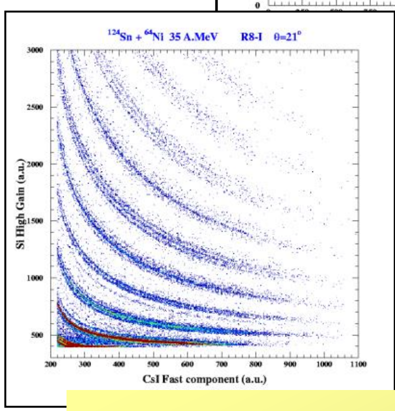

ΔE(Si)-E(CsI)

Charge Z and A for light ions (Z<9) punching throught the Si detector

ΔE(Si)-ToF

Mass for particles stopping in the Si detector

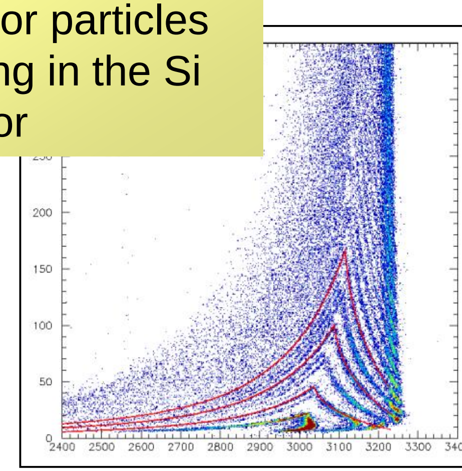

CHIMERA multi-detector

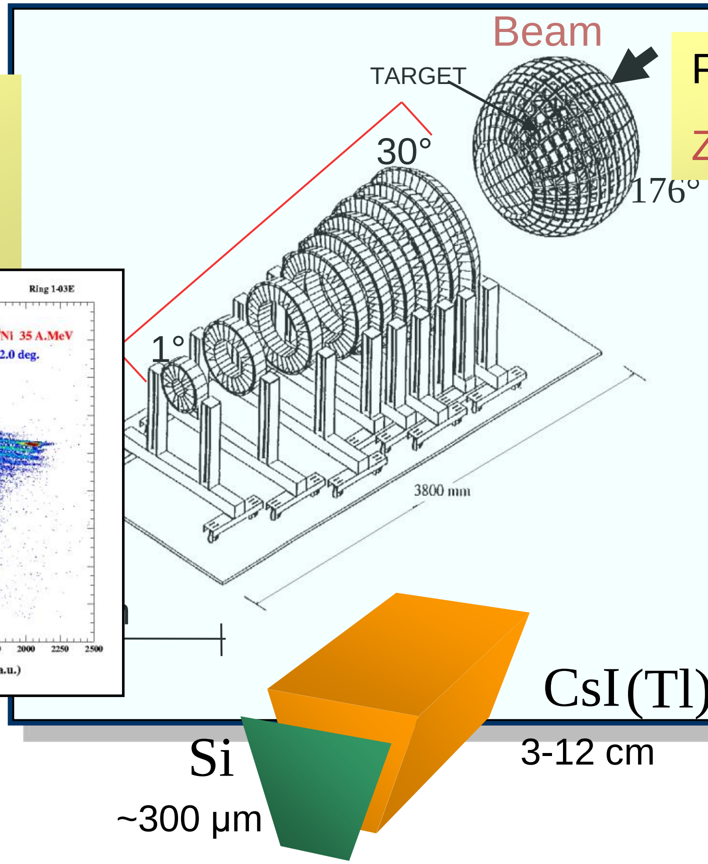

PSD in CsI(Tl)

Z and A for light charged particles

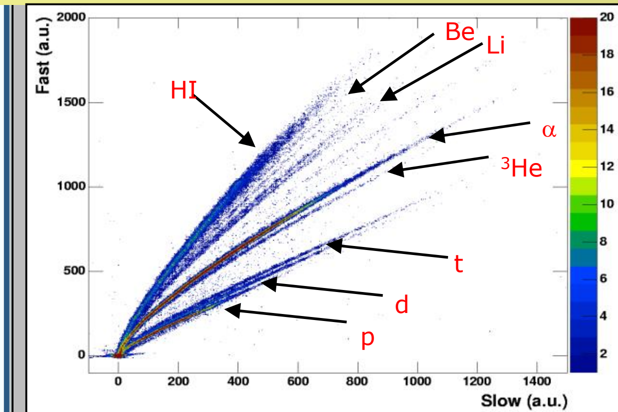

ΔE(Si)-E(CsI)

Charge Z for particles punching throught the Si detector

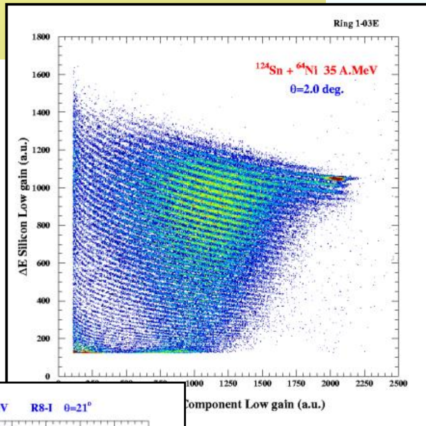

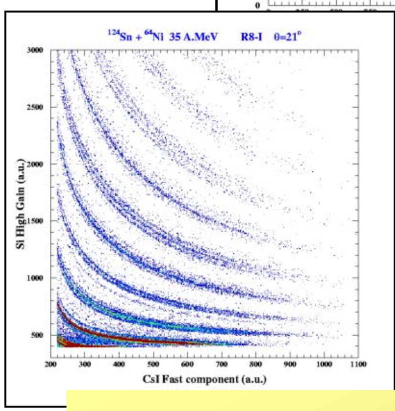

ΔE(Si)-E(CsI)

Charge Z and A for light ions (Z<9) punching throught the Si detector

ΔE(Si)-ToF

Mass for particles stopping in the Si detector

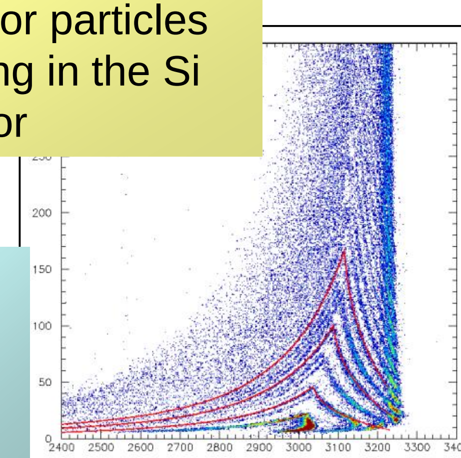

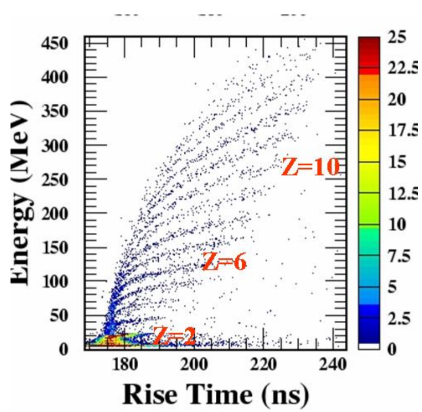

E(Si)-Rise time

Charge Z for particle stopping in Si detectors

Isospin transport through the "neck"

V. Baran et al., PRC 72 064620 (2005)

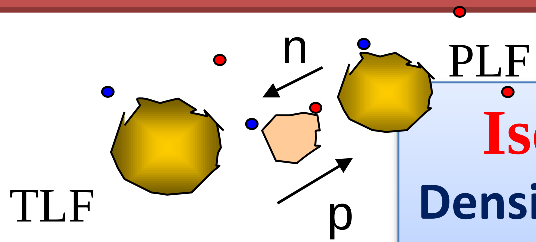

Isospin drift (fast timescale: around 100 fm/c

Density gradient

Depending on slope of the symmetry energy

Migration of neutrons in low density region

$$j_n - j_p \propto E_{sym}(\rho)\nabla I + \frac{\partial E_{sym}(\rho)}{\partial \rho} I \nabla \rho$$

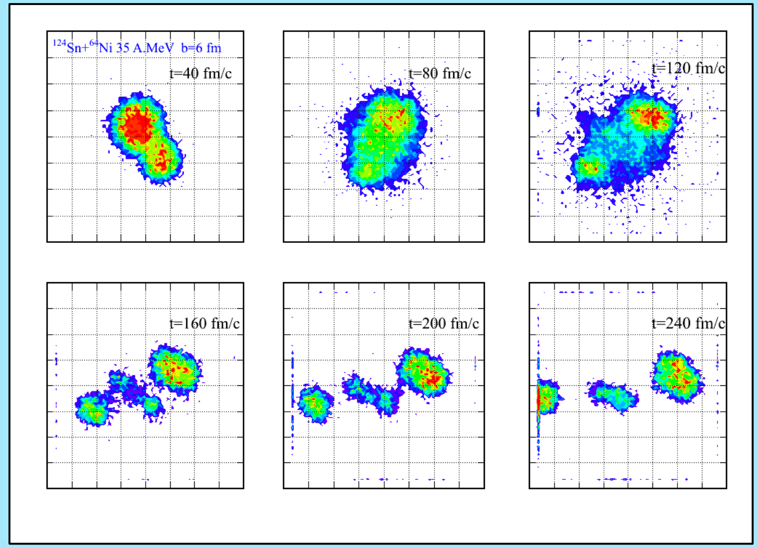

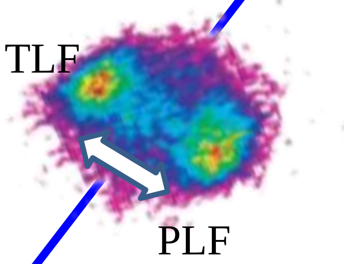

Isospin diffusion

Isospin gradient (N/Z asymmetry in the initial system)

Depending on absolute value of the symmetry energy

Isospin equilibration between projectile and target

Isospin transport through the "neck"

V. Baran et al., PRC 72 064620 (2005)

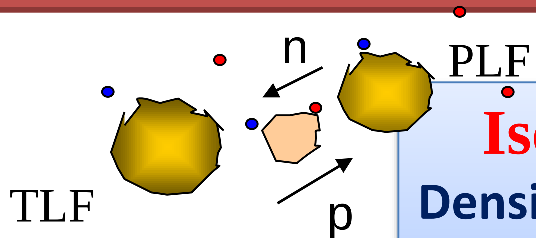

Isospin drift (fast timescale: around 100 fm/c

Density gradient

Depending on slope of the symmetry energy

Migration of neutrons in low density region

$$j_n - j_p \propto E_{sym}(\rho)\nabla I + \frac{\partial E_{sym}(\rho)}{\partial \rho} I \nabla \rho$$

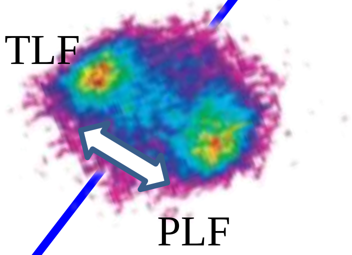

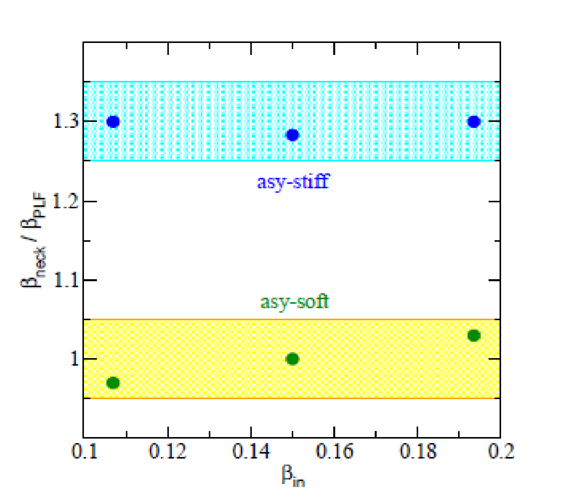

M. Colonna et al., J. Phys. CS, 413, 012018 (2013)

Isospin diffusion

Isospin gradient (N/Z asymmetry in the initial system)

Depending on absolute value of the symmetry energy

Isospin equilibration between projectile and target

Comparisons with SMF transport models

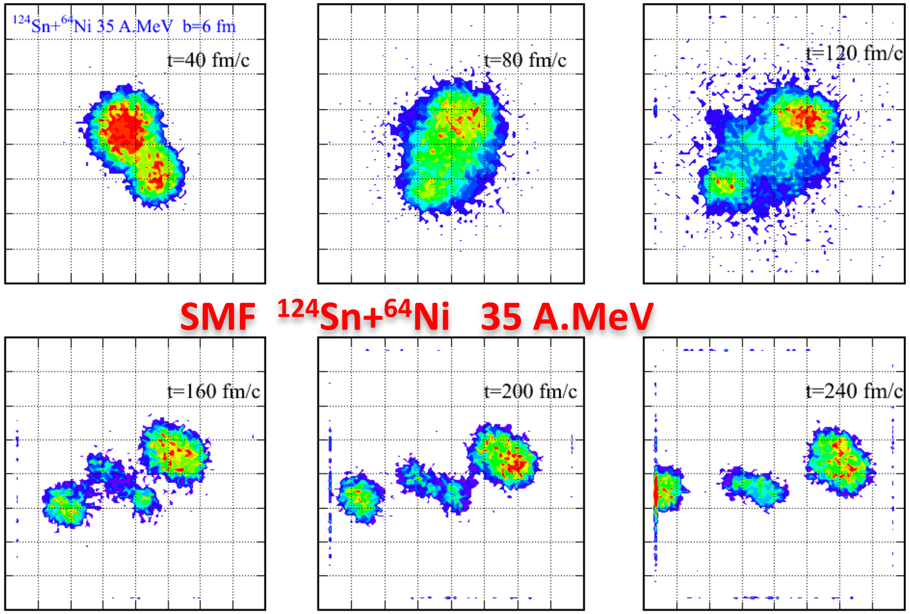

Stochastic Mean Field

V. Baran et al. Nucl. Phys. A730 329, 2004
M. Colonna et al.,J.Phys.CS, 413, (2013)

Comparisons with SMF transport models

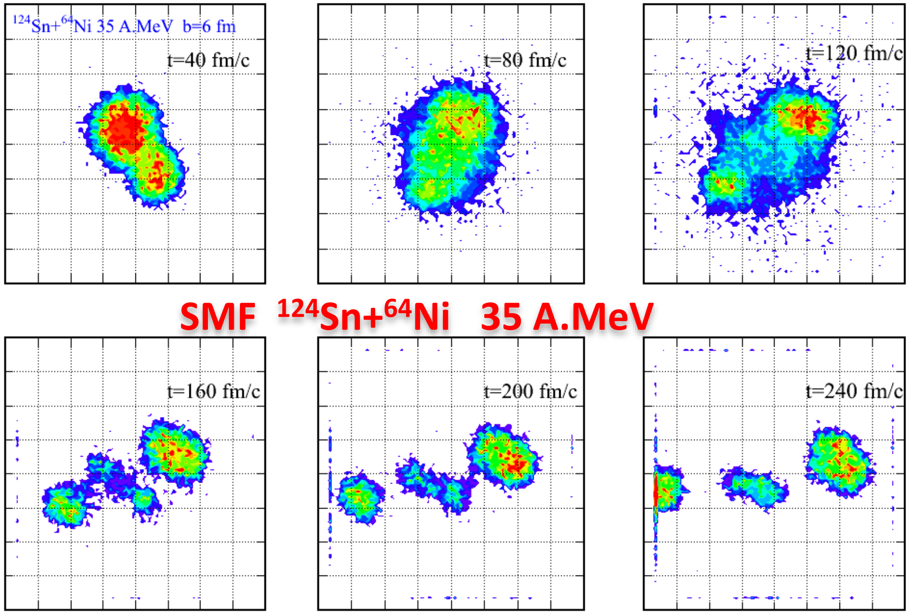

Stochastic Mean Field

V. Baran et al. Nucl. Phys. A730 329, 2004
M. Colonna et al.,J.Phys.CS, 413, (2013)

● Dynamically emitted
■ Statistically emitted

^{124}Sn+^{64}Ni 35 AMeV

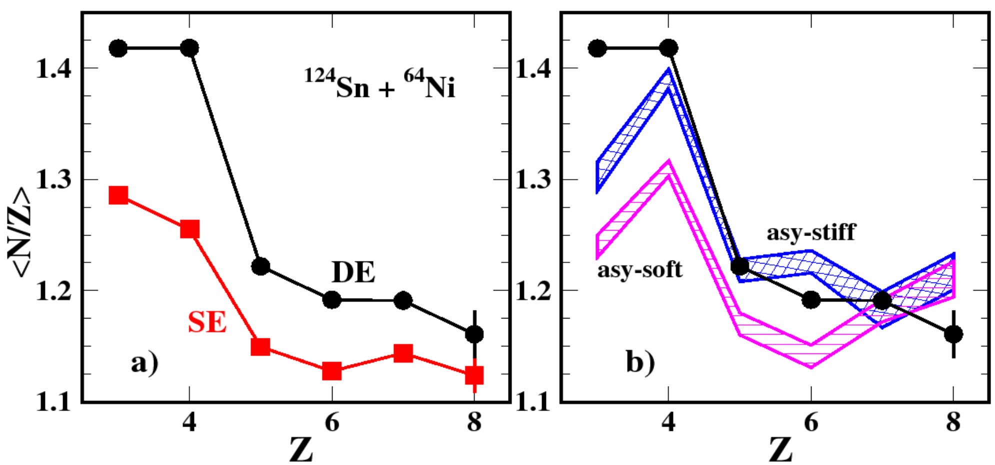

Experimental <N/Z> distribution of IMFs as a function of their atomic number compared with results SMF+GEMINI calculations (hatched area) for two different parameterizations of the symmetry potential (asy-soft and asy-stiff)

E. De Filippo et al., Phys. Rev. C 86 014610 (2012)
E. De Filippo & A. Pagano, EPJA 50 (2014)

R3BROOT

R3Broot simulations

Uniform momentum distribution between pmin and pmax
Uniform angular distribution inside the detector (surface)

particle	pmin (GeV/c)	pmax (GeV/c)
p,n	0.445	1.220
d	0.89	2.440
t,3He	1.335	3.660
4He	1.780	4.880

↑ Ekin/A=100 MeV (pmin)

↑ Ekin/A=600 MeV (pmax)

R3Broot simulations

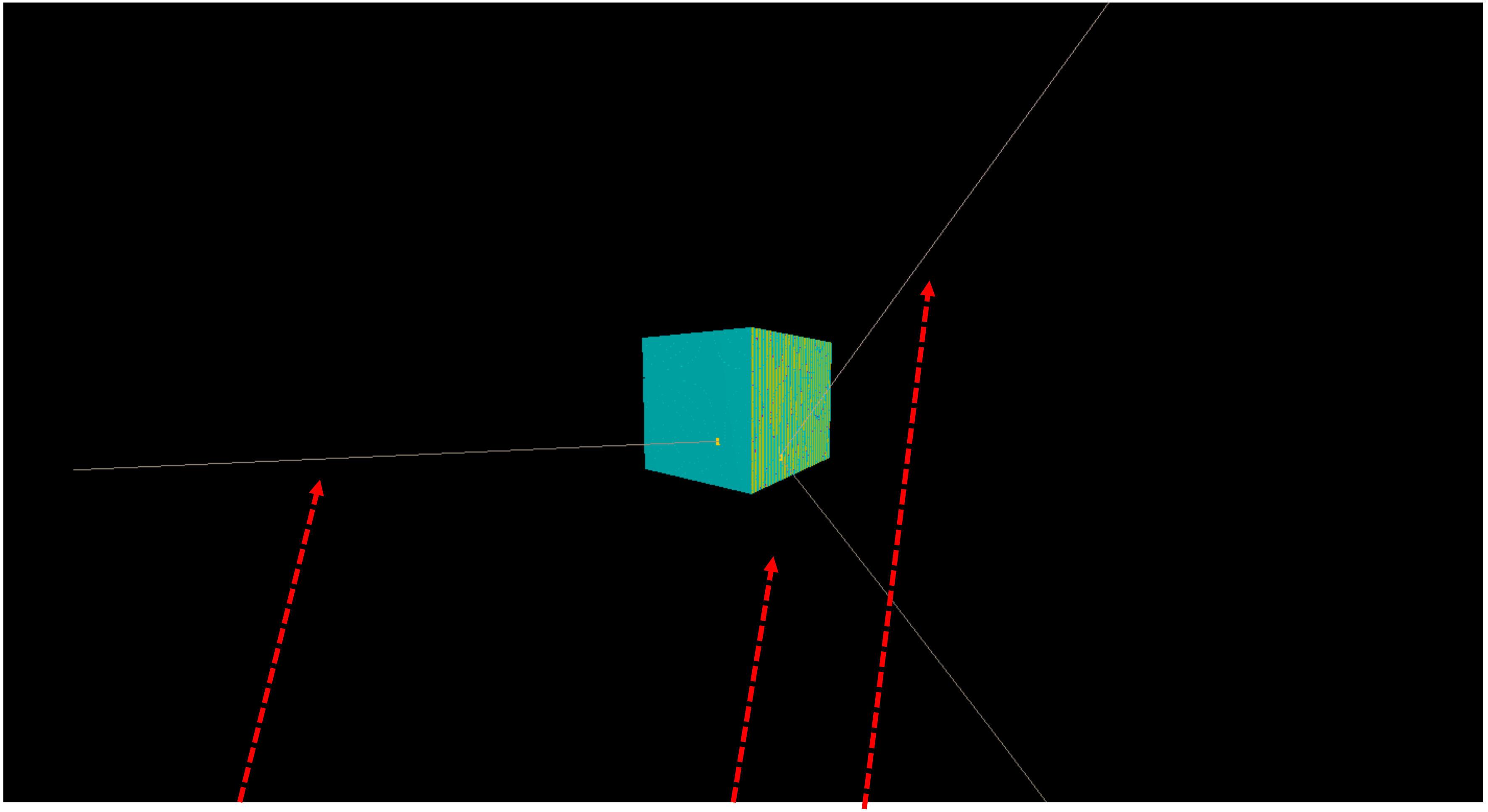

Incoming proton

Escaping gammas

R3Broot simulations

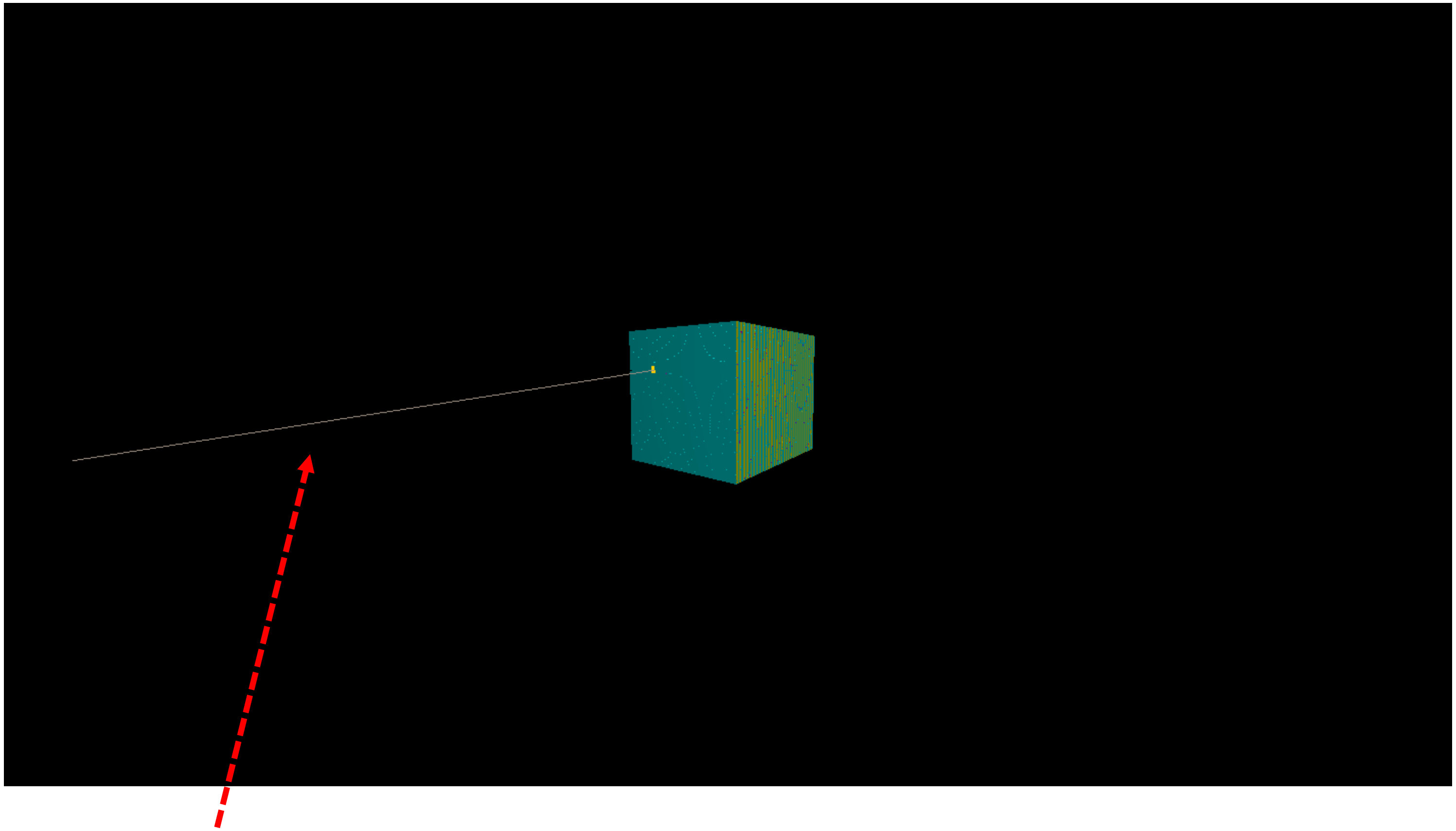

Incoming proton

QDC sum in 1st plane vs QDC sum in remaining planes (applyng clustering algorithm)

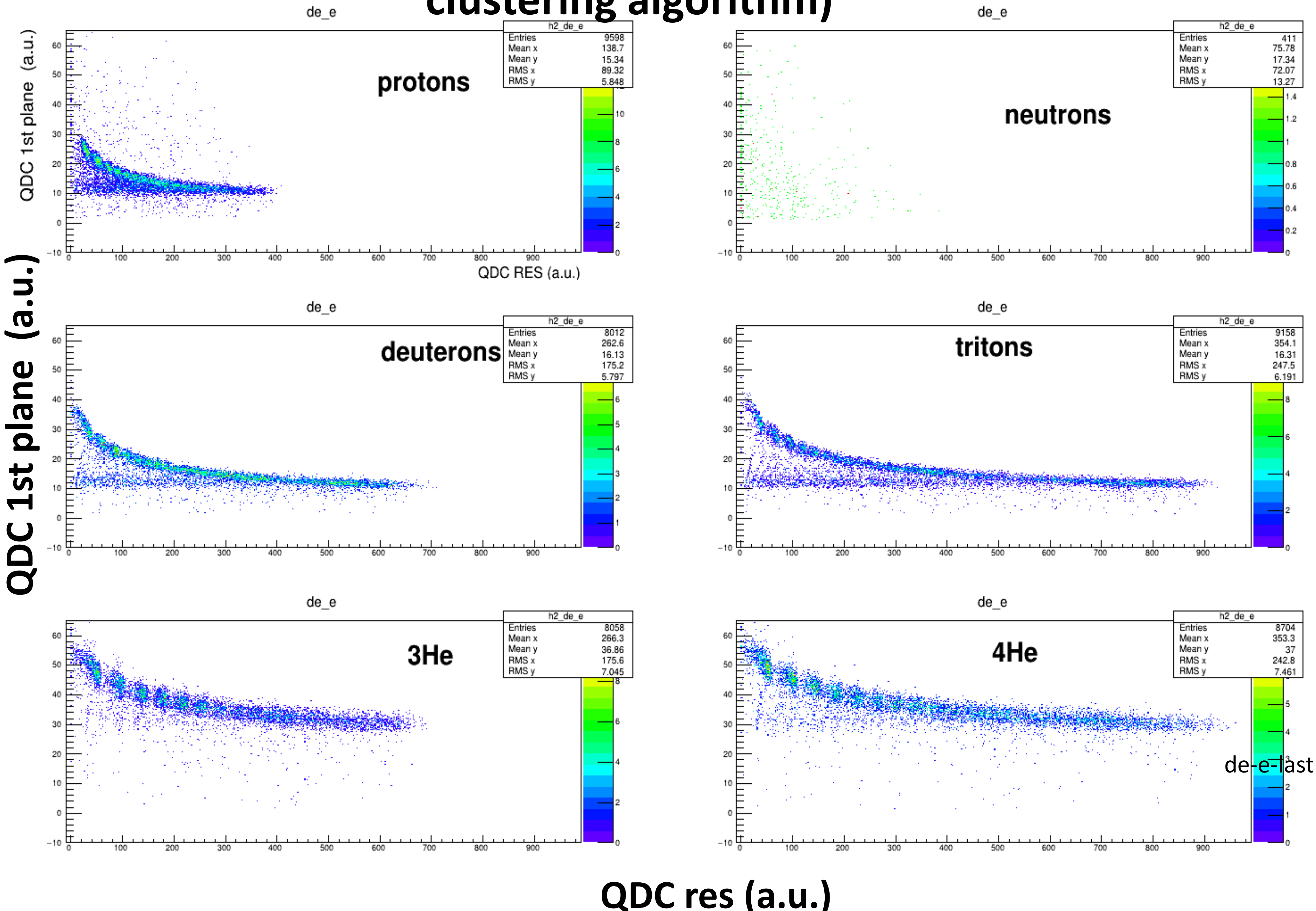

QDC sum in 1st plane vs QDC sum in remaining planes (applyng clustering algorithm)

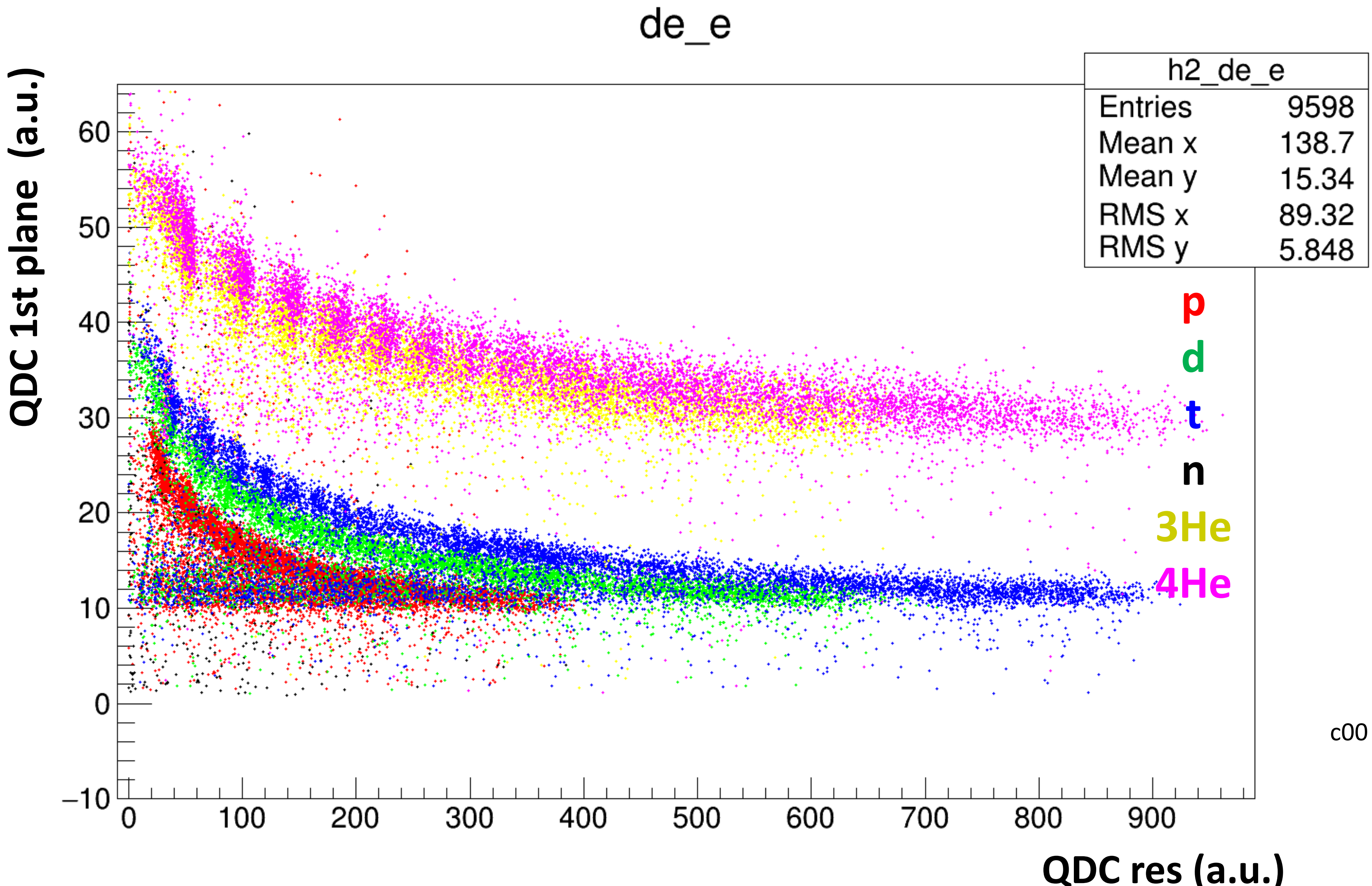

QDC sum in 1st plane vs velocity (applyng clustering algorithm)

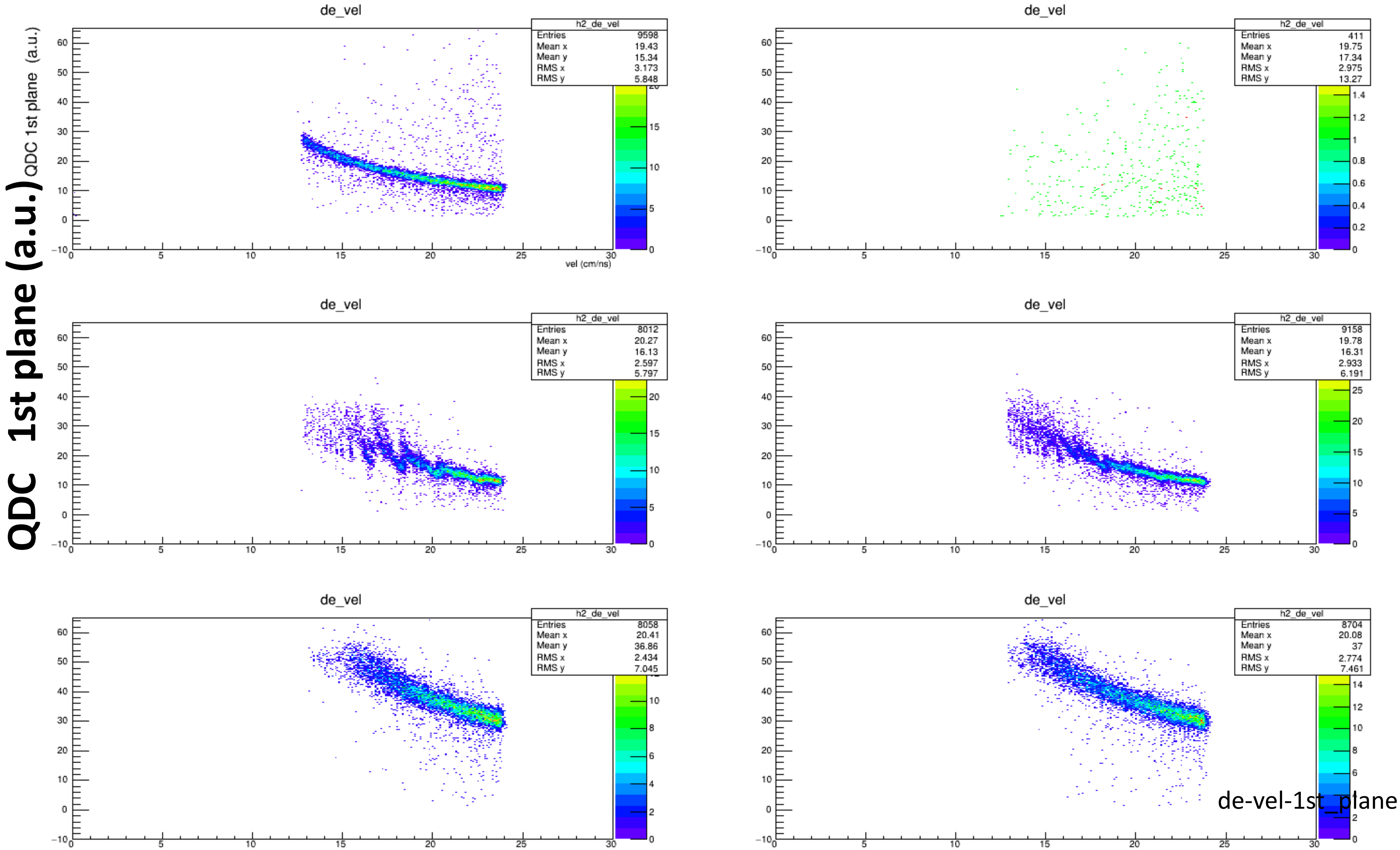

Vel (cm/ns)

QDC sum in 1st plane vs velocity (applyng clustering algorithm)

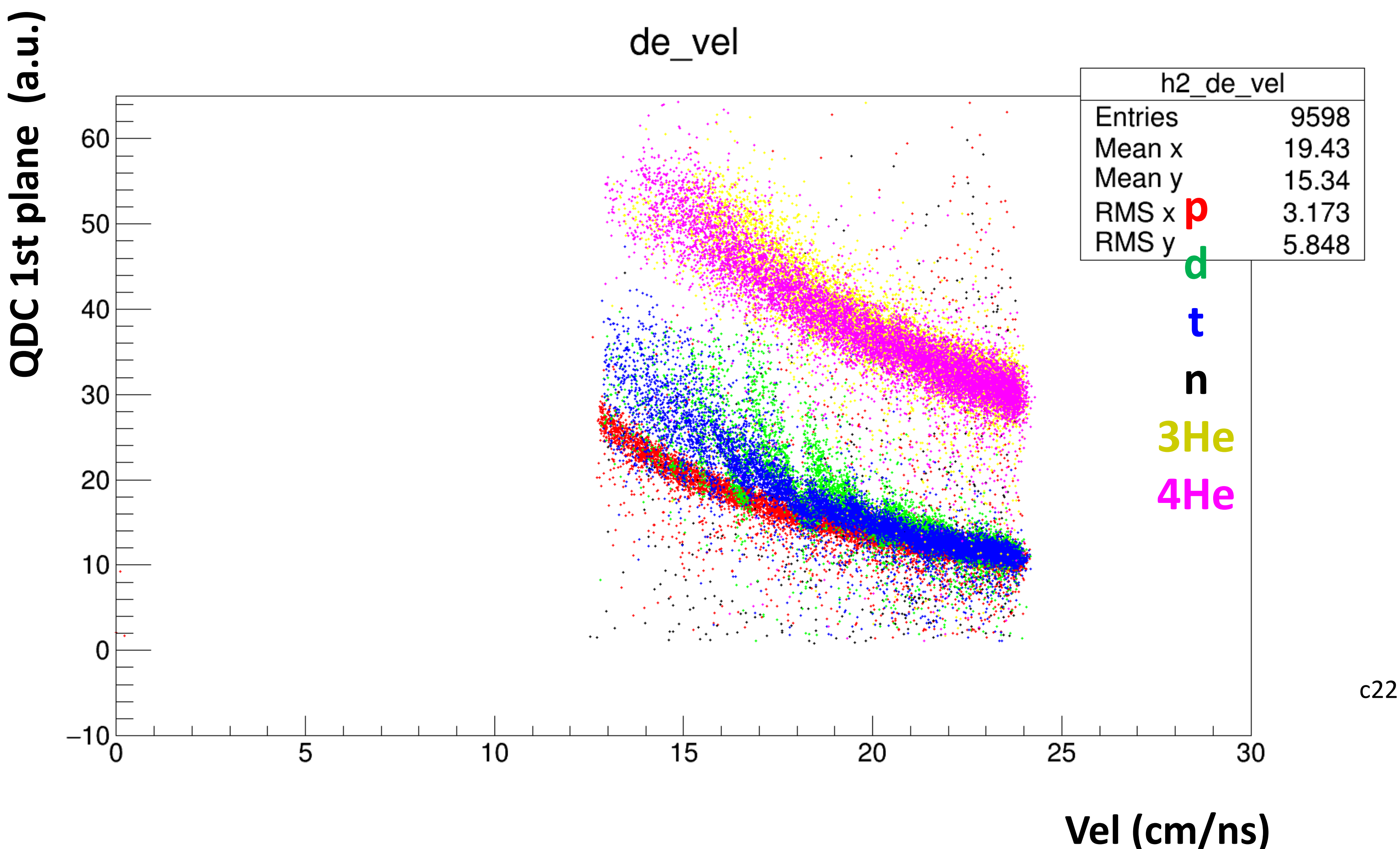

QDC sum vs velocity if 1st plane fired (applyng clustering algorithm)

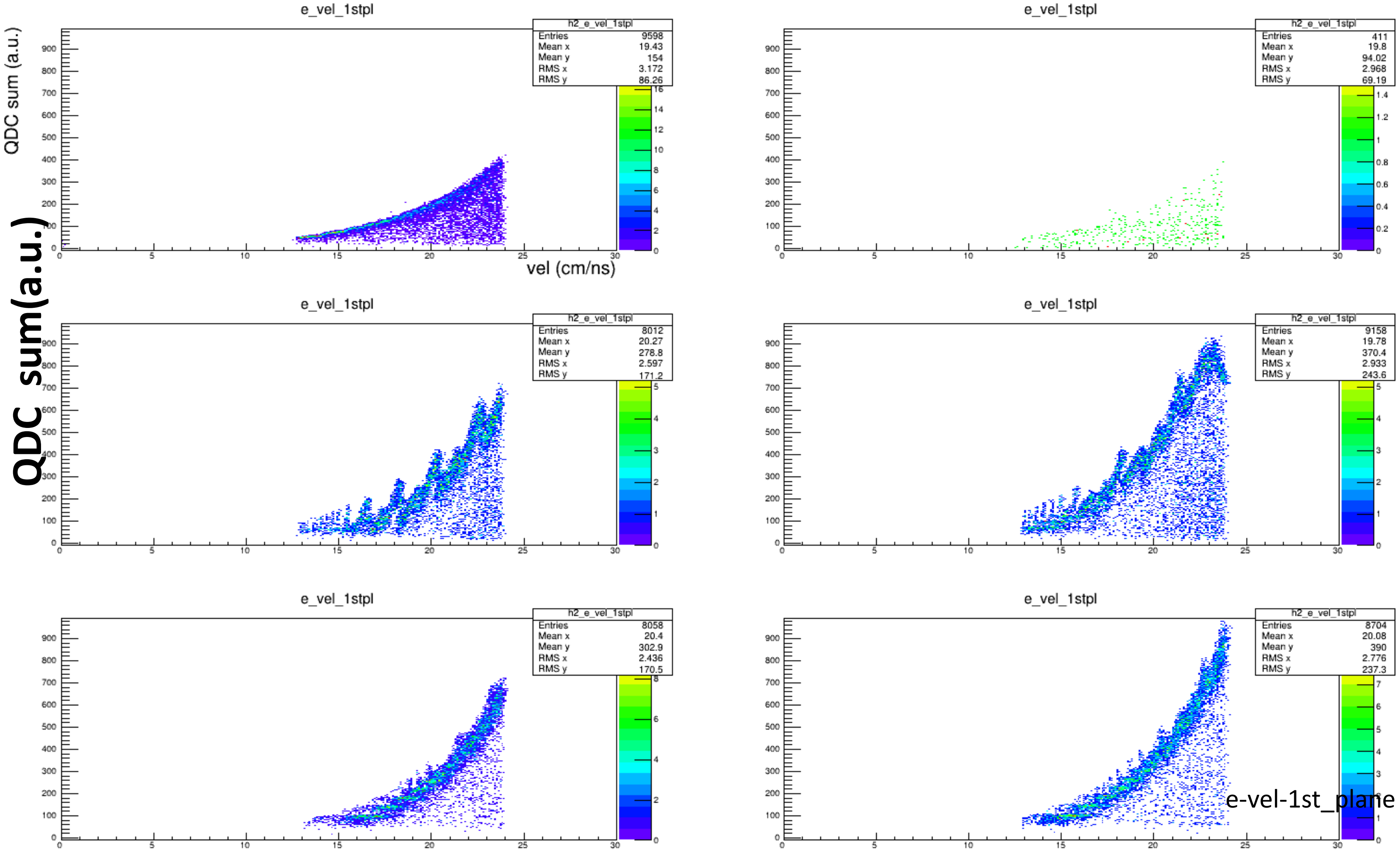

Vel (cm/ns)

QDC sum vs velocity if 1st plane fired (applyng clustering algorithm)

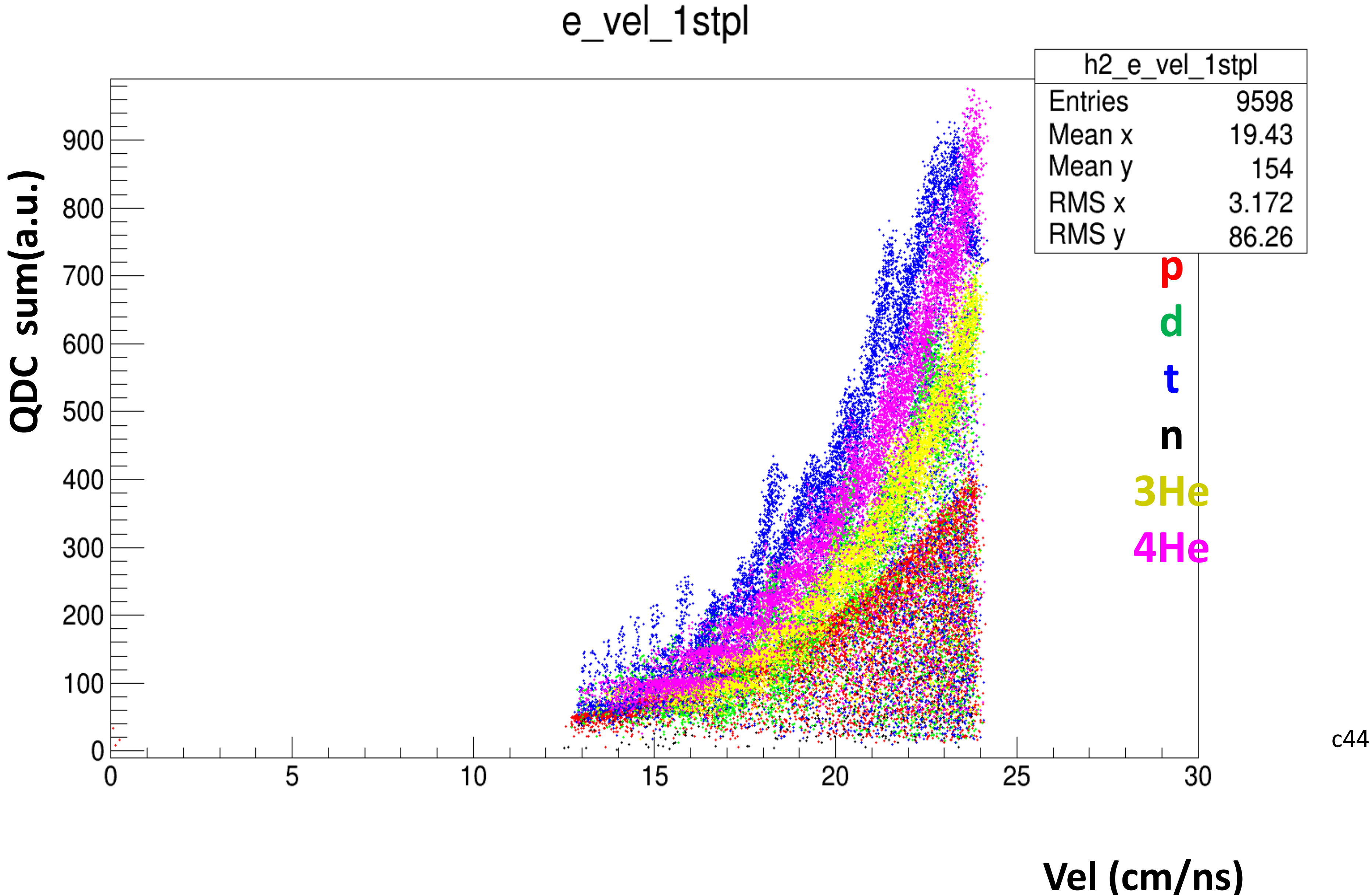

QDC sum vs velocity if 1st plane fired (applyng clustering algorithm)

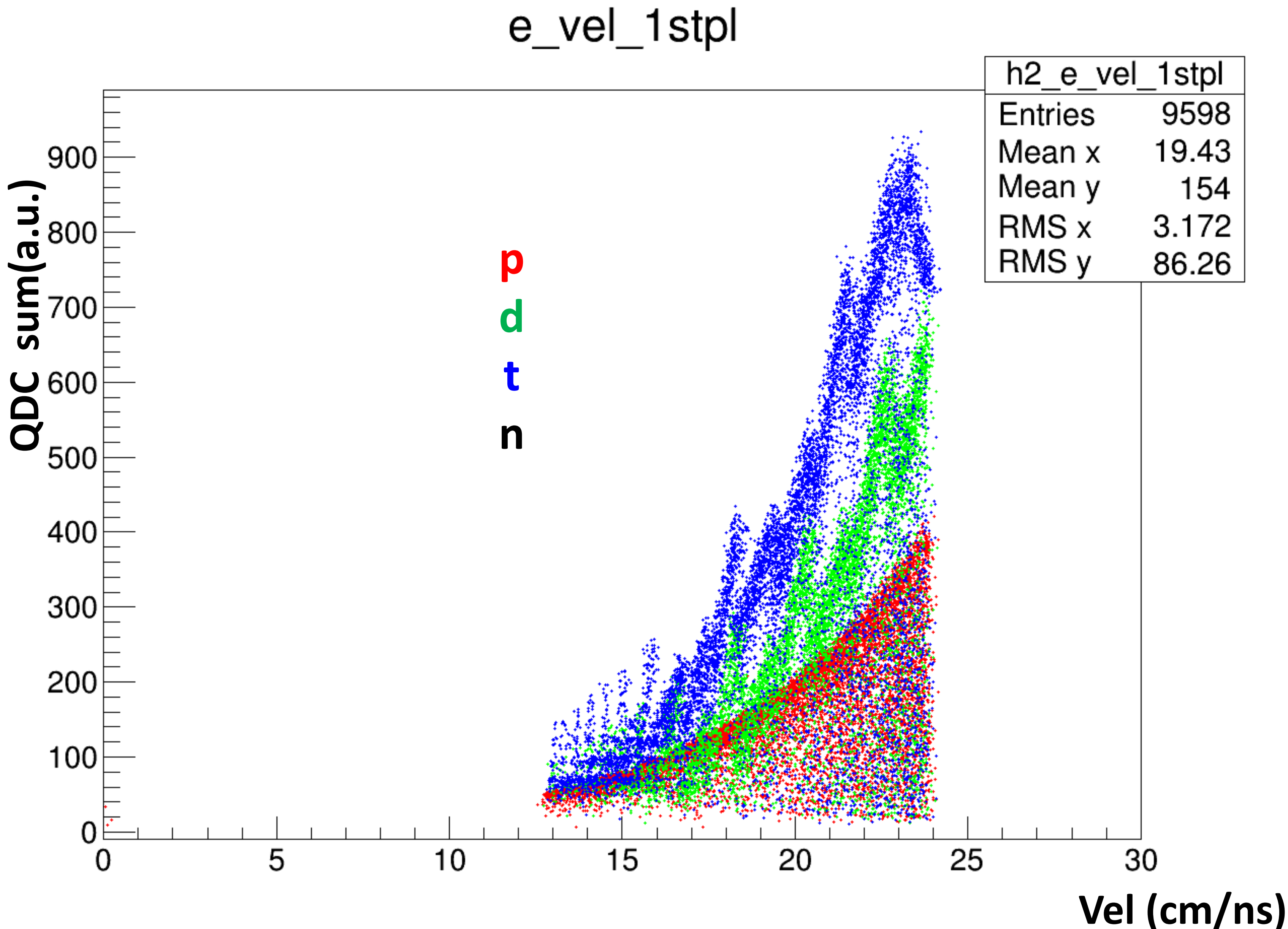

c44bis

QDC sum vs velocity if 1st plane not fired (applyng clustering algorithm)

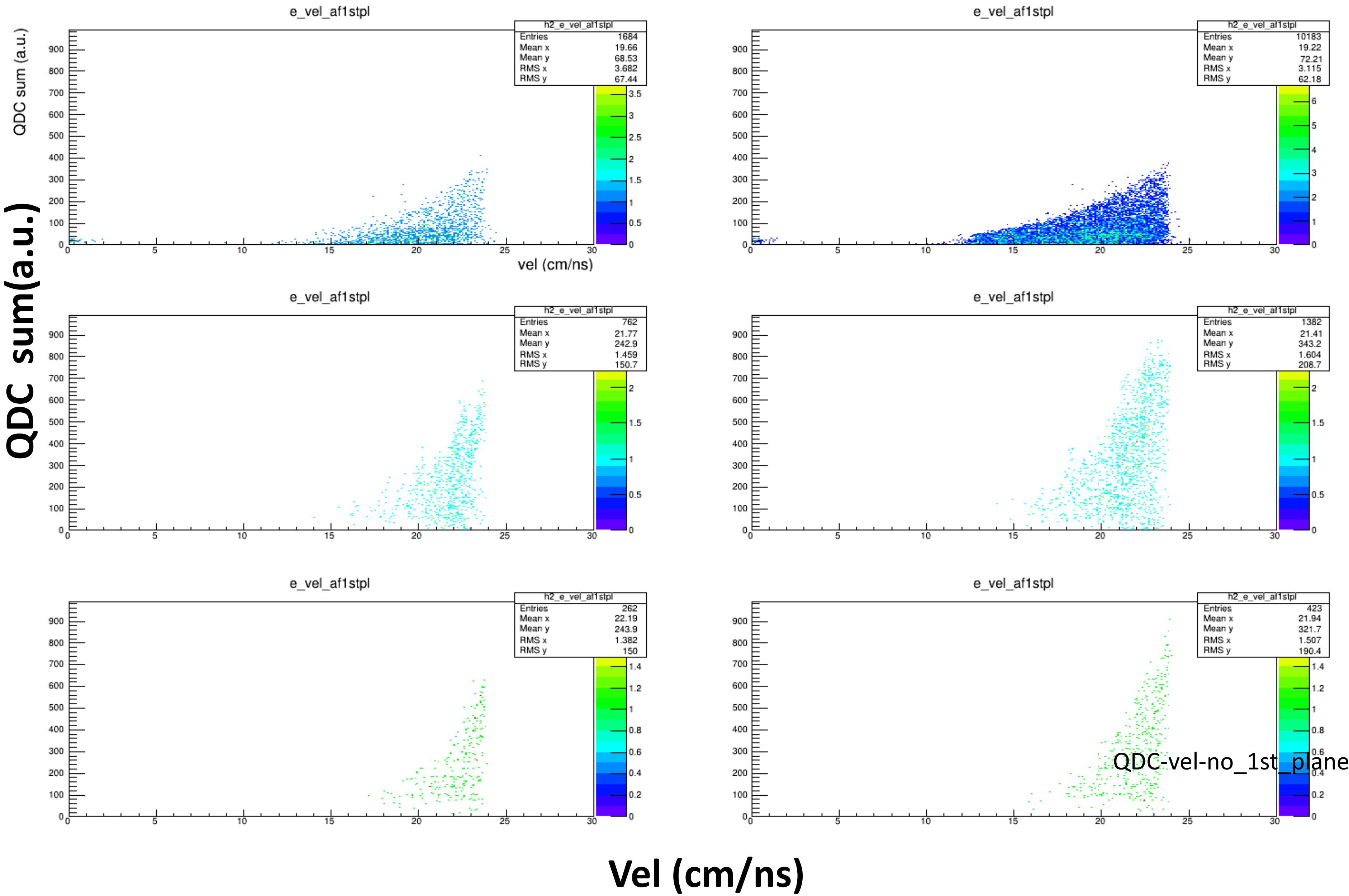

QDC sum vs velocity if 1st plane not fired (applyng clustering algorithm)

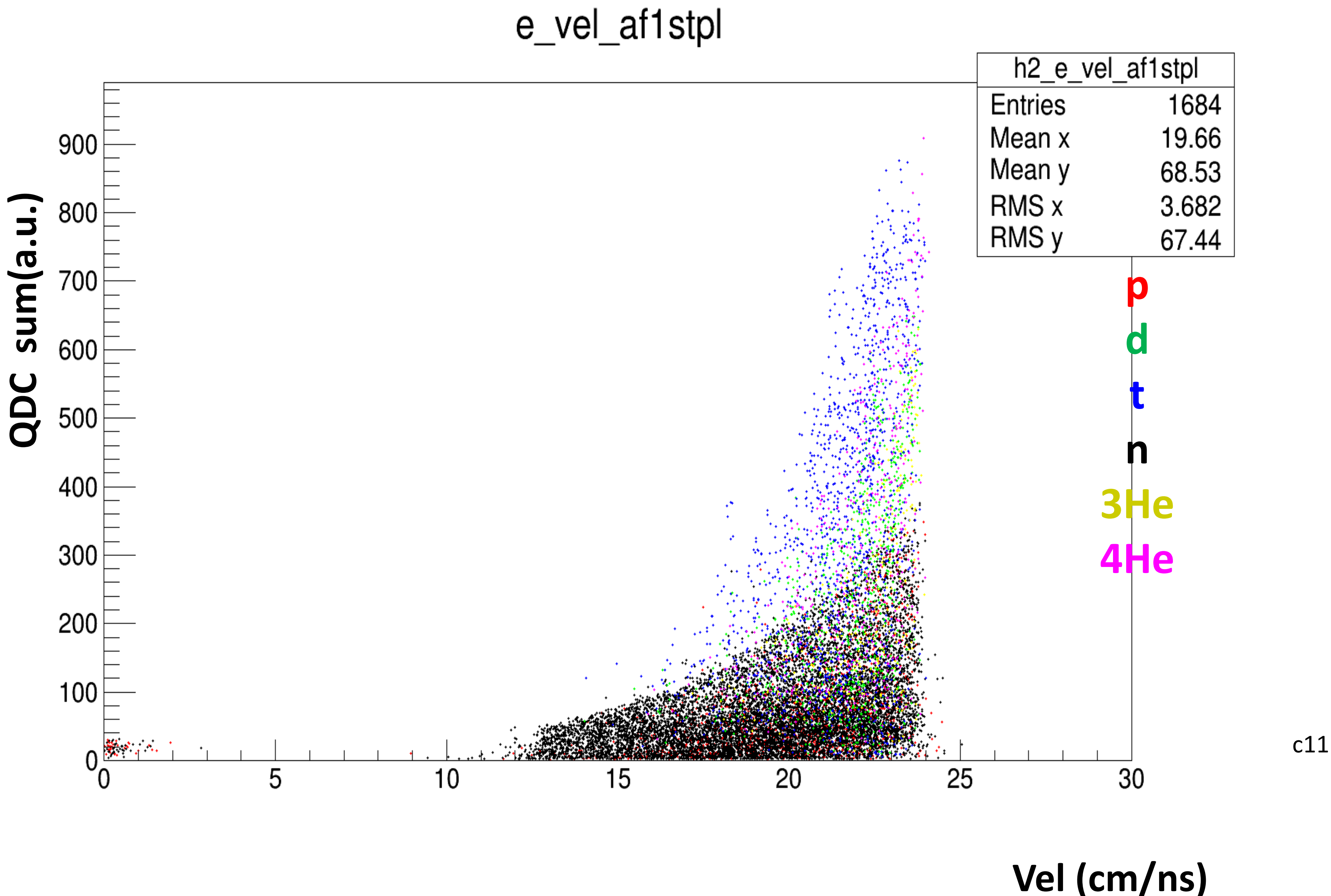

ESYM

Symmetry Energy

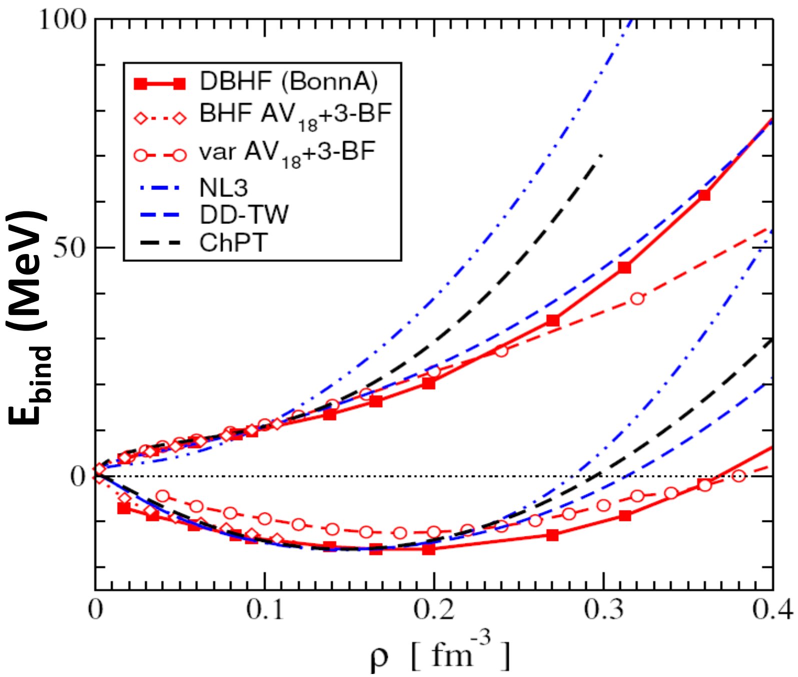

EOS of symmetric nuclear and neutron matter
from
Ab initio calculations (red)
and phenomenological approaches

Fuchs and Wolter, EPJA 30 (2006)

Symmetry Energy

$$E_{Sym}(\rho) = E_{Sym}(\rho, \delta = 1) - E_{Sym}(\rho, \delta = 0)$$

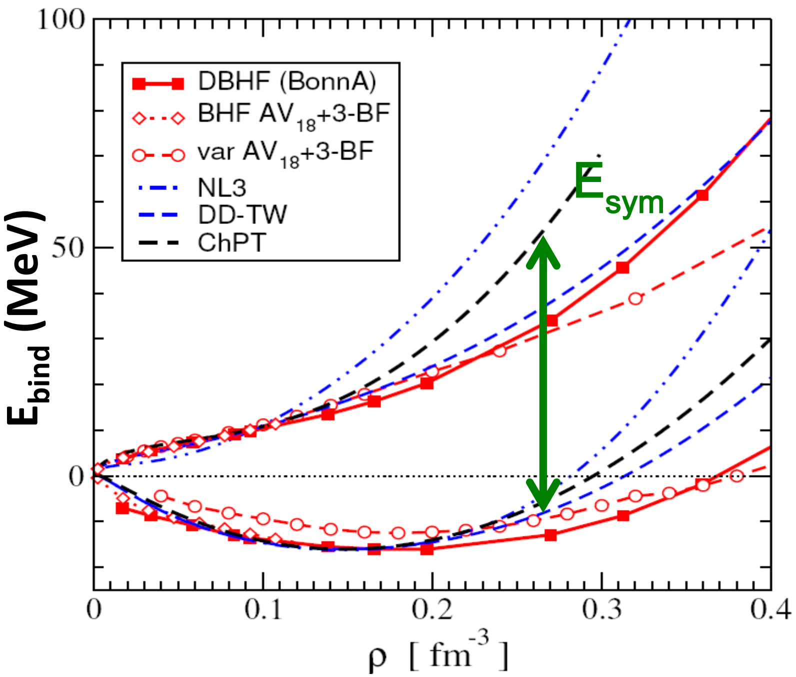

$$\delta = \frac{\rho_n - \rho_p}{\rho_n + \rho_p} = \frac{N - Z}{A}$$

EOS of symmetric nuclear and neutron matter from Ab initio calculations (red) and phenomenological approaches

Fuchs and Wolter, EPJA 30 (2006)

Symmetry Energy

$$E_{Sym}(\rho) = E_{Sym}(\rho, \delta = 1) - E_{Sym}(\rho, \delta = 0)$$

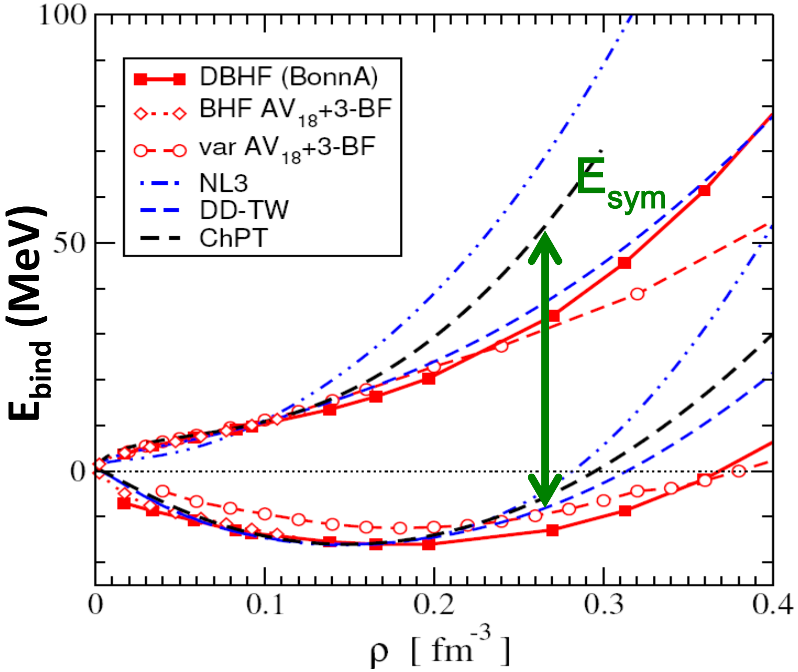

$$\delta = \frac{\rho_n - \rho_p}{\rho_n + \rho_p} = \frac{N - Z}{A}$$

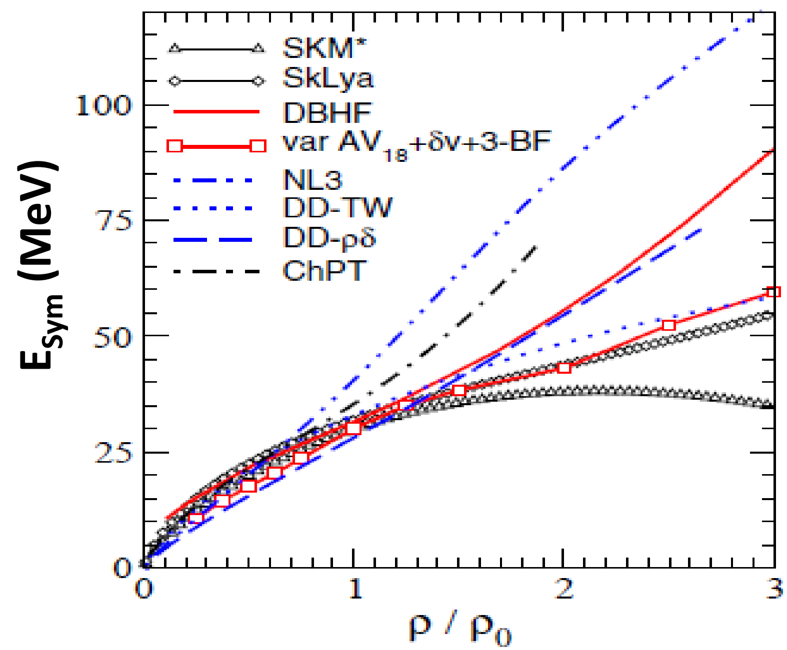

EOS of symmetric nuclear and neutron matter from Ab initio calculations (red) and phenomenological approaches

Fuchs and Wolter, EPJA 30 (2006)

Symmetry Energy

$$E_{Sym}(\rho) = E_{Sym}(\rho, \delta = 1) - E_{Sym}(\rho, \delta = 0)$$

$$\delta = \frac{\rho_n - \rho_p}{\rho_n + \rho_p} = \frac{N - Z}{A}$$

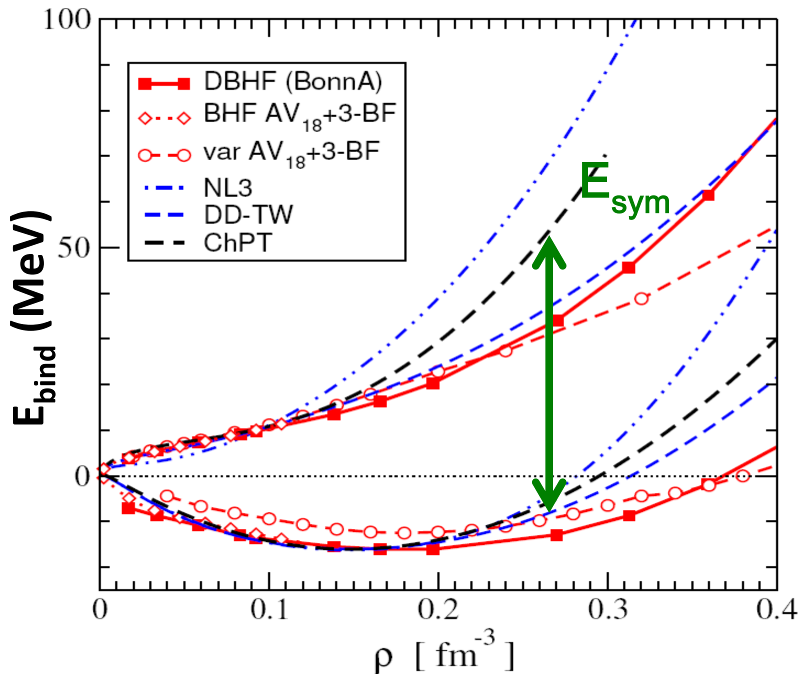

EOS of symmetric nuclear
and neutron matter
from
Ab initio calculations (red)
and phenomenological approaches

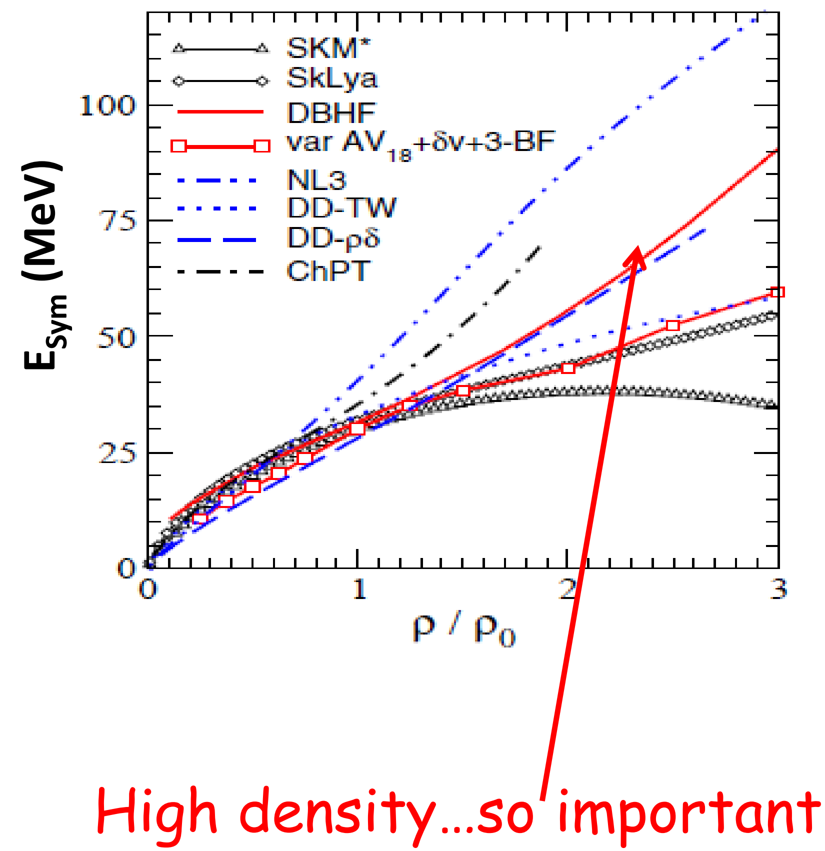

Fuchs and Wolter, EPJA 30 (2006)

High density symmetry energy and neutron stars

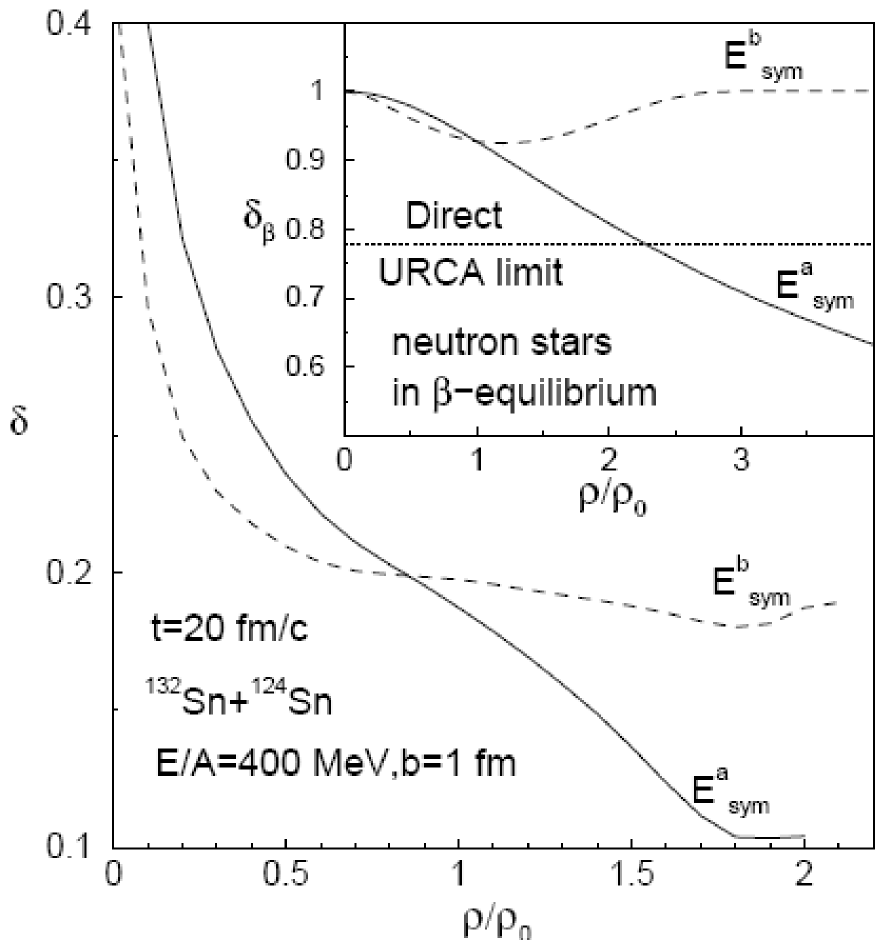

Relativistic HIC
supersaturation density:
neutron stars,
supernovae,

$$\delta \equiv (\rho_n - \rho_p)/(\rho_n + \rho_p)$$

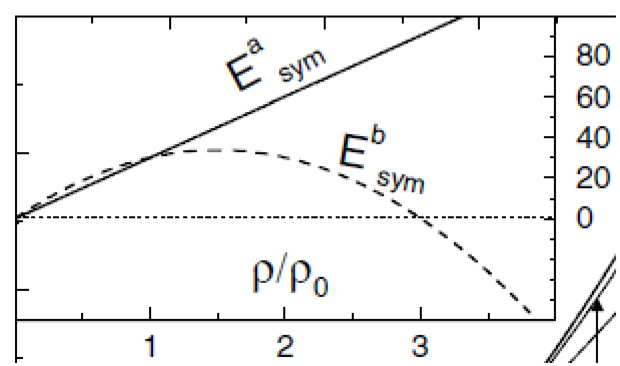

Bao-An Li, PRL 88 (2002)

Constraints of the Symmetry Energy

B.A. Li NuSym13 summary talk

$$E_{Sym}(\rho) = S(\rho) = S_0 + \frac{L}{3}\left(\frac{\rho-\rho_o}{\rho_o}\right) + \frac{K_{\rm sym}}{18}\left(\frac{\rho-\rho_o}{\rho_o}\right)^2 + \ldots,$$

Nusym13 constraints on $E_{sym}(\rho_0)$ and L based on 29 analyses of some data

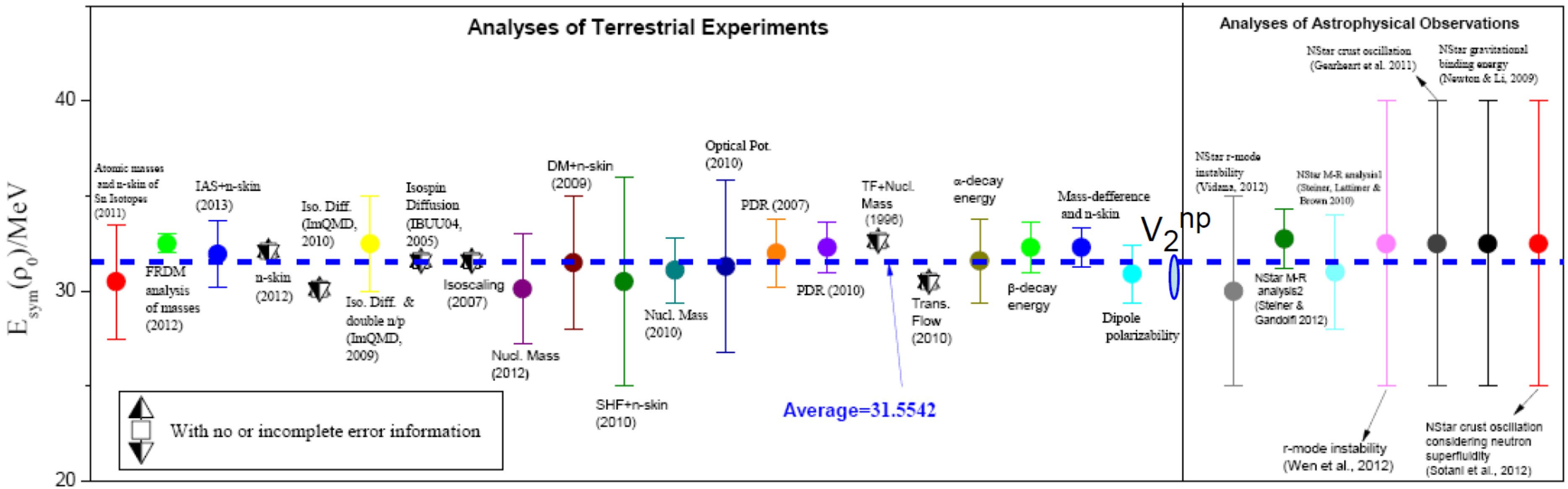

Constraints of the Symmetry Energy

B.A. Li NuSym13 summary talk

$$E_{Sym}(\rho) = S(\rho) = S_0 + \frac{L}{3}\left(\frac{\rho-\rho_o}{\rho_o}\right) + \frac{K_{\rm sym}}{18}\left(\frac{\rho-\rho_o}{\rho_o}\right)^2 + \ldots,$$

	S_0	L
average of the means	31.55415	58.88646
standard deviation	0.915867	16.52645

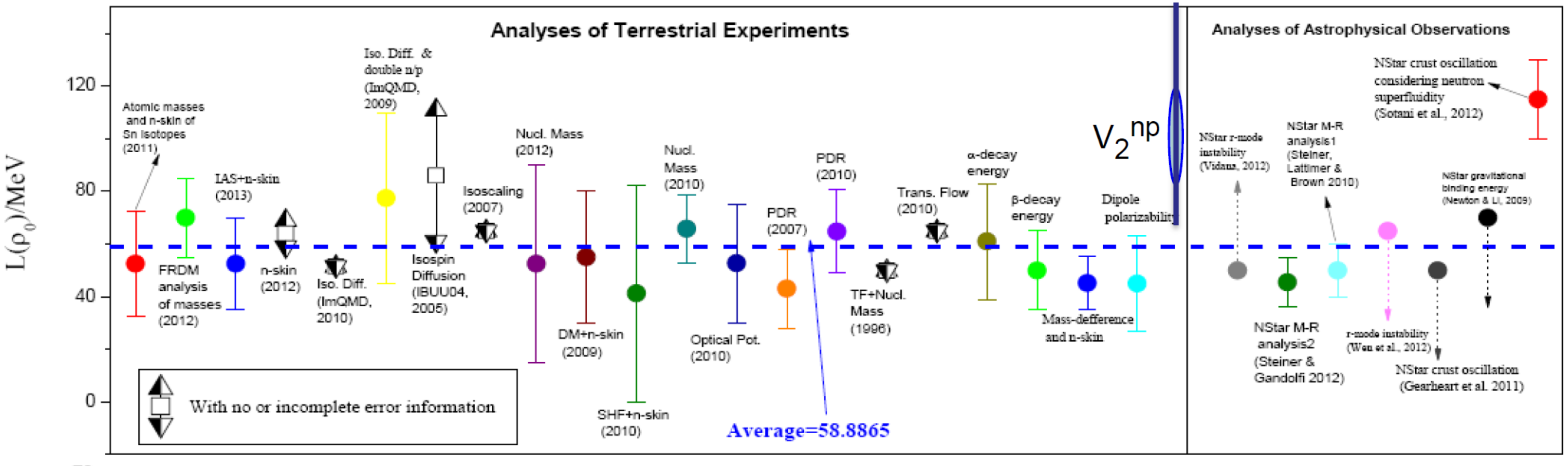

Constraints of the Symmetry Energy

B.A. Li NuSym13 summary talk

$$E_{Sym}(\rho) = S(\rho) = S_0 + \frac{L}{3}\left(\frac{\rho-\rho_o}{\rho_o}\right) + \frac{K_{\rm sym}}{18}\left(\frac{\rho-\rho_o}{\rho_o}\right)^2 + \ldots,$$

Nusym13 constraints on $E_{sym}(\rho_0)$ and L based on 29 analyses of some data

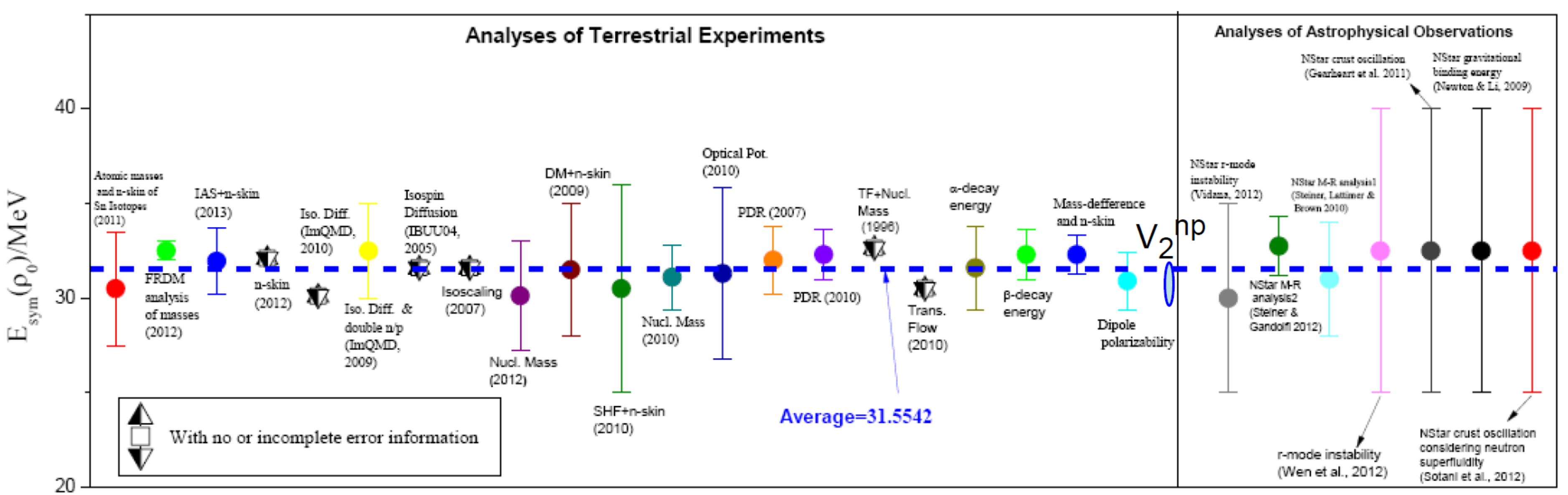

Constraints of the Symmetry Energy

B.A. Li NuSym13 summary talk

$$E_{Sym}(\rho) = S(\rho) = S_0 + \frac{L}{3}\left(\frac{\rho - \rho_o}{\rho_o}\right) + \frac{K_{\text{sym}}}{18}\left(\frac{\rho - \rho_o}{\rho_o}\right)^2 + \ldots,$$

	S_0	L
average of the means	31.55415	58.88646
standard deviation	0.915867	16.52645

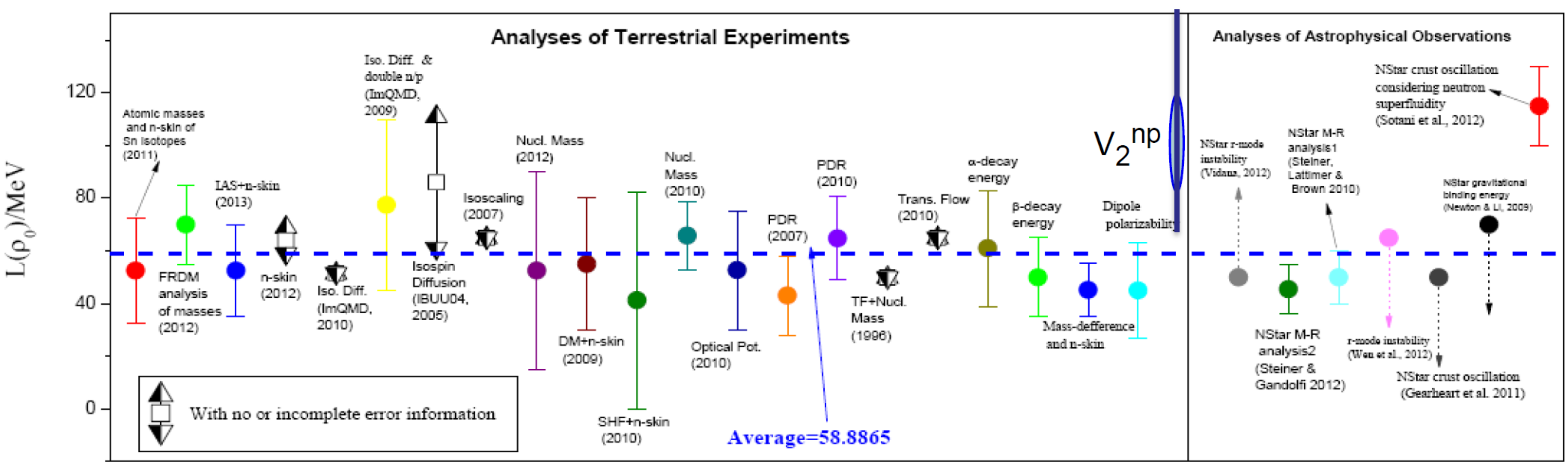

Constraints of the Symmetry Energy

B.A. Li NuSym13 summary talk

$$E_{Sym}(\rho) = S(\rho) = S_0 + \frac{L}{3}\left(\frac{\rho-\rho_o}{\rho_o}\right) + \frac{K_{\rm sym}}{18}\left(\frac{\rho-\rho_o}{\rho_o}\right)^2 + \ldots,$$

Terrestrial laboratories

	S_0	L
average of the means	31.55415	58.88646
standard deviation	0.915867	16.52645

- Several constraints (quite consistent among them) around and below ρ_0
- Few constraints above ρ_0

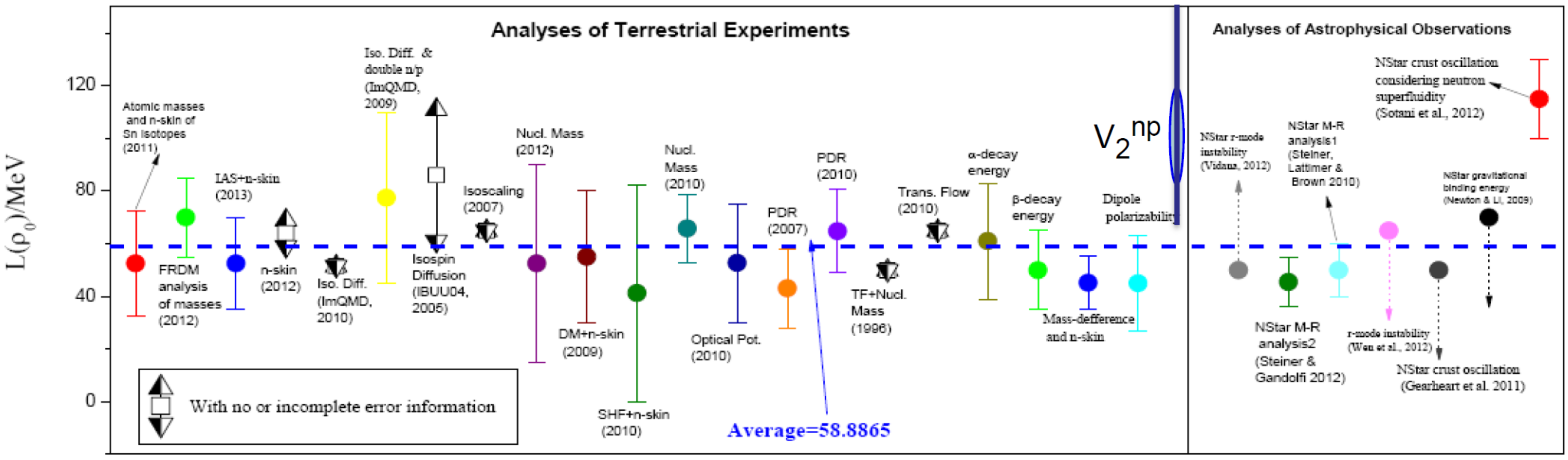

Constraints of the Symmetry Energy

B.A. Li NuSym13 summary talk

$E_{Sym}(\rho) = S(\rho$

average of the means

standard deviation

oratories

te consistent

below ρ_0

ρ_0

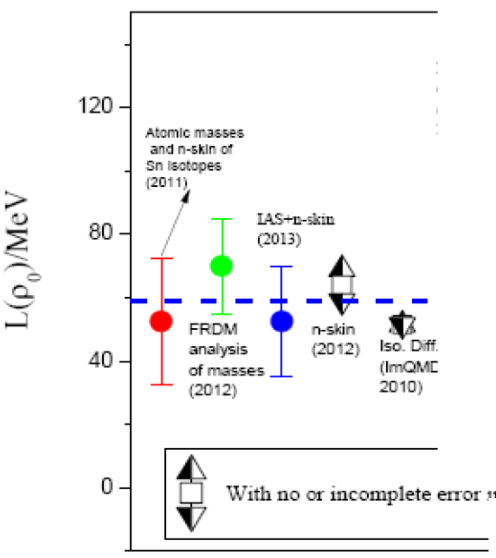

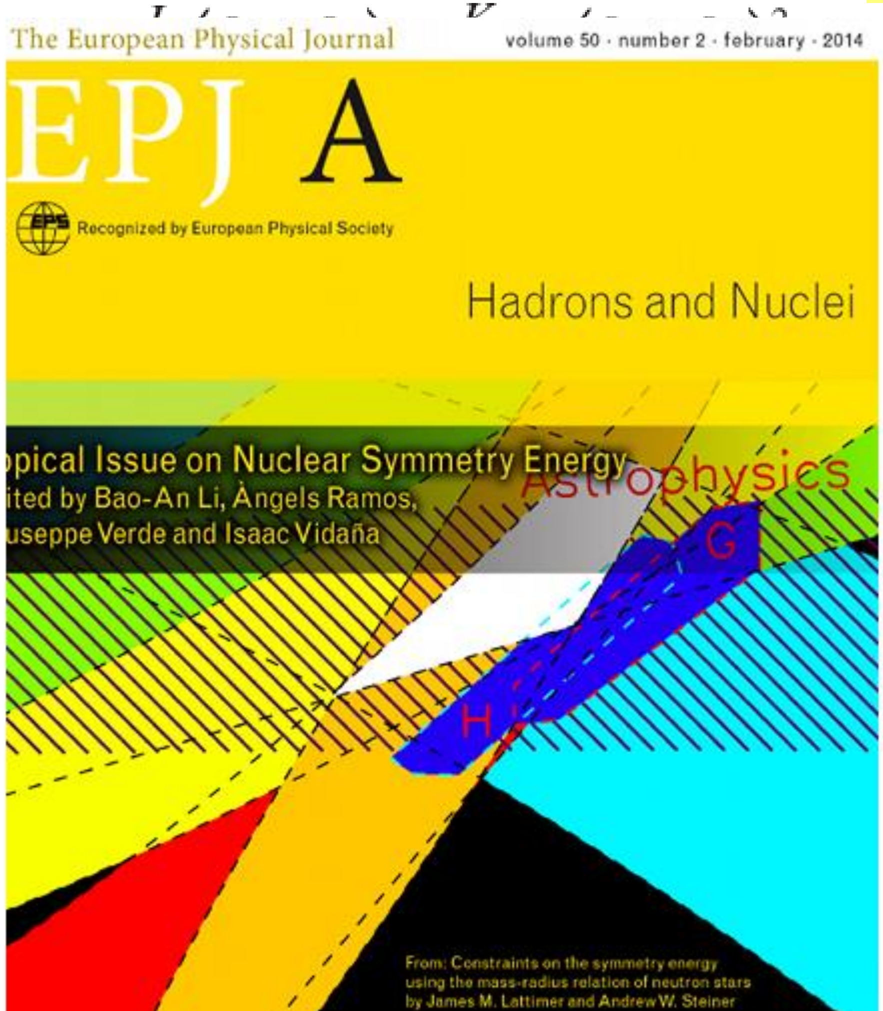

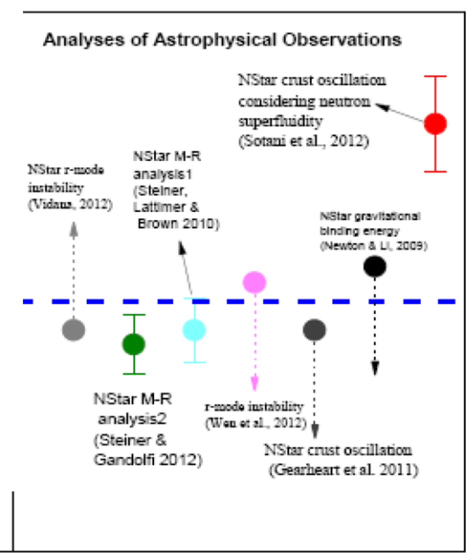

See Eur. Phys. J. A, 50 2 (2014) topical issue on Symmetry Energy

Access to high density

Heavy ion collisions (HIC) at GSI/SIS energies can give information on the Symmetry term of EOS at supra-saturation densities

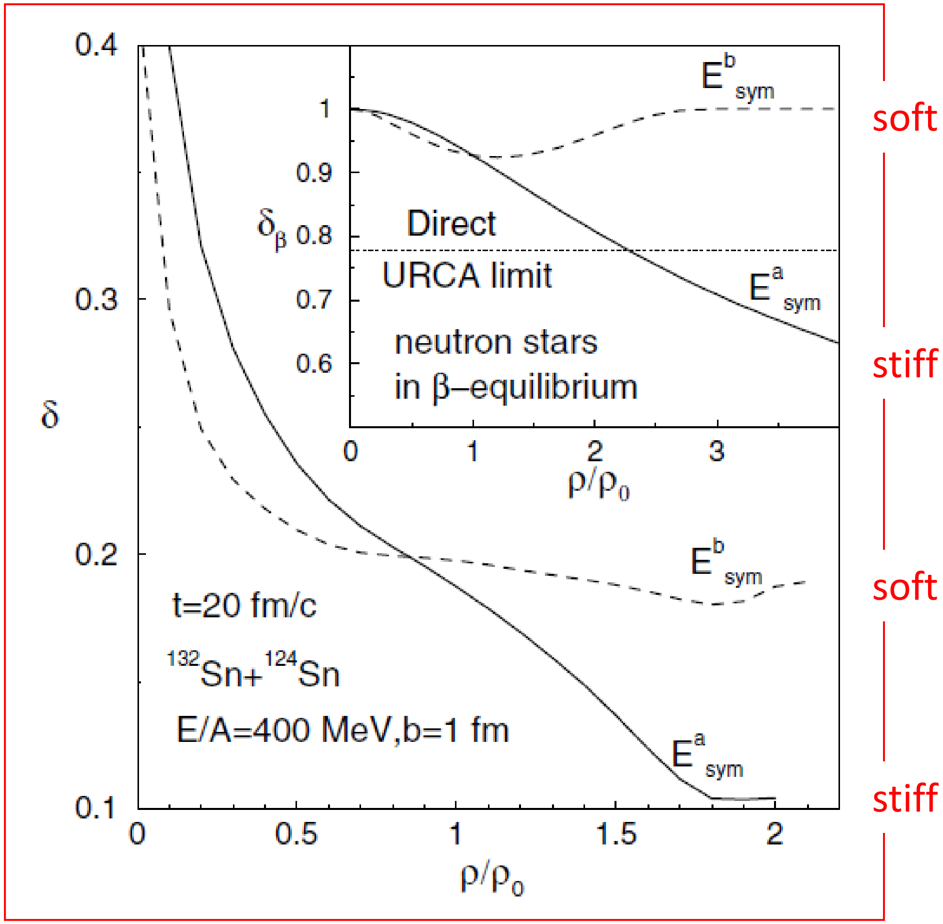

With HIC large density variations (density gradients) in nuclear matter can be obtained in a short timescale.

Bao-An Li, PRL 88 (2002):
differential flows in heavy ion reactions

Access to high density

Heavy ion collisions (HIC) at GSI/SIS energies can give information on the Symmetry term of EOS at supra-saturation densities

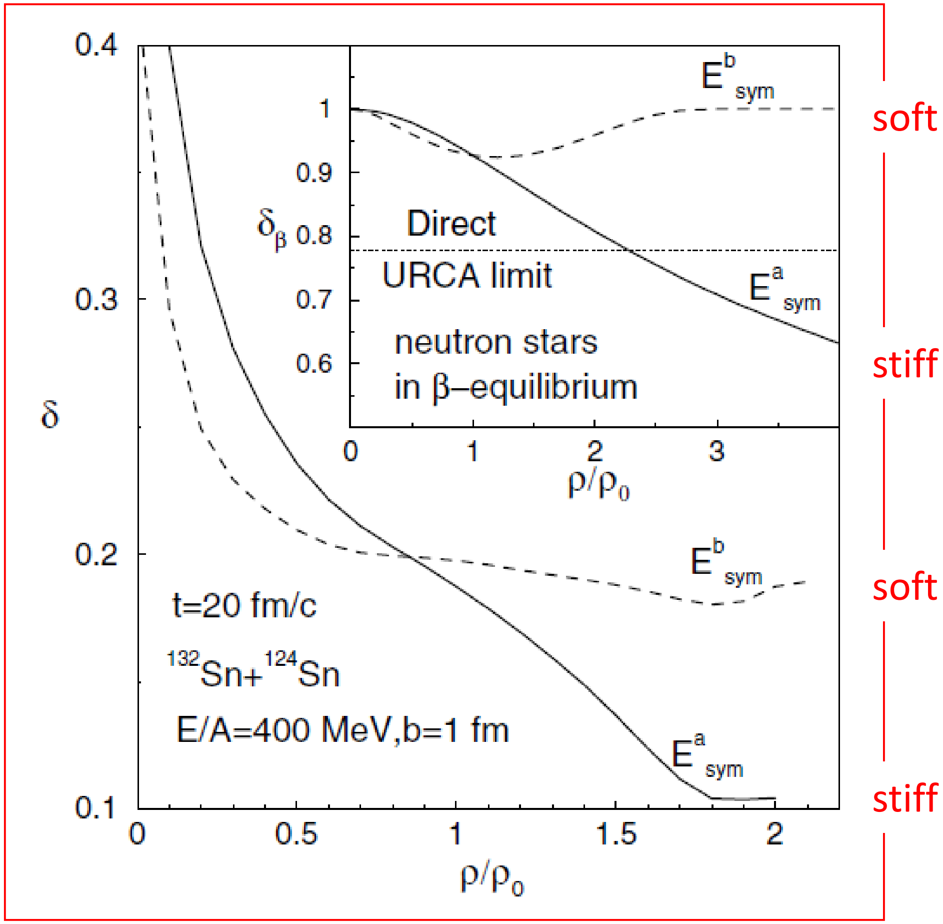

With HIC large density variations (density gradients) in nuclear matter can be obtained in a short timescale.

Bao-An Li, PRL 88 (2002):
differential flows in heavy ion reactions

Symmetry Energy

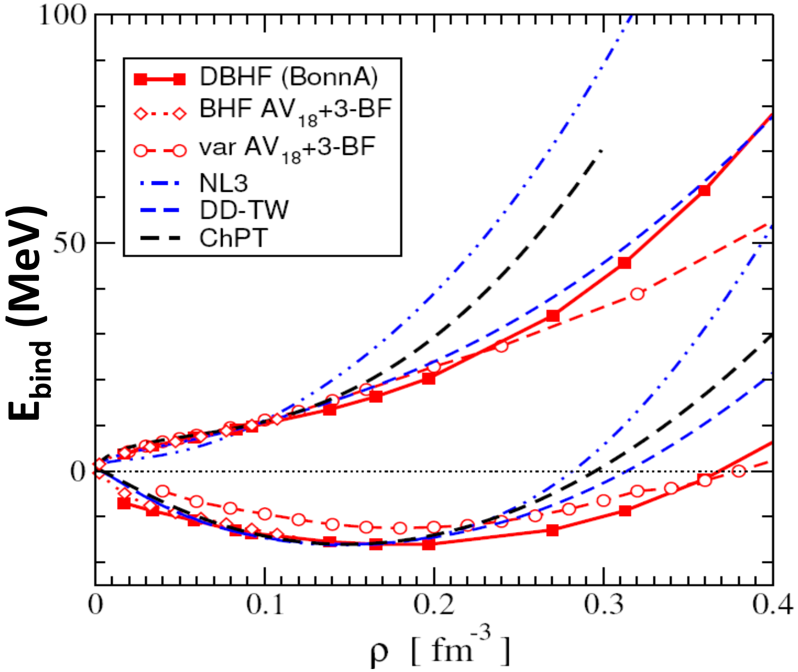

EOS of symmetric nuclear
and neutron matter
from
Ab initio calculations (red)
and phenomenological approaches

Fuchs and Wolter, EPJA 30 (2006)

Symmetry Energy

$$E_{Sym}(\rho) = E_{Sym}(\rho, \delta = 1) - E_{Sym}(\rho, \delta = 0)$$

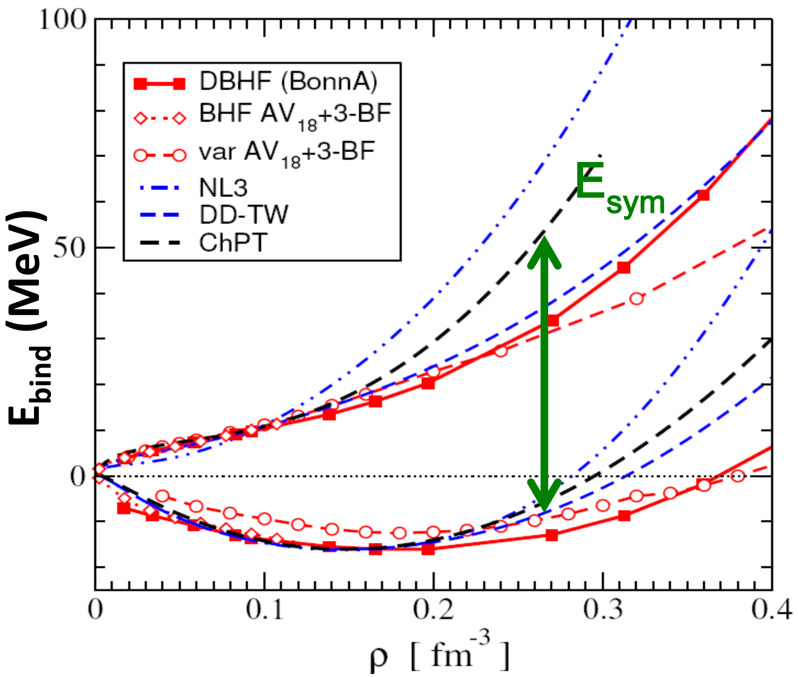

$$\delta = \frac{\rho_n - \rho_p}{\rho_n + \rho_p} = \frac{N - Z}{A}$$

EOS of symmetric nuclear
and neutron matter
from
Ab initio calculations (red)
and phenomenological approaches

Fuchs and Wolter, EPJA 30 (2006)

Symmetry Energy

$$E_{Sym}(\rho) = E_{Sym}(\rho, \delta = 1) - E_{Sym}(\rho, \delta = 0)$$

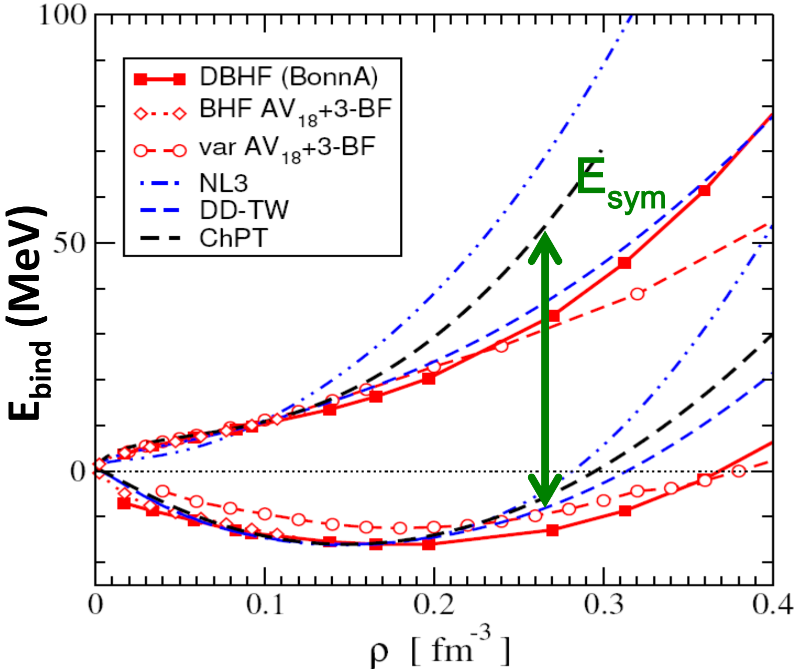

$$\delta = \frac{\rho_n - \rho_p}{\rho_n + \rho_p} = \frac{N - Z}{A}$$

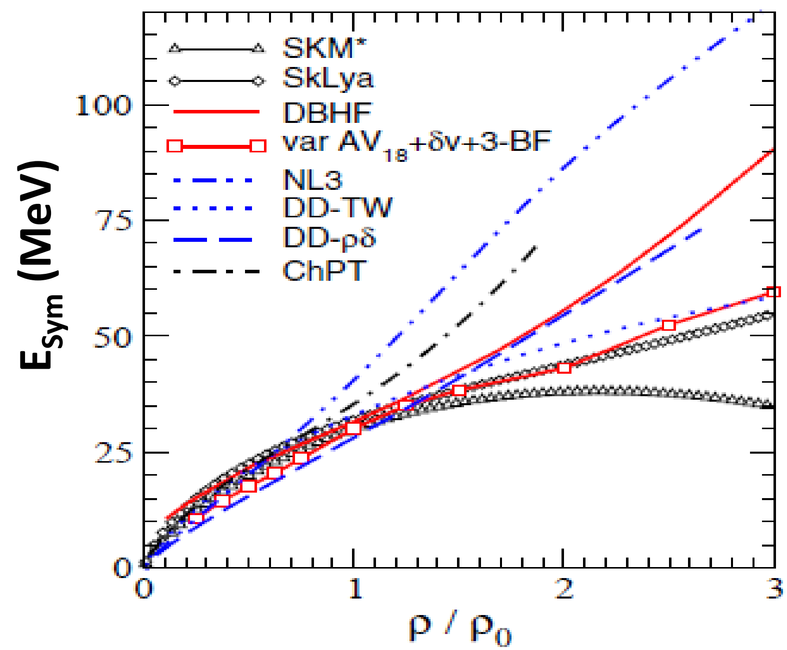

EOS of symmetric nuclear and neutron matter from Ab initio calculations (red) and phenomenological approaches

Fuchs and Wolter, EPJA 30 (2006)

Symmetry Energy

$$E_{Sym}(\rho) = E_{Sym}(\rho, \delta = 1) - E_{Sym}(\rho, \delta = 0)$$

$$\delta = \frac{\rho_n - \rho_p}{\rho_n + \rho_p} = \frac{N - Z}{A}$$

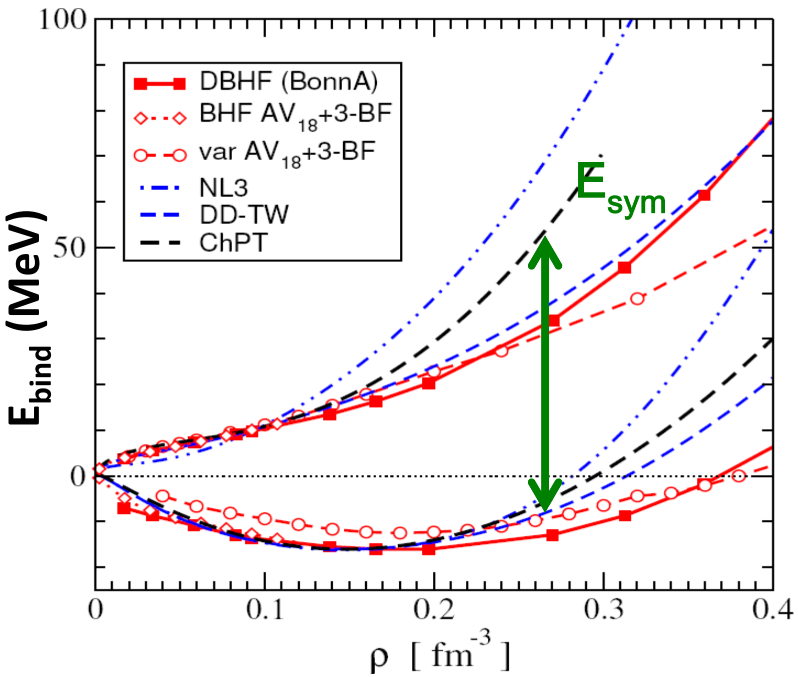

EOS of symmetric nuclear
and neutron matter
from
Ab initio calculations (red)
and phenomenological approaches

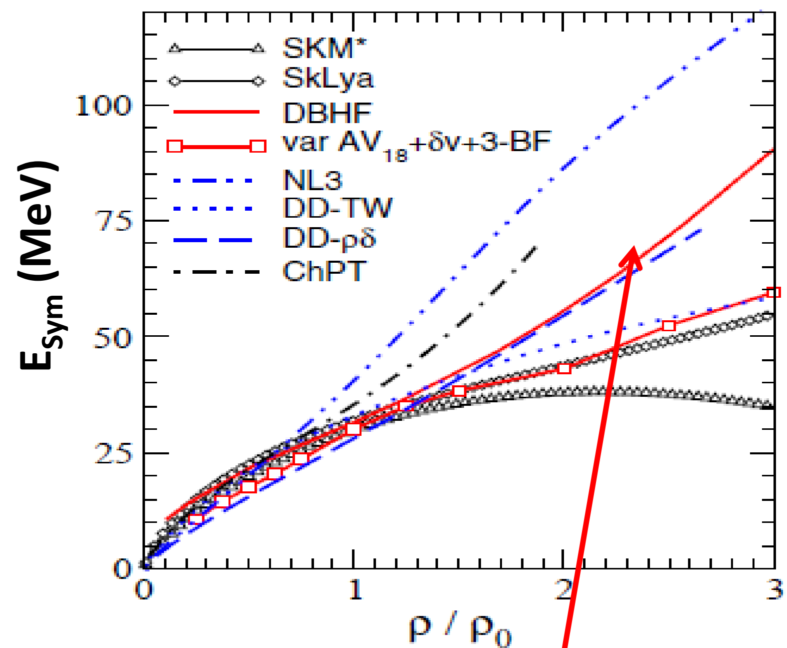

High density…so important!

Fuchs and Wolter, EPJA 30 (2006)

RISERVE

URQMD

parameterizations in UrQMD

Medium modifications (FU1, …) and momentum dependence (FP1, …) of **nucleon-nucleon elastic Xsects**
Qingfeng Li et al., PRC 83, 044617 (2011)

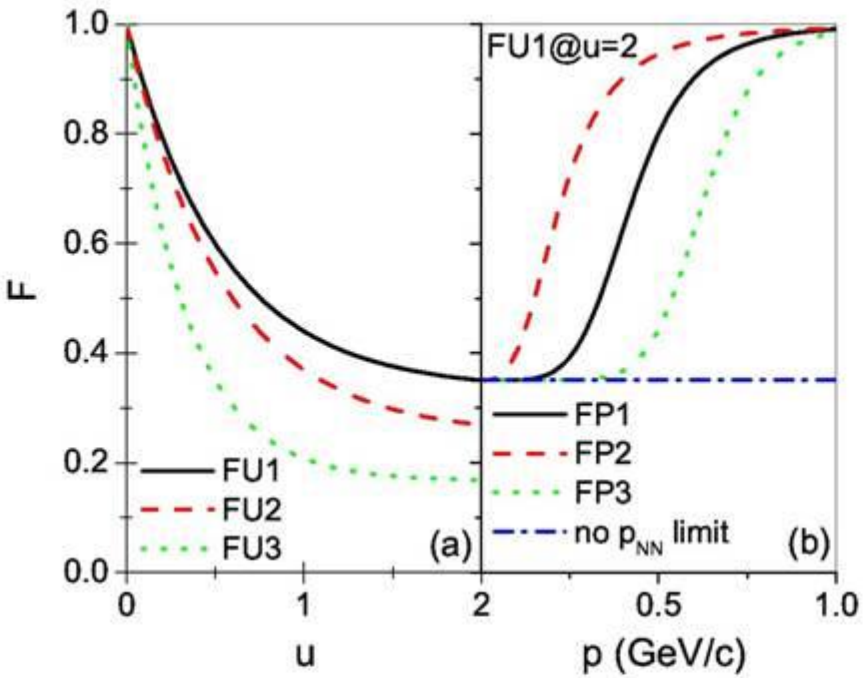

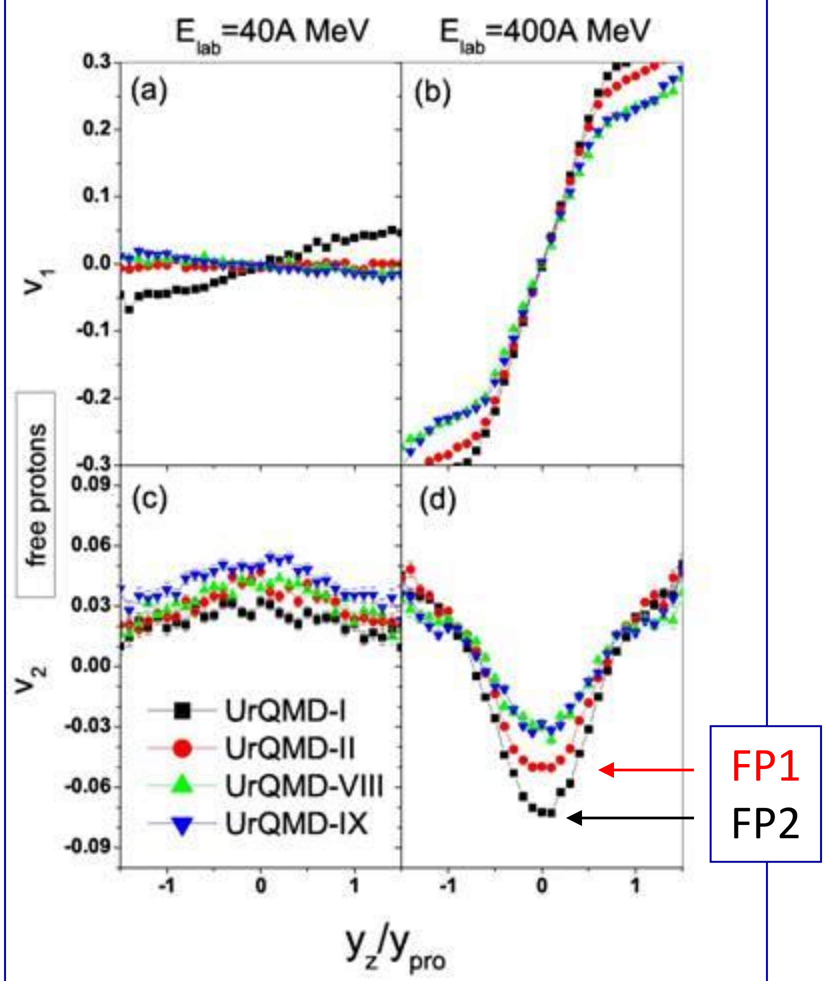

w/o momentum dep.

note change in color code black-red for FP1 and FP2 between left and right

INSTITUTE OF PHYSICS PUBLISHING JOURNAL OF PHYSICS G: NUCLEAR AND PARTICLE PHYSICS

J. Phys. G: Nucl. Part. Phys. **32** (2006) 407–415 doi:10.1088/0954-3899/32/4/001

Medium modifications of the nucleon–nucleon elastic cross section in neutron-rich intermediate energy HICs

Qingfeng Li[1,4], Zhuxia Li[2], Sven Soff[3], Marcus Bleicher[3] and Horst Stöcker[1,3]

[1] Frankfurt Institute for Advanced Studies (FIAS), Johann Wolfgang Goethe-Universität, Max-von-Laue-Str 1, D-60438 Frankfurt am Main, Germany
[2] China Institute of Atomic Energy, PO Box 275 (18), Beijing 102413, People's Republic of China
[3] Institut für Theoretische Physik, Johann Wolfgang Goethe-Universität, Max-von-Laue-Str 1, D-60438 Frankfurt am Main, Germany

E-mail: Qi.Li@fias.uni-frankfurt.de and lizwux@iris.ciae.ac.cn

Received 10 January 2006
Published 20 February 2006
Online at stacks.iop.org/JPhysG/32/407

Abstract

Several observables of unbound nucleons which are to some extent sensitive to the medium modifications of nucleon–nucleon elastic cross sections in neutron-rich intermediate energy heavy ion collisions are investigated. The splitting effect of neutron and proton effective masses on cross sections is discussed. It is found that the transverse flow as a function of rapidity, the Q_{zz} as a function of momentum, and the ratio of halfwidths of the transverse to that of longitudinal rapidity distribution $R_{t/l}$ are very sensitive to the medium modifications of the cross sections. The transverse momentum distribution of correlation functions of two nucleons does not yield information on the in-medium cross section.

(Some figures in this article are in colour only in the electronic version)

INSTITUTE OF PHYSICS PUBLISHING JOURNAL OF PHYSICS G: NUCLEAR AND PARTICLE PHYSICS

J. Phys. G: Nucl. Part. Phys. **32** (2006) 151–164 doi:10.1088/0954-3899/32/2/007

Probing the equation of state with pions

Qingfeng Li[1], Zhuxia Li[2], Sven Soff[3], Marcus Bleicher[3] and Horst Stöcker[1,3]

DDH3$\rho\delta^*$ > DDHρ^* > Fa3.

3. Momentum-dependent interactions for all baryons are introduced. The form of the momentum dependence is taken from the IQMD model [13, 38], which reads

$$U_{\rm md} = t_{\rm md} \ln^2[1 + a_{\rm md}(\Delta\mathbf{p})^2]u, \tag{1}$$

in which $\Delta\mathbf{p} = \mathbf{p}_i - \mathbf{p}_j$ represents the relative momentum of two nucleons i and j. The parametrizations of $t_{\rm md}$ and $a_{\rm md}$ are listed in table 1. We note that Li *et al* have used an isospin-dependent momentum-dependent parametrization in the BUU model, which

is guided by a Hartree–Fock calculation using the Gogny-effective interaction [39, 40]. However, here we do not consider the isospin dependence in the momentum-dependent part of the mean field.

RISERVE

V2

COLLECTIVE FLOWS

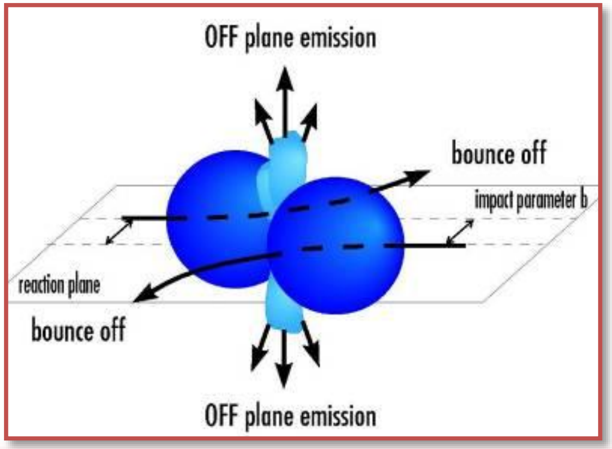

$$\frac{dN}{d(\phi-\phi_R)}(y,p_t)=\frac{N_0}{2\pi}\left(1+2\sum_{n\geq 1} v_n \cos n(\phi-\phi_R)\right)$$

Transverse flow

$$V_1(y,p_t)=\left\langle \frac{p_x}{p_t} \right\rangle$$

Elliptic flow

$$V_2(y,p_t)=\left\langle \frac{p_x^2-p_y^2}{p_t^2} \right\rangle$$

Elliptic flow: competition between in plane (**$V_2>0$**) and out-of-plane ejection (**$V_2<0$**)

Transverse flow: *it provides information on the azimuthal anisotropy in the reaction plane*

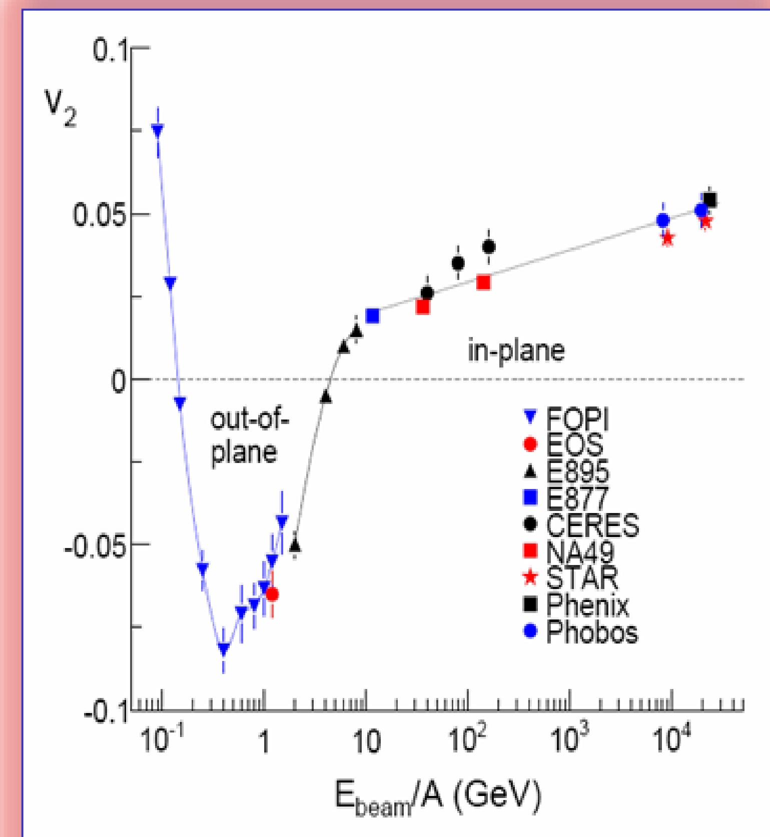

COLLECTIVE FLOWS

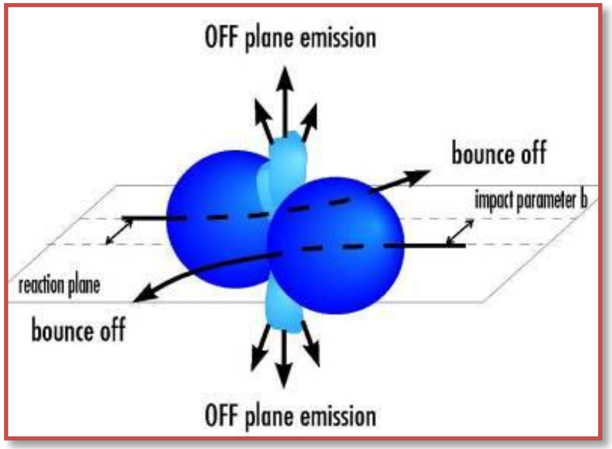

$$\frac{dN}{d(\phi-\phi_R)}(y,p_t)=\frac{N_0}{2\pi}\left(1+2\sum_{n\geq 1}v_n\cos n(\phi-\phi_R)\right)$$

Transverse flow

$$V_1(y,p_t)=\left\langle\frac{p_x}{p_t}\right\rangle$$

Elliptic flow

$$V_2(y,p_t)=\left\langle\frac{p_x^2-p_y^2}{p_t^2}\right\rangle$$

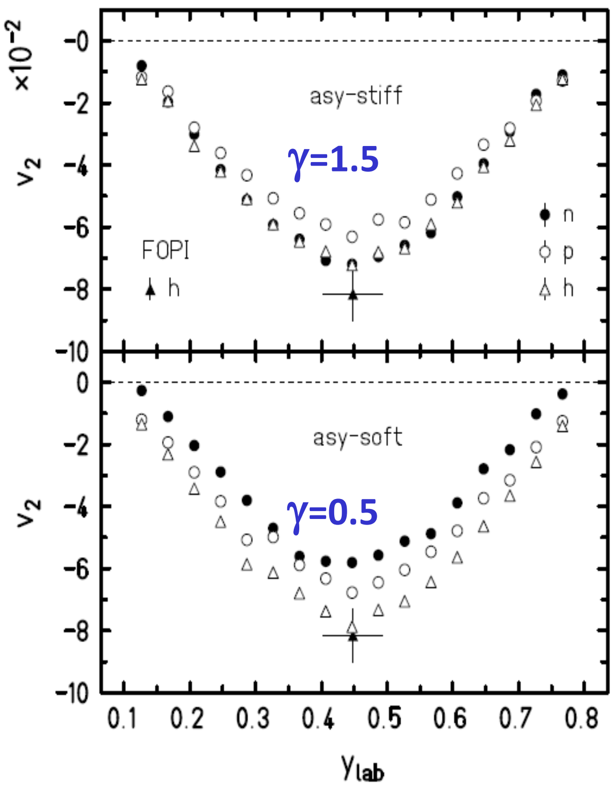

Elliptic flow: competition between in plane ($V_2>0$) and out-of-plane ejection ($V_2<0$)

Transverse flow: *it provides information on the azimuthal anisotropy in the reaction plane*

Elliptic flow from FOPI /LAND experiment Au+Au 400 A.MeV

UrQMD model: Au+Au @ 400 AMeV
5.5<b<7.5 fm

Qingfeng Li, J. Phys. G31 1359-1374 (2005)

P. Russotto et al., Phys. Lett. **B697,** 471 (2011)

Flows

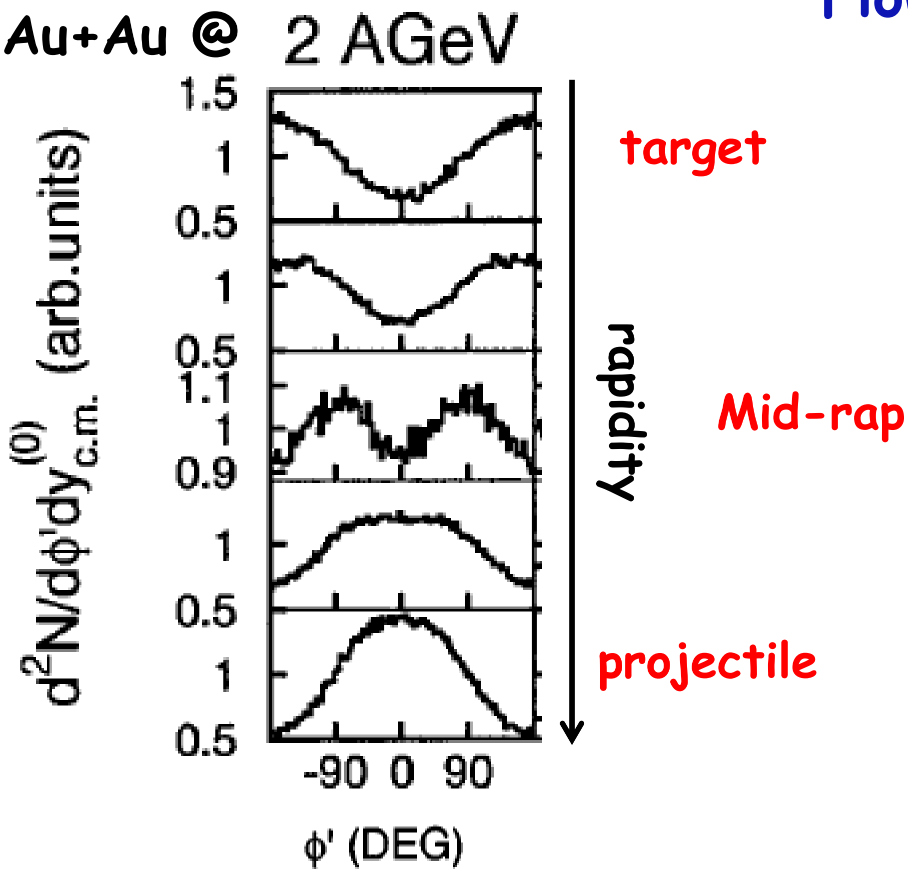

C.Pinkenburg et al., (E895),Phys.Rev.Lett. 83 (1999) 1295, *nucl-ex/9903010*

$$\frac{dN}{d(\phi-\phi_R)}(y,p_t)=\frac{N_0}{2\pi}\left(1+2\sum_{n\geq 1}v_n\cos n(\phi-\phi_R)\right)$$

Y = rapidity

pt = transverse momentum

Flows

Au+Au @

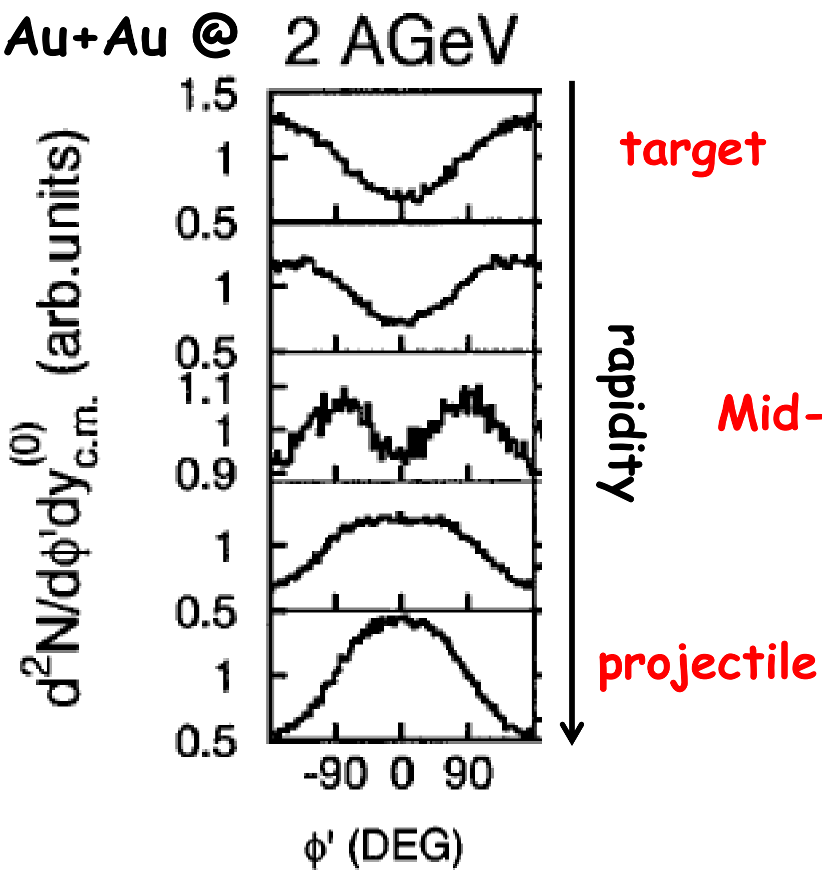

C.Pinkenburg et al., (E895),Phys.Rev.Lett. 83 (1999) 1295, *nucl-ex/9903010*

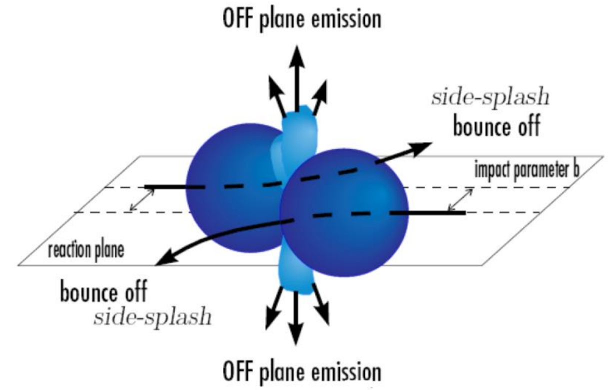

Not to scale: qualitative

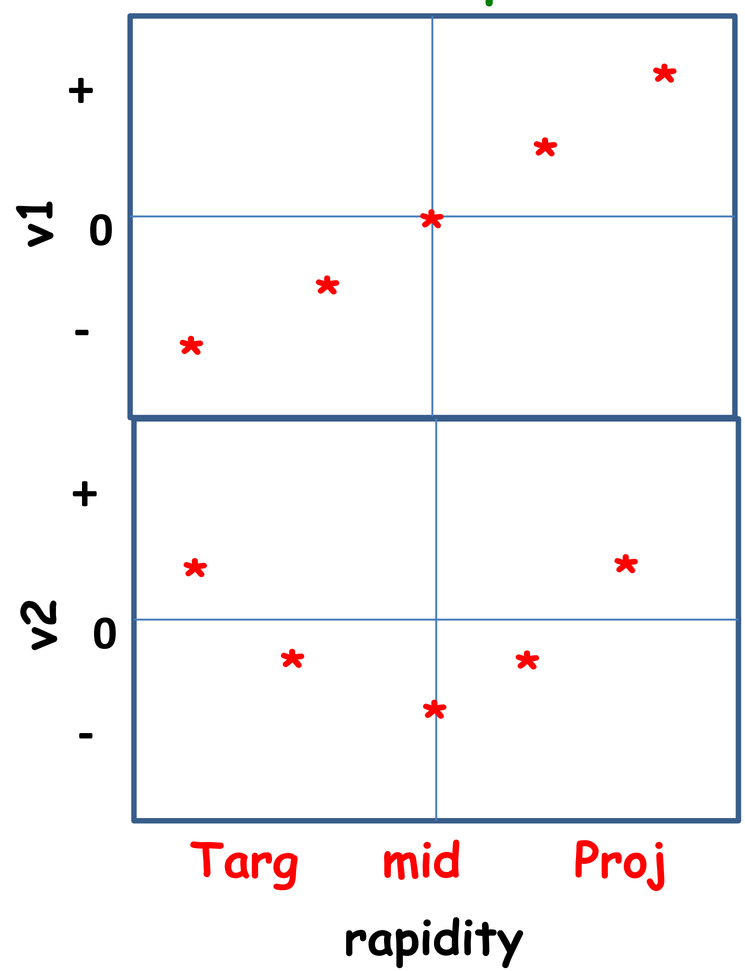

$$\frac{dN}{d(\phi-\phi_R)}(y,p_t)=\frac{N_0}{2\pi}\left(1+2\sum_{n\geq 1}v_n\cos n(\phi-\phi_R)\right)$$

Y = rapidity
pt = transverse momentum

Mass splitting impact on Elliptic Flow

$^{197}Au+^{197}Au$, 400 AMeV, b=5 fm, $y^{(0)} \leq 0.3$

From M.Di Toro talk at Asy-Eos2010

$m^*_n < m^*_p$: larger neutron squeeze out at mid-rapidity

- Larger neutron repulsion for asy-stiff

Increasing relevance of isospin effects for $m^*_n < m^*_p$

v_2 vs scaled rapidity

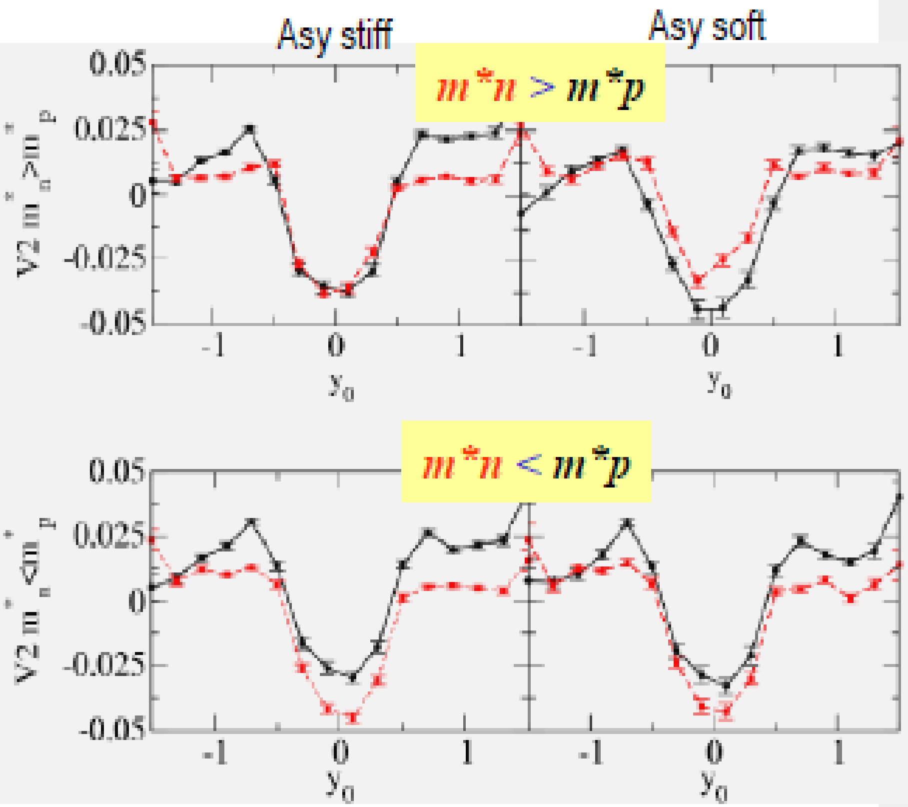

v_2 vs p_T

$y^{(0)} \leq 0.3$

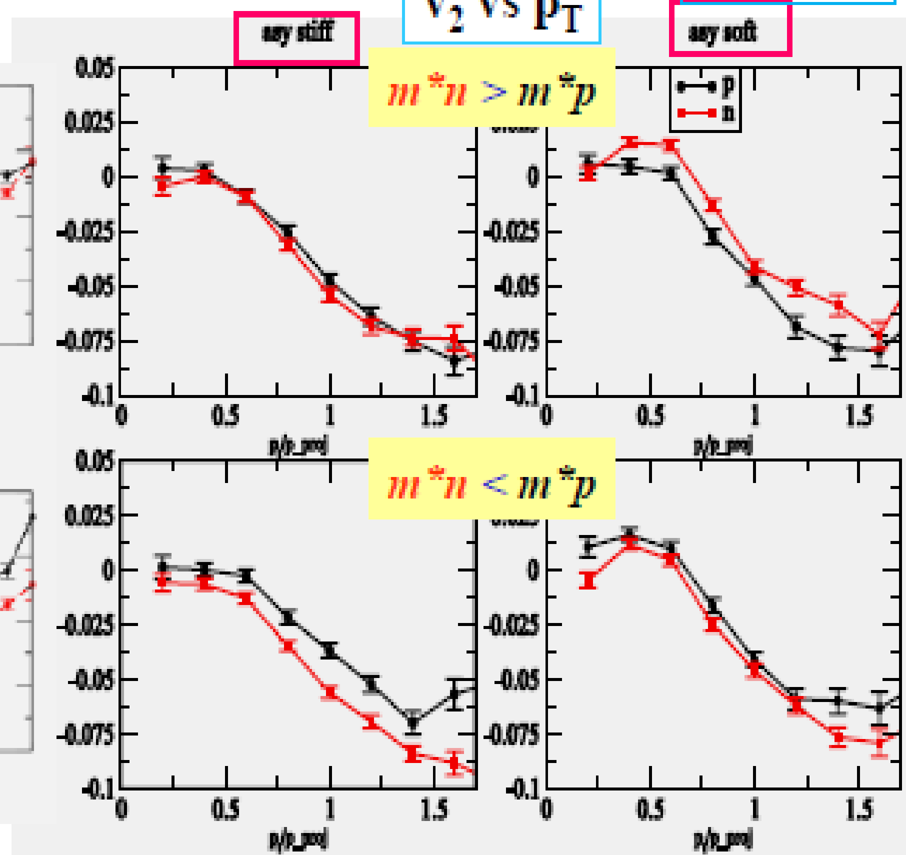

S394

High density over a long time

$\rho \cdot \Delta t$= maximum here

in the central region
of ^{132}Sn + ^{124}Sn central collisions
according to the isospin dependent
transport model of
Bao-An Li, NPA 708(2002)

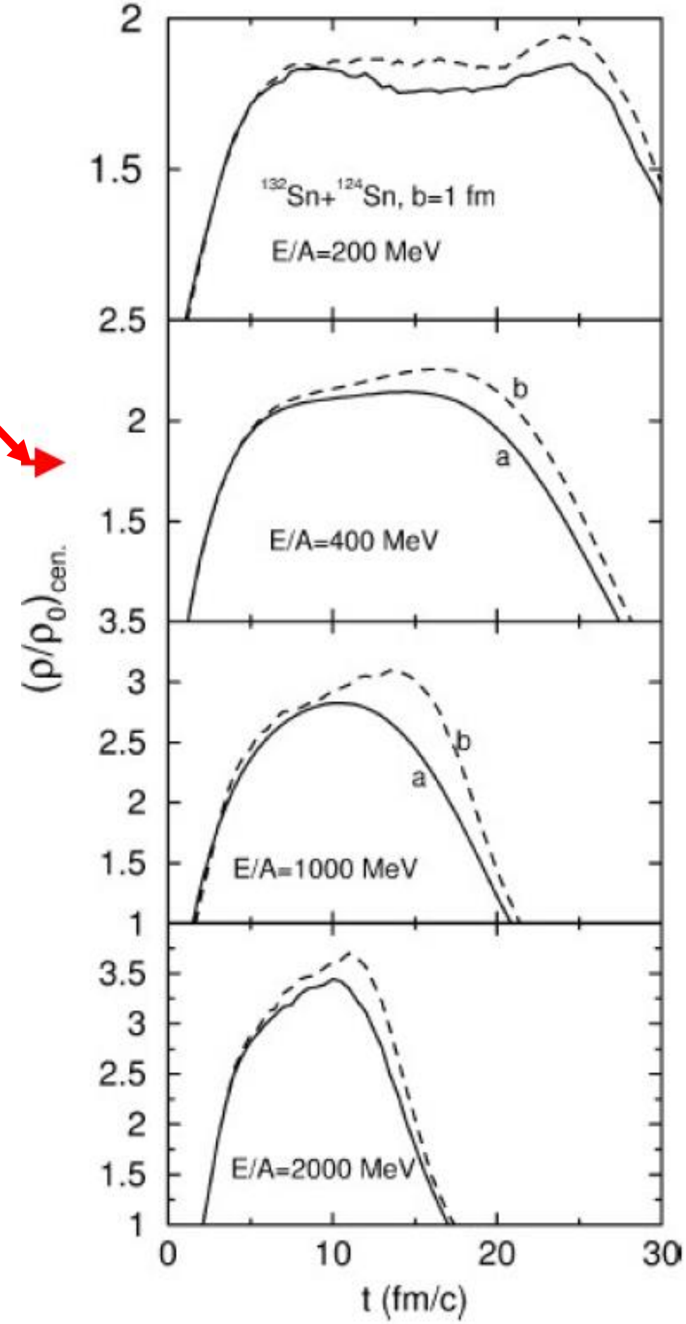

A. Andronic et al., Eur. Phys. J. A 30 (2006) 31.

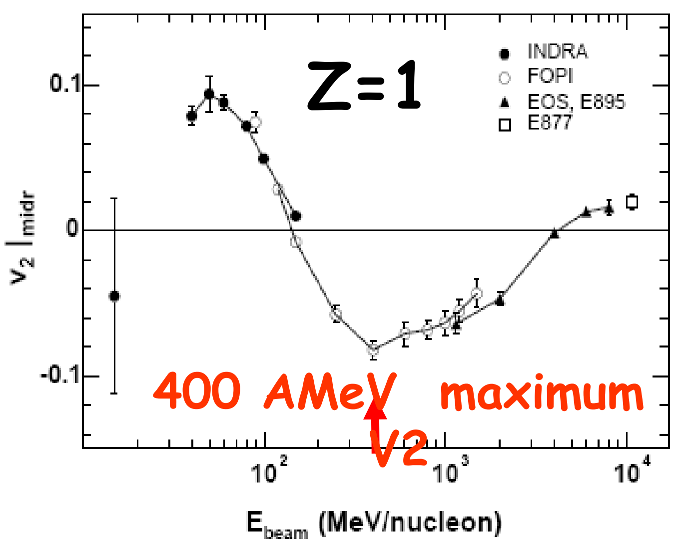

Aladin ToF-Wall

96 plastic bars 2.5X 100 cm
2 walls (front and rear) $\theta < 7°$
Z, velocity & X-Y position.
Impact parameter and
reaction plane determination

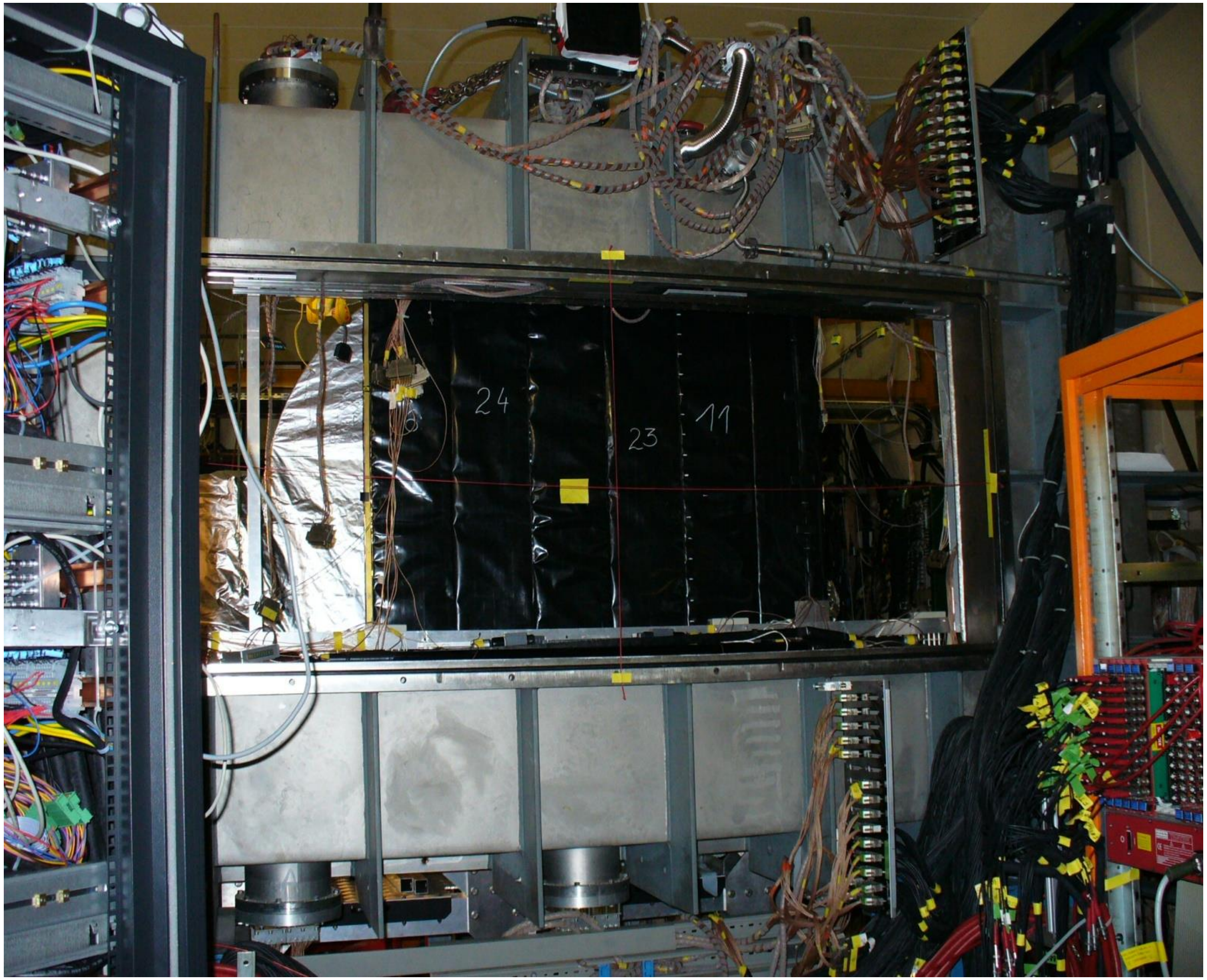

Aladin ToF-Wall

96 plastic bars 2.5X 100 cm
2 walls (front and rear) θ < 7°
Z, velocity & X-Y position.
Impact parameter and
reaction plane determination

TOF-Wall geometry

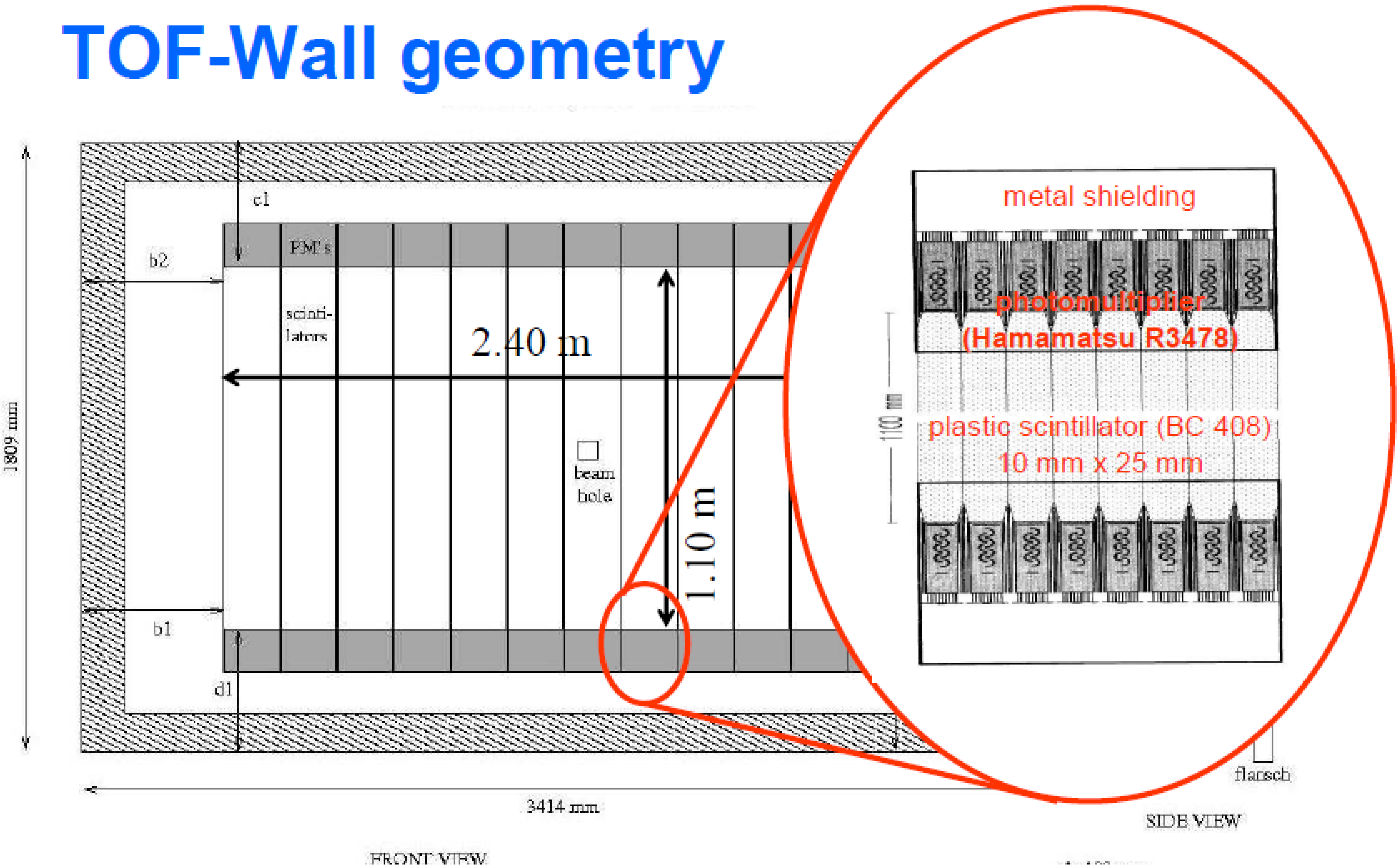

Time, charge and space resolution

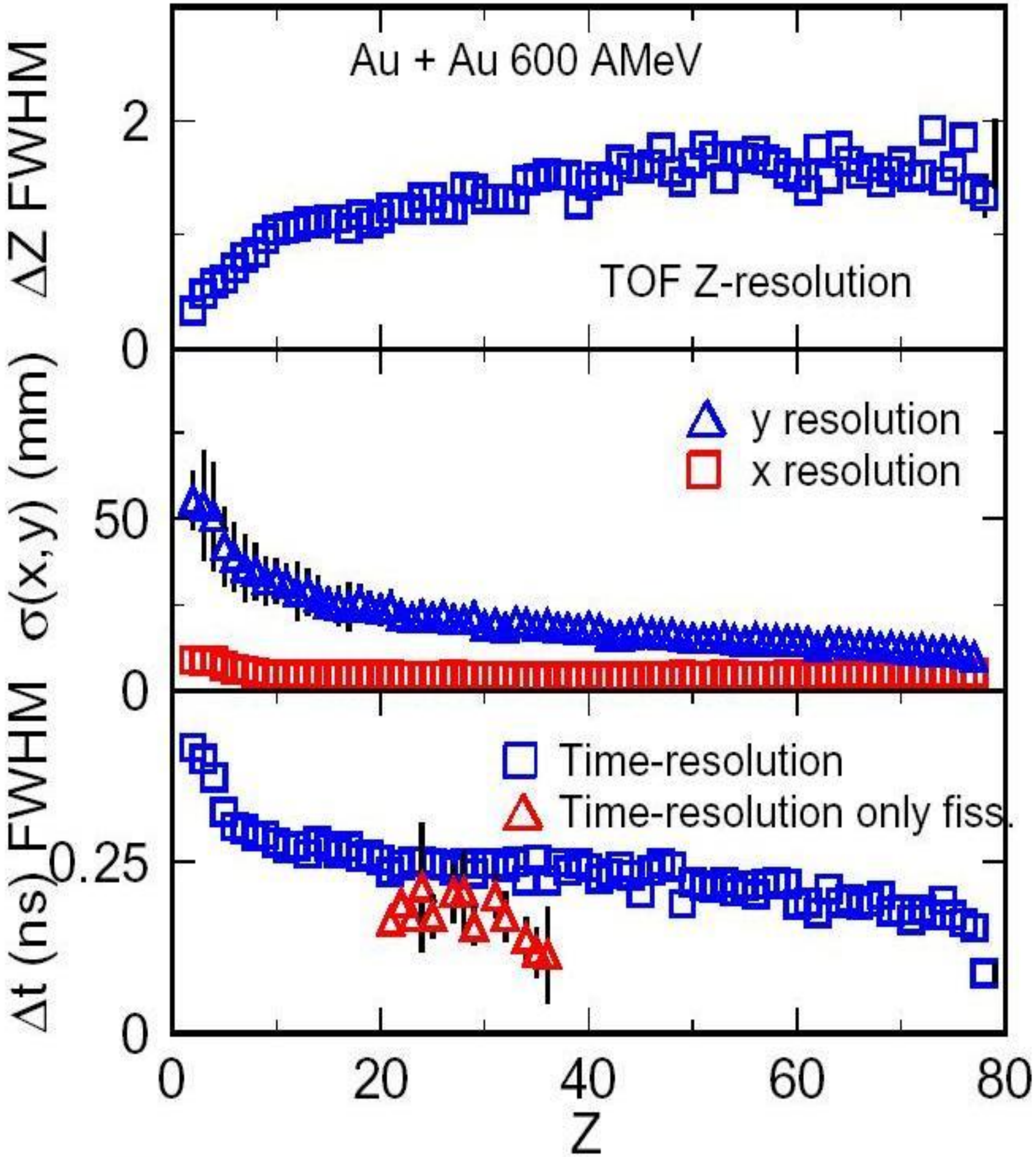

FWHM = 2.35 σ

A. Schüttauf

Aladin ToF-Wall (GSI)

96 plastic bars 2.5X 100 cm
2 walls (front and rear) $\theta < 7°$
Z, velocity & X-Y position.
Impact parameter and
reaction plane determination

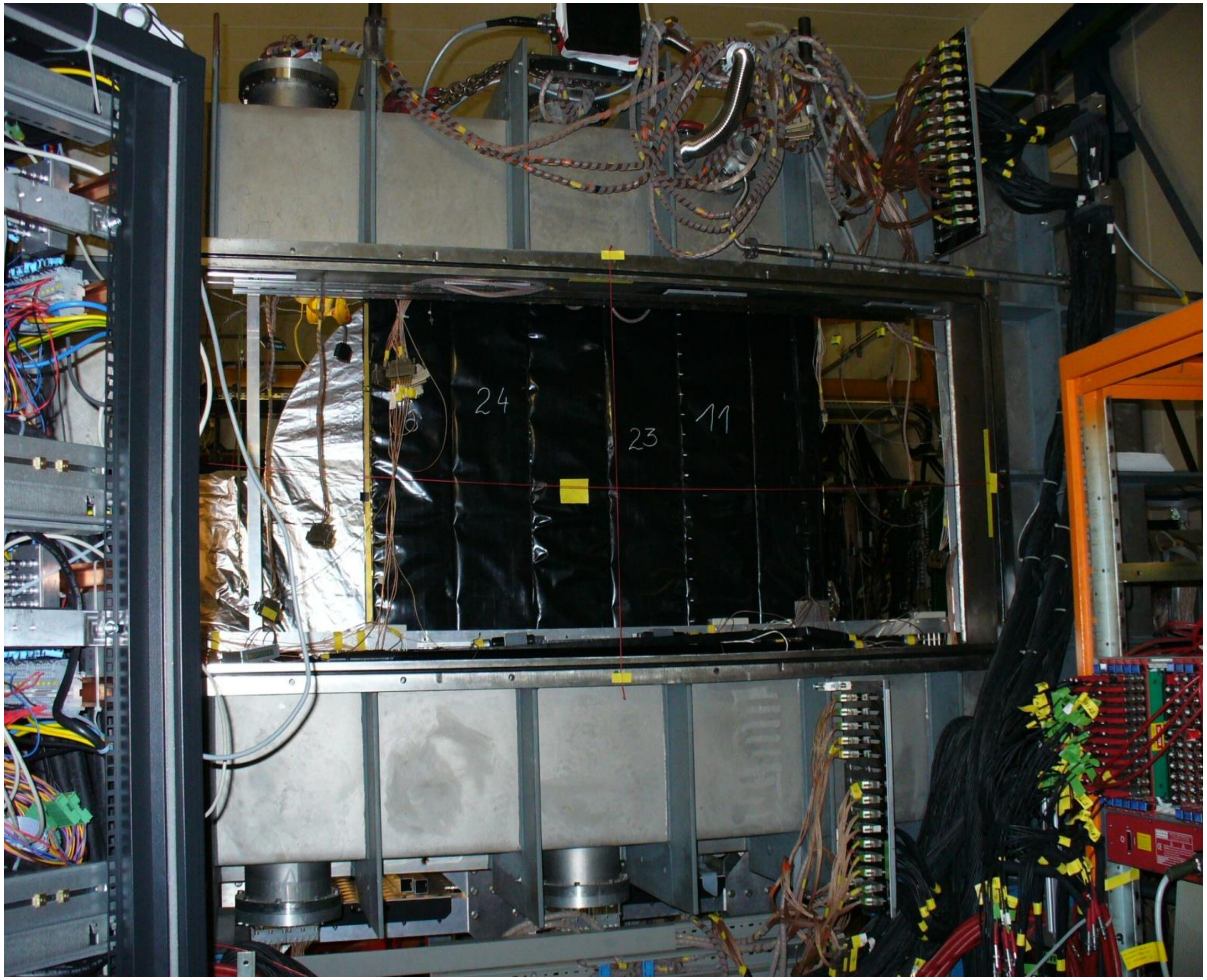

Aladin ToF-Wall (GSI)

96 plastic bars 2.5X 100 cm
2 walls (front and rear) θ < 7°
Z, velocity & X-Y position.
Impact parameter and
reaction plane determination

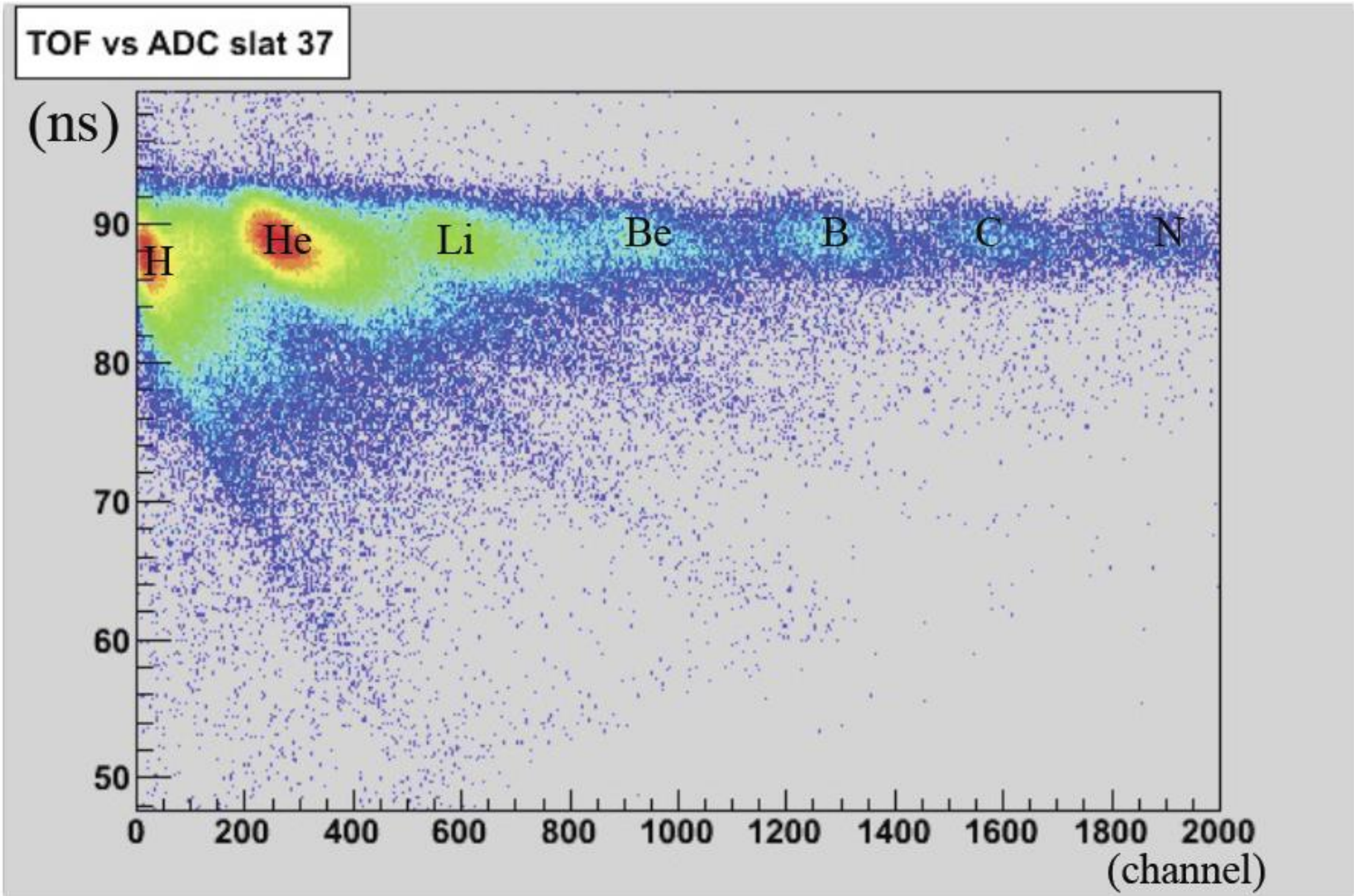

MicroBall (USA)

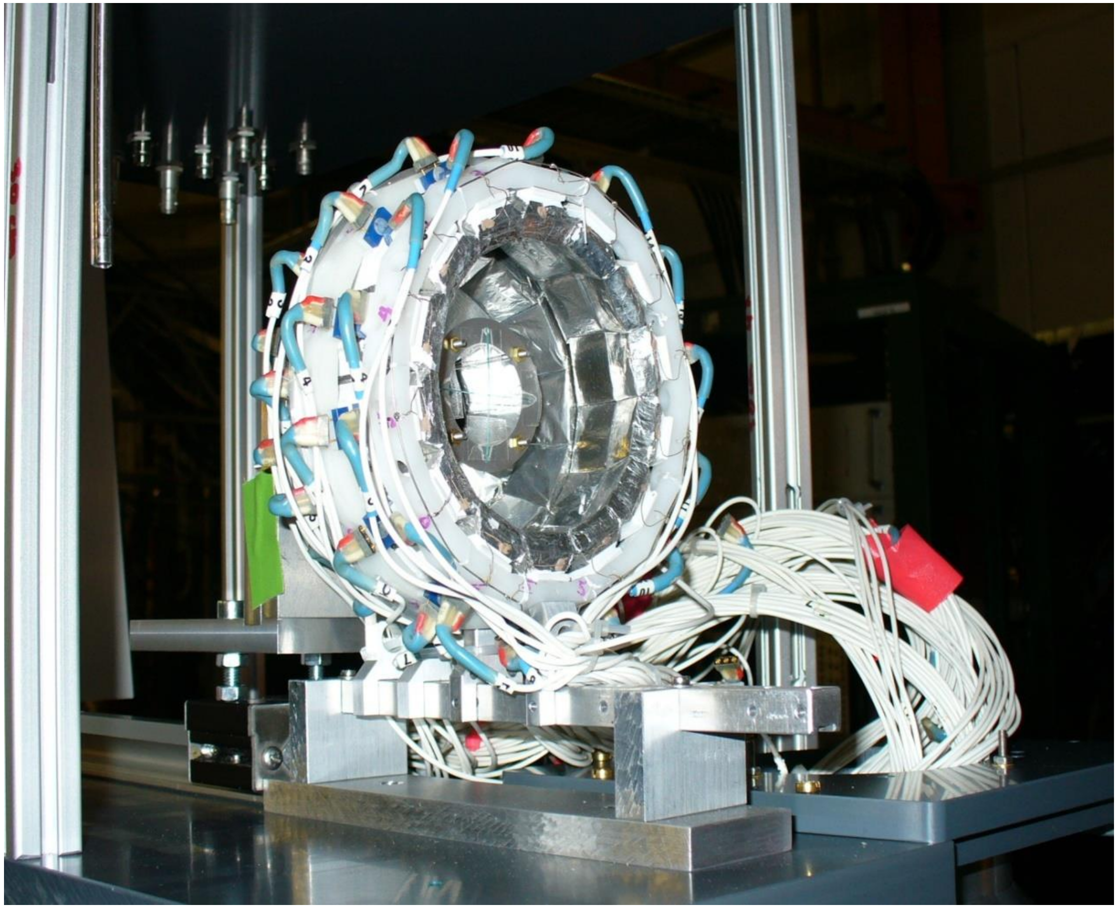

***μBall*:**

4 rings, 50 CsI(Tl)

~ 1 cm thick

60°<θ<147°.

Discriminate target vs. air interactions (backward angles).

Multiplicity measurements.

CHIMERA

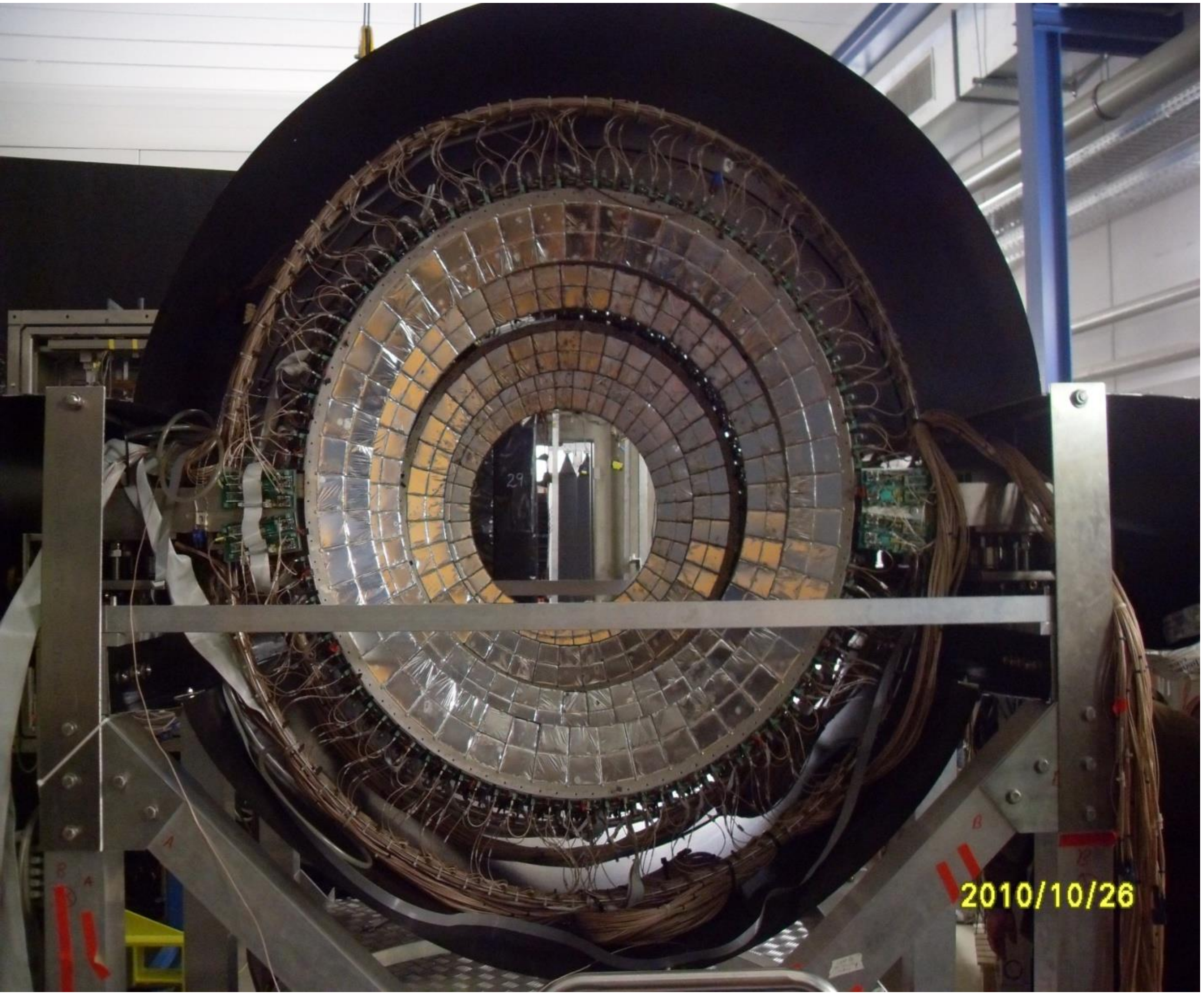

352 CsI 12 cm thick
+ 32 Si (telescopes)
8 Rings covering $7° < \theta < 20°$
Light ions
Z, Ekin & θ-ϕ.
Impact parameter and
reaction plane
determination

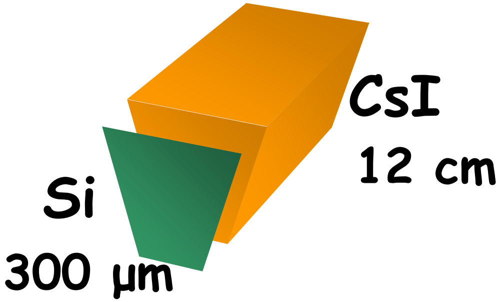

Identification in CHIMERA...

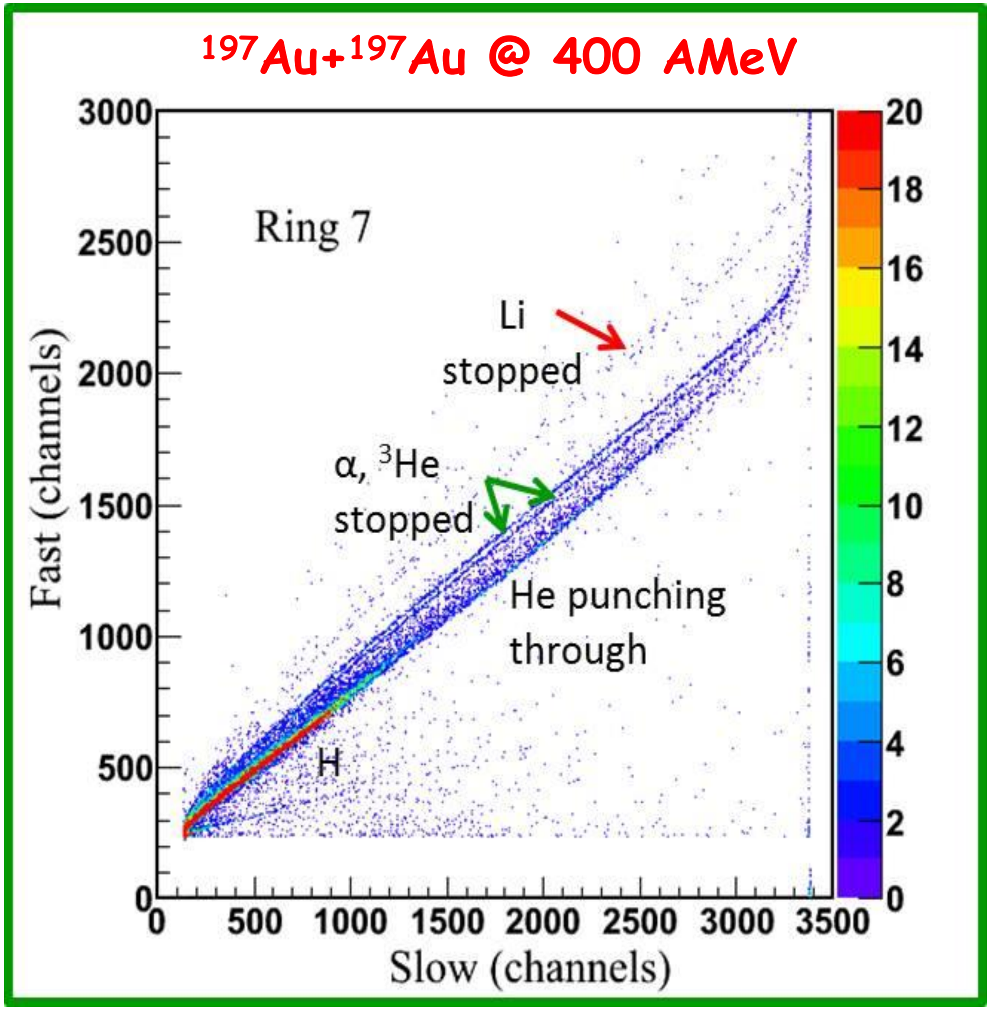

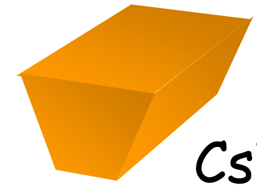

Identification in CHIMERA...

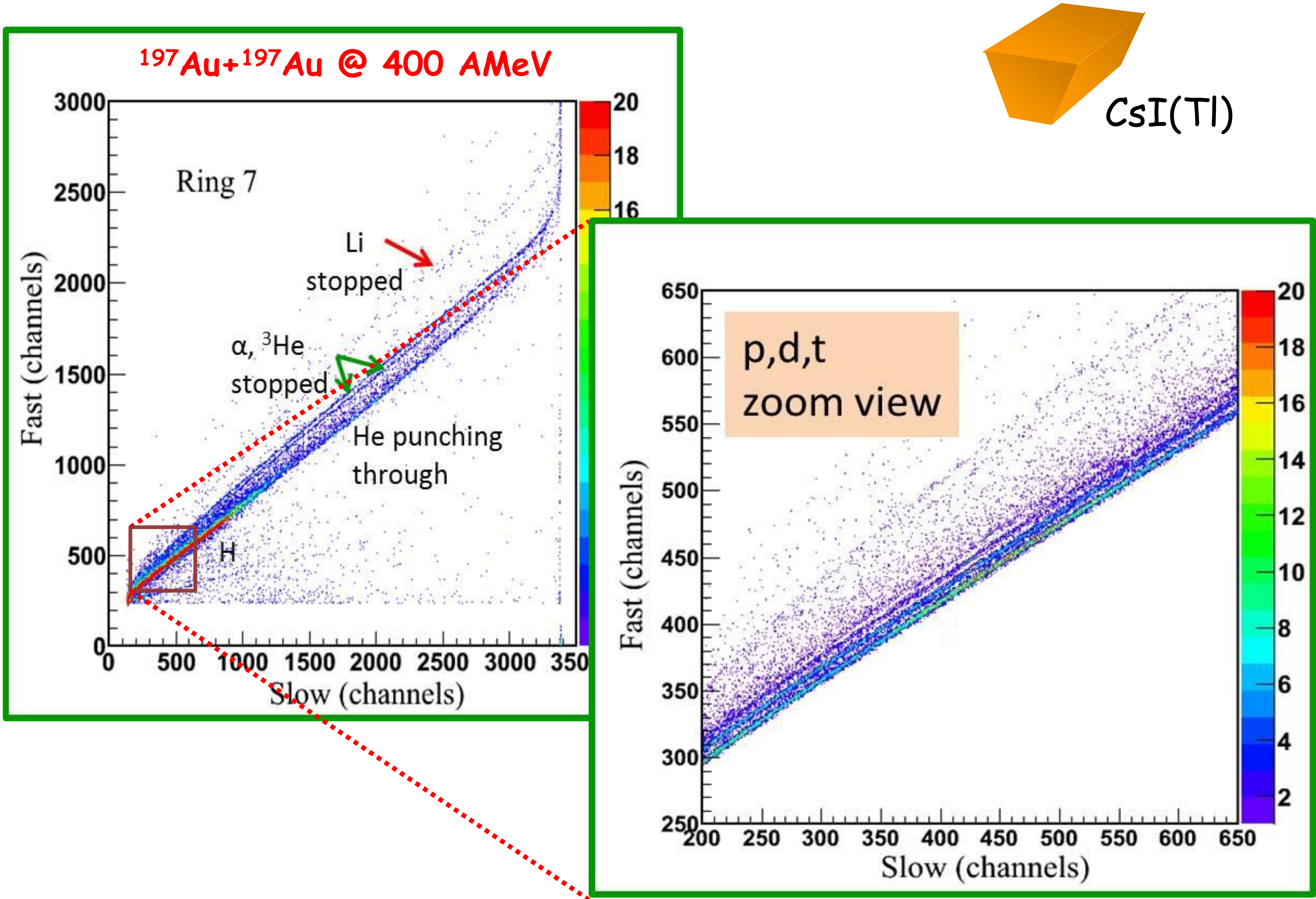

Identification in CHIMERA...

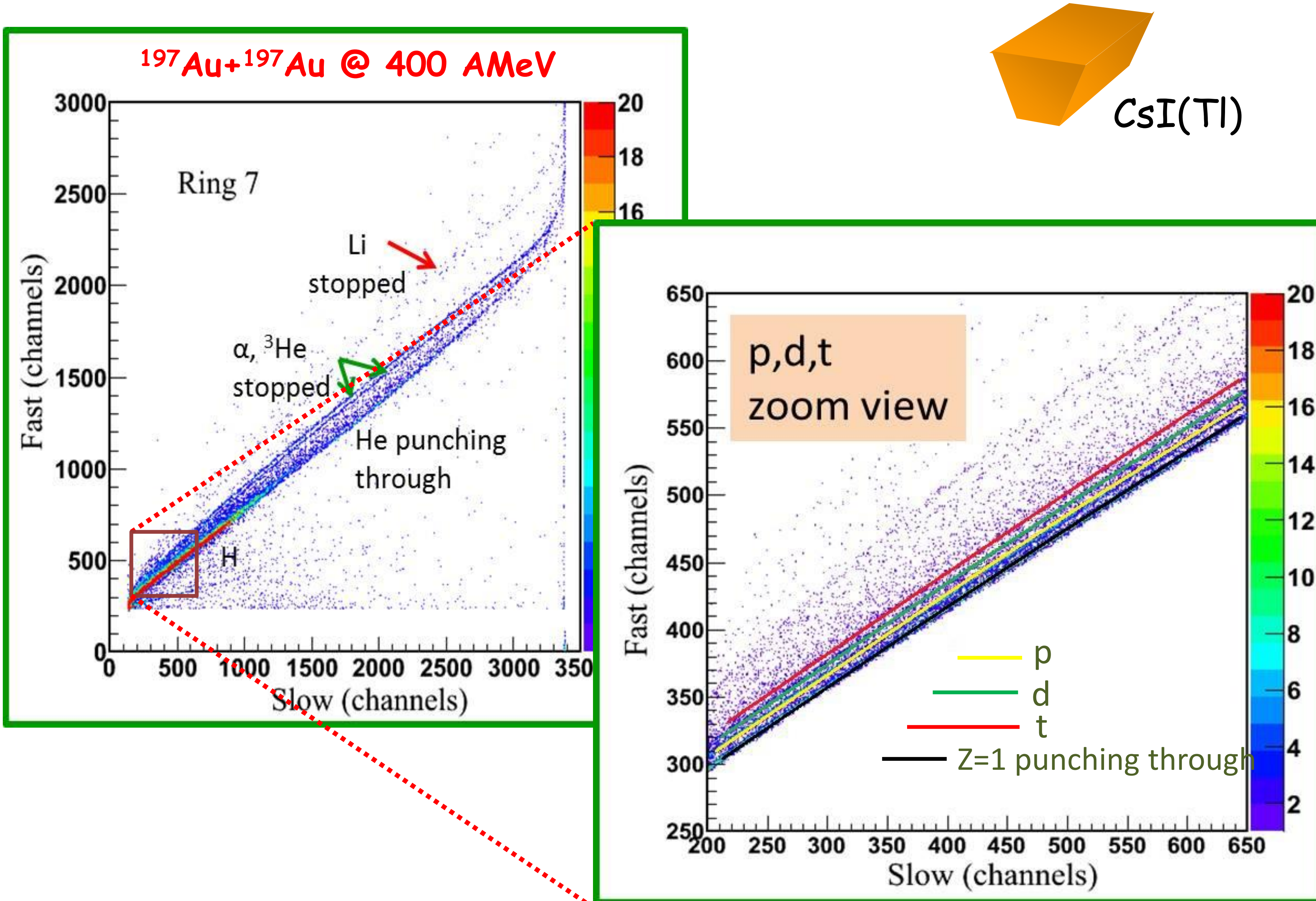

Timing problems in LAND

New pic

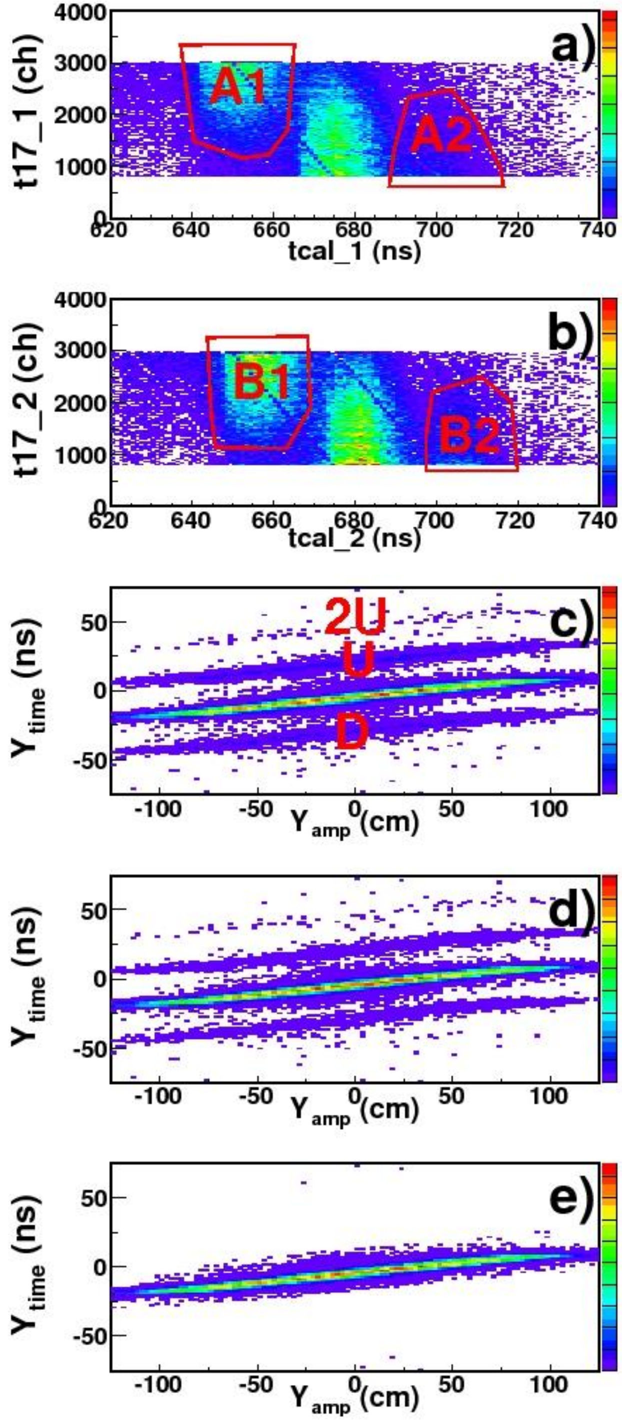

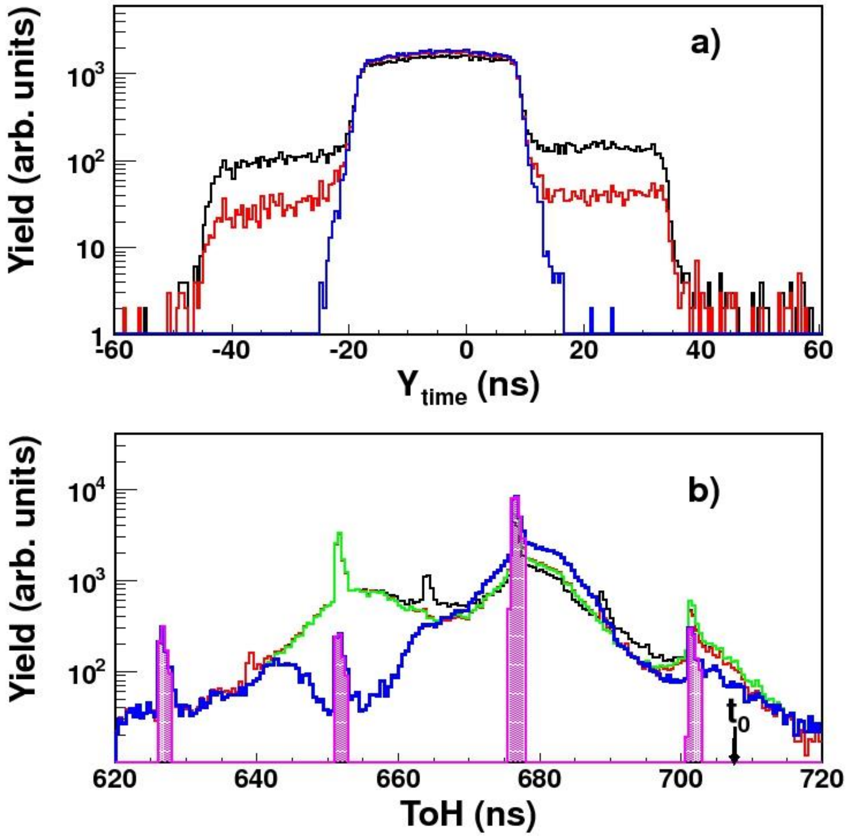

Timing problems in LAND

New pic

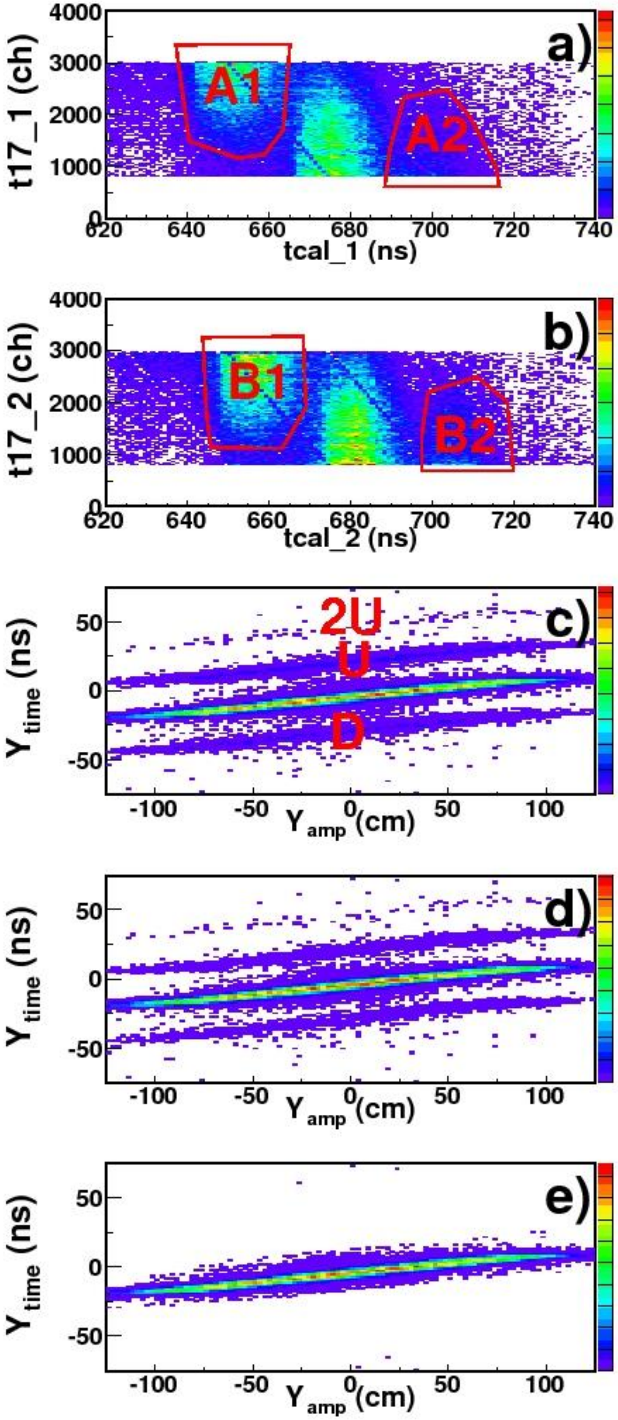

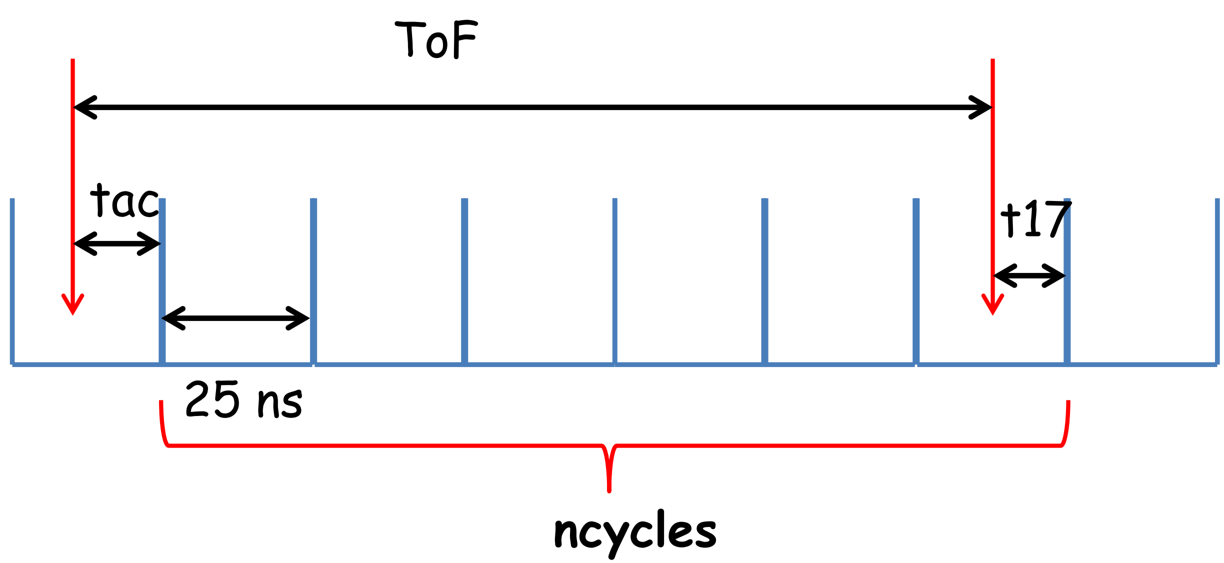

ToF= tac+25*ncycles-t17

Neutron azimuthal distributions from LAND

Au+Au @ 400 AMeV
b< 7.5 fm

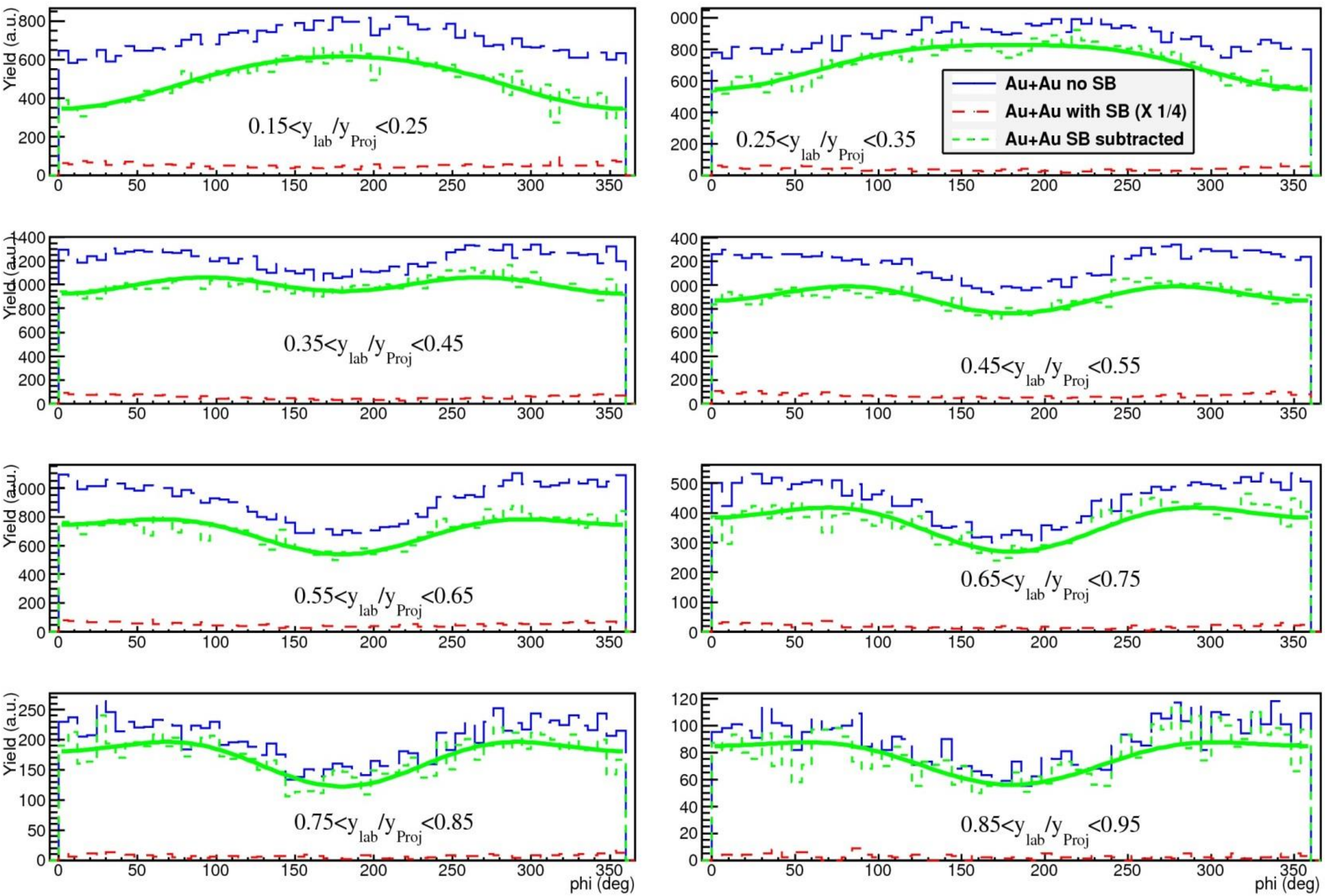

Yield and Flows of Charged Particles from FOPI

Au+Au @ 400 A.MeV

3.35<b<6 fm (c2)

θ_{lab} cut as in ASY-EOS set-up

Courtesy of W. Reisdorf

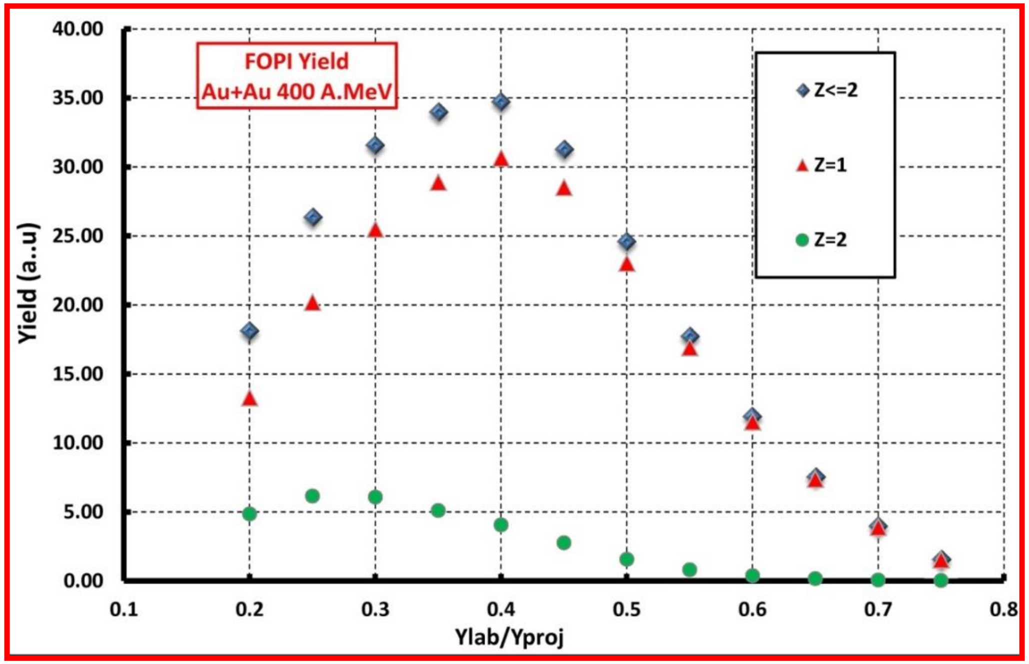

- Yield of Helium is small in such exp. conditions

- Although v2 of Helium is strong, v2 of charged particles is close to the Hydrogen one

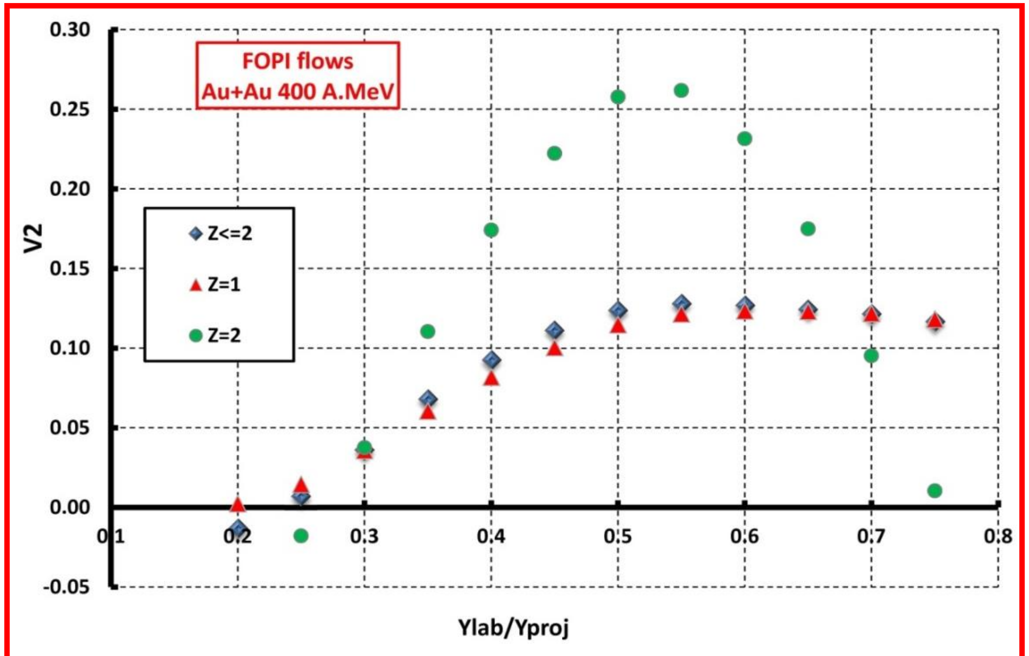

Comparing KraTTA* with FOPI: rapidity dep. of isotopes

35 modules (5 x7), 20.7°<θ<63.5°
40 cm from target.
Digitized with 100 MHz, 14 bits Flash ADCs

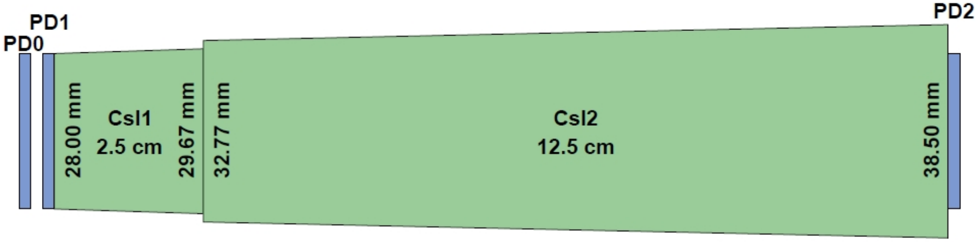

*J. Lukasik et al., NIM A 709, 120 (2013)

S. Kupny Ph. D (2014)

Comparing KraTTA* with FOPI: rapidity dep. of isotopes

35 modules (5 x7), 20.7°<θ<63.5°
40 cm from target.
Digitized with 100 MHz, 14 bits Flash ADCs

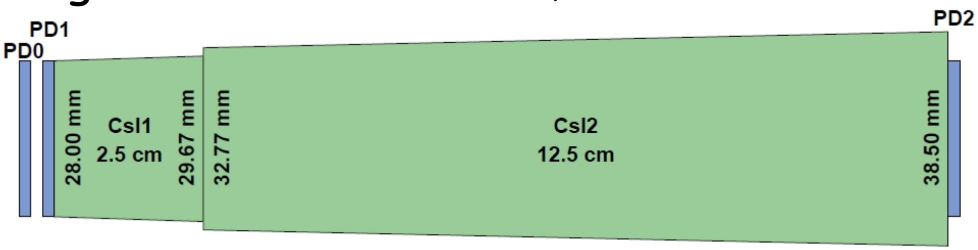

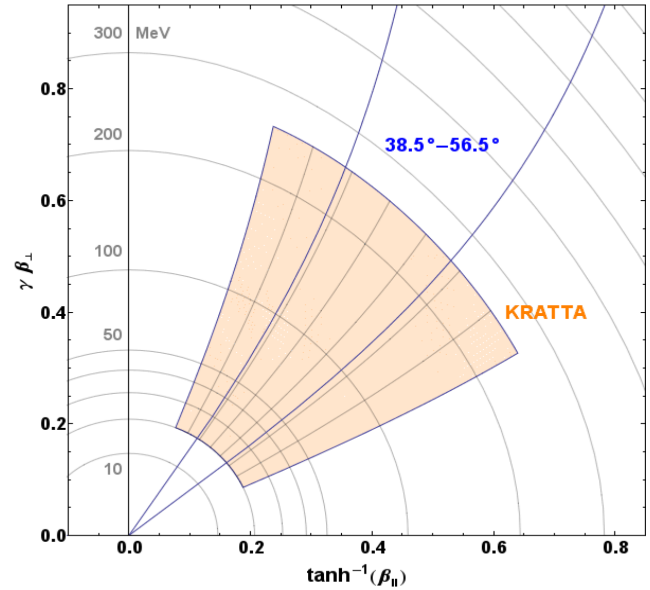

Au+Au @ 400 A.MeV
3.35<b<6 fm (c2)
θ_{lab} cut as LAND

*J. Lukasik et al., NIM A 709, 120 (2013)

S. Kupny Ph. D (2014)

Comparing KraTTA* with FOPI: rapidity dep. of isotopes

35 modules (5 x7), 20.7°<θ<63.5°
40 cm from target.
Digitized with 100 MHz, 14 bits Flash ADCs

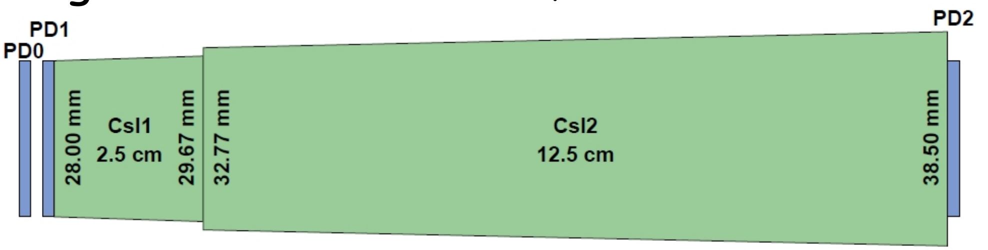

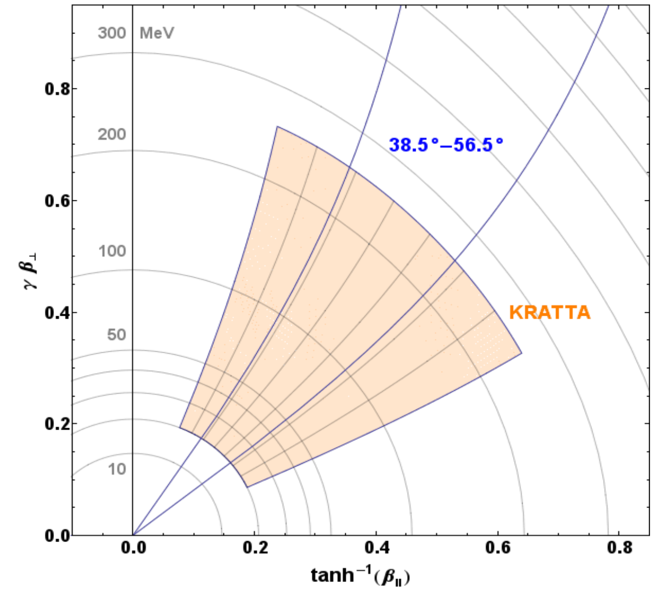

Au+Au @ 400 A.MeV
3.35<b<6 fm (c2)
θ_{lab} cut as LAND

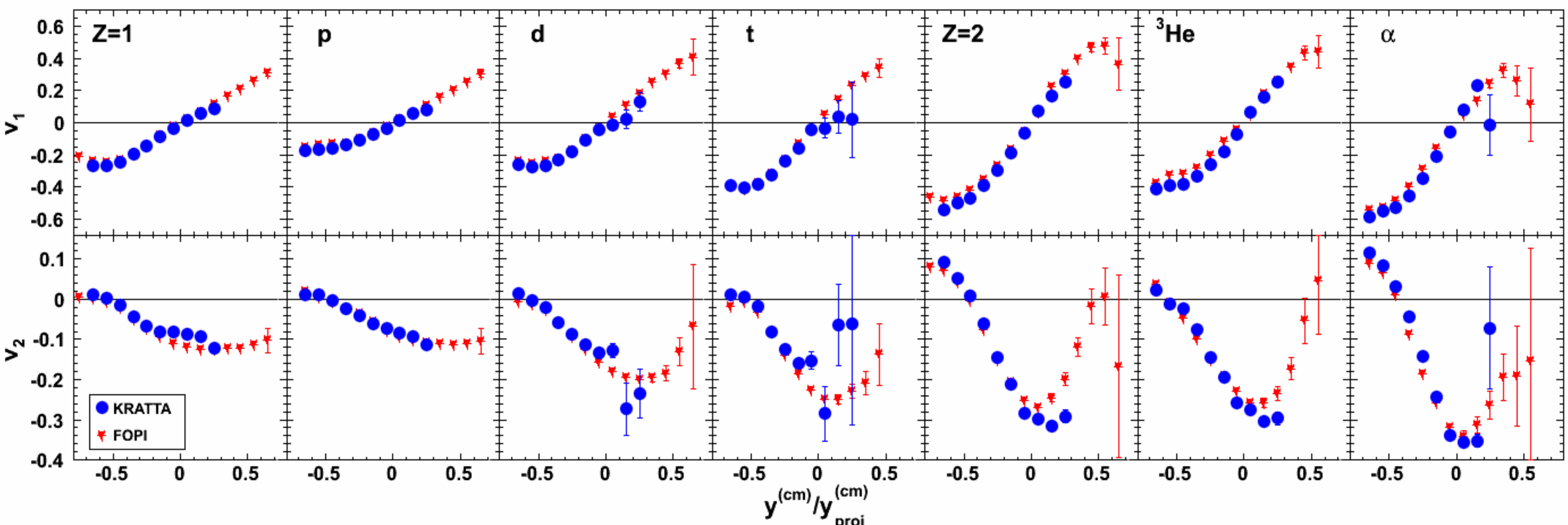

*J. Lukasik et al., NIM A 709, 120 (2013)

S. Kupny Ph. D (2014)

FUT

NeuLAND technical design

200 MeV	Generated					
Detected	%	1n	2n	3n	4n	5n
	1n	**88**	31	6	1	0
	2n	2	**62**	37	10	2
	3n	0	5	**49**	38	14
	4n	0	0	8	**48**	54
	5n	0	0	0	3	**26**

1000 MeV	Generated					
Detected	%	1n	2n	3n	4n	5n
	1n	**89**	12	1	0	0
	2n	7	**78**	23	3	0
	3n	0	8	**63**	26	5
	4n	0	0	12	**63**	40
	5n	0	0	0	7	**46**

The construction of the full detector will take about 3.5 years, and will be done in 3 steps. In the first step (November 2012), we will use a small assembly of 150 bars to determine time and position resolution with neutrons and validate simulation results. The neutrons of energies between 250 and 1500 MeV will be produced by proton knock-out reactions using a deuteron beam. In the second step, a 20% of detector will be available for physics experiments in the end of 2014 in Cave C at GSI, which will already profit from an improved resolution for neutron detection. The fully-equiped NeuLAND detector will be commissioned and available for the first experiments at Cave C in 2016. In 2017, the detector will move to its final

Califa
CALorimeter for the In Flight detection of γ rays and light charged pArticles

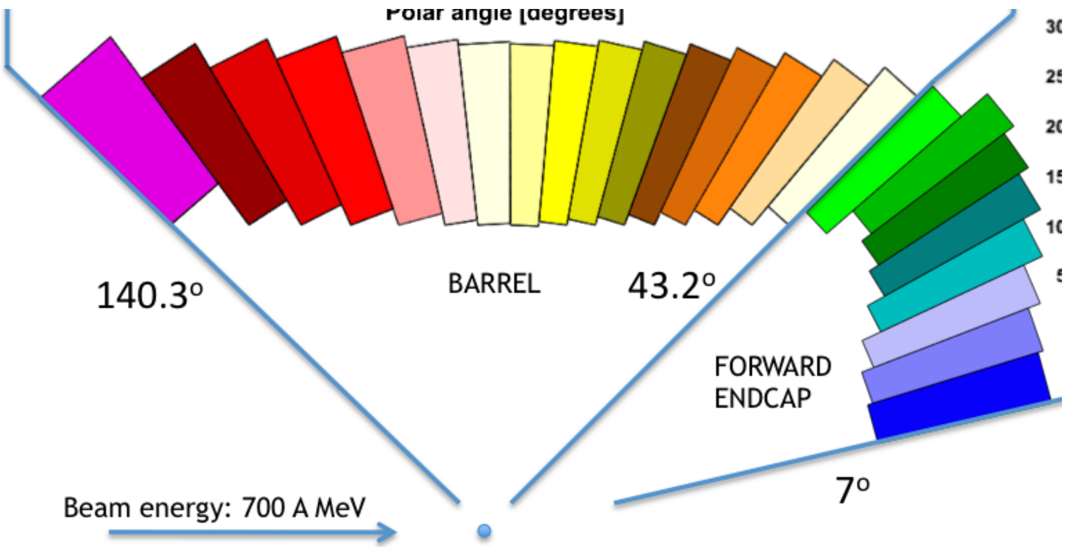

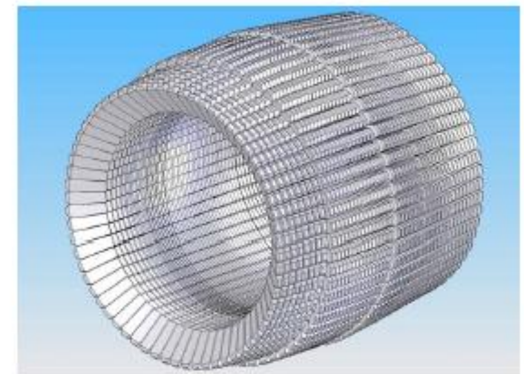

Fig. 2. Artistic view of the CALIFA calorimeter. The inner radius of the barrel is approximately 30 cm long.

CsI(Tl) read by APD with digital read-out

type	polar angle coverage °	azim. base mm	polar base mm	polar o. angle °	azim. o. angle °	height mm	weight kg	number of rings	number of pieces
I	43.2 - 55.5	29.36	15.32	92.20	94.02	220.0	0.73	3	384
II	55.5 - 70.4	29.39	15.34	92.27	94.90	180.0	0.58	3	384
III	70.4 - 87.6	29.25	15.35	92.39	95.48	170.0	0.55	3	384
IV	87.6 - 101.2	29.37	17.85	92.92	95.50	160.0	0.60	2	256
V	101.2 - 132.6	29.37	24.80	92.74	94.54	140.0	0.63	4	512
VI	132.6 - 140.35	67.77	69.69	95.00	94.54 - 93.90	120.0	3.14	1	32

Which densities are we exploring?

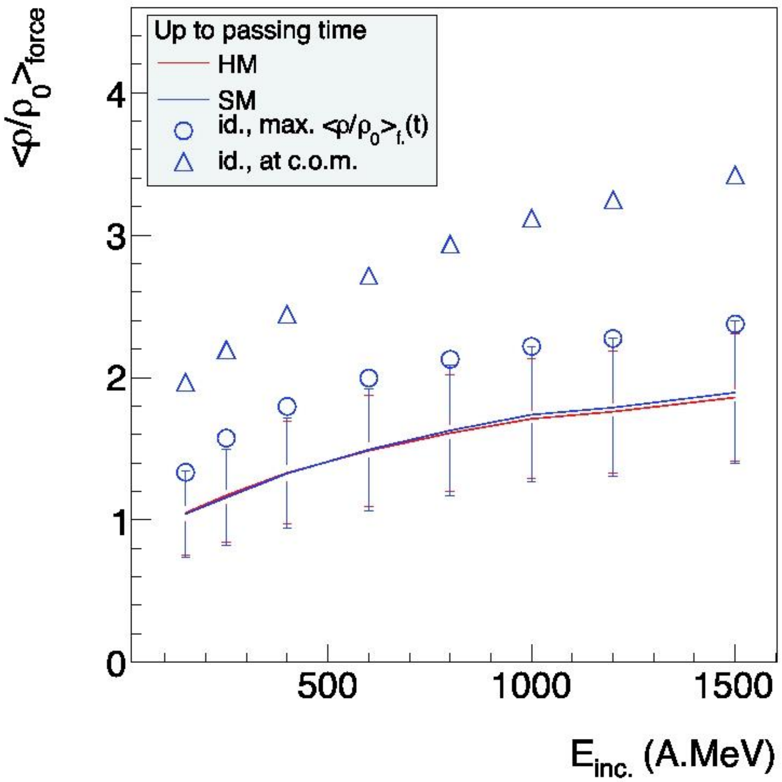

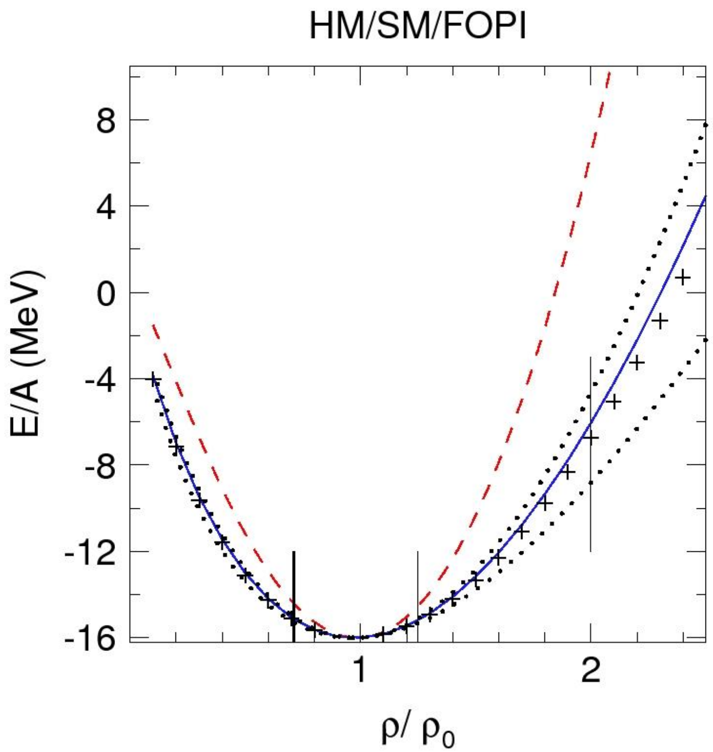

Mean value of the reduced density, computed up to the passing time, weighted by the force of the mean field seen by the participant protons, as a function of the incident energy as predicted by IQMD in Au+Au collisions at b=3 fm, for various EOS's. The error bars are the standard deviations. The blue symbols refer to the SM EOS: the circles depict the instantaneous maximum value of the force-weighted density reached over all times. The triangle is the same, restricted to the central compression zone.

See Constraining the nuclear matter equation of state around twice saturation density
A. Le Fevre, Y. Leifels, W. Reisdorf, J. Aichelin, Ch. Hartnack, and N. Herrmann
GSI Annual Report 2013 submitted

FAIR rates

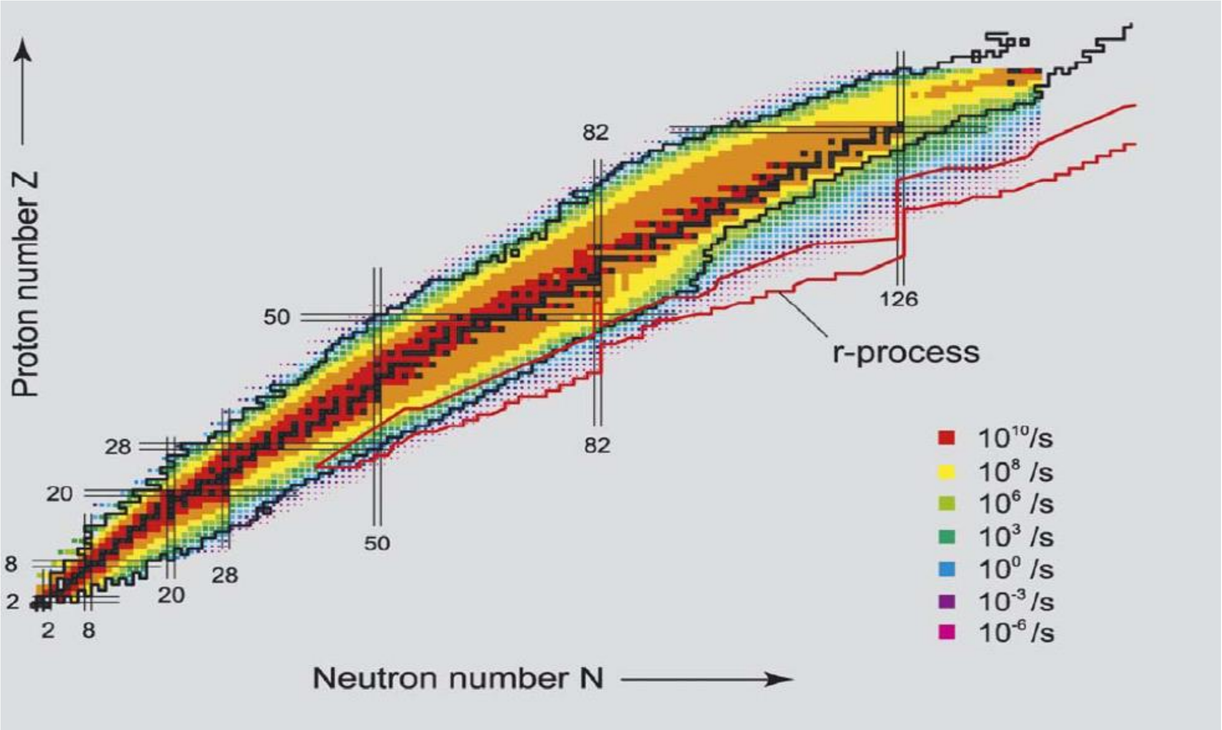

Proton number Z
Neutron number N
2
8
20
28
50
82
126
r-process
10^{10}/s
10^{8} /s
10^{6} /s
10^{3} /s
10^{0} /s
10^{-3} /s
10^{-6} /s

FAIR rates

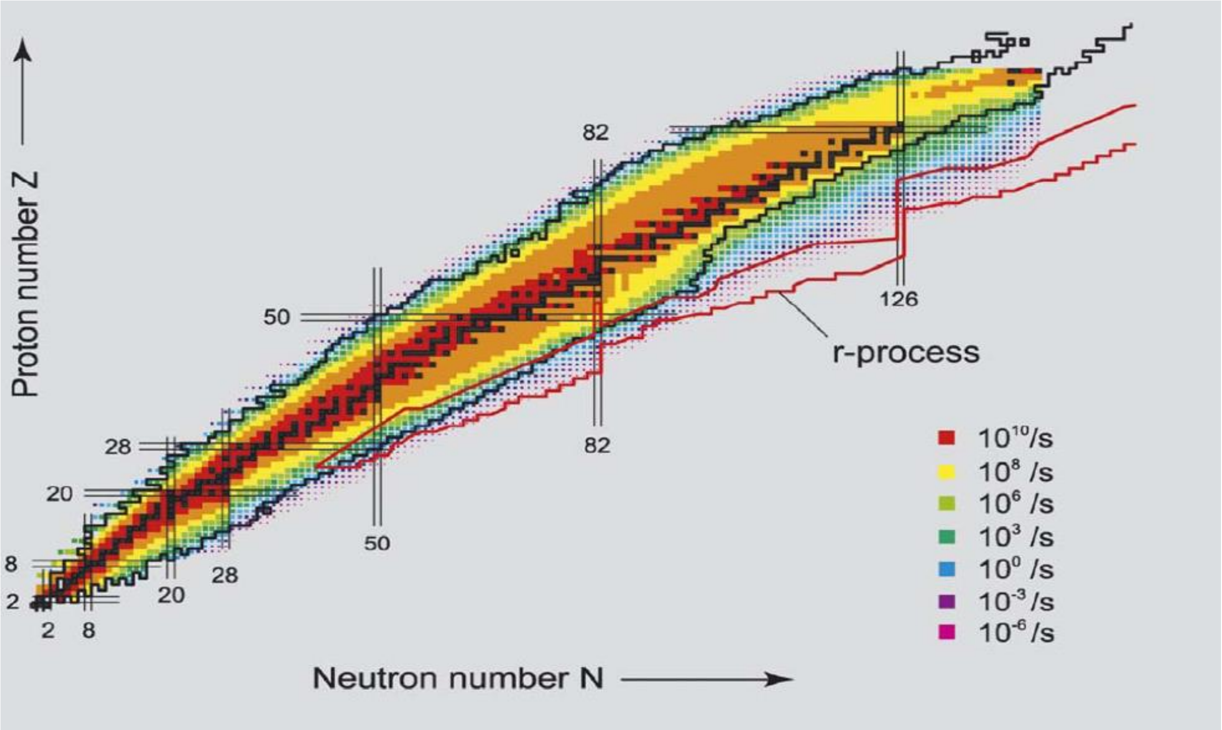

Some interesting beams (and I^2)

^{197}Au+^{197}Au @ 600,800,1000 AMeV (0.039+0.039)

^{132}Sn+^{124}Sn @ 400, 800, 1000 AMeV (0.059+0.037)

^{106}Sn+^{112}Sn @ 400, 800, 1000 AMeV (0.003+0.011)

Why ^{132}Sn?

B.-A. Li et al. / Physics Reports 464 (2008) 113–281

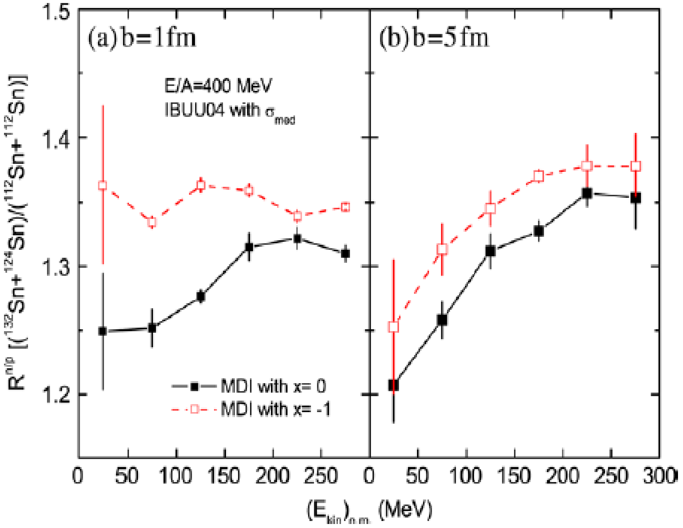

atio of free nucleons taken from the reactions of ^{132}Sn + ^{124}Sn and ^{112}Sn +
m (right panel). Taken from Ref. [67].

B.-A. Li et al. / Physics Reports 464 (2008) 113–281

Why ^{132}Sn?

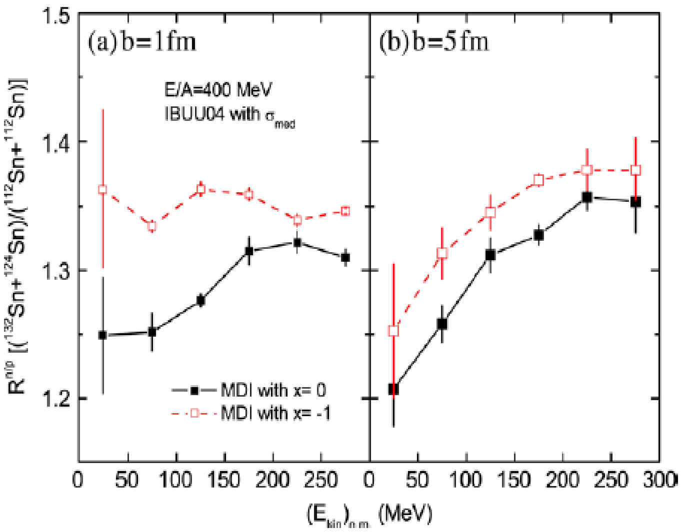

atio of free nucleons taken from the reactions of ^{132}Sn + ^{124}Sn and ^{112}Sn + ^{1}
m (right panel). Taken from Ref. [67].

B.-A. Li et al. / Physics Reports 464 (2008) 113–281

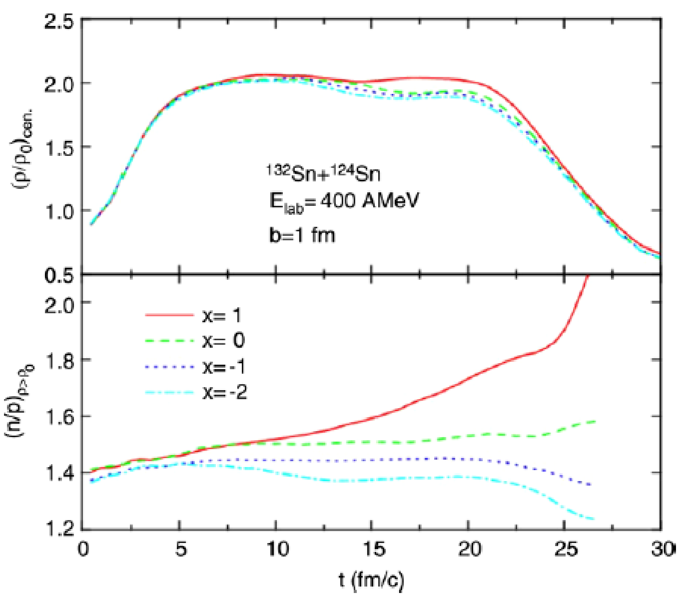

Why ^{132}Sn?

B.-A. Li et al. / Physics Reports 464 (2008) 113–281

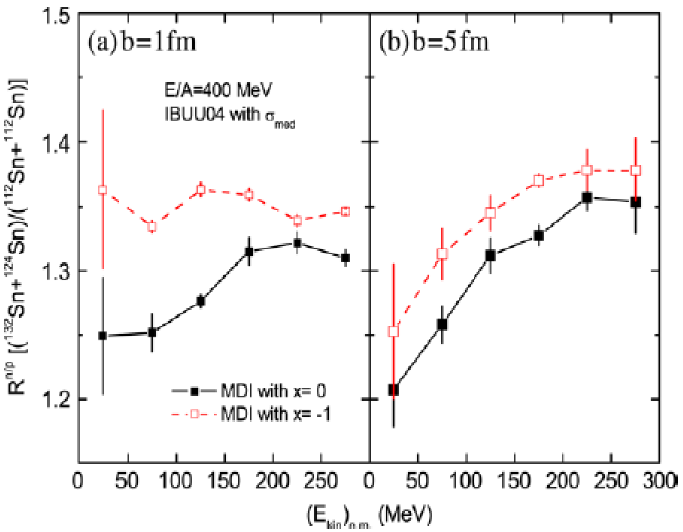

atio of free nucleons taken from the reactions of ^{132}Sn + ^{124}Sn and ^{112}Sn + ^{1}
m (right panel). Taken from Ref. [67].

B.-A. Li et al. / Physics Reports 464 (2008) 113–281

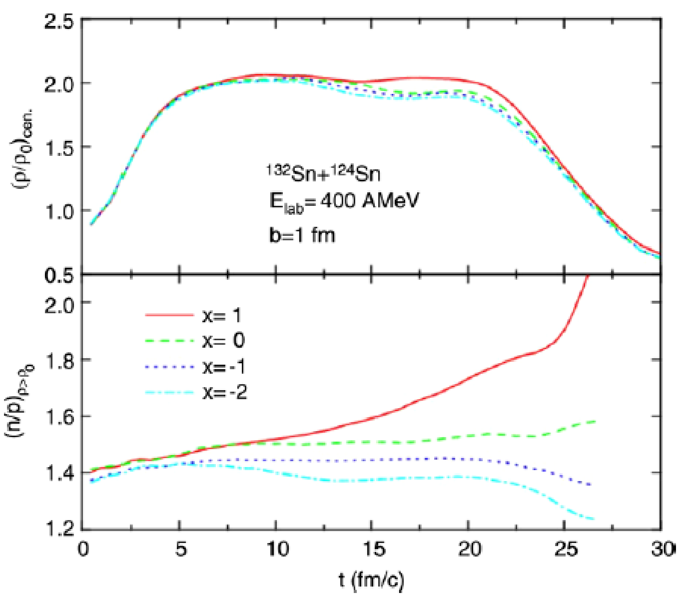

B.-A. Li et al. / Physics Reports 464 (2008) 113–281

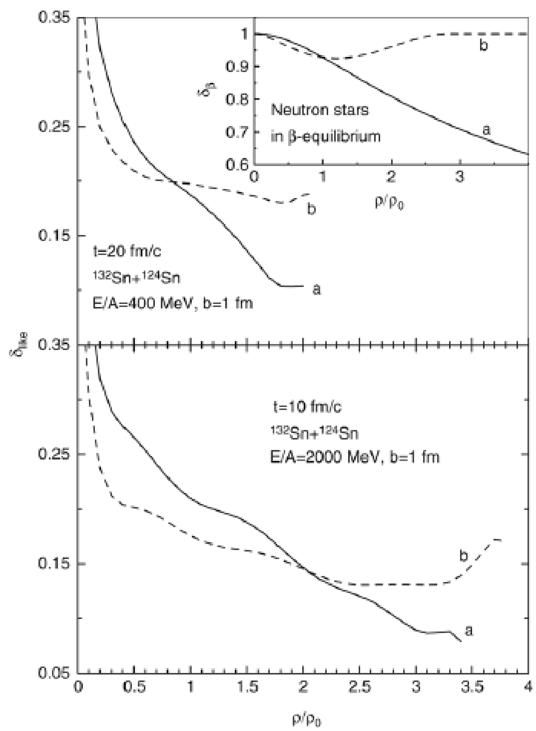

B.-A. Li et al. / Physics Reports 464 (2008) 113–281

Why ^{132}Sn?

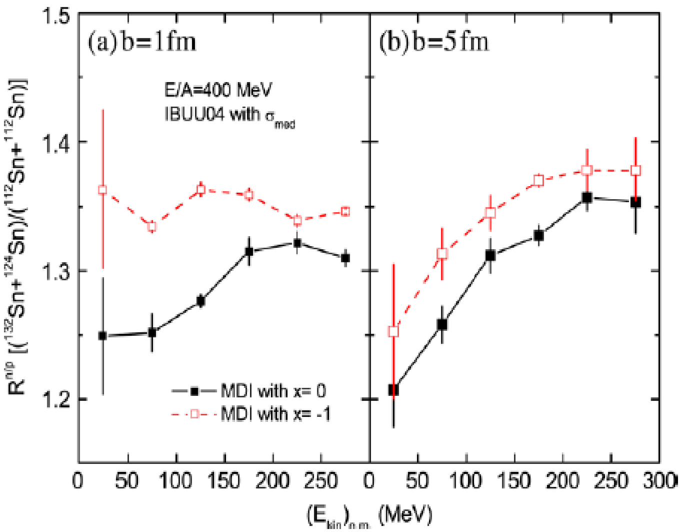

atio of free nucleons taken from the reactions of ^{132}Sn + ^{124}Sn and ^{112}Sn +
m (right panel). Taken from Ref. [67].

B.-A. Li et al. / Physics Reports 464 (2008) 113–281

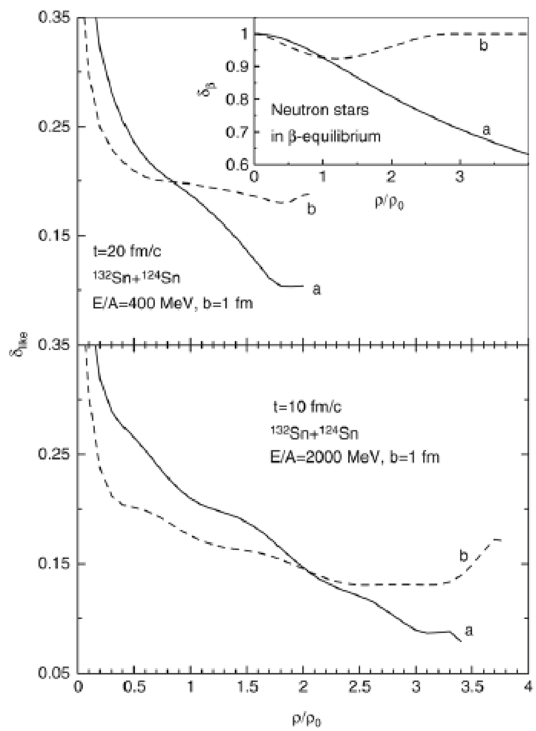

B.-A. Li et al. / Physics Reports 464 (2008) 113–281

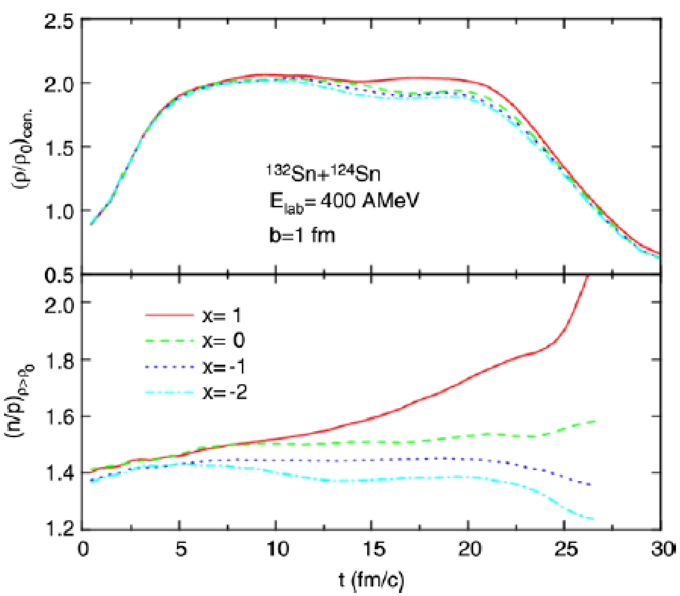

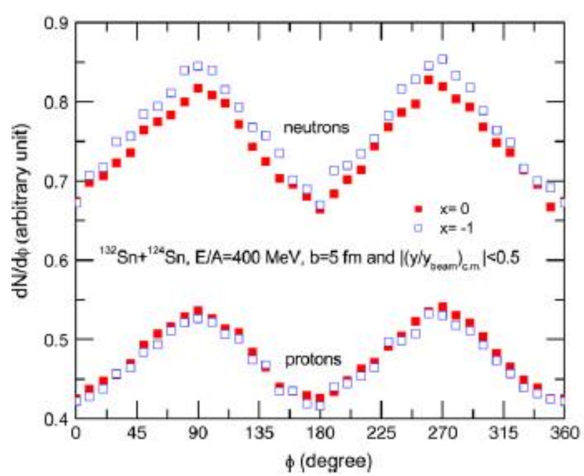

ics Reports 464 (2008) 113–281 233

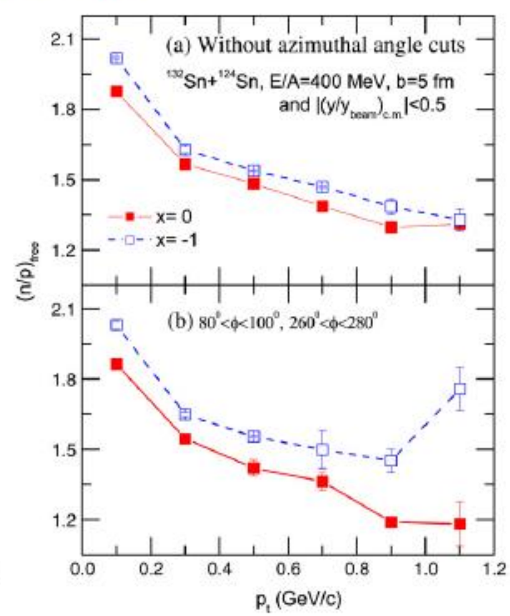

Why ^{132}Sn?

B.-A. Li et al. / Physics Reports 464 (2008) 113–281

V. Baran et al. / Physics Reports 410 (2005) 335–466

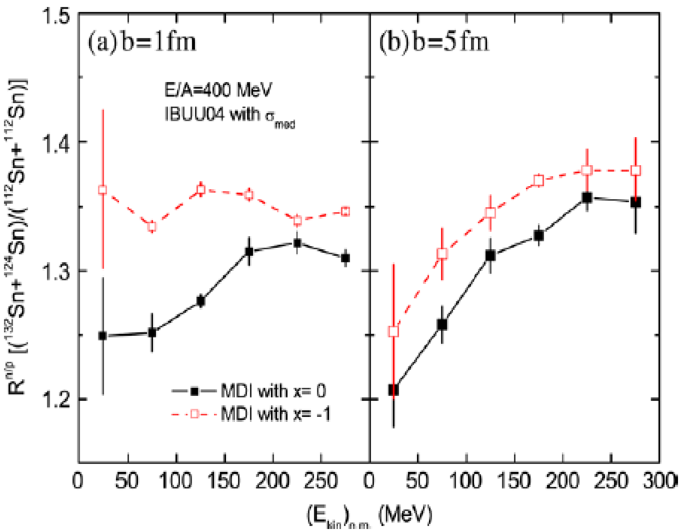

atio of free nucleons taken from the reactions of ^{132}Sn + ^{124}Sn and ^{112}Sn +
m (right panel). Taken from Ref. [67].

B.-A. Li et al. / Physics Reports 464 (2008) 113–281

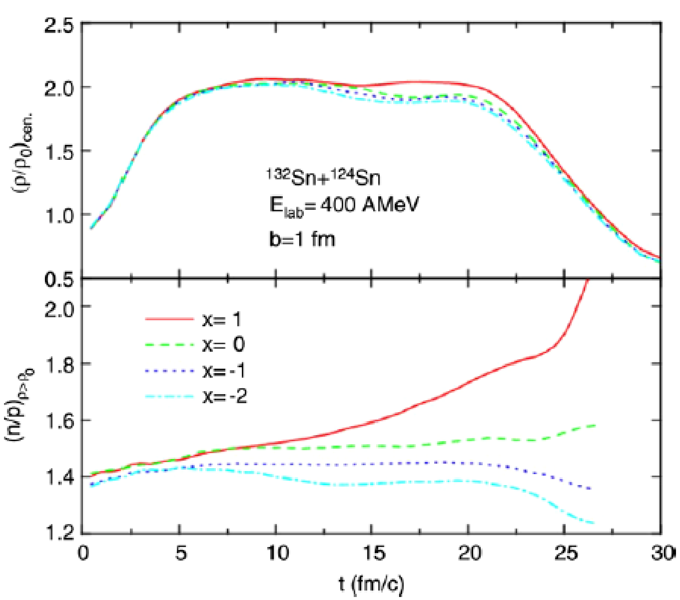

B.-A. Li et al. / Physics Reports 464 (2008) 113–281

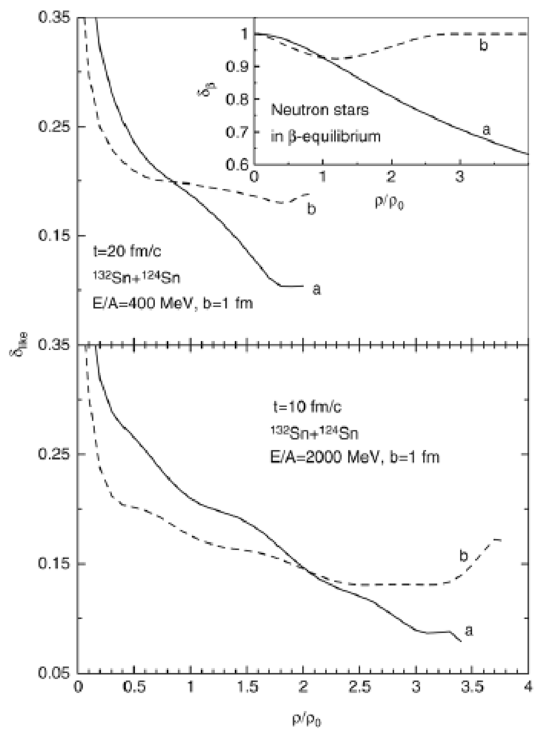

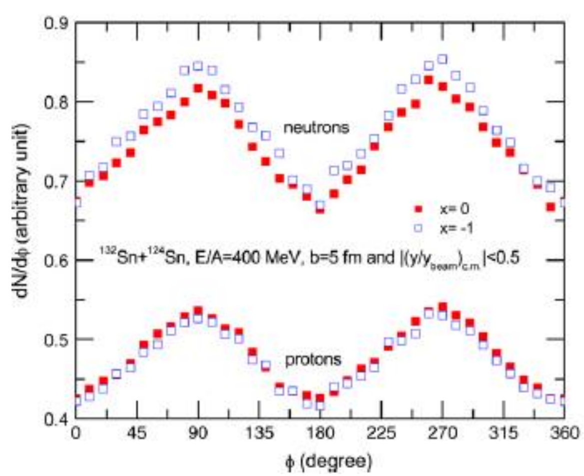

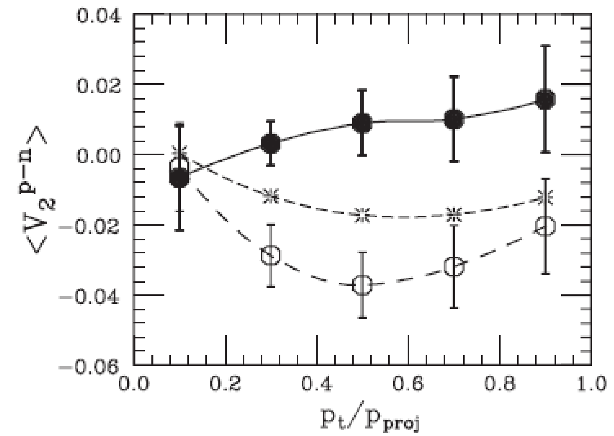

1.5 A GeV ($b = 6$ fm) from the three different models f
ll circles and solid line: $NL\rho\delta$. Open circles and dashe
ext and the previous caption.

ics Reports 464 (2008) 113–281 233

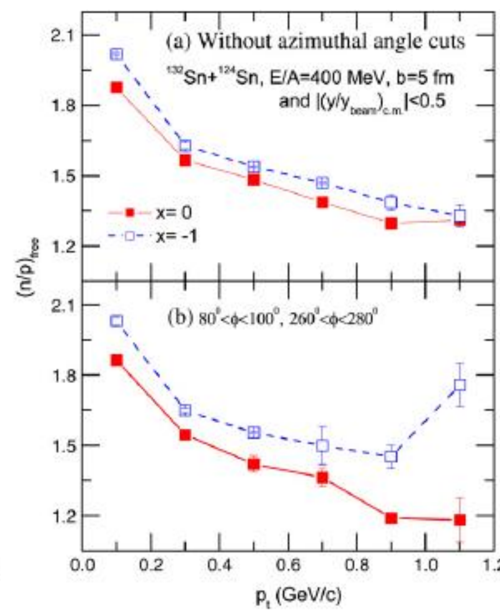

LAND

Large Area Neutron Detector :LAND (GSI)

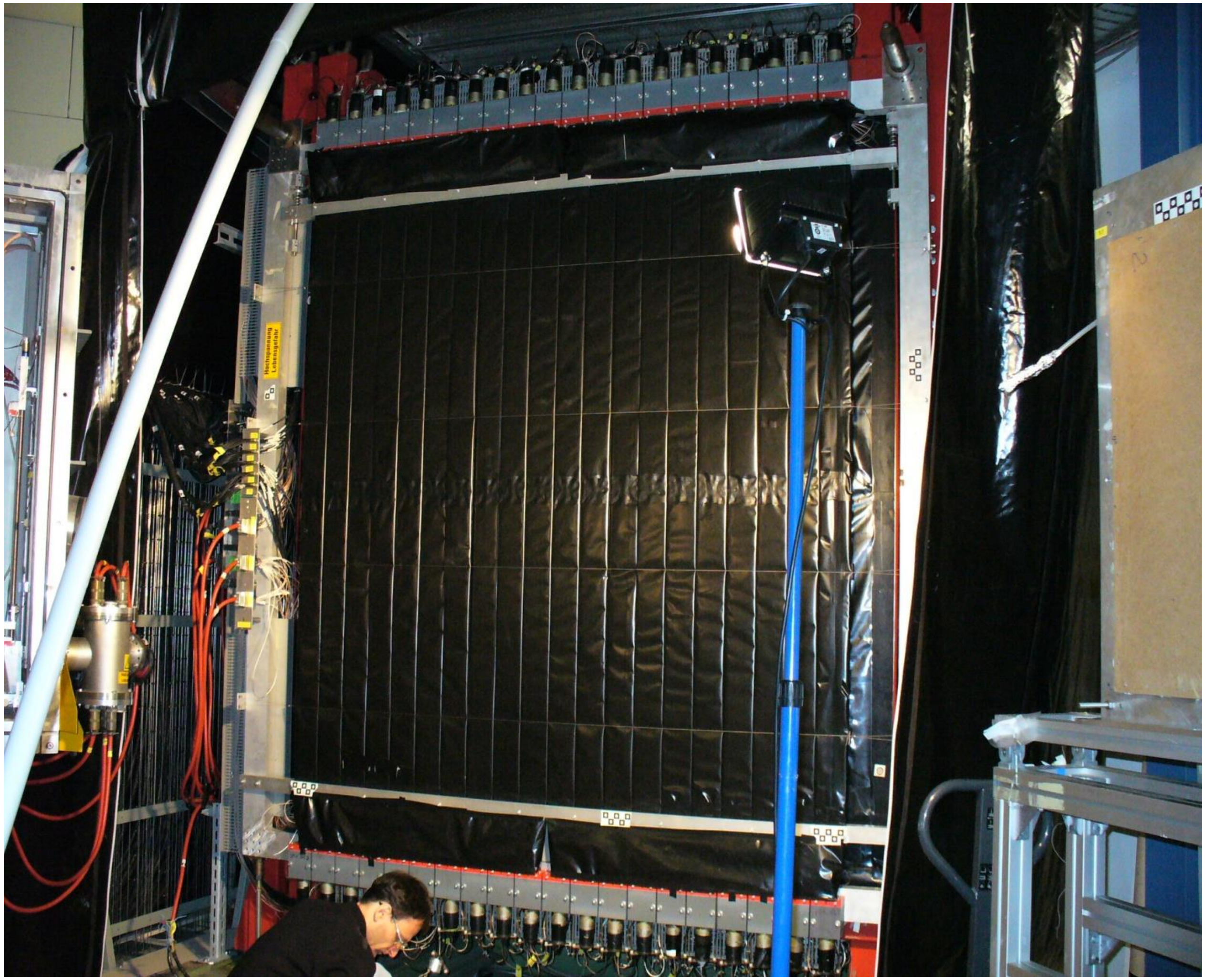

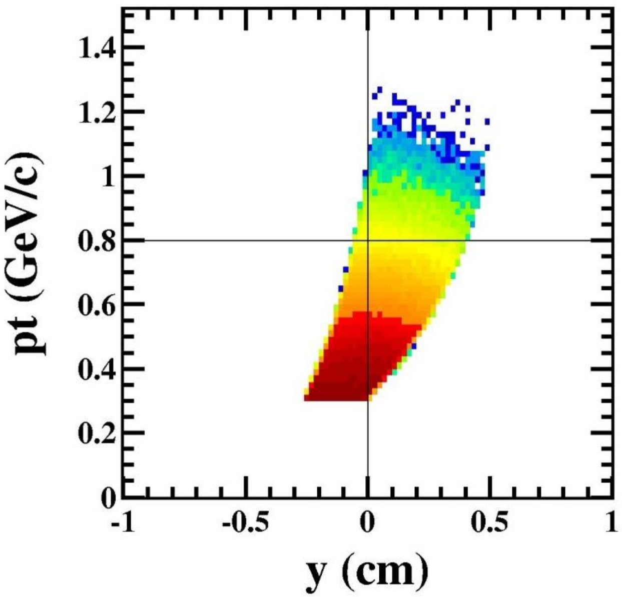

33.1<ϑ_{lab}<58 deg

Neutrons and Hydrogen detection.
Flow measurements

Th.Blaich et al.,NIM A314 (1992)

Large Area Neutron Detector :LAND (GSI)

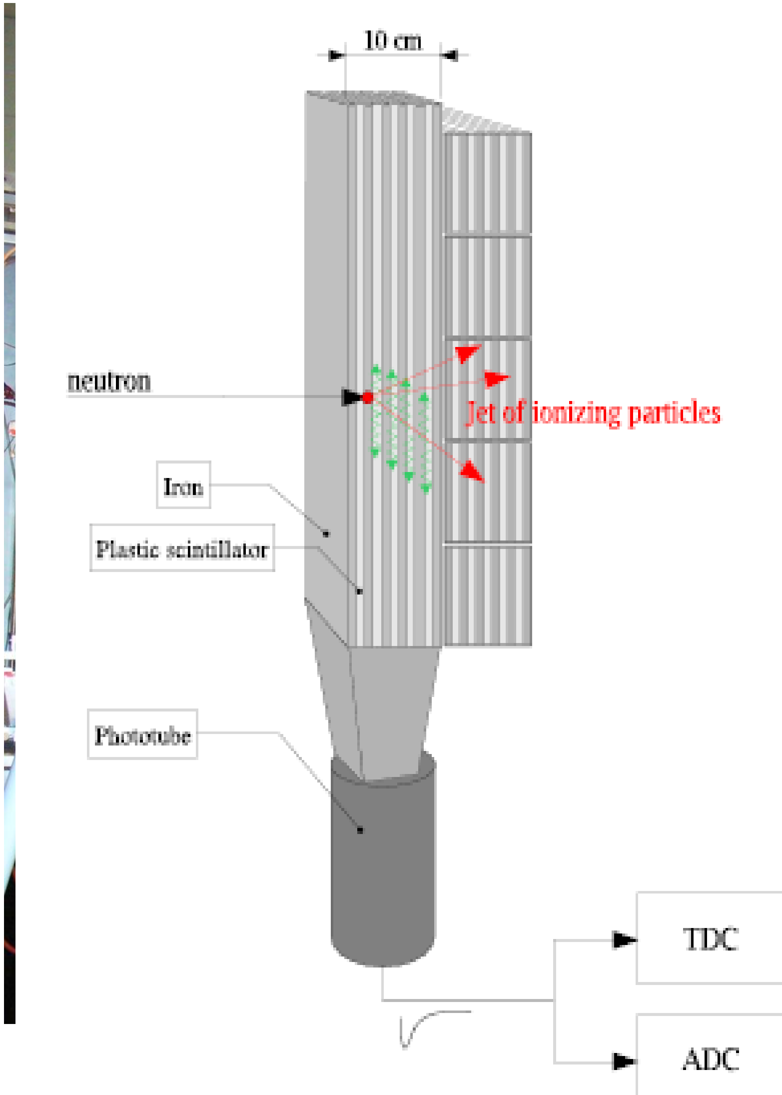

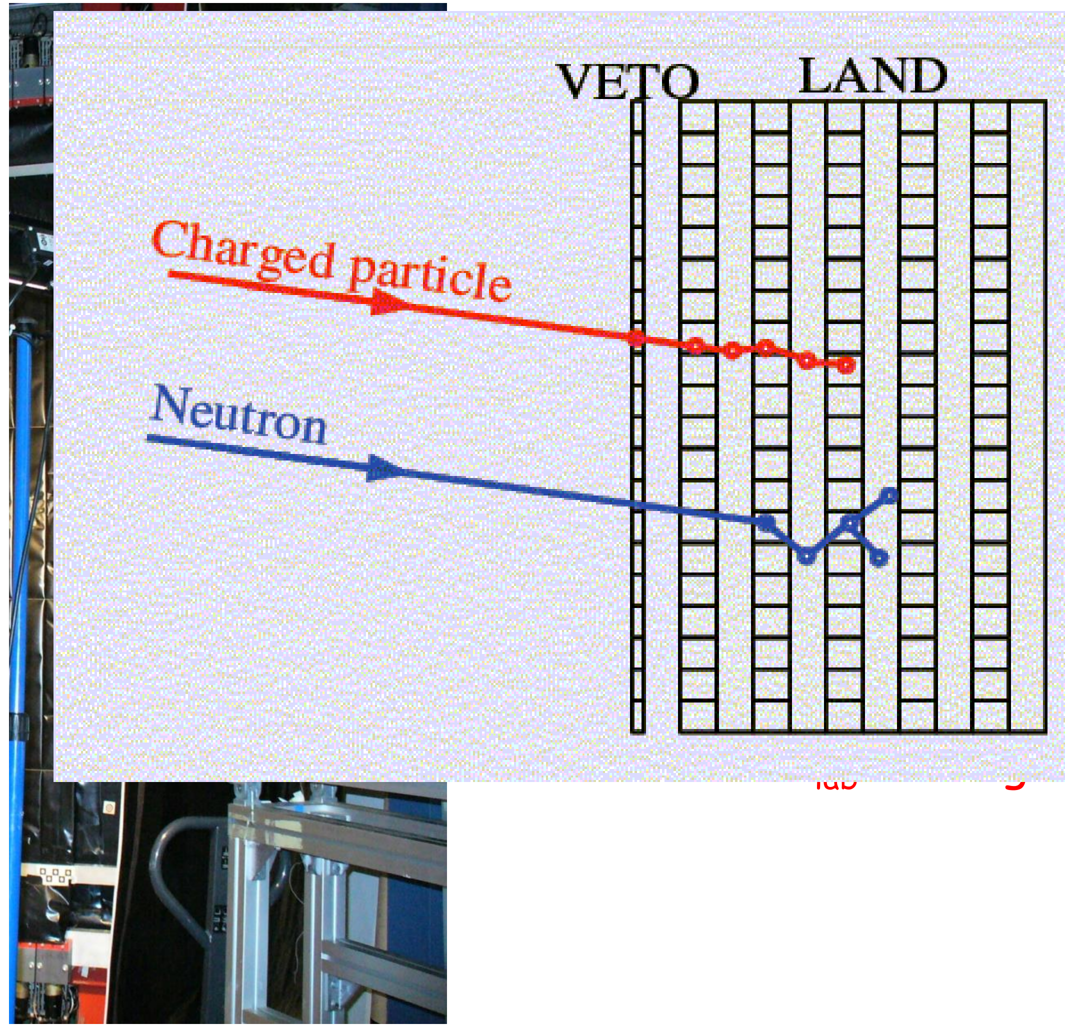

Neutrons and Hydrogen detection.
Flow measurements

Th.Blaich et al.,NIM A314 (1992)

Large Area Neutron Detector (LAND)

The Large Array Neutron Detector (LAND) is a device providing a valuable information on neutron multiplicities produced in relativistic nuclear reactions. It consists of **10 planes**, each plane containing **20 detectors**, called "paddles". Each paddle is made of 0.5 cm thick plastic scintillator layers separated by 0.5 cm thick iron layers. From each side of a paddle the ends of the plastic layers are joined to one common photo-multiplier. Each paddle is 10 cm large. The paddles are oriented either vertically or horizontally.

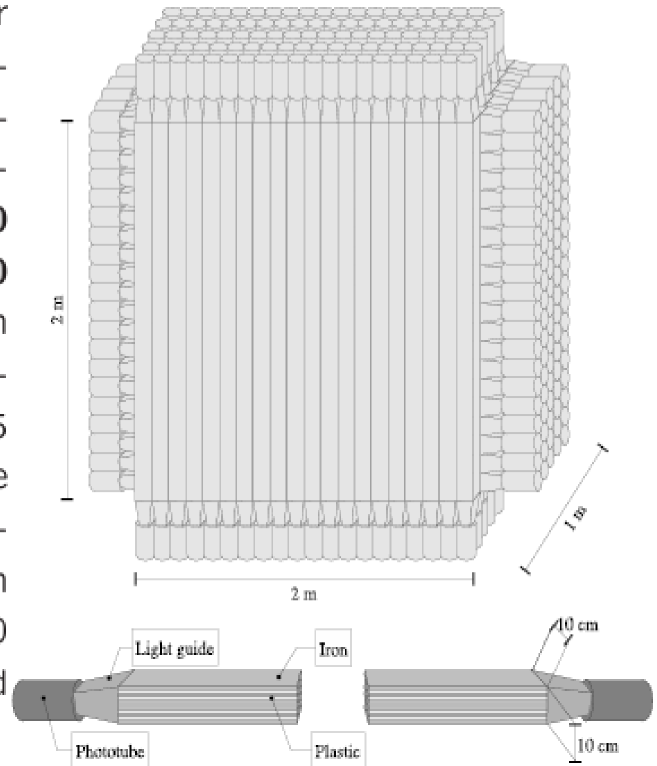

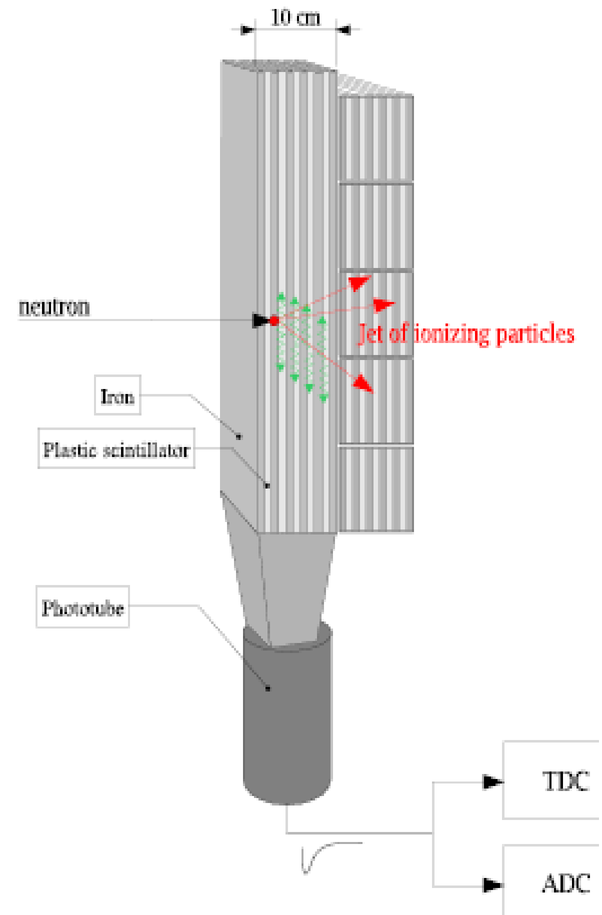

Th.Blaich et al.,NIM A314 (1992)

Adapted from P.Pawloski,IWM2007

Neutrons efficiency>80% (for E>400MeV)
No ^{1,2,3}H isotopic discriminations

Large Area Neutron Detector (LAND)

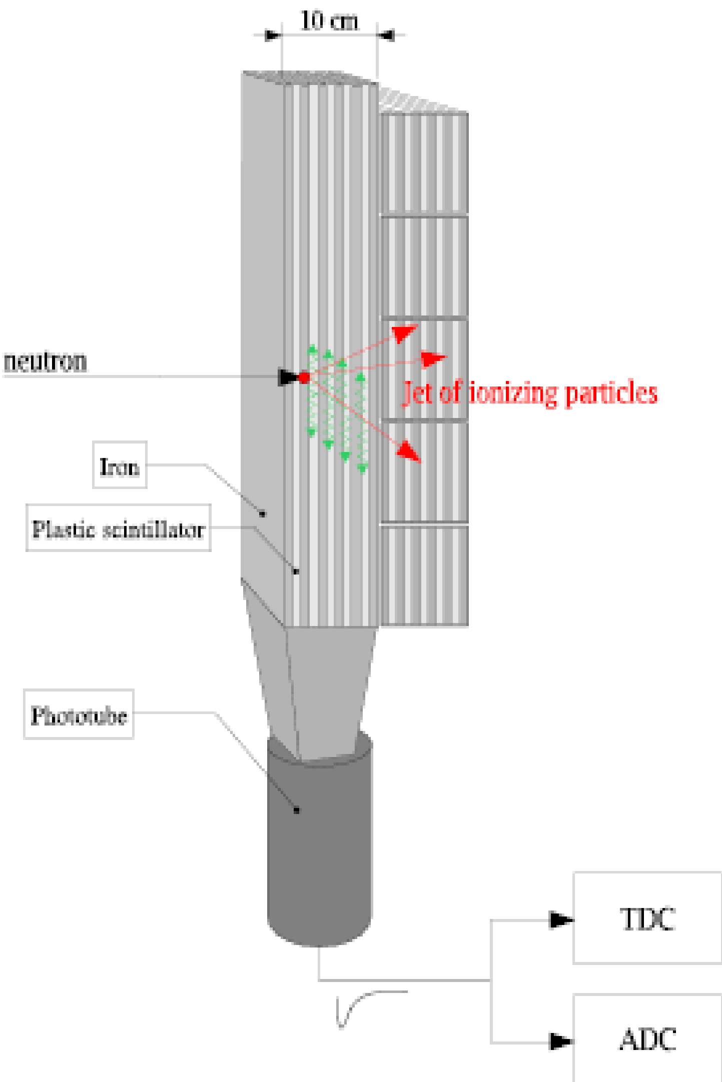

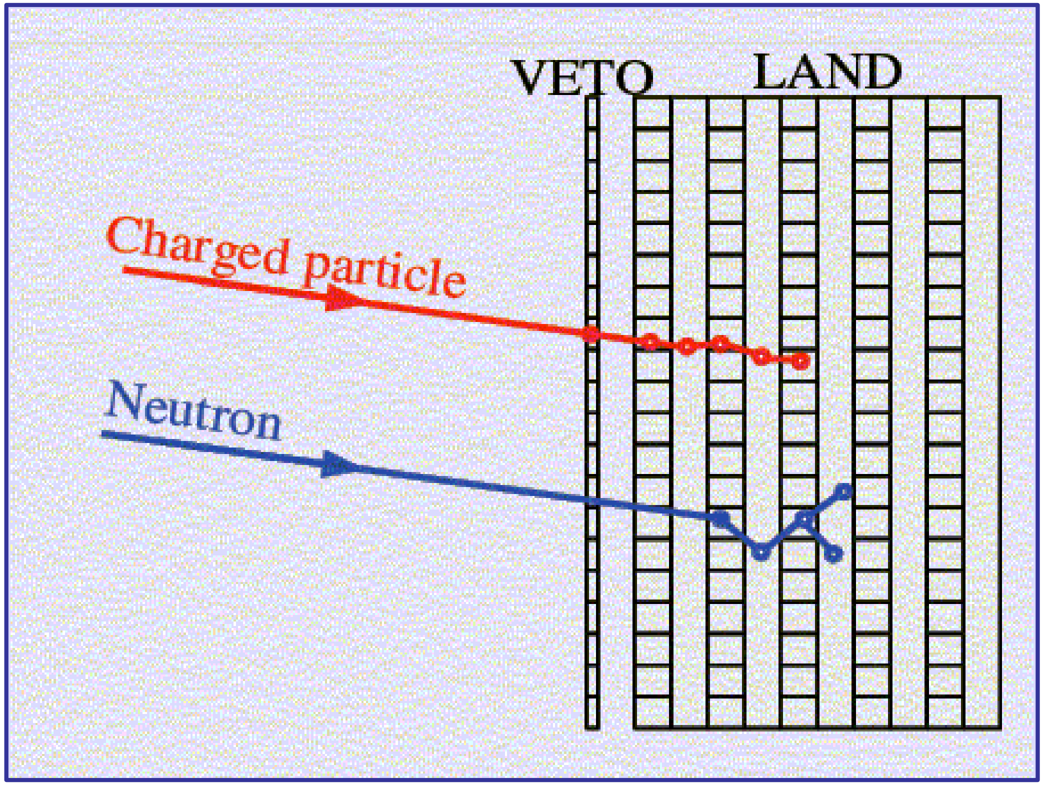

neutron <u>and</u> proton detection

Th.Blaich et al.,NIM A314 136-154 (1992)
P. Pawloski et al., "Study of neutron emission using Land detector", Procs of IWM2007

Large Area Neutron Detector (LAND)

A recursive procedure starts from a hit registered in the VETO wall and searches for a correlated hit in the first LAND plane. Then, for this hit, another correlated hit is searched in the 2 plane. The procedure is repeated until no more correlation can be found. The correlated hits are marked as "secondary" hits and are removed from total pool of the hits. The first hit ("primary" or "seed") determines the properties of a particle: its time and position give its velocity vector.

Next, one searches for the chains starting from one of hits registered in the first LAND plane (among that not correlated with the VETO hits), then from the second one, and so on. All these hits are considered to be generated by neutron.

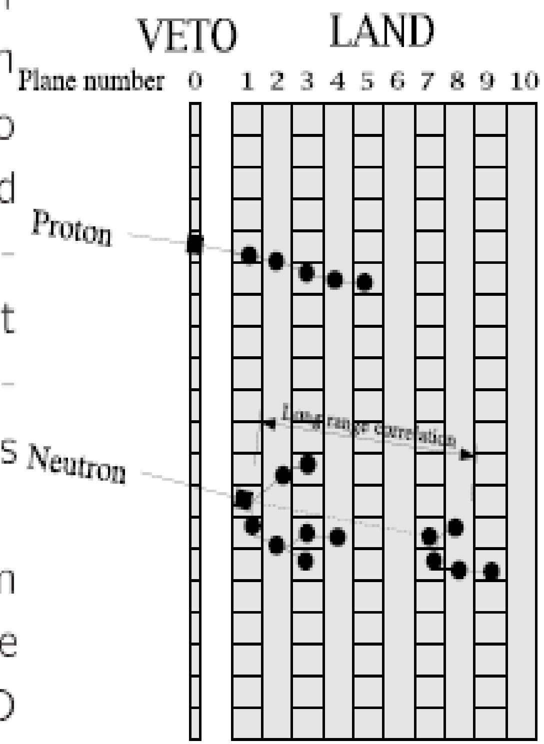

Adapted from P.Pawloski,IWM2007

Large Area Neutron Detector (LAND)

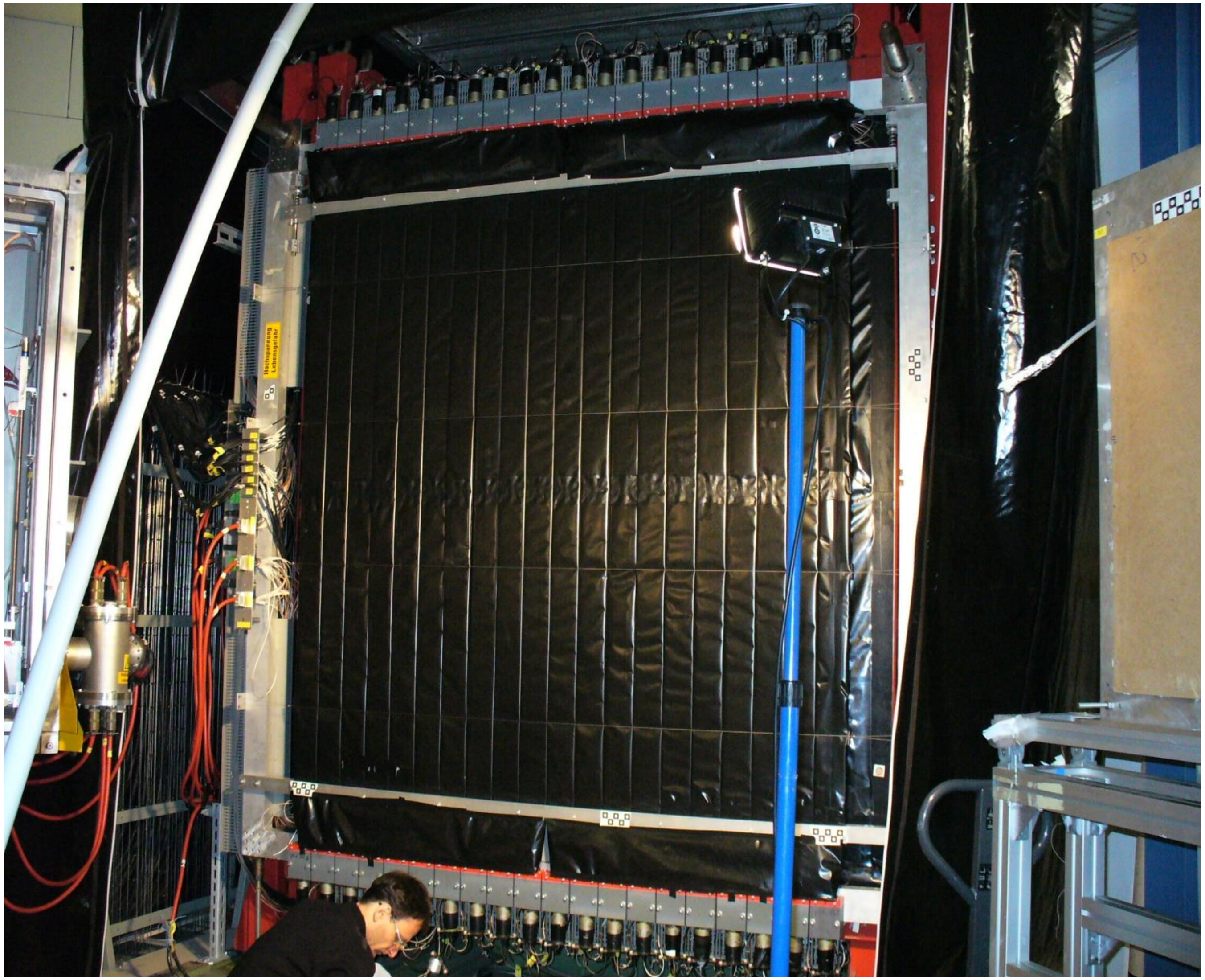

Neutrons and Hydrogen detection.
Flow measurements

Th.Blaich et al.,NIM A314 (1992)

Large Area Neutron Detector (LAND)

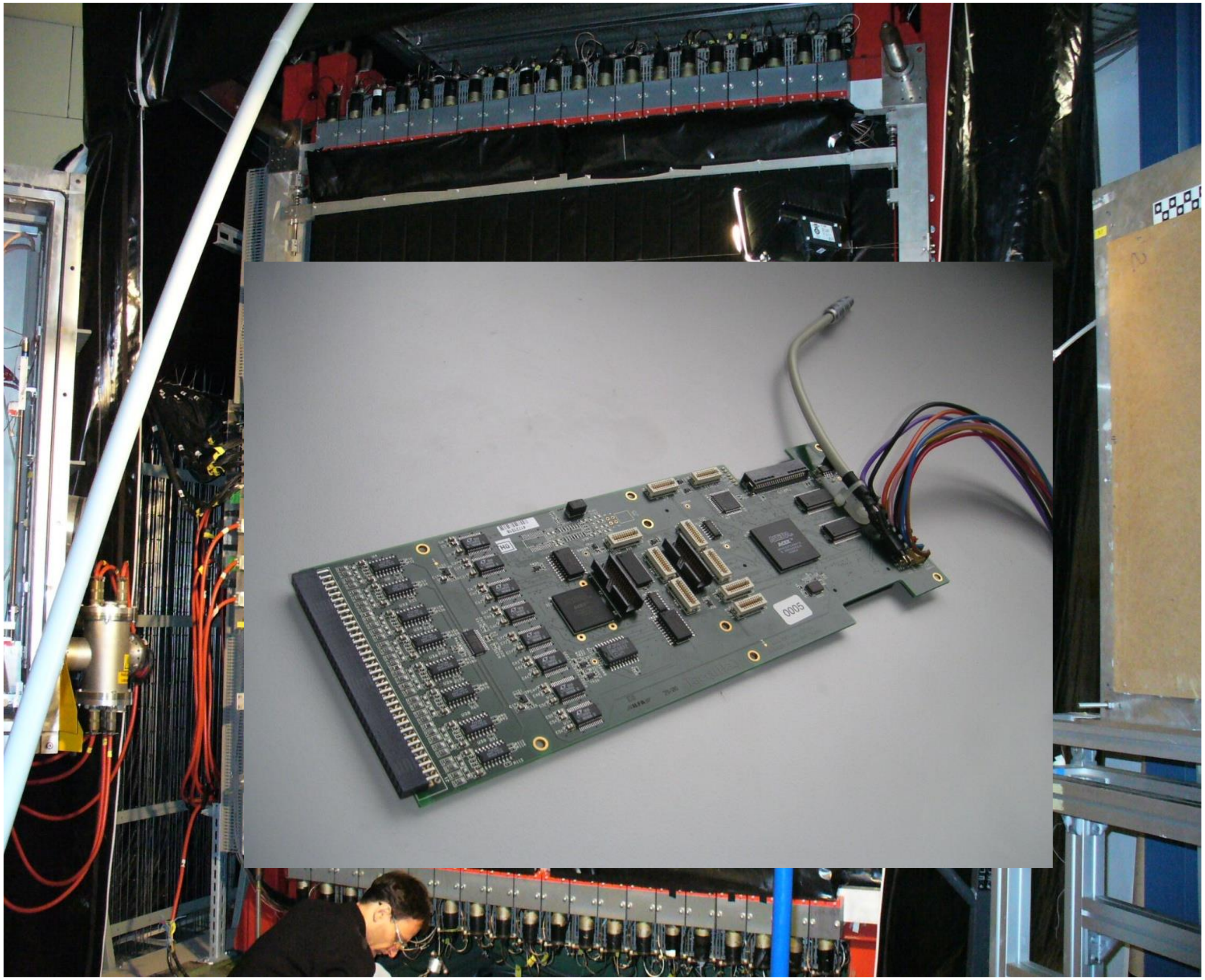

new TACQUILA electronic

A compact electronics for time measurements with very high resolution ~ 10ps RMS. Developed for the FoPi TOF-upgrade. The PCB consists of 16 channels based on the TAC GSI-ASIC. Optional with amplitude measurement card (QDC).

Neutrons and Hydrogen detection.
Flow measurements

Th.Blaich et al.,NIM A314 (1992)

RISERVE

PREV EXP

Main motivation: symmetry energy at supra-saturation densities

UrQMD simulations

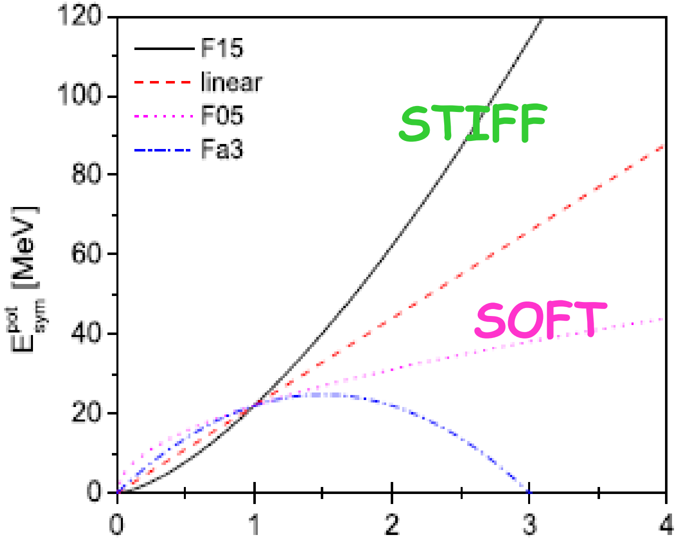

$$u = \rho/\rho_0$$

$$E_{sym} = E_{sym}^{pot} + E_{sym}^{kin}$$
$$= 22\,\text{MeV} \cdot (\rho/\rho_0)^{\gamma} + 12\,\text{MeV} \cdot (\rho/\rho_0)^{2/3}$$

UrQMD vs. FOPI data: Au+Au @ 400 AMeV b< 2.5 fm

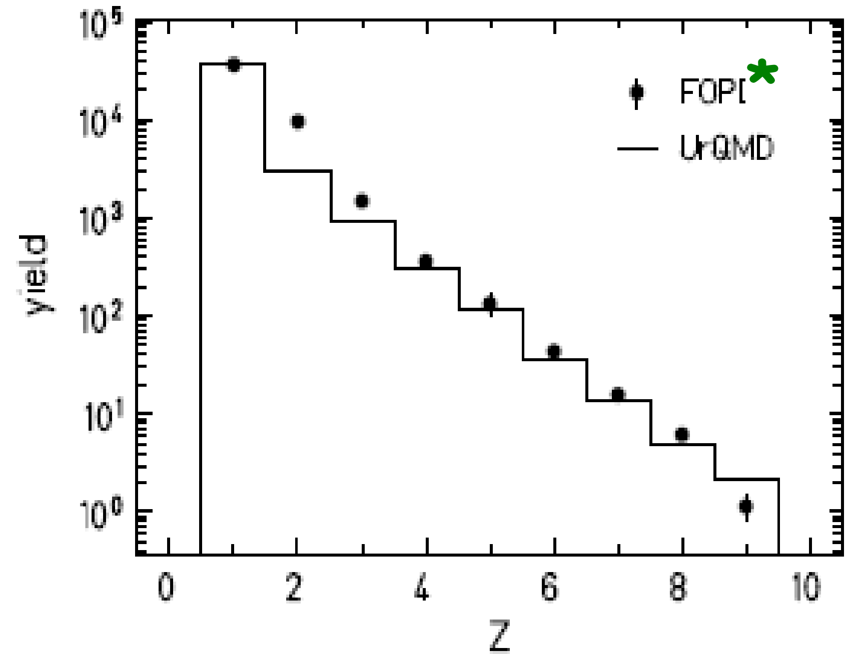

* W. Reisdorf, et al., Nucl. Phys. A 612 (1997) 493.

Coalescence condition:
Dr <3 fm and Dp< 275 MeV/c

See Qingfeng Li, J. Phys. G31 1359-1374 (2005) and references

FOPI/LAND experiment on neutron squeeze out (1991)

Au+Au 400 A MeV

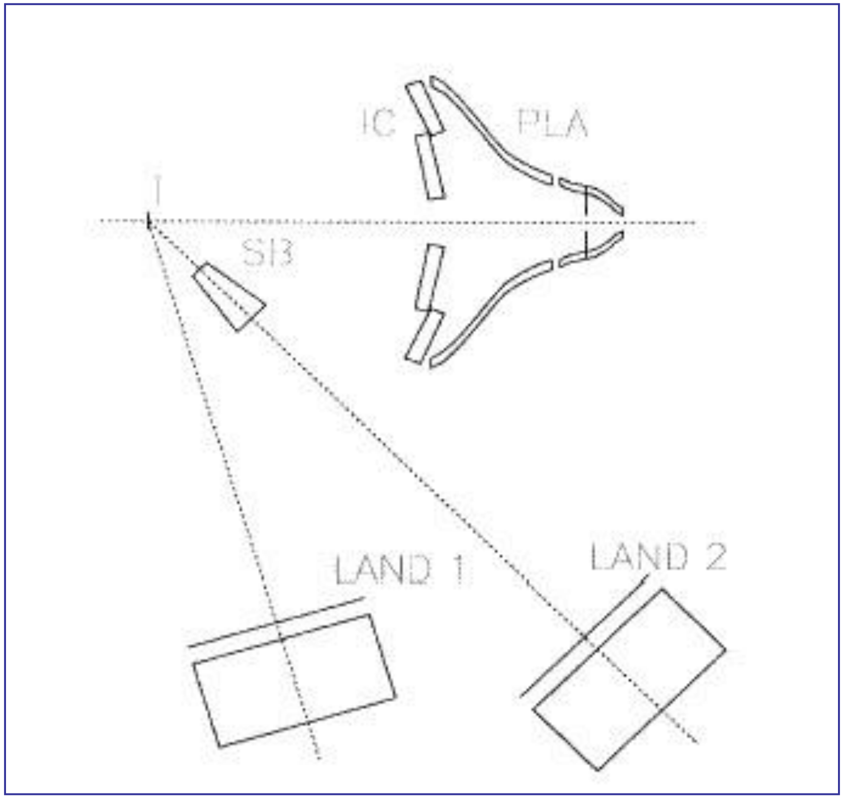

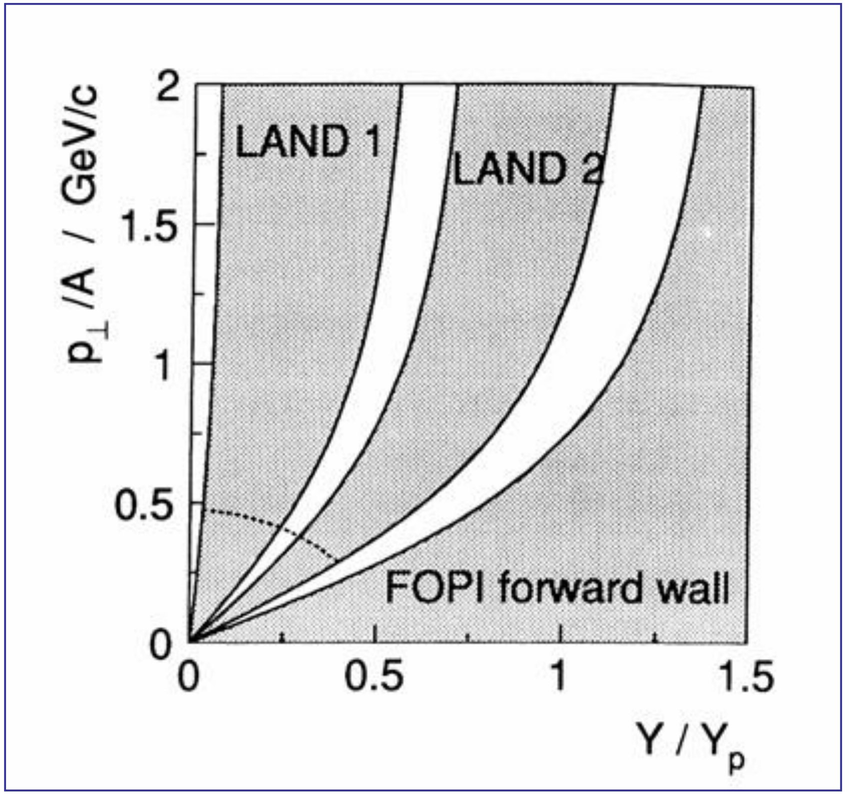

LAND coverage
$37° < \theta_{lab} < 53°$
$61° < \theta_{lab} < 85°$

Y. Leifels et al., PRL 71, 963 (1993)
P.Russotto et al., PLB 697 (2011)

FOPI/LAND experiment on neutron squeeze out (1991)

Au+Au 400 A MeV

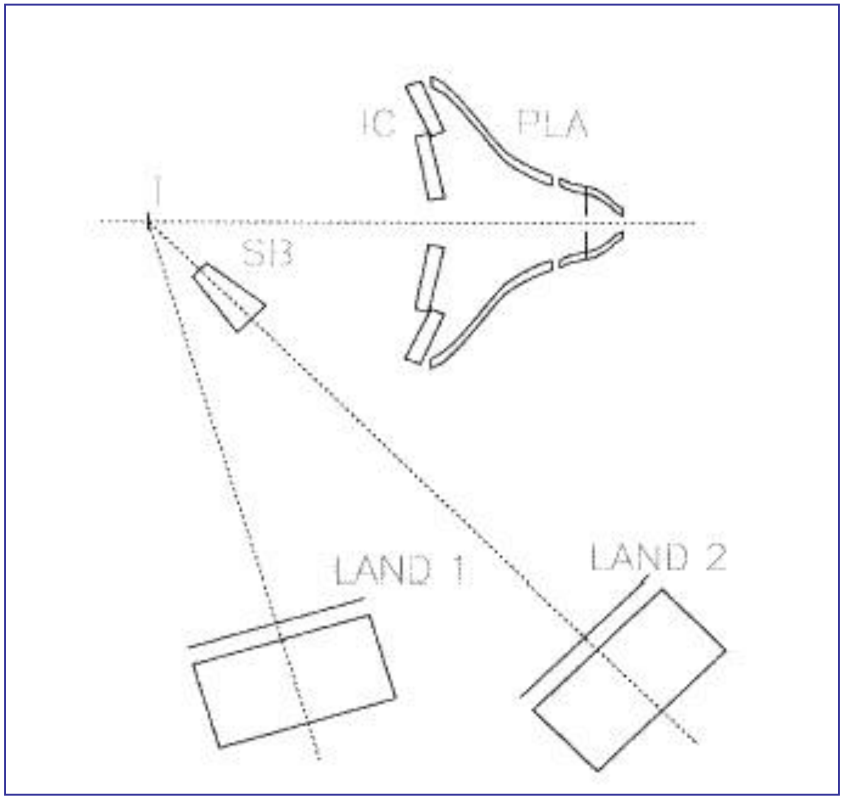

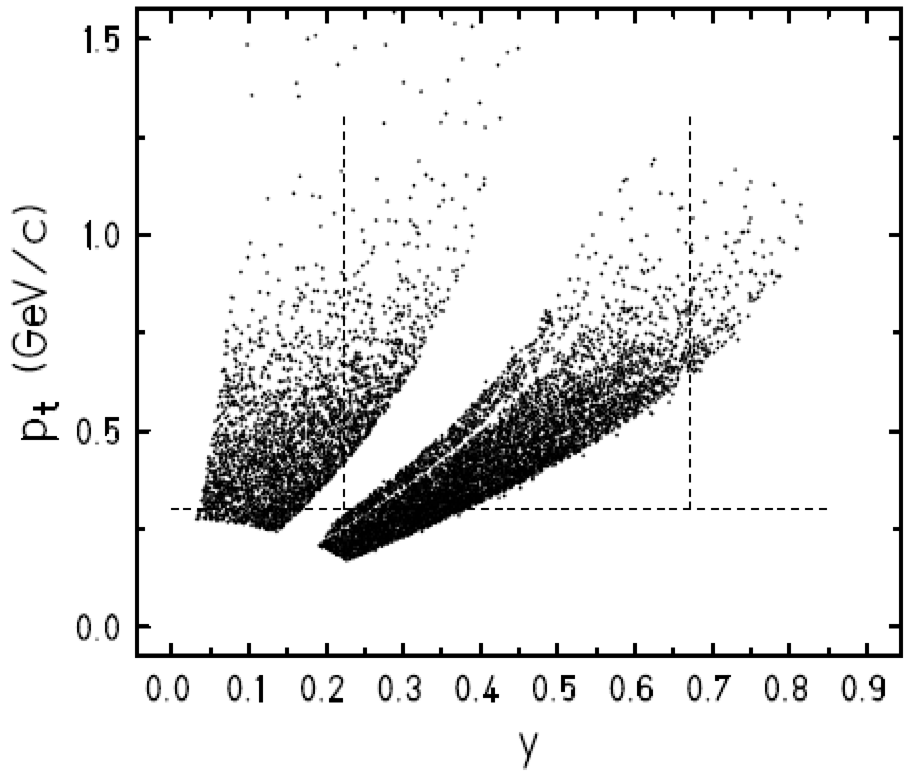

LAND coverage

$37° < \theta_{lab} < 53°$

$61° < \theta_{lab} < 85°$

Y. Leifels et al., PRL 71, 963 (1993)

P.Russotto et al., PLB 697 (2011)

High densities

n/p flow
LAND + FOPI

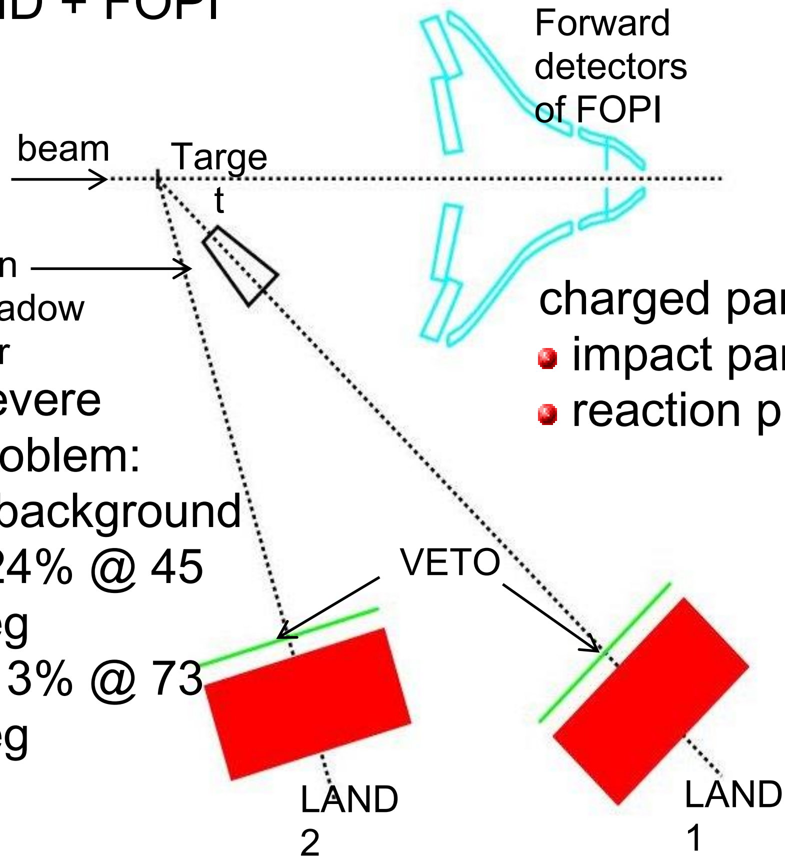

Severe Problem:
n-background
- 24% @ 45 deg
- 13% @ 73 deg

charged particle
- impact parame
- reaction plane

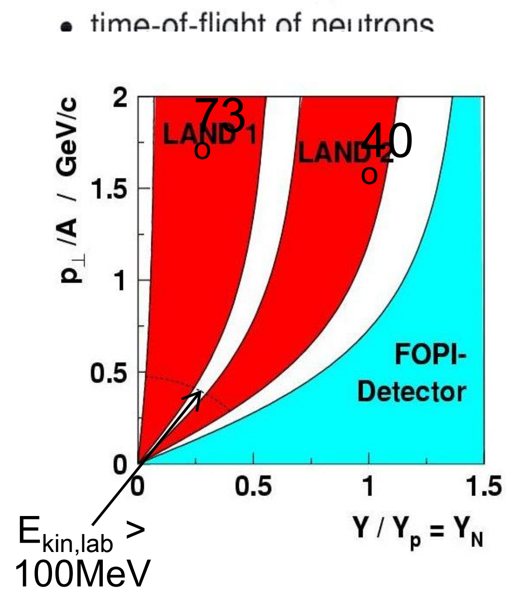

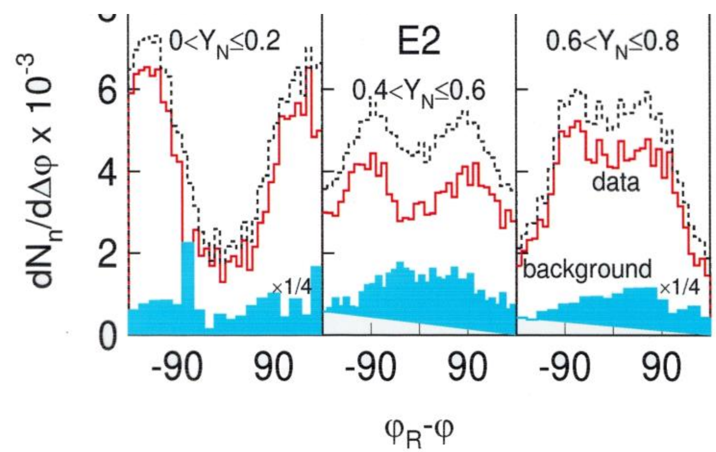

Analysys of FOPI/LAND data (1991)

Au+Au 400 A MeV
b< 7.5 fm

$$E_{sym} = E_{sym}^{pot} + E_{sym}^{kin}$$
$$= 22\mathrm{MeV}\cdot(\rho/\rho_0)^{\gamma} + 12\mathrm{MeV}\cdot(\rho/\rho_0)^{2/3}$$

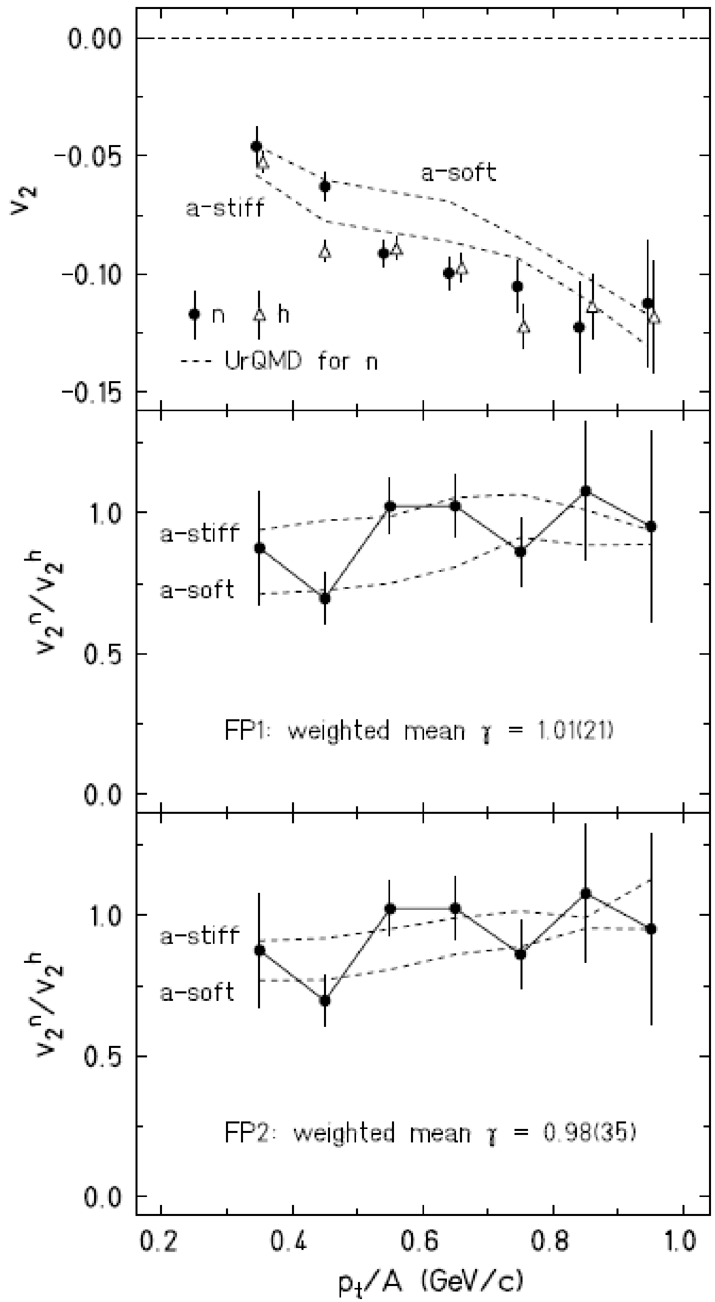

Y. Leifels et al., PRL 71, 963 (1993)
P.Russotto et al., PLB 697 (2011)

Analysys of FOPI/LAND data (1991)

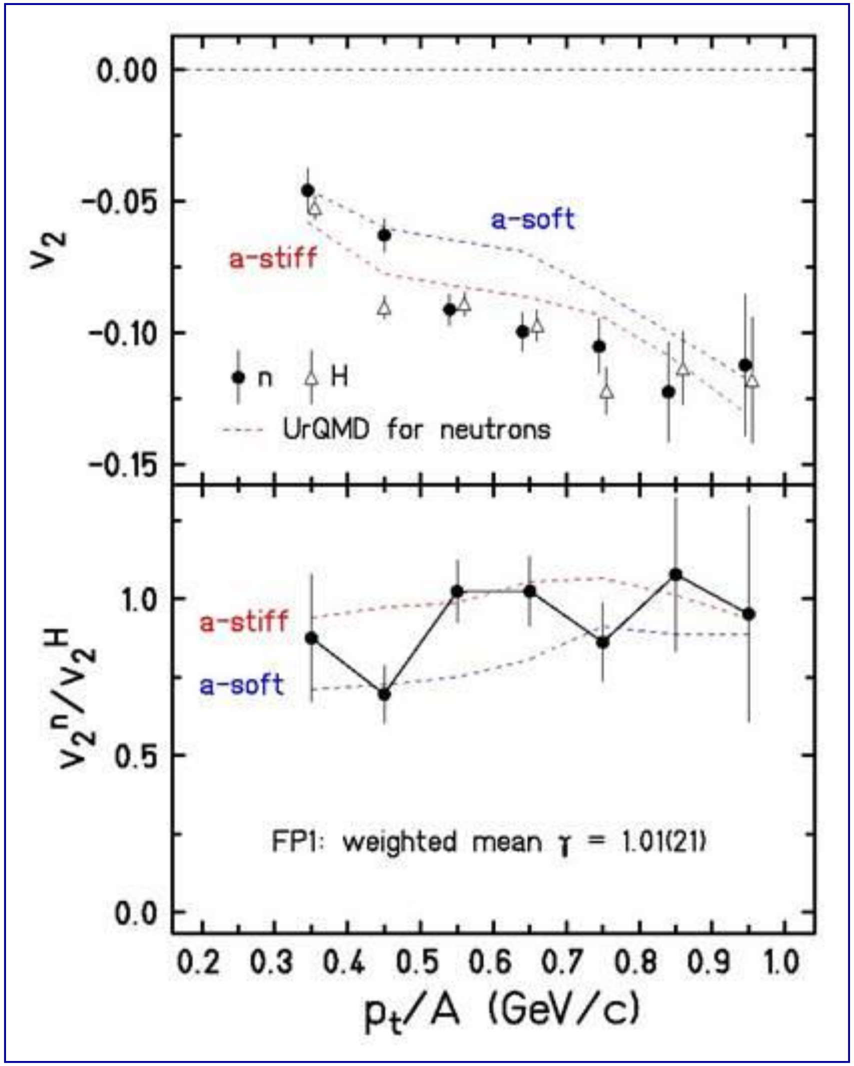

Au+Au 400 A MeV
b< 7.5 fm

$$E_{sym} = E_{sym}^{pot} + E_{sym}^{kin} = 22\,\text{MeV}\cdot(\rho/\rho_0)^{\gamma} + 12\,\text{MeV}\cdot(\rho/\rho_0)^{2/3}$$

Neutron/hydrogen
FP1: $\gamma = 1.01 \pm 0.21$
FP2: $\gamma = 0.98 \pm 0.35$
neutron/proton
FP1: $\gamma = 0.99 \pm 0.28$
FP2: $\gamma = 0.85 \pm 0.47$

adopted: $\gamma = 0.9 \pm 0.4$

Y. Leifels et al., PRL 71, 963 (1993)
P.Russotto et al., PLB 697 (2011)

test of systematic uncertainties

physical parameters:	
impact parameter	$\Delta\gamma = 0.43 \pm 0.32$ (PM3 vs. PM3-5)
transverse momentum	$\Delta\gamma < 0.1$ (p_t<0.8 vs. p_t<1.2 GeV/c)
rapidity	$\Delta\gamma < 0.15$ (for PM3-5)
	statistics not really sufficient to evaluate errors more precisely
data analysis:	
various sorting gates	$\Delta\gamma < 0.1$
include protons separately	$\Delta\gamma$ negligible (protons not sensitive)
background subtraction	$\Delta\gamma = 0.21$ (100% vs. 60% of measured background)
UrQMD:	
Pauli blocking (y/n)	$\Delta\gamma = 0.08$ (for PM3-5)
constant S_0 (=a_4)	$\Delta\gamma = 0.07$ (S_0=22 vs. S_0=18 MeV)

CUTS VARI

FOPI/LAND experiment on neutron squeeze out (1991)

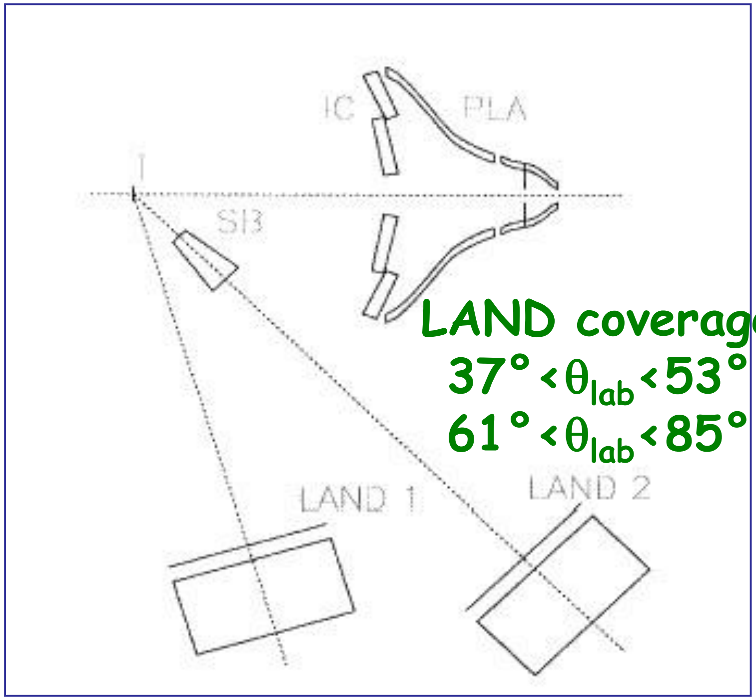

LAND coverage
$37° < \theta_{lab} < 53°$
$61° < \theta_{lab} < 85°$

Y. Leifels et al., PRL 71, 963 (1993)
P.Russotto et al., PLB 697 (2011)

FOPI/LAND experiment on neutron squeeze out (1991)

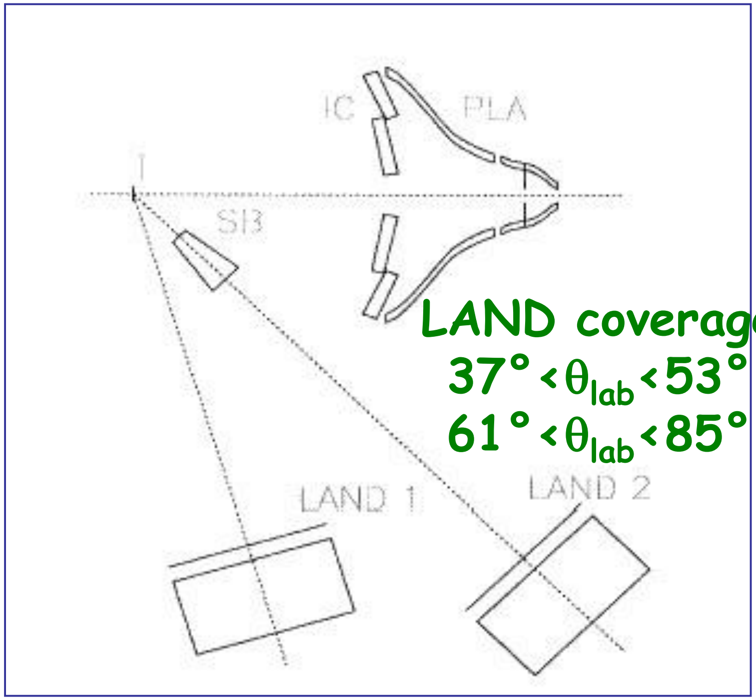

LAND coverage
$37° < \theta_{lab} < 53°$
$61° < \theta_{lab} < 85°$

Au+Au 400 A MeV
b< 7.5 fm

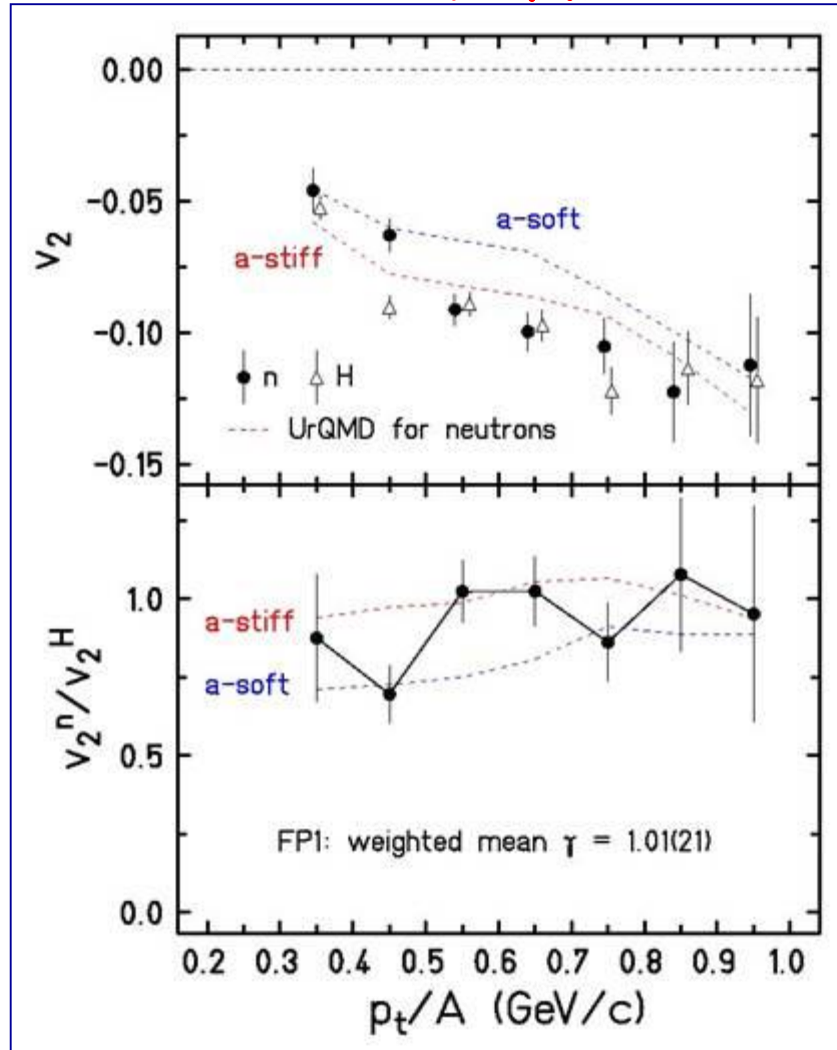

$$E_{sym} = E_{sym}^{pot} + E_{sym}^{kin}$$
$$= 22MeV\cdot(\rho/\rho_0)^{\gamma} + 12MeV\cdot(\rho/\rho_0)^{2/3}$$

Y. Leifels et al., PRL 71, 963 (1993)
P.Russotto et al., PLB 697 (2011)

FOPI/LAND experiment on neutron squeeze out (1991)

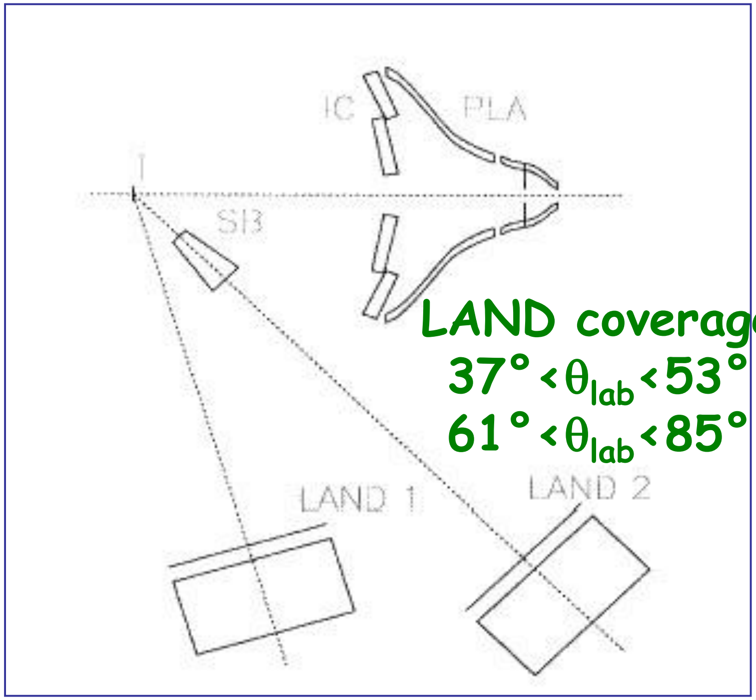

Au+Au 400 A MeV
b< 7.5 fm

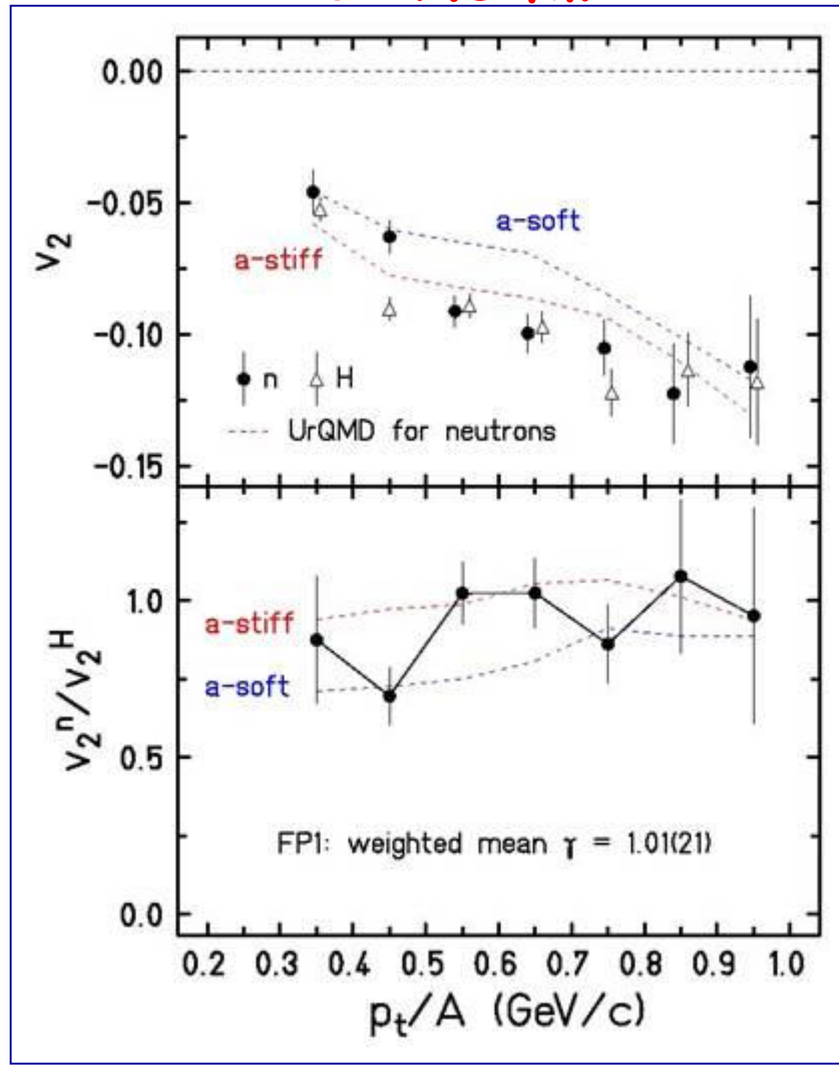

$\gamma = 0.9 \pm 0.4$

$L = 83 \pm 26$

$$E_{sym} = E_{sym}^{pot} + E_{sym}^{kin}$$
$$= 22\text{MeV}\cdot(\rho/\rho_0)^{\gamma} + 12\text{MeV}\cdot(\rho/\rho_0)^{2/3}$$

Y. Leifels et al., PRL 71, 963 (1993)
P.Russotto et al., PLB 697 (2011)

Results with Tübingen QMD

UrQMD:
momentum dep. of isoscalar field
momentum dep. of NNECS
momentum independent power-law
parameterization of the symmetry energy

Tübingen-QMD:
density dep. of NNECS
asymmetry dep. of NNECS
soft vs. hard EoS
width of wave packets
momentum dependent (Gogny inspired)
parameterization of the symmetry energy

M.D. Cozma, PLB 700, 139 (2011); arXiv:1102.2728

M.D. Cozma et al., Towards a model-independent constraint of the high-density dependence of the symmetry energy

arXiv:1305.5417 [nucl-th] PRC88 044912 (2013)

Results with Tübingen QMD

UrQMD:
momentum dep. of isoscalar field
momentum dep. of NNECS
momentum independent power-law
parameterization of the symmetry energy

Tübingen-QMD:
density dep. of NNECS
asymmetry dep. of NNECS
soft vs. hard EoS
width of wave packets
momentum dependent (Gogny inspired)
parameterization of the symmetry energy

M.D. Cozma, PLB 700, 139 (2011);
arXiv:1102.2728

Au+Au 400 A MeV b< 7.5 fm

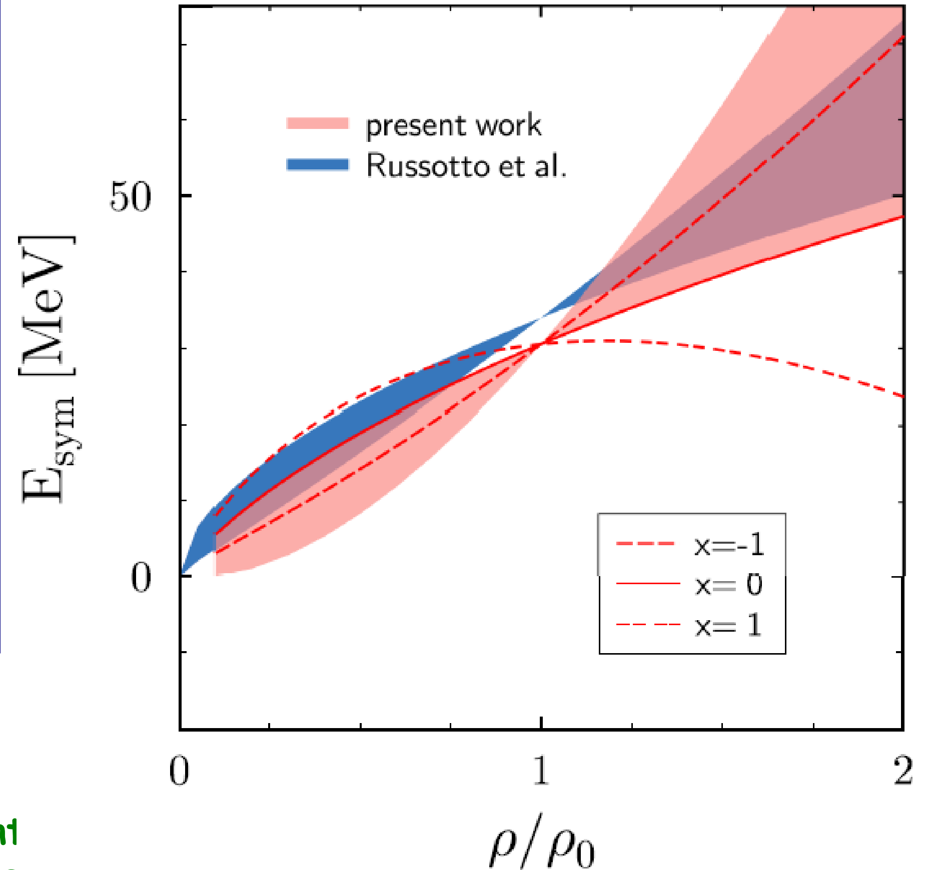

M.D. Cozma et al., Towards a model-independent constraint of the high-density dependence of the symmetry energy

arXiv:1305.5417 [nucl-th] PRC88 044912 (2013)

x =-1.0±1.0

Au+Au @ 400 A.MeV: Background rejection

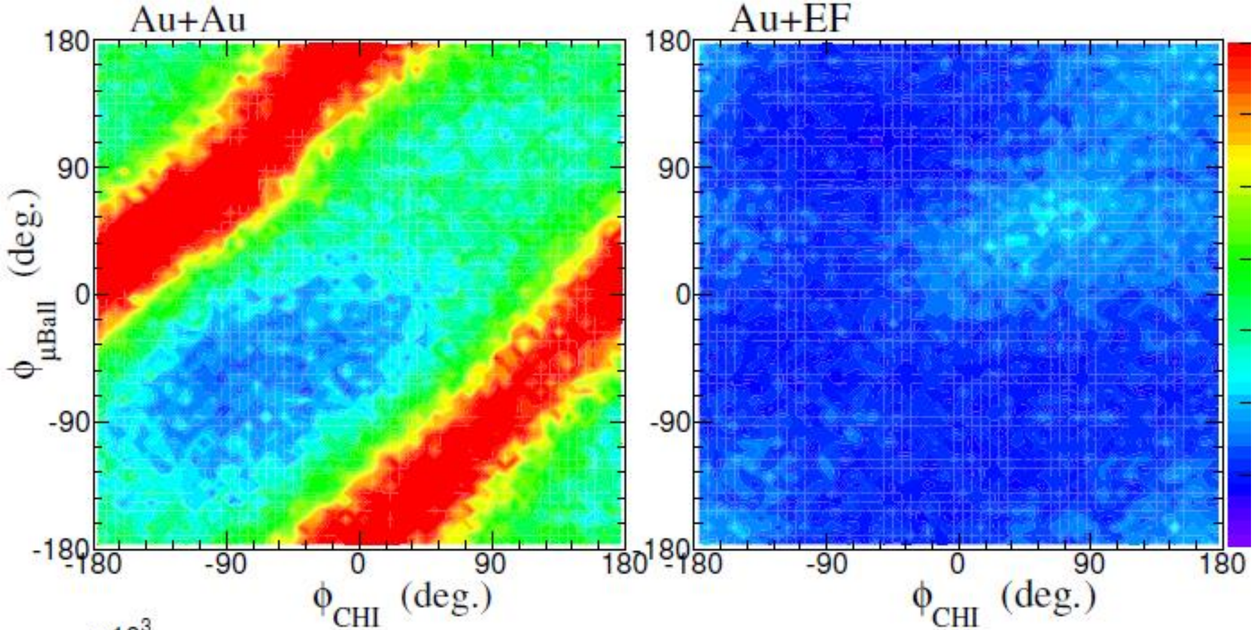

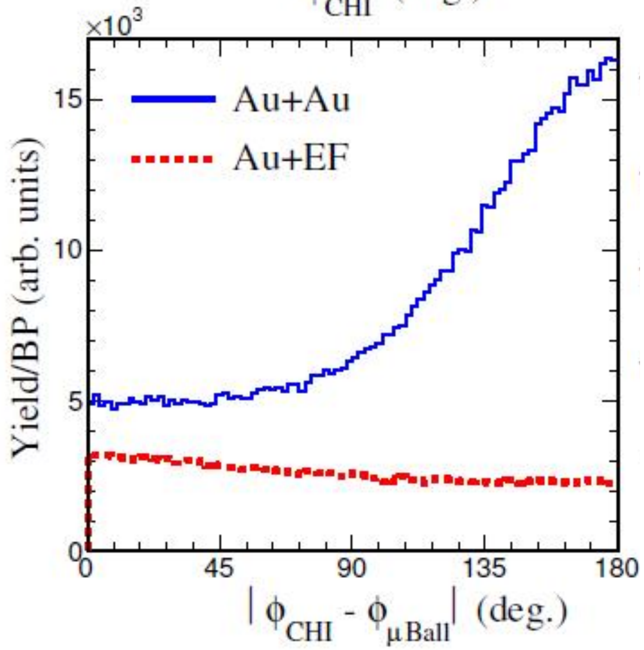

CHIMERA $M(Y_{cm}>0.1) \geq 4$

$$\vec{Q} = \sum_{i=1}^{M} w_i Z_i \gamma \vec{\beta}_t^{\,i} \qquad w_i = \begin{cases} 1 & \text{for } Y_{cm}>0.1 \\ 0 & \text{for } Y_{cm}<0.1 \end{cases}$$

μBall $M \geq 2$

$$\vec{Q} = \sum_{i=1}^{M} \hat{r}_t^{\,i}$$

ad. from P. Danielewicz et al., PLB 1985

Au+Au @ 400 A.MeV: Background rejection

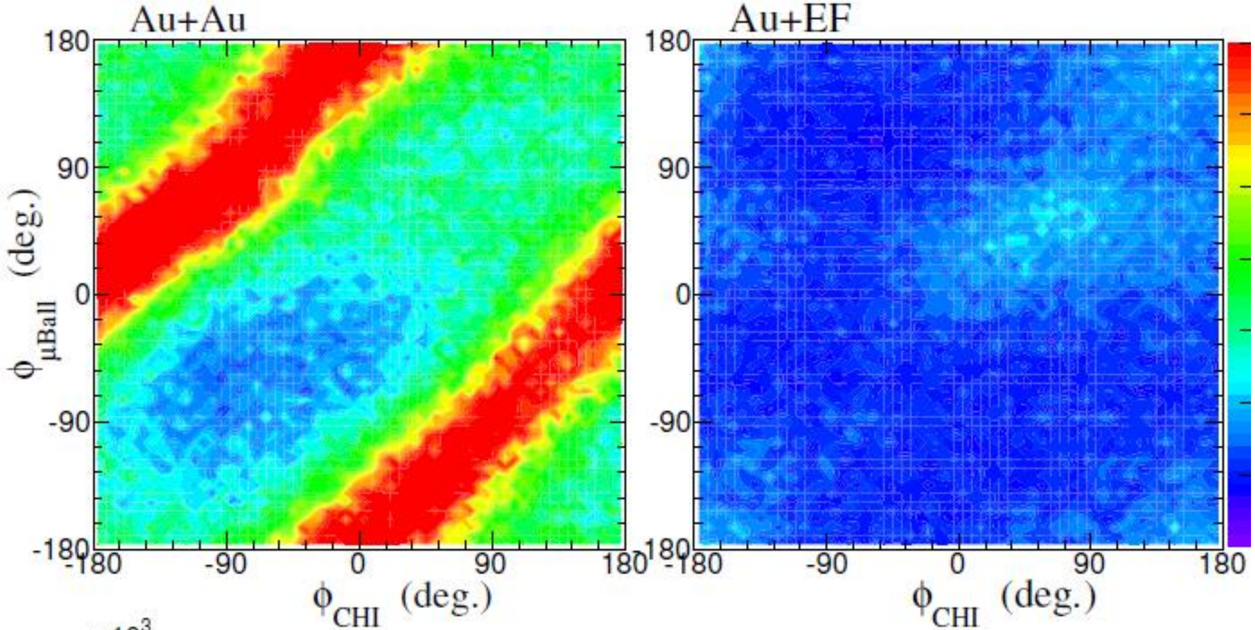

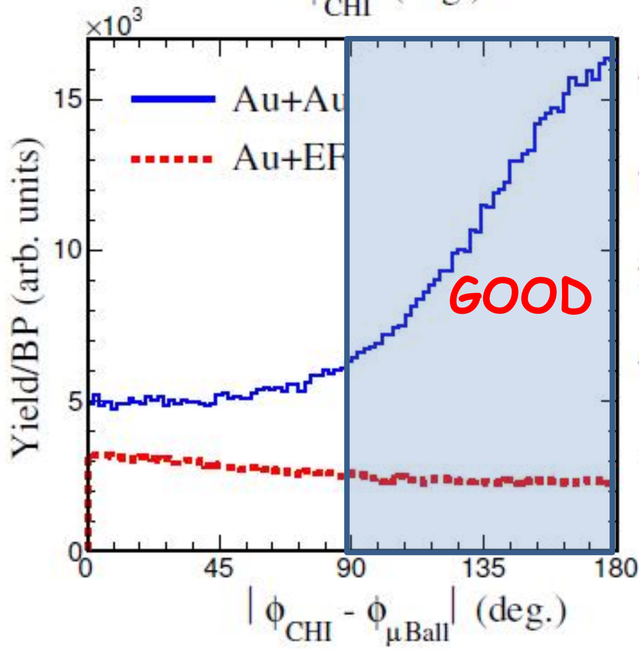

CHIMERA $M(Y_{cm}>0.1) \geq 4$

$$\vec{Q} = \sum_{i=1}^{M} w_i Z_i \gamma \vec{\beta}_t^i \qquad w_i = \begin{cases} 1 & \text{for } Y_{cm}>0.1 \\ 0 & \text{for } Y_{cm}<0.1 \end{cases}$$

μBall $M \geq 2$

$$\vec{Q} = \sum_{i=1}^{M} \hat{r}_t^i$$

ad. from P. Danielewicz et al., PLB 1985

Comparison with UrQMD

Au+Au @ 400 AMeV b<7.5 fm

Neutrons:
(Au+Au)-(Au+Au with SB)+
-(Au+EF)+(Au+EF with SB)

Charged Particles:
(Au+Au)-(Au+EF)

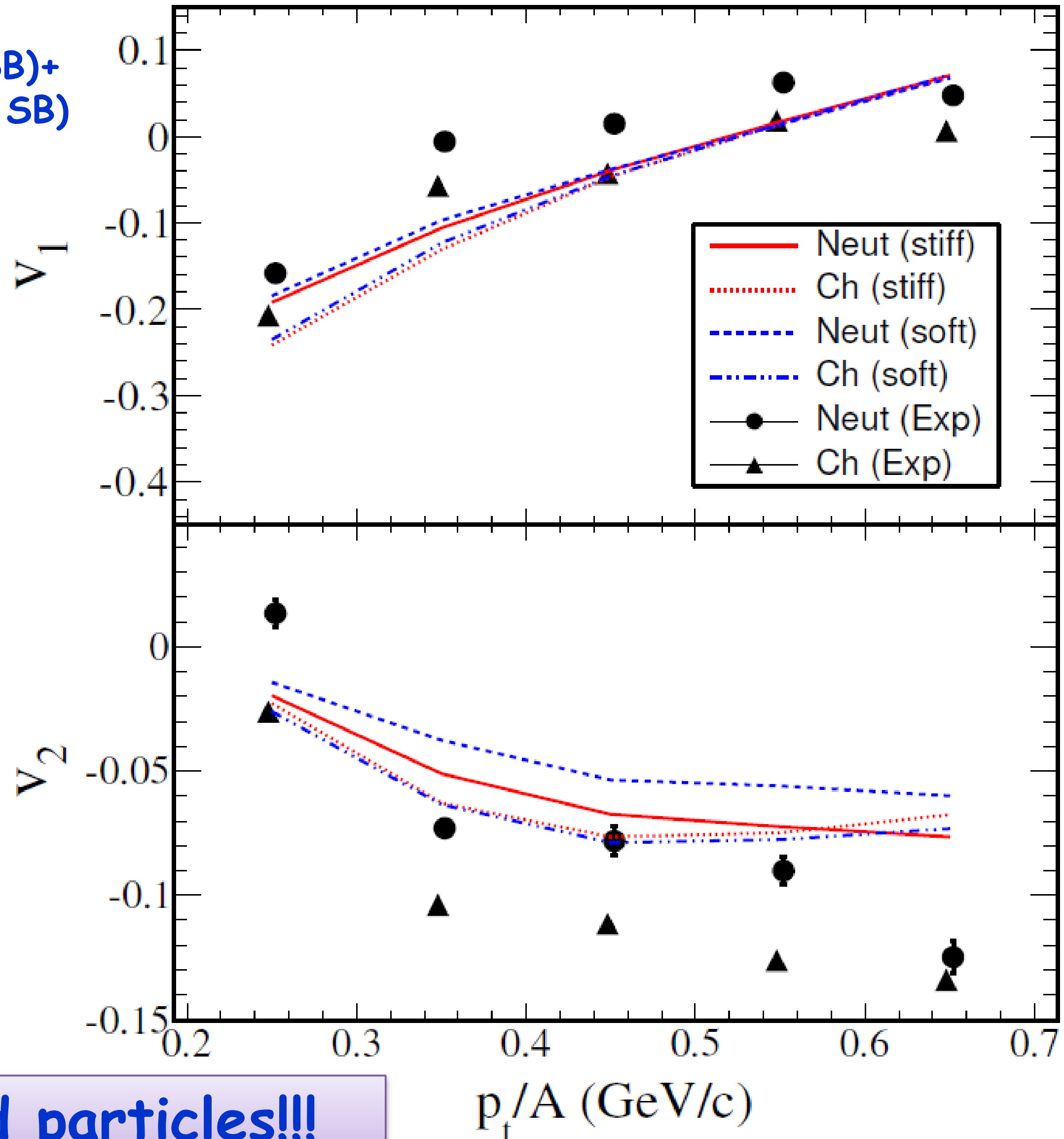

Only charged particles!!!

FUTURE Possibilities

UrQMD prediction for some interesting beams (and δ^2)

^{197}Au+^{197}Au @ 400, 600, 800, 1000,1500 AMeV (0.039+0.039)

^{132}Sn+^{124}Sn @ 400, 600, 800 AMeV (0.059+0.037)

^{106}Sn+^{112}Sn @ 400, 600, 800 AMeV (0.003+0.011)

At midvelocity b/bred <0.53

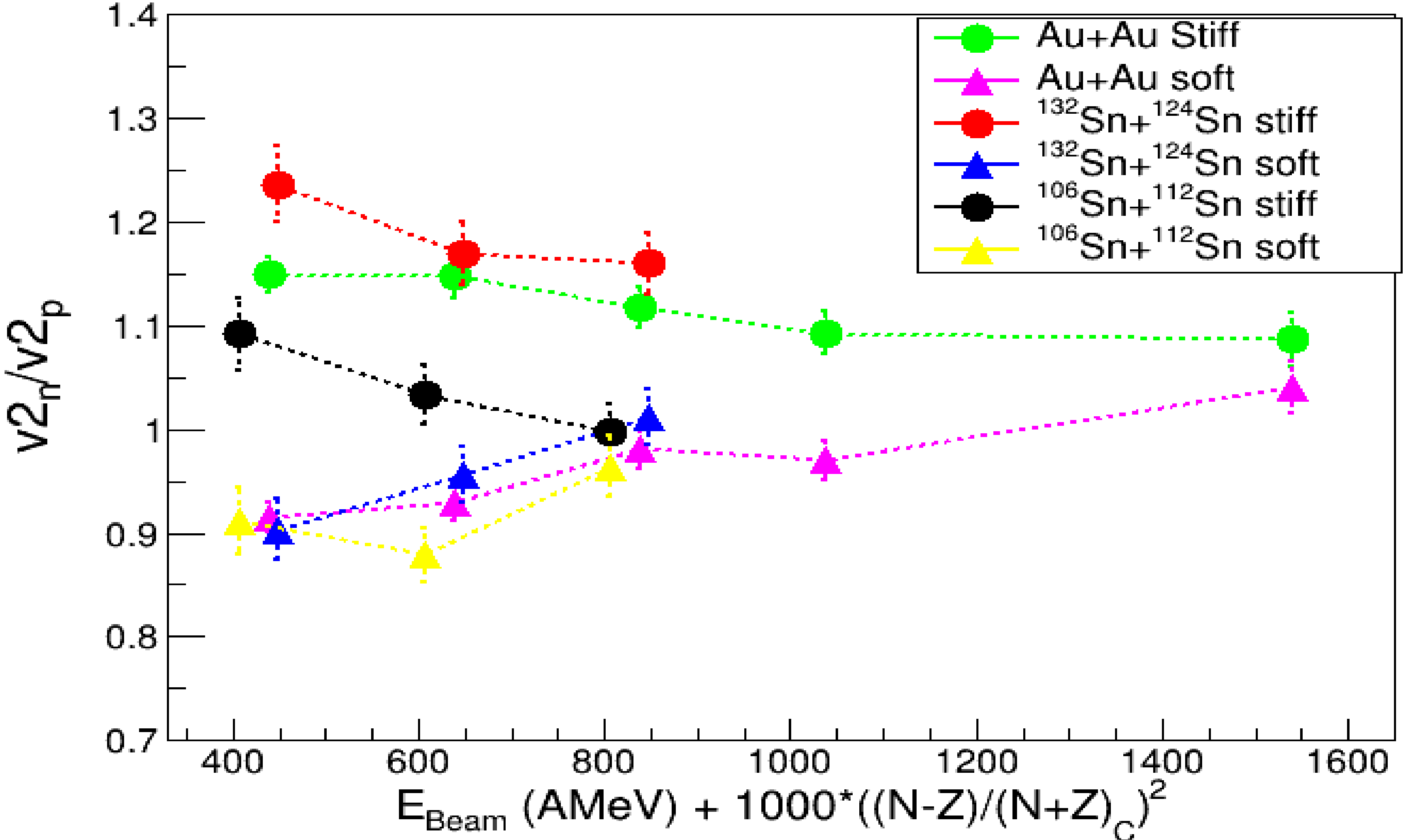

The Asy-Eos Collaboration

P. Russotto[1,a], M. Chartier[2], M.D. Cozma[3], E. De Filippo[1], A. Le Fèvre[4], S. Gannon[2], I. Gašparić[5,6], M. Kiš[4,5], S. Kupny[7], Y. Leifels[4], R.C. Lemmon[8], Q. Li[9], J. Łukasik[10], P. Marini[11,12], P. Pawłowski[10], S. Santoro[13,14], W. Trautmann[4], M. Veselsky[15], L. Acosta[16], M. Adamczyk[7], A. Al-Ajlan[17], M. Al-Garawi[18], S. Al-Homaidhi[17], F. Amorini[16], L. Auditore[13,14], T. Aumann[6], Y. Ayyad[19], V. Baran[16,20], Z. Basrak[5], R. Bassini[21], J. Benlliure[19], C. Boiano[21], M. Boisjoli[12], K. Boretzky[4], J. Brzychczyk[7], A. Budzanowski[10], G. Cardella[1], P. Cammarata[11], Z. Chajecki[22], A. Chbihi[12], M. Colonna[16], B. Czech[10], M. Di Toro[16,23], M. Famiano[24], V. Greco[16,23], L. Grassi[5], C. Guazzoni[21,25], P. Guazzoni[21,26], M. Heil[4], L. Heilborn[11], R. Introzzi[27], T. Isobe[28], K. Kezzar[18], A. Krasznahorkay[29], N. Kurz[4], E. La Guidara[1], G. Lanzalone[16,30], P. Lasko[7], I. Lombardo[31,32], W.G. Lynch[22], Z. Matthews[3], L. May[11], T. Minniti[13,14], M. Mostazo[19], A. Pagano[1], M. Papa[1], S. Pirrone[1], R. Pleskac[4], G. Politi[1,23], F. Porto[16,23], R. Reifarth[4], W. Reisdorf[4], F. Riccio[21,25], F. Rizzo[16,23], E. Rosato[31,32], D. Rossi[4,22], H. Simon[4], I. Skwirczynska[10], Z. Sosin[7], L. Stuhl[29], A. Trifirò[13,14], M. Trimarchi[13,14], M.B. Tsang[22], G. Verde[1], M. Vigilante[31,32], A. Wieloch[7], P. Wigg[2], H.H. Wolter[33], P. Wu[2], S. Yennello[11], P. Zambon[21,25], L. Zetta[21,26], and M. Zoric[5]

[1] *INFN-Sezione di Catania, Catania, Italy*
[2] *University of Liverpool, Liverpool, UK*
[3] *IFIN-HH, Magurele-Bucharest, Romania*
[4] *GSI Helmholtzzentrum, Darmstadt, Germany*
[5] *Ruder Boškoviċ Institute, Zagreb, Croatia*
[6] *Technische Universität, Darmstadt, Germany*
[7] *Jagiellonian University, Krakòw, Poland*
[8] *STFC Laboratory, Daresbury, UK*
[9] *Huzhou Teachers College, China*
[10] *IFJ-PAN, Krakow, Poland*
[11] *Texas A&M University, College Station, USA*
[12] *GANIL, Caen, France*
[13] *INFN-Gruppo Collegato di Messina, Messina, Italy*
[14] *Università di Messina, Messina, Italy*
[15] *Institute of Physics, Slovak Academy of Sciences, Bratislava, Slovakia*
[16] *INFN-Laboratori Nazionali del Sud, Catania, Italy*
[17] *KACST Riyadh, Riyadh, Saudi Arabia*
[18] *King Saud University, Riyadh, Saudi Arabia*
[19] *University of Santiago de Compostela, Santiago de Compostela, Spain*
[20] *University of Bucharest, Bucharest, Romania*
[21] *INFN-Sezione di Milano, Milano, Italy*
[22] *NSCL Michigan State University, East Lansing, USA*
[23] *Università di Catania, Catania, Italy*
[24] *Western Michigan University, USA*
[25] *Politecnico di Milano, Milano, Italy*
[26] *Università degli Studi di Milano, Milano, Italy*
[27] *INFN, Politecnico di Torino, Torino, Italy*
[28] *RIKEN, Wako, Japan*
[29] *Institute of Nuclear Research, Debrecen, Hungary*
[30] *Università Kore, Enna, Italy*
[31] *INFN-Sezione di Napoli, Napoli, Italy*
[32] *Università di Napoli, Napoli, Italy*
[33] *LMU, München, Germany*

Results with Tübingen QMD and UrQMD

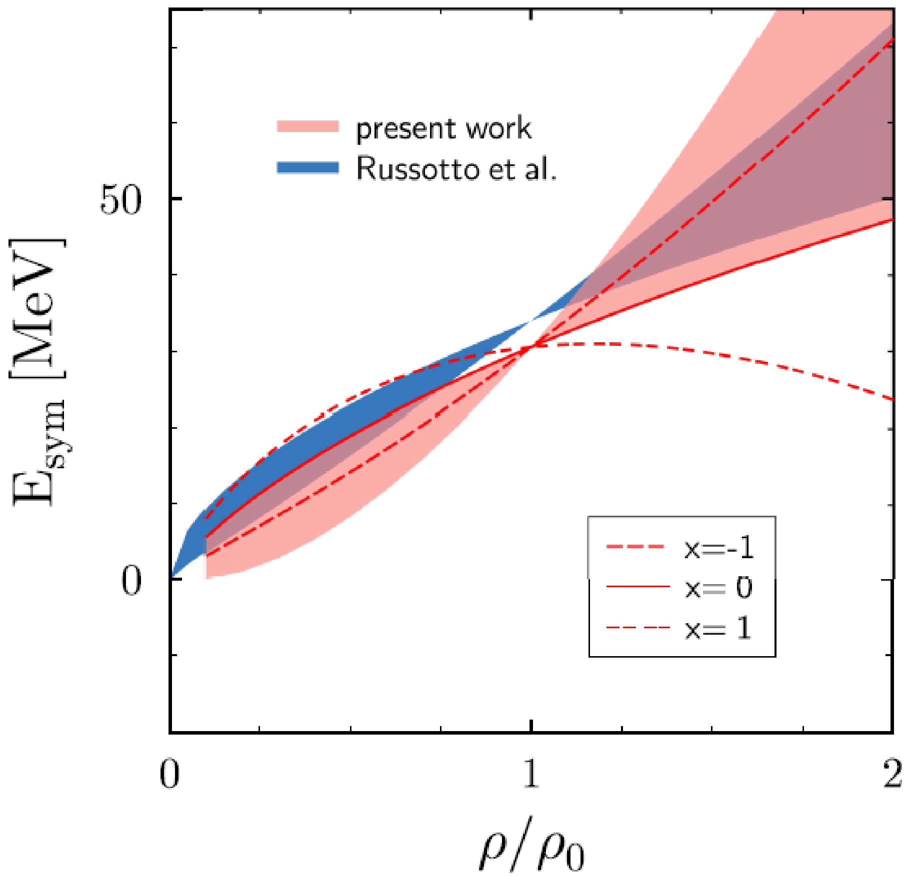

x =-1.0±1.0

M.D. Cozma et al., Towards a model-independent constraint of the high-density dependence of the symmetry energy,

arXiv:1305.5417 [nucl-th]

PRC88 044912 (2013)

Results with Tübingen QMD and UrQMD

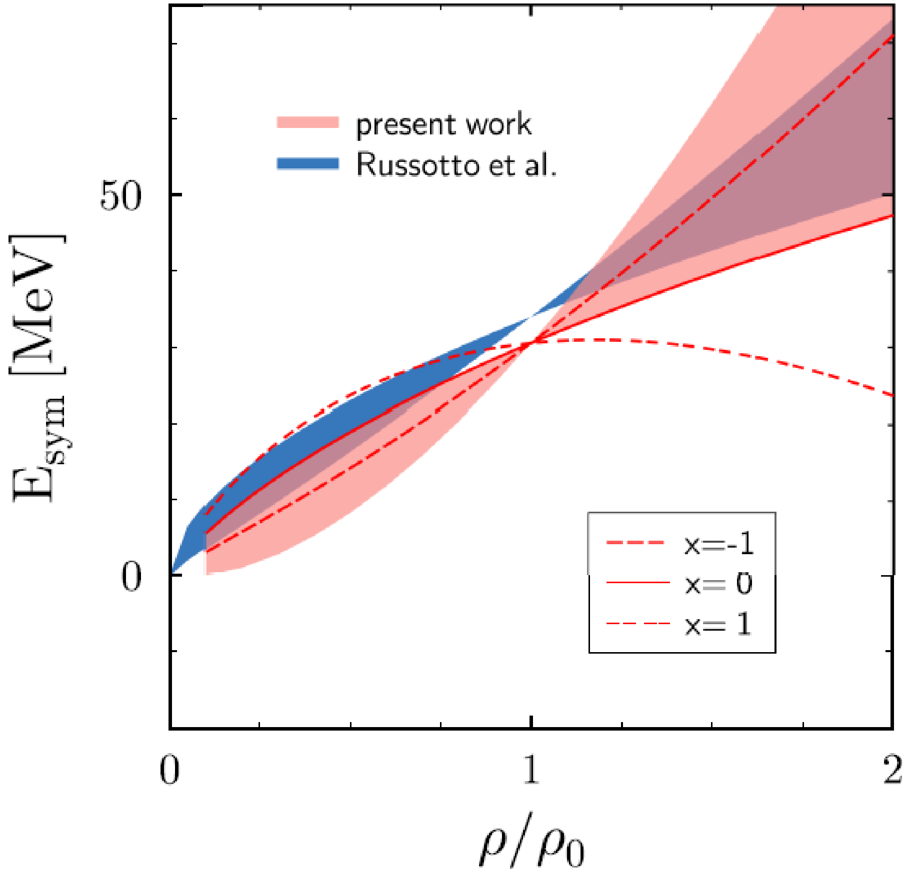

x =-1.0±1.0

M.D. Cozma et al.,
Towards a model-independent constraint of the high-density dependence of the symmetry energy,

arXiv:1305.5417 [nucl-th]

PRC88 044912 (2013)

See next talk (M.D. Cozma) about these results

Au+Au @ 400 A.MeV: Centrality selection

$$ZBound = \sum_i Z_i$$

with $Z_i \geq 2$

From AToF-Wall and CHIMERA

$$ZRat = \frac{Ztrans}{Zlong} = \frac{\sum_i Z_i \cdot \sin^2(\vartheta_i^{lab})}{\sum_i Z_i \cdot \cos^2(\vartheta_i^{lab})}$$

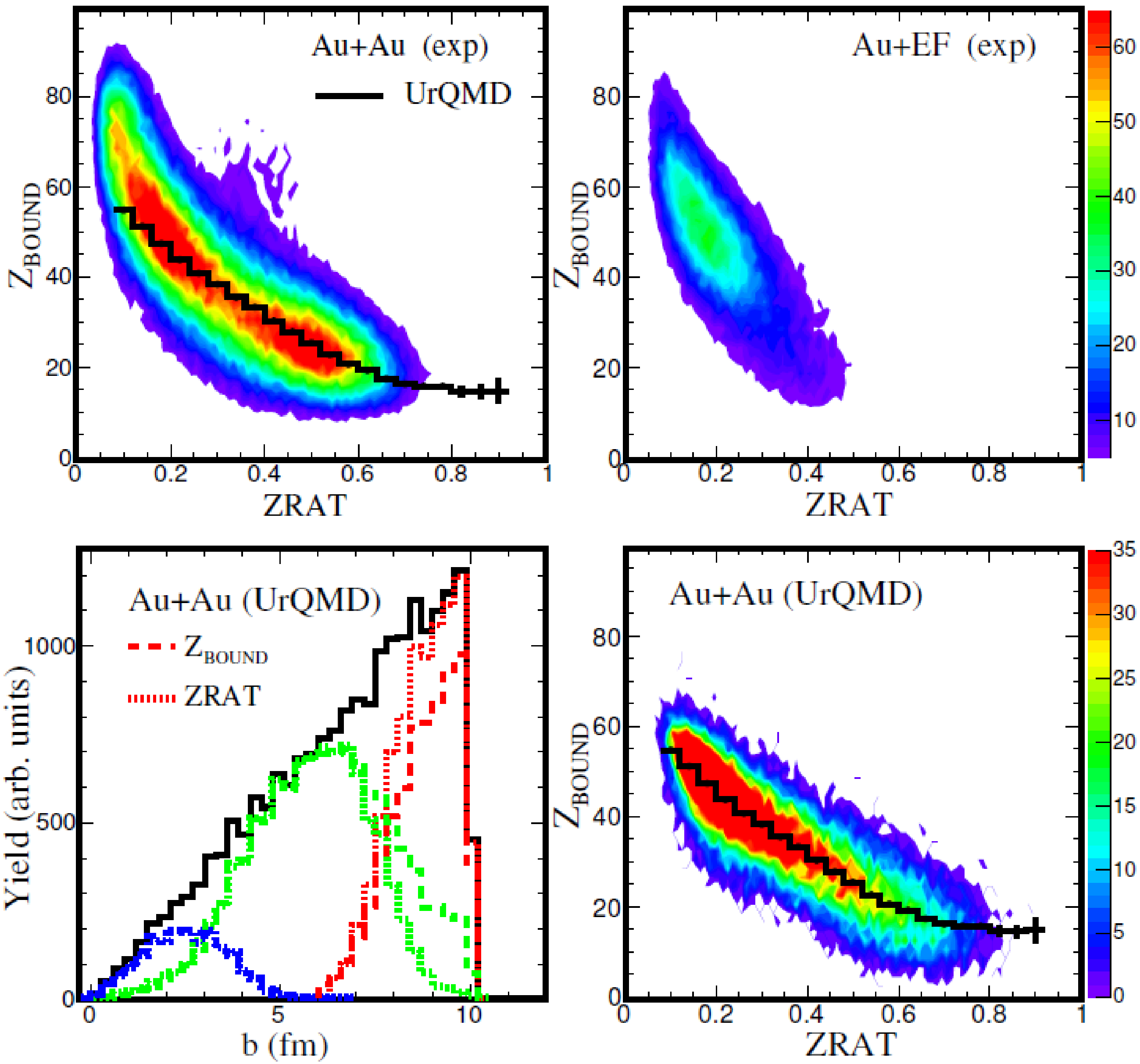

From MI28022014

Reaction Plane orientation

Au+Au @ 400 AMeV

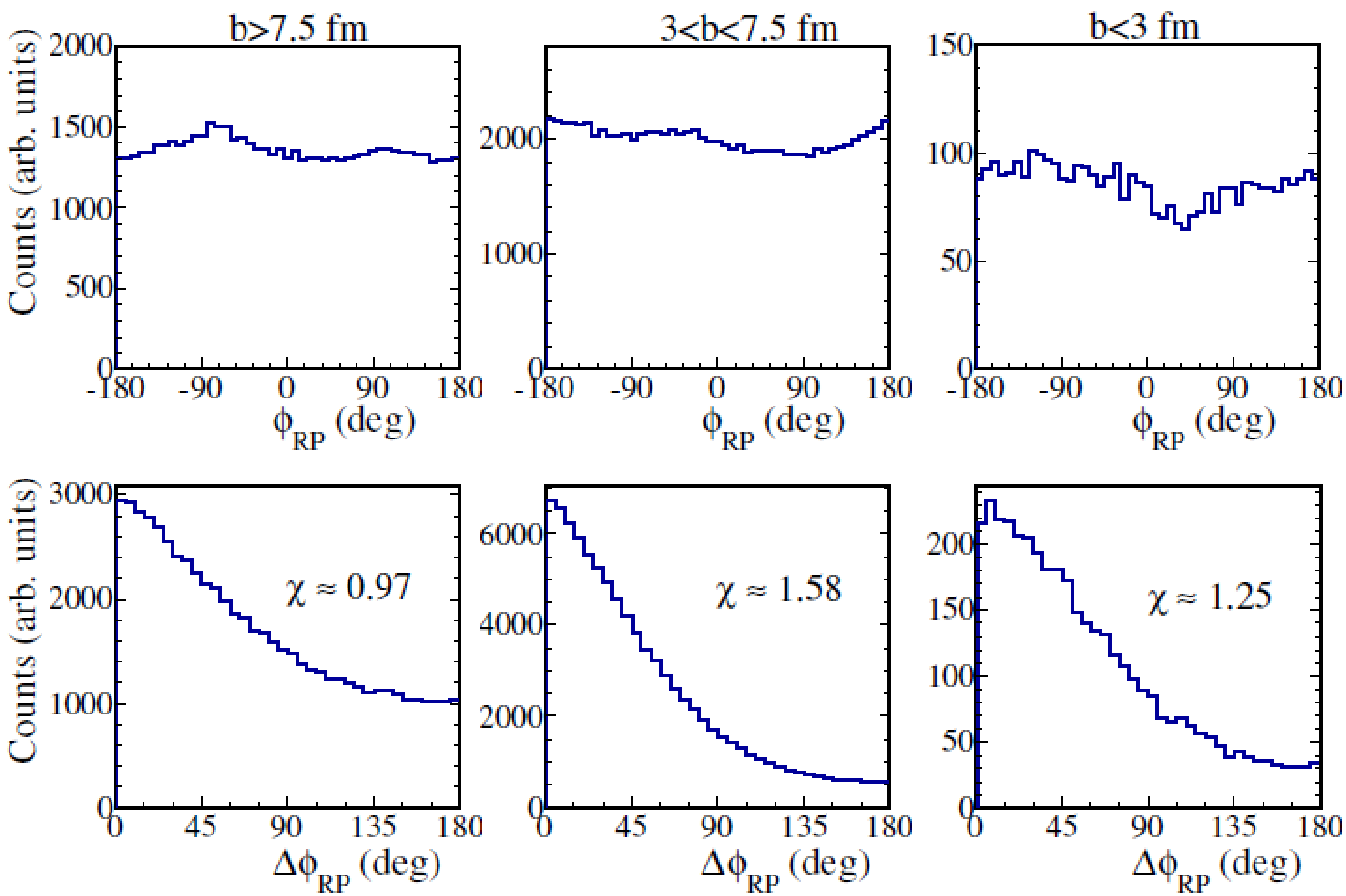

detectors and chosen weight	$y_{c.m.} > 0.1$	$y_{c.m.} > 0.2$
CHIMERA alone, equal weight	1.39	1.30
CHIMERA+AToF, equal weight	1.45	1.37
CHIMERA alone, Z	1.51	1.42
CHIMERA+AToF, Z	1.58	1.50
CHIMERA alone, $Z\beta_t\gamma$	1.52	1.42
CHIMERA+AToF, $Z\beta_t\gamma$	1.59	1.49

Reaction Plane orientation

Au+Au @ 400 AMeV

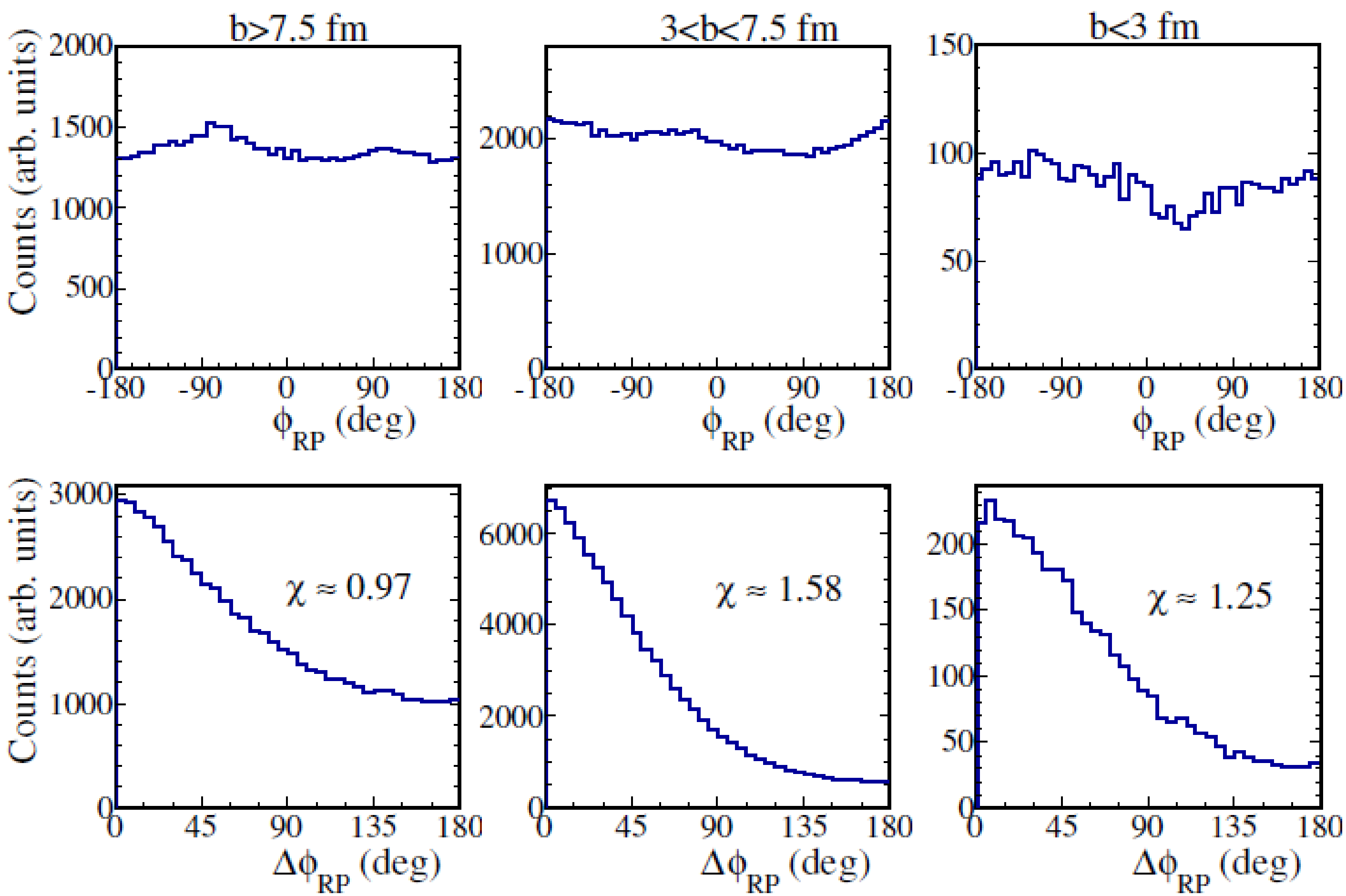

CHIMERA *$M(Y_{cm}>0.1) \geq 4$ + AToF $M(Y_{cm}>0.1) \geq 4$*

$$\vec{Q} = \sum_{i=1}^{M} w_i Z_i \gamma \vec{\beta}_t^i \qquad w_i = \begin{cases} 1 \text{ for } Y_{cm}>0.1 \\ 0 \text{ for } Y_{cm}<0.1 \end{cases}$$

detectors and chosen weight	$y_{c.m.} > 0.1$	$y_{c.m.} > 0.2$
CHIMERA alone, equal weight	1.39	1.30
CHIMERA+AToF, equal weight	1.45	1.37
CHIMERA alone, Z	1.51	1.42
CHIMERA+AToF, Z	1.58	1.50
CHIMERA alone, $Z\beta_t\gamma$	1.52	1.42
CHIMERA+AToF, $Z\beta_t\gamma$	1.59	1.49

ad. from P. Danielewicz et al., PLB 1985

J-Y Ollitrault arXiv:nucl-ex/9711003v2

Comparing ASY-EOS with FOPI: rapidity dep. of charged particles

Main uncertainty due to timing problems in LAND

ToF ±25 ns

Au+Au @ 400 A.MeV

3.35<b<6 fm (c2)

θ_{lab} cut as LAND in ASY-EOS exp

Courtesy of W. Reisdorf

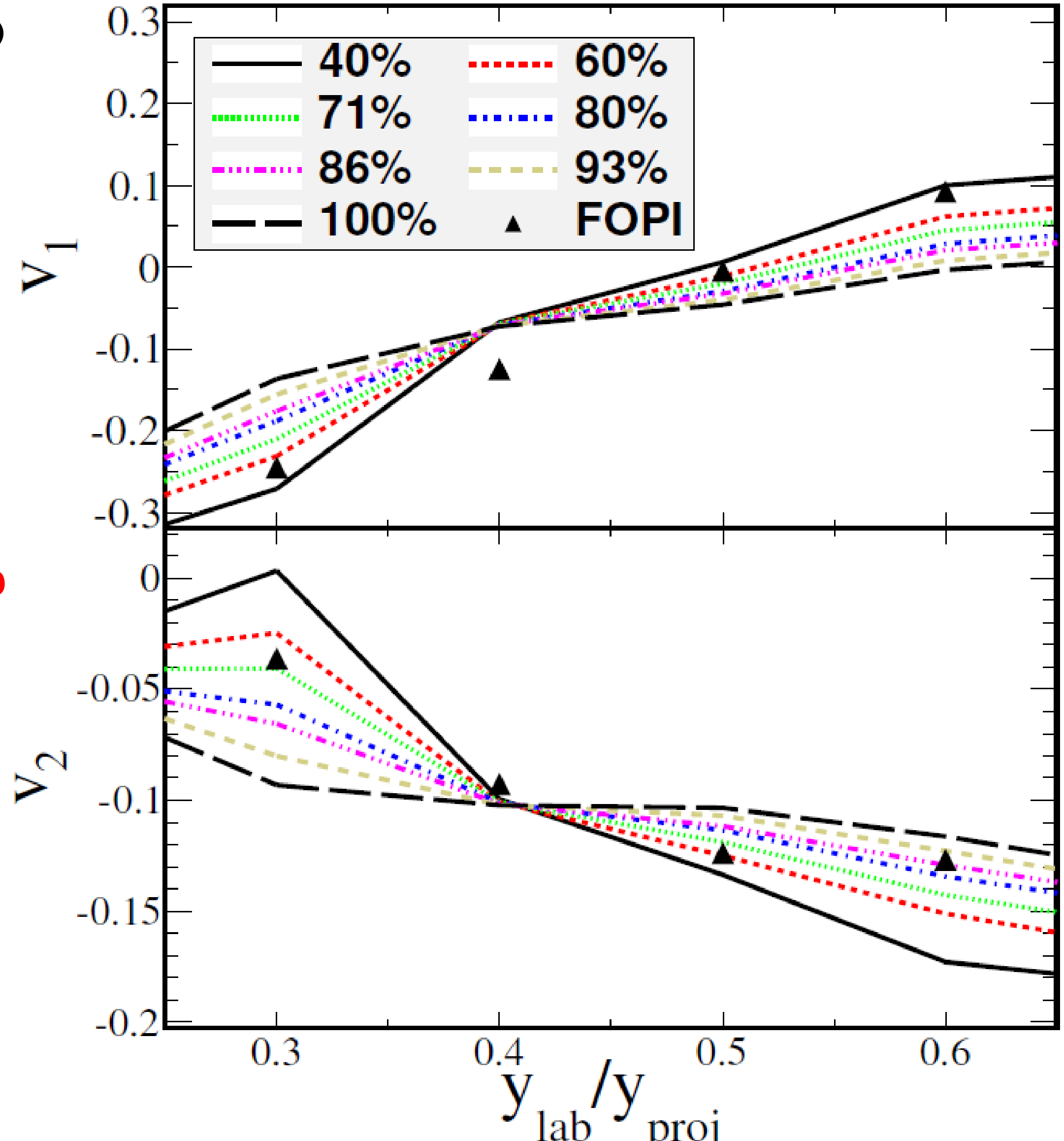

V2n/V2H vs V2n/V2ch

Au+Au @ 400 AMeV b<7.5 fm
but
FOPI-LAND data compared with UrQMD

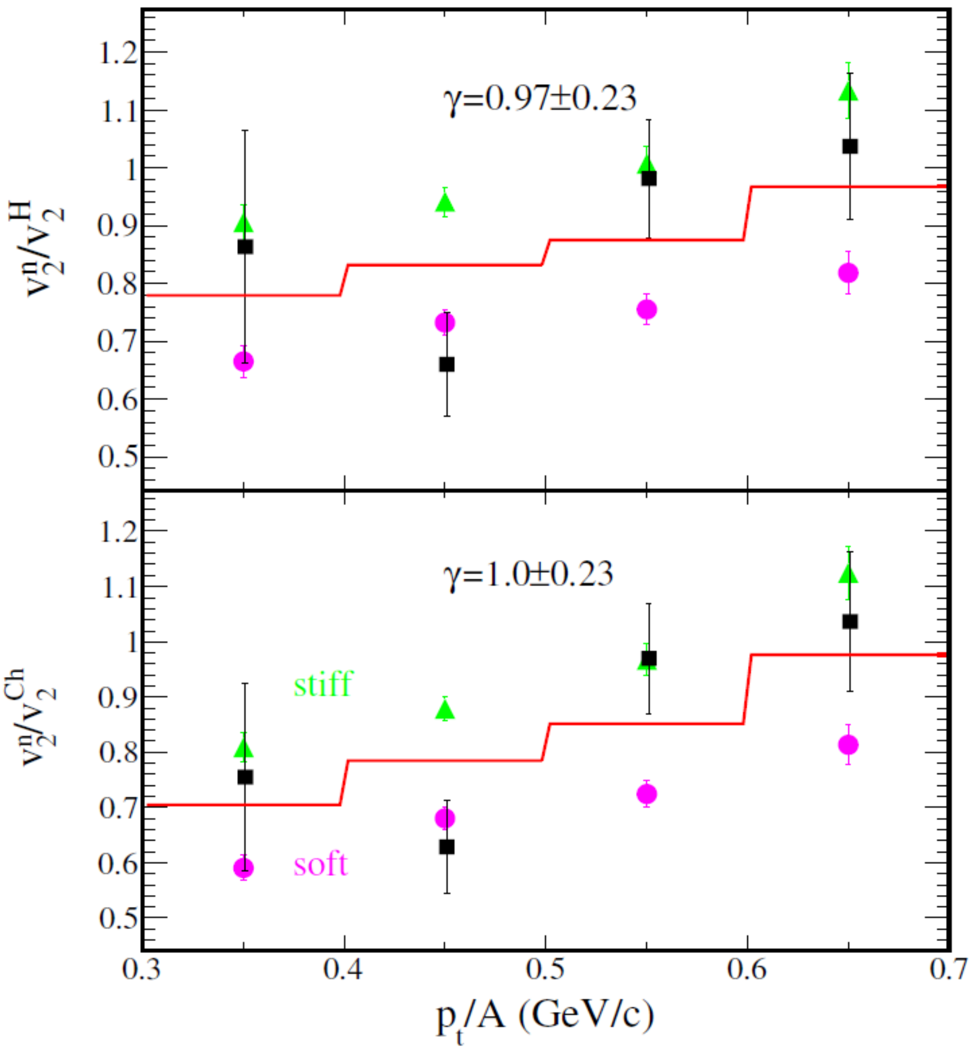

Gamma extrapolation II

Au+Au @ 400 AMeV
b<7.5 fm

Neutrons:
(Au+Au)-(Au+Au with SB)+
-(Au+EF)+(Au+EF with SB)

Charged Particles:
(Au+Au)-(Au+EF)

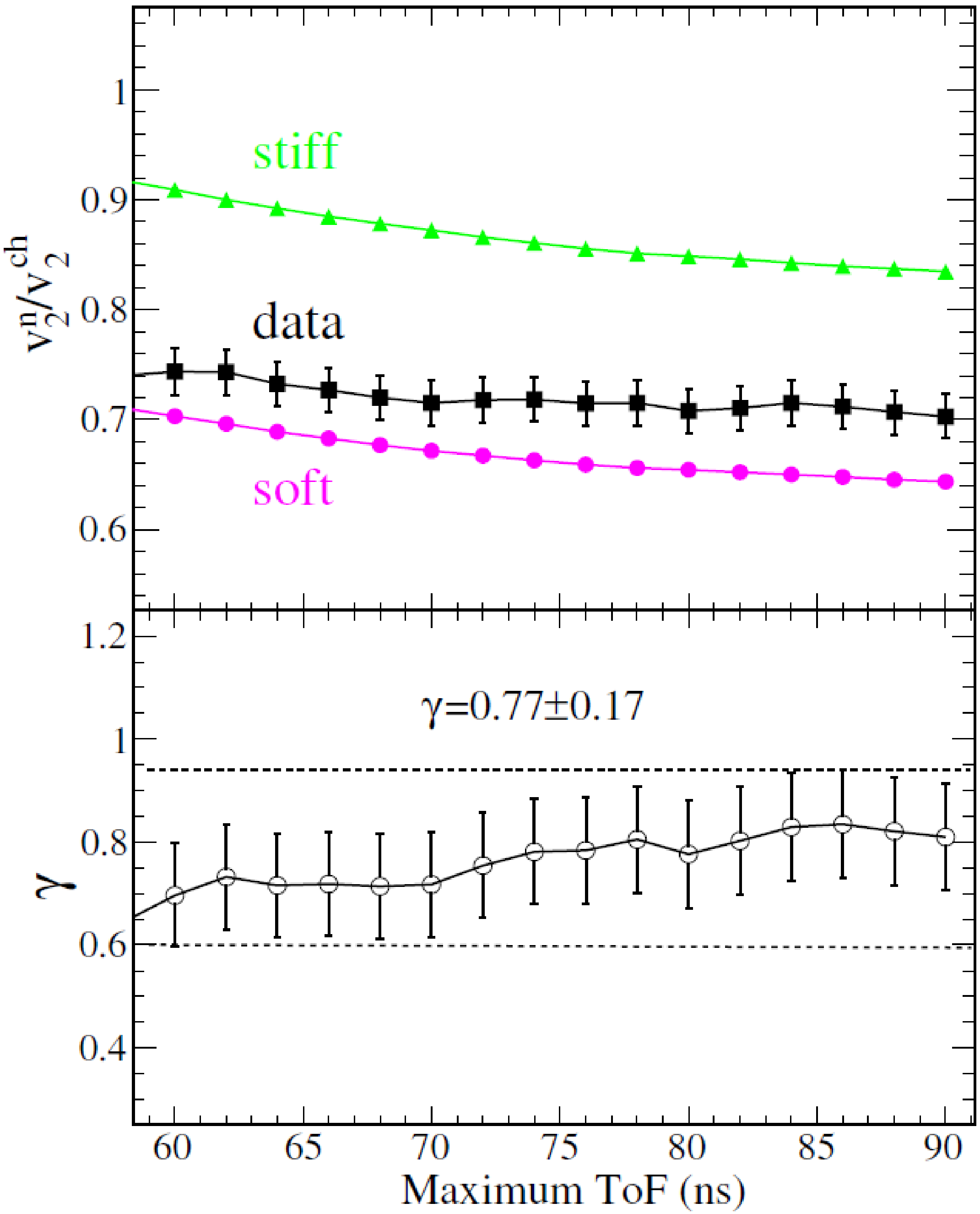

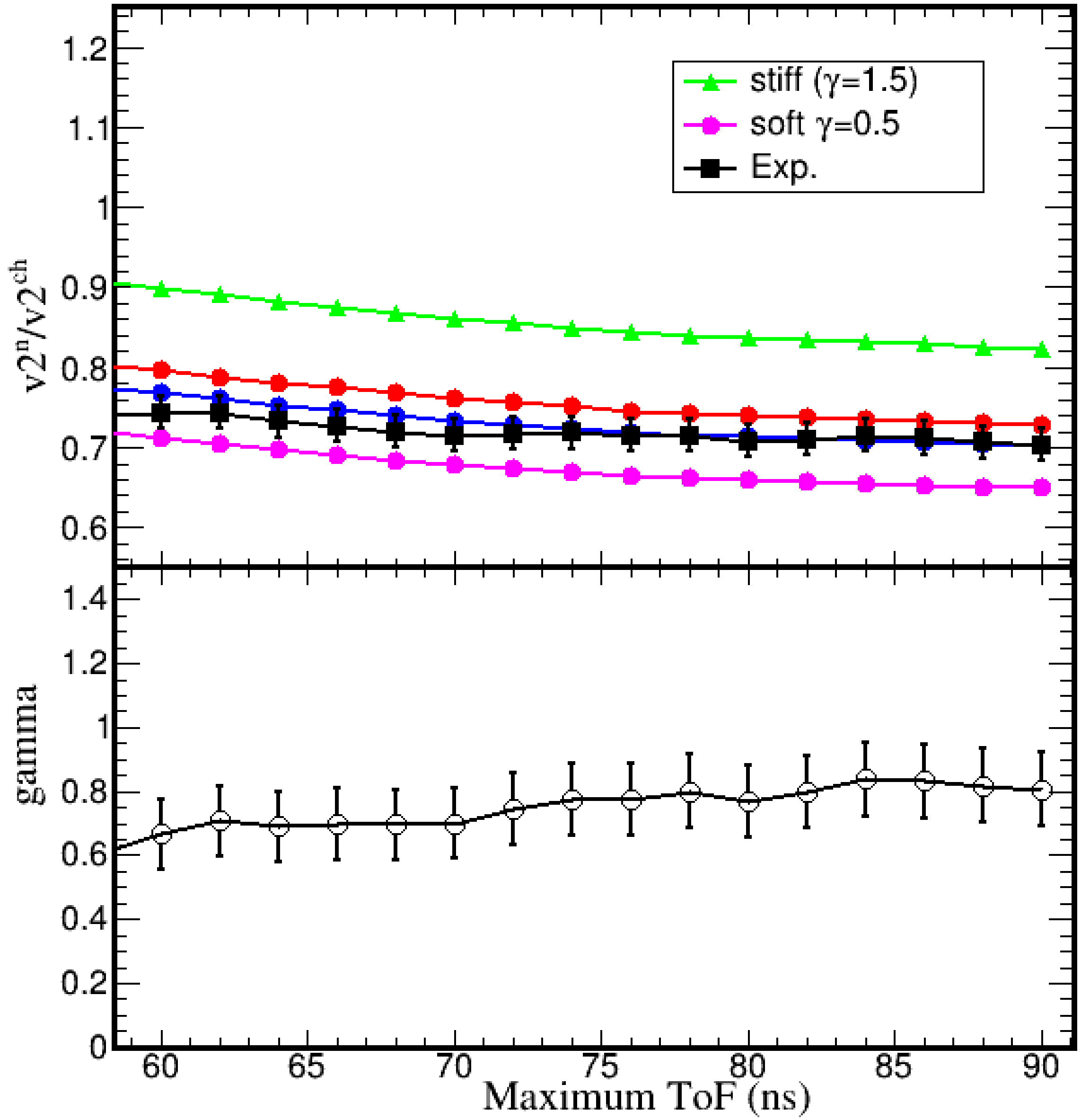

stiff (γ=1.5)
soft γ=0.5
Exp.
v2^n/v2^ch
gamma
Maximum ToF (ns)
1.2
1.1
1
0.9
0.8
0.7
0.6
1.4
1.2
1
0.8
0.6
0.4
0.2
0
60
65
70
75
80
85
90

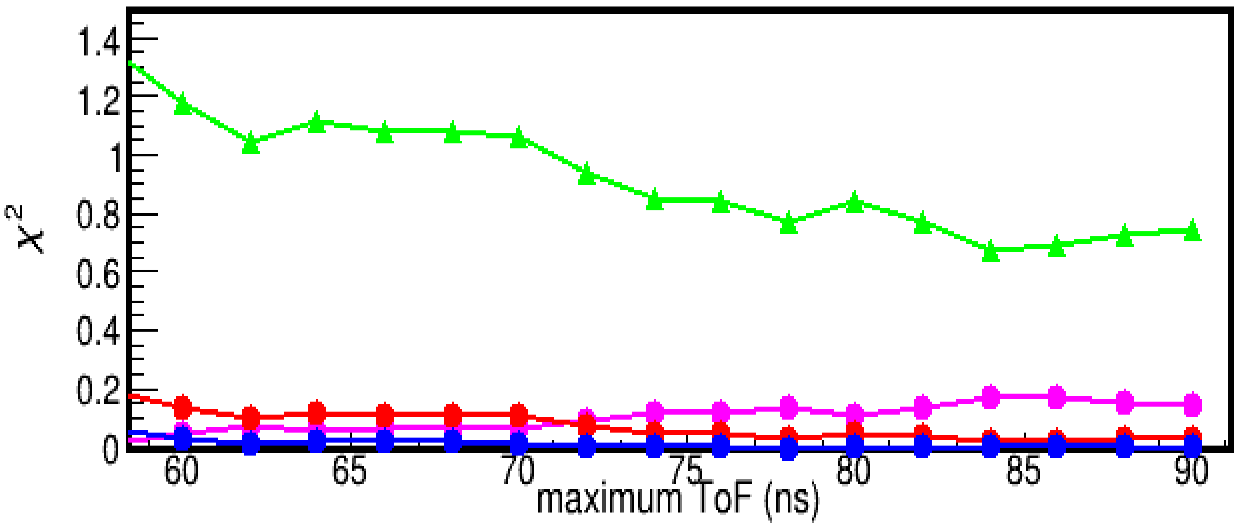

χ^2
1.4
1.2
1
0.8
0.6
0.4
0.2
0
60
65
70
75
80
85
90
maximum ToF (ns)

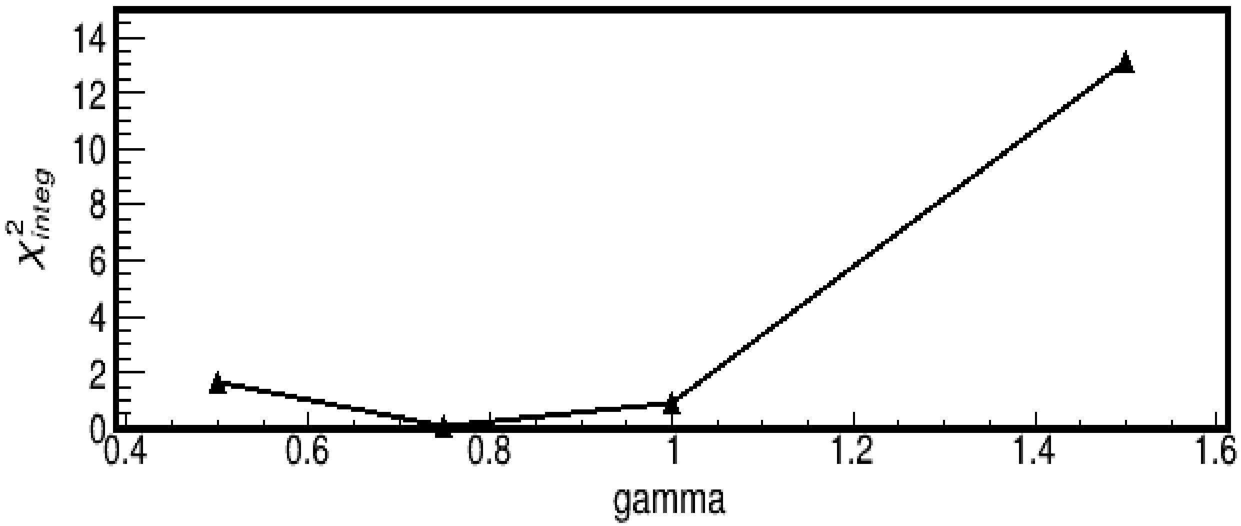

χ^2_{integ}
14
12
10
8
6
4
2
0
0.4
0.6
0.8
1
1.2
1.4
1.6
gamma

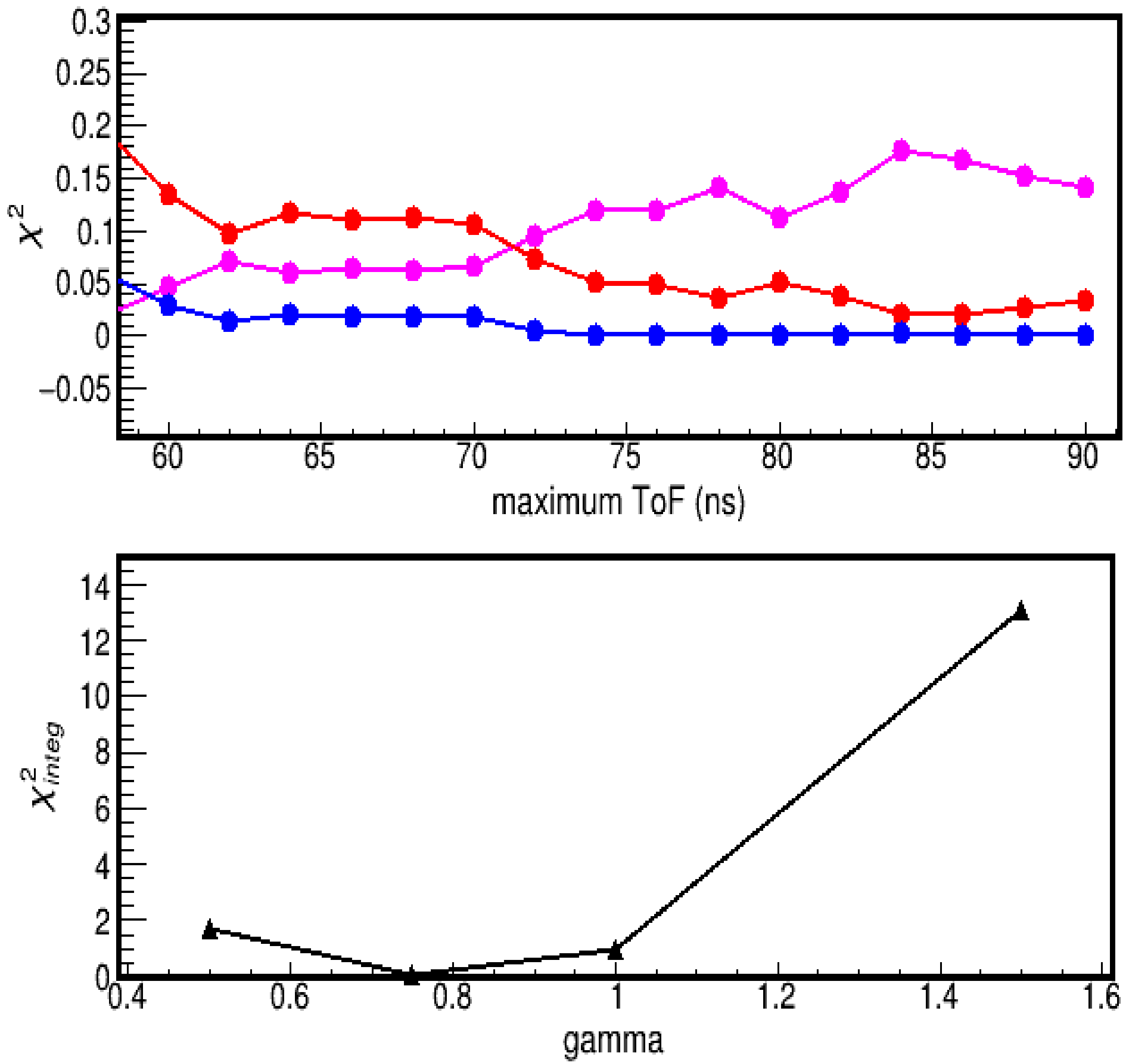

0.3
0.25
0.2
0.15
0.1
0.05
0
−0.05
χ2
60
65
70
75
80
85
90
maximum ToF (ns)
14
12
10
8
6
4
2
0
χ2integ
0.4
0.6
0.8
1
1.2
1.4
1.6
gamma

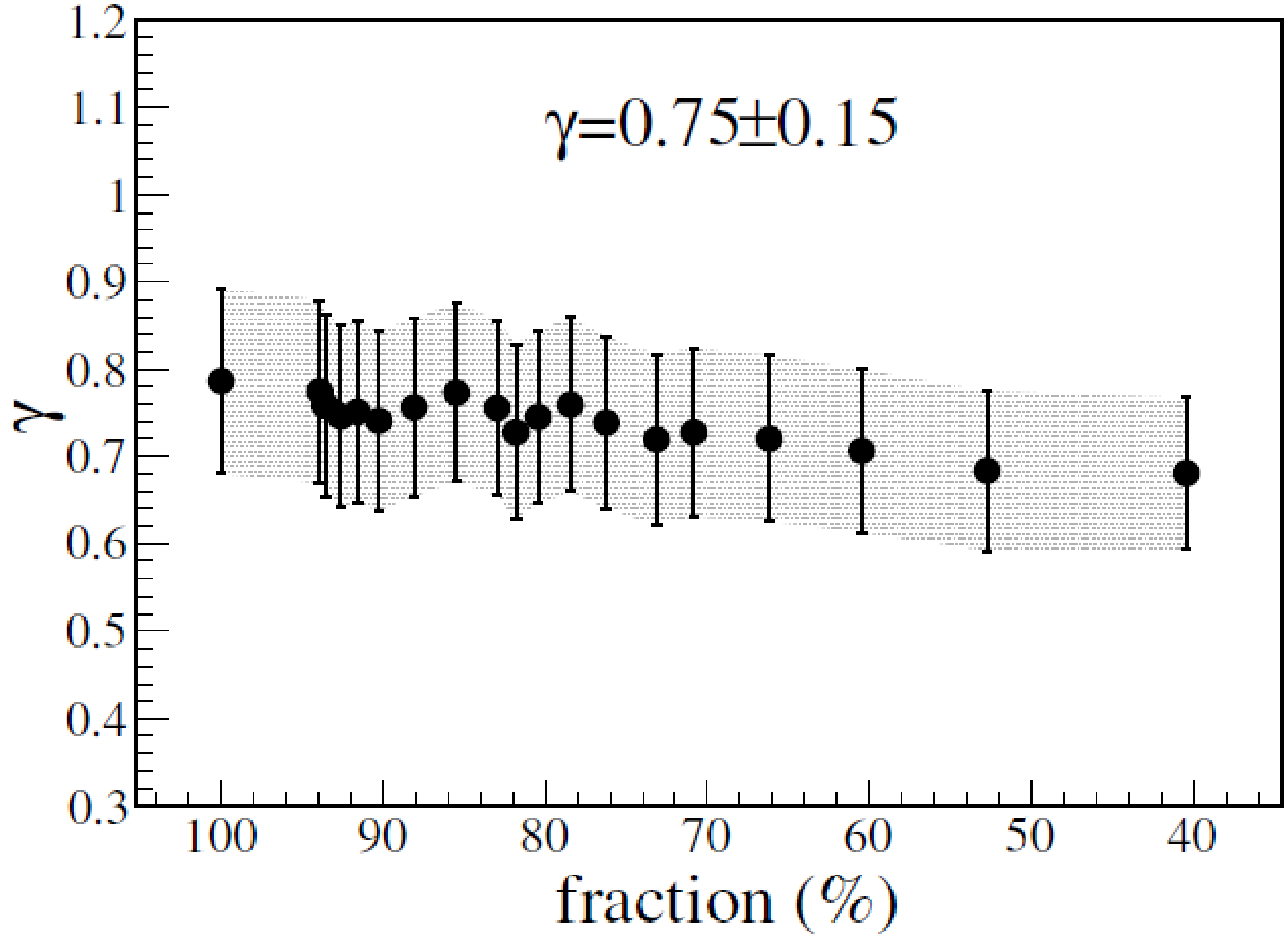

γ=0.75±0.15
γ
1.2
1.1
1
0.9
0.8
0.7
0.6
0.5
0.4
0.3
100
90
80
70
60
50
40
fraction (%)

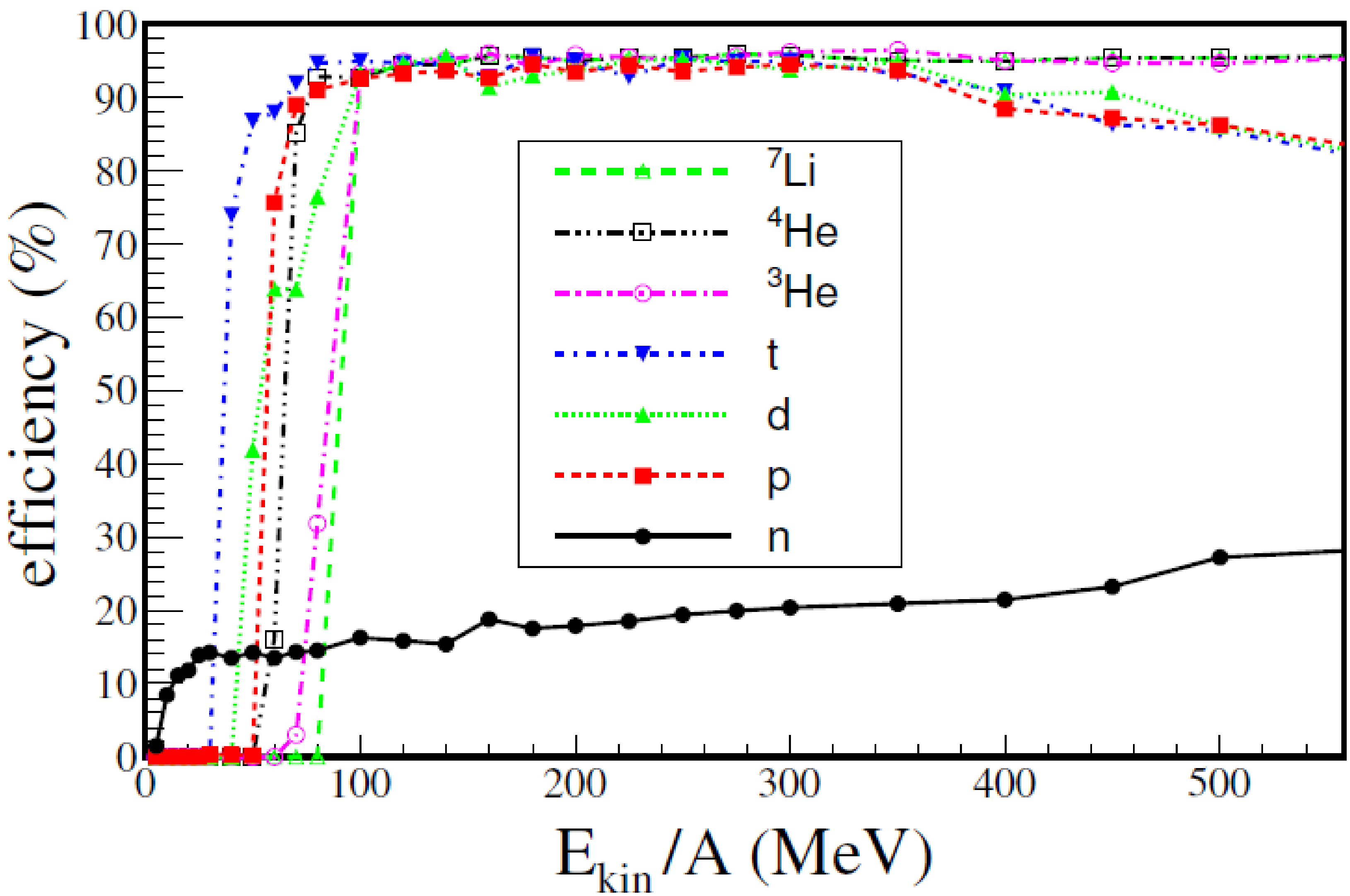

efficiency (%)
E_{kin}/A (MeV)
^{7}Li
^{4}He
^{3}He
t
d
p
n
0
10
20
30
40
50
60
70
80
90
100
0
100
200
300
400
500

FUTURE Possibilities

UrQMD prediction for some interesting beams (and δ^2)

$^{197}Au+^{197}Au$ @ 600,800,800,1000,1500 AMeV (0.039+0.039)

$^{132}Sn+^{124}Sn$ @ 400, 600, 800 AMeV (0.059+0.037)

$^{106}Sn+^{112}Sn$ @ 400, 600, 800 AMeV (0.003+0.011)

FUTURE Possibilities

UrQMD prediction for some interesting beams (and δ^2)

^{197}Au+^{197}Au @ 600,800,800,1000,1500 AMeV (0.039+0.039)

^{132}Sn+^{124}Sn @ 400, 600, 800 AMeV (0.059+0.037)

^{106}Sn+^{112}Sn @ 400, 600, 800 AMeV (0.003+0.011)

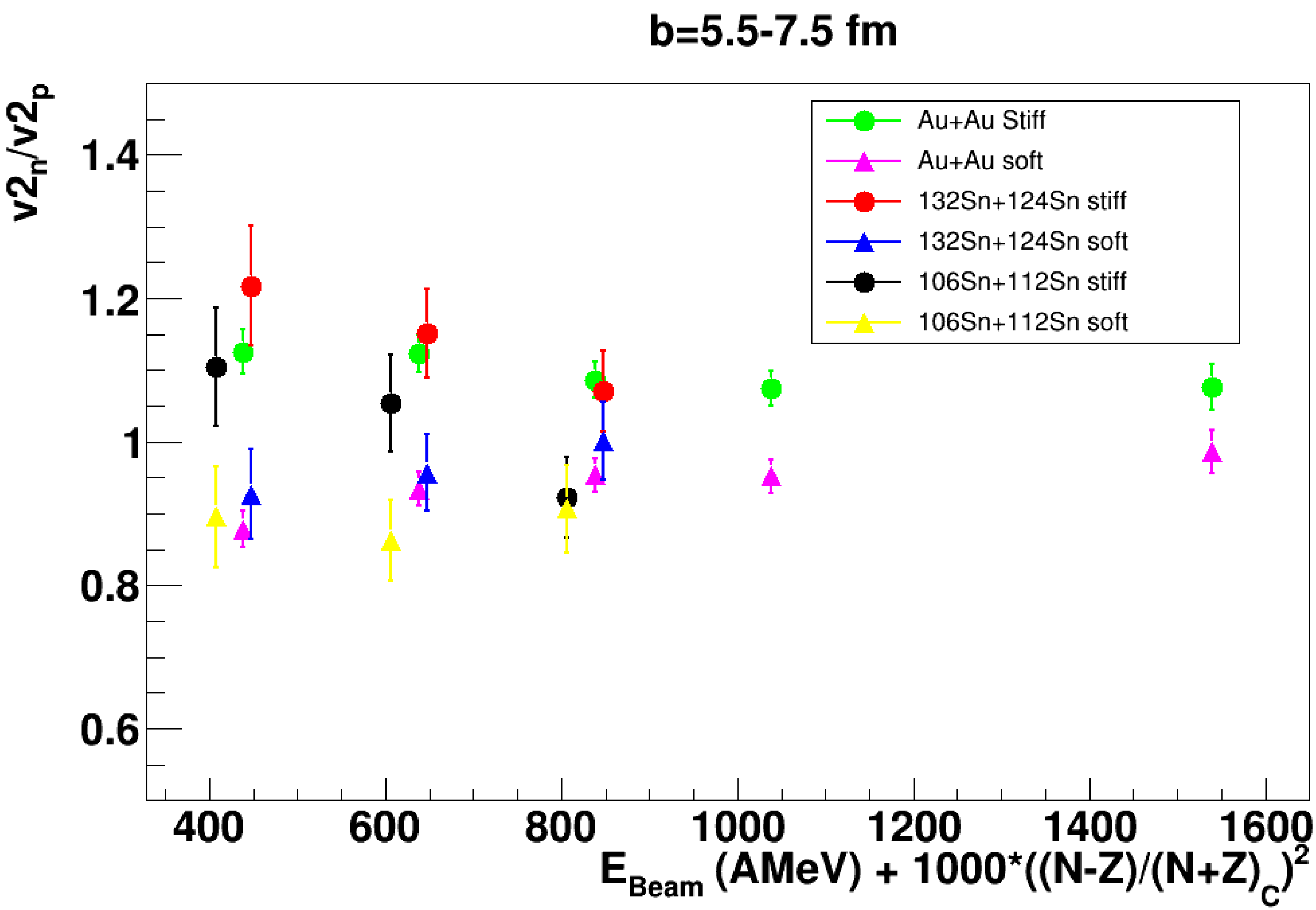

RIKEN

FUTURE Possibilities

UrQMD prediction for some interesting beams (and δ^2)

^{197}Au+^{197}Au @ 400, 600, 800, 1000,1500 AMeV (0.039+0.039)

^{132}Sn+^{124}Sn @ 400, 600, 800 AMeV (0.059+0.037)

^{106}Sn+^{112}Sn @ 400, 600, 800 AMeV (0.003+0.011)

At midvelocity b/bred <0.53

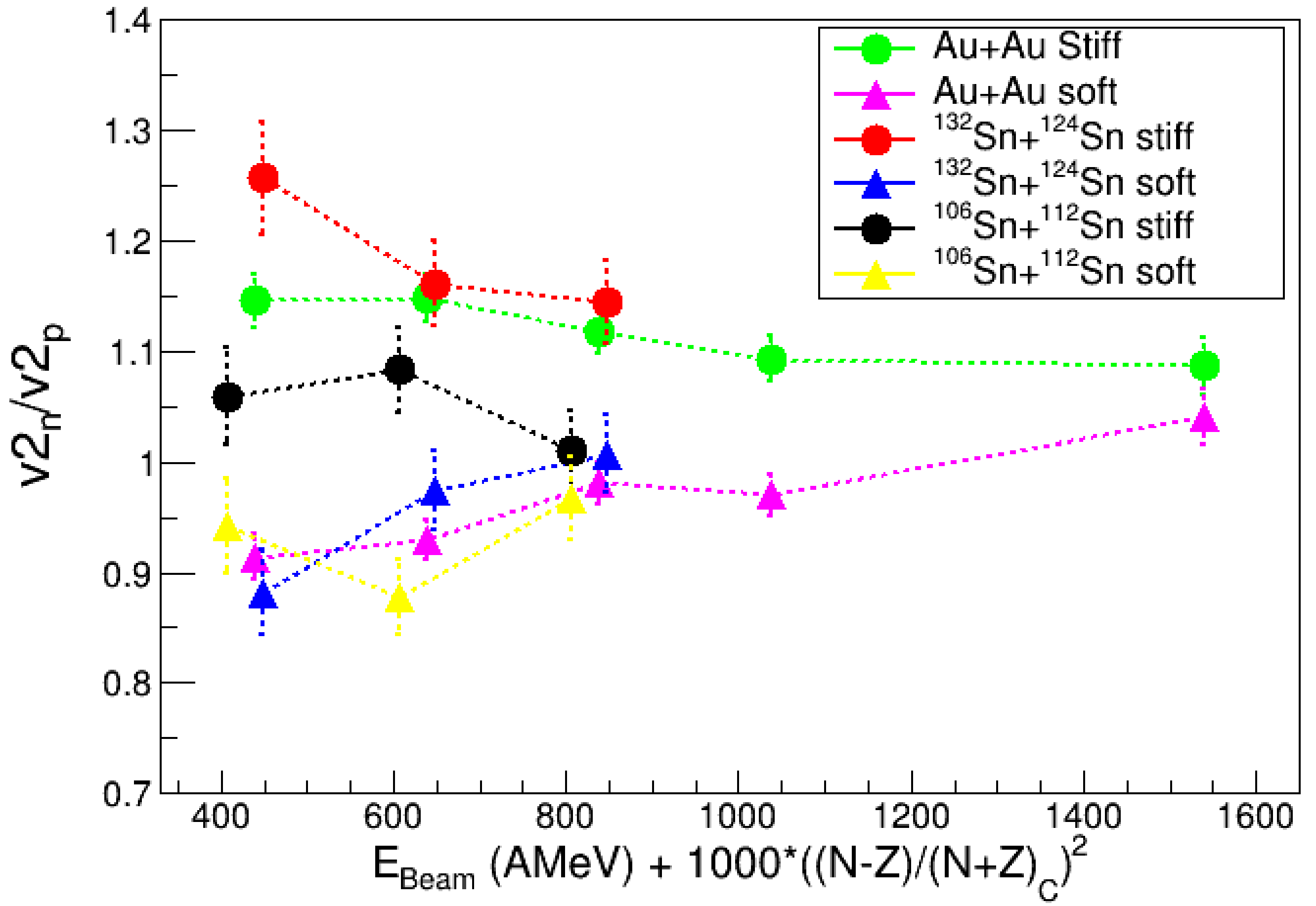

FUTURE Possibilities

UrQMD prediction for some interesting beams (and δ^2)

$^{197}Au+^{197}Au$ @ 400, 600, 800, 1000,1500 AMeV (0.039+0.039)

$^{132}Sn+^{124}Sn$ @ 400, 600, 800 AMeV (0.059+0.037)

$^{106}Sn+^{112}Sn$ @ 400, 600, 800 AMeV (0.003+0.011)

At midvelocity b/bred <0.53

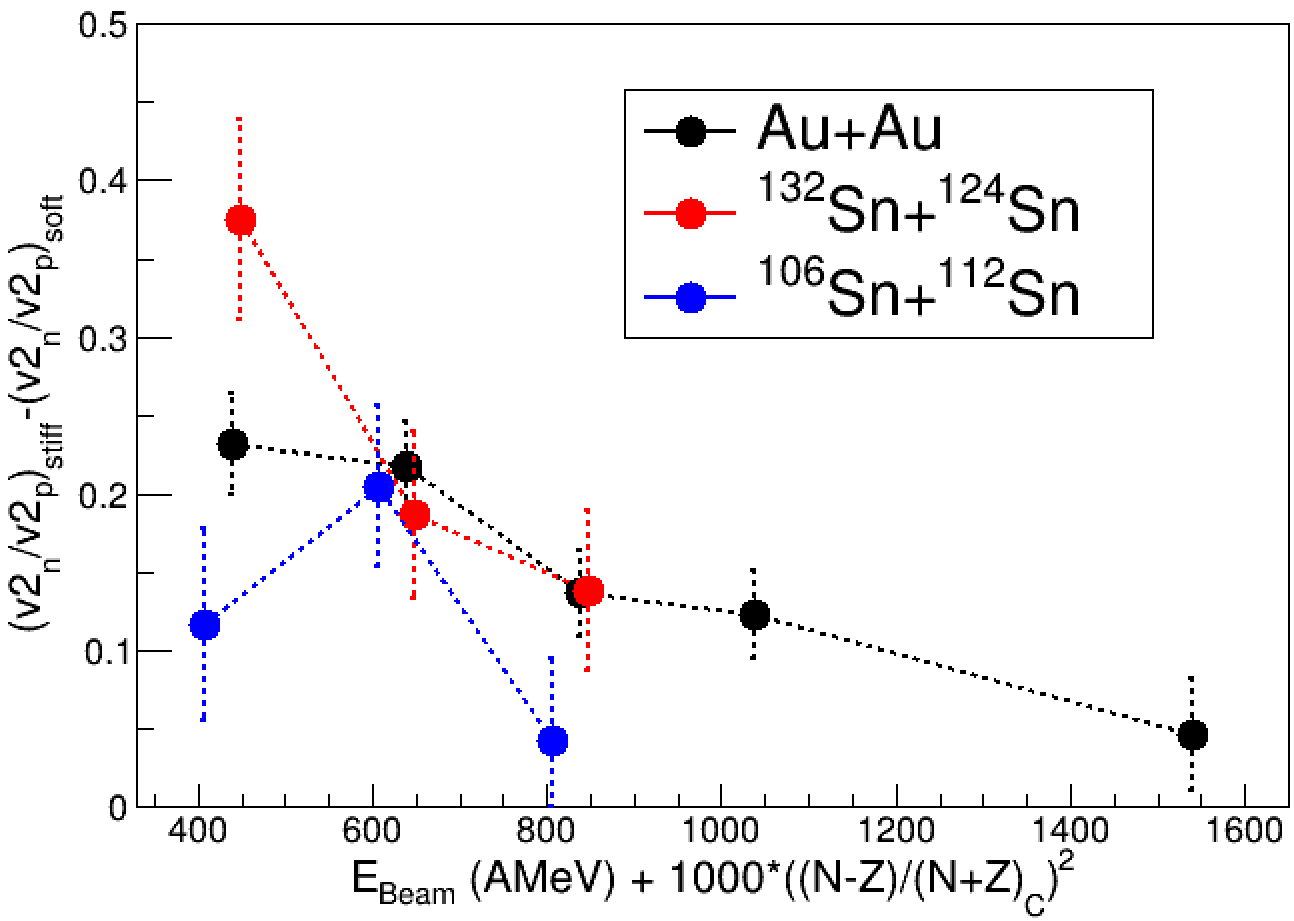

FUTURE Possibilities

UrQMD prediction for some interesting beams (and δ^2)

^{197}Au+^{197}Au @ 400, 600, 800, 1000,1500 AMeV (0.039+0.039)

^{132}Sn+^{124}Sn @ 400, 600, 800 AMeV (0.059+0.037)

^{106}Sn+^{112}Sn @ 400, 600, 800 AMeV (0.003+0.011)

At midvelocity 0.4<b/bred <0.53

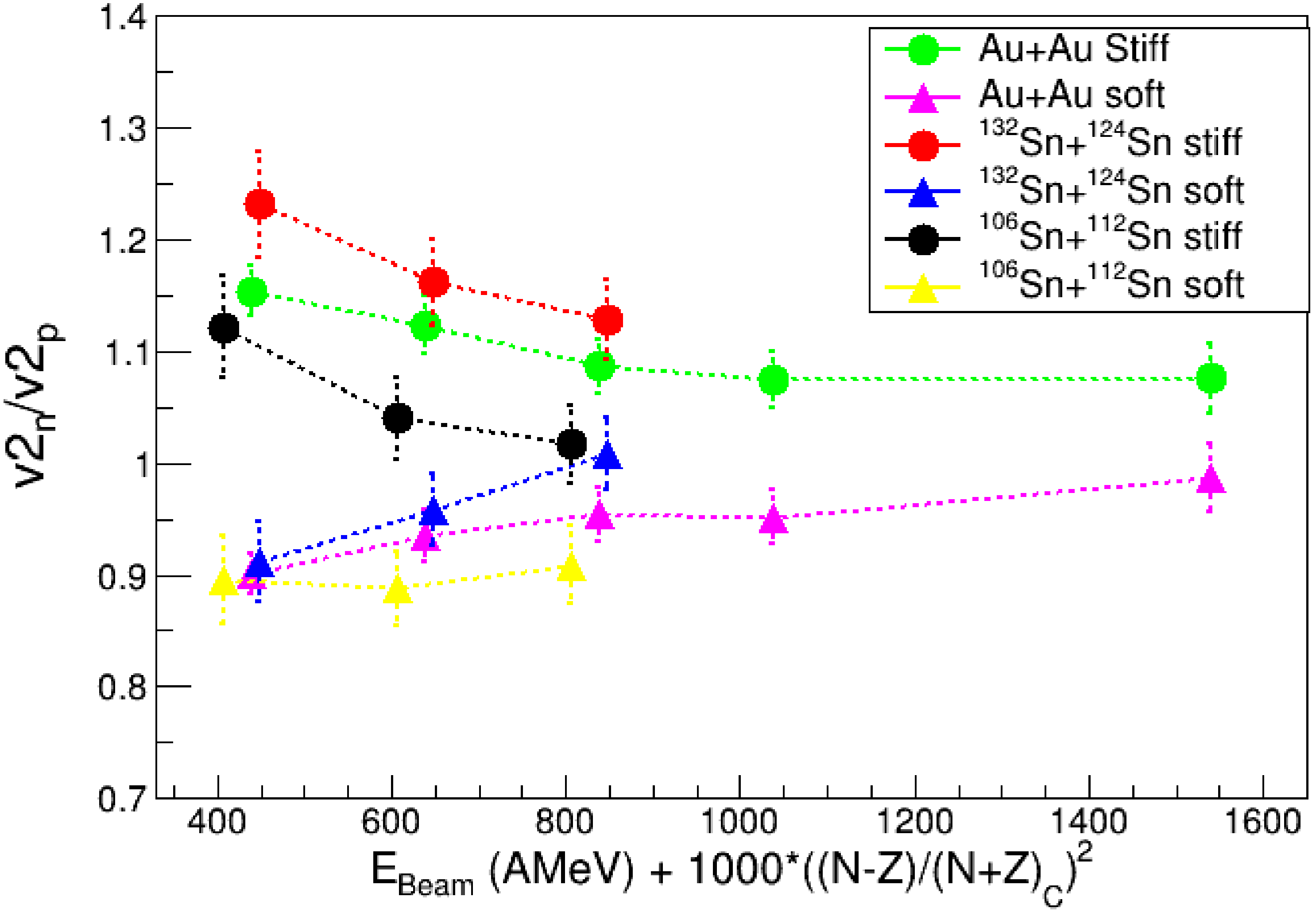

FUTURE Possibilities

UrQMD prediction for some interesting beams (and δ^2)

$^{197}Au+^{197}Au$ @ 400, 600, 800, 1000,1500 AMeV (0.039+0.039)

$^{132}Sn+^{124}Sn$ @ 400, 600, 800 AMeV (0.059+0.037)

$^{106}Sn+^{112}Sn$ @ 400, 600, 800 AMeV (0.003+0.011)

At midvelocity 0.4<b/bred <0.53

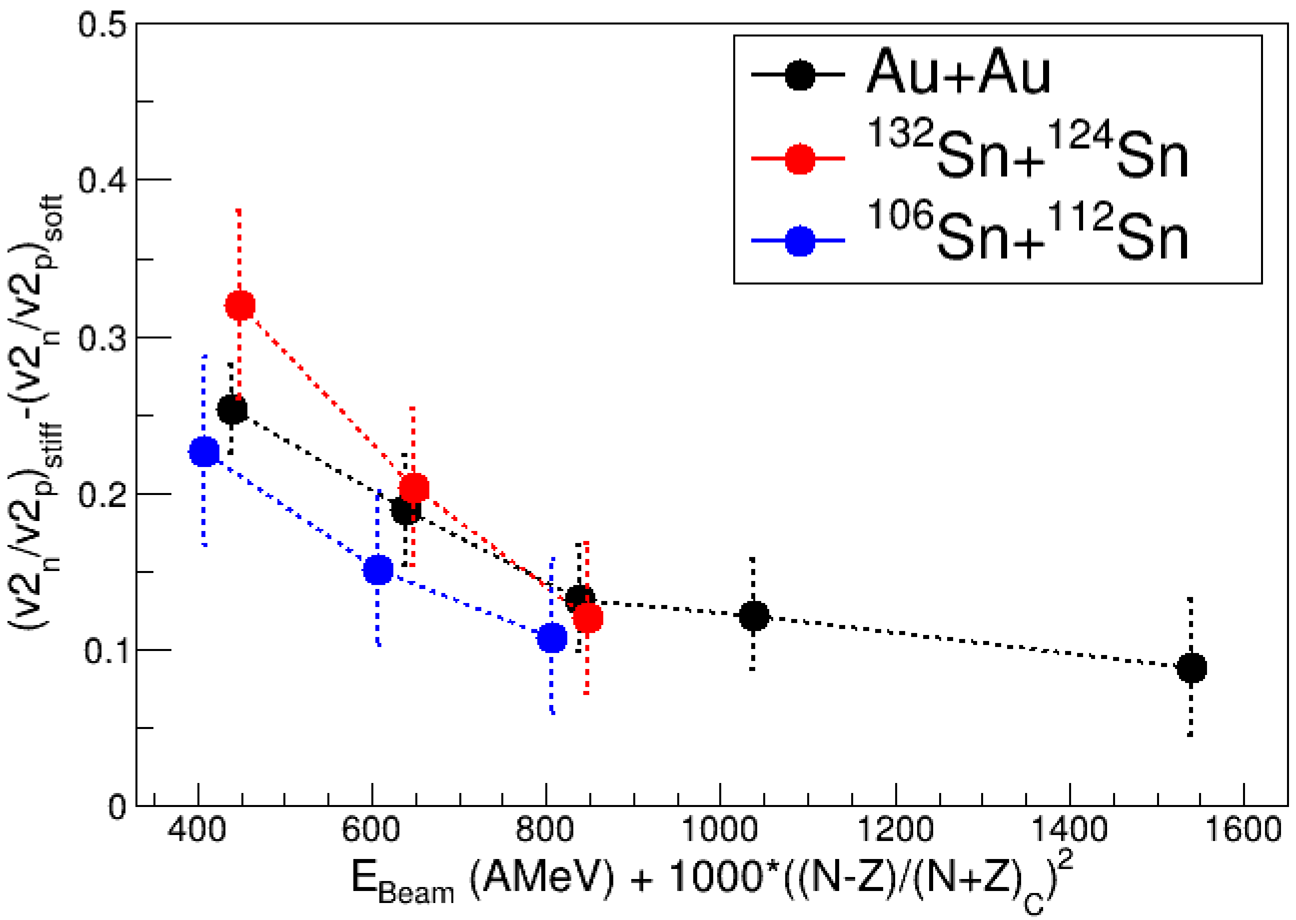

FUTURE Possibilities

UrQMD prediction for some interesting beams (and δ^2)

$^{197}Au+^{197}Au$ @ 400, 600, 800, 1000,1500 AMeV (0.039+0.039)

$^{132}Sn+^{124}Sn$ @ 400, 600, 800 AMeV (0.059+0.037)

$^{106}Sn+^{112}Sn$ @ 400, 600, 800 AMeV (0.003+0.011)

At midvelocity 0.4<b/bred <0.53

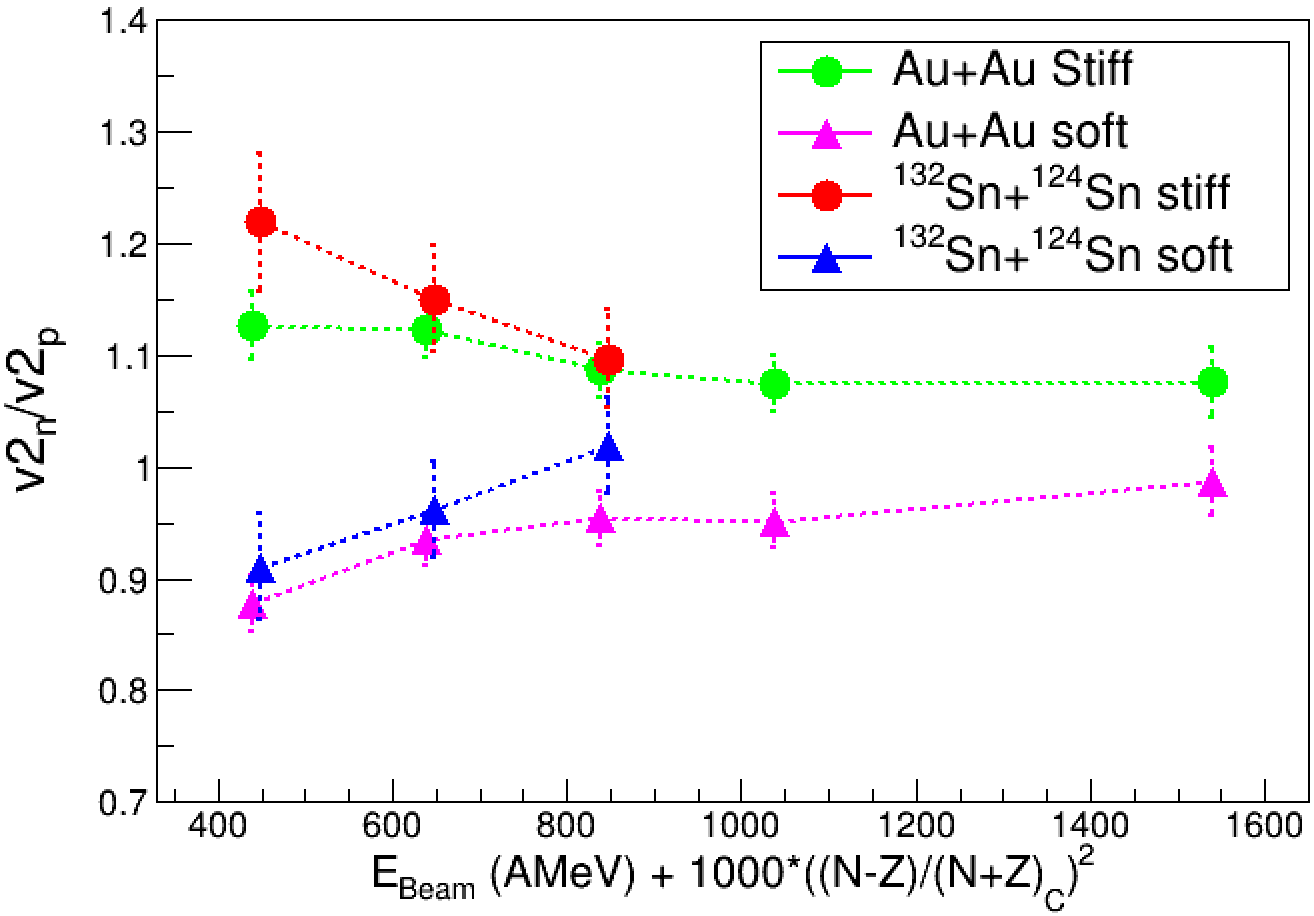

FUTURE Possibilities

UrQMD prediction for some interesting beams (and δ^2)

$^{197}Au+^{197}Au$ @ 400, 600, 800, 1000,1500 AMeV (0.039+0.039)

$^{132}Sn+^{124}Sn$ @ 400, 600, 800 AMeV (0.059+0.037)

$^{106}Sn+^{112}Sn$ @ 400, 600, 800 AMeV (0.003+0.011)

At midvelocity 0.4<b/bred <0.53

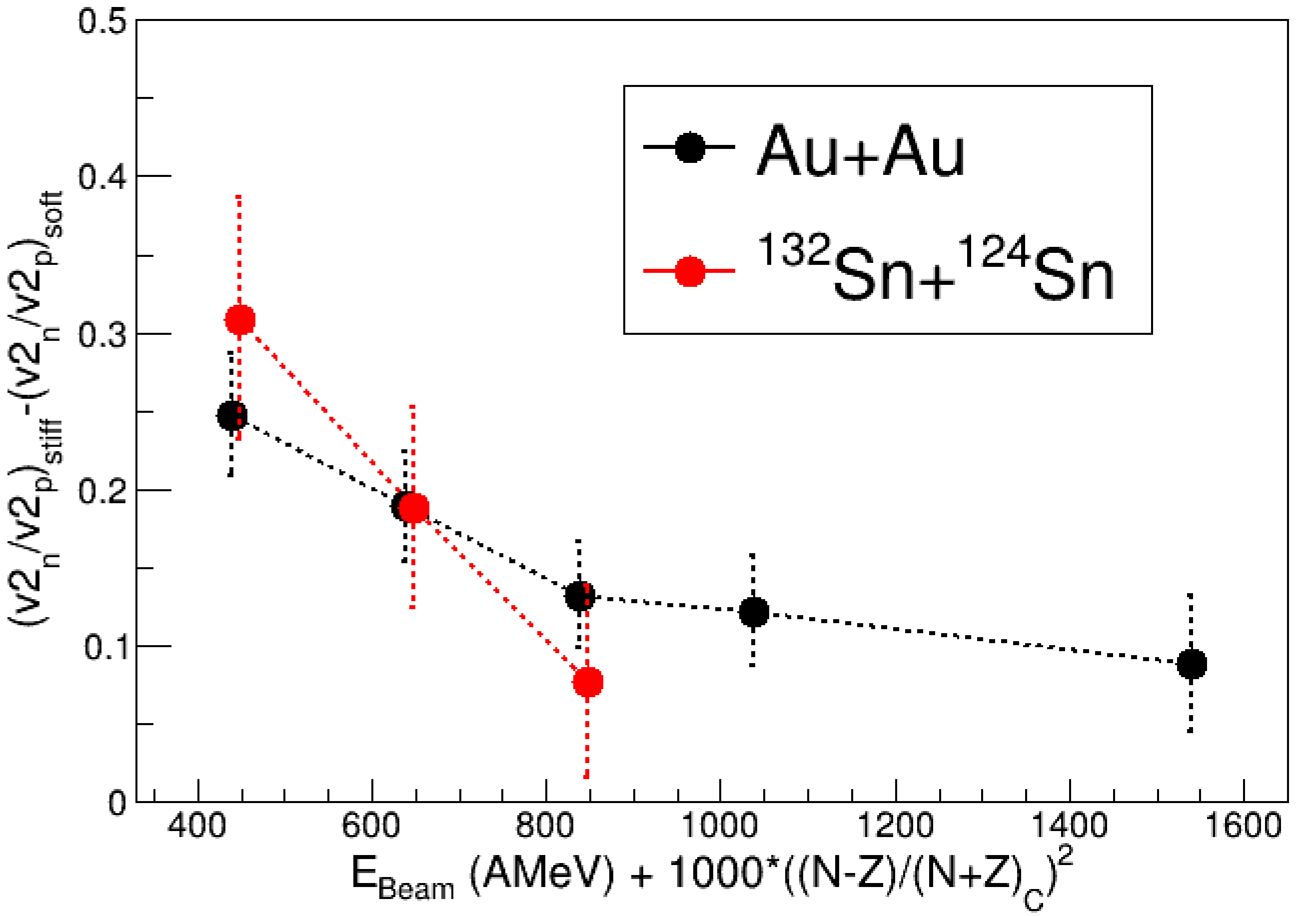

PION && KAONS

sistemare

Esym at high density: pions

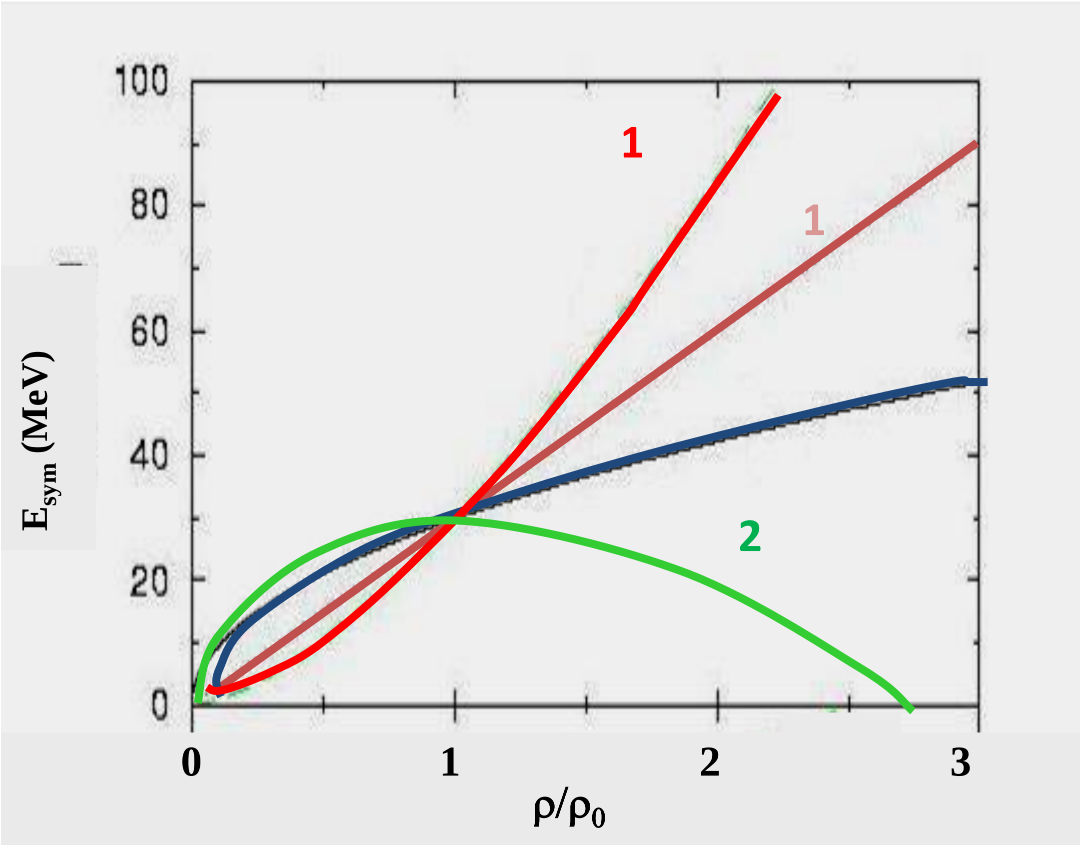

See:

Z. Xiao et al., PRL 102 (2009) IBUU04

Z.Q. Feng, PLB 683 (2010) ImIQMD

W.J. Xie , et al., PLB 718 (2013) ImIBL

G. Ferini, et al., NPA 762 (2005) RMF

From IWM 2011 – Y. Leifels

Esym at high density: pions

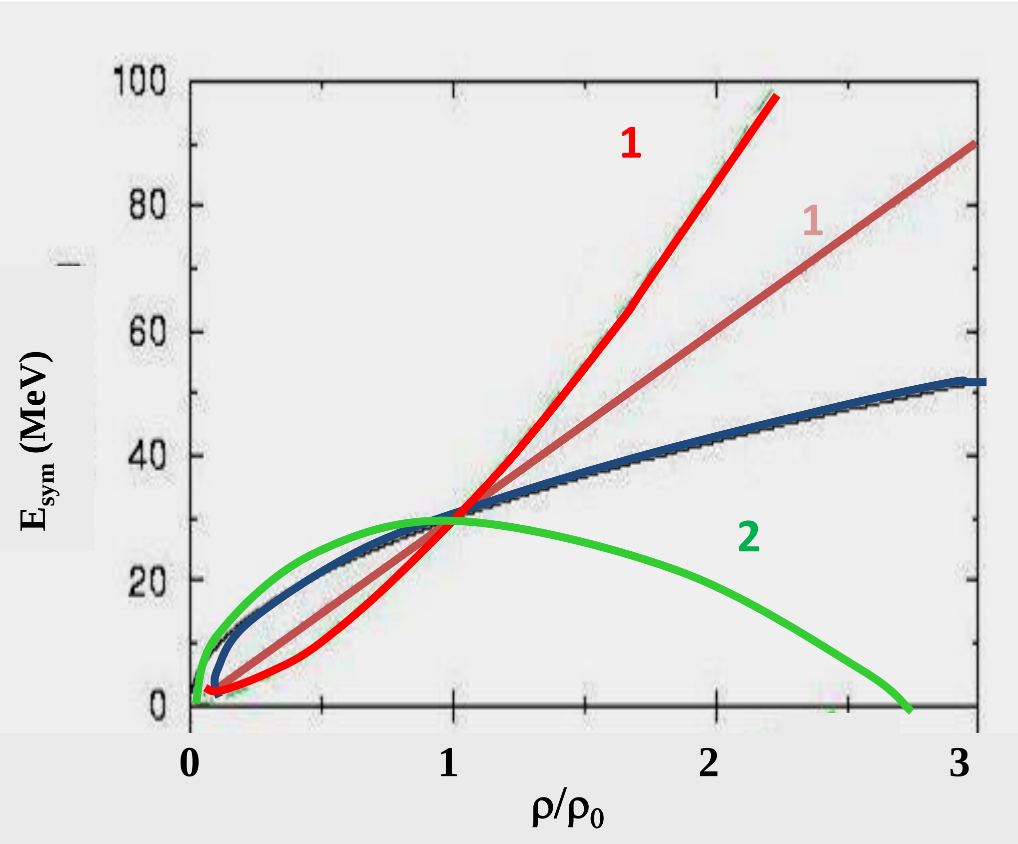

- Results model dependent
- Density dependence of symmetry energy unambiguously soft or hard
- BUT
- symmetry energy → n/p ratio, number of nn, np, pp collisions

$$\text{asystiff} \frac{n}{p} \downarrow \Rightarrow \frac{Y(\Delta^{0,-})}{Y(\Delta^{+,++})} \downarrow \Rightarrow \frac{\pi^-}{\pi^+} \downarrow$$

- medium → effective masses (N, π, Δ), cross sections → thresholds

$$\text{asystiff} \Rightarrow \frac{\pi^-}{\pi^+} \uparrow$$

→ Interpretation of pion data not straight forward

See:

Z. Xiao et al., PRL 102 (2009) IBUU04

Z.Q. Feng, PLB 683 (2010) ImIQMD

W.J. Xie , et al., PLB 718 (2013) ImIBL

G. Ferini, et al., NPA 762 (2005) RMF

From IWM 2011 – Y. Leifels

Esym at high density: pions

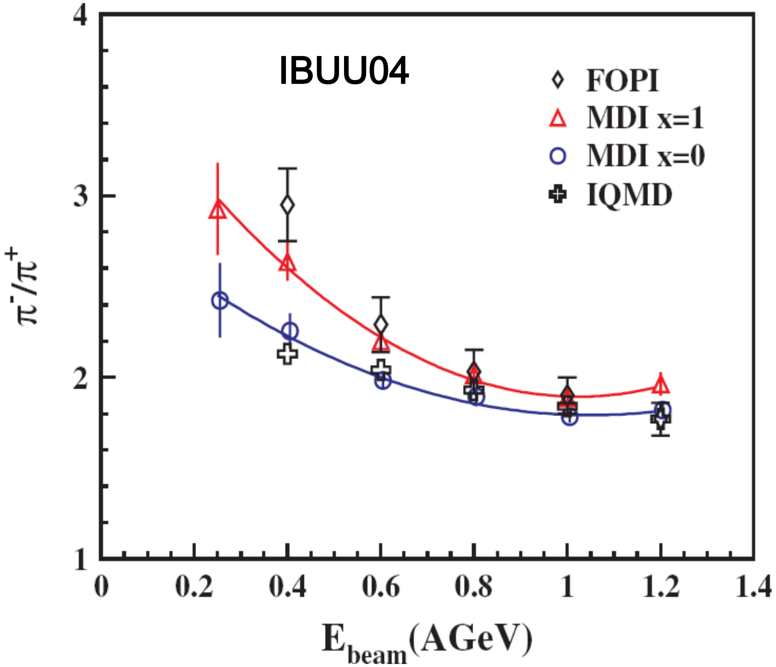

Z. Xiao et al., PRL 102 (09)

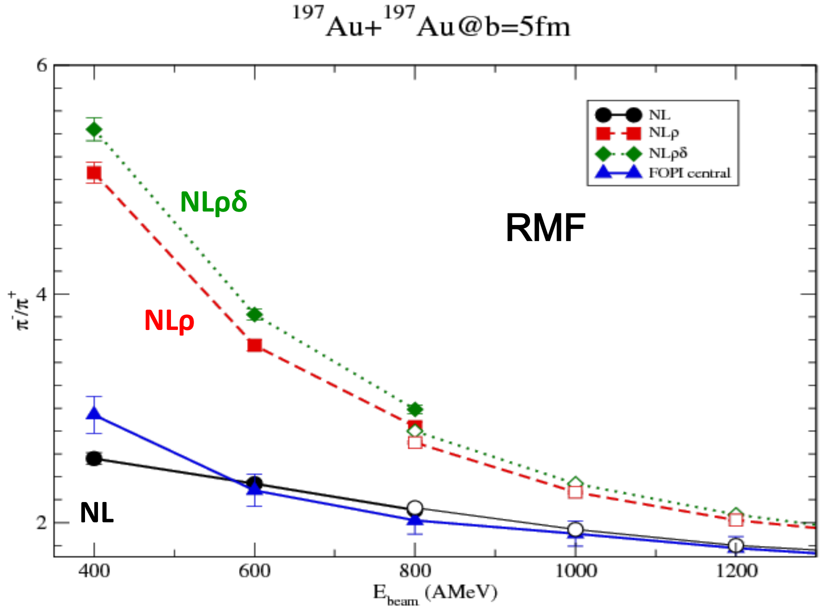

Ferini, at al., NPA 762 (2005)

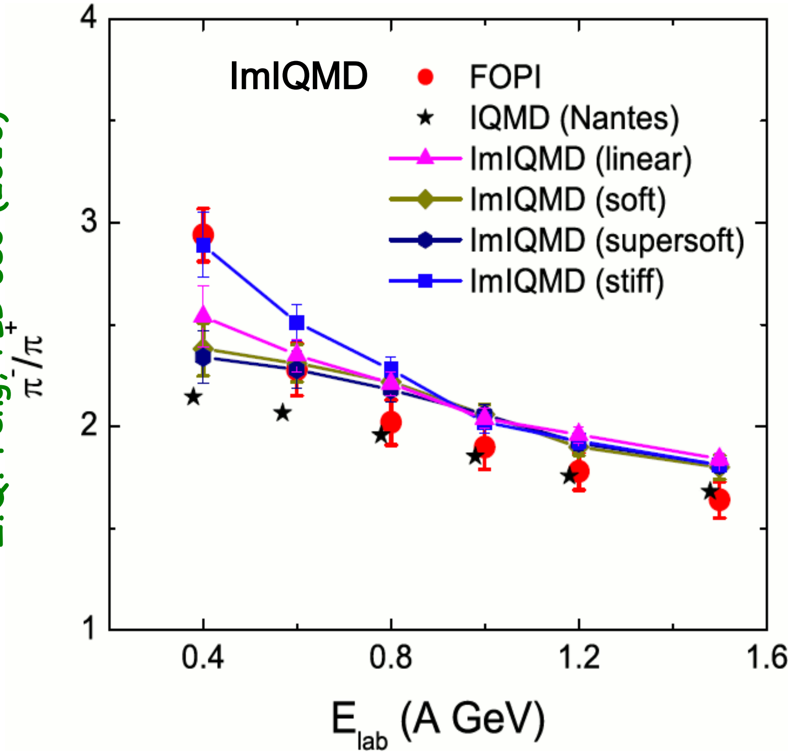

Z.Q. Feng, PLB 683 (2010)

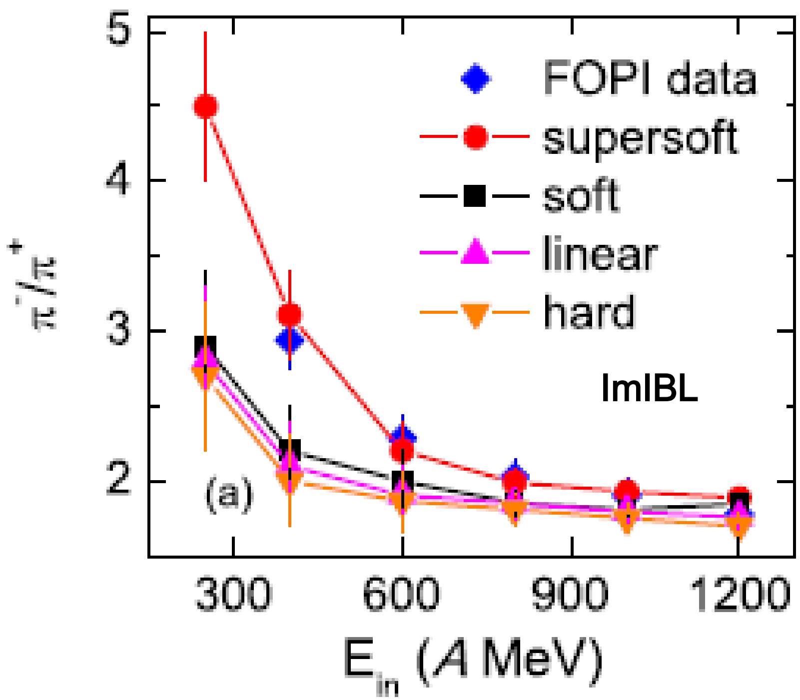

W.J. Xie , at al., PLB 718 (2013)

Device: SAMURAI TPC (U.S. Japan Collaboration)

T. Murakami[a], Jiro Murata[b], Kazuo Ieki[b], Hiroyoshi Sakurai[c], Shunji Nishimura[c], Atsushi Taketani[c], Yoichi Nakai[c], Betty Tsang[d], William Lynch[d], Abigail Bickley[d], Gary Westfall[d], Michael A. Famiano[e], Sherry Yennello[g], Roy Lemmon[h], Abdou Chbihi[i], John Frankland[i], Jean-Pierre Wieleczko[i] , Giuseppe Verde[j], Angelo Pagano[j], Paulo Russotto[j], Z.Y. Sun[k], Wolfgang Trautmann[l]

[a]Kyoto University, [b]Rikkyo University, [c]RIKEN, Japan, [d]NSCL Michigan State University, [e]Western Michigan University, [g]Texas A&M University, USA, [h]Daresbury Laboratory, [i]GANIL, France, UK, [j]LNS-INFN, Italy, [k]IMP, Lanzhou, China, [l]GSI, Germany

The SAMURAI TPC would be used to constrain the density dependence of the symmetry energy through measurements of:

- Pion production
- Flow, including neutron flow measurements with the nebula array.

The TPC also can serve as an active target both in the magnet or as a standalone device.

- Giant resonances.
- Asymmetry dependence of fission barriers, extrapolation to r-process.

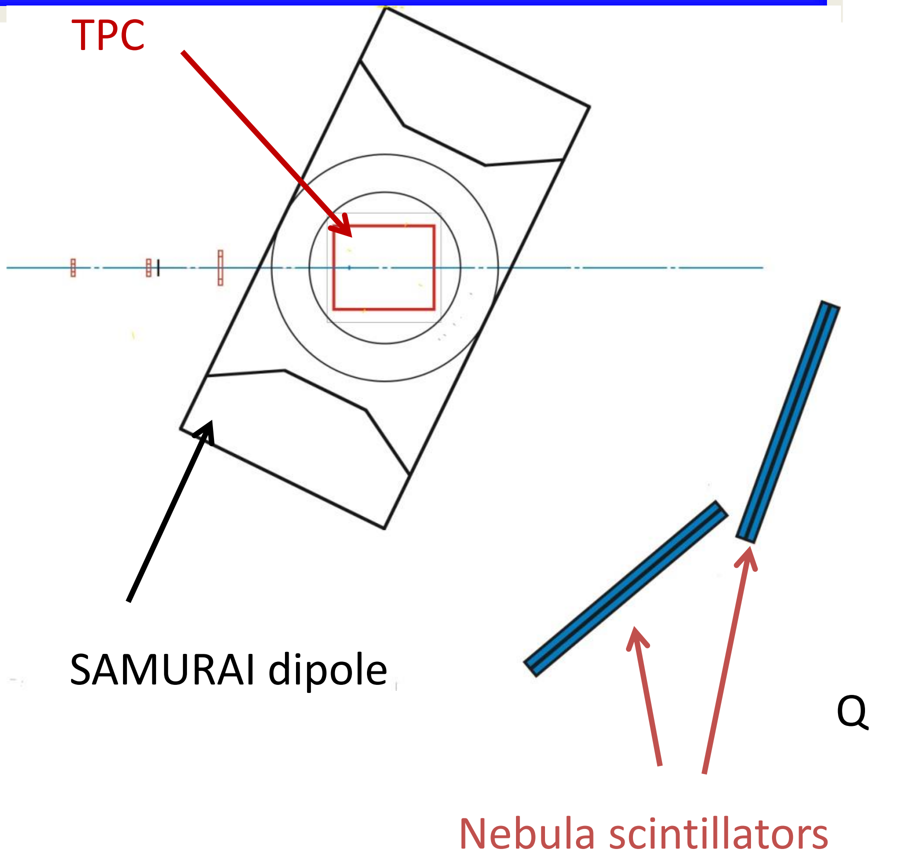

Difference between $^{132}Sn+{}^{124}Sn$ and $^{108}Sn+{}^{112}Sn$ collisions

W.G. Lynch talk @ NuSym 2014

E/A =120 MeV

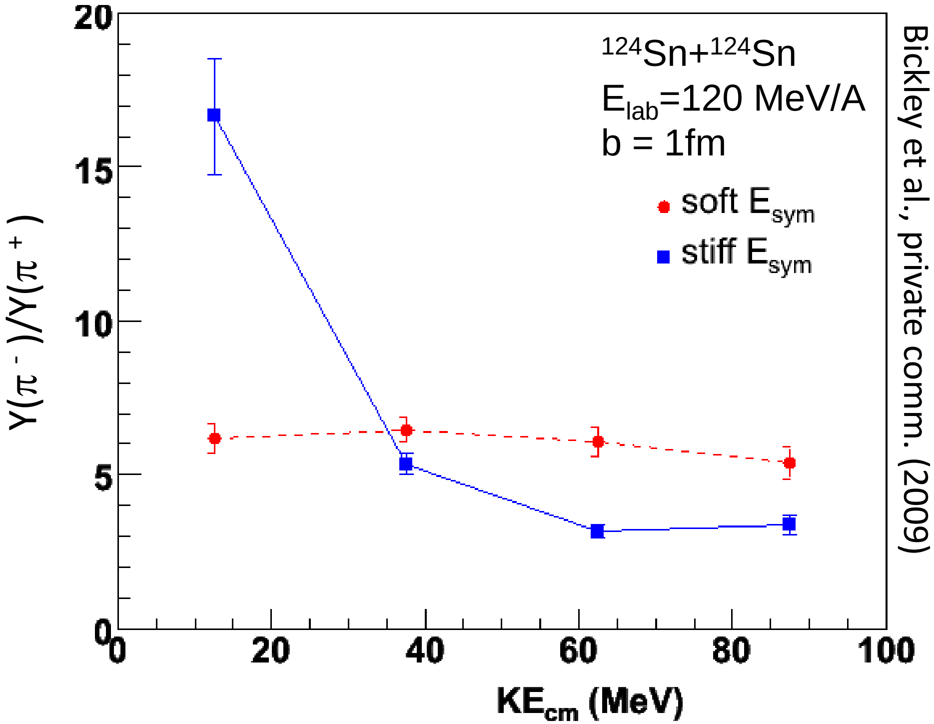

Bickley et al., private comm. (2009)

E/A = 300 MeV

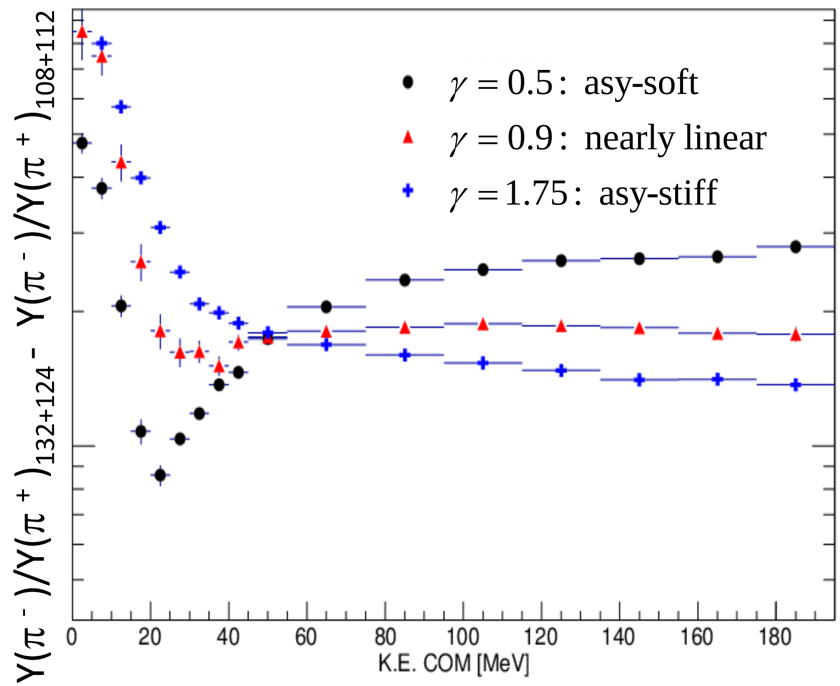

J. Hong, P. Danielewicz, private commicatons (2013)

- Pion ratio depends strongly on the symmetry energy.
- Ratios of spectra are more sensitive than ratios of integrated yields.
  - Integrated yields at E/A≥400 MeV suggest soft symmetry energy at $\rho \geq 2.5\rho_0$ (Xiao PRL, 102, 062502 (2009)
- Built two TPC's to probe these observables
  - E/A<150 MeV at MSU and E/A=200-350 MeV at RIKEN (probes $\rho \approx 2\rho_0$).

Pion and Kaon freeze-out in HIC

π^+, π^-

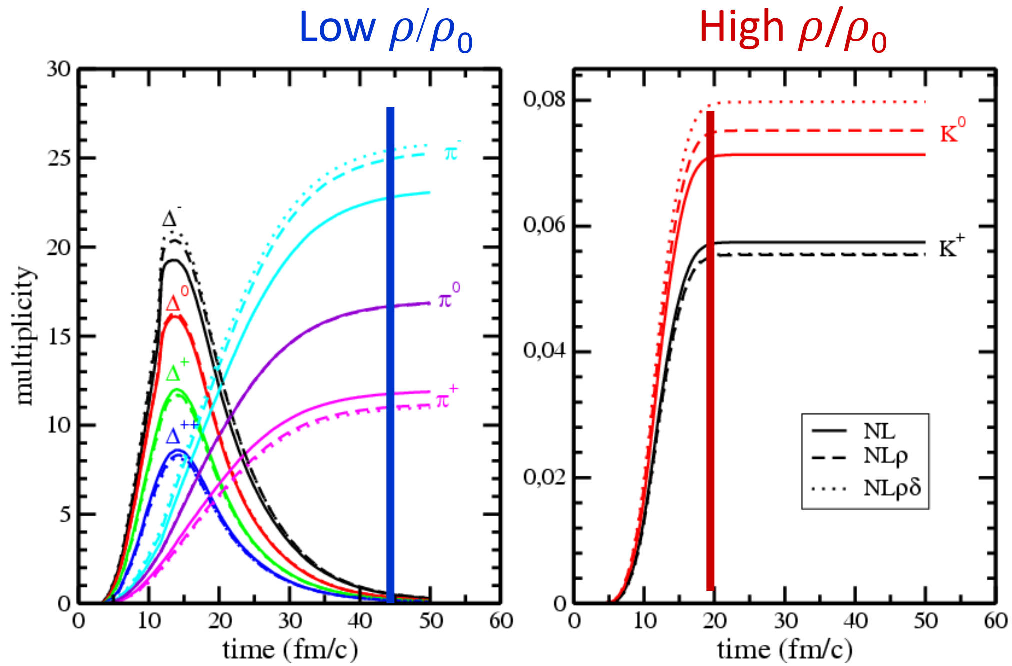

K^+,K^0

Ferini et al., PRL97, 202301

Warning with pions:

- Strongly interacting in medium
- Freeze-out at late times (low ρ/ρ_0)
- Difficult to isolate π^+ and π^- produced in the high density stage

Kaons: more sensitive probes?

- Higher thresholds
- Weakly interacting in medium
- Freeze-out already at 20 fm/c: more reliable as high ρ probes

FIG. 1 (color online). Time evolution of $\Delta^{\pm,0,++}$ resonances, pions $\pi^{\pm,0}$ (left), and kaons $K^{0,+}$ (right) for a central ($b = 0$ fm impact parameter) Au + Au collision at 1*A* GeV incident energy. Transport calculation using the NL, NLρ, NL$\rho\delta$, and DDF models for the isovector part of the nuclear EOS are shown.

For exp. results see
X.Lopez et al. (Fopi coll.) PRC 75, 011901 2007

Pion and Kaon freeze-out in HIC

Low ρ/ρ_0 High ρ/ρ_0

π^+, π^-

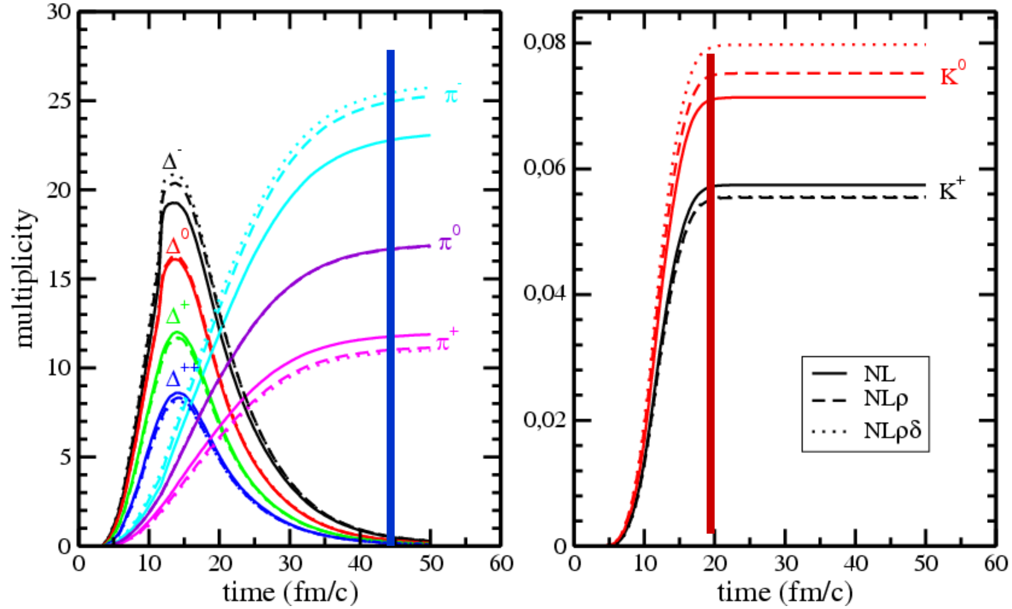

K^+,K^0

Ferini et al., PRL97, 202301

Warning ?

FOR OTHER INTERESTING OBSERVABLE SEE:

Zhi-Gang Xiao et al., Eur. Phys. J. A (2014) 50: 37

- Strong
- Freeze-out at late times (low ρ/ρ_0)
- Difficult to isolate π^+ and π^- produced in the high density stage

- Weakly interacting in medium
- Freeze-out already at 20 fm/c: more reliable as high ρ probes

FIG. 1 (color online). Time evolution of $\Delta^{\pm,0,++}$ resonances, pions $\pi^{\pm,0}$ (left), and kaons $K^{0,+}$ (right) for a central ($b = 0$ fm impact parameter) Au + Au collision at 1*A* GeV incident energy. Transport calculation using the NL, NLρ, NL$\rho\delta$, and DDF models for the isovector part of the nuclear EOS are shown.

For exp. results see
X.Lopez et al. (Fopi coll.) PRC 75, 011901 2007

particella	*massa* (MeV/c^2)	*decadimento*	*vita media* (s)
$K^{\pm}$	494	$K^{\pm} \rightarrow \pi^{\pm}\pi^{0}$	$1.24\ 10^{-8}$
K^{0}	498	$K^{0} \rightarrow \pi^{-}\pi^{+}$	$0.89\ 10^{-10}$
Λ^{0}	1116	$\Lambda^{0} \rightarrow p\pi^{-}$	$2.63\ 10^{-10}$

$$\pi^{-}p \rightarrow K^{0}\Lambda^{0} \qquad \pi^{-}p \rightarrow K^{0}K^{-}p$$
$$\pi^{+}n \rightarrow K^{+}\Lambda^{0} \qquad \pi^{+}n \rightarrow K^{+}K^{-}p$$

ma *non si osserva* $\pi^{-}n \rightarrow K^{-}\Lambda^{0}$. Un'altra peculiarità osservata è

$$\text{probabilità di produzione di } K^{+} \gg \text{probabilità di produzione di } K^{-}$$
$$\text{probabilità di interazione di } K^{+} \ll \text{probabilità di interazione di } K^{-}$$

$\pi^0 \rightarrow \gamma\gamma$	0.988	*interazione elettromagnetica*
$\pi^0 \rightarrow e^+e^-\gamma$	0.012	$\tau = 0.84\ 10^{-16}\ s$
$\pi^0 \rightarrow e^+e^-$	$6.2\ 10^{-8}$	
$\pi^+ \rightarrow \mu^+\nu_\mu$	1.000	*interazione debole*
$\pi^+ \rightarrow e^+\nu_e$	$1.2\ 10^{-4}$	$\tau = 2.60\ 10^{-8}\ s$

I modi di decadimento dei mesoni K carichi e le probabilità di decadimento sono

$K^+ \rightarrow$	$\mu^+\nu_\mu$	0.635	*decadimenti*
	$e^+\nu_e$	$1.6\ 10^{-5}$	*leptonici*
	$\pi^0 e^+\nu_e$	0.048	*decadimenti*
	$\pi^0\mu^+\nu_\mu$	0.032	*semileptonici*
	$\pi^+\pi^0$	0.212	*decadimenti*
	$\pi^+\pi^+\pi^-$	0.056	*adronici*
	$\pi^+\pi^0\pi^0$	0.017	

$$K^+ = u\bar{s} \qquad K^- = d\bar{s} \qquad \pi^+ = u\bar{d}$$
$$K^0 = \bar{u}s \qquad \bar{K}^0 = \bar{d}s \qquad \pi^+ = \bar{u}d$$

Probing the Nuclear Equation of State by K^+ Production in Heavy-Ion Collisions

C. Fuchs, Amand Faessler, and E. Zabrodin
Institut für Theoretische Physik der Universität Tübingen, Auf der Morgenstelle 14, D-72076 Tübingen, Germany

Yu-Ming Zheng
China Institute of Atomic Energy, P.O. Box 275 (18), Beijing 102413, China
(Received 10 July 2000; revised manuscript received 15 November 2000)

In the energy range considered here, the nucleon-nucleon inelastic channels can be restricted to the excitation of the lowest mass resonance $\Delta(1232)$ and perturbative kaon ($K^{+,0}$) production through baryon-baryon collisions $BB \rightarrow BYK$, where B stands for nucleons or resonances and Y for hyperons (Λ, $\Sigma^{\pm,0}$). Pions are produced via the decay of the $\Delta(1232)$ resonance and—after propagation and rescattering—can contribute to the kaon yield through collisions with baryons: $\pi B \rightarrow YK$. All of

Circumstantial Evidence for a Soft Nuclear Symmetry Energy at Suprasaturation Densities

Zhigang Xiao,[1] Bao-An Li,[2,*] Lie-Wen Chen,[3] Gao-Chan Yong,[4] and Ming Zhang[1]
[1]Department of Physics, Tsinghua University, Beijing 100084, P.R. China
[2]Department of Physics, Texas A&M University-Commerce, Commerce, Texas 75429-3011, USA
[3]Institute of Theoretical Physics, Shanghai Jiao Tong University, Shanghai 200240, P.R. China
[4]Institute of Modern Physics, Chinese Academy of Sciences, Lanzhou 730000, P.R. China
(Received 1 August 2008; revised manuscript received 1 December 2008; published 13 February 2009)

Among the most sensitive probes of the $E_{sym}(\rho)$ at suprasaturation densities proposed in the literature [6], the π^-/π^+ ratio in heavy-ion collisions is particularly promising. Qualitatively, the advantage of using the π^-/π^+ ratio is evident within both the $\Delta(1232)$ resonance model [38] and the statistical model [39] for pion production. Assuming only first chance inelastic nucleon-nucleon collisions produce pions and neglecting their reabsorptions, the Δ resonance model predicts a primordial π^-/π^+ ratio of $(\pi^-/\pi^+)_{res} \equiv (5N^2 + NZ)/(5Z^2 + NZ) \approx (N/Z)^2_{dense}$, where the N and Z are neutron and proton numbers in the participant region of the reaction. The π^-/π^+ ratio is thus a direct measure of the isospin asymmetry $(N/Z)_{dense}$ of the dense matter formed. The latter is determined by the $E_{sym}(\rho)$ through the dynamical isospin fractionation [40], namely, the high (low) density region is more neutron-rich (poor) with a lower $E_{sym}(\rho)$ at suprasaturation densities. Since effects of the $E_{sym}(\rho)$ are

Circumstantial Evidence for a Soft Nuclear Symmetry Energy at Suprasaturation Densities

Zhigang Xiao,[1] Bao-An Li,[2,*] Lie-Wen Chen,[3] Gao-Chan Yong,[4] and Ming Zhang[1]

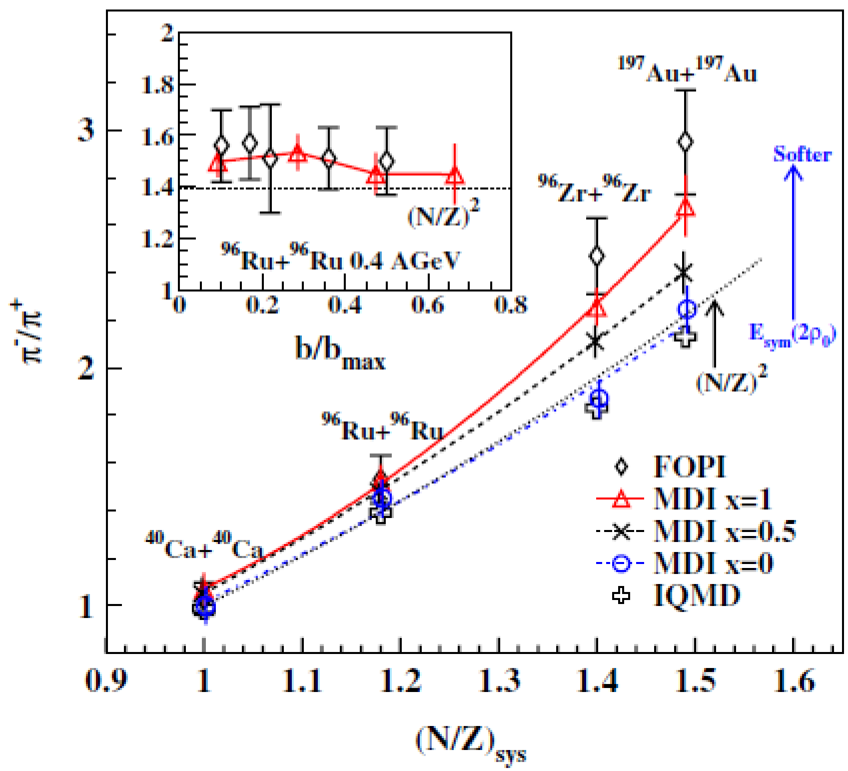

FIG. 2 (color online). The π^-/π^+ ratio as a function of the neutron/proton ratio of the reaction system at 0.4A GeV with the reduced impact parameter of $b/b_{max} \leq 0.15$. The inset is the impact parameter dependence of the π^-/π^+ ratio for the ^{96}Ru + ^{96}Ru reaction at 0.4A GeV.

PHYSICS REPORTS (Review Section of Physics Letters) 135, No. 5 (1986) 259–315. North-Holland, Amsterdam

PARTICLE PRODUCTION IN HIGH ENERGY NUCLEUS–NUCLEUS COLLISIONS

	π^+	π^0	π^-
nn	0	1	5
pp	5	1	0
np = pn	1	4	1

For collisions of identical nuclei, $N/Z^{\text{fireball}} = N/Z^{\text{proj}} = N/Z^{\text{targ}}$. We have N^2 nn collisions, Z^2 pp collisions and $2NZ$ collisions of np or pn type. The latter contribute to Δ production with half the weight of nn and pp because the np amplitude has a 50%, $T = \frac{1}{2}$ component, non-productive for single Δ formation. Summing with proper weights, we find

$$\frac{\sigma(\pi^-)}{\sigma(\pi^+)} = \frac{\langle \pi^- \rangle}{\langle \pi^+ \rangle} = \frac{5N^2 + NZ}{5Z^2 + NZ} \approx \left(\frac{N}{Z}\right)^2 . \tag{4.3}$$

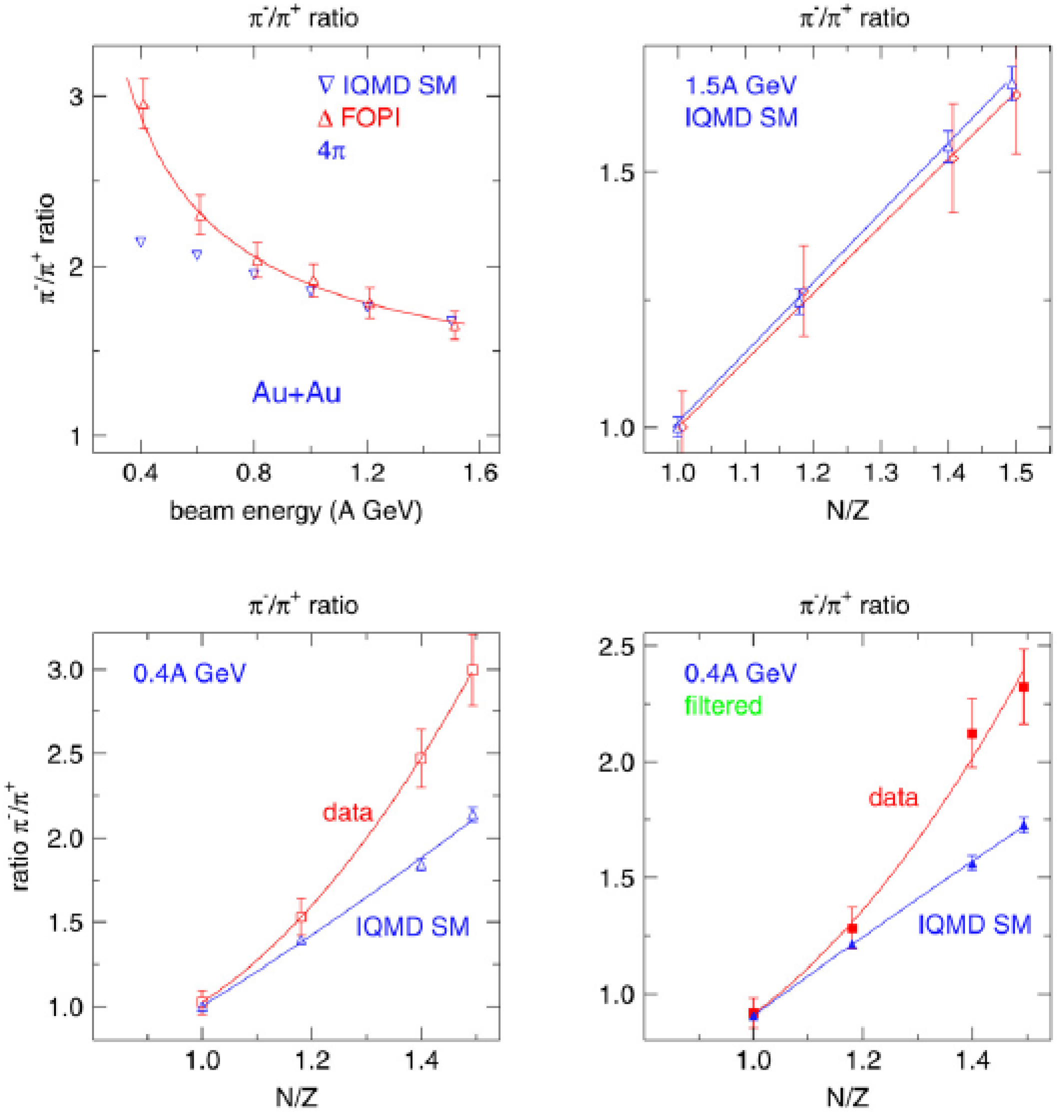

Fig. 25. Upper left panel: excitation function of the 4π-integrated ratio of π^-/π^+ yields in central Au + Au collisions. The experimental data are joined by a least squares fit of the function $c_0 + c_{-1}(E/A)^{-1}$ excluding the lowest energy point. The IQMD SM prediction (triangles) is also given. Upper right and lower left panels: the N/Z dependence at 1.5 A, respectively 0.4 A GeV of the π^-/π^+ ratio. The solid lines are least squares fits of linear or quadratic (N/Z) dependence. Lower right panel: same as lower left panel, but for filtered data.

Physics Letters B 683 (2010) 140–144

Contents lists available at ScienceDirect

Physics Letters B

www.elsevier.com/locate/physletb

Probing high-density behavior of symmetry energy from pion emission in heavy-ion collisions

Zhao-Qing Feng *, Gen-Ming Jin

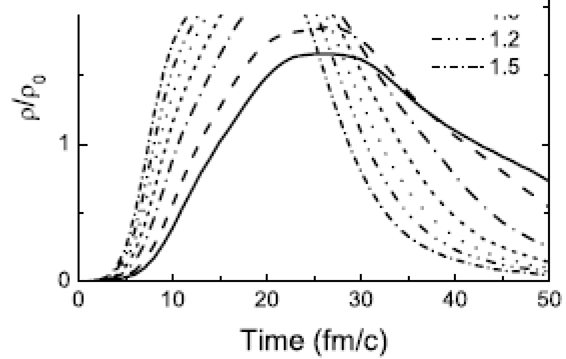

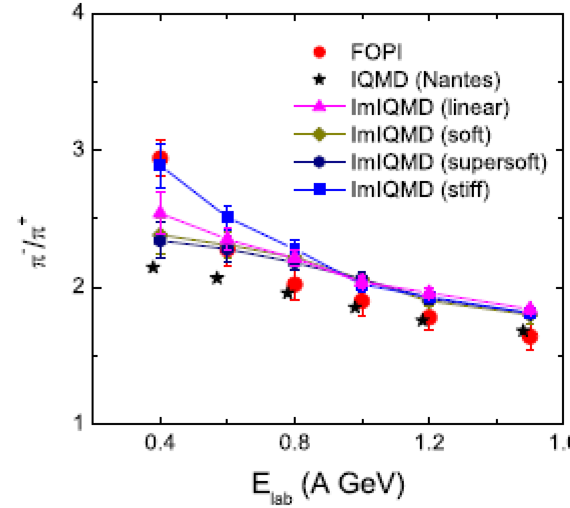

Fig. 3. Evolution of average central density at different incident energies (left panel) and the excitation functions of the π^-/π^+ ratios at different stiffness of the symmetry energy (hard, linear, soft and supersoft), and compared with IQMD results [10] as well as the FOPI data [3] (right panel).

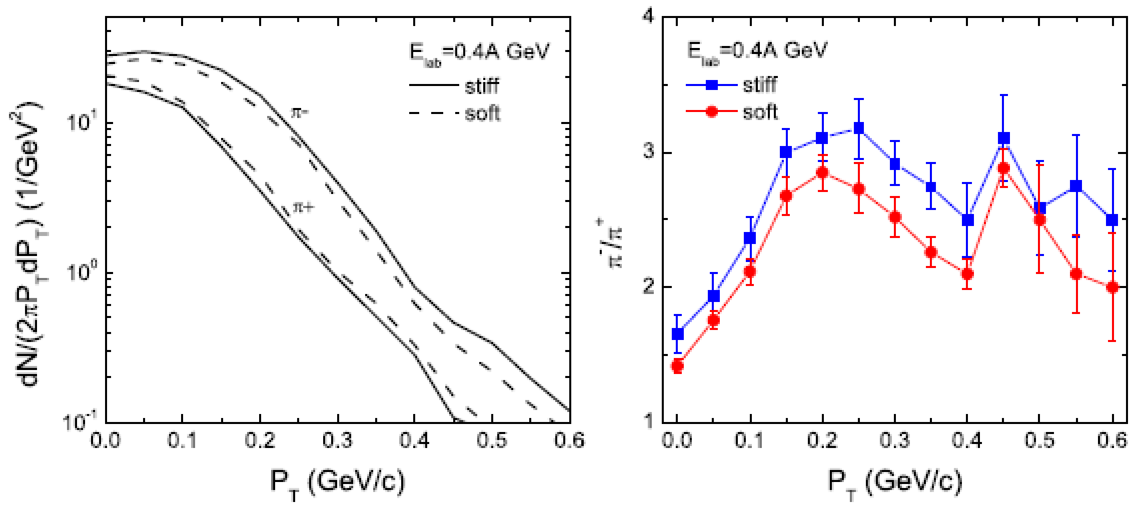

Fig. 4. Distributions of transverse momentum of final π^- and π^+ and the ratio π^-/π^+ for the cases of stiff and soft symmetry energies in the reaction ^{197}Au + ^{197}Au at incident energy $E_{lab} = 0.4$ A GeV.

Physics Letters B 683 (2010) 140–144

Contents lists available at ScienceDirect

Physics Letters B

www.elsevier.com/locate/physletb

Probing high-density behavior of symmetry energy from pion emission in heavy-ion collisions

Zhao-Qing Feng*, Gen-Ming Jin

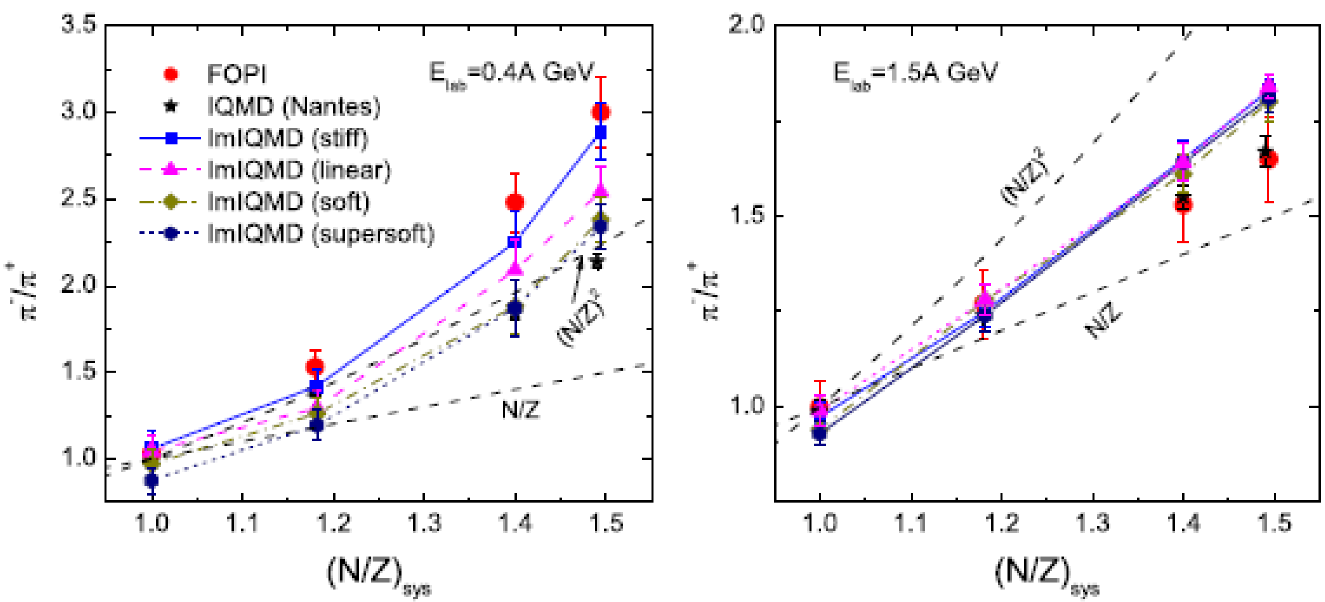

Fig. 5. The π^-/π^+ yields as a function of the neutron over proton N/Z of reaction systems for head on collisions at incident energy $E_{\text{lab}} = 0.4$ A GeV and 1.5 A GeV, respectively.

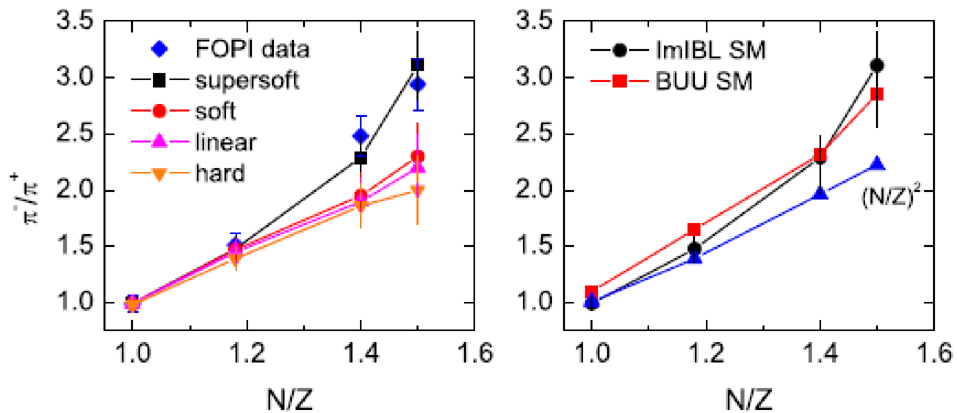

Fig. 3. (Color online.) The π^-/π^+ ratio as a function of the neutron/proton ratio of reaction systems for central ^{40}Ca + ^{40}Ca, ^{96}Ru + ^{96}Ru, ^{96}Zr + ^{96}Zr and ^{197}Au + ^{197}Au collisions at 400*A* MeV. The results are calculated by different stiffness of the symmetry energy using the ImIBL model with the SM (left panel) and different transport theories (right panel).

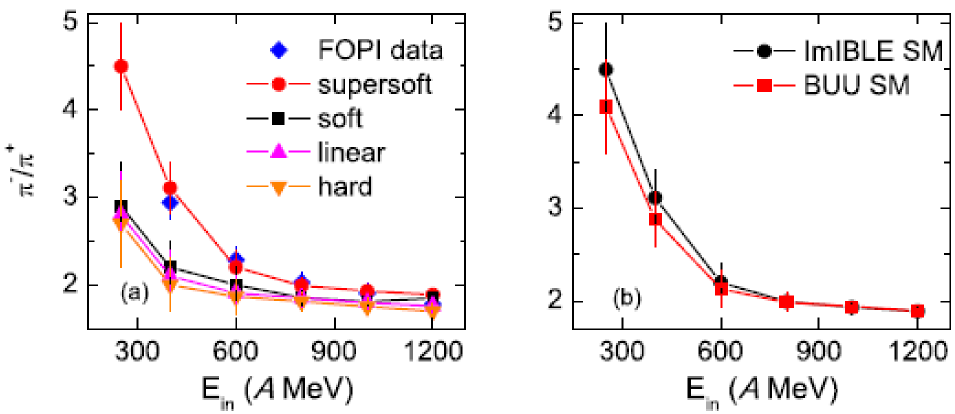

Fig. 4. (Color online.) Excitation functions of the π^-/π^+ ratio in central ^{197}Au + ^{197}Au collisions for different stiffness of the symmetry energy using the ImIBL model with the SM (left panel) and different transport theories (right panel).

High densities: π^-/π^+ ratio

FOPI Data,

W.Reisdorf et al. NPA781 (2007)

Z.Q. Feng, PLB 683 (2010)

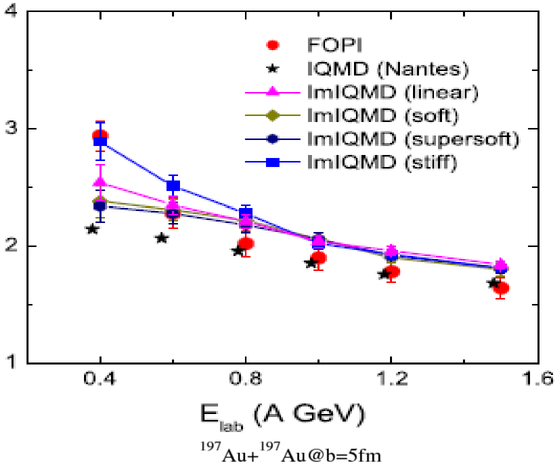

Ferini, at al., NPA 762 (05)

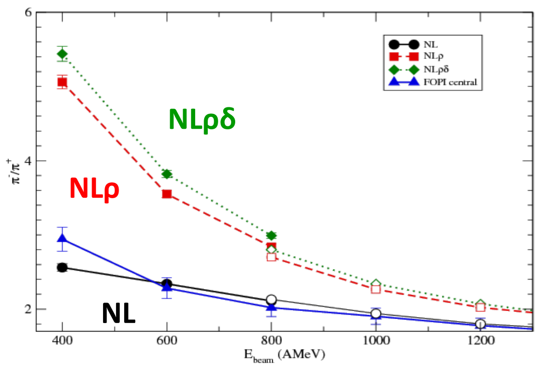

Z. Xiao et al., PRL 102 (09)

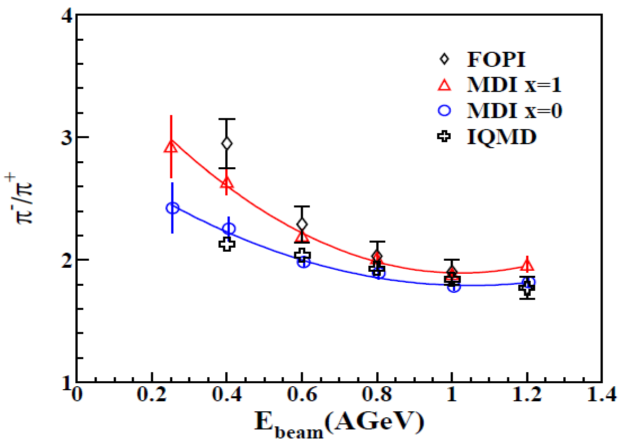

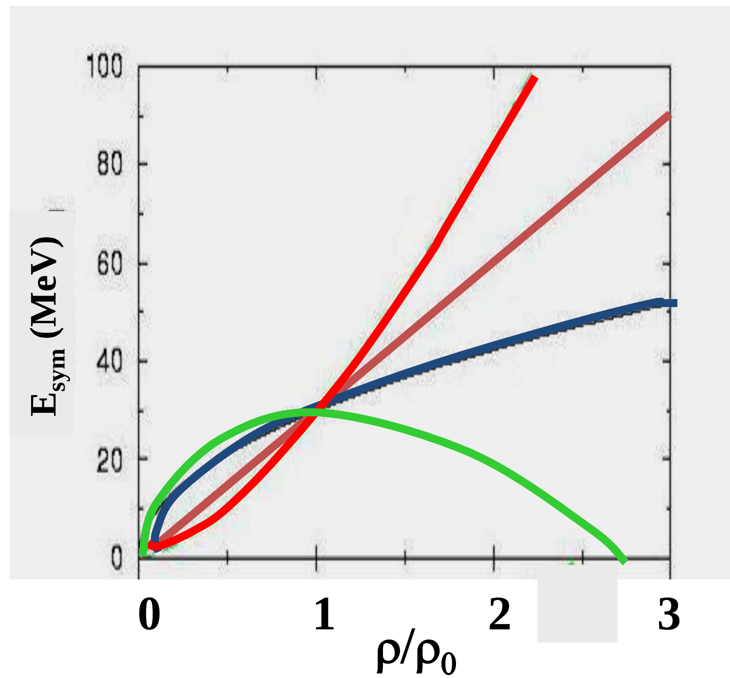

High densities: π^-/π^+ ratio

FOPI Data,

W.Reisdorf et al. NPA781 (2007)

Z.Q. Feng, PLB 683 (2010)

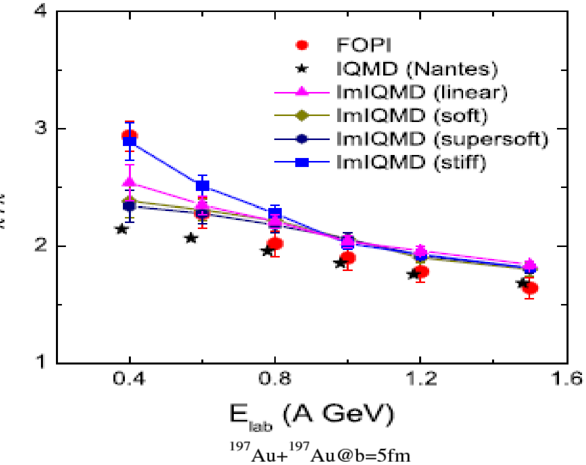

Ferini, at al., NPA 762 (05)

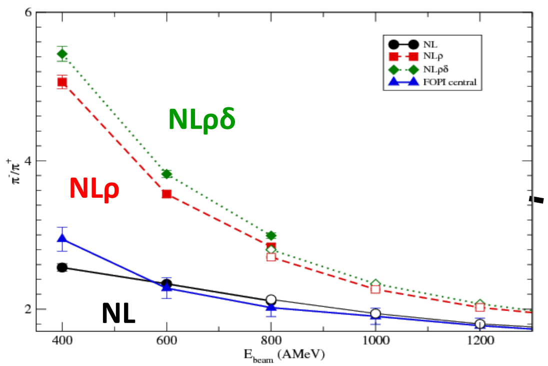

Z. Xiao et al., PRL 102 (09)

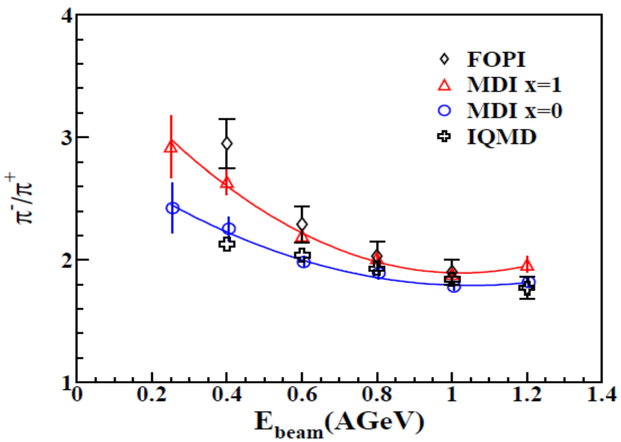

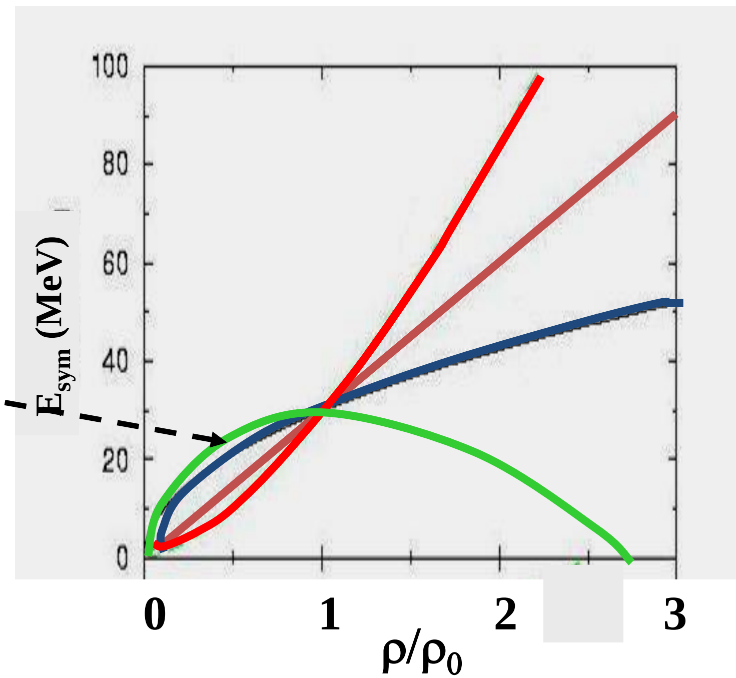

High densities: π^-/π^+ ratio

FOPI Data,

W.Reisdorf et al. NPA781 (2007)

Z.Q. Feng, PLB 683 (2010)

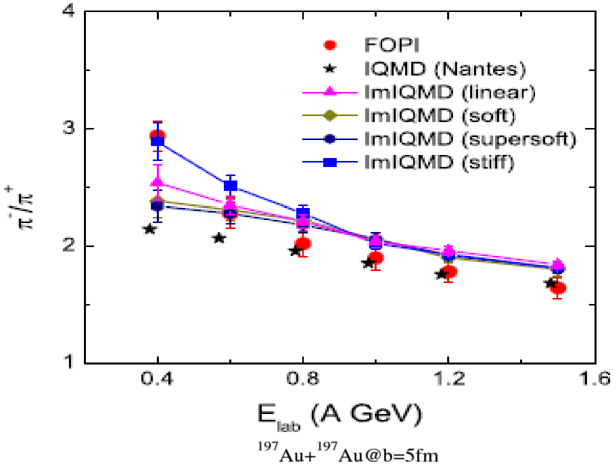

Ferini, at al., NPA 762 (05)

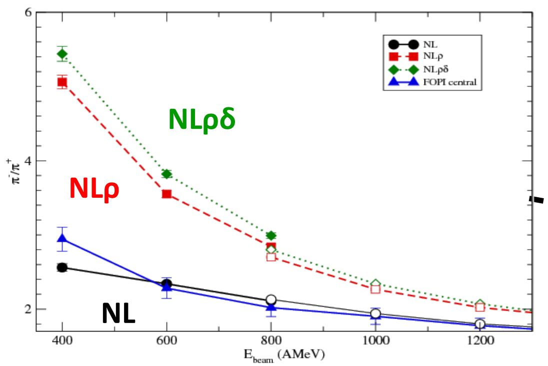

Z. Xiao et al., PRL 102 (09)

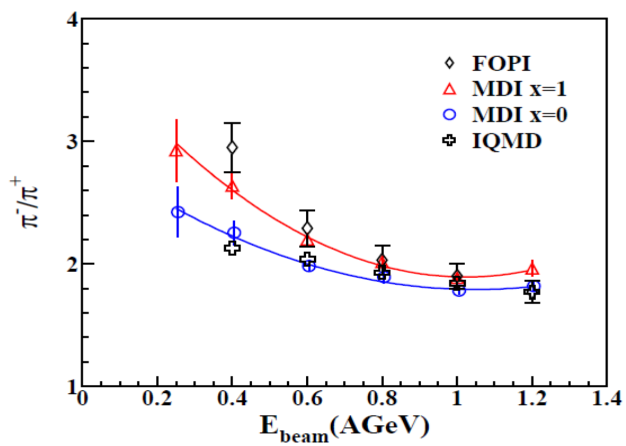

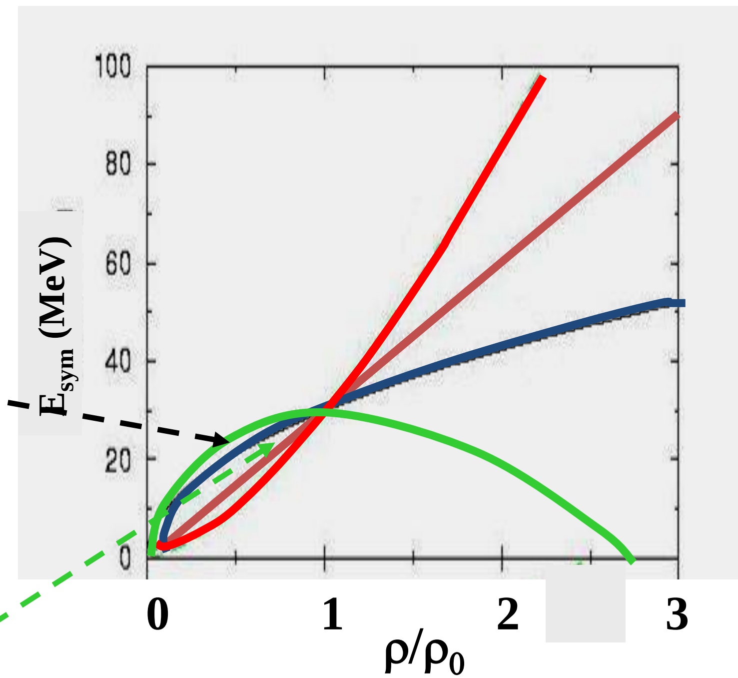

High densities: π^-/π^+ ratio

FOPI Data,

W.Reisdorf et al. NPA781 (2007)

Z.Q. Feng, PLB 683 (2010)

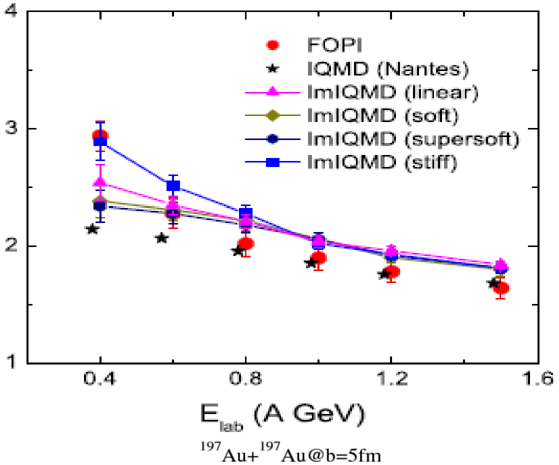

Ferini, at al., NPA 762 (05)

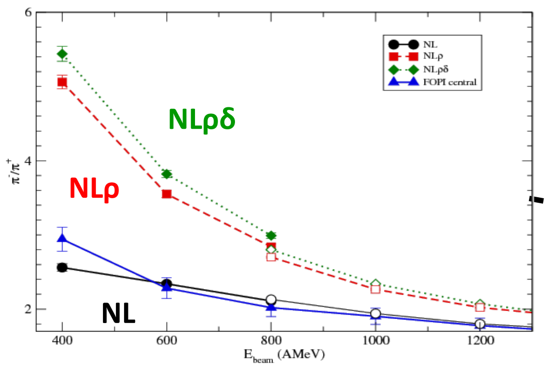

Z. Xiao et al., PRL 102 (09)

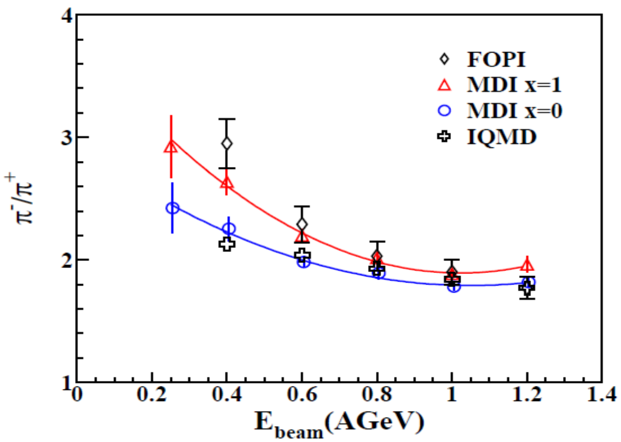

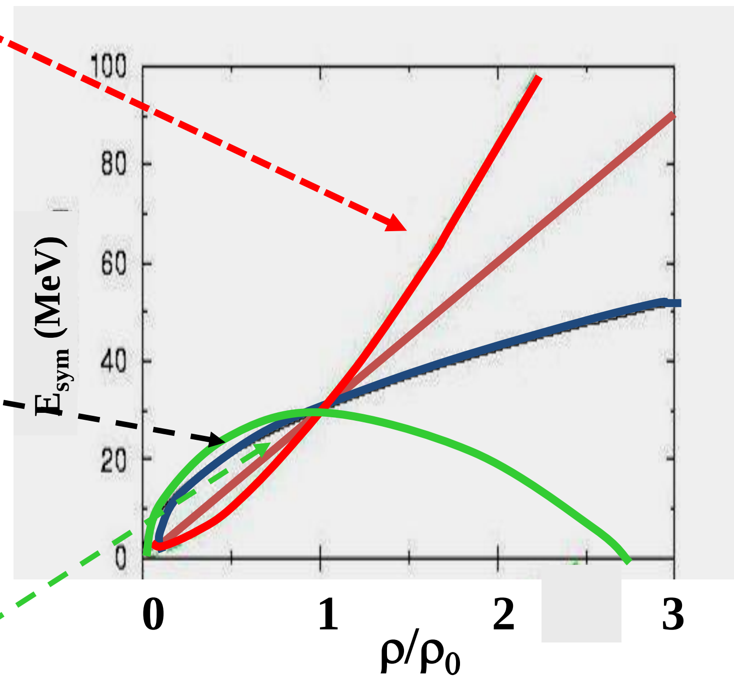

High densities: π^-/π^+ ratio

FOPI Data,

W.Reisdorf et al. NPA781 (2007)

Z.Q. Feng, PLB 683 (2010)

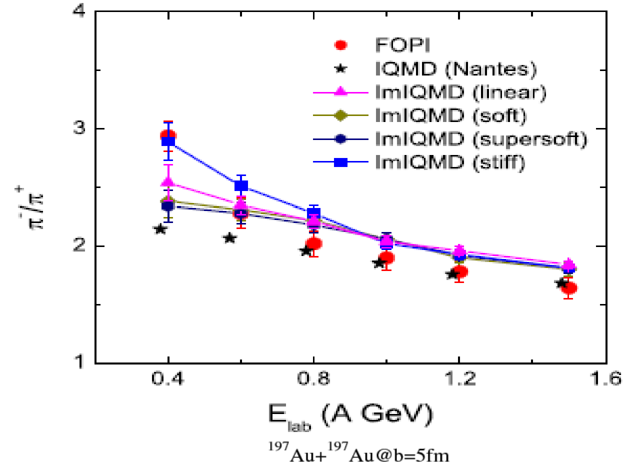

Ferini, at al., NPA 762 (05)

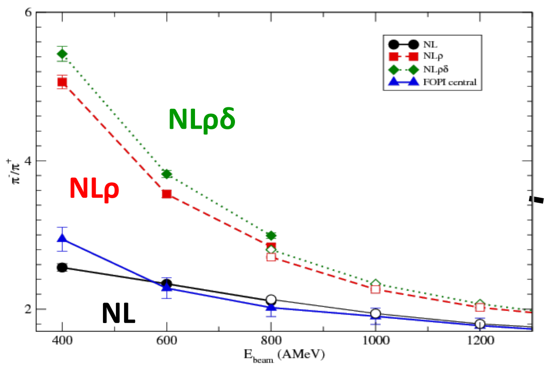

Z. Xiao et al., PRL 102 (09)

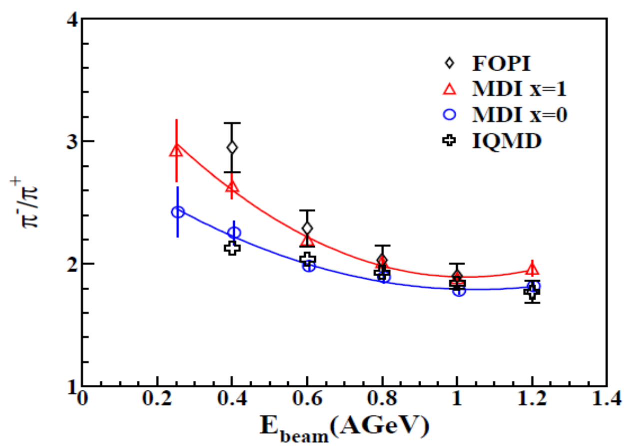

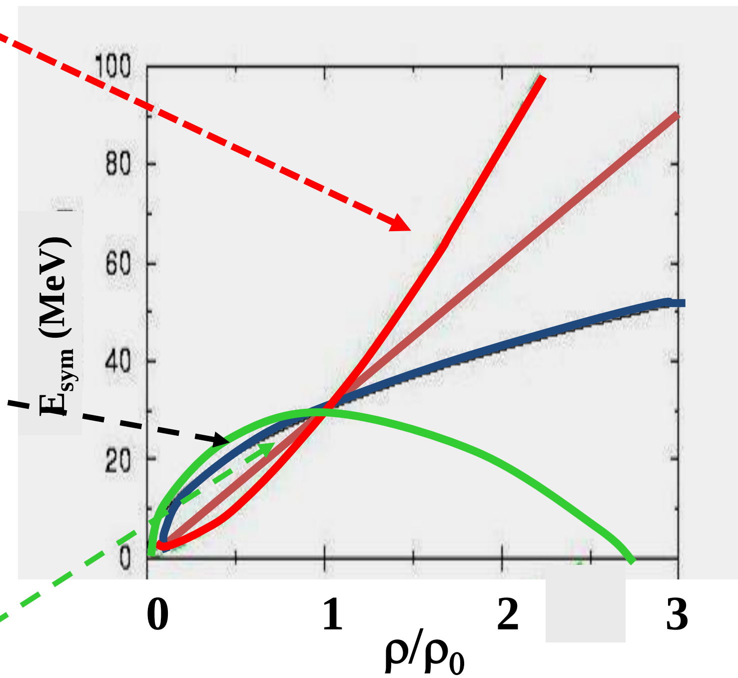

Pion ratio->High densities???:

Inconsistent with each

High-density Symmetry Energy: Particle Production

Difference in neutron and proton potentials

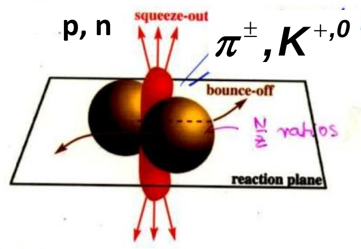

1. „direct effects“: difference in proton and neutron (or light cluster) emission and momentum distribution

2. „secondary effects“: production of particles, isospin partners $\pi^{-,+}$, $K^{0,+}$

G.Ferini et al.,PRL 97 (2006) 202301

High-density Symmetry Energy: Particle Production

Difference in neutron and proton potentials

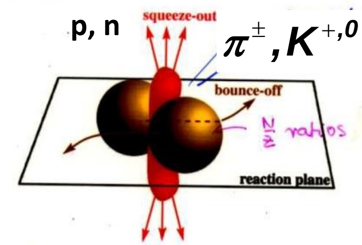

1. „direct effects“: difference in proton and neutron (or light cluster) emission and momentum distribution

2. „secondary effects“: production of particles, isospin partners $\pi^{-,+}$, $K^{0,+}$

   NN → NΔ

G.Ferini et al.,PRL 97 (2006) 202301

High-density Symmetry Energy: Particle Production

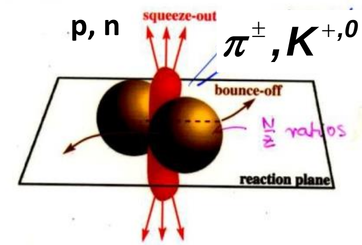

Difference in neutron and proton potentials

1. „direct effects“: difference in proton and neutron (or light cluster) emission and momentum distribution

2. „secondary effects“: production of particles, isospin partners $\pi^{-,+}$, $K^{0,+}$

NN → NΔ → Nπ

G.Ferini et al.,PRL 97 (2006) 202301

High-density Symmetry Energy: Particle Production

Difference in neutron and proton potentials

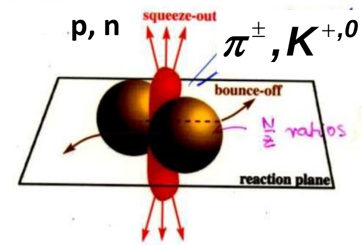

1. **„direct effects“: difference in proton and neutron (or light cluster) emission and momentum distribution**

2. **„secondary effects“: production of particles, isospin partners $\pi^{-,+}$, $K^{0,+}$**

NN → **NΔ**

↳ **Nπ** → **ΛK**

G.Ferini et al.,PRL 97 (2006) 202301

High-density Symmetry Energy: Particle Production

Difference in neutron and proton potentials

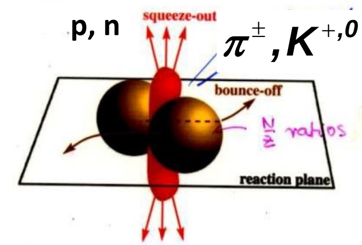

1. „direct effects“: difference in proton and neutron (or light cluster) emission and momentum distribution

2. „secondary effects“: production of particles, isospin partners $\pi^{-,+}$, $K^{0,+}$

NN → NΔ

NΔ → Nπ → ΛK

NΔ → NΛK

G.Ferini et al.,PRL 97 (2006) 202301

High-density Symmetry Energy: Particle Production

Difference in neutron and proton potentials

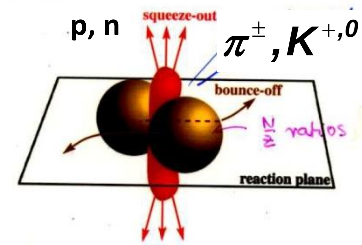

1. „direct effects“: difference in proton and neutron (or light cluster) emission and momentum distribution

2. „secondary effects“: production of particles, isospin partners $\pi^{-,+}$, $K^{0,+}$

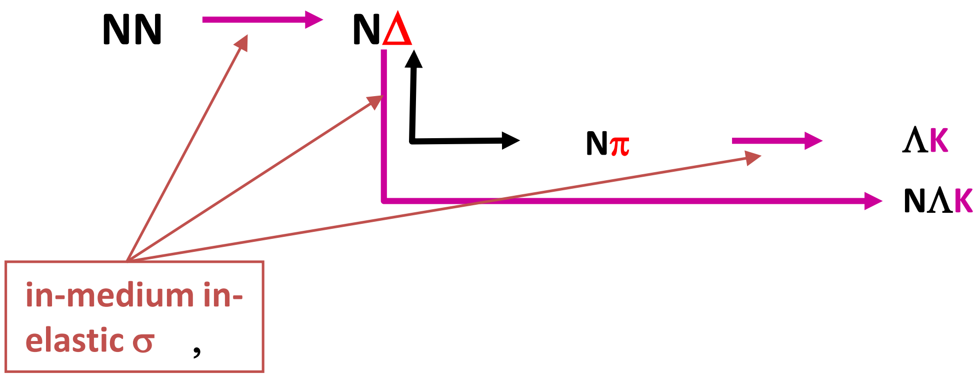

G.Ferini et al.,PRL 97 (2006) 202301

High-density Symmetry Energy: Particle Production

Difference in neutron and proton potentials

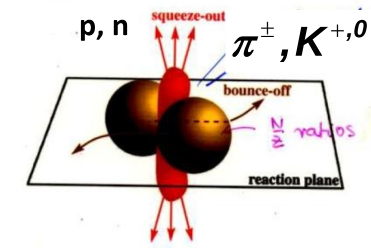

1. „direct effects“: difference in proton and neutron (or light cluster) emission and momentum distribution

2. „secondary effects“: production of particles, isospin partners $\pi^{-,+}$, $K^{0,+}$

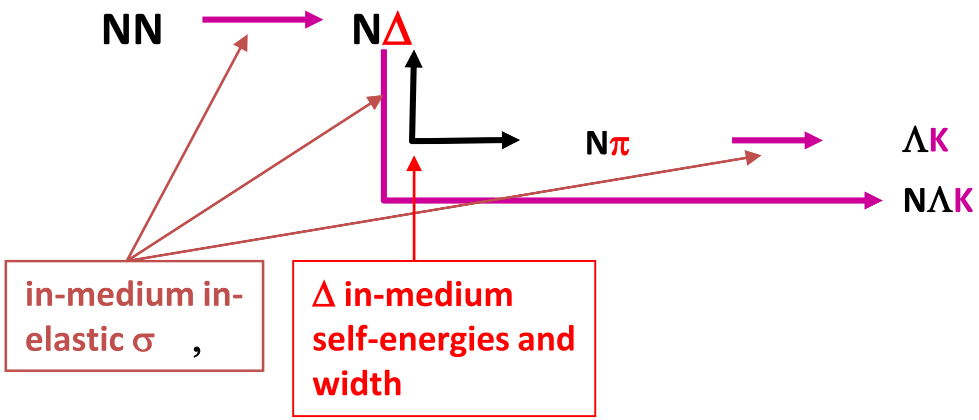

G.Ferini et al.,PRL 97 (2006) 202301

High-density Symmetry Energy: Particle Production

Difference in neutron and proton potentials

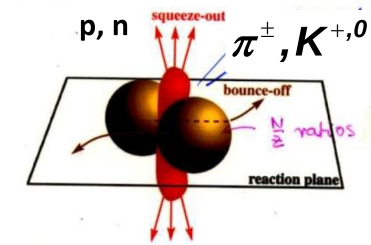

1. „direct effects“: difference in proton and neutron (or light cluster) emission and momentum distribution

2. „secondary effects“: production of particles, isospin partners $\pi^{-,+}$, $K^{0,+}$

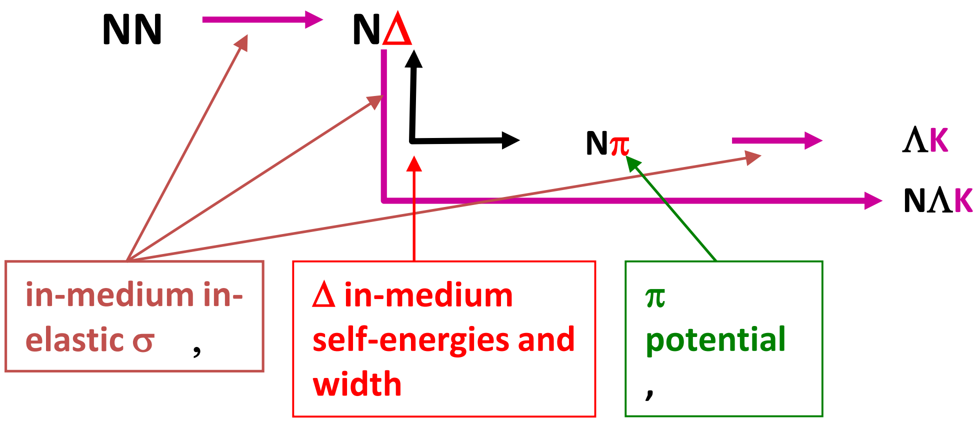

G.Ferini et al.,PRL 97 (2006) 202301

High-density Symmetry Energy: Particle Production

Difference in neutron and proton potentials

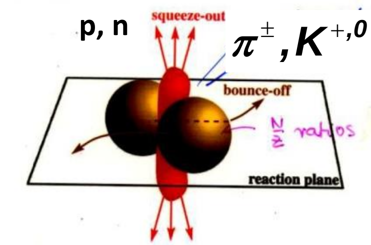

1. „direct effects“: difference in proton and neutron (or light cluster) emission and momentum distribution

2. „secondary effects“: production of particles, isospin partners $\pi^{-,+}$, $K^{0,+}$

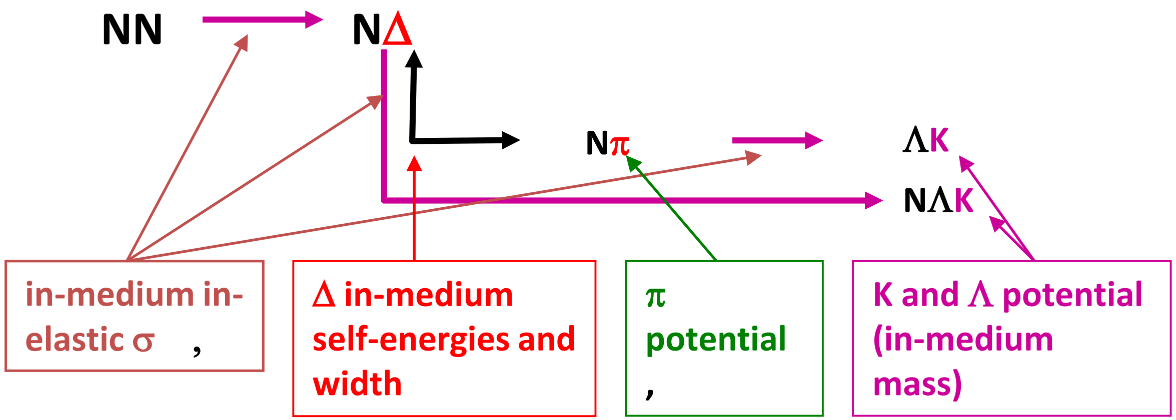

G.Ferini et al.,PRL 97 (2006) 202301

High-density Symmetry Energy: Particle Production

Difference in neutron and proton potentials

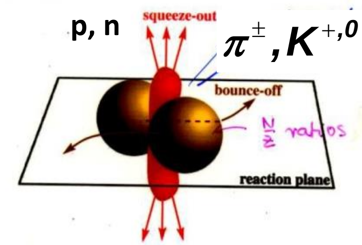

1. „direct effects“: difference in proton and neutron (or light cluster) emission and momentum distribution

2. „secondary effects“: production of particles, isospin partners $\pi^{-,+}$, $K^{0,+}$

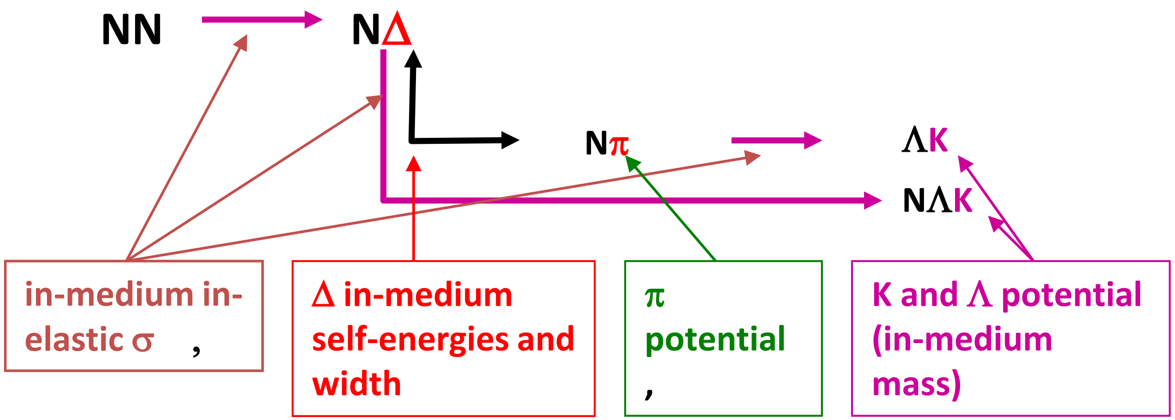

1. Mean field effect: U_{sym} more repulsive for neutrons, and more for asystiff
→ pre-equilibrium emission of neutron, reduction of asymmetry of residue

$$\frac{n}{p}\downarrow \Rightarrow \frac{Y(\Delta^{0,-})}{Y(\Delta^{+,++})}\downarrow \Rightarrow \frac{\pi^-}{\pi^+}\downarrow$$

$$\textit{decrease with asy-stiffness}$$

G.Ferini et al.,PRL 97 (2006) 202301

High-density Symmetry Energy: Particle Production

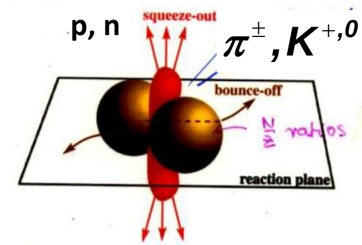

Difference in neutron and proton potentials

1. „direct effects“: difference in proton and neutron (or light cluster) emission and momentum distribution
2. „secondary effects“: production of particles, isospin partners $\pi^{-,+}$, $K^{0,+}$

NN → NΔ

Nπ → ΛK

NΛK

in-medium in-elastic σ ,

Δ in-medium self-energies and width

π potential ,

K and Λ potential (in-medium mass)

1. Mean field effect: U_{sym} more repulsive for neutrons, and more for asystiff

→ pre-equilibrium emission of neutron, reduction of asymmetry of residue

2. Threshold effect, in medium effective masses:

→ m^*_{N}, m^*_{Δ}, contribution of symmetry energy; m^*_{K}, models for K-potentials

$$\frac{n}{p}\downarrow \Rightarrow \frac{Y(\Delta^{0,-})}{Y(\Delta^{+,++})}\downarrow \Rightarrow \frac{\pi^-}{\pi^+}\downarrow$$

decrease with asy – stiffness

$$\sigma = \sigma\left(s_{in} - s_{th}\right) \quad \frac{\pi^-}{\pi^+}\uparrow \textit{ increase with asy – stiffness}$$

G.Ferini et al.,PRL 97 (2006) 202301

High-density Symmetry Energy: Particle Production

Difference in neutron and proton potentials

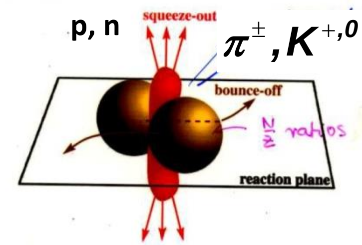

1. „direct effects“: difference in proton and neutron (or light cluster) emission and momentum distribution

2. „secondary effects“: production of particles, isospin partners $\pi^{-,+}$, $K^{0,+}$

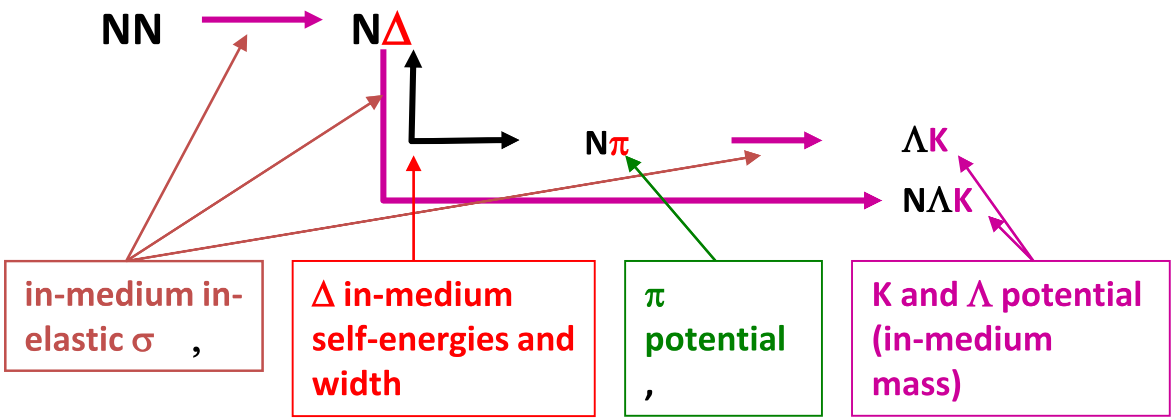

1. Mean field effect: U_{sym} more repulsive for neutrons, and more for asystiff
→ pre-equilibrium emission of neutron, reduction of asymmetry of residue

$$\frac{n}{p} \downarrow \Rightarrow \frac{Y(\Delta^{0,-})}{Y(\Delta^{+,++})} \downarrow \Rightarrow \frac{\pi^-}{\pi^+} \downarrow$$
$$decrease\ with\ asy-stiffness$$

2. Threshold effect, in medium effective masses:
→ m^*_{N}, m^*_{Δ}, contribution of symmetry energy; m^*_{K}, models for K-potentials

$$\sigma = \sigma(s_{in} - s_{th}) \quad \frac{\pi^-}{\pi^+} \uparrow increase\ with\ asy-stiffness$$

s_{thres} independent of isospin, due to simple model of Δ self energies

$$\Sigma_i(\Delta^-) = \Sigma_i(n)$$
$$\Sigma_i(\Delta^0) = \frac{2}{3}\Sigma_i(n) + \frac{1}{3}\Sigma_i(p)$$
$$\Sigma_i(\Delta^+) = \frac{1}{3}\Sigma_i(n) + \frac{2}{3}\Sigma_i(p)$$
$$\Sigma_i(\Delta^{++}) = \Sigma_i(p) \quad ,$$

G.Ferini et al.,PRL 97 (2006) 202301

PION PRODUCTION

G.Ferini et al., NPA 762 (2005) 147, NM Box
PRL 97 (2006) 202301, HIC

Main mechanism $NN \Rightarrow N\Delta \searrow \pi N$

nn → $p\Delta^-$ → $n\pi^-$
nn → $n\Delta^0$ → $p\pi^-$

pp → $p\Delta^+$ → $n\pi^+$
pp → $n\Delta^{++}$ → $p\pi^+$

n→p "transformation"

$$\Rightarrow \frac{\pi^-}{\pi^+}$$

Vector self energy more repulsive for neutrons and more attractive for protons

1. C.M. energy available: "threshold effect"

$$\varepsilon_{n,p} = E^*_{n,p} + f_\omega \rho_B \mp f_\rho \rho_{B3} \longrightarrow \begin{array}{l} s_{nn}(NL) < s_{nn}(NL\rho) < s_{nn}(NL\rho\delta) \\ s_{pp}(NL) > s_{pp}(NL\rho) > s_{pp}(NL\rho\delta) \end{array}$$

π(-) enhanced
π(+) reduced

2. Fast neutron emission: "mean field effect"

$$\frac{n}{p}\downarrow \Rightarrow \frac{Y(\Delta^{0,-})}{Y(\Delta^{+,++})}\downarrow \Rightarrow \frac{\pi^-}{\pi^+}\downarrow \Rightarrow decrease: NL \rightarrow NL\rho \rightarrow NL\rho\delta$$

Some compensation in "open" systems, HIC, but "threshold effect" more effective, in particular at low energies

⇒ No evidence of Chemical Equilibrium!!

Esym at high density: kaons

Kaon production

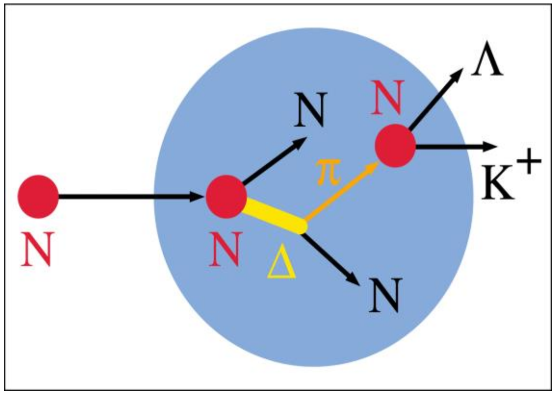

stiffness

Au+Au, b < 1 fm

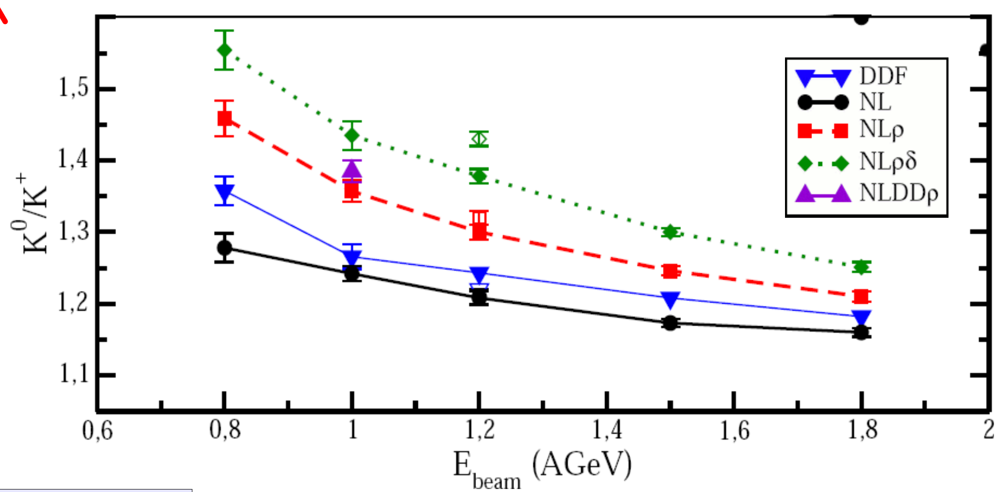

- Production of kaons at energies below the pp production threshold

$$.(NN \rightarrow K^+ + \Lambda + N) = 1.6($$
$$NN \rightarrow K^- + K^+ + NN) = 2.5$$

- Multistep production process
- Sensitive to isospin of the primary collision partners
- K^+/K^0 ratio sensitive to EOS

Ferini et al., PRL 97, 202301 (2006)

RMF calculations

INM: T=60 MeV and ρ_B=2.5ρ_0

RBUU: transport simulation

From IWM 2011 – Y. Leifels

Meson production: Pions

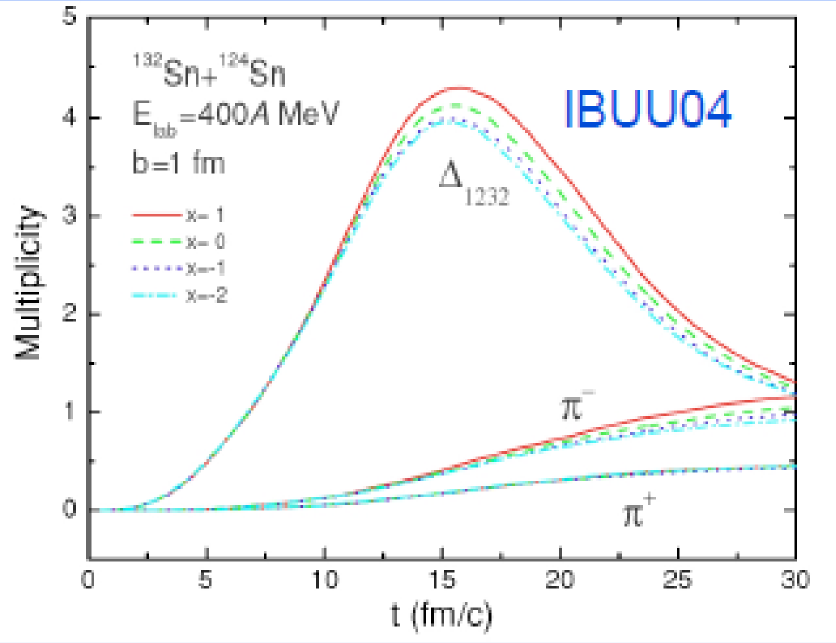

B.A. Li, PRC71, 014608 (2005)

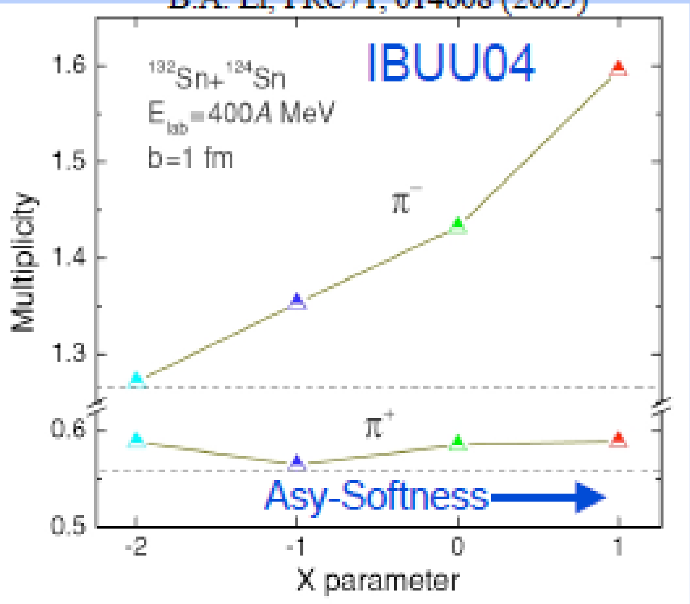

nn → $p\Delta^-$ → $n\pi^-$; nn → $n\Delta^0$ → $p\pi^-$

pp → $p\Delta^+$ → $n\pi^+$; pp → $n\Delta^{++}$ → $p\pi^+$

π-/π+ sensitive to $E_{sym}(\rho)$ at high ρ

NN collisions in high density regions

π^-/π^+ reflecting the $(N/Z)_{dense}$

Esym at high density: kaons

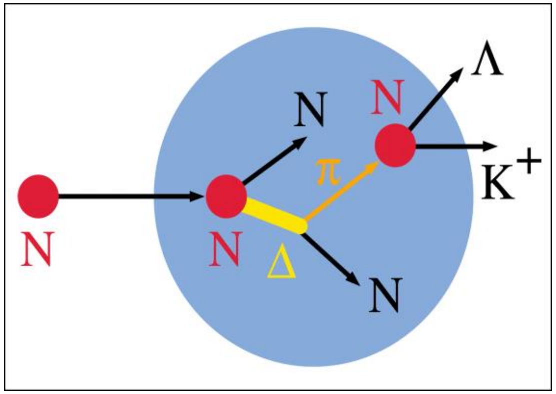

Ferini et al., PRL 97, 202301 (2006)

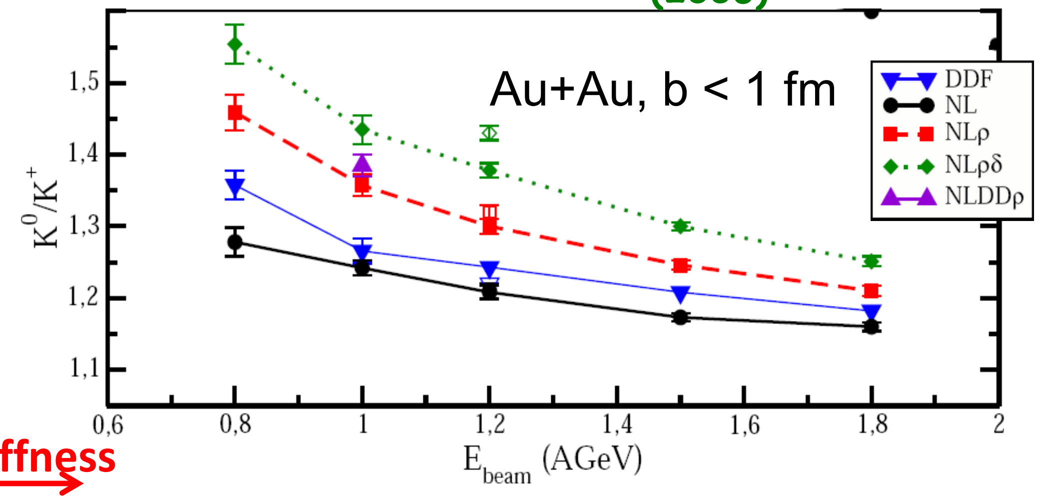

stiffness

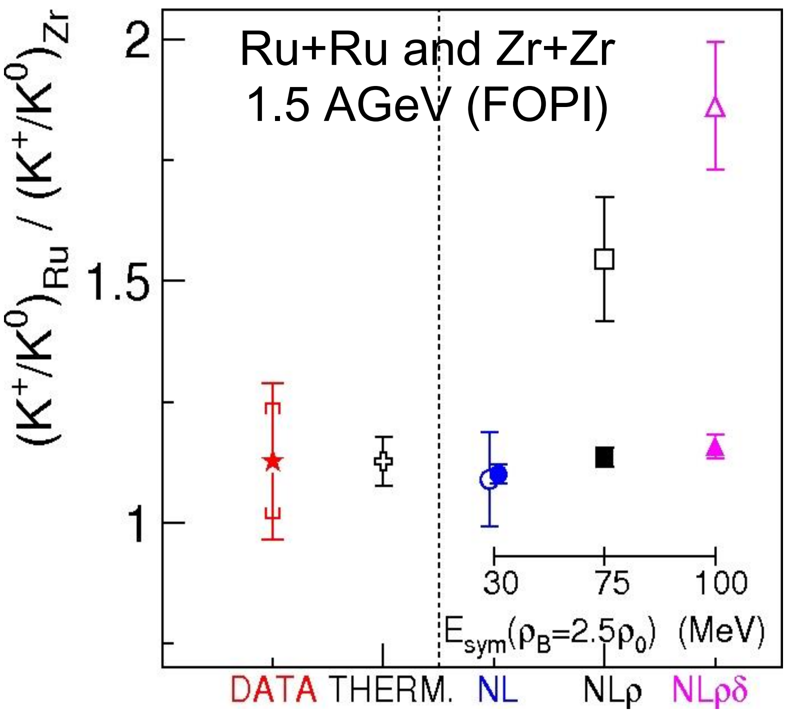

X. Lopez et al. 2007

RMF calculations

INM: T=60 MeV and $\rho_B=2.5\rho_0$

RBUU: transport simulation

- higher sensitivity at lower energies
- requires excellent kaon identification and long beam times

From IWM 2011 – Y. Leifels

Pion and Kaon freeze-out in HIC

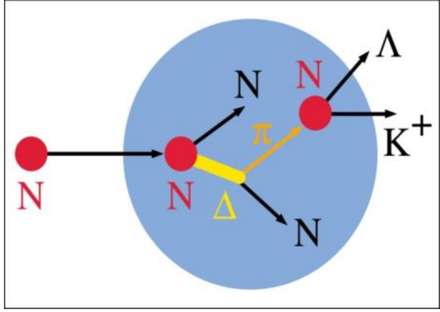

Low ρ/ρ_0 High ρ/ρ_0

π^+, π^-

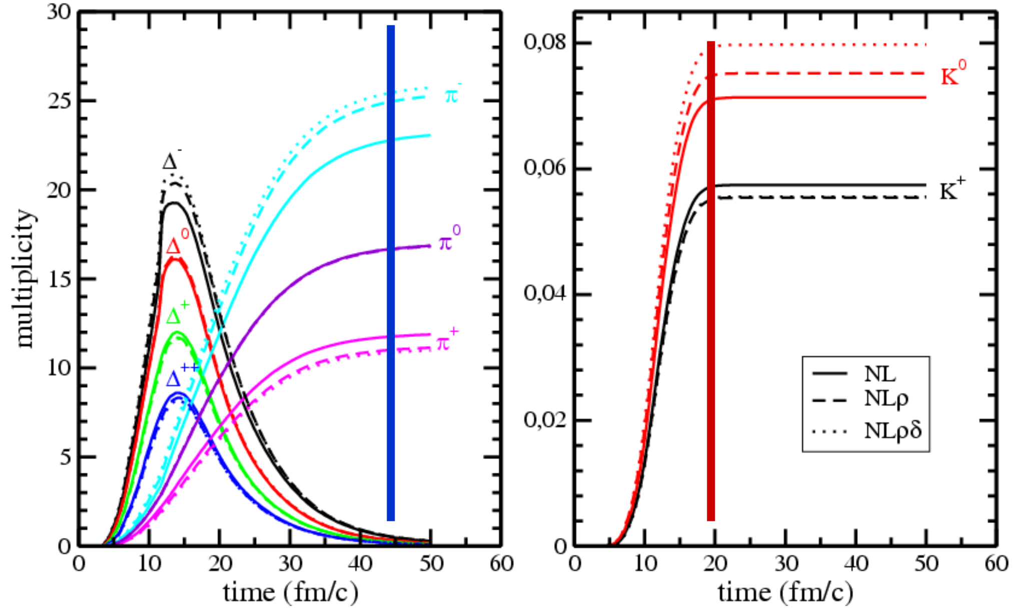

K^+, K^0

RBUU, Ferini et al., PRL97, 202301

Warning with pions:

- Strongly interacting in medium
- Freeze-out at late times (low ρ/ρ_0)
- Difficult to isolate π+ and π- produced in the high density stage

Kaons: more sensitive probes?

- Higher thresholds
- Weakly interacting in medium
- Freeze-out already at 20 fm/c: more reliable as high ρ probes